CONF - 670305
HEALTH AND SAFETY
(TID - 4500)

PROCEEDINGS

of the

FIRST INTERNATIONAL SYMPOSIUM ON THE BIOLOGICAL INTERPRETATION OF DOSE FROM ACCELERATOR-PRODUCED RADIATION

held at the

LAWRENCE RADIATION LABORATORY

BERKELEY, CALIFORNIA

March 13 - 16, 1967

Edited by Roger Wallace

Sponsored by

Division of Operational Safety

United States Atomic Energy Commission

Washington, D. C.

DISCLAIMER

DISCLAIMER

Portions of this document may be illegible in electronic image products. Images are produced from the best available original document.

FOREWORD

The "First International Symposium on the Biological Interpretation of Dose from Accelerator-Produced Radiation" was sponsored by the United States Atomic Energy Commission's Division of Operational Safety. The Symposium was held at the Lawrence Radiation Laboratory in Berkeley, California, March 13-16, 1967.

The objective of the meeting was to provide a companion meeting to the "First Symposium on Accelerator Radiation Dosimetry and Experience" which was held November 3-5, 1965, at the Brookhaven National Laboratory. This first symposium was limited in scope to an intensified discussion of dosimetry techniques. The biology which is associated with high energy radiation was specifically excluded, since it was the original plan to hold a second symposium devoted entirely to biology. Thus the present Symposium was a sequel to the first and they were inseparable in their objectives.

Since those attending the BNL Symposium were almost entirely health physicists with a background in physical science and actively engaged in the solution of radiation protection problems at high energy accelerators, it was felt that it would be necessary to begin the BID Symposium with a general review session on radiation biology, in order to provide a biological background for the proper understanding of the later sessions. This first session was arranged to give the health physicist a meaningful transition from fundamental radiobiological considerations to current new research activities in high energy biology.

In our opinion, and also based on the comments of several of those attending these objectives were quite well attained. The talks by Bond, Robertson, Brustad, Wolff, and Patt were quite exhaustive as an introduction to the several areas of specialization in radiobiology.

The overall purpose of the meeting was of course to inform the health physicists about the state of knowledge in advanced biological research as it might apply to their problems. It has often been said that it takes a long time for laboratory findings to be applied in practical situations, but this is certainly not true in radiobiology. Through this conference and others like it, the most recent understanding of high energy radiobiology is available to the practicing health physicist and is probably used fairly effectively. In addition, much of this material applies equally well to reactor and space radiation problems, and some of the participants were from these areas as well.

It is difficult for one discipline to know what another is doing. Such a lack of knowledge sometimes leads to duplication of effort. There were one or two times at the Symposium when the radiobiological speakers were able to inform a questioner in the audience that information was already available on a point which the questioner thought was an unknown area. This was true of the area of proton biology. It would seem, from the content of some of the questions and comments, that the Symposium was able to somewhat reduce the isolation between the physical and biological sciences.

One of the desires, often expressed in the planning of the meeting, was to try to get the biologists to be very explicit in describing what the health physicists should be measuring to be of maximum use to the biologist. This desire was expressed to most of the speakers beforehand, and several of them tried to satisfy this special request. While this is a complex question and there is still no general agreement on the instruments and measurements that should be used and made at high-energy accelerators, the Symposium seemed to throw much new light in this area. Of all the meetings and symposia that we have attended, this one made the most definite attempt to clear up the controversy between those who measure dose and those who try to measure distribution of ionization density or spectra. The measurement-of-dose school of thought had no supporters who were willing to speak out.

A further conclusion that can be drawn from the Symposium is that the AEC should be a leader in this area, since radiation is its prime concern, and the progress in radiobiology made by the national laboratories shows that this responsbility has been well met.

The success of this meeting is largely due to the many persons who participated in its organization and conduct. We give special thanks to Miss Charlotte Mauk, editor in the LRL Technical Information Division, for the many hours she spent assisting in the editing of these proceedings, and to members of:

Program Committee:

Edward J. Vallario, Chairman
Division of Operational Safety, USAEC

Miguel Awschalom, Princeton University
William W. Burr, Division of Biology and Medicine, USAEC
J. F. Fowler, Postgraduate Medical School, London
Lawrence H. Lanzl, University of Chicago
John T. Lyman, Lawrence Radiation Laboratory, Berkeley
James S. Robertson, Brookhaven National Laboratory
Roger Wallace, Lawrence Radiation Laboratory, Berkeley

Arrangements Committee:

H. Wade Patterson, Chairman
Lawrence Radiation Laboratory, Berkeley

L. J. Beaufait, SAN, USAEC
Ruth Block, Livermore
Ellen E. Cimpher, Lawrence Radiation Laboratory, Berkeley
Alexander Grendon, Donner Laboratory, UC Berkeley
Calvin Jackson, SAN, USAEC
John H. Kane, Division of Technical Information, USAEC
Alan R. Smith, Lawrence Radiation Laboratory, Berkeley
Lloyd D. Stephens, Lawrence Radiation Laboratory, Berkeley

Session Chairmen:

Victor P. Bond (I) - Brookhaven National Laboratory
P. Bonet-Maury (II) - Laboratoire Joliot-Curie, France
E. F. Oakberg (III) - Oak Ridge National Laboratory
J. Fowler (IV) - Postgraduate Medical School, London
Lawrence H. Lanzl (V) - University of Chicago
Charles A. Sondhaus (VI) - UC California College of Medicine
Burton J. Moyer (VII) - Lawrence Radiation Laboratory, Berkeley

Gratefully, appreciation is expressed to Edward J. Vallario, whose help went far beyond that of Chairman of the Program Committee and who has made a major contribution to every phase of the planning and organization of the Symposium. Special mention should be made of the untiring devotion to the details necessary for the successful holding of the Symposium and the secretarial work necessary both before and after the meeting and in connection with the preparation of these proceedings made by Mrs. Ellen E. Cimpher.

Roger Wallace
Symposium Chairman

Contents

Introductory Remarks

Martin Biles

Division of Operational Safety
USAEC, Washington, D. C.

Before I give my prepared comments I would like on behalf of the AEC, to join with our host and Dr. McMillan and welcome you to this Conference. I feel this is a double pleasure, since I am a native of this area and still consider Berkeley as my home; therefore it is a real satisfaction to welcome you to one of the truly pleasant areas of the world.

As you are aware, in more recent years particle accelerator technology has advanced extremely rapidly. Large particle acclerators have been created--the Bevatron, AGS, SLAC, and others--which provide the physicist with particle beams of high intensity and energy. As these higher-energy accelerators have become operational new problems of evaluating and interpreting the radiation environment have evolved.

The areas of uncertainty, then, are felt to be twofold: one, measuring the stray radiation environment, and, two, interpreting the effects of radiation. In the former instance some commendable work has been accomplished in the past few years in particle spectroscopy with high-energy neutron detectors, among other things. Many of the techniques were presented at the Symposium on Accelerator Radiation Dosimetry and Experience held at Brookhaven Laboratory in November of 1965. In the next few days this Conference will be concerned with the second area of uncertainty, that is, the biological effects.

The need for such a Conference as this became apparent during the initial planning of the dosimetry Symposium at Brookhaven, when it was decided to limit the scope of that conference to an intensified discussion of dosimetry techniques and give the biology consideration a thorough review at a later date. Therefore this meeting is a sequel to the first Symposium, and the two are virtually inseparable in their objectives.

Although there has been considerable progress in the field of radiation safety, some salient problems still remain to be resolved by the expertise of the radiobiologist. As an example: dose equivalent cannot be accurately determined in many cases, since the rem or dose equivalent depends on several factors, including the quality factor, dose distribution, and build-up factor. Although the absorbed dose in rads is a measurable quantity, the values for quality factor and build-up factor can only be estimated. The latter factors are dependent largely on biological information. Some of the investigations which were intended to improve our knowledge in these areas of uncertainty included seeking a better understanding of the linear energy transfers, quality factors, and energy absorption at microscopic dimensions. Much of this work will be discussed at this meeting.

To provide proper focusing of the problems in resolving these uncertainties in dose-effect relationships, the following few prerequisites must be included:

(a) A routine exchange of information is needed between biologist and physicist.

(b) Attempts should be made to narrow the gap between physicist and biologist, to establish a common basis for developing physical and biological parameters.

(c) Management should be willing to allot a portion of machine time for pertinent biological research on a routine basis.

Thank you.

CELLULAR RADIOBIOLOGY IN THE MAMMAL

V. P. Bond and C. V. Robinson

Brookhaven National Laboratory
Upton, New York

In the course of this Symposium a number of papers dealing with radiobiology, from the most basic physical, chemical, and cellular levels to the intact mammal, are presented. In selection of material most suitable to this introductory lecture, it seemed appropriate to attempt to show that work conducted at these various levels is indeed related, and that the radiobiological principles developed in so-called "simple systems," particularly cell systems, can be utilized in predicting (even quantitatively) the effects of radiation in the intact mammal, including man. Hence this presentation deals principally with examples designed to illustrate that results derived from studies on cell populations can be utilized in dealing with effects on the intact mammal. Initially, early effects in the mammal are dealt with, where the data and theses are on relatively firm ground. Late effects are then dealt with, in which the data are less secure and the hypotheses more speculative.

Before the principal subjects of this paper are put forth, several introductory statements are appropriate. First, radiobiology and radiological physics constitute the basic sciences of applied radiation protection, as they constitute the basic sciences for applied radiation therapy. Health physicists deal with a set of guide lines or numbers for routine work that are "legislated" by appropriately constituted bodies such as the NCRP and the ICRP. One can operate by utilizing these numbers without being at all concerned with their origin or how well their values may be rooted in radiobiology and radiological physics. However, the guide lines provided do not cover all situations. The more one understands of the origins of these numbers in radiobiology, and the radiobiological principles upon which they are based, the greater the flexibility the operational individual has in applying the established rules of radiation protection. The myriad of situations encountered in radiation protection are best and most intelligently dealt with if the individuals concerned have a firm appreciation of the present strengths and limitations of radiobiology and radiological physics.

In radiation protection it is frequently stated that an effort is made to balance possible risk versus possible gain. "Risk" entails the probability of effect, and may encompass also some estimate of the relative seriousness of different types of harm. In any event, the concept entails quantitative dose-effect relationships. If this concept is taken at all seriously, then it is absolutely mandatory that quantitative dose-effect relationships in the mammal be known to the best degree possible.

Also, in radiation protection one deals with perhaps the most complicated situation imaginable. This contrasts with radiobiological experimentation, in

which both biological and physical factors are designed to keep variables down to a minimum. In routine radiation protection work, on the other hand, all factors are almost as wholly undesirable as one could imagine. The absorbed dose at any location is only poorly known at best. One deals with one of the more complicated biological specimens, the intact human being. Nonuniform exposure or even partial-body exposure is the rule, and the dose rates encountered are highly variable and frequently unknown. An entire spectrum of radiation qualities, only poorly defined, is frequently encountered. The complexity is perhaps best illustrated in the subject matter of this Conference. In dealing with accelerator beams and their effects, one is dealing with nonuniform exposure, with markedly different doses derived from radiations of markedly different quality, to different organs or portions of the same organ. Quantification of the effects of such radiations is difficult, to say the least.

There are two approaches to dealing with the highly unsatisfactory conditions encountered in routine radiation protection. The one encompasses the completely empirical approach, in which one can attempt to guess at or evaluate dose-effect relations under the various degrees of uniformity of exposure, dose rates, and radiation qualities encountered. In the other, one can attempt to develop and understand principles of dose-effect relationships at the most basic levels of biological organization, and utilize these principles in attempting to deal quantitatively with the exposures and exposure conditions encountered in routine radiation protection. This latter approach involves the essence of the disciplines of radiobiology and radiological physics.

Generally speaking, a great deal is known about the effects of radiation at the level of the cell, the organ, and the mammal, as well as at the physical and chemical levels. A hiatus exists, however, between our knowledge of effects at the very basic level, and from the cell on up. As is shown below, effects on the mammal are understandable and predictable on the basis of effects on underlying cell populations. Eventually it may even be possible to predict satisfactorily effects in the intact mammal on the basis of events occurring at the most basic physical and chemical levels.

Body Cell Populations; Radiosensitivity

All organs of the body are composed basically of cells. For purposes here, the organs can be further divided into two categories, those in which in the adult the cells continue to divide or "turn over" at a rapid rate, and those in which in the adult the cells divide rarely if at all. The process of division of course involves mitosis, and it is a fact of radiobiology that most cells that do not divide are resistant to inactivation or killing by radiation (classical exceptions are the small lymphocytes and oocytes), and that those that do divide are exquisitely sensitive to radiation in terms of reduced or destroyed ability to further proliferate or to produce additional daughter cells. With large doses of radiation, and when early effects are considered, it is damage to those organs with a "rapid turnover rate"--principally the bone marrow and the gastrointestinal tract--that lead to significant damage and the so-called acute radiation syndromes that are seen.[1]

It is profitable to look at a specific organ whose cells turn over rapidly, the bone marrow. In Fig. 1 is shown schematically the cellular structure of

this organ. Cells are produced and allowed to mature in the bone marrow, and the mature cells are fed to the peripheral blood, where they serve their function and die. Only the granulocyte series is dealt with here, although the principles involved apply also to the red cell and megakarocyte series. The stem cell that produces ultimately the mature granulocyte can be defined as a cell capable of producing its own kind (another stem cell) as well as cells that are destined to mature through the granulocytic series and become functional granulocytes in the peripheral blood.

The granulocytic stem cells and the entire granulocytic marrow series can be regarded as the "factory" whose sole function is to produce the mature granulocytes in the blood which serve the critical function of protecting the individual against infectious disease. It can be seen immediately that if for any reason the stem cell population is suddenly reduced to small numbers, the effects will be felt successively in the more mature compartments, and then in the peripheral blood. Following high-dose exposure of the entire body it is the sudden effective reduction in the number of stem cells in the marrow that is the critical event that leads in time to the serious symptoms and signs associated with such exposure.

Uniform Whole-Body Exposure, $LD_{50/30\ days}$

A dose-effect relationship for marrow stem cells has been determined,[2] and the type of function obtained, shown in Fig. 2, is similar to that obtained with cells in tissue culture. (The curve is for a population of stem cells capable of producing at least red and white cell precursors. A curve for granulocyte precursors alone has not yet been determined.)

Note that there is an initial "shoulder" on the curve, followed by what appears to be an exponential falloff. Note the sensitivity of the cells--some 50% of the cells are rendered incapable of proliferation at doses of the order of 100 R or less. At the medium lethal dose for an animal--i.e., the dose that will kill approximately half of animals exposed to radiation--the number of surviving stem cells is reduced to low levels. Specifically in the mouse, when the number of stem cells is reduced to some 2 to 3 per thousand of the normal population, the animal has a 50-50 chance of surviving or dying.

Thus it is clear that with uniform whole-body radiation we are dealing with effects of radiation on populations of cells. When the size of a population is reduced to some fixed number for a given species, the remaining number of cells is no longer able to provide the functions of that organ, and if the functions of that organ system are critical to survival, the animal dies.

Bone-marrow failure has been implicated as the primary damage leading to death. It should not be inferred that other organs go unscathed, or that impaired function of other organs does not contribute in some measure to death. Some organs such as the lymphopoietic system and the testis, in which cells are renewed rapidly, are also severely injured. However, either such organs are not critical for survival, or the stem cells are able to regenerate fast enough so that the overall function of the organ is not critically impaired. Damage to the bowel or other organs may be contributory to lethality from the

bone-marrow syndrome. However, there is little question that these are second-order effects, and that the significant damage in terms of mortality or survival in the range from LD_0 to LD_{100} is damage to the bone marrow.

Time Factors in Granulocyte Depletion

In the above examples it was shown that one could predict the organs in the body which would play the greatest role in lethality in the animal exposed to whole-body radiation, on the basis of radiobiological principles involving the nature of the responses of dividing and nondividing cell populations to radiation. In addition, one can anticipate the time course of response on the basis of the same principles.[1] The granulocyte renewal system can be used as an example.

In Fig. 1 it will be noted that the granulocyte renewal system consists of dividing cells in the marrow, and nondividing cells in the marrow and peripheral blood. One would expect the dividing cells in the marrow to be quite radiosensitive, the nondividing cells in both the marrow and the blood to be quite radioresistant. One might further expect a continuing supply of granulocytes to the peripheral blood, for a time equal to the time from the "last" mitosis in the maturing cell series to the time of emergence of granulocytes into the peripheral blood. This time has been determined precisely[1] by administering a single dose of tritiated thymidine to the mammal, and noting the time of appearance of labeled neutrophils in the peripheral blood. This time varies with species, from the order of 1.5 days in the rodent to the order of 3.5 to 4 days in man.

Thus, one would expect a "shoulder" on the curve depicting the granulocyte count in the peripheral blood versus time after exposure of the mammal to whole-body radiation. In Fig. 3 is shown the time course of response of the granulocytes in the blood of the pig, as a function of dose after exposure. It has been observed in a number of species that the width of the shoulder is in fact equal to the time from the last mitosis to emergence of neutrophils in the peripheral blood. At the end of this time, there is a precipitous drop in the granulocyte count, and as the dose is increased the slope approaches more and more closely that of the normal disappearance rate of the granulocytes from the blood, or a half-disappearance time of about 6 or 7 hours. At lower doses, the slope is less, due to the easily observed continued entrance of some cells young enough to undergo mitosis at the time of exposure, which were injured but not sufficiently severely to prevent their maturation to the granulocyte stage. As the dose is increased, the ratio of injured to killed cells in mitosis decreases.

The remaining portion of the granulocyte response, the "abortive rise" and final recovery, have also been explained to a degree on the basis of the known changes in the underlying cell population.[1] The explanations are at present somewhat more speculative than for the initial "degenerative phase" of the granulocyte response, and more work must be done before the precise cellular basis for the latter two phases of the overall response are satisfactorily documented.

Nonuniform Exposure; $LD_{50/30\ days}$

With nonuniform exposure of the body, the degree of effect (mortality for present purposes) is, generally speaking, less per given maximum dose. The

extreme of nonuniform exposure is partial-body exposure, such as that used in radiotherapy. It is this reduction in effectiveness that accounts in part for the fact that doses of many thousands of R are routinely employed in radiotherapy, despite the fact that it requires only about 400 R delivered uniformly to the entire body to cause death.

The effect of nonuniform exposure can be quantified by introducing a factor, the "distribution effectiveness factor," DEF, analogous to RBE (relative biological effectiveness). RBE takes into account the effect of radiations of different quality, which can be regarded as reflecting different degrees of uniformity of energy disposition in micro volumes of tissue. RBE takes into account differing degrees of effect per unit of average absorbed dose of different quality radiations, and is determined empirically in the biological system of interest. The ratio of the dose of the most uniformly distributed radiation (the standard or low-LET radiation) needed to produce a given effect, divided by the average absorbed dose of the given (usually high-LET) radiation required to give the same degree of the same biological effect, is taken as the RBE of the given radiation.

A similar approach can be used for nonuniform exposure. One can start with the dose of uniform radiation required to give a certain degree of biological effect (LD_{50}, for instance), and divide this by the average dose (gram-rads per gram) of nonuniform radiation that gives the same degree of the same biological effect. This yields an empirically determined DEF, which could serve in practical situations in the same fashion as does RBE (or QF or "quality factor" in radiation protection).

This empirical approach has serious limitations when the subject of primary interest is the human being and the variety of dose distributions to be considered is essentially infinite. An approach that could allow calculation of the DEF would have obvious advantages. The cellular basis of radiation death described above provides such an approach for obtaining the required DEF, which can be applied to a variety of distributions of dose to the bone marrow of the body. The usefulness of the model in nonuniform exposure of rats, dogs, and swine has been tested.[5] An outline of the approach is given below.

It is assumed that the survival of the animal depends upon survival of the same critical fraction of the total number of marrow stem cells in the body, independent of their distribution among the subunits of the total marrow mass. The distribution of active marrow throughout the unirradiated individual can be determined by administration of radioactive isotopes that localize in the marrow, such as ^{59}Fe in the form of the ferrous salt or technetium-99m (^{99m}Tc) incorporated into particulate material that is taken up by the reticuloendothelial cells of the bone marrow (Fig. 3). It is reasonable to assume that the relative number of stem cells follows the same distribution, and that the stem cells in different parts of the bone marrow are subject to the same dose-survival relationship determined for uniform exposure of the marrow and illustrated in Fig. 2. The dose to each subunit of marrow can then be determined.

Knowing the dose to each subunit of marrow, the amount of marrow per subunit, and the dose-effect curve for stem cells (Fig. 2), one can calculate the DEF as follows: For the given pattern of nonuniform dose and for an exposure

that is known empirically to yield the specified degree of the given biological effect of interest (50% lethality rate in this instance), the number of surviving stem cells in each subunit of marrow can be calculated. This can then be summed over the entire marrow, to determine the number of surviving stem cells in the total marrow mass. The average absorbed dose to the marrow (gram-rads per gram) for this nonuniform exposure can then be calculated. The ratio of this value to the dose of uniform whole-body radiation required to reduce the number of stem cells in the total marrow mass to the same fraction as that calculated for the nonuniform exposure will indicate the expected effectiveness of the particular dose distribution in producing mortality, the DEF.

A comparison of the DEF so calculated with that found empirically is a check on the validity of the approach. The agreement has been found to be good in the cases so far (Ref. 5 and Fig. 4); however, additional data for further evaluating the approach are required.

It should be noted that whereas values of RBE are usually greater than unity, values of DEF are usually less than unity.

The above discussions indicate that integral dose/gram (gram-rads/gram) alone, even if calculated for the marrow mass only, is not the significant parameter in terms of which death from the hemopoietic syndrome can be predicted. The integral dose to kill will obviously vary with the distribution of dose in the body, so that integral dose becomes significant only as a step in finding the meaningful parameter, average marrow dose, in terms of which the DEF can be determined.

Bowel Exposure

Although in principle rapidly turning over cell systems of the bowel are similar to those of the bone marrow, real differences exist. In Fig. 5 is shown schematically a histological section of the wall of the bowel, with the crypts in which the stem cells are located, and the villi covered with the mature functional cells. The stem cells serve to continuously feed mature cells to the villi, where their existence is terminated by their being sloughed into the bowel lumen at the tips of the villi.

With whole-body uniform exposure, a phenomenon similar to that seen in the bone marrow exists. Radiation affects primarily the stem cells, which results effectively in a failure of delivery of mature cells to the villi. If the stem cells have been reduced to a critical level, breaks in the covering of the villi occur before the stem cell population can regenerate adequately, and death ensues.

It should be pointed out that, although all portions of the bone marrow pour mature granulocytes into the common pool, the blood, the stem cells in each crypt feed mature cells only into those villi directly associated with this crypt. Thus it is impossible for the crypts of a portion of the bowel unexposed or lightly exposed to feed mature cells into nonadjacent villi in bowel portions that may have received a higher exposure. With nonuniform exposure, those portions of the bowel that have received a very high dose become depleted of mature villus cells, and the animal will die even if a large portion of the gut received no, or very little, exposure. Thus the approach outlined for the bone marrow for

calculating effectiveness of the distribution factor does not apply to the bowel, or only to a very limited extent. It should be pointed out also that similar reasoning applies to the number of surviving crypts, and that a dose-effect curve in terms of number of surviving crypts rather than surviving stem cells has little meaning in this context.

Fortunately, lethal damage to the bowel occurs only at relatively high doses, well above those leading to death from the bone marrow syndrome. Thus the approach outlined for the marrow is applicable in the dose range of most interest, that is, in the sublethal ranges or in dose ranges where survival is possible or where enhanced survival is possible by means of suitable therapy.

Late Effects, Uniform Exposure

A number of late effects may occur, such as cancer, leukemia, cataract formation, life shortening, etc. It is important to point out that the basic lesion most probably is still at the cellular level. Now, however, instead of primarily death of the cell or lack of proliferative capacity, the injury to cells that are still capable of continued proliferation is likely of major interest. Also, unlike early effects, there is no evidence that the organs with rapidly turning over cells are especially susceptible to late effects. Thus cells in nonproliferating organs such as the liver may be injured, and there is evidence to indicate that such injury may lead to life shortening.[6] There is also evidence that such injury may stimulate the cell to divide or to proliferate independent of regulatory mechanisms that prevail over the normal cell. This may result in uncontrolled proliferation, namely leukemia or cancer. Thus the effects of interest probably are not the depletion of a cell population with resultant lack of function of that organ as a result of failure of the stem cells to supply mature functional cells in adequate numbers. Rather, a sublethal injury to cells may result in abnormal growth or other malfunction, leading in time to a process lethal to the individual.

It is pointed out, however, that although the basic lesion leading to significant late effects may well be cell injury, a number of difficulties must be dealt with before quantitative relationships can be developed that approach those possible with early effects. The cell population at risk is unknown for many effects of interest, particularly leukemia, and the numbers at risk may well vary with age. Hormonal factors are known to be at least a complicating if not a primary factor in the genesis of many malignancies. The probability of cell injury leading to malignancy may well be a function of age, hormonal state, or other factors. The fact that partial-body shielding appears to protect against radiation induction of some forms of leukemia may indicate additional complicating factors as yet unknown. It is not yet clear if these additional factors represent complications that must be taken into account over and above basic cell injury, or whether these factors may be of considerable and general significance or even of overriding importance. These difficulties, however, should not deter one from attempting to deal with late effects at the cellular or finer level of organization, making assumptions that certainly oversimplify. Such an approach will be outlined below, with leukemia induction as an example. Efforts of this nature have been made previously.[7,8]

Leukemia Production, Uniform Exposure

Although dose-effect curves at the cellular level for leukemia (or other neoplasia) induction are not available, dose-effect curves indicating the rate of leukemia (or other neoplasia) production vs dose have been determined in a number of species.[7-9] Such a curve for leukemia induction in individuals exposed to atomic bomb radiation in Japan is indicated in Fig. 6. The exposure in Japan was received over a very short interval of time, and the dose-effect relationship might well be different at lower dose rates. In addition, more recent calculations of the dose received by individuals in Japan would alter the dose scale shown in Fig. 5; however, this would not alter the shape of the curve. The data are consistent with a straight-line relationship between dose and effect, although the data are far from adequate to indicate if this is in fact the correct function. Also, data are absent at very low doses, and it cannot be stated whether or not a "threshold" exists below which the incidence of leukemia would be zero. Because some data, such as those shown, are compatible with a straight-line dose-effect relationship, because there is increasing thought that leukemia and other cancer may result from injury in a single cell ("somatic mutation"), and because a straight-line relationship represents a simple and conservative approach, the so-called "no threshold, linearity" hypothesis is commonly taken as the dose-effect relationship to apply to the induction of leukemia and other neoplasia and to the cells responsible. It is stressed that this remains hypothesis, however, and it is not clear at present how good it is, or the extent to which it agrees or disagrees with experiment.

In Fig. 5 the relative number of individuals developing leukemia is plotted vs dose, i.e., the curve represents a leukemia-incidence-vs-dose relationship. The curve would also represent the relationship between dose and the number of surviving affected cells of interest vs dose, provided that the following assumptions apply: (a) leukemia following irradiation arises from injured but surviving cells, i.e., its origin lies in "somatic mutation," (b) only one affected cell is necessary to produce leukemia, (c) all individuals exposed have approximately the same number of cells of interest at risk in the body, (d) the number of cells affected is at most a very small fraction of the number of surviving cells (well below 1%), and (e) the highest incidence considered is small, i.e., below approximately 10%.

The dose-incidence curve shown in Fig. 5 also represents a plot of dose vs number of cells at risk (as opposed to just surviving cells at risk), provided additionally that virtually every cell affected also survives and may potentially produce leukemia, i.e., there is negligible cell death in the irradiated cell population of interest.

Additional factors must be taken into account. If the given disease--in this case leukemia--is thought of as caused by a single affected cell, it would seem at first glance that the incidence I of this disease, expressed as a fraction, should equal the probability that an animal has such a cell, which in turn is equal to the average number of such cells per animal. This is true, however, only if two corrections are taken into account, either of which may be quite significant. First, one must find the incidence I' which would have been observed in the absence of other causes of death. This corrected incidence may be determined by

an integration involving the age-specific incidence of the disease. Necessarily $I' > I$, and the magnitude of the correction depends in general on the degree to which deaths from other causes predominate over and precede those from the given disease. The second correction is for the occurrence of animals with more than one affected cell. As a consequence of such "redundancy" the average number of cells, m, is greater than I'. Assuming a Poisson distribution of probabilities that an animal has no cell, one cell, etc., one has $I' = 1-e^{-m}$. At low incidence, I' and m approximate each other closely, whereas for higher values the difference may be considerable. When $I' = 0.5$, for example, the value of m is ln 2 or 0.693.

Thus, although only incidence-vs-dose curves for late effects such as leukemia are available, this type of curve can be used, together with certain assumptions, to infer the nature of the dose-effect curve for the cells at risk. Or, alternatively, one can simply assume the nature of this curve. The curve is commonly assumed to be linear, with no threshold.

Nonuniform Exposure, Leukemia Production

If the curve for net affected cells vs dose is assumed or is known, and if the distribution of the cells at risk within the body is known, then the same cellular approach outlined above for dealing with nonuniform exposure of the marrow can be used to yield the total risk to the individual for a given type of nonuniform exposure as compared with the uniform exposure.

Further, however, if the net-affected-cells–vs–dose curve is assumed or known to be linear, and if the cells of interest are known to be uniformly distributed in the organ of interest, then the calculation reduces to a calculation of integral dose per gram, or gram-rads/gram, that is, the average dose to the organ of interest. To say this in another way, the incidence for a given nonuniform distribution of dose, with a given average dose, is the same as that for uniform exposure with the same given average dose. This means in effect that the DEF is unity.

Summary

In this introductory presentation an effort has been made to show that if one knows (a) the distribution of absorbed dose throughout the body, (b) the distribution of cells of interest, and (c) the dose-effect curves for these cells and the effects of interest, one can effectively and quantitatively translate the principles and knowledge obtained at the basic cellular level into expected effects in the intact mammal. Several illustrations have been used to show that this is true. Data are available for exact evaluation with respect to early effects. It has been shown that the same approach may be applied more generally, and perhaps even with long-term effects such as the development of malignancies. However, data are now insufficient for adequate evaluation and the approaches at present are highly hypothetical. Throughout, the paramount importance of obtaining more quantitative data, particularly dose-effect curves, and especially at the cellular level, is stressed. The more data of this nature that are obtained, the more it will be possible to use radiobiological principles in applied health protection work.

References

1. V. P. Bond, T. M. Fliedner, and J. O. Archambeau, Mammalian Radiation Lethality; A Disturbance in Cellular Kinetics, Academic Press., N. Y. and London, 1965.

2. E. A. McCulloch and J. E. Till, The Sensitivity of Cells from Normal Mouse Bone Marrow to Gamma Radiation, in Vitro and in Vivo, Radiation Res., 16: 822-832, 1962.

3. Warren K. Sinclair, X-Ray-Induced Heritable Damage (Small-Colony Formation) in Cultured Mammalian Cells, Radiation Res., 21: 584-611, 1964.

4. E. P. Cronkite, F. W. Ulrich, D. C. Eltzholtz, C. R. Sipe, and P. K. Schork, The Response of the Peripheral Blood of Swine to Whole-Body X-Ray Radiation in the Lethal Range, U. S. Naval Medical Res. Inst. Report, Proj. NM 007039, Report No. 21, April 1949.

5. V. P. Bond and C. V. Robinson, A Mortality Determinant in Nonuniform Exposures of the Mammal, Presented at the Workshop Conference on Space Radiation Biology, University of California, Berkeley, California, Sept. 7-10, 1965, unpublished data.

6. H. K. Curtis, A Composite Theory of Aging, The Gerontologist, 6 [3]: Part 1, Sept. 1966.

7. V. P. Bond, E. P. Cronkite, C. A. Shellabarger, and G. Aponte, Radiation-Induced Mammary Gland Neoplasia in the Rat, Mammalian Cytogenetics and Related Problems in Radiobiology, 361-382, Pergamon Press, Oxford, 1964.

8. L. H. Gray, Symposium on Fundamental Cancer Research, 18th, Anderson Hospital & Tumor Inst., Radiation Biology and Cancer, in Cellular Radiation Biology, 7-25, Williams & Wilkins, Baltimore, 1965.

9. A. C. Upton, V. K. Jenkins, and J. W. Conklin, Myeloid Leukemia in the Mouse, Annals N. Y. Acad. Sci., 114: 189-202, 1965.

10. E. P. Cronkite, W. Moloney, and V. P. Bond., Radiation Leukenogenesis: An Analysis of the Problem, Am. J. Med., 28: 673-682, 1960.

Table 1. Calculation of fraction of total bone marrow stem cells surviving at the $LD_{50/30\ day}$ exposure level for dogs irradiated with uniform (bilateral) and nonuniform exposure patterns.

Type of exposure	Name of part of stem-cell pool	Fraction of pool in part	Average dose to part, rads	Calculated fraction survival in part	Relative number of surviving stem cells
unilateral	Proximal	0.306	530	0.006	0.002
	Middle	0.427	337	0.043	0.018
	Distal	0.267	168	0.256	0.068
	Whole	1.000	351[a]	-	0.088
bilateral	Middle	0.427	280	0.079	0.034
	Outer	0.573	266	0.091	0.052
	Whole	1.000	272[a]	-	0.086

a. Gram rads per gram.

Effectiveness factor for unilateral exposure is 272/351 = 0.78.

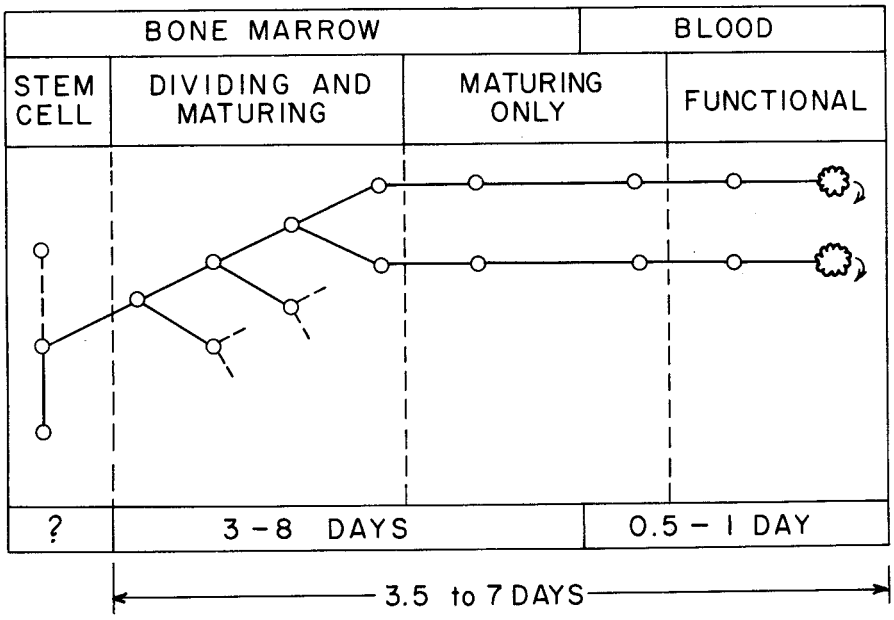

Fig. 1. Schematic representation of the bone marrow–blood granulocyte cell-renewal system. The bone marrow is the "factory" supplying mature functional granulocytes to the blood at a steady rate in the normal individual.

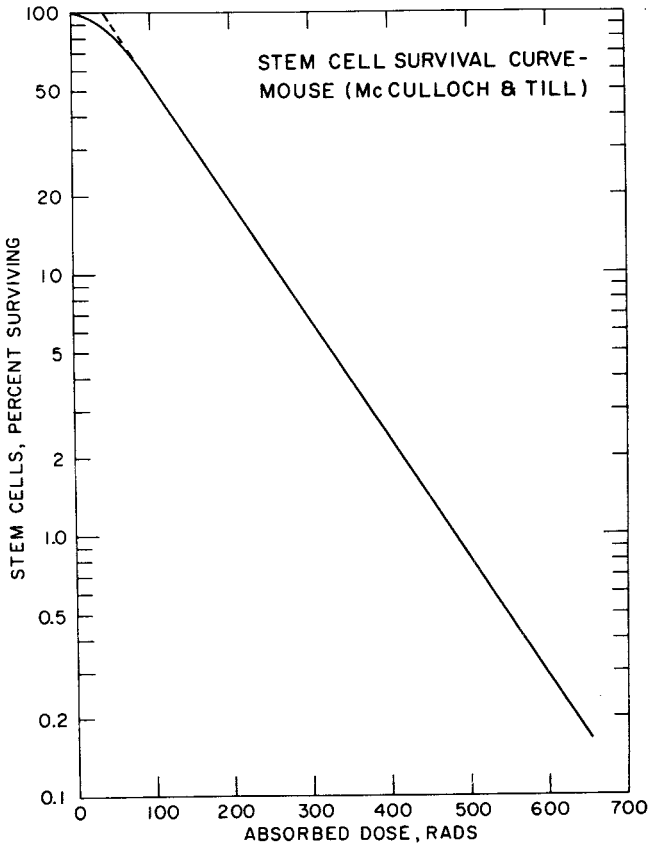

Fig. 2. Dose-survival curve of "stem cells" of the mouse bone marrow (data from Ref. 2).

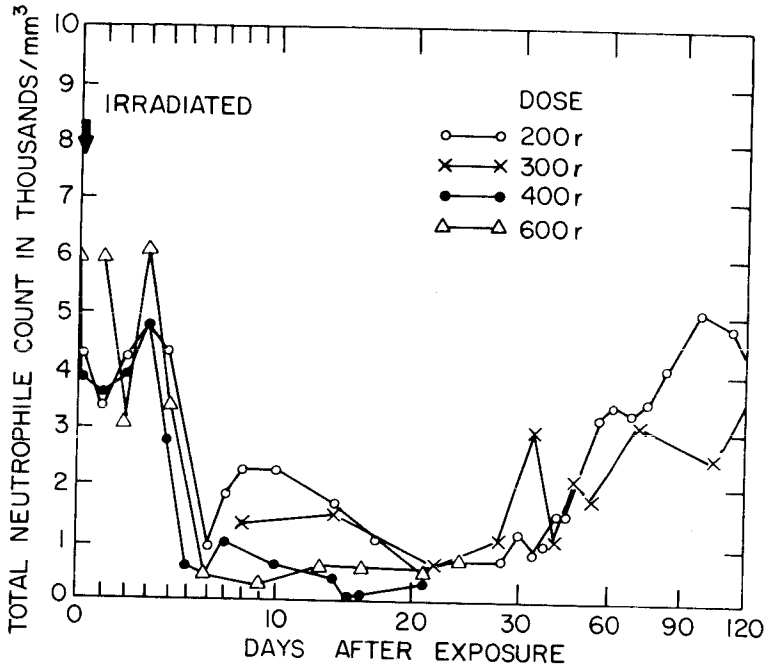

Fig. 3. Granulocyte response of the swine to various doses of radiation to the whole body (data from Ref. 4).

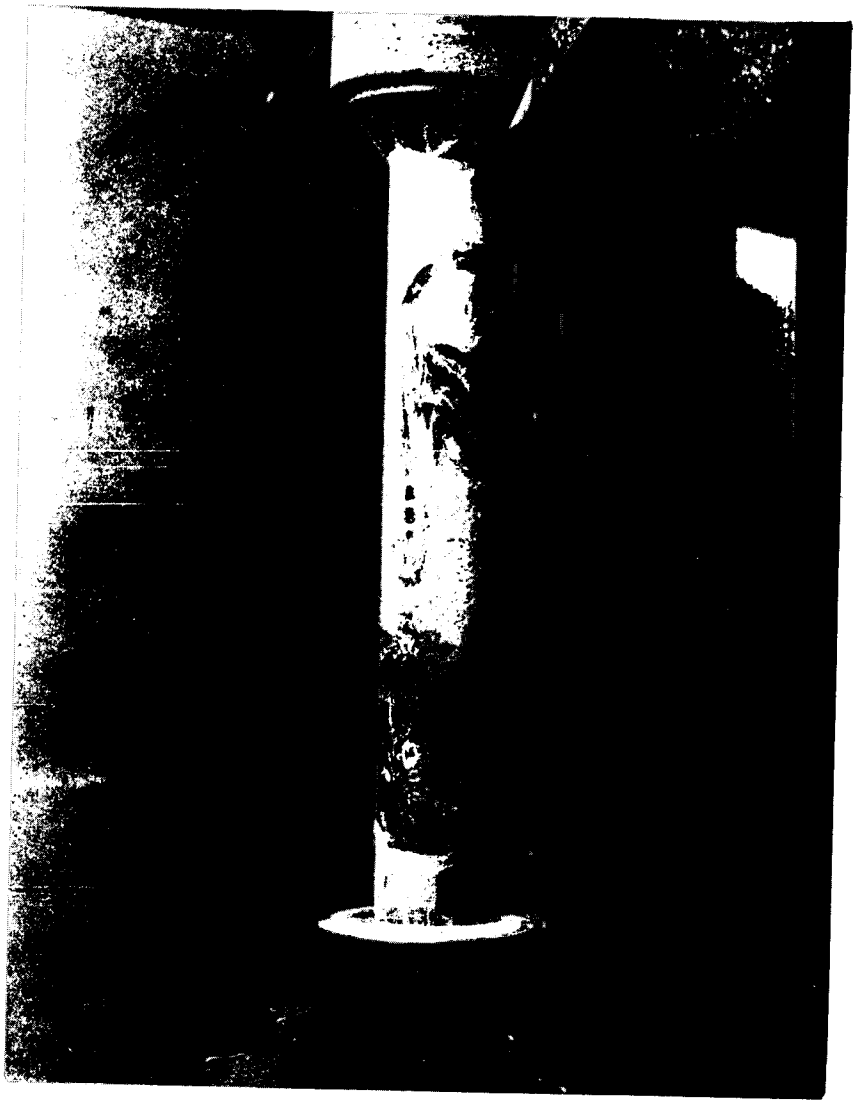

Fig. 4. Method of determining precisely the distribution of active bone marrow in the rat as a function of distance from the animal's surface. A ^{99m}Tc colloid was administered intravenously. The animal was then frozen and turned down on a lathe. The activity per cut reflects the amount of active marrow at the corresponding depth.

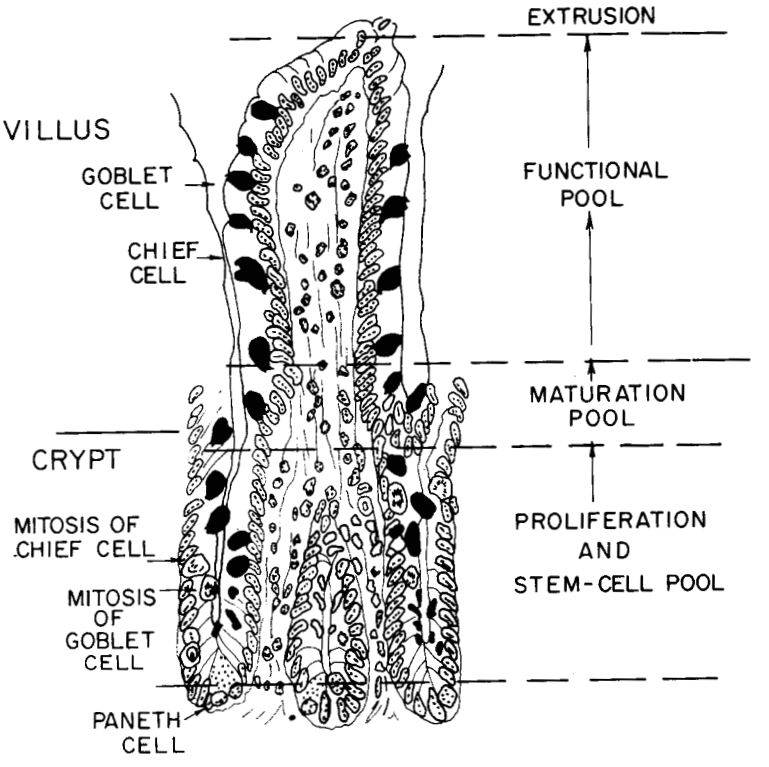

Fig. 5. Schematic of the cell-renewal system of the bowel epithelium. The dividing cell populations of the crypts furnish mature nondividing functional cells continuously to the villi.

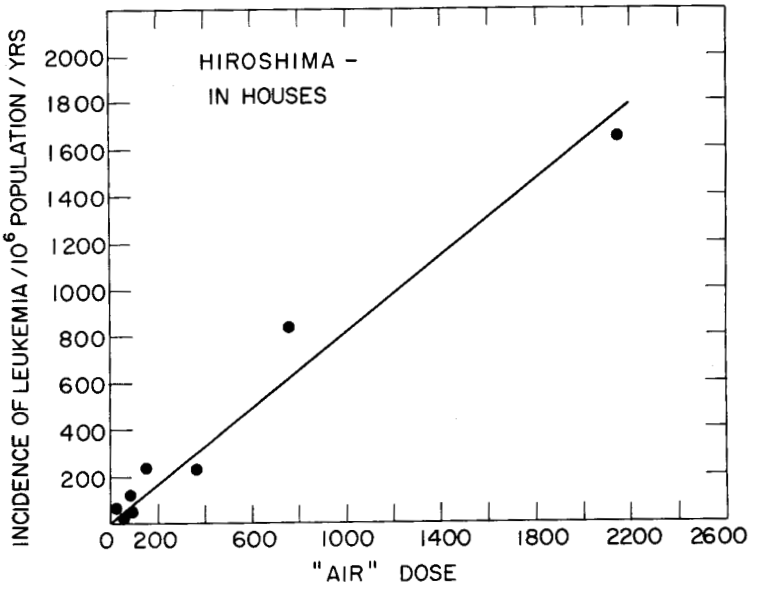

Fig. 6. Incidence of leukemia in Hiroshima populations, vs estimated dose (dose estimates have been revised downward after collection of data shown).

Basic Physical Mechanisms in Radiobiology

J. S. Robertson
Brookhaven National Laboratory

I.2

1: Introduction

One of the principal objectives of this symposium is to relate the radiation dose to the biological effects that ensue as consequences. In so doing we begin with the assumptions that ultimately the biological effects are caused, at least stochastically if not deterministically, by the initial physical events that are associated with exposure to ionizing radiation, and that these initial events are followed by a chain of chemical and biochemical reactions that translate the physical events into the biological effects.

Of the physical parameters, the absorbed dose, expressed in terms of energy absorbed per gram at the point of interest, is of prime importance. Experience, however, indicates that the radiation dose *per se* does not determine the biological effects. Instead, many factors must be considered. These include other physical parameters such as dose rate and ion track density, and many biological factors such as species, age, sex, and end point. In particular, for the same end point it has been found that the dose required to produce a given degree of effect depends upon the nature or type of radiation. The ratio of the dose of a standard radiation, usually 250-kvp x rays or ^{60}Co gamma rays, to the dose of the test radiation required to produce a given effect has been defined as the RBE, or relative biological effectiveness of the test radiation, as mentioned by Dr. Bond in the preceding paper.

In health physics work it is often necessary to accept the existence of RBE's as an empirical fact, and arbitrary or "legislated" values dependent on the LET, or linear energy transfer rate, are used. The values assigned, however, may be based on exposure conditions in which

many of the variables, particularly the dose, the dose rate, and the end point, are quite different from those involved in the situation being evaluated, and may not be directly applicable.

One of the problems in radiobiology is to seek a theoretical explanation of RBE's. To insure general validity, this requires determining the RBE's for a wide variety of exposure conditions and end points. We may epitomize the problem by asking, "Why aren't all RBE's equal to unity?"

In the present paper we shall review the basic physicochemical mechanisms involved in the interaction between ionizing radiation and the absorbing material, but may as well admit at the beginning that at present there is no completely satisfactory answer to the above question. In part this is because although much is known about the effects at each of several stages—physical, physicochemical, chemical, biological, clinical—the mechanisms of transition between the stages is often not well understood.

2. Physical Phase

Ionization and excitation

In the passage of ionizing radiations through any absorbing medium, the primary processes that occur are ionization or ion-pair production and excitation, which are distinguished by whether an electron is removed from an atom or merely elevated to an abnormally high energy state. In ion pair production there is removal of an electron from one atom and electron attachment to another. The ionization potential varies with the material, and is about 16 eV air, 13 eV for water. However, on the average, about 32.5 eV are dissipated per ion pair, so for each ion

pair there is another 10-20 eV to be accounted for and which is dissipated by excitation. The excitation energy is disposed of by dissociation, fluorescence, or energy transfer. In complex molecules it may appear as vibrational or oscillatory energy. Although direct measurements in water are difficult to achieve, it is inferred from other results that in aqueous media the energy is roughly equally divided between excitation and ionization. The relative importance of excitation in producing biological effects is not known.

Although, at least in such devices as roèntgen meters, only the ionization is actually measured, dosimetric values are usually expressed in terms of the total energy absorbed.

Ionization tracks may be studied in cloud chambers, bubble chambers, and emulsions. The separation of ion clusters depends on the nature of the radiation, with gamma rays producing relatively sparse tracks having only about 10 ion pairs/μ of path length, whereas alpha particles may have, typically, about 5000 ion pairs/μ, and uranium fission fragments over 100 000 ion pairs/μ. In terms of LET, the values run 0.28 keV/μ for 20-MeV γ rays, 2.8 keV/μ for 200-kvp x rays, 150 keV/μ for 5.14-MeV α particles, and 4000 keV/μ for uranium fission products. Highly accelerated heavy charged particles, however, have low LET values. A more detailed consideration of specific types of radiation follows.

Heavy charged particle

In their passage through absorbing material, the heavy charged particles transfer their kinetic energy to the medium mostly by inelastic collision reactions with electrons. This process is described by the Bethe formula:

$$-\frac{dE}{dx} = \frac{4\pi z^2 e^4}{mv^2} NZ \ln \frac{2mv^2}{I},$$

where $\frac{dE}{dx}$ = rate of loss of energy by primary particle,

e = charge of electron (4.8025×10^{-10} abs esu),

ze = charge of particle (z an integer),

v = velocity of particle,

m = mass of electron (9.1091×10^{-28} g),

Z = electrons/molecule in medium,

N = density of molecules in medium,

I = mean excitation potential.

The above formula is a simplification of the more complete form, which includes additional terms for corrections for very low and for very high velocities. Since the velocity appears in the denominator, $-\frac{dE}{dx}$ becomes smaller for high velocities, which in turn means high energies. In the GeV energy range, protons and other accelerated particles have $\frac{dE}{dx}$ values that may be as low as those for gamma rays. Minimal $\frac{dE}{dx}$ values are about 0.22 keV/μ.

Protons with energies of 0.5 to 1.5 MeV have short, thick, straight paths, with $\frac{dE}{dx}$ values typically 30 to 40 keV/μ in water. This rate of energy loss produces about 1000 ion pairs/μ in water. Alpha particles of the same or somewhat higher energy typically have $\frac{dE}{dx}$ values of 150 keV/μ and produce 5000 ion pairs/μ in water. As may be seen from the stopping formula, the most intense ionization is produced near the end of the particle's range, where the velocity is low. Near the end of the track a maximum value is reached, after which the $\frac{dE}{dx}$ falls rapidly to zero as the particle comes to rest. This peak is known as the Bragg peak.

Some examples of particle energies that may be encountered are:

Radioactive nuclides	5-6-MeV alpha particles,
BNL AGS	33-GeV protons,
Proposed Weston AGS	200 GeV,
Berkeley Omnitron	(1.4-GeV protons, (70-GeV uranium nuclei.

The above energies are, of course, those of the primary particles in the main beam. Since direct exposure of personnel to the beam is not ordinarily permitted, consideration of the biologic effects of such exposures is more of radiobiological than of health physics interest. In practice, a more frequent source of radiation hazard is the secondary radiation that arises from the reactions of the main beam with shielding and other materials in its path.

In a cloud chamber α-particle tracks may be seen to include short, faint straggling tracks branching from the main track. These are due to recoil electrons and are known as delta rays. The recoil electrons can receive a maximum energy corresponding to twice the α-particle velocity,

$$E_{MAX} = 2mv^2.$$

For a 10-MeV α particle, the most energetic delta ray will have an energy of about 6.3 keV.

Thus not only does the $\frac{dE}{dx}$ for a given type of radiation vary along the track length as a function of the residual energy, but there is also spectrum of LET values within any small segment of the track. This aspect of the problem is discussed more extensively in other papers at this symposium, as is the relationship between LET and $\frac{dE}{dx}$.

3. Electrons, Positrons, and Mesons

The absorption of the energy of the lighter charged particles involves essentially the same mechanisms as have been described for the heavy particles. However, because of their lower masses, the velocities for electrons and positrons are much higher for given energies, and the necessity for relativistic velocity corrections arises at lower energies. Positrons and π^- mesons have the additional feature of energy-releasing reactions at the ends of their tracks. Positrons react with electrons to produce two 0.511-MeV gamma rays which are emitted in opposite directions. The π^- mesons react with atomic nuclei to disrupt them and produce "stars," or multiple tracks associated with the nuclear fragments.

The deceleration of high-speed electrons, particularly in dense target materials, results in another kind of radiative emission called bremsstrahlung, or braking radiation. This is a continuous spectrum of x rays, the characteristics of which depend on the electron energy and on the composition of the absorbing medium. For electron energies above 50 MeV this mechanism becomes competitive with inelastic collision as a mechanism of energy loss, but at lower energies it is of minor importance in radiobiology.

4. Electromagnetic Radiations

Electromagnetic radiations are generally present as a "contaminant" of other kinds of beams and are produced by many reactions of accelerated particles with shielding materials. They are characterized by their wavelength, which is related to their energy:

$$\lambda = \frac{c}{\nu} \qquad \text{cm},$$

$$E = h\nu = \frac{hc}{\lambda} \qquad \text{ergs},$$

$$E = \frac{0.12354}{\lambda'} \qquad \text{MeV},$$

where λ = wavelength (cm),

λ' = wavelength in Angstrom units, A^{o},

c = velocity of light (cm/sec),

E = energy,

h = Planck's constant, 6.6256×10^{-27} erg sec.

It is important to note that as the energy increases, the wavelength decreases. As a rough rule, the wavelength determines the size of the object with which an electromagnetic wave will interact. Thus radio waves, with λ's in cm to many meters (1.2×10^{-16} to 0.025 eV) react with antennas, whereas infrared rays (0.025 to 1.75 eV) react with molecules, and in the visible region (1.75 to 3.55 eV) is found the beginning of excitation in atoms. The photoelectric effect, in which the incident photon disappears and an electron is removed from an atom, begins in the ultraviolet region (3.55 to 90 eV). In the x- and γ-ray regions of 0.5 to 5 MeV, Compton scattering becomes the predominant energy-absorbing mechanism. In this process the energy of the incident photon is divided between that of a recoil photon of lower energy and a recoil electron. With λ = incident photon, λ' = recoil photon, φ = scattering angle, m_o = electron rest mass, and e = electron charge, the change in wavelength is given by the formulas

$$(\lambda' - \lambda) = \frac{h}{m_o e}(1 - \cos\varphi) = 0.0242\,(1 - \cos\varphi),$$

where the final numerical value is for $(\lambda' - \lambda)$ in A^{o}.

Figure 1 shows the Compton scattering photo energy patterns for 500-keV, 1-MeV, and 10-MeV incident photons. It can be shown that for the directly backscattered photons ($\varphi = 180^{\circ}$) the limiting energy is $\frac{m_o c^2}{2} = 0.255$ MeV, where m_o is the electron rest mass.

At gamma-ray energies above 1.022 MeV, pair production becomes possible. In this process 1.022 MeV of energy is transformed into a β^-, β^+ pair, and the remaining energy appears as kinetic energy of the particles.

For low-Z materials nuclear reactions, (γ,p), (γ,n), and (γ,α), occur at gamma-ray energies above 10-15 MeV.

Figure 2 shows the total absorption, μ, and the true absorption, μ_a, curves in water for photons in the 0.01- to 100-MeV energy range, and the contributions due to scatter σ_a, the photoelectric effect τ, Compton scattering σ_a, and pair production k, components of the curves. Since the density, ρ, of water is 1, the ordinate values may also be given units of cm^{-1}, or fractional linear absorption. The values for water are approximately correct for soft tissues.

Neutrons

Because of their lack of charge and much greater mass, neutrons do not react appreciably with electrons. Their absorption in matter thus involves nuclear reactions only. There are three main processes:

1. Inelastic scattering.
2. Elastic scattering.
3. Neutron capture.

Neutrons may be classified according to their energy:

Slow (including thermal)	0 — 0.1 keV,
Epithermal	0.1 keV — 0.02 MeV,
Fast	0.02 — 10 MeV,
High energy	> 10 MeV.

Inelastic scattering occurs only for neutrons of several keV or more and leaves the nucleus in an excited state.

Elastic scattering is the only process effective in reducing neutrons to thermal energies. With fast neutrons below 20 MeV and in tissue, where hydrogen is the most important constituent, elastic scattering accounts for 85-95% of the energy transfer. The energy transferred in a collision is

$$\Delta E = \frac{4m}{(m+1)^2} E \cos^2 \theta,$$

where m = neutron energy,

θ = recoil angle.

After n collisions the neutron energy is

$$T_{n1} = T_o e^{-n\xi},$$

where T_o = initial kinetic energy of neutron,

T_{n1} = median energy of degraded spectrum,

$$\xi = \frac{(A = 1)^2}{2A} \ln \frac{A + 1}{A - 1},$$

where A is the atomic weight of the scattering medium.

At energies exceeding 20 MeV, neutrons have sufficient energy to disintegrate nuclei on collision, leading to spallation or star formation.

Below 20 keV, in the epithermal region, the most important mode of energy transfer is by elastic collision. Here the recoiling nuclei do not ionize, but initiate atomic and molecular excitations. Neutron capture by nitrogen and hydrogen does lead to ionization, but at energies above 100 eV the cross sections are low. Both of these processes follow the 1/v law, so at lower energies the probability of capture increases with $1/\sqrt{E}$. Neutrons are usually slowed to thermal energies before being captured. Table I lists data pertinent to neutron capture in normal tissue.

TABLE I

Neutron Capture in Normal Tissues

Element and isotope	Element fraction in tissue, %	Isotope abundance, %	Reaction cross section, barns	Energy, MeV
O 17	65.	0.037	(n,α) 0.4	1.6
H 1	10.	99.98	(n,γ) 0.352	2.2255
N 14	3.	99.6	(n,p) 1.75	.660
Cl 35	0.15	75.5	(n,γ)30.	8.58

Factors affecting dose-effect relationships

The above considerations indicate the principal mechanisms by which the energy of various kinds of radiation is absorbed in matter, and the reasons for there being differences in track density. To a large extent RBE's are associated with these differences, with the denser tracks in general giving the higher RBE's. It is still not entirely clear, however, why the same amount of energy absorbed in a dense track is more effective than in a sparse track.

The explanation appears to lie at the physicochemical level, and involves a complicated interation of many factors. Among these are free-radical diffusion rates, the oxygen effect, target theory, and the sensitivity of the irradiated system.

Free-radical diffusion rates and the oxygen effect are most important with indirect effects, those which depend on the initial absorption of energy by solvent atoms rather than directly by target molecules. In the denser tracks the irradiation products of water, the free radicals H and OH, have a higher probability of reacting with each other and forming oxidative radicals such as H_2O_2, than of diffusing and reacting with solutes which may act as protective agents. The presence of oxygen in solution increases the production of oxidative radicals by radiations having relatively sparse tracks, but has little or no effect in association with the denser tracks.

The survival curves for cells, bacteria, etc. irradiated with high-LET-type radiations are typically exponential, whereas those for low-LET radiations often have a shoulder before becoming exponential. This phenomenon is usually interpreted in terms of various forms of the hit theory, with either multiple hits being required to affect a single

target or multiple targets having to be hit to produce the observed effect. Evidently if the required number of hits are too widely separated in time, recovery from the first hits is possible and the later hits are less effective. Thus the denser tracks may be more effective in part because the required number of hits are closer together in time. Very large doses are required for the tracks of low-LET radiations to be close enough together in space and time to simulate high-LET tracks. Studies with low-LET radiations show that the effects of high-LET radiation begin to be simulated at dose rates of over 10^8 rad/sec. Even this is somewhat lower than had been expected by theory, indicating that some of the free radicals have longer lives than had been expected. More recent data with electron spin resonance methods support the concept of longer-lived radicals.

In summary, it appears that an explanation of RBE in physical and physicochemical terms is going to be possible, but considerably more data on track structure, free-radical production, dose-rate effects, and other related parameters are needed. Several of the other papers presented at this symposium are concerned with recent data and theories in this area.

Bibliography

Lea, D. E.: Actions of Radiations on Living Cells, MacMillan, New York, 1947.

Siri, W. E.: Isotopic Tracers and Nuclear Radiations, McGraw-Hill, New York, 1949.

Bacq, Z. M., and Alexander, P.: Fundamentals of Radiobiology, Academic Press, New York, 1955.

Hine, G. J., and Brownell, G. L.: Radiation Dosimetry, Academic Press, New York, 1956.

Kaplan, I.: Nuclear Physics, Addison-Wesley, Cambridge, Mass., 1956.

Claus, W. D.: Radiation Biology and Medicine, Addison-Wesley, Reading, Mass., 1959.

Haissinsky, M. (Ed.): The Chemical and Biological Actions of Radiation, Vol. V, Academic Press, New York, 1961.

Hart, E. J.: Hydrated electron, Science 146, 19, 1964.

Behrens, C.: Atomic Medicine, 4th Ed., Williams and Wilkins, Baltimore, 1964.

I.2

COMPTON SCATTER

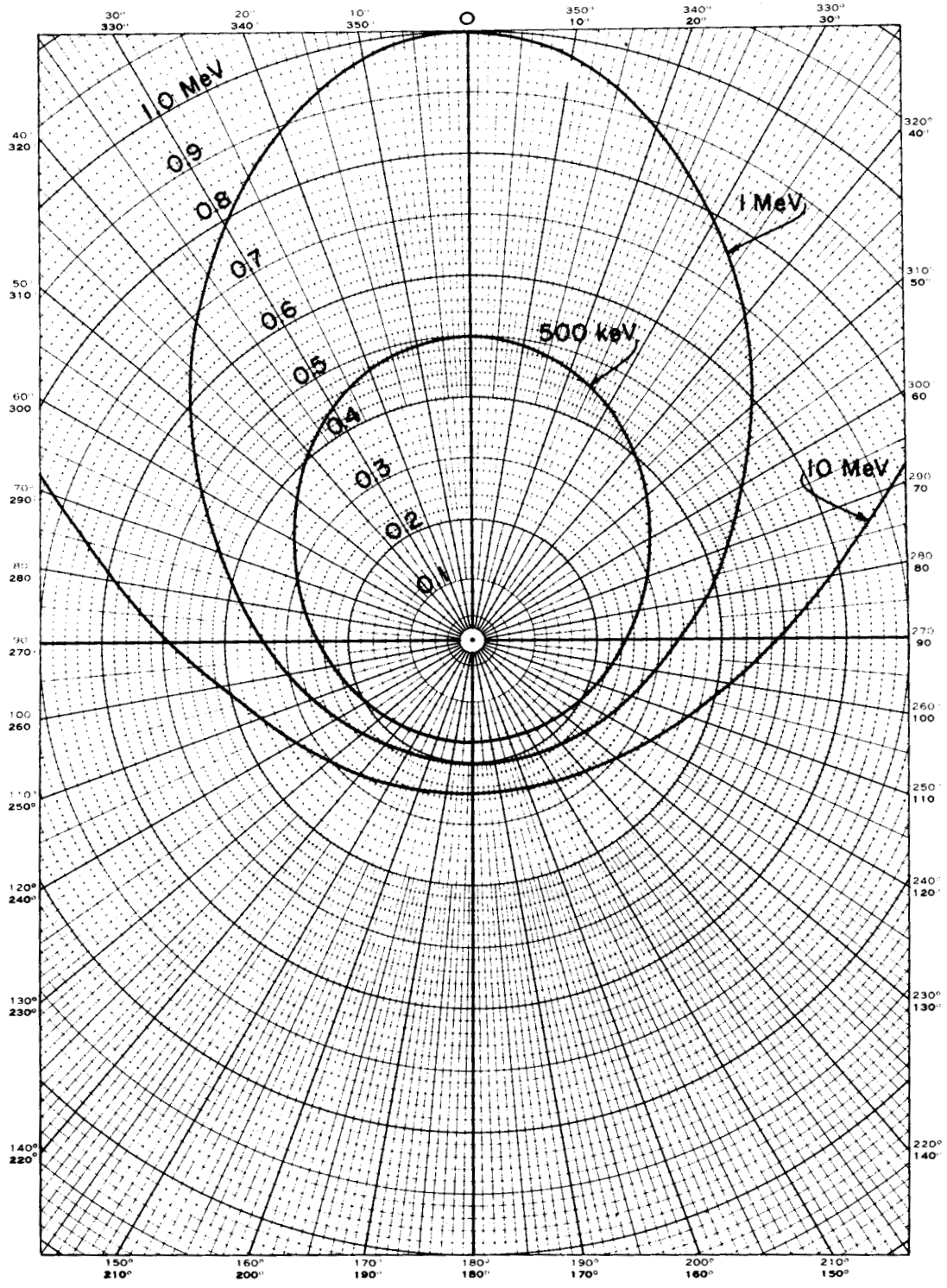

FIGURE 1

Compton scatter energy distribution patterns for 500-keV, 1-MeV, and 10-MeV gamma rays.

I.2

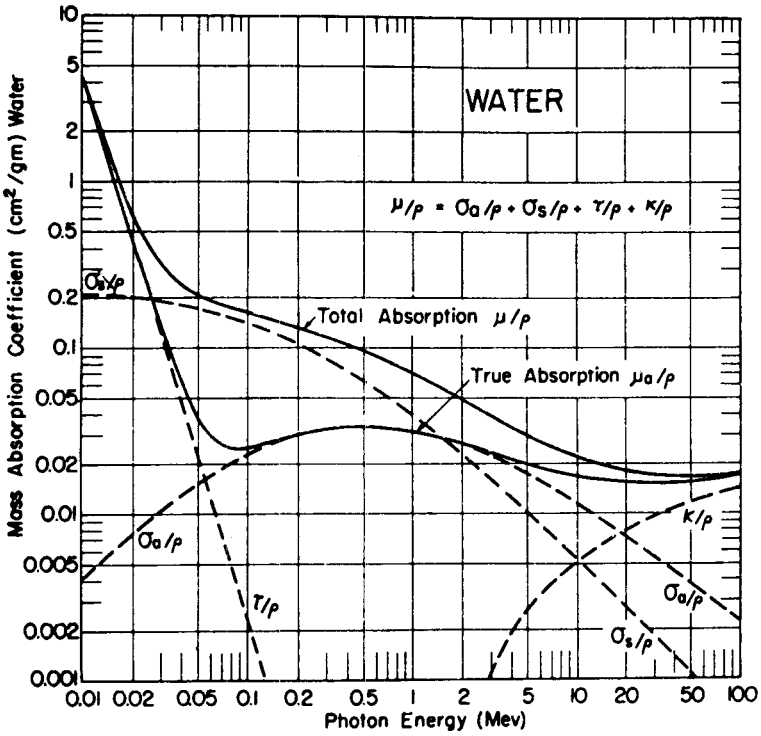

FIGURE 2

Mass absorption coefficients in water for photon energies 0.01 to 100 MeV. The true absorption curve differs from the total absorption curve in not including the elastic scattering component, σ_s. From Hine and Brownell, Radiation Dosimetry.

EFFECTS OF ACCELERATED HEAVY IONS ON ENZYMES IN THE DRY STATE AND IN AQUEOUS SOLUTIONS

Tor Brustad

Norsk Hydro's Institute for Cancer Research
Montebello, Norway

Introduction

Most of the studies of accelerator-produced radiations on biological macromolecules have been concerned with effects of protons, deuterons, and helium ions on dried materials. Ions heavier than helium ions, with energies up to about 10 MeV/amu produced either by cyclotrons, linear accelerators, or tandem Van de Graaffs are, however, now becoming more commonly available. Because of the short range of such particles, few investigations have been conducted to elucidate the mechanisms of heavy-ion-induced injury on macromolecules in dilute aqueous solutions. It is therefore felt appropriate here to recapitulate only briefly some of the results obtained with accelerated particles on dried enzymes. Emphasis will instead be placed on some recent studies of inactivation of enzymes in aqueous solutions with radiations of different LET, although the results obtained in this field so far are only fragmentary.

Effects on Macromolecules Exposed in the Dry State

The pioneer work of Lea[1] and the subsequent extensive investigations by Pollard et al.[2] led to the general conclusions that (a) an enzyme molecule becomes inactivated when a primary ionization occurs anywhere within the confines of the molecule, (b) ionizations occurring outside the enzyme molecule contribute only little to the radiation damage, and (c) excitations are unimportant for the inactivation processes. Based on this simplest form of a "one hit" target theory, a clear relationship is expected between the radiosensitivity of an enzyme and its size or molecular weight. This relationship has been studied extensively by the Yale group; results are summarized in Fig. 1.[3] A log plot of the radiosensitivity, expressed as the "radiation molecular weight" vs the accepted molecular weight, is shown. The data are clearly somewhat scattered, but nevertheless, they provide impressive evidence for a strong correlation between the radiosensitivity and the molecular weight of dried enzymes.

Experiments by the Yale group and others, however, showed the radiosensitivity to be modified by a number of physical and chemical factors, such as assay methods, presence of oxygen, and the nature of the solutions from which the enzymes are dried as well as properties of the media in which the enzymes are dissolved after the exposure.[2] It was also found that admixtures of various molecules affected the radiosensitivity of enzymes when exposed to radiations of low LET[4] as well as to radiations of high LET.[5]

In Fig. 2 are shown the inactivation cross sections of trypsin exposed to C ions when the enzymes are mixed with certain foreign molecules in various

concentrations.[5] As seen, the enzyme radiosensitivity can be affected by the added molecules so that it becomes greater or smaller than that characteristic of the pure enzyme.

Figure 3 shows still another factor which modifies the enzyme radiosensitivity.[6] Here the relationship between the inactivation cross section of trypsin is plotted as a function of the temperature of the sample during the irradiation. Results are presented for six different radiations, and each point on the graph is based on a dose-effect curve. As seen, the shape of the curve is similar for all radiations. From about 10°K to about 100°K the radiosensitivity is independent of the temperature. From about 100°K the radiosensitivity increases with increasing sample temperature up to the highest temperatures studied. On the average, the radiosensitivity at room temperature is about 2 to 3 times that observed in the temperature-independent region below about 100°K.

A problem of considerable interest at present is to what extent the radiation-induced radicals in, say, dried enzymes are responsible for the observed enzyme inactivation. To shed more light on this problem, attempts have been made to search for correlations between the yield of enzyme inactivation and the yield of induced free radicals, when the latter are measured by ESR technics after the end of the exposure to ionizing radiation.[7-9] The ESR centers thus observed may, however, in a complicated way be affected more or less by secondary radical reactions during and after the exposure, but prior to the measurement on the ESR spectrometer. Such secondary reactions are known to be slowed down by lowering of the sample temperature. Unfortunately, qualitative and quantitative studies are not yet reported of enzyme radicals which are induced at temperatures as low as that of liquid helium and measured in the ESR spectrometer at the same temperature.

In his work Henriksen decided to look for correlations between the yields of those radicals which are trapped at room temperature and the yields of enzyme inactivation, after exposure at various temperatures to different accelerator-produced radiations.[8] He found that the free radicals induced in trypsin and lysozyme were essentially identical and nearly independent of the ionization density of the radiation. The ESR signal consists of a doublet and a broad resonance when irradiated in vacuum and measured in the ESR spectrometer at room temperature. Evidence is now available for the interpretation that the broad resonance is due to a sulfur radical in which the unpaired electron is localized mainly on the sulfur atom in the cysteine residue and that the doublet is due to a radical in which the unpaired electron is localized in a π-orbital on an α carbon atom in the protein backbone:[8]

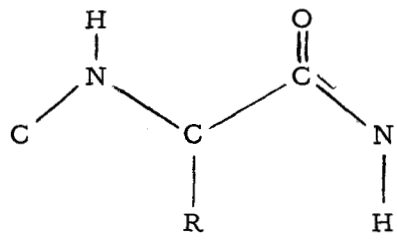

The group R is primarily a hydrogen atom.

In Fig. 4 are shown two different effects on dried trypsin exposed to C ions, namely the relative yields for (a) inactivation of the enzymatic activity (data due to the present author) and (b) induction of free radicals (data due to Henriksen[8]) as a function of the sample temperature during the exposure. As seen from the graph, the yields for induced radicals depend on the irradiation temperature in the same way as do the yields for inactivation, discussed above.

In Fig. 5 are also shown two different effects on dried trypsin, namely the relative yields for (a) inactivation of the enzymatic activity (data due to the present author) and (b) induction of free radicals (data due to Henriksen[8]), as a function of the stopping power of various radiations. Here it is seen that the yields for induced radicals depend on the stopping power in the same way as do the yields for inactivation, discussed above.

Figures 4 and 5 show pronounced correlations between yields of radicals trapped at room temperature and enzyme inactivation for varying sample temperatures and for radiations of different LET. Although our understanding of relations between induced radicals and the biological damage is very incomplete, the data presented suggest that the loss of enzymatic activity of dried enzymes exposed to various types of ionizing particles is the result of a sequence of events in which free radicals are important intermediates.[8]

Inactivation of Enzymes in Aqueous Solutions

Studies of x-irradiated biological macromolecules in aqueous solutions have led to the conclusion that the injury is caused predominantly by indirect action due to the radiolysis products of water, namely:

$$H_2O \xrightarrow{\text{x rays}} OH,\ H,\ e^-_{aq},\ H_2,\ H_2O_2.$$

The radical species OH, H, and e^-_{aq} are assumed to be of particular importance for the injury resulting from radiations of low LET. Our knowledge of the exact amount of radiation injury caused by any of these radiolysis products, however, is rather scanty for radiations of low LET[10] and almost nonexistent for radiations of high LET.

In the following some preliminary results will be presented of an investigation aiming at a comparison of the enzyme inactivation caused by x rays and by various heavy ions.[11]

Heavy ions of energy up to 10 MeV/amu were accelerated in the Berkeley heavy-ion accelerator. An irradiation chamber as shown in Fig. 6 was designed. The beam entered the chamber through a 1/4-mil Mylar window over which area the particle fluence was constant. The thickness of the chamber in the direction of the beam is about 4 mm. The heavy ions, which have a range in water less than 1 mm, are therefore all stopped in the solution in the chamber. The enzyme solution was bubbled either with oxygen or with nitrogen during the exposure, by flushing the gas through the inlet tube and the sintered glass filter, shown in the figure. The bubbling action was insufficient, however, to ensure homogeneous irradiation of the entire enzyme solution in the chamber. A small magnet stirrer

shown in the figure was therefore used. The dose delivered to an irradiated sample was calculated from (a) the number of heavy ions stopped in the sample, (b) the energy of the heavy ions then entering the solution, and (c) the thickness of the chamber holding the enzyme solution. The average dose rate was kept at about 85 krad/min. The enzymes were dissolved in a concentration of 0.1 mg/ml in a buffer made up from citric acid and sodium phosphate. Details of the experimental procedures are described elsewhere.[11]

The dose-activation curves of lysozyme irradiated in oxygen-saturated solution with x rays were usually exponential. When exposures were made in solutions saturated with nitrogen, on the other hand, the curves were always found to be of the type shown in Fig. 7a, e.g., a low efficiency for inactivation in the low-dose region, followed by an exponential or nearly exponential portion with higher inactivation efficiency as the dose increased. On the other hand, when the enzyme solution was irradiated with heavy ions, the dose-inactivation curves were always exponential. Sometimes the exponential portion extended over the entire dose range investigated, as shown in Fig. 7b, whereas under other conditions a "resistant tail" was observed in the high-dose region. We have not studied the conditions under which these tails appear, but they may, at least in part, be ascribed to insufficient mixing of the enzyme solution during the irradiation.

The present finding, that densely ionizing radiations result in exponential dose-inactivation curves under conditions that cause sparsely ionizing radiation to give rise to "multiple hit" curves, parallels results obtained on the cellular level, for instance for inactivation of the reproductive capacity of human kidney "T1" cells.[12]

Figure 8 shows the radiosensitivity of lysozyme in N_2-saturated solution as a function of the average stopping power of the solution for x rays and for three different types of accelerated particles; the different heavy ions all entered the solution with nearly the same velocity. These experiments show that the radiosensitivity decreases considerably with increasing stopping power. It is known that the radiosensitivity of dried enzymes decreases by less than a factor of 3 over the same range of stopping power.[5] Thus, the data show that for increasing stopping power a greater fraction of the enzyme inactivation is caused by the so-called "direct effect."

Figure 9 shows the radiosensitivity of lysozyme exposed to various radiations as a function of the pH of the enzyme solution. Shown also is the radiosensitivity of lysozyme exposed in the dry state to C ions. The pH in this latter case refers to the medium from which these samples were dried. The curves of the radiosensitivities in aqueous solutions are all similar in shape in the sense that they show a broad minimum in the middle of the pH range studied. In aqueous solutions at neutral pH the radiosensitivity decreases by somewhat less than 2 orders of magnitude when the stopping power is increased from that of x rays to that of Ar ions. The figure also shows that the sensitivity of lysozyme, exposed in aqueous solutions to Ar ions, even at neutral pH, is at least 2 orders of magnitude greater than that of dried enzymes. In other words, even for the very densely ionizing Ar ions, a considerable degree of the enzyme inactivation in aqueous solution is due to the presence of water.

Figure 10 shows the radiosensitivity at pH = 2.5 as a function of the average stopping power of helium, carbon, and argon ions. The curve drawn through the open circles refers to different heavy ions of approximately equal velocity (8 to 9 MeV/amu). The curve through the filled circles refers to carbon ions of different velocities (9 to 0.8 MeV/amu). From the data here presented it can be concluded that heavy ions which, by virtue of differences in charge state and velocity, have equal average stopping power do not produce the same degree of enzyme injury per unit energy absorbed. This result may have an important bearing on problems encountered in radiation protection, in the sense that it underlines the difficulty involved in assigning meaningful tolerance doses for charged heavy ions. In this connection it should, however, be pointed out that Todd has shown that lithium ions of various velocities appear to have the same effectiveness in inhibiting the colony-forming ability of human kidney "T1" cells as do heavier ions having similar stopping powers.[12]

Figure 11 shows the radiosensitivity of lysozyme as a function of the pH of the enzyme solution, saturated either with oxygen or with nitrogen, during the exposure. Contrary to what applies in cellular radiobiology the present results show that the radiosensitivity is greater in nitrogen than in oxygen atmosphere, for x rays as well as for carbon ions. These results show that compared with nitrogen, oxygen acts as a radioprotective compound over the entire pH range studied, but the degree of this oxygen protection is smaller for carbon ions than for x rays.

The data presented in the preceding figure show therefore that it is possible by chemical means to provide protection against enzyme injury resulting from radiations of high LET. These results prompted an investigation of the effectiveness of various known chemical radioprotectors in reducing the degree of enzyme inactivation caused by heavy ions. Studies were performed of the effect of ethanol, glycerol, histidine, and cysteine on the radiation injury of lysozyme irradiated in oxygen-free solutions. Dose-effect curves were determined for three or more concentrations of each of the chemicals under investigation. From such curves plots of the radiosensitivity as a function of the protector concentrations were obtained. Figure 12 shows an example of how the radiosensitivity of lysozyme depends on the concentration of glycerol during the exposure to C ions. It is seen that the radiosensitivity decreases considerably even for rather moderate concentrations of glycerol, and levels off as the protector concentration is increased. At the highest concentrations tested the sensitivity is reduced to about 5% of that of an unprotected enzyme solution. It is of interest to note that the radiosensitivity at neutral pH, in the presence of such a high concentration of glycerol, still is about 35 times that of dry enzyme. In Table 1 are shown for each of the four protectors tested the concentrations required to reduce the radiosensitivity of lysozyme to 50% of that value characteristic of the unprotected enzyme solution. From this table two conclusions can be drawn: (a) all four compounds protect lysozyme against radiation injury resulting from x rays as well as from C ions. Surprisingly, less than double the concentration of protector appears to be required to provide the same degree of protection against injury from C ions as from x rays. (b) Ethanol and glycerol are about equally effective radioprotectors. Histidine is about one order of magnitude more effective, whereas cysteine (which also is known to participate in repair processes) is more effective than glycerol by almost two orders of magnitude.

Table 1. Concentrations of protectors which reduce sensitivity to 50%.

Protector	Concentration (10^{-4} M)				
	pH = 2.5		pH = 5.0		pH = 9.4
	x Rays	C^{6+}	x Rays	C^{6+}	C^{6+}
Ethanol	60	75	90	135	
Glycerol	60	100	90	125	
Histidine		21	7	12	4
Cysteine	1	1	1	1	1

Discussion

When radiations act "indirectly" upon enzyme molecules (e.g., through water radicals like H, OH, or e^-_{aq}) the major reaction presumably involves the removal of a hydrogen atom from the molecule forming a free radical in which the free bond lies on a carbon or, perhaps, a nitrogen atom. When radiations act "directly" upon enzyme molecules similar enzyme radicals are presumably also formed. When enzyme solutions are irradiated by x rays, enzyme radicals are formed almost uniformly throughout the volume, mainly by indirect action of water radicals which under these conditions pervade the entire solution. It is not unreasonable, therefore, that oxygen or other radical scavengers can act efficiently as protectors against x-ray-induced injury. That oxygen provides a strong protection against the x-ray-induced injury of lysozyme (Fig. 11) has been interpreted to indicate that lysozyme is sensitive to attack by diffusible reducing species, in particular H and e^-_{aq}.[10]

From studies of simple solutions, such as ferrous sulphate, exposed to polonium α particles it is known that very few water radicals escape the tracks of such radiations.[13] Since the average stopping powers of water for C and Ar ions, used in the present investigation, are greater than that of polonium α particles, it may be suspected that very few water radicals escape from the "core" of the tracks of these heavy ions also. However, heavy ions of energy about 10 MeV/amu produce secondary electrons of energy up to 21 keV.[5] These secondaries, which have relatively low LET, extend out of the core of the track of the heavy particle. The "track anatomy" of different heavy particles is illustrated in Fig. 13, which shows that the apparent diameter of the track decreases as the heavy ion is slowed down.[14] In line with this reasoning it may be expected that C or Ar ions create enzyme radicals by direct action to a much greater extent than do x rays, and more so the lower the energy of the heavy ions. The observation that the radiosensitivities in nitrogen atmosphere at neutral pH after exposure to Ar ions and C ions are respectively 2% and 5% of that for x rays (Fig. 9),

and, furthermore, that the radiosensitivity decreases with decreasing energy of the carbon ions (Fig. 10) is in line with this reasoning. Since the injury to the enzyme molecules after heavy-ion exposure (which is greater than injury after x-ray irradiation) is assumed to stem from direct action, one expects here less protection by radical scavengers. This expectation is borne out in the data presented (Fig. 11). The surprising observation that a number of chemical protectors provide considerable protection against heavy-ion-induced injury may possibly suggest certain cooperating mechanisms:

Hypothesis 1: Fast heavy ions produce high-energy δ rays of low LET, which in turn create reactive water radicals which can escape from the track of the primary heavy ion. Radical scavengers can protect enzymes against heavy-ion injury by inactivation of the water radicals formed by the δ rays.

Hypothesis 2: Enzyme radicals, formed by direct action of heavy ions, may be able to diffuse in time out of the tracks where they are formed and here react with oxygen or other solute molecules present in low concentrations. This is possible because the enzyme radicals have a longer lifetime than the highly reactive water radicals. Oxygen molecules, for instance, are known to react very rapidly with carbon radicals to form peroxy radicals. Subsequent reactions of such peroxy radicals may be such that the activity of the enzyme is not destroyed, whereas in the absence of oxygen the enzyme radicals may undergo some spontaneous rearrangement which has a certain degree of probability of destroying the enzymatic activity.

Further experiments are being planned to shed more light on the mechanisms of protection against heavy-ion-induced injury.

Acknowledgments

I am very grateful to Professor C. A. Tobias for the opportunity to work in his group and for his interest in this work, to Dr. John Lyman for discussions of heavy-ion dosimetry, and to Mr. David Love, Mr. Jerry Howard, and Mrs. Jean Luce for their unfailing help and support during the arduous Hilac experiments. The work was jointly supported by the U. S. Atomic Energy Commission, the National Aeronautics and Space Administration, and Norsk Hydro's Institute for Cancer Research. A travel grant from The Royal Norwegian Council for Scientific and Industrial Research is gratefully acknowledged.

References

1. D. E. Lea, Actions of Radiations on Living Cells, Cambridge University Press, London, 1946.

2. E. C. Pollard, W. R. Guild, F. Hutchinson, and R. B. Setlow, The Direct Action of Ionizing Radiation on Enzymes and Antigens, Progr. Biophys. Biophys. Chem., 5: 72-108 (1955).

3. E. Pollard, Radiation Inactivation of Enzymes, Nucleic Acids, and Phage Particles, Rev. Mod. Phys., 31: 273-281 (1959).

4. R. Braams, Changes in the Radiation Sensitivity of Some Enzymes and the Possibility of Protection Against the Direct Action of Ionizing Particles, Radiation Res., 12: 113-119 (1960).

5. T. Brustad, Heavy Ions and Some Aspects of Their Use in Molecular and Cellular Radiobiology, Advan. Biol. Med. Phys.,8: 161-224 (1962).

6. T. Brustad, Inactivation at Various Temperatures of the Esterase Activity of Dried Trypsin by Radiations of Different LET, in Proceedings of the Workshop Conference on Space Radiation Biology, Berkeley, 1965, Radiation Res., Suppl. 7 (in press).

7. J. W. Hunt and J. F. Williams, Radiation Damage in Dry Ribonuclease: Yields of Free Radicals and Other Chemical Lesions Compared with Inactivation Efficiency, Radiation Res., 23: 26-52 (1964).

8. T. Henriksen, Electron Spin Resonance Signals in Irradiated Proteins, in Electron Spin Resonance and Effects of Radiation on Biological Systems. Wallace Snipes, (Ed.) Nuclear Science Series, Report No. 43, pp. 81-100, National Academy of Sciences, National Research Council, Washington D. C., 1966.

9. T. Brustad, H. B. Steen, and J. Dyrset, Inactivation and Induction of Free Radicals in Dried Trypsin, Radiation Res., 27: 217-228 (1966).

10. T. Brustad, The Effects of Radical Scavengers on the Radiosensitivity of Lysozyme in Dilute Aqueous Solutions of Varying pH, Radiation Res., 27: 456-473 (1966).

11. T. Brustad, On the Mechanisms of Radiation Inactivation of Enzymes in Dilute Solutions, in Proceedings of the Third International Congress of Radiation Research, Cortina, 1966 (in press).

12. P. W. Todd, Reversible and Irreversible Effects of Ionizing Radiations on the Reproductive Integrity of Mammalian Cells Cultured in vitro, USAEC Report UCRL-11614, Lawrence Radiation Laboratory, Aug. 1964.

13. A. O. Allen, The Radiation Chemistry of Water and Aqueous Solutions, D. Van Nostrand Company, 1961.

14. H. H. Heckman, B. L. Perkins, W. G. Simon, F. M. Smith, and W. H. Barkas, Ranges and Energy-Loss Processes of Heavy Ions in Emulsion, Phys. Rev., 117: 544 (1960).

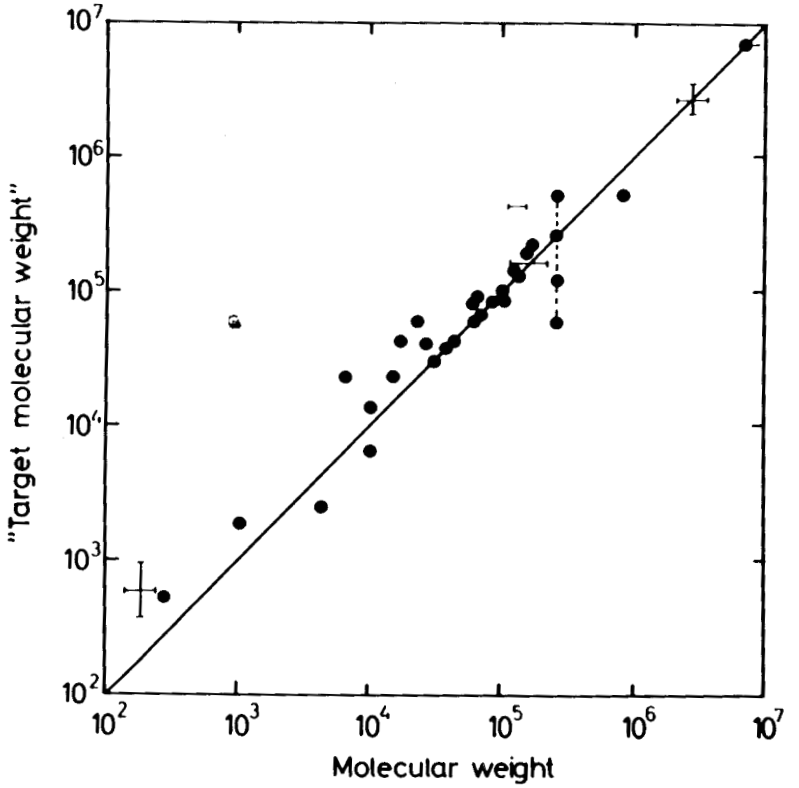

Fig. 1. The observed relationship between molecular weight and "target molecular weight" for a wide variety of dried biological macromolecules. This graph is due to Pollard (Ref. 3).

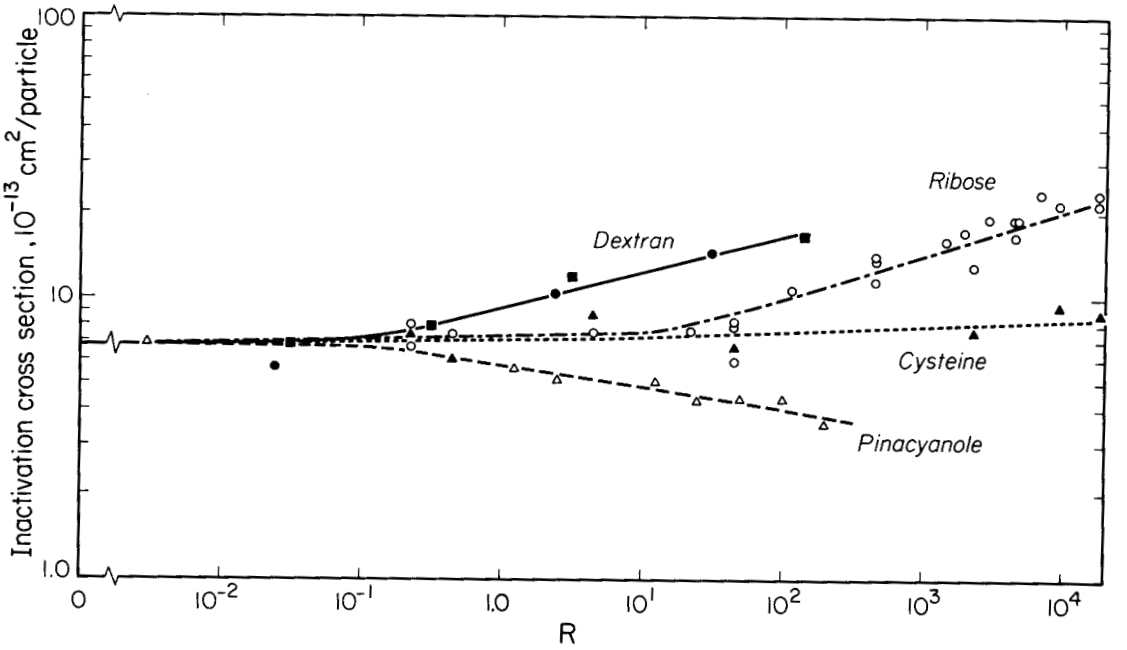

Fig. 2. Inactivation cross section of trypsin mixed with dextran, ribose, cysteine, and pinacyanol as a function of the ratio of number of foreign molecules per trypsin molecule. The samples were exposed in high vacuum to 115-MeV carbon ions (Ref. 5).

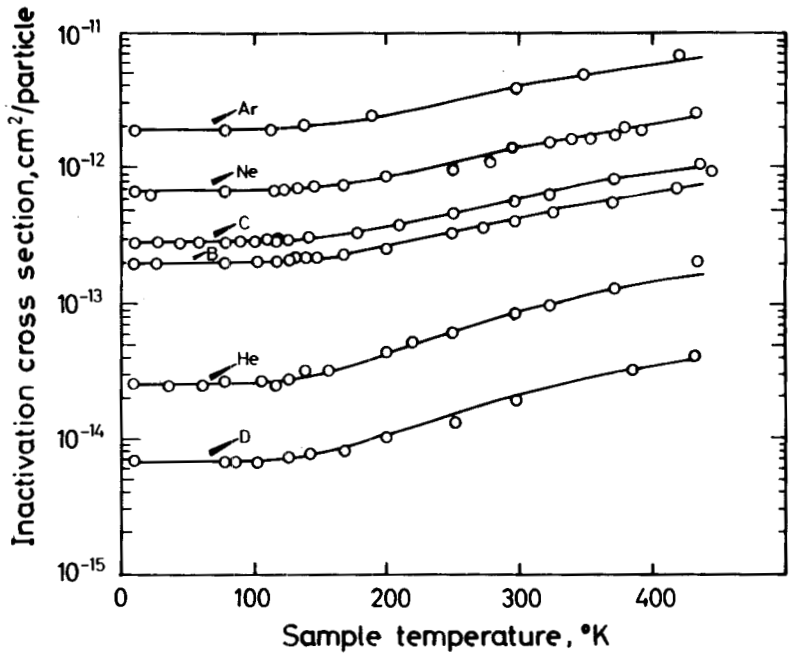

Fig. 3. Inactivation cross section of trypsin, irradiated in vacuum at various temperatures with stripped nuclei of deuterium, helium, boron, carbon, neon, and argon. The energy of the deuterons was 10.2 MeV/amu. All the other ions impinged upon the samples with an energy of 8.3 MeV/amu.

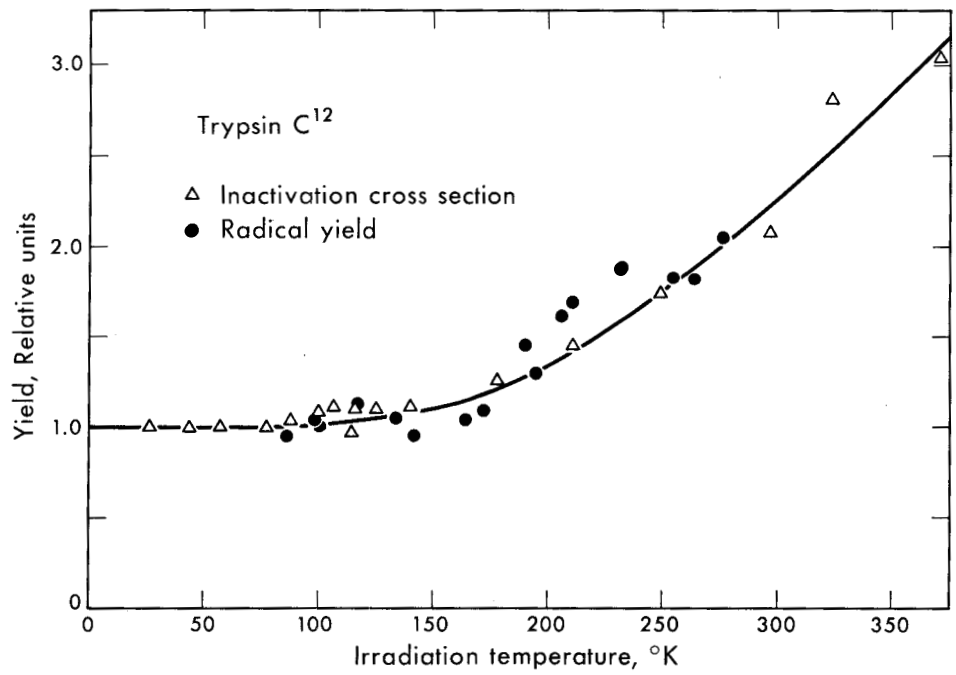

Fig. 4. Effect of the temperature of dried trypsin samples during irradiation with C^{6+} ions on
(a) relative yields of induced secondary radicals (data due to Henriksen, Ref. 8), and
(b) relative yields of enzyme inactivation (data due to this author).

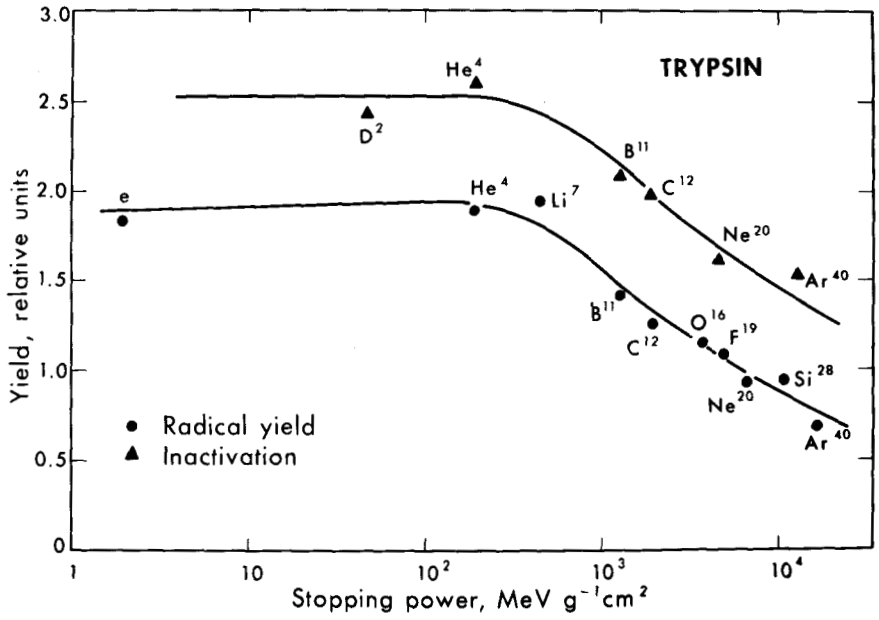

Fig. 5. Effect of the stopping power of dried trypsin for various radiations on
(a) relative yields of induced secondary radicals (data due to Henriksen, Ref. 8), and
(b) relative yields of enzyme inactivation (data due to this author).

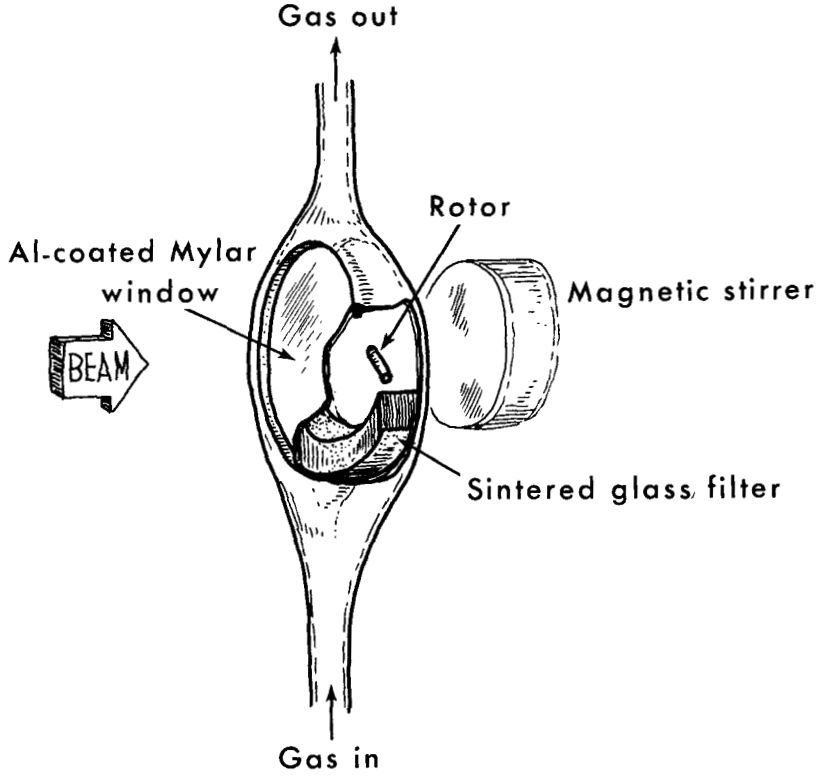

Fig. 6. Drawing of the exposure chamber used when irradiating enzyme solutions with heavy ions. The heavy ions entered the chamber through a 1/4-mil Mylar window.

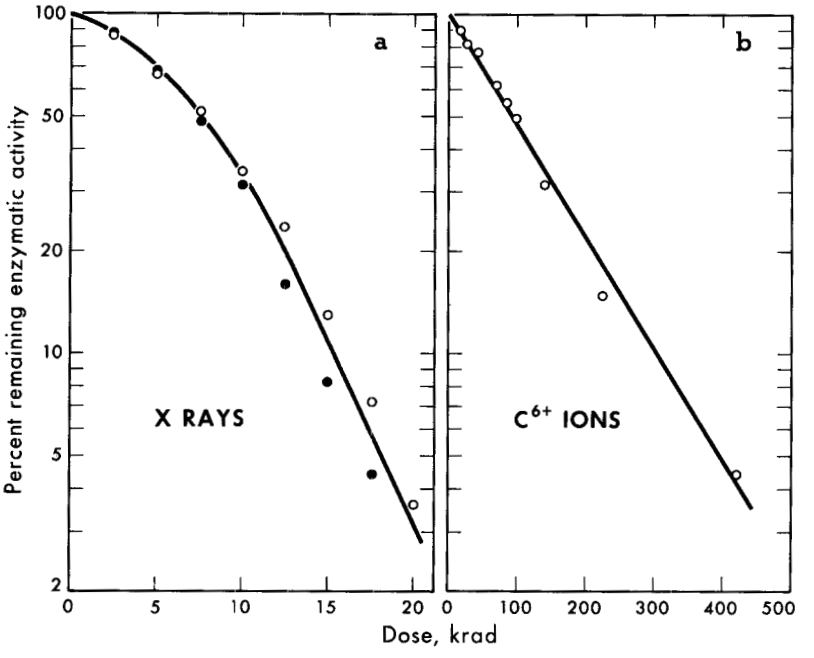

Fig. 7. Dose-inactivation curves of lysozyme, exposed in N_2-saturated aqueous solution of pH 3.5: (a) 150-kV x rays, (b) 120-MeV C^{6+} ions.

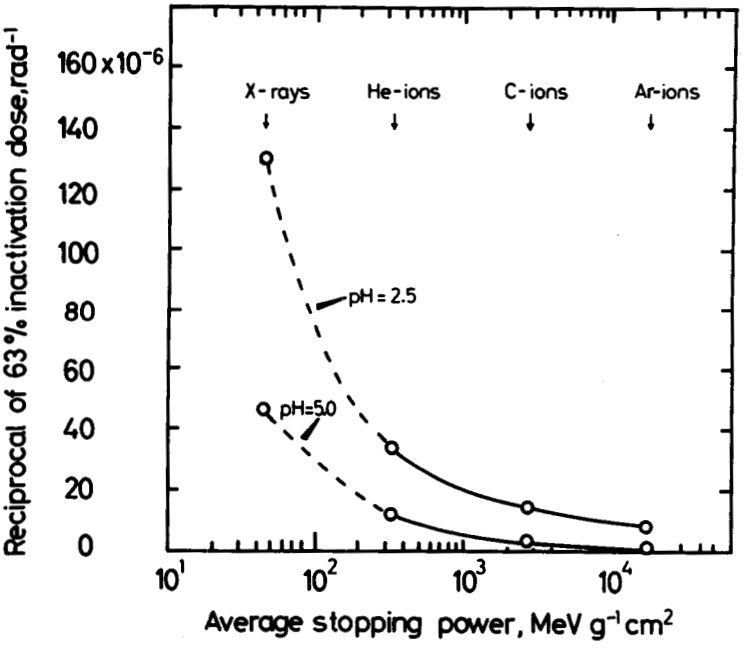

Fig. 8. The radiosensitivity of lysozyme in N_2-saturated solution as a function of the average stopping power of the solution for x rays (150 kVp), He ions (9.2 MeV/amu), C ions (9.2 MeV/amu), and Ar ions (7.8 MeV/amu). The average stopping power (E/R) is calculated as the ratio between the energy of the particles when entering the solution (E) and the range of the particles (R).

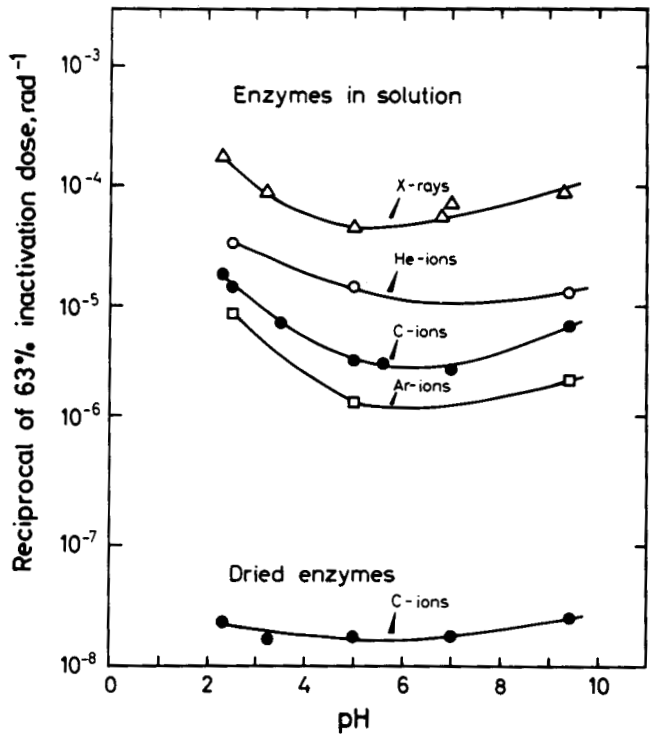

Fig. 9. The radiosensitivity of lysozyme in N_2-saturated solutions of various pH, for x rays (150 kVp), He ions (9.2 MeV/amu), C ions (9.2 MeV/amu), and Ar ions (7.8 MeV/amu). The radiosensitivity of lysozyme, dried from solutions of various pH and irradiated in high vacuum with C ions, is shown for comparison.

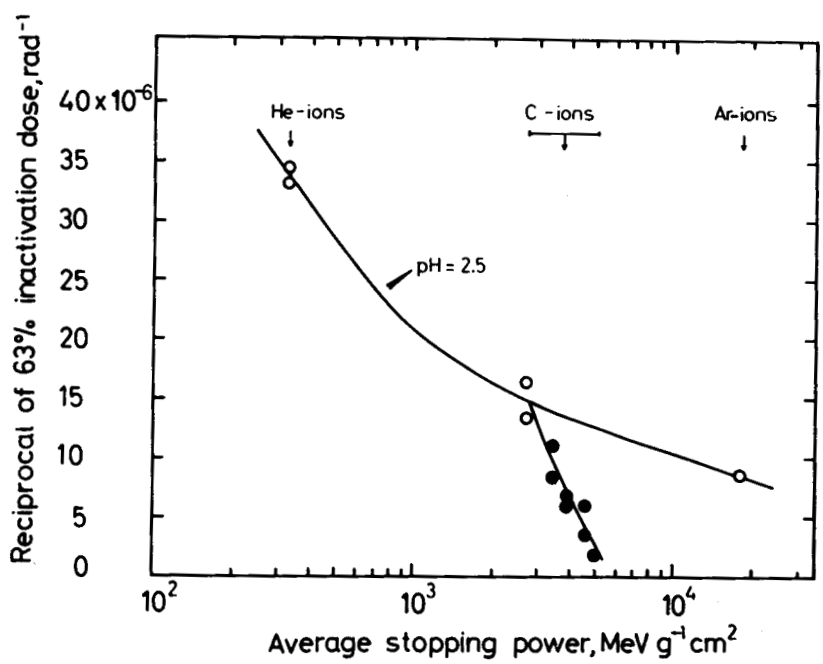

Fig. 10. The radiosensitivity of lysozyme in N_2-saturated solution of pH ≅ 2.5 as a function of the average stopping power of the solution. The curve through the open circles refers to ions of nearly equal velocity (He ions: 9.2 MeV/amu; C ions: 9.2 MeV/amu; and Ar ions: 7.8 MeV/amu). The curve through the filled circles refers to C ions of different velocities (9.2 to 0.8 MeV/amu).

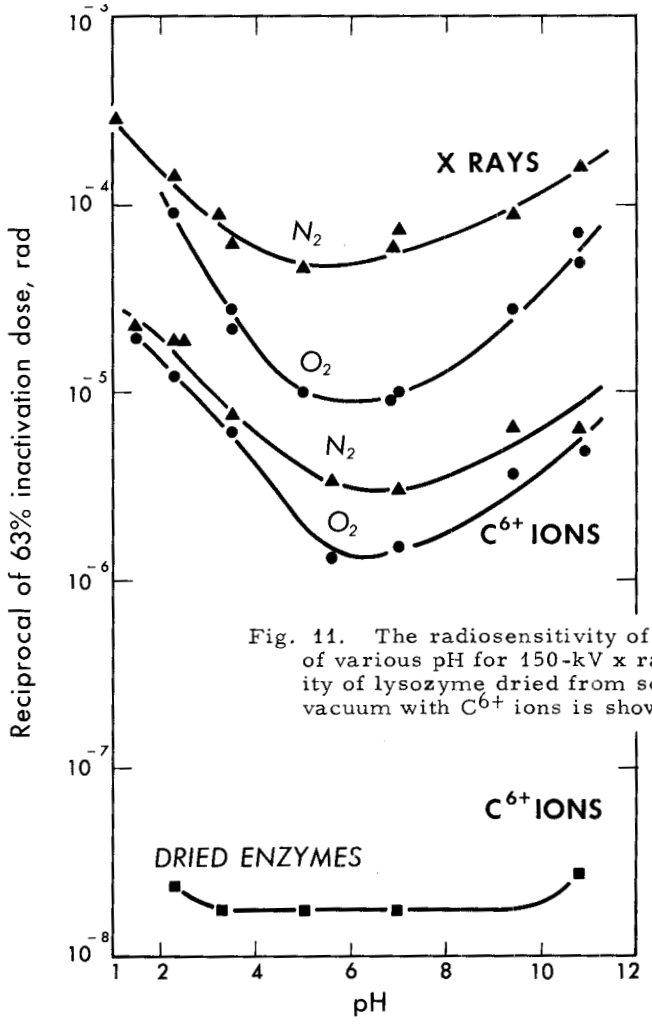

Fig. 11. The radiosensitivity of lysozyme in N_2- and in O_2-saturated solutions of various pH for 150-kV x rays and 110-MeV C^{6+} ions. The radiosensitivity of lysozyme dried from solutions of various pH and irradiated in high vacuum with C^{6+} ions is shown for comparison.

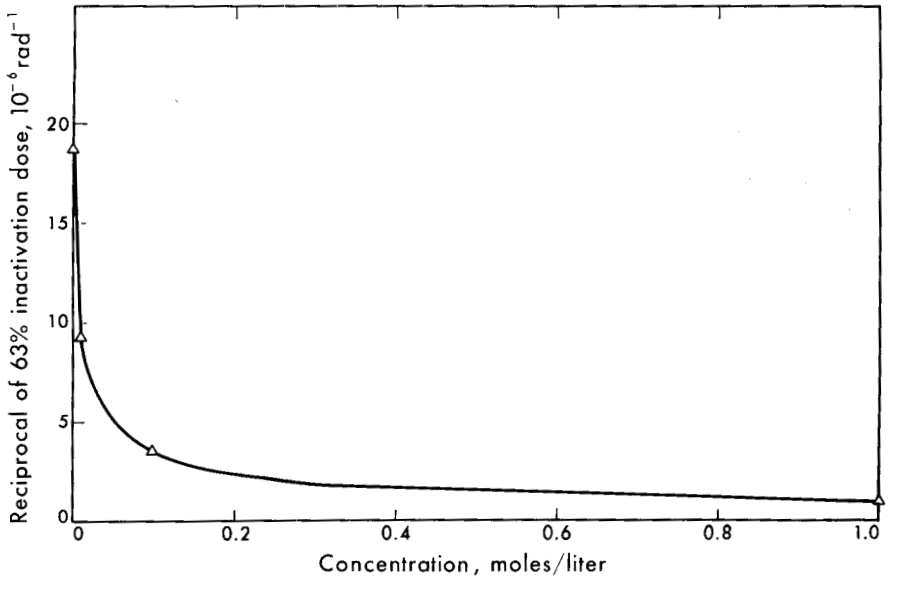

Fig. 12. The reciprocal of the 63% inactivation dose of lysozyme, irradiated with 110-MeV C ions in a N_2-saturated solution of pH 2.5 as a function of the concentration of glycerol in the solution.

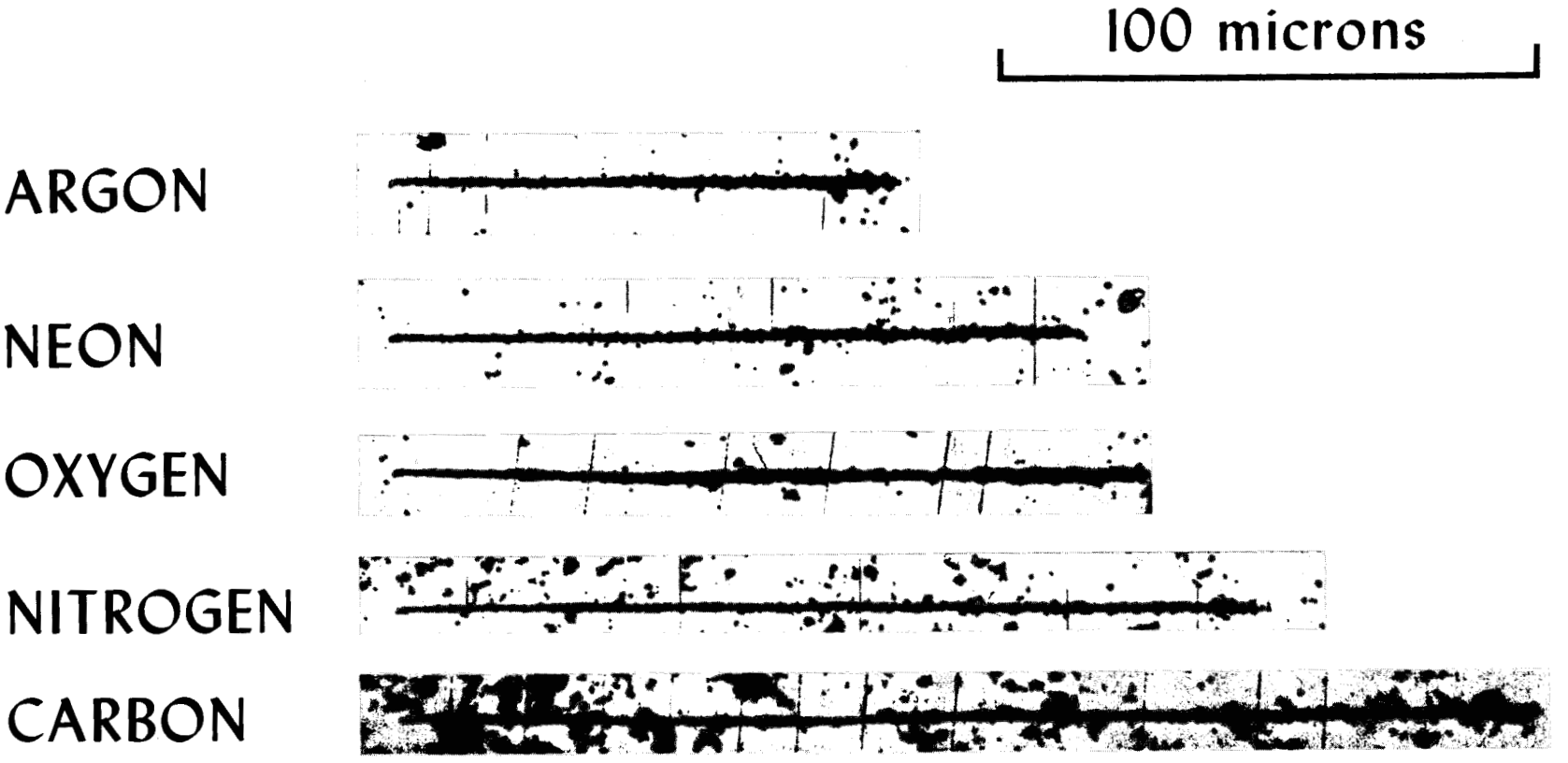

Fig. 13. Tracks in nuclear emulsions of accelerated ions of argon, neon, oxygen, nitrogen, and carbon of energy about 10 MeV/amu (Ref. 14). The particles penetrate from right to left.

II.4

CHROMOSOME DAMAGE

Sheldon Wolff

Laboratory of Radiobiology and Department of Anatomy
University of California Medical Center
San Francisco, California

Because a large segment of the audience does not consist of biologists, Dr. Wallace asked me to give an introductory lecture on the effects of radiation on chromosomes rather than to go into detail on experiments that are presently being carried out. I think a good way to follow his injunction is to point out that when cells are irradiated, one of the things that is readily noticed is that radiation can break the chromosomes that are found in the nucleus of the cell. As a matter of fact, studies on the induction of different types of chromosomal aberrations have been important in the development of at least two fields, biophysics and genetics.

In the field of biophysics, these studies have been invaluable in the development of the target theory, which explains the effects of radiations in terms of a simple direct interaction of the radiation with certain specific loci, or targets, within the cell. In the usual target experiment, cells are irradiated and then the survivors are studied to obtain dose action curves for killing. Since in these studies only survivors are observed, we look at cells that are not hit, and then make inferences about those that have been hit and about what targets have been inactivated. If, however, in an experiment we look at the chromosomes, which are essentially giant molecules that can be seen with the compound microscope, we see the targets right before our eyes and do not have to make any inferences at all. Because of this, about a third of the classical book on target theory, Douglas Lea's The Actions of Radiations on Living Cells, deals with the effects of radiations on genetic material.

In the field of genetics, radiation studies have been important because radiation can induce gene mutations. The genetic variability that is manifested as mutations has been the stuff upon which genetic studies are made. The mutations induced can be classified broadly into two groups, those that are supposedly true point mutations, or intragenic changes, and the much broader class, the so-called intergenic mutations that come about from the breakage of the chromosomes and the subsequent rearrangement of the broken ends into new configurations.

I think that at the outset it should be pointed out that when an organism is irradiated, very low doses can be lethal. For instance, doses as low as 400 rads may very well be the LD_{50} (the dose that will kill one-half of the organisms) for mammals that are given such a dose. Such low doses can also kill soaked seeds. At these low doses we are not causing any general sytemic effects or putting in enough ionizations to knock out enzyme systems. At one time Patt made a calculation for one large group of enzymes, the SH enzymes that require sulfhydryl groups for their activity, and found that it would take the ionizations

from about a million rads to inactivate all of these enzymes in the cell. The reason that such a large number of ionizations is required is that Avogadro's number is such a big number. That is, although there will be a low molar concentration of enzymes within the cell, there will be a very large number of molecules present. Since we cannot, therefore, reasonably expect cell death to be caused by a direct effect on enzyme systems at these low doses, we have to look for a system that is going to be sensitive to the radiation and also going to be capable of magnifying any effect that has been inflicted upon it so as to lead to the drastic systemic effects that cause death. The genetic apparatus, the genes and the chromosomes, are just such a system. Cells can be irradiated with low doses, and the chromosomes damaged, i.e., broken. The cells then cannot exist without the genes that were lost, because it is the genetic apparatus that controls all the chemical reactions that go on within the cell.

If we irradiate an unreplicated interphase chromosome, we can induce chromosome breakage. After the chromosome replicates, it shortens and contracts and becomes a metaphase chromosome. At metaphase, when the chromosomes can be seen, we find the fragments induced by the radiation. If the numbers of such fragments induced are plotted against the dose of radiation, it is found that they generally increase linearly with the dose of radiation, indicating that there is a certain probability (P) that a chromosome can be broken, and P is directly proportional to dose. The yield (Y) will then simply be equal to kD. Furthermore, it is found that the numbers of aberrations induced in a given experiment are distributed randomly within the cells, that is, the distribution fits the Poisson formula of $E^{-m}(m^r)/r!$, where m is the mean number induced in the experiment and r indicates whether the cell has 1, 2, 3, etc., aberrations.

There is another group of aberrations that are induced. This consists of the two-break aberrations that arise when two chromosomes close by each other are broken. If this happens, sometimes the broken ends can rejoin with one another so that the genes that were on one chromosome become translocated to the other. This is a true intergenic mutation, with changes in linkage relations and resultant genetic consequences. Occasionally we can find that, by chance, instead of rejoining to form a symmetrical translocation, the broken ends can rejoin to form a dicentric chromosome. If the numbers of these dicentric chromosomes are plotted against the dose of sparsely ionizing radiations, such as x or γ rays, it is found that the yield increases as the square of the dose (at least as a first approximation). This is very much what we would expect, since the probability of producing a single break would be P, and, therefore, the chance of producing another break would also be P, making the chance of obtaining both breaks concurrently P^2, which would be proportional to the square of the dose.

Many years ago, Karl Sax found that there are two factors involved in the production of these two-break, or two-hit, aberrations that increase as the square of the dose. These two factors are not noticed in studies on one-hit aberrations. One of the factors is a time factor and the other a space or distance factor.

The time factor reveals itself in dose fractionation, or dose intensity studies. One-hit aberrations have been found to be independent of the intensity of the radiation exposure, or independent of whether or not the dose is

fractionated. For two-break aberrations, however, this is not the case. The rationale is that if the radiation is given at low intensities or split into two portions, it will produce only part of the breakage, and repair of the breaks can occur in which the broken ends rejoin in the original configuration (restitution). Therefore, by the time the rest of the dose, or the second fraction, is given, it is possible to find that all the breaks were not open in the cell concurrently and so not capable of rejoining with one another to form two-hit aberrations. As a matter of fact, the time during which breaks remain open can be measured in these studies. For instance, if breaks stay open 5 minutes, you can break the chromosome at the beginning of an experiment and then break another nearby 5 minutes later, and it is just as though the dose were never fractionated. If, however, breaks have closed within this period of time, then the two groups cannot interact with each other and the yield is somewhat less.

The distance factor was noticed in experiments that have shown that although breakage occurred randomly within the cell and was distributed according to the Poisson formula there was a nonrandomness in the rejoining of the broken ends. Breaks that were close to each other could rejoin with each other, but those farther away could not. This was first shown in some experiments Sax performed on Tradescantia microspores. Tradescantia is a plant, the spiderwort, that has very large chromosomes. The microspore, which is a cell that is to become the pollen grain, is haploid and has only six of these instead of the twelve that are usually found in normal somatic tissue. Each of the chromosomes had two arms that were of about equal length, that is, they all had median centromeres. When Sax checked the numbers of dicentric versus ring chromosomes formed, he found that instead of observing 10 dicentric chromosomes for every ring, as would be expected if rejoining were random, he found only two or three dicentrics per ring. Some 10 to 1 was expected, because for any given break, there would be ten other arms with which it could rejoin to form a dicentric whereas there was only one other arm with which it could rejoin to form a ring chromosome. Sax attributed the excess number of rings to the fact that only breaks close to each other could rejoin and that the two arms of the same chromosome would be closer to each other than would be two arms from separate chromosomes.

Other evidence that rejoining is not random comes from the shape of curves obtained when we irradiate cells with more densely ionizing radiation than x or γ rays. When cells are irradiated with neutrons (which produce their ionizations by projecting protons within the cell), it is found that the two-break aberrations increase linearly with dose instead of as the square of the dose. This indicates that both breaks that take part in the exchange are produced by the same ionizing particle. If rejoining were a random process, then we might not expect to find linear kinetics, because a break that is produced in one part of the nucleus might very well wander around and find a break that was induced in another part of the nucleus by another proton projected by a neutron. This should give rise to some two-hit kinetics. Actually, the curve is linear over a large range of doses, which essentially rules out random rejoining of breaks.

We performed some experiments in which we looked not at the simple breaks that were produced by the radiation, but at the two-break chromosome aberrations induced in the early part of interphase before the chromosomes replicated. We found that although most chromosome breaks are distributed

according to the Poisson formula, this group that requires both breakage and rejoining for their formation were not distributed according to the formula, and therefore were not distributed randomly among the cells. We always found that there were too few cells having multiple aberrations, indicating to us that in addition to the formation of the aberrations not being random there was only a limited number of places within the nucleus where the chromosomes did come close enough to rejoin if broken. The earlier experiments had indicated the chromosomes had to be close to each other to rejoin, and this present result indicated there were not many places in the nucleus where this happened.

There is something else in neutron experiments that was notable other than that the curve was linear. It was found that the numbers of aberrations induced by a given dose of neutrons was far greater than those induced by the same dose of x or γ rays, that is, that there was a higher relative biological effect (RBE) of neutrons in producing aberrations. This is an indication that the production of a break is going to take more than one ionization. The argument is that if the effect observed took only one ionization (and this is true for the true point mutations), we would find that as we changed the linear energy transfer (LET) of the radiation, there would be no RBE effect, but if it required more than one ionization, there would be. One way to visualize this is to consider the target to be a sphere. If it required two ionizations to produce the effect, then more densely ionizing radiation would be more likely to deposit two ionizations within the volume hit, and therefore more densely ionizing radiations would be more efficient at producing mutations. If, however, it required only one ionization to produce the effect, then more densely ionizing radiation would not be more efficient, and, as a matter of fact, might be found to be less efficient than sparsely ionizing radiations in that they might deposit all of their energy within a single target and so effectively waste ionizations or dose. True point gene mutations did not show an RBE effect, but chromosome breakage did. From such studies, calculations have been made of the numbers of ionizations that are necessary to break a chromosome. Some of the calculations made by Lea indicated that it took approximately 15 to 20 ionizations to produce a break, even with x rays. The belief was that the breaks came not from individual ionizations, but from clusters of ionizations that were formed in the densely ionizing tails of the radiation tracks. The trouble with this kind of calculation is that what we observe are really only those aberrations or breaks that end up as aberrations at metaphase. This does not really reflect the primary breakages induced because, as we noted from the intensity experiments, breaks can restitute, i.e., repair can occur. Thus, we do not see in our aberration studies every single break that the radiation produced. We only see those that rejoin in such a way as to become visible as an aberration at metaphase.

Rather careful RBE studies for chromosome aberrations were carried out by Conger, who plotted the coefficient of aberration production at various LET's. With densely ionizing radiations this was rather easy to do, since the aberrations increase linearly with dose and the coefficient, k, was the same at all dose points. For sparsely ionizing radiations, however, in which the aberrations increased as the square of the dose, the calculations became a little more difficult because the yield of aberrations changed according to where one was on the dose curve. Therefore, at low doses, the RBE might very well be high, but would become negligible at higher doses, since the aberrations induced by sparsely ionizing radiations are increasing more rapidly than the first power

of the dose. It is even possible to find RBE's less than 1 at extremely high doses. In order to obtain his RBE's while working with two-break chromosome aberrations, Conger found it necessary to use a biological criterion and to look always at the point where only 50% of the cells had aberrations. When he did the experiment, he found that as LET increased he got an increase in RBE up to a certain point. From that point on with even more densely ionizing radiations he found the RBE curves fell, that is, it took more than one ionization to produce a break, but that when the radiations were sufficiently densely ionizing, dose would be wasted.

There was something else that came out of studies on chromosome aberrations and that is that their formation is subject to the well-known oxygen effect. As a matter of fact, it was while working with Vicia faba chromosomes that Thoday and Read first found the oxygen effect, whereby there is an increased yield of biological damage (in this case chromosome aberrations) when material is irradiated with sparsely ionizing radiations in the presence of oxygen rather than under anoxic conditions. Thoday and Read and others who then followed in the study of this phenomenon found that the numbers of aberrations induced by a given dose of radiation increased as the oxygen tension increased from zero to 20% oxygen, which is just about the amount of oxygen that is present in air. At this point the curve saturated, and there was only a slight increase as the oxygen tension increased to 100%. It has been found that this particular saturation point is really an artifact because the cell is respiring constantly, burning up oxygen as it does. Therefore, the outside concentration is not the same as that inside the cell and, as a matter of fact, there are oxygen gradients within the cell. If, however, cellular respiration is poisoned so the cell cannot burn up the oxygen, then the inside of the cell can equilibrate with the outside and we find the saturation point really occurs at about 2% rather than 20% oxygen.

With α rays that are very densely ionizing, we find there is no oxygen effect. One of the arguments for this is that the oxygen effect itself is caused by the production of HO_2 or even hydrogen peroxide, and with sparsely ionizing radiations, far less of these compounds is produced when cells are irradiated under anoxic conditions. When they are irradiated with α rays, however, we find that there is essentially just as much peroxide produced anoxically as in the presence of oxygen. Therefore, with α rays we don't find any oxygen effect. With neutrons that are not so densely ionizing as α rays we find that there is an oxygen effect, but not nearly so great as that seen with sparsely ionizing radiations. Ordinarily, we find about a two- or threefold increase in oxygen effects when x or γ rays are used, whereas in a neutron experiment the increase might be only about 1.4-fold.

The foregoing, I think, does give some idea of the types of things that can be done and have been done in experiments on chromosome aberrations. I did not, however, present much about effects found with more densely ionizing radiations, although from the title of this symposium, this latter might very well be one of the major concerns of the people who are in attendance. One of the reasons, however, that I did not spend much time considering these effects is that in the past, at least, there just has not been so much work done with these more densely ionizing radiations as has been done with x and γ rays.

References

1. A. D. Conger, M. C. Randolph, C. W. Sheppard, and H. J. Luippold, Quantitative Relation of RBE in Tradescantia and Average LET of Gamma Rays, X-rays, and 1.3-, 2.5-, and 14.1-MeV Fast Neutrons, Radiation Res., 9: 525-547 (1958).

2. H. J. Evans, Chromosome Aberrations Induced by Ionizing Radiations, Intrn. Rev. Cytol., 13: 221-321 (1962).

3. D. E. Lea, Actions of Radiations on Living Cells, Cambridge University Press, 1955.

4. S. Wolff, Radiation Genetics, in Mechanisms in Radiobiology, M. Errera and A. Forssberg, Eds., Academic Press, New York, 1961, pp. 419-475.

II.5

FUNDAMENTAL ASPECTS OF THE DEPENDENCE OF BIOLOGICAL RADIATION DAMAGE IN HUMAN CELLS ON THE LINEAR ENERGY TRANSFER OF DIFFERENT RADIATIONS

G.W. Barendsen

INTRODUCTION

Ionizing radiations are capable of producing a variety of effects in living cells. When germ cells of an intact organism are irradiated, mutations may arise which can be transmitted to offspring. These effects are therefore called genetic effects. Irradiation of other cells in an organism may result in the development of tumors or death of the organism due to damage to the reproductive capacity of cells in some specific tissues. These types of effects are called somatic effects.

Sufficient knowledge with respect to the action of ionizing radiations on living cells is not yet available about whether various types of effects are initiated by the same mechanism. It appears likely that at least for the effects mentioned, the chromosomal material in the cell is the primary target. This does not imply however that dose-effect relations for the various types of effects must be similar. Nevertheless in the present paper dose-effect relations will be discussed concerning impairment of the reproductive capacity of cultured mammalian cells and it is suggested that insight gained from these studies may be useful for the interpretation of available data with respect to other effects as well.

Interest in the comparison of biological effects produced by different radiations stems from the well-known fact that for equal absorbed doses of two types of radiations the degrees of damage may be different, though no fundamental differences have been demonstrated between the types of effects produced by various radiations. In general any type of biological effect produced by X-rays or γ-rays can also be produced by other ionizing radiations, be it with a lower or higher degree of effectiveness.

The variations observed in the effectiveness of different radiations are generally assumed to be due to differences between the spatial distributions on a submicroscopic scale of the energy deposition in the irradiated material. The absorption of ionizing radiation in a given material results in energy-dissipation events which are not distributed at random, but are localized along the tracks of individual charged particles. The distribution along the tracks of the individual energy-

dissipation events is dependent on the charge and velocity of the particle. In order to evaluate the biological effects of different radiations it is necessary to characterize the pattern of energy deposition of different radiations. For this purpose the concept of LET has been introduced[1] which is commonly expressed in keV/μ of unit density tissue. Because all radiations will show a spread in LET, a single value of the LET is certainly not sufficient to characterize a given type of radiation, and a complete analysis of the distribution of dose in LET presents many fundamental and practical difficulties[2]. The concept of local energy density distribution, introduced by Rossi, is certainly preferable for fundamental as well as practical reasons, but insufficient data for very small volumes are yet available to compare the biological effects in mammalian cells with these distributions. In the present paper we will therefore use the LET concept, but it is important to note that it is only a first approximation.

Two different methods of calculating mean LET values have been commonly used, yielding the track-average LET and the dose-average LET respectively. These have been discussed in detail elsewhere[3, 4, 5, 6]. Mean LET values are obviously of greatest value if relatively narrow distributions of dose in LET are obtained. This can be attained if the irradiated object is thin and if monoenergetic heavy charged particles are used in conditions whereby only a small part of their track traverses the cell.

In the next sections we will first consider dose-effect relations obtained with experimental conditions in which these narrow distributions of dose in LET are attained, and subsequently we will discuss effects of other radiations with wide LET distributions.

RBE-LET RELATIONS FOR IMPAIRMENT OF THE PROLIFERATIVE CAPACITY OF CULTURED HUMAN CELLS

In order to describe quantitatively the differences in effectiveness between different radiations, the concept of "relative biological effectiveness" has been introduced. The RBE of a radiation Y for a specified biological effect is defined as the ratio of two absorbed doses of different radiations which yield equal effects:

$$\text{RBE (Y)} = \frac{\text{dose of "standard radiation" required for specified effect}}{\text{dose of radiation Y required for equal effect}}. \qquad (1),$$

The effect for which the RBE-LET$_\infty$* relations will be discussed is usually described as: impairment of the proliferative capacity of individual cells. The cells we have investigated have been derived originally from a human kidney[6]. The cell culture technique employed has been introduced by Puck and Marcus in 1956[7] and during the past ten years the application of this method has yielded a vast amount

*LET$_\infty$ implies that δ rays are all included[8].

of radiobiological data. Briefly this technique consists in the plating of a known number of cells in a suitable environment, followed by an incubation period after which the clones which have developed are counted. Figure 1 shows the results of a typical experiment, in which the number of clones obtained decreases as a function of the dose. The results of these experiments are usually plotted as a survival curve which represents the fraction of surviving cells as a function of the dose.

A selection of the many survival curves obtained with this technique is presented in Figure 2. From these curves it is possible to derive RBE values for the different radiations employed, but it will be clear that no single value can be assigned to each radiation. With radiations which correspond to LET_{∞} values of 60 keV/μ or more, exponential survival curves are obtained, whereas with radiations which have LET_{∞} values of less than 20 keV/μ the curves show a distinct curvature which is most pronounced in the low dose region. As a consequence of these differences in shape between the survival curves and because 200-kV X rays are taken as a standard of reference in the definition of the relative biological effectiveness, the RBE of densely ionizing α particles, deuterons, protons, and neutrons changes with the level of damage considered.* This variation of the RBE as a function of LET is presented in Figure 3 for respectively 80%, 20%, 5%, and 1% survival. The RBE values for all percentages survival increase sharply between 10 and 100 keV/μ of tissue to a maximum at 110 keV/μ and followed by a decrease beyond 120 keV/μ of tissue. In addition, however, the RBE values are shown to be highest at high percentages survival, which correspond to low levels of damage and low doses. In relation to Health Physics problems the question must be considered whether at the still lower doses and at low dose rates, which are relevant to conditions encountered in radiation protection, the RBE increases further and whether or not a limiting value does exist. On the basis of general considerations concerning energy-dissipation characteristics of different radiations it is possible to conclude that a limiting value must exist[9]. These general considerations lead to the conclusion that sparsely ionizing radiations, e.g. X and γ rays, dissipate part of their energy through low energy electrons which have LET's sufficiently high to cause a "single event" type of damage in the same way as produced by densely ionizing α-particles and deuterons. Thus for X and γ rays an initial negative slope at low doses must exist, and the limiting maximum value of the RBE is equal to the ratio of this initial negative slope and the slope of the exponential survival curve obtained with a radiation which has a LET of 110 keV/μ. The experimental results obtained with doses of 25 and 50 rads of 200-kV X rays show survival percentages of 94.3 ± 2.3 and 89.7 ± 2.1 respecticely. From these data a D_{37} of 450 ± 100 rads can be calculated. The D_{37} of

* No significant difference has been observed to exist between the RBE of 200-kV X rays and 250-kVp X rays.

a radiation at a LET of 110 keV/μ is 57 ± 4 rads and from these values a maximum RBE of 8 ± 2 may be calculated. It may be concluded from these data that the maximum RBE value obtained for cells in oxygenated conditions is not much in excess of the value of 8 obtained at 80% survival.

VARIATIONS OF THE RBE DUE TO VARIOUS EXPOSURE CONDITIONS

a. Dose Fractionation and Dose Rate

From the definition of the RBE it is evident that any factor which influences the effectiveness of the standard radiation and the effectiveness of the radiation considered to a different extent, will cause a variation of the RBE. One of these factors is the distribution of dose in time. As first demonstrated by Elkind and Sutton[10] for Chinese hamster cells and subsequently shown by others [9, 11] for a variety of cell lines, fractionation of the dose and variation of the dose rate may profoundly influence the effectiveness of radiations with a low mean LET. An example of an experiment designed to demonstrate this effect is given in Figure 4. This phenomenon is interpreted to result from repair of sublethal damage which occurs within a few hours after exposure. As a result the effect of a given total dose is less in fractionated exposures as compared with single exposures[10]. This also will apply to exposures at very low dose rates which are equivalent to a small dose per cell generation. It has further been demonstrated that the recovery phenomenon does not occur with radiations of high LET, which give exponential survival curves. This implies that, in contrast with low LET radiations, the effectiveness of high LET radiation does not decrease with decreasing dose rate. Consequently the RBE of densely ionizing radiations will be higher at low dose rates as compared with high dose rates. As discussed earlier, however, even with low LET radiation a fraction of the damage will be produced by a "single event" type of mechanism and this fraction, which should also be independent of the dose rate, will determine the ultimate maximum RBE obtained. This value cannot be higher than about 8, as calculated from the ratio of the initial slopes of the survival curves a and b of Figure 4, i.e., equal to the ratio of slopes of a and c.

b. Environmental Conditions of Cells

In addition to dose rate, several environmental conditions, e.g. temperature, oxygen concentration and protective compounds, are known to modify the effects of ionizing radiations on biological systems. In general it is found that the effectiveness of sparsely ionizing radiations, e.g. X or γ rays, can be affected to a greater extent than the effectiveness of densely ionizing radiations, e.g. α radiation or fast neutrons. This is shown in Figure 5 where the effect of anoxia on radiation-induced damage to cultured cells is demonstrated. With densely ionizing α particles a protection factor of only 1.15 is found, i.e. a 1.15 times higher dose is required to produce the same level of damage in cells equilibrated with

nitrogen as compared with air. With 250-kV X rays a protection factor of 2.6 is obtained. These factors are called "oxygen enhancement ratio s" (OER). As a consequence of these differences in the OER values, the RBE of 3.4-MeV α particles in these extreme conditions is increased by a factor of 2.6/1.15 = 2.26. Thus the maximum RBE value of about 7 for α particles of 140 keV/μ of tissue at low doses with oxygenated cells is found to be increased to about 16 for anoxic cells.

The OER values have been measured for a variety of radiations and the relation between OER and LET_∞ is given in Figure 6. It is shown that the OER decreases with increasing LET from about 2.6 at a LET_∞ of 5.6 keV/μ of unit density tissue to a value of 2.05 at 61 keV/μ, followed by a more rapid decrease of 1.0 at 165 keV/μ[12].

With protective compounds in high concentrations the differences in effectiveness may become even larger. Protection factors of 1.2 and 3.7 have been measured with 25 mM cysteamine for cultured cells irradiated with α particles at 140 keV/μ of tissue and 200-kV X rays with an average LET of 3.5 keV/μ of tissue respectively[13]. Thus the RBE of 3.4-MeV α radiation under these conditions may be calculated at about 21. It will be clear, however, that this value is of little practical importance, because the extreme variations attained in these experiments will not be attained in conditions with which we are concerned in radiation protection.

c. General Aspects of RBE-LET Relations

From the experimental data discussed an insight has been obtained with regard to the RBE-LET relations and their variations with dose, dose-fractionation, dose rate, and various experimental conditions. It is possible to divide the total LET interval in five main parts. In the lowest LET range, i.e., below about 10 keV/μ, designated I in Figure 7, the energy dissipated can contribute to cell killing only through accumulation of damage and the OER is high, usually between 2.5 and 3.0. In region III, between 20 and 80 keV/μ, damage is produced by traversals of single particles resulting in exponential survival curves. In this region the OER is still relatively high but already decreases from about 2.5 to 1.8. The RBE-LET curve rises sharply in this region. In region V, in excess of about 160 keV/μ, damage is produced by traversals of single particles, resulting in exponential survival curves. The RBE-LET curve decreases in this region and the effectiveness per unit dose is almost independent of oxygen. Between these regions we have regions II and IV in which rapid variations in RBE or OER occur, which may be called transition regions.

RBE AND OER VALUES FOR RADIATIONS WITH WIDE DISTRIBUTIONS OF DOSE IN LET

The radiations discussed in the preceding parts were used in conditions in which

narrow LET distributions are attained except for the 200-kV X rays which are taken as a standard of reference. A characteristic property of the energy dissipation by indirectly ionizing radiations, e.g. X rays, γ rays, neutrons, mesons as well as of directly ionizing particles in conditions where the track is not much longer than the dimension of the irradiated object, is the presence of a wide distribution of dose in LET. It will be clear that the RBE as well as the OER and the effect of fractionation and dose rate of these radiations will depend on the distribution of the dose in LET. With X rays, γ rays, and fast electrons this distribution will extend from a minimum determined by the maximum energy of the electrons liberated in the biological material up to a maximum determined by the LET of electrons at the end of their paths where they are slowed down. The minimum theoretically possible is about 0.2 keV/μ, the maximum is about 50 keV/μ[6]. This implies that the OER of these radiations is uniformly high and that a considerable part of the damage corresponding to the energy dissipated in region I is dependent on dose rate. The RBE may vary depending on the distribution of the dose in regions I, II, and III.

Data which have been obtained with fast neutrons are more difficult to classify because the distribution of the dose in LET is even more complex and may extend over an even wider range than is the case for γ rays or fast electrons. The minimum of this distribution is determined by the maximum energy of protons set in motion in the irradiated biological material, and the maximum depends on the LET of heavy nuclei, e.g. C, N, and O. Thus for 15-MeV neutrons the minimum value is 3 keV/μ while the maximum may be as high as 1000 keV/μ. Depending on the exact distribution of the dose in LET, the RBE, the OER, and the effects of fractionation may vary. A surprising fact is, however, that the OER and the RBE vary relatively little between about 1 and 15 MeV as shown in Figure 8[14, 15]. This does not correspond at all with either the track-average LET value or the energy-average LET values which have been calculated[4]. This again indicates the necessity to obtain adequate measurements of local energy density distribution as discussed by Rossi[16]. The same remark applies to radiations about which even less is known, e.g. mesons, which may produce also wide distributions of dose in LET.

REFERENCES

1. R.E. Zirkle, D.F. Marchbank, and K.D. Kuck, Exponential and sigmoid survival curves resulting from alpha- and X-irradiation of Aspergillus spores, J.Cell.Comp.Physiol., 39: 75 (1952).
2. H.H. Rossi, Correlation of radiation quality and biological effect, Ann.N.Y. Acad.Sci., 114: 4 (1964).
3. P. Howard-Flanders, Physical and chemical mechanisms in the injury of cells by ionizing radiations, in Advances in Biological and Medical Physics, Vol. 6, pp. 553-603, Academic Press, New York, 1958.
4. A.D. Conger, M.L. Randolph, C.W. Sheppard, and H.J. Luippold, Quantitative relation of RBE in Tradescantia and average LET of gamma-rays, X-rays, and 1.3-, 2.5-, and 14.1-MeV fast neutrons, Radiat.Res., 9: 525 (1958).
5. T. Brustad, Heavy ions and some aspects of their use in molecular and cellular radiobiology, in Advances in Biological and Medical Physics, Vol. 8, pp. 161-224, Academic Press, New York, 1962.
6. G.W. Barendsen, Mechanism of action of different ionizing radiations on the proliferative capacity of mammalian cells, in Theoretical and Experimental Biophysics, Vol. 1, pp. 167-231, Marcel Dekker, New York, 1967.
7. T.T. Puck and P.I. Marcus, Action of X-rays on mammalian cells, J. Exp. Med., 103: 653 (1956).
8. Report of the RBE Committee to the International Commissions on Radiological Protection and on Radiological Units and Measurements 1963, Hlth.Phys., 9: 357 (1963).
9. G.W. Barendsen, Dose-survival curves of human cells in tissue culture irradiated with alpha-, beta-, 20-kV X- and 200-kV X-radiation, Nature, 193: 1153 (1962).
10. M.M. Elkind and H. Sutton, Radiation response of mammalian cells grown in culture I. Repair of X-ray damage in surviving Chinese hamster cells, Radiat. Res., 13: 556 (1960).
11. R.J. Berry and J.R. Andrews, Quantitative studies of radiation effects on cell reproductive capacity in a mammalian transplantable tumor system in vivo, Ann.N.Y.Acad.Sci., 95: 1001 (1961).
12. G.W. Barendsen, C.J. Koot, G.R. van Kersen, D.K. Bewley, S.B. Field, and C.J. Parnell, The effect of oxygen on impairment of the proliferative capacity of human cells in culture by ionizing radiations of different LET, Int.J.Radiat.Biol., 10: 317 (1966).
13. G.W. Barendsen and H.M.D. Walter, Effects of different ionizing radiations on human cells in tissue culture. IV. Modification of radiation damage, Radiat. Res., 21: 314 (1964).
14. G.W. Barendsen and J.J. Broerse, Dependence of the oxygen effect on the energy of fast neutrons, Nature, 212: 722 (1966).

15. J.J. Broerse, Effects of Energy Dissipation by Monoenergetic Neutrons in Mammalian Cells and Tissues, Thesis, University of Amsterdam, 1966.
16. H.H. Rossi, Microdosimetry, in Biophysical Aspects of Radiation Quality, I.A.E.A., Vienna, Technical Reports Series No. 58, pp. 81-95, (1966).

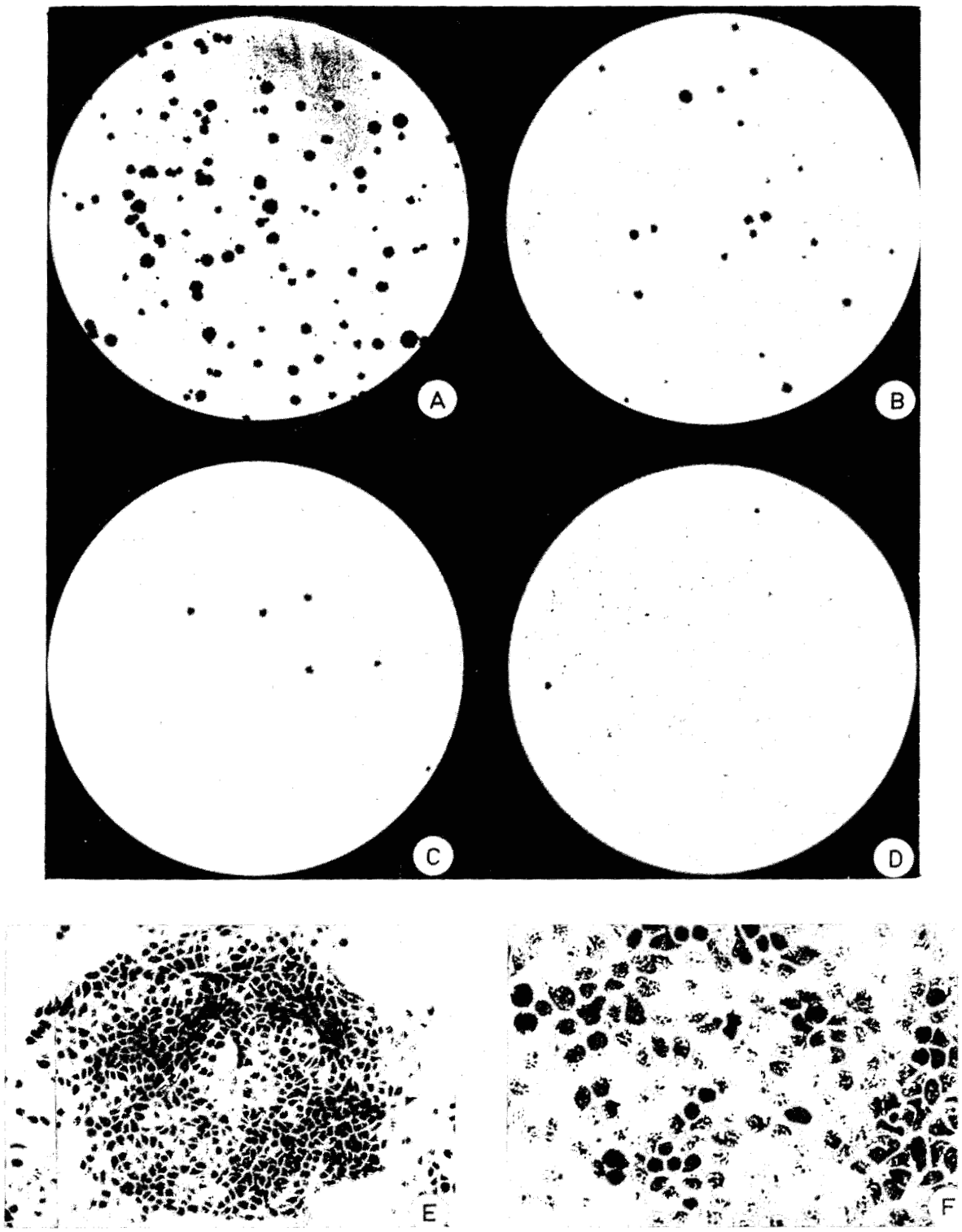

Figure 1: Pictures of dishes with clones developed from cells irradiated with 3.4-MeV α particles, LET_{∞} 140 ± 30 keV/μ. A, B, C, and D are examples of dishes irradiated with 0, 100, 200, and 300 rads respectively, E represents a magnification of one clone, F is a larger magnification of part of this clone which shows individual cells more clearly.

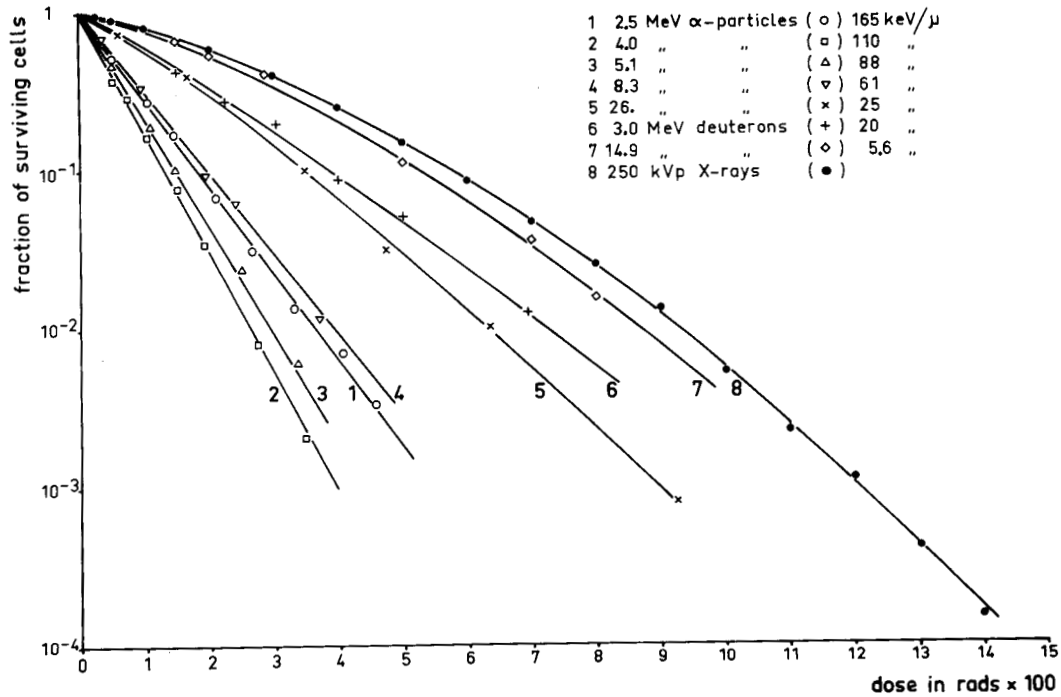

Figure 2: Survival curves for cultured cells of human origin obtained with radiations of different LET_{∞}.

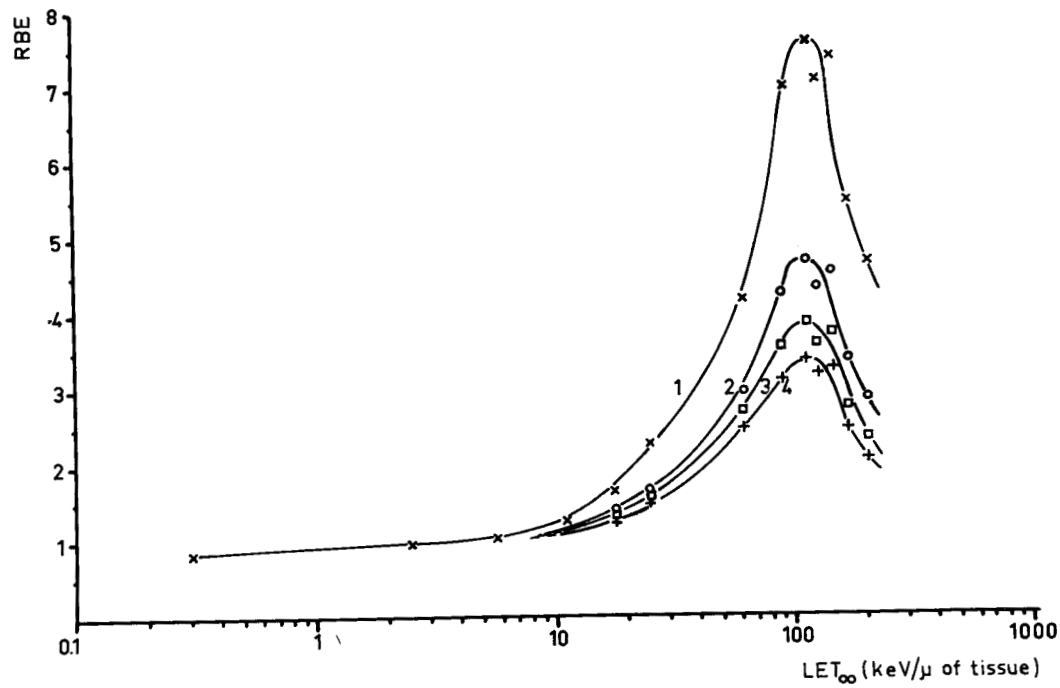

Figure 3: Relative Biological Effectiveness as a function of LET_{∞} of different ionizing radiations with respect to impairment of the proliferative capacity of human kidney cells (T-1 cells) in culture. Curves 1, 2, 3, and 4 correspond to surviving fractions of 0.8, 0.2, 0.05, and 0.01.

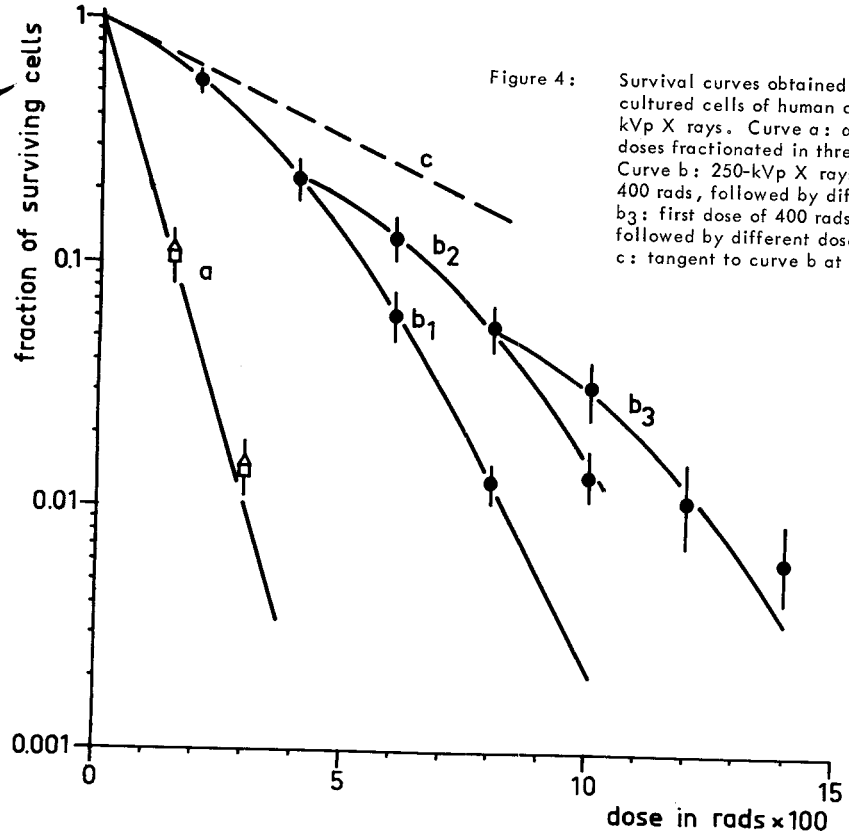

Figure 4: Survival curves obtained with single and fractionated exposures of cultured cells of human origin to 3.4-MeV α particles and to 250-kVp X rays. Curve a: α radiation, □ single exposures, Δ total doses fractionated in three equal parts with intervals of 6 hours. Curve b: 250-kVp X rays, b_1: single exposures, b_2: first dose of 400 rads, followed by different doses after an interval of 6 hours, b_3: first dose of 400 rads, after 6 hours a second dose of 400 rads followed by different doses after another interval of 6 hours. Curve c: tangent to curve b at dose zero.

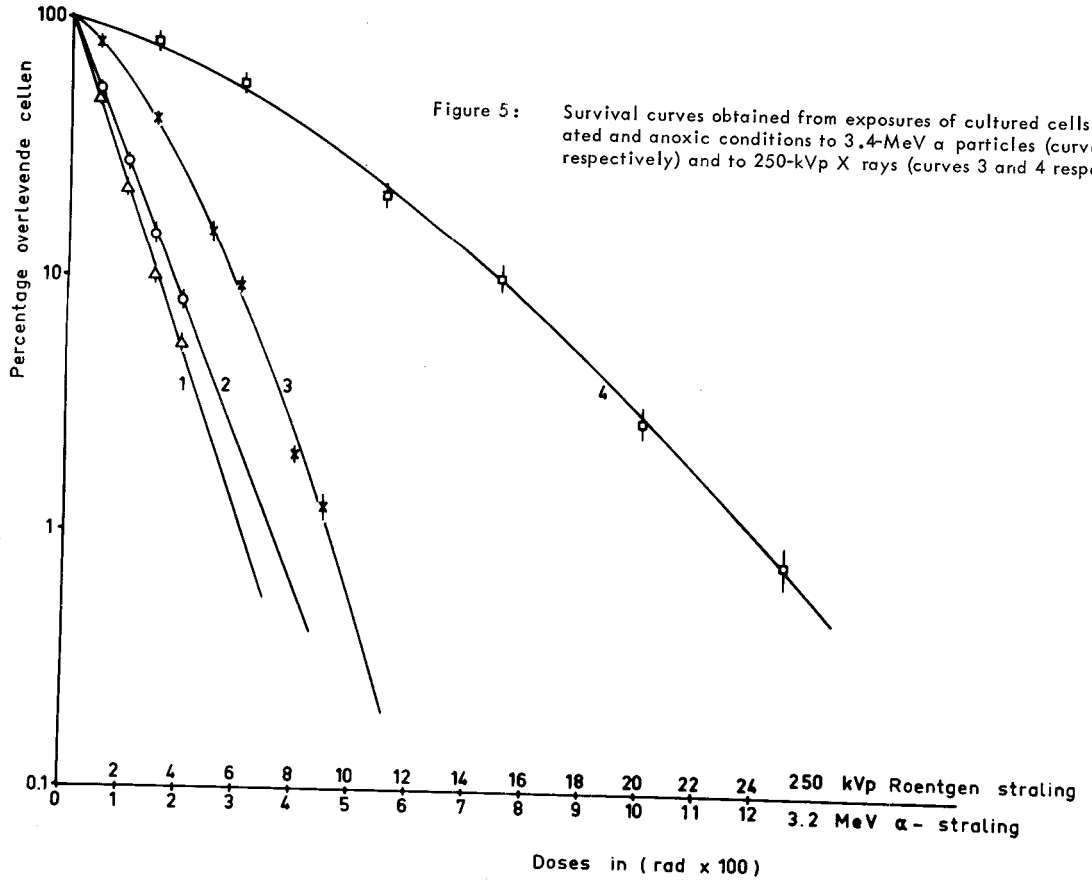

Figure 5: Survival curves obtained from exposures of cultured cells in oxygenated and anoxic conditions to 3.4-MeV α particles (curves 1 and 2 respectively) and to 250-kVp X rays (curves 3 and 4 respectively).

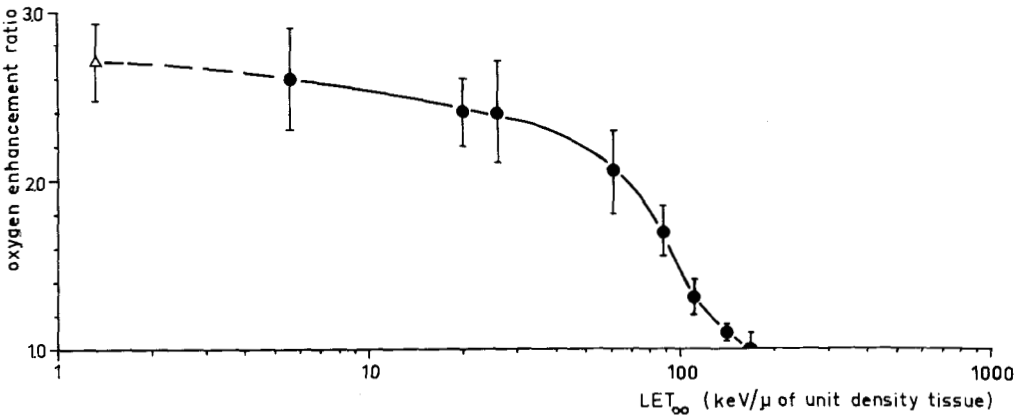

Figure 6: *Oxygen enhancement ratio as a function of* LET_{∞} *for impairment of the proliferative capacity of cultured cells of human origin by different radiations. Circles: monoenergetic charged particles employing the track-segment method, triangle: 250-kVp X rays assumed mean LET 1.3 keV/μ (after Barendsen, Koot, van Kersen, Bewley, Field and Parnell 1966).*

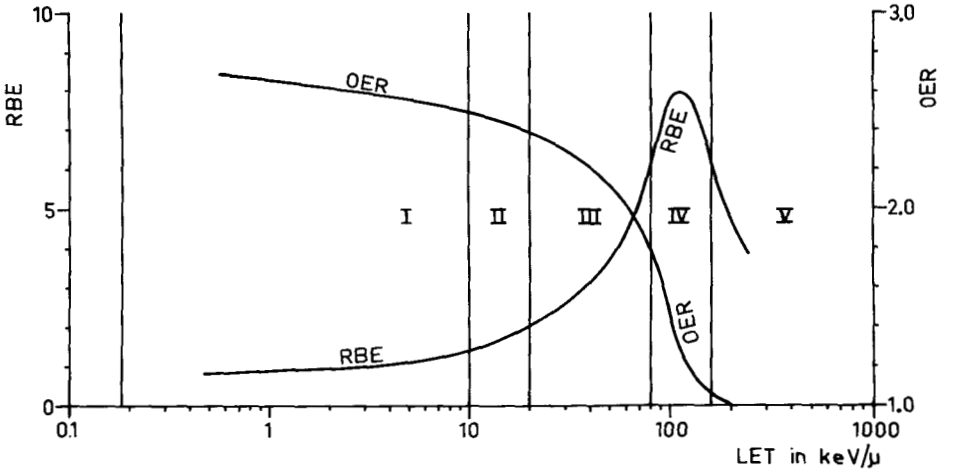

Figure 7: The relation of RBE and OER with LET in different regions of LET. RBE curve is identical with curve 1 of Figure 3. OER curve is identical with the curve of Figure 6.

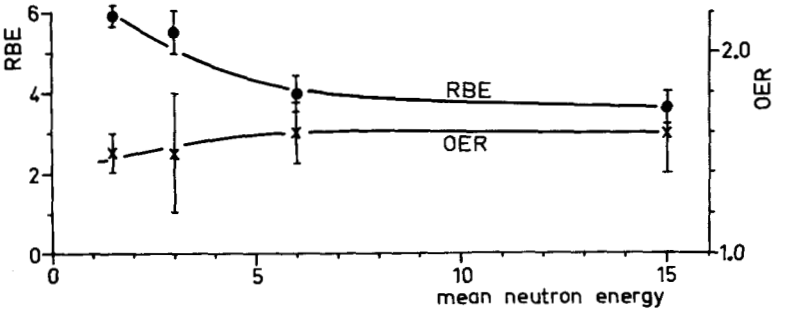

Figure 8: Relative Biological Effectiveness and Oxygen Enhancement Ratio of fast neutron beams as a function of the mean energy with respect to impairment of the proliferative capacity of cultured cells of human origin. RBE values correspond to a dose level producing a surviving fraction of cells of 0.8, i.e. equivalent to 100 rads of 250-kVp X rays. Specification of the beams: "Fission spectrum" fast neutrons from ^{235}U, spectrum with a maximum intensity at 1.5 MeV; 3-MeV monoenergetic neutrons produced by bombarding Deuterium with 400-kV deuterons; fast neutrons produced by bombarding Be with 15-MeV deuterons, spectrum with a maximum intensity at 6 MeV; 15-MeV monoenergetic neutrons produced by bombarding Tritium with 400-kV deuterons.

II.6

FRACTIONAL LINEAR ENERGY TRANSFER

Richard Madey
Department of Physics
Clarkson College of Technology
Potsdam, New York 13676

Abstract

The concept of linear energy transfer (LET) was introduced in radiation dosimetry to describe the local density of energy deposition along the path of an ionizing particle. There is a certain fuzziness about the LET concept which arises from the interpretation of the word "local" insofar as biological radiosensitivity is concerned. It is possible to specify the extent of a local region around the path of an ionizing particle by restricting the energy transferable to the electrons in the atoms of the stopping medium.

The fractional linear energy transfer (FLET) is the ratio of the restricted stopping power to the total stopping power. The restricted stopping power of a medium for a charged particle moving at a given velocity is proportional to the total stopping power. The proportionality factor is essentially independent of the velocity of a heavy charged particle if the restricted energy transfer is equal to the root-mean-square (rms) energy transfer, and it has only a slight dependence on the primary particle velocity if the restricted energy transfer is equal to the mean energy transfer. In these circumstances, the fact that the FLET is insensitive to the velocity of a heavy charged particle means that only a scale factor distinguishes the restricted stopping power from the total stopping power; hence, a biological effect that depends on some function of the total stopping power will have the same functional dependence on the restricted stopping power with energy transfers restricted either to the rms or to the mean energy transfer.

II.6

FRACTIONAL LINEAR ENERGY TRANSFER

Richard Madey
Department of Physics
Clarkson College of Technology
Potsdam, New York 13676

It is well known that a charged particle moving through matter loses energy primarily by inelastic collisions with the electrons in the atoms of the material. In an inelastic collision, the charged particle transfers energy to a bound electron and thereby raises it either to an excited bound state or to an unbound state. The final state of the struck electron depends on the amount of energy transferred in the collision. The term ionization refers to both degrees of excitation. In ionizing collisions involving large energy transfers to a single electron, the struck electron ionizes other atoms outside the path of the original charged particle. It is this situation which led to the introduction of the concept of linear energy transfer (LET) in radiation dosimetry to describe the local density of energy deposition along the path of an ionizing particle. There is a certain fuzziness about the LET concept which arises from the interpretation of the word "local" insofar as biological radiosensitivity is concerned. It is possible to specify the extent of a local region around the path of an ionizing particle by restricting energy transfers to values less than some arbitrary value W_o; hence, W_o represents the maximum energy transfer that contributes to the "local" ionization.

The maximum energy transferable to an atomic electron of mass m by an incident particle of mass M, momentum P, and total energy E is given by

$$W_m = 2mc^2 \frac{c^2P^2}{m^2c^4 + M^2c^4 + 2mc^2E} \tag{1}$$

For incident heavy $(M >> m)$ particles with energies satisfying the condition $(E/Mc^2) << 1/2\ (M/m)$, the maximum energy transfer is

$$W_m = 2mc^2\ (P/Mc)^2 = 2mc^2\ \beta^2/(1-\beta^2). \tag{2}$$

where β is the particle velocity in units of the light velocity c. In Table I, we list values of W_m versus β. The maximum energy transfer is about 22 kev for a 10-Mev proton, 196 kev for an 100-Mev proton, and 3340 kev for an 1000-Mev proton.

We use the symbol $(LET)_{W_m}$ to refer to the LET that admits all possible energy transfers upto W_m. The literature usually refers to $(LET)_{W_m}$ as $(LET)_\infty$. It includes the ionization from both the primary particle and all of the secondary electrons ejected by the primary particle. $(LET)_{W_m}$ is the same as the "stopping power" of the medium for the particle, which is equal to $\frac{dT}{dx}$, the loss of kinetic energy per unit path length of the particle in the medium. Hence, for charged particles heavier than electrons,

$$(LET)_{W_m} \equiv \frac{dT}{dx}\left(\frac{\text{Mev}}{\text{g-cm}^{-2}}\right) = \frac{N_o}{A}\,\frac{4\pi r_e^2\, mc^2\, z^2}{\beta^2}\, B, \qquad (3)$$

$$B \equiv Z\,[\ln (W_m/I) - \beta^2\,] = \frac{Z}{2}\,[\ln (W_m/I)^2 - 2\beta^2\,], \qquad (4)$$

where

N_o = Avogadro's number = 6.023×10^{23} atoms/mole,

A = mass number of the medium,

β = v/c = particle velocity in units of the velocity of light,

mc^2 = rest energy of the electron = 0.5110 Mev,

r_e = e^2/mc^2 = classical electron radius = 2.818×10^{-13} cm,

z = charge of the particle,

Z = atomic number of the absorbing medium,

I = average of the excitation potential over all electrons in the atoms of the medium.

Note that we have written Eq. (4) for the stopping number B without the shell correction term and the density effect correction term. The shell correction term has a small effect at low energies where the particle velocity is of the order of the velocity of the atomic electrons in the K and L shells. The density effect term does not become significant until the particle velocity approaches the extremely relativistic region. Barkas (1960) has tabulated numerical values for the sum of the two correction terms for protons in nuclear track emulsion with an ionization potential I = 331 ev. For this calculation, the density effect correction is negligible for 1-BeV ($\beta = 0.87504$) protons and is about 4.5 per cent for 10-BeV ($\beta = 0.99631$) protons.

We use the symbol $(\mathrm{LET})_{W_o}$ to refer to the LET when the energy transfer is restricted to values less than W_o. $(\mathrm{LET})_{W_o}$ is the same as the "restricted stopping power" $(dT/dx)_{(W < W_o)}$ of the medium for the particle. It neglects ionization from secondary electrons greater than W_o. Bethe (1930; 1932) developed the theory of the "restricted stopping power" and obtained the following result in the approximation that $W_o << W_m$:

$$(\mathrm{LET})_{W_o} \equiv \left(\frac{dT}{dx}\right)_{(W < W_o)} = \frac{N_o}{A} \frac{4\pi r_e^2 mc^2 z^2}{\beta^2} B_1, \tag{5}$$

$$B_1 \equiv \frac{Z}{2} [\ln(W_m W_o / I^2) - \beta^2]. \tag{6}$$

The stopping number B_1 in Eq. (6) is for charged particles heavier than electrons.

It is convenient now to introduce the fractional linear energy transfer with the notation $(\mathrm{FLET})_{W_o}$:

$$(\mathrm{FLET})_{W_o} \equiv \frac{(\mathrm{LET})_{W_o}}{(\mathrm{LET})_{W_m}} \equiv \frac{\left(\frac{dT}{dx}\right)_{(W < W_o)}}{\left(\frac{dT}{dx}\right)}. \tag{7}$$

In terms of the well-known stopping-power theory, the fractional linear energy transfer is simply the ratio of the stopping number for the "restricted stopping power" to that for the total stopping power; thus, for charged particles heavier than electrons, the fractional linear energy transfer is

$$(\mathrm{FLET})_{W_o} = \frac{B_1}{B} = \frac{1}{2}\left[1 + \frac{\ln (W_o/I)}{\ln(W_m/I) - \beta^2}\right]. \qquad (8)$$

For $\beta^2 << \ln (W_m/I)$, we may rewrite the fractional linear energy transfer:

$$(\mathrm{FLET})_{W_o} \cong \frac{1}{2}\left[1 + \frac{\ln (W_o/I)}{\ln (W_m/I)}\right]. \qquad (9)$$

In Table I, we list values of $\ln (W_m/I)$ for water with a mean excitation potential $I = 65.1$ eV versus the particle velocity β. We note that β^2 is always small compared to $\ln (W_m/I)$; for water, the ratio $\beta^2/\ln (W_m/I)$ is 0.2 percent at $\beta = 0.100$, 2 percent at $\beta = 0.400$, 6.2 percent at $\beta = 0.800$, 7.3 percent at $\beta = 0.900$ and 7.2 percent at $\beta = 0.990$.

The above expressions for the fractional linear energy transfer contain the restricted energy transfer W_o. In order to evaluate the fractional linear energy transfer, it is necessary to specify W_o. First, we note that in the inelastic coulomb scattering collisions of the primary charged particle of velocity v with an atom, the atomic electrons are ejected with a distribution of kinetic energies given by the classial Rutherford formula; thus, the number of delta rays (or ejected electrons) with kinetic energies between T and T + dT produced per unit differential path length of a heavy particle (of charge ze and velocity βc in a material of atomic number ~~Z~~ and ρ_n nuclei per unit volume) is

$$n(T)\,dT = 2\pi r_e^2 mc^2 \rho_n Z \frac{z^2}{\beta^2}\frac{dT}{T^2} = W_s \frac{dT}{T^2}, \qquad (10)$$

where

$$W_s \text{ (Mev/gm-cm}^{-2}) = \frac{2\pi r_e^2 mc^2}{\beta^2} \quad \frac{N_o}{A} Z z^2 = \frac{0.153}{\beta^2} \quad \frac{Z}{A} z^2. \quad (11)$$

Since the derivation of the classical Rutherford formula neglects the binding energy of the atomic electrons, it applies to the ejection of atomic electrons with energies large compared to the ionization potential. Integration of the Rutherford formula, Eq. (10), over the electron kinetic energies gives the total number of δ rays produced per unit path; thus,

$$N(>I) = \int_I^{W_m} n(T)\, dT = \frac{W_s}{I} \left[1 - \frac{I}{W_m}\right]. \quad (12)$$

The lower limit of this integral is the minimum kinetic energy transfer, which is of the order of the mean excitation potential I, since I is a measure of the least energy that can be transferred on the average to a bound electron.

For large energies of the primary particle and for very close collisions, Bhabha (1938) showed quantum-mechanically that the classical Rutherford formula needed an additional term dependent also on the spin σ of the primary particle:

$$n(T)\, dT = W_s \left[1 + f(T, \sigma, \beta, z)\right] \frac{dT}{T^2} \quad (13)$$

For simplicity, we shall restrict our present treatment to primary particle velocities such that $f(T, \sigma, \beta, z) << 1$.

The absorbed dose D is the energy deposited per unit mass Δm of the medium by delta rays produced per unit path of the primary particle; hence,

$$D = \frac{1}{\Delta m} \int_I^{W_m} T\, n(T)\, dT = \frac{1}{\Delta m} \bar{T}\, N(>I), \quad (14)$$

where N(>I), the total number of delta rays produced per unit path of the primary particle, is

$$N(>I) \equiv \int_{I}^{W_m} n(T)\, dT \tag{15}$$

and where $\bar{T}$, the average kinetic energy of a delta-ray, is

$$\bar{T} \equiv \frac{\int_{I}^{W_m} T\, n(T)\, dT}{\int_{I}^{W_m} n(T)\, dT}. \tag{16}$$

If we evaluate the integrals in Eq. (16), we find that

$$\bar{T} = \left(\frac{I\, W_m}{W_m - I}\right) \ln \left(\frac{W_m}{I}\right). \tag{17}$$

Stopping power theory is valid for values of the primary particle velocity β large compared with the velocity of atomic electrons. Stopping power theory begins to breakdown near $\beta = 0.04$. We see from Table I that $W_m/I >> 1$ is a good approximation for $\beta \gtrsim 0.04$. If we set the restricted energy transfer W_o equal to the mean energy transfer $\bar{T}$, we find that the value of W_o is given in good approximation by

$$W_o = \bar{T} = I \ln (W_m/I) = I \ln (2mc^2/I)\, (P/Mc)^2, \tag{18}$$

where the right-hand member follows by substituting Eq. (2) for W_m. In this form, we see that the mean energy transfer depends on the natural logarithm of the momentum P of the primary ionizing particle expressed in units of its rest mass. The possible role of momentum in radiation dosimetry has been discussed by Turner and Hollister (1962), Ivanov (1963), and Turner (1965).

With W_o specified by the mean energy transfer, we find upon substitution of Eq. (18) into Eq. (9) that the fractional linear-energy-transfer is given by

$$(FLET)_{W_o = \bar{T}} = \frac{1}{2} \left[1 + \frac{\ln \ln (W_m/I)}{\ln (W_m/I)}\right]. \tag{19}$$

We find that the $(FLET)_{W_o} = \bar{T}$ has a value which varies only slightly with the velocity of the primary particle from 0.69 for $\beta = 0.040$ to 0.60 for $\beta = 0.990$.

The mean-squared energy transfer is

$$\bar{T}^2 \equiv \frac{\int_I^{W_m} T^2\, n(T)\, dT}{\int_I^{W_m} n(T)\, dT} = W_m I . \tag{20}$$

If we set the restricted energy transfer W_o equal to the root-mean-square (rms) energy transfer T_{rms}, we find that the value of W_o becomes

$$W_o = T_{rms} \equiv (\bar{T}^2)^{1/2} = (W_m I)^{1/2} = (2mc^2 I)^{1/2} (P/Mc), \tag{21}$$

where the right-hand member of Eq. (21) follows from Eq. (2) for W_m. In this form, we see that the root-mean-square energy transfer is proportional to the momentum of the primary ionizing particle expressed in units of its rest mass. From Eq. (21) also, we see that the root-mean-square energy transfer is equal to the geometric mean of the maximum and least energy transfers. Comparison of Eqs. (18) and (21) reveals the following simple relation between the mean and rms energy transfers:

$$\bar{T}/I = 2 \ln (T_{rms}/I). \tag{22}$$

In Table II, we list the maximum, the mean, and the root-mean-square energy transfers to an atomic electron by heavy charged particles versus the particle velocity. We see that the mean energy transfer $\bar{T}$ and the root-mean-square energy transfer T_{rms} are both small in comparison with the maximum energy transfer W_m. Since we have evaluated the restricted stopping power for values of the restricted energy transfer W_o

equal either to $\bar{T}$ or T_{rms}, we have verified that these choices satisfy the condition of the theory of the restricted stopping power that $W_o << W_m$. With W_o specified by the root-mean-square energy transfer, we find upon substitution of Eq. (21) into Eq. (9) that the fractional linear-energy transfer has a value equal to 3/4, independent of the velocity of the primary ionizing particle.

The restricted stopping power of a medium for a charged particle of velocity β is proportional to the total stopping power. The proportionality factor is essentially independent of the velocity of the heavy charged particle if the restricted energy transfer is equal to the rms energy transfer, and it has only a slight dependence on the primary particle velocity if the restricted energy transfer is equal to the mean energy transfer. In these circumstances, the fact that the ratio of the restricted to the total stopping power is insensitive to the velocity of a heavy charged particle means that only a scale factor is involved between these two quantities; hence, a biologial effect that depnds on some function of the total stopping power will have the same functional dependence on the restricted stopping power with energy transfers restricted either to the rms or to the mean energy transfer. Since extensive tabulations of the total stopping power have been compiled by physicists, it is more convenient to relate biological effects to the total stopping power rather than to the restricted stopping power.

Acknowledgements

This paper was stimulated by discussions, particularly with Dr. N. Barr, at the conference on "Accelerator Radiation Dosimetry and Experience" held at Brookhaven National Laboratory in November 1965. The author is grateful to Yan Pong Yu for performing calculations on the IBM-1620 computer at Clarkson College of Technology. This work was supported in part by the Health and Safety Laboratory of the Atomic Energy Commission.

References

Barkas, W. H.

1960: National Academy of Sciences - National Research Council Publication 742, Nuclear Science Series Report Number 29

Bethe, H. A.

1930: Annalen d. Physik 5, 325

1932: Zeits. f. Physik 76, 293

Ivanov, V. I.

1963: Biological Effects of Neutron and Proton Irradiations, Proceedings of the International Atomic Energy Agency Symposium held at Brookhaven National Laboratory, 7-11 October 1963, I, 35.

Turner, J. E.

1962: and H. Hollister, The Possible Role of Momentum in Radiation Dosimetry, Health Physics 8, 523-532 (1962).

1965: The Possible Role of Momentum in Radiation Dosimetry-II. Extension to Charged or Uncharged Particles and Implications, Health Physics 11, 1163-1175 (1965).

TABLE I

The Maximum Energy Transferable to an Atomic Electron by an Incident Heavy Particle, the Ratio and the Natural Logarithm of the Ratio of the Maximum Energy Transfer to the Mean Excitation Potential I (=65.1 ev) for Water versus the Particle Velocity

Particle Velocity $\beta \equiv v/c$	Maximum Energy Transfer to an Atomic Electron W_m (kev)	W_m/I I=65.1 ev	$\ln (W_m/I)$ I = 65.1 ev
.010	0.102	1.57	.45
.020	0.409	6.28	1.84
.040	1.64	25.2	3.23
.050	2.56	39.3	3.67
.080	6.58	62.6	4.62
.090	8.35	101	4.85
.100	10.32	128	5.06
.200	42.58	159	6.48
.400	194.6	654	8.00
.500	340.6	2990	8.56
.800	1817	5233	10.24
.900	4357	27,909	11.11
.990	50335	66.927	13.56

TABLE II

The Maximum, the Mean, and the Root-Mean-Square Energy Transfers to an Atomic Electron by Heavy Charged Particles versus the Particle Velocity

Particle Velocity $\beta = v/c$	Mean Energy Transfer $\bar{T}$ (kev)	Root-Mean-Square Energy Transfer T_{rms} (kev)	Maximum Energy Transfer W_m (kev)
.010	.0809	.0816	0.102
.020	.142	.163	0.409
.040	.219	.326	1.64
.050	.245	.408	2.56
.080	.303	.654	6.58
.090	.318	.736	8.35
.100	.331	.818	10.32
.200	.420	1.65	42.58
.400	.511	3.42	194.6
.500	.540	4.41	340.6
.800	.625	8.97	1817
.900	.671	13.0	4357
.990	.819	40.9	50335

$$W_m = 2mc^2 \beta^2/(1-\beta^2)$$

$$\bar{T} = \frac{I\left[\ln (W_m/I) - \beta^2 (1 - I/W_m)\right]}{\left[1 - (I/W_m) - \beta^2 \ln (W_m/I)\right]} \cong I \ln W_m/I$$

$$T_{rms}^2 = \bar{T}^2 = W_m I \frac{\left[(W_m/I) - 1 - \frac{1}{2}\beta^2\left(\frac{W_m}{I} - \frac{I}{W_m}\right)\right]}{\left[(W_m/I) - 1 - \beta^2 \ln (W_m/I)\right]} \cong W_m I$$

TISSUE, ORGAN, AND ORGANISM EFFECTS

Harvey M. Patt

Laboratory of Radiobiology
University of California Medical Center
San Francisco, California

The disturbance of the organism consequent to irradiation assumes a distinctive time course, which depends upon the dosage and manner of exposure, and upon the temporal relation between the various processes or injury and recovery. There is a series of possible lethal syndromes after whole-body irradiation. With a massive exposure, e.g., 10^5 rads, death occurs within seconds or minutes and is believed to involve effects on the central nervous system. The dose required for immediate killing is sufficient to denature protein and to cause wide-spread injury to membranes. With doses of the order of 10^4 rads, death occurs within several hours to a day, with signs of circulatory collapse. Early circulatory disturbances and death may occur in some species, e.g., rabbit and chicken, after even smaller doses. Renal failure can be an additional factor in the 1-day lethality in birds. Exposures of one or a few thousand rads lead to death in a few days which is associated with wide-spread denudation of intestinal epithelium. With doses of a few hundred rads, lethality occurs some 2 to 3 weeks later and is referable to bone marrow damage. Granulocytopenia and, to a lesser extent, thrombocytopenia are leading factors in this mode of death. The immediate survivors of an acute whole-body exposure do not necessarily escape unscathed; there are subacute and chronic effects which can lead to a shortening of the life span.

Of the several acutely lethal syndromes, those associated with "intestinal death" and "marrow death" are of the greatest interest, since they require only moderate doses of radiation. Lethality in these instances is a direct reflection of what Quastler and I referred to as the aplastic cytopenia syndrome, a term which characterizes the acute radiation responses of cell-renewal systems in general. For the most part, my remarks will be oriented to radiation effects on such systems after a total-body exposure to x rays. The aplastic cytopenia syndromes provide an excellent example of the interplay of cellular and mammalian radiobiology.

The intimate connection between radiation and processes of growth and development was appreciated very early in the history of radiobiology. In 1906, Bergonie and Tribondeau suggested that x ray sensitivity varied directly with the rate of proliferation and the number of future divisions, and inversely with the degree of morphological and functional differentiation. This formulation, although not absolute (there are exceptions), is a useful generalization which can be derived from an association of radiosensitivity with activity pattern.

Although radiation in the proper amount can depress any biological activity, activities in progress are generally less susceptible than the preparations for such activities. This means that a biological system should be most

sensitive at a time preceding the change from one activity pattern to another, since during this period the new activity pattern must be implemented. This rule applies both to the original causation of damage and to the unmasking of a previously caused latent damage, and it applies to a variety of noxious agents including radiation. Viewed in this light, it is not surprising that perturbations of growth and development can be brought about most dramatically by exposure to ionizing radiation. Both proliferation and differentiation involve sharp transitions in patterns of activity. The association of radiosensitivity with reorganization is a useful concept. Although it does not tell us much about specific mechanisms, it brings the problem into sharper focus by telling us where to look further.

Cell production is notoriously susceptible to interference by radiation. The interference may be very brief or quite prolonged. It may result from (a) early necrobiosis, i.e., interphase death or cell killing without regard to the mitotic process itself, (b) blockage of different transitions in the proliferative cell cycle, or (c) asymmetric mitoses, e.g., incomplete or unequal separation of chromosomes at anaphase.

Considerable attention has been given to analysis of radiation effects on the proliferative cell cycle. Indeed, present concepts of the cell cycle are an outgrowth of such studies. The early interest in effects on DNA metabolism led to the development of autoradiographic techniques for study of DNA labeling in individual cells, first with ^{32}P and then with ^{14}C and ^{3}H thymidine. The staging of the cell cycle--i.e., G_1, S, G_2, and M--which was first described by Howard and Pelc, provides a useful framework for analysis of basic parameters of proliferation, chromosomal aberrations, and mitotic abnormalities generally. For example, by marking the periods of chromosome replication, i.e., the S period, it has been possible to analyze the types of aberrations in relation to the position of a cell in its proliferative cycle. Thus, irradiation in G_1 leads to chromosome aberrations; irradiation in S or G_2 leads to chromatid aberrations. It has also been learned that the sensitivity of a cell as measured by its reproductive capacity can differ by a factor of 3 to 4 depending on the stage of the cycle at which it is irradiated. In general, the periods just prior to DNA synthesis (late G_1) and mitosis (G_2) are the most sensitive. With comparatively low radiation doses, cells will not initiate DNA synthesis or mitosis for a time, but cells in synthesis or mitosis will continue at normal rates. This phenomenon is dose-dependent; with large doses, ongoing activities of DNA synthesis and mitosis will also be depressed.

The proliferation rate, i.e., the reciprocal of the cell cycle time, can be an important factor in the development and repair of lesions. There are several reasons for this. Cells may differ in radiosensitivity at different stages of the cell cycle, i.e., G_1, S, G_2, or M. Possible changes in stage distribution depending on whether the cell cycle is long or short could therefore influence the overall sensitivity of the cell population. Variations in cell-cycle times among normal mammalian cells are due largely to variation in the G_1 phase (this may not be so with tumor cells). Thus, the "differential count" of the population in respect to cell cycle stage would shift toward the G_1 when the proliferation rate is low, and G_1 on the whole is a less sensitive stage than, for example, G_2. There is another consideration owing to the fact that some forms of damage are manifest only after the cell resumes mitosis. The

duration of the initial mitotic block is related to the cell cycle time. Mitoses return earlier (and the cell cycle time is shorter) in tissues considered to be more radiosensitive. Recovery of cells may also depend on the proliferation rate.

There are many systems in the body in which cell production and loss are in dynamic equilibrium. Such steady-state populations are easily perturbed by irradiation and, in first approximation, the acute response can be reduced to a simple basic scheme: impaired cell production, with little change in rate of cell decay, leading to cell depletion; the degree of depletion will depend on the degree to which production is impaired. In other words, radiation causes aplastic cytopenia or, if a cell population vanishes completely, acytosis. This should not suggest that radiation, in doses sufficient to interfere with cell production, does not affect other aspects of a cell-renewal system. In some cases, e.g., in the lymphoid system, effects on mature cells are important. Indeed, in analyzing the response of a tissue to a perturbation such as irradiation, the sensitivity of individual cells must be distinguished from that of the system as a whole. In the blood lymphocytes, there is a biphasic time response: rapid depletion during the first day followed by a much slower depletion. The initial rapid phase is due mainly to direct killing of lymphocytes, and the slower subsequent phase to the disturbed lymphopoiesis.

Although effects on individual cells can be significant, in the majority of renewal systems it is the impairment of cell production that is of critical physiologic importance. The evolution of the response that leads first to depletion, and then to restoration, of the mature functional components is related to the normal kinetics of the system. Within this framework, however, there are complexities owing to the general fact that the kinetics of irradiated systems can deviate in a number of ways from normal. The "first approximation model" of aplastic cytopenia is complicated by the fact that radiation-damage proliferative cells may still be capable of some proliferative activity; moreover, such cells can mature. A succession of abortive attempts at proliferation and subsequent maturation can give rise to abnormal mature cells which may deviate from normal kinetics. Since the interplay between depletion and regeneration is crucial for the system as a whole, minor proliferative activity and minor deviations from normal kinetics can decide the fate of the system. The fate of the organism in which the system is located will, of course, be determined by the essentialness of the functional cell whose production has been impaired. The death of an organism is hardly a simple mirror image of the death of its stem cells. When a minimum number of functional cells--e.g., villus cells or blood granulocytes--is needed for survival, what really matters is the number of viable stem cells that remain in relation to the manner in which the developmental pathway between stem cell and functional cell is structured and controlled.

All steady-state populations can be structured into compartments or classes with specific attributes of form, function, or location. The minimum structure resulting from this separation is: proliferation $\longrightarrow$ maturation $\longrightarrow$ function. The proliferation compartment can be subdivided further into self-maintaining elements. In some irradiated systems, the periods of proliferative deficiency and functional deficiency overlap. This happens in the intestinal epithelium and bone marrow. In other systems, e.g., spermatogenic

epithelium, there may be a distinct separation such that the functional deficit occurs some time after repopulation of the proliferating elements has begun. These differences reflect differences in length of the developmental pathway, which is known to increase from intestinal epithelium to bone marrow to testes.

The rate of release of maturing elements from a renewal system is not a simple matter of growth pressure. As a rule, onset of depletion of functional cells after moderate irradiation depends on the time normally required for completion of maturation of the postmitotic cells. A cytokinetic basis of this latency period is clearly shown by the correspondence between the time needed for onset of granulocytopenia and the time required for postmitotic granulocyte maturation in various species. This relationship suggests that there is little, if any, disturbance of the turnover kinetics of the functional, as well as of the maturing, cells during the initial period after irradiation.

The correspondence between depletion rate and normal turnover rate of functional cells may become complex with the passage of time. As the organism reacts to the injury and the system attempts to recover, the kinetics can deviate from normal. For example, in the intestinal epithelium, there is a discrepancy by a factor of two between the time when complete denudation is expected (no production--normal exit) and the time when it actually occurs. This comes about mainly because radiation-damaged proliferative cells are still capable of some proliferative activity and because such cells can mature into normal and abnormal forms.

The depletion of functional cells from a steady-state population is influenced by a number of cytokinetic factors. The relative depletion is increased if the potential for stem cell turnover and recruitment is small. This also occurs if there is normally a long transit time, large number of divisions, or small potential for amplification in the proliferation compartment. The transit time in the maturation compartment enters the kinetic equation only by determining the time for onset of functional cell depletion, i.e., the latency period. On the other hand, the transit time in the functional compartment is an important factor in the relative magnitude of depletion, the latter being increased when the transit time is short.

It is of interest that sensitivity to acute lethal action among the various species seems to be related more to differences in rates of recovery than to differences in the extent of initial injury. This may apply also to the relative response of certain critical systems, e.g., intestinal epithelium and bone marrow, in a given species. The phenomenon of early intracellular recovery is by now well known. However, I am inclined to believe that the differences in recovery to which I have alluded are a reflection mainly of the nature of the system and of the essentialness of the functional cell.

The restitution of a depleted cell population after irradiation poses some important basic questions. A cell renewal system can recover only if a fraction of the progenitor cells have retained their reproductive integrity. Under normal conditions, progenitor or stem cells are induced to differentiate at a certain rate. When the progenitor compartment is reduced in size, there must be a compensatory increase in proliferation rate or a decrease in the rate of

withdrawal of cells by maturation if the system is to recover. The latter is known to occur in some systems and if the dose of radiation has been severe enough, the focus of regeneration may show hyperplastic tendencies suggestive of neoplasia. This hyperplastic phase may be fleeting, as in the intestine, or persist for a considerable time, as in cartilage. In other systems, e.g., bone marrow, the requirement for functional cells may be such that the pressure for differentiation may take precedence for a time over the pressure for stem cell reconstitution. Thus, it is necessary to think in terms of a pull as well as of a push in the maintenance of a steady-state population.

Apropos of recovery, it is instructive to consider briefly some adaptive patterns of response to a second exposure or to a sustained irradiation. Several lines of evidence are indicative of a transient radioresistance in respect of acute lethality and the response of systems such as the intestine and bone marrow after a single irradiation. With continuous irradiation, damage, instead of increasing progressively, appears to reach a steady state, at least for a time. This has been seen with indices such as blood counts, organ weights, renewal of intestinal epithelium, and male fertility. The compensatory response may reflect an increased stem cell turnover or recruitment. An adaptive response is not seen in the ovary, apparently because there are no stem cells from which depleted cells can be replaced.

RECENT STUDIES ON THE GENETIC EFFECTS OF RADIATION IN MICE

W. L. Russell

Biology Division, Oak Ridge National Laboratory
Oak Ridge, Tennessee

The genetic hazards of radiation have been estimated by many individuals and repeatedly by both national and international committees. For example, the United Nations has published three extensive scientific reports on the genetic effects of atomic radiation.[1-3] It therefore seemed sensible to devote the space available here to a discussion of results of recent experiments, with emphasis on current studies in my own laboratory.

My work has been concerned primarily with factors that affect mutation frequency. Significant recent advances have been made in our knowledge of the effect of radiation dose rate, the effect of the interval between irradiation and conception, and the effect of low doses. All of these have a strong bearing on the estimation of the genetic risks of radiation exposure.

In the experiments described here, mutation frequency was scored by our standard specific locus method.[4]

Dose Rate

When the first United Nations report on the biological effects of radiation was prepared, it was generally believed that the radiation induction of point mutations was independent of dose rate. This had been regarded as a basic principle of radiation genetics for several years. Extensive work with Drosophila spermatozoa had shown that the mutation frequency induced by a given total dose of radiation is the same regardless of whether that dose is delivered in a few seconds or spread out over hours, days, or weeks.

Our first experiments on the effect of dose rate in the mouse showed the contrary to be true for spermatogonia and oocytes (the reproductive cell stages important in human hazards).[5] Spreading the dose out gave a marked reduction in mutation frequency. All of our subsequent experiments have supported the results of the original ones.[6] Further confirmation of an effect of dose rate on mutation has come from independent work on mouse spermatogonia by Phillips,[7] from studies on silkworms by Tazima, Kondo, and Sado,[8] and from experiments by Baldwin[9] on the wasp Dahlbominus.

The extensive information on the mouse that has already been published will be reviewed briefly here as a background for the presentation of the new results.

Radiation-induced mutation frequency from x and γ rays in spermatogonia was measured with dose rates ranging from approximately 90 R/min to 0.001 R/min. Mutation frequency at 9 R/min is significantly lower than that at

90 R/min. At 0.8 R/min the mutation frequency is further reduced to between one-third and one-quarter of that at 90 R/min. Reducing the dose rate to 0.009 R/min and even to 0.001 R/min gives no further reduction in mutation frequency.

In oocytes only three dose rates have been tested: 90, 0.8, and 0.009 R/min. The difference between the mutation frequencies at 90 R/min and 0.8 R/min is similar to that observed in spermatogonia, but, unlike spermatogonia, the oocytes show a further reduction in mutation frequency to a very low value when the dose rate is lowered to 0.009 R/min.

There are two new sets of data. One of these, which will be reported in detail elsewhere, came from a repetition of the 0.001-R/min dose-rate experiment on spermatogonia. This is a tedious experiment, the 600-R dose used requiring an exposure time of more than a year, but it was important to obtain as reliable a figure as possible at this low dose rate. The new results are in close agreement with those obtained earlier, and therefore support the conclusion that lowering the dose rate below 0.8 R/min gives no further reduction in mutation frequency in spermatogonia.

The second new set of data is presented in Table 1. The experiment was our first test of the effect of an x-ray dose rate higher than 90 R/min. The observed mean mutation frequency per locus of 9.0×10^{-5} is not significantly different from the frequency of 8.7×10^{-5} (40 mutations in 65 548 offspring) obtained from earlier experiments with the same x-ray dose of 300 R delivered at a dose rate of 90 R/min. Thus, raising the dose rate above 90 R/min appears to give no noticeable increase in mutation frequency in mouse spermatogonia.

Analysis of the cause of the dose-rate effect is important for the clues it may provide to an understanding of the nature of the mutation process and for the application of the mouse results to the estimation of genetic hazards in man. Evidence is mounting in support of the view that the dose-rate effect, or at least a large part of it, is due to repair of mutational or premutational damage.[10] At the higher doses and dose rates the repair process is postulated to be saturated or itself damaged by the radiation. If repair is the mechanism responsible for the dose-rate effect, then the important question arises as to whether complete repair might be possible at very low dose rates, such as those to which man is exposed as a result of peacetime radioactive fallout.

There would, of course, be no possibility for complete repair if some of the mutations were of a qualitatively irreparable type. An interesting piece of information that bears on this problem has come out of the work on mice. In spermatogonia, where the data are extensive enough for comparisons, it is found that the distribution of mutations among the seven loci tested is not affected by dose rate even though the distribution itself is characterized by marked differences between loci.[10] In other words, the relative frequencies of mutations at the seven loci are constant regardless of dose rate. This suggests that the mutations that fail to be repaired at low dose rates are not qualitatively different from those that are repaired. Of course, without further information, it could still be argued that the unrepaired mutations and the repaired ones are qualitatively of different types, but then a further assumption would be required, namely, that the ratio of the two types is the same at all loci. There is,

however, the important additional observation that when the conditions (e.g., cell stage) are changed so that the proportions of qualitatively different types of mutation (e.g., deficiencies versus nondeficiencies) are affected, then the relative frequencies of mutations among the seven loci are also affected. This would seem to support the tentative conclusion reached above that, since change in dose rate does not alter the relative frequencies of mutations among the loci, the unrepaired mutations occurring at low dose rates may be qualitatively like the repaired ones, i.e., originally capable of repair.

If this conclusion is correct, then the way is theoretically open for the occurrence of complete repair at very low dose rates. There is nothing in the experimental results on oocytes that argues against this possibility. The mutation frequency drops progressively with reduction in dose rate, and at the lowest dose rate tested (0.009 R/min) the mutation frequency, even with moderately large total doses, is not significantly higher than the spontaneous rate in males. (The spontaneous rate in females has not yet been accurately determined.) In spermatogonia, on the other hand, the mutation frequency is still appreciable at 0.8 R/min, and it is not reduced by further lowering of the dose rate as far as 0.001 R/min. Why is this so if all mutations are potentially reparable? One can, of course, imagine several possible mechanisms that would account for an irreducible minimum mutation frequency. To give just one example, one could invoke the evidence obtained by Kimball[11] in Paramecium that mutational damage is fixed when DNA replication occurs and that the probability of mutational damage not being repaired is large when the time interval between irradiation and DNA replication is short. Thus it could be postulated that in the dividing spermatogonial population there may always be some cells so close to DNA replication that if mutational damage occurs there may not be enough time for repair.

In summary, it can be stated that, so far as hazards are concerned, application of the experimental results for spermatogonia seems to be uncomplicated. The data at the very low dose rate of 0.001 R/min have been augmented and still show no reduction in mutation frequency compared with that at 0.8 R/min. Furthermore, since plausible hypotheses can be advanced to account for such a result in spermatogonia, there is no reason for not believing that the minimum mutation frequency has been reached in spermatogonia with the dose rates already tested. The realistic conclusion suggested by the data is that, although mutation frequency may be very low in females exposed to low dose rates, in males there is evidence against a threshold dose rate, and the irreducible minimum mutation frequency occurring even at lowest dose rates is an appreciable one, namely, between one-third and one-quarter of the maximum frequency obtained at high dose rates.

Effect of the Interval Between Irradiation and Conception

Extensive data on spermatogonia show no significant change in mutation frequency with time after irradiation. In contrast, recently published results on female mice exposed to fission neutrons show that the interval between irradiation and conception has a tremendous effect on mutation frequency.[12] Conceptions in the first seven weeks after irradiation with approximately 63 rads yielded 59 specific locus mutations in 89 301 offspring. After that, no mutations were found in a total of 120 483 offspring.

It was obviously important to find out whether the result was a peculiarity of neutron irradiation or a general radiation effect. Experiments with x rays were accordingly started, despite the handicap of having to work with a dose no higher than 50 R. With higher doses the females become sterile too soon after irradiation. This difficulty was greatly reduced in the neutron work because the relative biological effectiveness for mutation induction was much higher than that for effects on fertility. An additional handicap was discovered during the x-ray experiment which was, however, of great importance in itself. This was the finding that the mutation frequency in the early mating period was lower than expected from the frequencies at higher doses on the assumption of a straight-line relation between mutation frequency and dose. This will be discussed in the next section.

The extensive data collected to overcome these difficulties are presented in Table 2. They have finally reached the point where the mutation frequency in the later period is significantly below that in the early period ($P = 0.028$). Thus, the phenomenon appears to be general, and therefore of much greater importance than if it had been solely a neutron effect.

The cause of the effect presumably lies in the nature of the oocyte follicle stages involved. The early period is long enough for the conception of two litters. The low mutation frequency in the later period must have come from oocytes that were in less mature follicle stages at the time of irradiation. It is not yet known whether the marked difference in mutation frequencies is due to a low mutational sensitivity of oocytes in early follicle stages, to an efficient repair mechanism in these stages, or to cell selection.

Whatever the cause, it is extremely effective. It was pointed out[12] that in the neutron data even the upper 99% confidence limit of the zero mutation frequency in the later period is lower than the spontaneous rate in male mice. Almost half as many offspring in this period have now been added by the x-ray experiment, and still no mutations have been observed.

Application of this result to the estimation of genetic effects in women should be made with great caution until more is known about the comparability of the oocyte stages involved in the two species. Some information might be obtained by analyzing the genetic data from human radiation exposures in terms of the time interval between irradiation and conception.

Small Doses

In describing the new x-ray experiment on females, brief mention was made of the fact that, in the early mating period, the mutation frequency induced by 50 R of 90-R/min x rays was lower than expected on the basis of results at higher doses. This finding has already been reported at an earlier stage in the experiment.[13] The pooled data from several experiments on females exposed to a single dose of 400 R of 90-R/min x rays gave 23 specific locus mutations in 14 842 offspring from conceptions occurring in the first 7 weeks after irradiation. On the assumption of a straight-line relation between mutation frequency and dose, approximately 25 mutations would have been expected in the 127 391 offspring now recorded in the early mating period in the 50-R

experiment. Only 10 were actually observed. This is significantly lower than the expected number (P = 0.011). Since the offspring in the 400-R experiments came mostly from conceptions occurring within the first 3 weeks after irradiation, a more rigorous comparison can be made by restricting both sets of data to this period. In the 400-R experiments there were 21 mutations in the 14 591 offspring conceived in this period. In the same period in the 50-R experiment there were 4 mutations in 67 391 offspring. Although this reduces the numbers for comparison, the difference from the frequency expected on the basis of the 400-R results is still significant (P = 0.022).

This finding was not entirely unexpected. In the first publication in which a repair mechanism was suggested as a possible cause for the dose-rate effect on mutation, it was postulated[5] that repair might occur with small doses of acute irradiation as well as with irradiation at low dose rates. A hypothetical curve was drawn to illustrate this.[5] However, no attempt was made to speculate on the dose level below which repair would be noticeably effective. The new results indicate a substantial effect at 50 R in females.

This finding is obviously of great importance in the estimation of genetic hazards, and an attempt has been made to check it in an experiment designed to avoid the vast numbers of animals required to establish a reliable mutation frequency with a dose as low as 50 R. In this new experiment a total dose of 400 R of 90-R/min x irradiation was given to female mice in eight fractions of 50 R spaced 75 minutes apart. The rationale was that, since females exposed to a continuous dose of 400 R of 0.8-R/min irradiation give a reduced mutation frequency compared to that from 90-R/min irradiation, perhaps 50-R fractions of 90-R/min irradiation distributed over the same total time of exposure as that required in the 0.8-R/min irradiation might also give a low mutation frequency.

The results obtained for conceptions occurring within the first 3 weeks after irradiation are shown in Table 3. The data were restricted to the 3-week interval for comparison with the data from single 400-R exposures which were similarly restricted. The observed number of mutations, 13, is significantly (P = 0.005) below the approximately 34 that would have been expected on the basis of the frequency obtained from single 400-R exposures (21 mutations in 14 591 offspring).

Thus the fractionation experiment confirms the finding from the 50-R single-dose experiment that small doses of high-dose-rate irradiation give fewer mutations than would be expected on the basis of a straight-line relation with the mutation frequency from large doses at the same dose rate.

In estimating human genetic hazards it would now appear that the risk from small doses of acute irradiation may, in females at least, be lower than had been estimated on the basis of large doses.

Table 1. Mutation frequency in mouse spermatogonia exposed to a dose of 300 R of 1000-R/min x irradiation.

Number of offspring	Number of mutations at 7 loci	Mean number of mutations per locus
38 207	24	9.0×10^{-5}

Table 2. Mutation frequency in female mice exposed to a dose of 50 R of 90-R/min x irradiation.

Interval between irradiation and conception	Number of offspring	Number of mutations at 7 loci
Up to 7 weeks	127 391	10
More than 7 weeks	54 621	0

Table 3. Mutation frequency in conceptions occurring in the first 3 weeks after irradiation of female mice with 90-R/min x rays.

Total dose	Fractionation	Number of offspring	Number of mutations at 7 loci
400 R	8×50 R at 75-min intervals	23 387	13

References

1. United Nations Scientific Committee on the Effects of Atomic Radiation. Report to the General Assembly. Official Records: Thirteenth Session, Supplement No. 17 (A/3838), United Nations, New York, 1958.

2. United Nations Scientific Committee on the Effects of Atomic Radiation. Report to the General Assembly. Official Records: Seventeenth Session, Supplement No. 16 (A/5216), United Nations, New York, 1962.

3. Report of the United Nations Scientific Committee on the Effects of Atomic Radiation. General Assembly. Official Records: Twenty-first Session, Supplement No. 14 (A/6314), United Nations, New York, 1966.

4. W. L. Russell, X-Ray-Induced Mutations in Mice, Cold Spring Harbor Symposium on Quantative Biology, 16: 327 (1951).

5. W. L. Russell, L. B. Russell, and E. M. Kelly, Radiation Dose Rate and Mutation Frequency, Science, 128: 1546 (1958).

6. W. L. Russell, The Effect of Radiation Dose Rate and Fractionation on Mutation in Mice, in Repair from Genetic Radiation Damage, Ed. Sobels, pp. 205-217, 231-235, Pergamon Press, Oxford, 1963.

7. R. J. S. Phillips, A Comparison of Mutation Induced by Acute x and Chronic Gamma Irradiation in Mice, Brit. J. Radiology, 34: 261 (1961).

8. Y. Tazima, S. Kondo, and T. Sado, Two Types of Dose-Rate Dependence of Radiation-Induced Mutation Rates in Spermatogonia and Oogonia of the Silkworm, Genetics, 46: 1335 (1961).

9. W. F. Baldwin, Visible Mutation Frequencies in Dahlbominus Oogonia Produced by Acute x Rays and Chronic γ Radiation, Mutation Res., 2: 55 (1965).

10. W. L. Russell, The Nature of the Dose-Rate Effect of Radiation on Mutation in Mice (Conference on Mechanisms of the Dose Rate Effect at the Genetic and Cellular Levels, Oiso, Japan, November 1964), Suppl., Jap. J. Genetics, 40: 128 (1965).

11. R. F. Kimball, The Relation of Repair to Differential Radiosensitivity in the Production of Mutations in Paramecium, Repair from Genetic Radiation Damage, Ed. Sobels, pp. 167-178, Pergamon Press, Oxford, 1963.

12. W. L. Russell, Effect of the Interval Between Irradiation and Conception on Mutation Frequency in Female Mice, Proc. Natl. Acad. Sci. U. S., 54: 1552 (1965).

13. W. L. Russell and Elizabeth M. Kelly, Mutation Frequency in Female Mice Exposed to Small x-Ray Dose at High Dose Rate, Genetics, 52: 471 (1965).

DATA FROM VARIOUS OCCUPATIONAL GROUPS

Howard Parker

Lawrence Radiation Laboratory
University of California
Berkeley, California

Despite the word "data" in its title, I must warn that my talk will be a hard one for you to draw definite conclusions from. It will be particularly difficult for me to approach the subject systematically, since I do not want to repeat descriptions of a number of radiation accident cases that have already been covered in excellent fashion by talks earlier in the week. However, I will be content if I can leave you with certain general impressions. I want to describe the radiation protection problems, particularly with accelerators, as they are seen by an occupational physician for Lawrence Radiation Laboratory in Berkeley, one of the AEC prime contractors.

From the cases that I see and know about, I have the impression that the larger accelerators must, with present safeguards, be very safe machines. We know that the principal population risk throughout the world from external radiation results from the use of x-ray machines. We also know that the bulk of low-level radiation exposure of an occupational sort is due to industrial radiography and occupational exposures to medical x rays.

From histories that I have heard, it seems evident that in the early days of the modern accelerators there was some tendency to line such machines up by eye, and in other ways to disregard the risks, in contrast to our present practice. In a number of the important accelerator accidents it appears that the victim had some good, though not sufficient, reason to think that the machine was off at the time the accidental exposure took place. The complicated nature of the larger machines, and the long distances that there sometimes are between the operator and the point of delivery of the radiation, have contributed to the confused circumstances that have caused some of the accidents.

As was pointed out by Dr. Lushbaugh in his talk, there are some 75 accident cases that we can study, collected from USAEC and other sources in this country during approximately the last 20 years. From them we can learn profitable lessons about radiation accidents. It should be noted that relatively few of these cases are the result of accelerator-produced radiation.

One knows, of course, that there are from time to time some lesser episodes of radiation exposure from which the physician and health physicist might be able to learn, and I think it was on that basis that Dr. Wallace asked me to informally present to you our experience and impressions.

I am going to try to put the radiation accidents and other data that can be obtained from occupational groups in perspective against the broader viewpoint

of occupational health in general at Lawrence Radiation Laboratory. What risks does one actually accept in coming to work at LRL here in Berkeley? To dramatize rather than exhaustively cover this point, I am going to read to you some of the "serious injuries" that occurred from October through December, 1966, as listed in the Laboratory Safety News:

"A machine operator received a contusion to his finger when a co-worker started a machine while the injured had his hands in it.... A custodian received a contusion and a fracture of his finger when a windblown door shut on his finger.... A biochemist fractured her arm when she slipped in a corridor.... A laborer cut his finger seriously on the rough edges of a tamper.... A laborer developed a painful left upper arm after using a jackhammer and dragging a hose.... An electrician received a laceration of his forearm when he fell and struck his arm on a step.... An electrician severely lacerated his finger while trying to keep a manhole cover from falling.... An electrician received a painful left knee, preventing him from walking, after crawling inside the magnet platform in the Bevatron.... A machinist struck a chip with his finger and received a severe laceration.... A machinist struck and lacerated his right hand on a tool bit.... An assembly machinist sustained a serious laceration to his right hand when he bumped it against a tool bit.... A machinist sliced his finger on a brass bar."

Well, I read to you about half of the items in this particular issue of the Safety News. It seems quite typical of our experience with accelerators that the only item concerning one of them in this 3-month period was the one about the electrician who injured himself crawling inside the magnet platform of the Bevatron. This, of course, did not involve radiation, but on a week-to-week, month-to-month basis you must realize that we do not see medical problems related to radiation from the accelerators.

Let me list briefly some statistics on visits to our department: There were 14 100 visits to the Medical Facility in Fiscal year 1966. Of these, 8 011 were for first aid. Of them 831 were industrial first visits and 806 were re-visits, totalling 1 637 visits related to occupational illness or injury out of the slightly more than 8 000 first aid visits. During this same time 2 319 visits were for routine physical examination. I want to emphasize that in this particular period none of the visits listed was for a radiation exposure or radiation injury of significance.

In order to show our experience over a longer time span, and from another point of view, I would like to now summarize the accident history of LRL - Berkeley as it appears to the University's insurance carrier for industrial accidents and illnesses. During this same fiscal year, 1966, the insurer dealt with 80 cases.

Thirty-seven of them were so-called lost-time injuries, and 13 have necessitated temporary disability payments. There were approximately $7 900 in temporary disability payments during the fiscal year. And, actually, three of these are cases held over from previous years, as it is necessary to do in this insurance work and three of them account for $4 790 of the total. These cases consist of two back injuries, one in lifting and one from a fall, and one injury of a hip from a fall suffered by a clerical worker. The remaining $3 100 was spread among 13 cases. Based on that experience, the insurer can at this time project his probable cost for medical care, hospitalization, payments on

permanent and temporary disability, and the various administrative costs. It will all add up to between $10 000 and $45 000 in that particular fiscal year. The advance premium paid by the Laboratory was approximately $58 000 during that fiscal year, and eventually a fraction of it will be refunded.

I have reviewed some of these figures to sketch for you the nature of occupational health in an organization like ours. There are other statistics that might be helpful, but these have caught my eye in recent months. The big point is that none of these costs has to do with radiation injuries or exposure to beryllium, an associated problem.

Now let us look for a moment at total LRL experience from 1940 to date, 27 years. Here I am moving from Berkeley LRL experience to that of LRL as a whole, in Berkeley and Livermore, and I will be discussing only the radiation cases. The insurer reports he has had to deal with some 20 cases. Six of them involved litigation, and all six were closed on the basis of no proof. They were radiation injury claims made by various people against the University. There were 14 cases that were not litigated, and the insurer accepted liability for radiation injury in 13 of them during these 27 years. Seven of them were at Livermore, and six here in Berkeley. We have about 3 500 people working here in Berkeley currently, and Livermore has about 5 500 employees. Both laboratories have, of course, grown very much in those 27 years. I haven't tried to base this presentation on total man-years for you, but those are our present employee population figures, and they have been fairly stable at that level for the last few years. So, as I mentioned, the insurer accepted some liability in 13 of these cases of radiation accident. I looked through them to see if they had anything to do with accelerators, your particular interest, and I was able to find five that do. There was one case of an exposure to what is estimated to be 41 rem in an accelerator at Livermore. You can find that case in the AEC Summary of Operational Accidents in 1964. There was a case here in Berkeley of a man exposed to about 5 rem of moderately energetic β radiations to one of his eyes from an accelerator. He has no observable injury, but is listed by the insurer because it is necessary to pay for examination by an ophthalmologist from time to time. There was one case of radiation cataract in Livermore, which I unfortunately cannot tell you more about at this time. There was an x-ray burn of the hand that has taken place fairly recently at Livermore. The fifth case is a case of leukemia in a researcher who worked here for many years in Berkeley, and who had substantial exposure to both accelerator-produced radiation with the 60-inch cyclotron, various radioisotopes, and x rays. In this case a death benefit was paid by the insurer. That, briefly, summarizes the kind of experience LRL has had.

Many of you are familiar with the summaries that the Division of Operational Safety of the USAEC prepares from time to time about their operational accidents, including radiation exposure. There is much to be learned from their experience because of the greater number of man-years accumulated in it, and I am going to briefly present here today some pertinent material from their 1965 report.[1] The report covers 22 years of experience and lists a number of things deserving of study that I can only briefly touch on here. First they point out that the death rate of the AEC and its contractor personnel, as compared with the United States in general, runs about one-half to one-third during these years.

They list the causes of fatalities in AEC programs and, of course, they list separately the construction workers, those in plant and in laboratory operations or in direct governmental activities. In the construction area, of the 251 deaths during these 23 years, 71 are due to falls or falling objects, 38 to motor vehicles, and 20 electric shock. Actually the distribution of causes in plant and laboratory operation is rather similar to the construction figures. In all categories only three radiation deaths are listed. (Perhaps one should add in the other three people from the SL1 accident, who were irradiated, but who are listed under death due to explosion.) The publication lists approximately 15 800 lost-time injuries in this 22-year period. Thirty-six radiation injuries are listed. So 1/2 of 1% of the injuries in the AEC experience are due to radiation. It also lists such things as time lost from radiation injuries, also a very tiny amount of the total. It lists some interesting things about property damage which underline some of the points I am making here today. For example, if you look at fire loss you see that these losses are quite substantial in comparison with any loss due to radiation accident. If you then look at the radiation accidents listed, to see which have to do with accelerators, you find very little useful information. They are primarily criticality accidents. In one section of the publication there is a list of 24 known criticality accidents.

Then they list all their fatalities, as well as the radiation exposures over 15 rems. There is also a small chart here of radiation exposure broken down according to the size of the rem dose recorded on the personnel film badge. When you are thinking about long-term effects of radiation, you might be more interested in that than in the accident statistics. From 0 to 1 rem they list a total of 922 000 exposures, from 1 to 5 rem only 50 000, and then from 5 to 10 rem, 13 000; from 10 to 15 rem it is 110 cases, and above 15 rem, 42 such situations are listed. This material is well-known now, but I think it helps to review it for you in this context.

People often say "here you have this long experience in a laboratory like LRL and surely there must be some statistics on leukemia incidence that have come from it; something of that kind would be useful information for all of us." Well, it appears there are not actually enough people working for the entire AEC and its contractors during these 22 years to give a really adequate picture of leukemia incidence or help to elucidate the problem of radiation-induced leukemia. Dr. Mancuso has begun a pilot study for the Atomic Energy Commission to study the morbidity and mortality experience of AEC contractor personnel. I personally think this will be largely nonproductive scientifically, and there are many people who agree. However, it may nonetheless be of considerable value to be able to say from such data, for example, that, with a high degree of probability, the leukemia incidence in the AEC and its contractors was not tripled. The statistical information that you can gather from examination of your employees does not so far seem to be very helpful in comparison with the other epidemiological and experimental studies we've talked about earlier this week.

George Barr, who is working with us now, has done some thesis work, looking at about 100 people who have the highest radiation exposures in this Laboratory (incidentally, a sizable fraction of those are people who worked with the 60-inch cyclotron or radiation generators of that kind, who have actually worked fairly close to permissible levels for some years.) He is not able to

show a definite decline due to radiation (that is, correlated with dosimetric information) in such things as total white blood count or total lymphocytes. There is some kind of a decline in these figures, but the radiation effect and the age effect and probably some other things are mixed, so it is almost impossible to make any determination of the effect of radiation. He does feel that he may have turned up a definite age effect in studying the population in a vertical way through the years. That is, an age effect on such things as total white blood count--they slowly decrease. This effect is very slight. Indeed, it may be a time effect related to something about the Laboratory's program rather than aging of the employees.

It appears that when karyotype analysis can be done widely on radiation workers, it will be a very sensitive test, and perhaps helpful in making radiation protection decisions; this is not yet the case, however. Since Dr. Norman will be talking to you on that subject, I will certainly not try to go further into its implications now.

Well then, from the point of view of long-term results, what kind of information does presently come from occupational exposure? From a historical point of view the original information did come from occupational exposure. The broad base of our experience in those early years was occupational exposure and the dangers were very clear. Books have been written about the so-called "martyrs to science through the Roentgen rays." The tendency to repeat all this with accelerators seems to have so far been minimal, so the idea of being a martyr to science in this way seems to have gone out of style in the late 30's and 40's and is fine testimony to increasing awareness during those years of what constitutes adequate occupational health practice. There is, of course, information from radium dial painters which is helpful when dealing with permissible levels of radioactivity. Most of you are probably familiar with the story. These data are still being improved and refined. There is some information from miners, but if you look through the UNSCEAR reports you see that quantitative information from miners is very sparse. It seems to be enough to be able to say that it is probably the radon and its daughters that are the principal troublemakers, and not the various other things that can happen to you in the mines. It is very hard to get quantitative data about lung cancer from this type of exposure.

One type of occupational exposure that is still providing interesting information is that described in the studies on leukemia incidence and life span of radiologists in the United States. There is a definite increase in leukemia incidence and a definite shortening of life span of radiologists. This has not been confirmed in British radiologists, a difference which may be real. In the Archives of Environmental Health, October, 1966, Dr. Shields Warren summarizes his recent studies on the radiologists.[2] The thing that is especially interesting now is that the life-span-shortening effect on U. S. radiologists seems to be disappearing.

When he plots the average age at death in 5-year periods from 1930 through 1965, it can be seen that although the average age at death of the U. S. male population is rising slightly during this period, the age at death of radiologists is lower but increasing more steeply, and is indistinguishable from the

rest of the population in the final 5-year period. This appears to lend weight to the earlier conclusion that radiologists did die younger, and suggests in addition that they are probably no longer doing so.

Bibliography

1. United States Atomic Energy Commission, Division of Operational Safety: Operational Accidents and Radiation Exposure Experience, April, 1965, U. S. Government Printing Office, Washington, D. C.

2. S. Warren and O. M. Lombard, New Data on the Effects of Ionizing Radiation on Radiologists, Arch. Environ. Health, 13; 415 (1966).

III. 3

SOME BIOLOGICAL END POINTS OF DOSIMETRIC VALUE DERIVED FROM CLINICAL DATA

C. C. Lushbaugh, M. D.

Medical Division
Oak Ridge Institute of Nuclear Studies, Inc.
Oak Ridge, Tennessee

Since the discovery of radioactivity late in the 19th Century, man has become increasingly aware of the potential for this type of energy to cause biologic damage. This aspect of ionizing radiation was not anticipated at first. One year after the discovery of x rays, reports of their harmful effects began to appear in medical journals. Becquerel and Pierre Curie produced radiation dermatitis and ulcers on themselves in one of the first experiments with radiation in man in 1901.[1] Gastrointestinal distress (now called the prodromal response) occurred first in an x-ray technician in 1898, and Walsh reported[2] that the man unwittingly cured himself by wearing a lead apron while another man who at the same time had headaches while working alongside a Crookes tube was unable to prevent them by using a block of wood as a shield! Radiobiology has come a long way since then and we have explanations for some of these historical clinical events, but most are still not completely understood and some not at all.

Nonetheless, the vast amount of clinical data that has been accumulated in the last 70 years is rife with information that defines the radiosensitivity of man in practical terms mutually understandably by physician and physicist. These observations are used by the one group to avoid irreparable damage to the whole patient receiving radiotherapy for cancer, and by the other to avoid acute or chronic occupational exposures that could lead to premature death by acceleration of aging and other degenerative processes.

This large clinical experience has been used extensively to provide a firm basis for our occupational radiation health program that has proven so remarkably successful since exploitation of atomic forces was begun. It has also been useful in retrospect in interpreting biologic damage in atomic disasters--intentional, accidental, or incidental. In our time this biologic dosimetric information has been put to the test in about 14 accidents, involving more than 50 individuals. Few recent observations have changed the radiobiological concepts founded on past clinical observations, although many have helped establish more precise dose-response relations than have previously been known to man. All of the studies show that, without doubt, all mammals including man react in a similar fashion to radiation exposure, differing apparently only in relation to amount of exposure.[3]

Unfortunately, accidents by definition are not designed, but occur in spite of the best precautions. Since they occur only when they are not anticipated, they usually occur when the film badge is in the victim's locker, the gamma alarms and interlocks are not working, or the victims have ignored warning signs. As a result dosimetry immediately after an accident is either nonexistent or so poor that no physician can base his plan of therapy upon it.[4] Instead, his treatment of the victim is reactive to the sequence and progress of anatomical and physiological events and in this sense these events have become "biological dosimeters."

Most biologic radiation effects at the morphologic or anatomical level can be used as dosimetric end points, because most of them require direct exposure and few result from the exposure of some other organ. The outstanding exceptions to this statement are, of course, (a) the changes in numbers of circulating blood cells, since these reflect total (or average) lymphocytic and bone marrow damage, and the consequences of radiation-induced failure to replenish the constant loss of blood cells; (b) the symptoms and signs of the gastrointestinal prodromal responses that appear to reflect irradiation of a diffusely distributed autonomic nervous system, and (c) radiation death, which we all know reflects many different lesions that are determined by whether the whole body or a particular part of the body was exposed, by the radiation dose given, and by the rate or number of fractions of the total exposure. So, what do I mean when I say that biologic responses can be used as dosimeters? I mean even considering all these variables, complicated as they are by unpredictable variations in the radiosensitivity of individuals, a physician can make a meaningful, accurate dose analysis from the course of clinically observable events and the changes that occur in radiation-exposed tissues.

Historically, this ability to appraise dose was found true first for the skin and its component parts. The production of erythema was so constant a postirradiation event that in the absence of physical dosimetry and of any international agreement on the definition of a physical unit the radiologist coined his own unit--the S. E. D. or skin erythema dose. It is now well known that the slow appearance of erythema within 4 weeks after exposure to a single radiation dose indicates that 400 to 750 rads was deposited in the skin. In half the cases the dose will have been less than 575 rads. Most radiologists consider an S. E. D. $\approx$ 600 rads. A more rapid appearance of erythema followed by blisters, moist desquamation, and ulceration follows doses between 1600 and 2000 rads. In half the patients, skin exposed to 2000 rads or less will heal in 4 to 6 weeks with only moist dressings for treatment--defining the so-called skin tolerance dose for man ($TD_{50} \approx$ 2000 rads). This effect is dependent on the area of skin irradiated only if the area is less than 400 cm^2. It is also dependent on the energy and quality

of the radiation and upon the dose rate and number of fractions in which the dose is given. The knowledge that man can repair radiation damage was also learned first from studying the skin responses clinically after fractionated exposures. Strandquist showed in a now classical study[5] that the size of the skin-tolerated dose was increased as a power of the number of daily dosage fractions administered, according to the formula

$$TD_{50} = 2000\ t^{0.32}\ \text{(days)}.$$

The hands of a technician who handled filters contaminated by an unknown amount of fission products are shown in Fig. 1. This appearance of blisters, within a week after erythema that occurred almost immediately after about 2 hours of exposure, was followed by ulceration that required years of plastic surgery for repair. The dose here is unknown, but was obviously much greater than the TD_{50} of 2000 rads, and is estimated to have been between 20 000 and 30 000 rads. Figure 2 shows the right hand of a man who was manipulating a part of a fissionable assembly when it reached criticality. The ulcerated blisters, edema, and lifeless appearance is now known to reflect a dose far in excess of 50 000 rads. I hope Dr. Sagan will tell us later about a similar lesion that occurred recently in a man who made the mistake of adjusting a target while it was being exposed to accelerated particles. The two most recent victims of fatal reactor accidents, who received whole-body average doses in excess of 4400 and 8800 rads respectively, each showed intense erythema within 15 minutes of exposure.[6] They both also had intensely scarlet-appearing conjunctivae "welder's eyeballs" a sign of radiation exposure of the eyes after exposures equivalent to or greater than 10 000 R.

Among the oddities of medical practice that I am afraid are still being practiced is the exposure of the scalps of children suffering from "ringworm" to 300 R of 80- to 100-kVp x rays. Because the fungus grows in the hair follicle and because 300 R stops skin mitosis, hair growth stops and epilation then occurs. The disease is cured (providing the child's hat is also destroyed and reinfection is not allowed). So, temporary loss of hair is another biologic dosimeter that says the dose in the skin at the level of the hair follicle was about 300 rads. The permanence of the baldness is a direct measure of an excessive epilating dose and an embarrassment to the radiotherapist or dermatologist.

Permanent baldness cannot always be avoided when a deep-seated tumor is treated. Before leaving the skin as a radiation dosimeter, I would like to mention that an atrophic skin lesion thought to be due to radiation damage can be considered as such only if the small smooth-muscle bundles that erect the hair during fright have been spared. These microscopic muscles, like the muscle in our hearts and extremities, are resistant to

radiation doses even in excess of 20 000 rads. If surgical biopsy fails to demonstrate their selective survival, ionizing radiation was not involved in producing the dermal lesion.[7]

Let us go on now to the prodromal responses as dosage indicators. By prodromal we mean medically a prognostically useful group of symptoms that protends the severity of things to come. In human radiobiology today, "prodromal response" is used instead of the old term "radiation sickness" because this term has been used loosely to mean almost anything that happens after radiation exposure and no longer has the original meaning of the German "Strahlenkater" which means, as far as I can determine, "radiation hangover." Who would not define a "hangover" as a combination of anorexia, nausea, vomiting, diarrhea, and fatigue? This combination of symptoms and signs also defines the human prodromal response to clinically significant amounts of radiation exposure.

Because the threat of radiation exposure in space also carries with it the threat of the occurrence of the prodromal response in a weightless, artificial environment where aspirated vomitus could be fatal, an attempt has been made recently to establish as precisely as possible the population distribution for the probability for this type of response to increment radiation dosages.[8]

To establish this biologic response as a predictable human radiation dosimetry system, we have had more than 35 collaborators who have contributed more than 1600 case studies where total-body irradiation was used as a means of treating disseminated malignant diseases.[9] By studying the clinical charts of 800 patients who have received single total-body exposures, we have found dose-response relations for the various symptoms of the prodromal response.

In the paper that follows, concerning an important segment of these patients, the differences between total-and partial-body irradiation will be emphasized. In the study reported here, only total-body irradiation of patients treated for widely desseminated malignant disease is considered.

Figure 3 shows that with radiation exposures in excess of 300 R, the average time to emesis is about 144 minutes. In this distribution of response the highest doses caused the earliest responses. In more recent studies we have found that total-body irradiation with exposures of less than 300 R have a remarkably constant 120-minute latent period, and that if vomiting occurs it is most likely to occur within an 8-hour period after exposure. Vomiting in less than 2 hours indicates an exposure in excess of 300 R, or a midline dose greater than 200 rads. Figure 4 shows that

the incidence of emesis in a previous study of 163 patients exposed to various amounts of radiation (expressed as the average dose in the upper abdominal compartment) indicated that the effective dose (ED_{50}) for this symptom was close to 200 rads.[9] The other line lying within the 95 percent fiducial limits of the slope variance of these data is the probit regression line for the incidence of vomiting in respect to dose for normal men accidentally exposed to total-body irradiation in nuclear accidents. The ED_{50} is about the same. The increased slope of their dose-response line implies a decreased variance in responsiveness, as would be interested in healthy men.

So far we have determined the single dose-response relationships for five prodromal responses as shown in the table.

In addition, we have attempted to test the hypothesis first stated by Warren in 1948,[10] after study of the Hiroshima and Nagasaki experiences, that the lethal radiation dose (LD_{50}) for man is approximately 450 R (300 rads). Obviously to use these clinical data in this way it must be remembered that all of these patients had a large, unknown probability because of their diseases that they might die unexpectedly and soon in spite of therapy. The statement that a dose-response relationship for human radiation death has been developed from these data requires, therefore, that the investigators have a firmly entrenched faith in the magic of statistics. If, however, deaths between 10 and 60 days after radiation exposure are assumed to be both "naturally" and radiation-induced, then the results can be used to test whether Warren's lethal dose estimate of 450 R (300 rads) for normal man is too low. The results shown in the table and Fig. 5 indicate that his estimate is remarkably close to that made by probit analysis of the patient's data here in which a significant but unknown incidence of non-radiologic deaths occurred. Even though nonrealistic for healthy man, these data define the most sensitive or worst situation for man and make him appear more radiosensitive than he really is. Such a death probability line could, however, be used as the upper probability bound for clinically serious hematopoietic damage. The lowest bound in this hematopoietic death syndrome would be the dose-response probability for loss of appetite (anorexia), the most innocuous symptom of the prodromal symptom complex. The resulting dose-response probability "envelope" is shown along with confidence limits in Fig. 6.

As with the skin, dose protraction of fractionation will increase the total dose necessary to produce these end points and will displace the entire dose-response "envelope", as in Fig. 7. A decrease in its slope would indicate that greater increments in fractionated doses than of instantaneous single doses would be required to obtain the same proportion of responses

in the populace. A study of fractionated total-body doses of about 700 patients, exposed over about 30 years of radiologic practice, led Drs. Focht, Nickson, and Langham[11] to conclude recently that dose fractionation permits radiation repair, and requires total dose for lethal effect to be increased as a power function just as in the case of necrotizing skin dose. This relationship is shown in Fig. 8. Only the experience of one normal man affords us an approximate confirmation of this model: a Mexican man who inadvertently was exposed about 8 hours each day for 116 days in the now famous Mexican cobalt-60 accident and survived exposure to about 1000 rads (minimal estimate).[12] His fit to the LD_{50} curve, where his survival chances at the time his exposures were stopped were less than 50:50, may be fortuitous, but his hospital course was that of a severe aplastic anemia. From all of this and from what you heard yesterday from Dr. Bond concerning the radiation death syndromes, the time of death of an irradiated normal person is also a measure of his dose. This temporal relation for the various syndromes has not been developed so well for man as for other animals, but is loosely accepted as shown in Fig. 9.

Doses up to 600 rads cause death if untreated within a 20-to 60-day time period; more than 600 but less than 2000 rads cause death between 7 and 20 days; more than 2000 but less than 10 000 rads within 36 to 72 hours, and greater doses within one day. All of these dose-related lethal syndromes have typical histopathologic lesions or combination of them that can be documented surgically or at autopsy. Most of these are so well known that they need not be mentioned.[3] Among many others, I would like to show you two that intrigue me:

(a) the death of the acid-secreting cell of the stomach that occurs after exposure to about 800 R (Fig. 10); and

(b) the development of a myocarditis and meningitis (Fig. 11) that occurs in man at doses of about 4000 rads and greater in a recently described human vascular death syndrome.[6]

However, among all the morphologically based response-versus-dose relations none is considered more quantitative than the temporal changes in the peripheral lymphocyte count, as shown in Fig. 12. The change in absolute lymphocyte count during the first 48 hours has many times the prognostic value of the first film badge reading. It has a much greater veracity than the first sodium-24 estimate, which in the past has been off by a factor of 10 because of failure to exclude residual radiochloride counts or because of errors in arithmetic. This reliability is the result of the invariable way that lymphocyte death begins at about 50 rads and is virtually

complete at about 1000 rads after a single prompt dose-a dose beyond which no man has survived without injection of foreign marrow grafts.

At 1000 rads the temporal sequence of events occurs in the peripheral blood as shown in Fig. 13. The degree of change is progressively proportional to dose, as shown in Fig. 14, and led to the generalization for biological dosimetry, shown in Fig. 12, that in essence shows that the lower the lymphocyte count at 48 hours the worse the prognosis, and that the complete disappearance of lymphocytes within 48 hours of exposure indicates a hopeless prognosis. In the two most recent accident victims this prognosis was borne out by their deaths within 33 and 49 hours respectively.[6]

I have not been able in this rapid review to spend much time on any one facet of the problem, and have had to pass lightly over the biological dosimetric information of the various death syndromes and their basis in tissue damage, hoping that Dr. Bond and others would have indoctrinated you in these areas. I passed over completely discussion of the germinal epithelium, spermato-genesis, cataractogenesis, carcinogenesis, and leukemogenesis. But lest you forget, allow me to remind you that early radiologists found it convenient to test their machines by taking a daily x ray picture of their left hands, and thereby discovered that the skin erythemic dose has no relation to the epidermal carcinogenic dose; but daily minute doses to the skin that do not cause erythema can be extremely carcinogenic and quite fatal.

III.3

Probit analysis of effective doses for gastrointestinal and systematic clinical responses to total-body irradiation in man (using arithmetic dose).

Clinical Response	Equation P = a (dose) + b		ED50 ± S. E. (m)	
	Probit (a)	Units (b)	Epigastric dose (rads)	Midline air dose[a] (R)
Anorexia[b]	0.017	3.609	82 ± 32	124
Nausea[b]	0.008	3.837	138 ± 20	209
Vomiting[b]	0.008	3.588	173 ± 18	262
Fatigue[c]	0.004	4.428	136 ± 36	206
Diarrhea[c]	0.008	3.441	194 ± 19	294
Death[d]	0.006	3.347	281 ± 44	425

a. As if all doses were from cesium-137 γ rays, so 66 absorbed tissue rads = 100 R measured in air at theoretical midline without the patient present.

b. Incidence of response through 2 days.

c. Incidence of response through 42 days.

d. Incidence of response through 60 days.

References

1. H. Becquerel, and P. Curie, Action physiologique des rayons du radium, comptes rendus, 132: 1290 (1901).

2. D. Walsh, Deep Tissue Traumatism from Roentgen-Ray Exposure, Brit. Med. J., 2: 272 (1897).

3. V. P. Bond, T. M. Fliedner, and J. O. Archambeau, Mammalian Radiation Lethality, a Disturbance in Cellular Kinetics, pp. 101-114, Academic Press, New York, 1965.

4. G. A. Andrews, J. A. Auxier, and C. C. Lushbaugh, The Importance of Dosimetry to the Medical Management of Persons Accidentally Exposed to High Levels of Radiation, in Personnel Dosimetry for Radiation Accidents, International Atomic Energy Agency, Vienna, pp. 3-16, 1965.

5. M. Strandqvist, A Study of the Cumulative Effects of Fractionated X-Ray Treatment Based on the Experience Gained at the Radiumhemmet With the Treatment of 280 Cases of Carcinoma of the Skin and Lip, Acta Radiol., 55: 300 (1944).

6. Herbert Fanger, and C. C. Lushbaugh, Radiation Death from Cardiovascular Shock Following a Criticality Accident: Report of a Second Death from a Newly Defined Human Radiation Death Syndrome, Arch. Path., 83: 446-460 (1967).

7. C. C. Lushbaugh and J. F. Spalding, The Natural Protection of Sheep from External Beta Radiation, Am. J. Vet. Res., 18:345-361 (1957).

8. C. C. Lushbaugh, Frank Comas, and Ruth Hofstra, Clinical Studies of Radiation Effects in Man: A Preliminary Report of a Retrospective Search for Dose-Response Relationships in Man, Rad. Res. 30, Suppl. 7 (in press).

9. C. C. Lushbaugh, Frank Comas, E. L. Saenger, M. Jacobs, Ruth Hofstra, and G. A. Andrews, Radiosensitivity of Man by Extrapolation from Studies of Total-Body Irradiation of Patients, Radiation Res., 27 3: 487-488 (1966) (abstr.).

10. S. Warren, and J. Z. Bowers, The Acute Radiation Syndrome in Man, Ann. Intern. Med, 32: 207-216 (1950).

11. Wright Langham and Douglas Grahn, Eds., Radiobiological Effects in Manned Space Flight: Report of the Space Radiation Study Panel of the Life Sciences Committee, pages 109-127, NAS-NRC, Washington, D. C. D. C., 1966 (in press).

12. G. R. Martinez, et. al., Z. D. Knowles, Translator (1-21-66) (TR-1-23-66), Accident from Radiation: Observations on the Accidental Exposure of a Family to a Source of Cobalt-60, Rev. Medica, Inst. Mex. Seguro Social, 3, Suppl. 1 : 14-69 (1964).

13. Norman T. Knowlton, Jr., E. Leifer, J. R. Hogness, L. H. Hempelmann. L. F. Blaney, D. C. Gill, Wm. R. Oakes, and C. L. Shafer, Beta Ray Burns of Human Skin, J. Am. Med. Assoc., 141: 239-246 (1949).

14. L. H. Hempelmann, H. Lisco, and J. G. Hoffman, The Acute Radiation Syndrome: A Study of Nine Cases and a Review of the Problem, Ann. Internal Med. , 36[2]: 279-510 (1952).

15. H. B. Gerstner, Reaction to Short-Term Radiation in Man, Ann. Rev. Med., 11: 289-302 (1960).

16. G. A. Andrews and R. J. Cloutier, Accidental Acute Radiation Injury, Arch. Environ. Health, 10: 498-507 (1965).

17. C. C. Lushbaugh, Gross and Microscopic Pathology and Neuropathology, in Acute Radiation Death Resulting from an Accidental Nuclear Critical Excursion, T. L. Shipman, Ed., J. Occup. Med. 3: 160-168, Special Suppl. (March 1961).

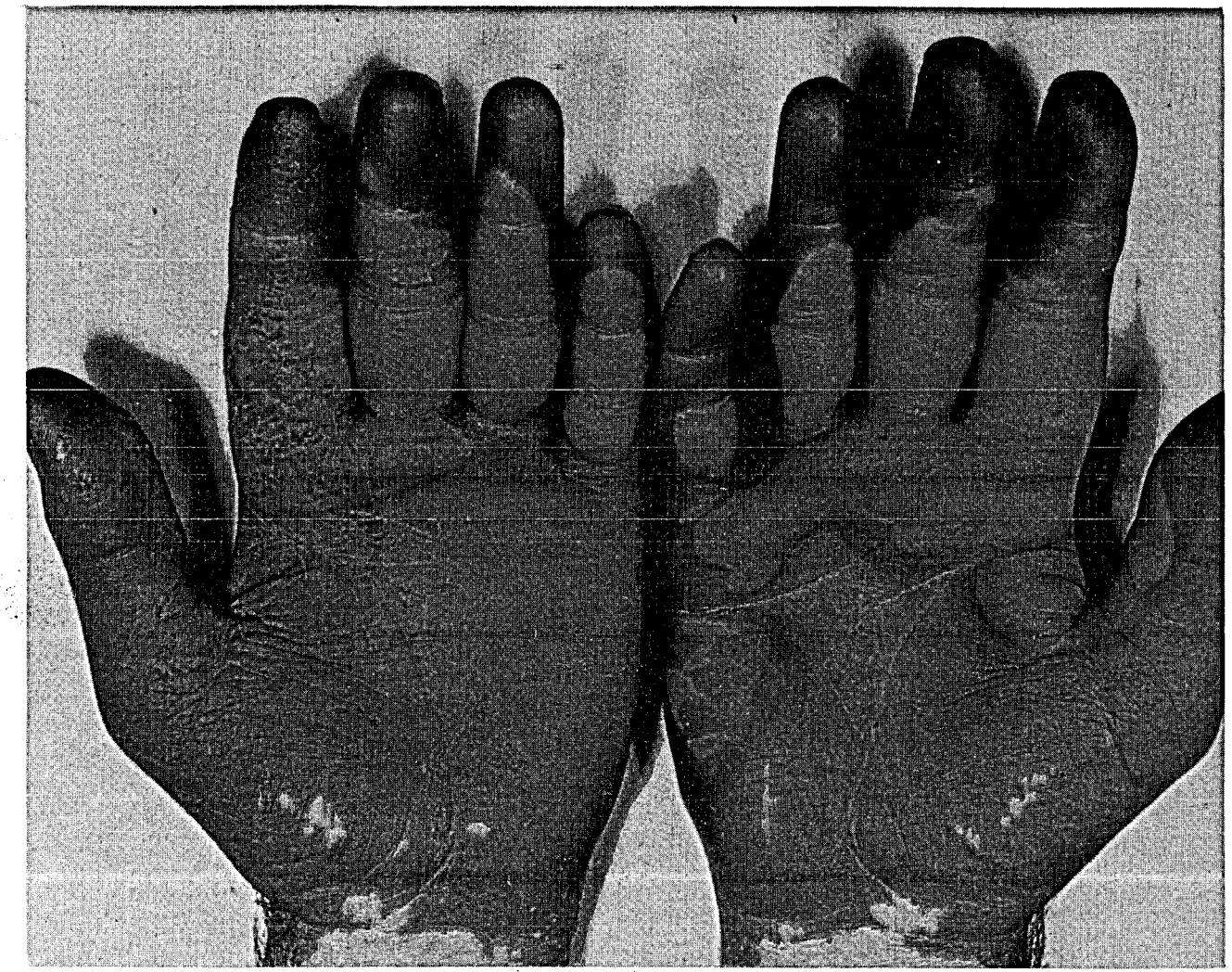

Fig. 1. Erythema and blistering from accidental exposure of the hands 18 days after beta radiation in excess of 20 000 rem from fission products (Ref. 13).

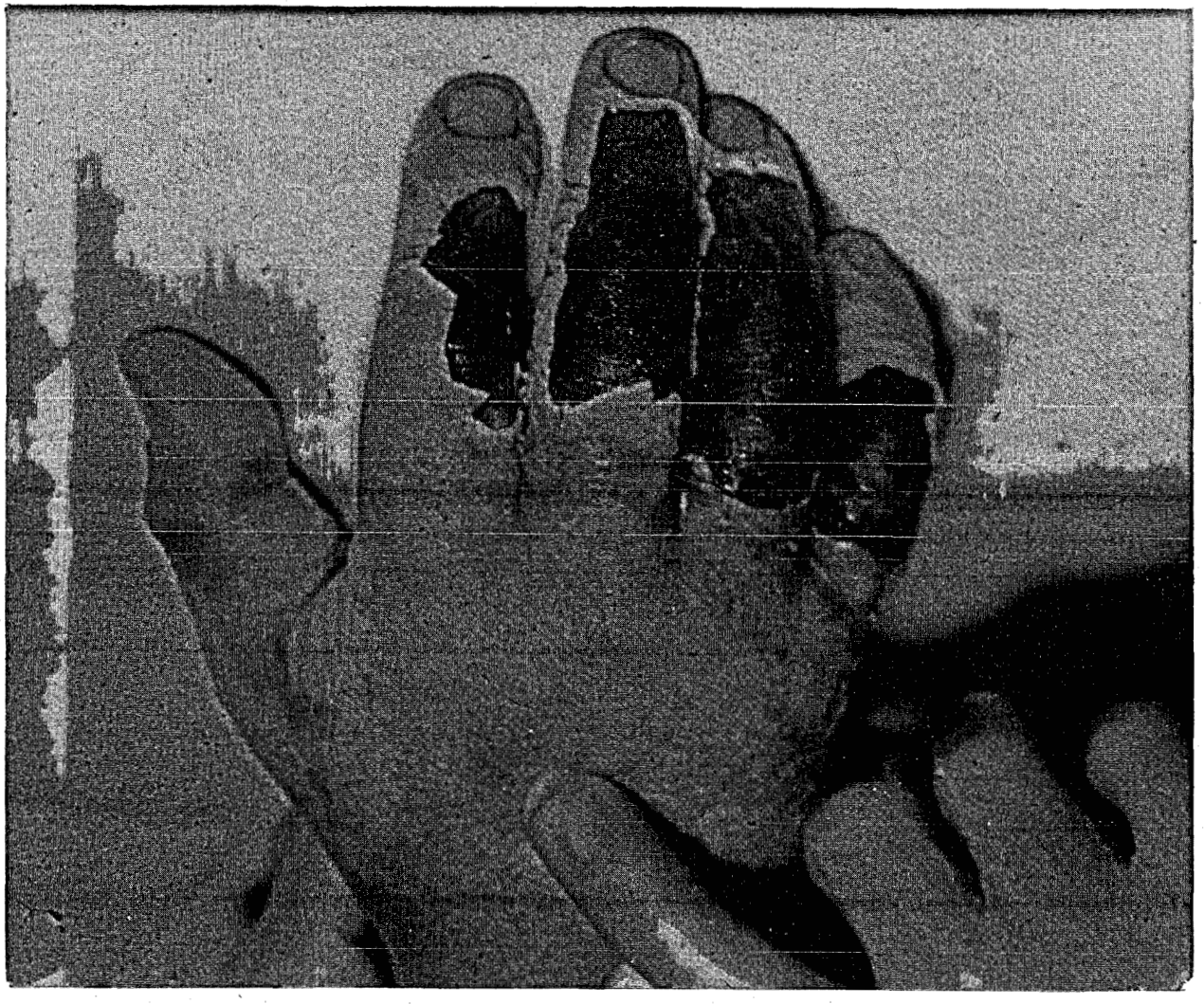

Fig. 2. Ulcerations about 2 weeks after exposure to radiations from fissionable material in an inadvertent criticality excursion. The details of this accident were described by Hempelmann et al (Ref. 14).

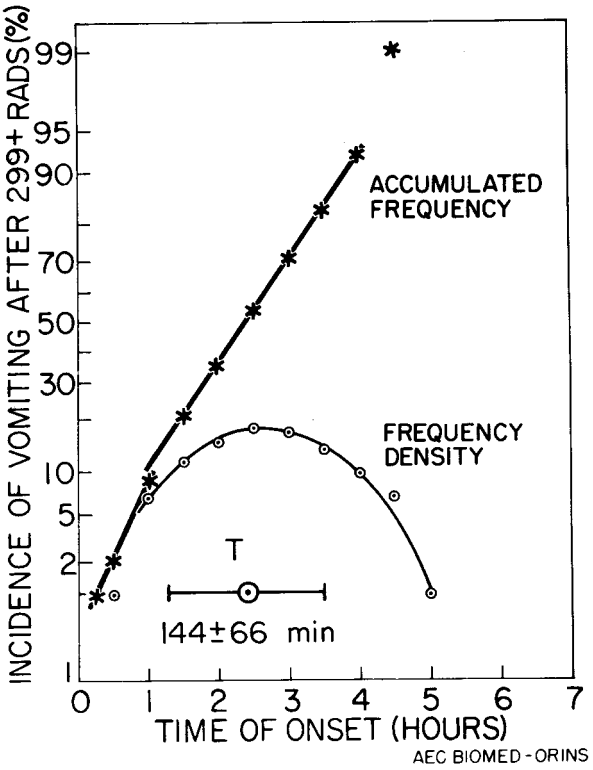

Fig. 3. The distribution of time of occurrence of first emesis in men exposed to greater than 300 R of whole-body irradiation (redrawn from data from Gerstner, (Ref. 15).

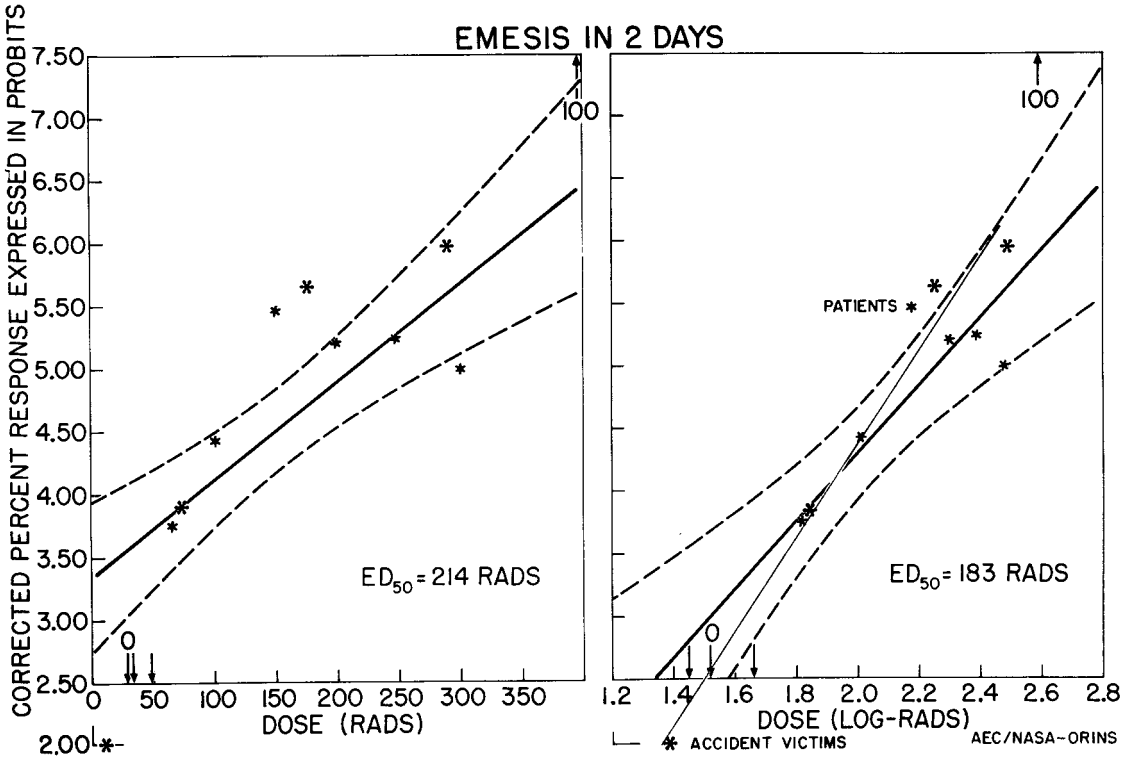

Fig. 4. Probit regression analyses of percent of exposed patients that vomited after radiation exposure in respect to dose in rads and log-rads. The resulting ED_{50}'s are shown. The thinnest line is the regression line obtained with data from studies made by others of 45 atomic accident victims.

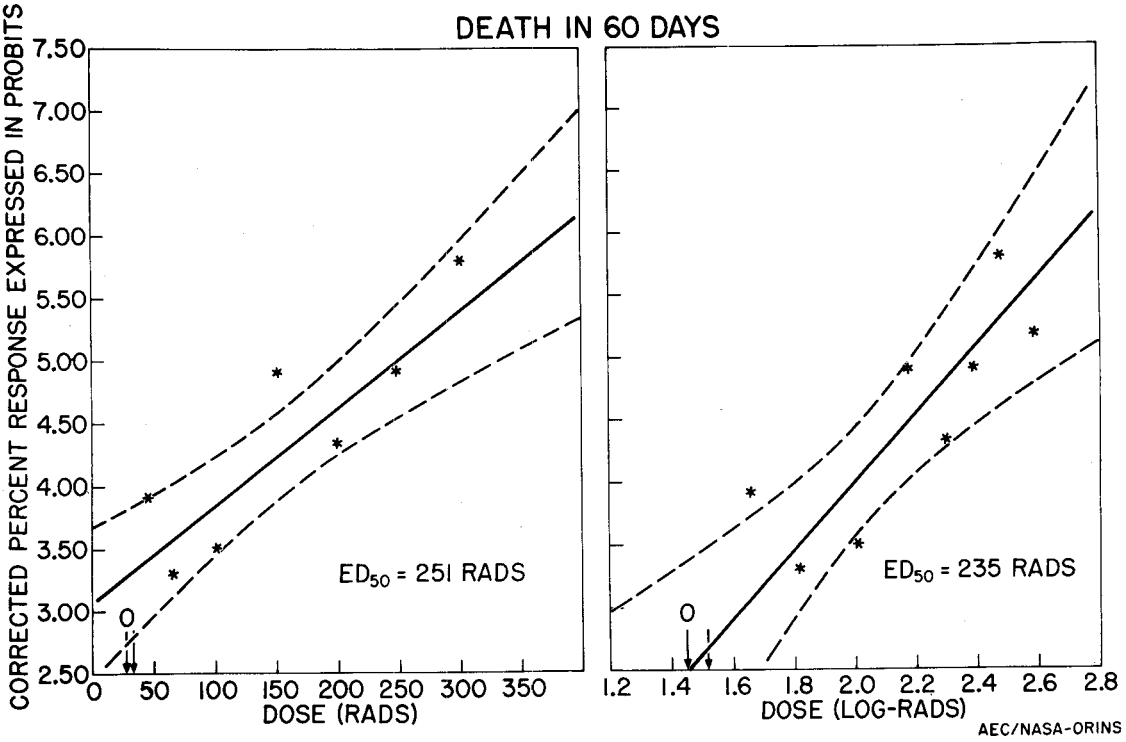

Fig. 5. Probit regression analyses of percent of exposed cases where death from any cause occurred within 60 days of exposure, showing corrected estimates of lethal radiation dose using linear and logarithmic dosage scales.

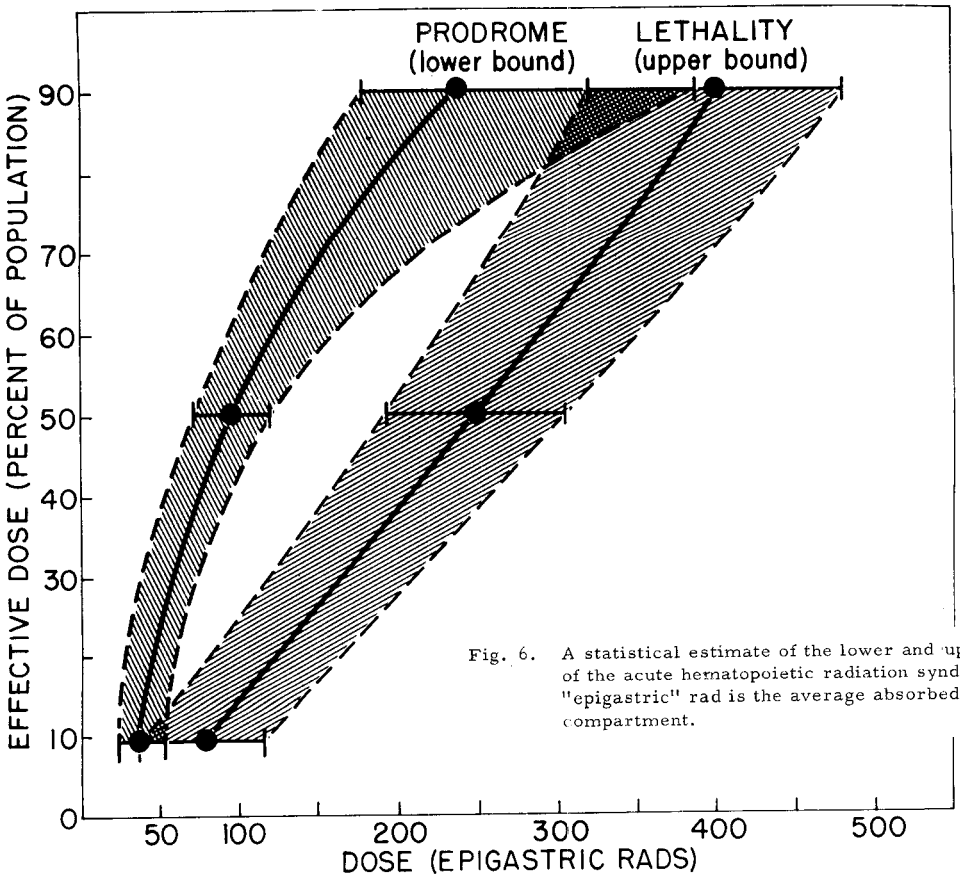

Fig. 6. A statistical estimate of the lower and upper dose-response bounds of the acute hematopoietic radiation syndrome in man. The "epigastric" rad is the average absorbed dose in the upper adominal compartment.

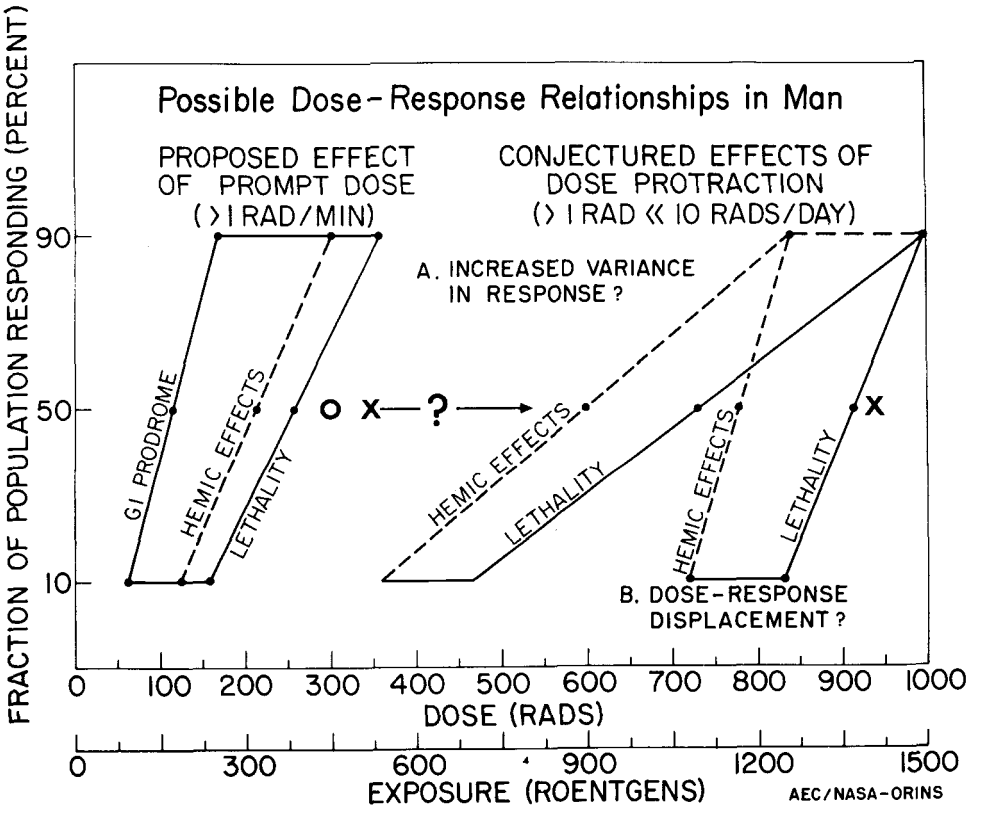

Fig. 7. The conjectured effects of dose protraction or fractionation upon the dose-response probability envelope for the hematopoietic syndrome. In (A) the envelope is shifted chiefly because low-dose rate and fractionation magnify the variance in radioresistance by allowing repair. In (B) the entire envelope shifts due to threshold of Irreparable damage being reached in the bone marrow or other organs as might be expected with high-LET particles. The large 0 denotes the position of the Warren LD_{50} estimate. The first X indicates the possible shift in LD_{50} after 1 week of dose protraction, and the second X locates the LD_{50} displaces by 52 weeks of intermittent exposures as estimated by the LASL model (Fig. 8).

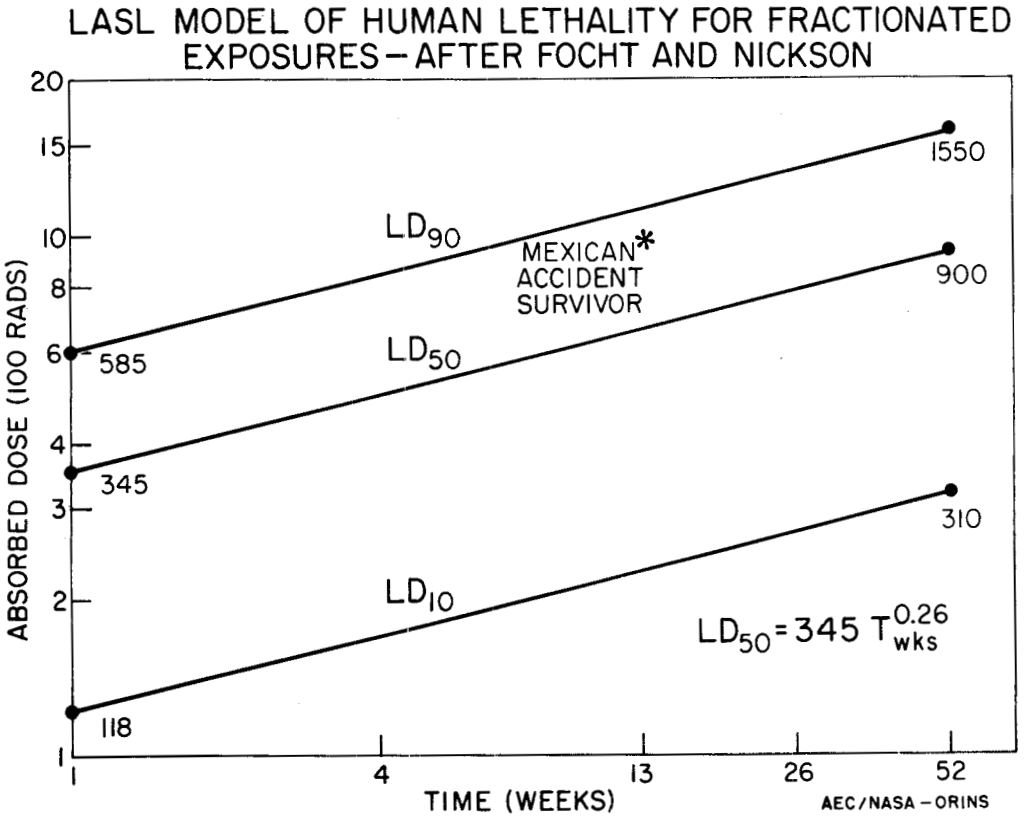

Fig. 8. The effect of fractionation of total-body radiation exposures upon the estimated human LD_{50}. The Mexican accident survivor "fits" fortuitously within the schema. The 10% and 90% probability estimates are based on the slope of the probit-regression line in Fig. 5A.

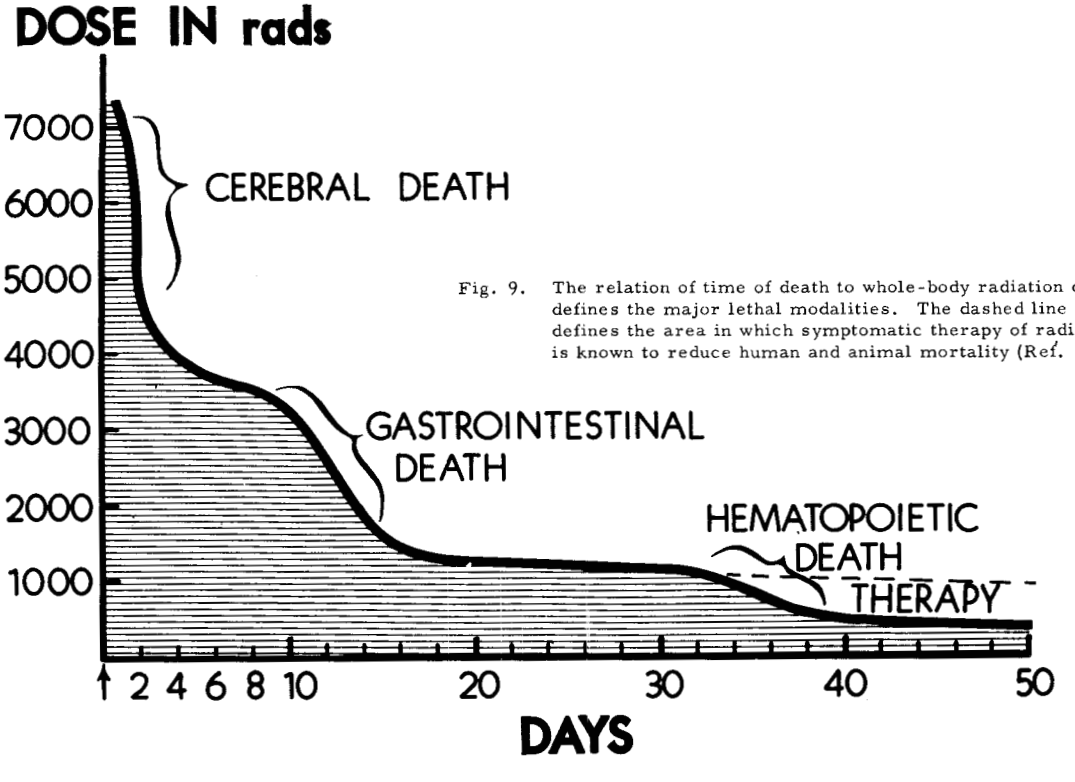

Fig. 9. The relation of time of death to whole-body radiation dose that defines the major lethal modalities. The dashed line over "therapy" defines the area in which symptomatic therapy of radiation damage is known to reduce human and animal mortality (Ref. 16).

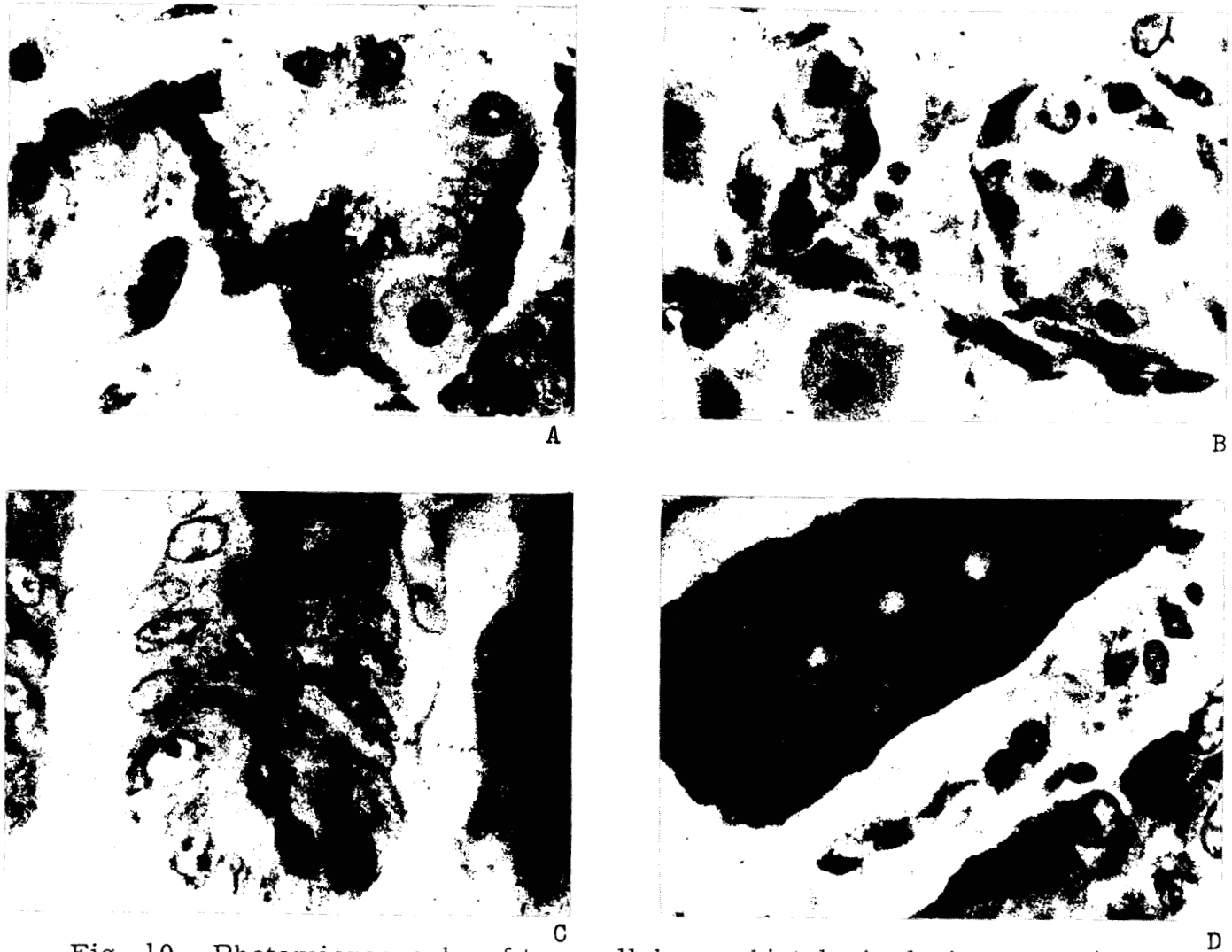

Fig. 10. Photomicrographs of two well-known histologic dosimeters: (A) normal human gastric gland contrasted with that (B) of a man who received greater than 800 rads to the stomach, causing parietal cell necrosis; (C) a colonic gland crypt and (D) a jejunal gland crypt, showing mitotic arrest at doses greater than 400 rads (Ref. 17).

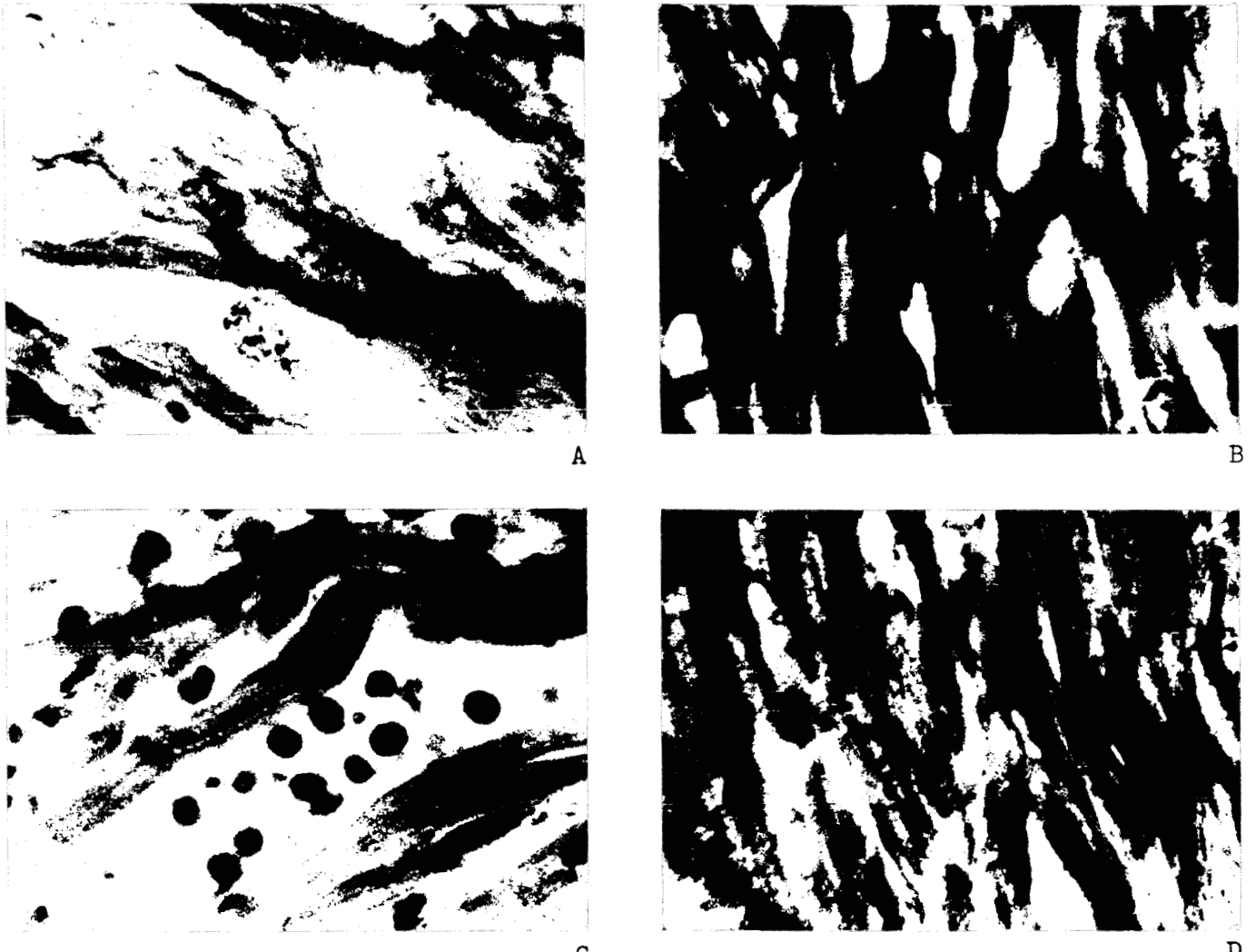

Fig. 11. Photomicrographs of human myocardium, showing in A and B the normal appearance and in (C) the severe edema of the myocardial fibers and in (D) the interstitial exudation of leukocytes that occurs in the heart of human radiation accident victims exposed to greater than 4000 rads average whole-body dose (Ref. 17).

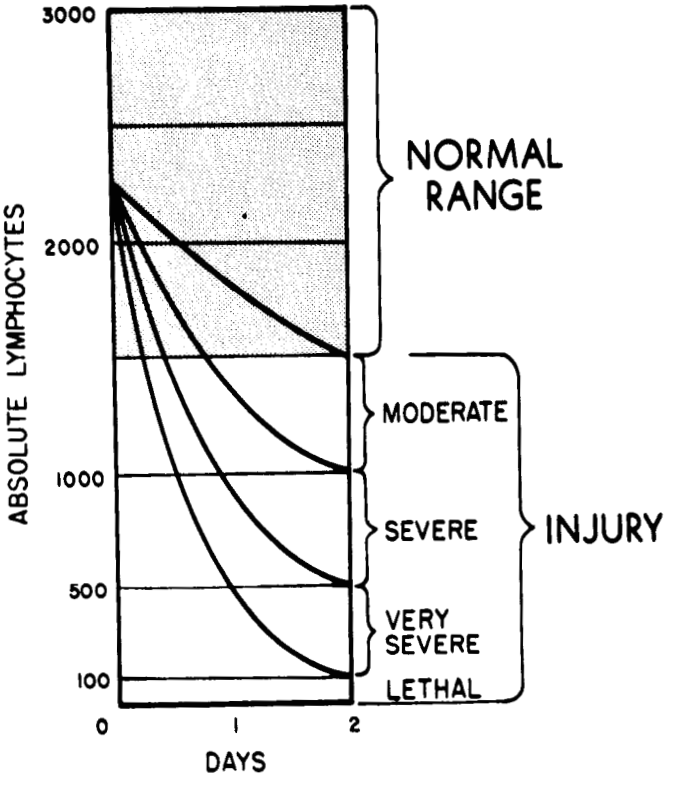

Fig. 12. Graphic prognosis chart based on clinical experience, showing that depression in degree of peripheral lymphocyte count is a measure of severity of whole-body radiation injury (Ref. 4).

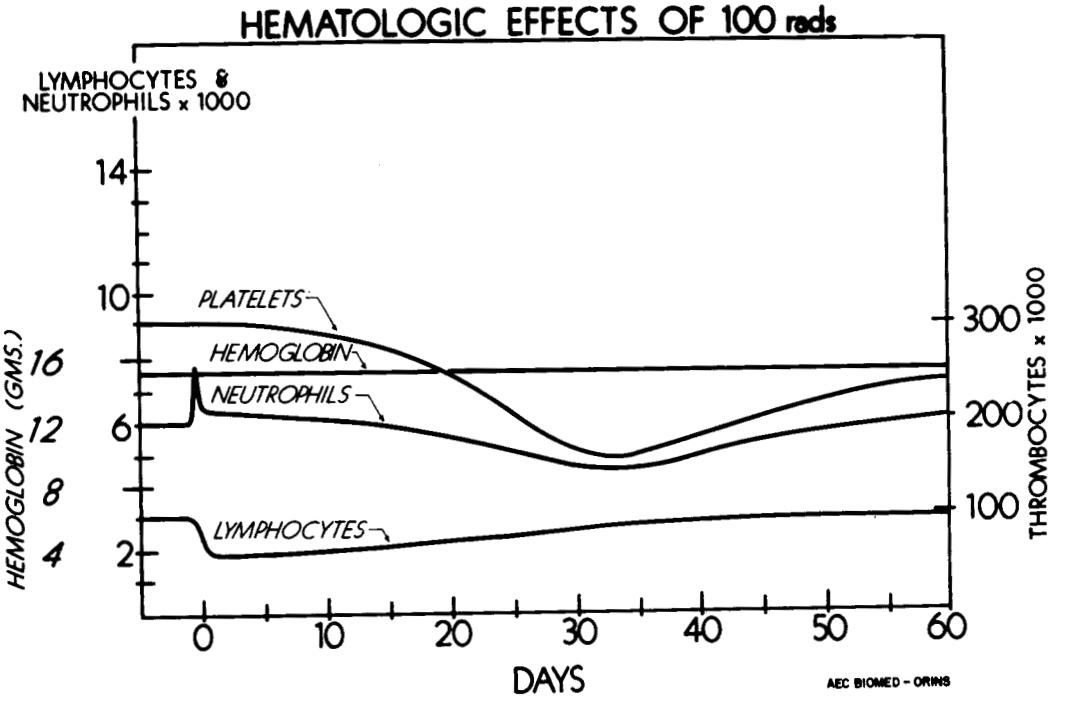

Fig. 13. Chart of the usual changes in parameters of peripheral blood morphologic contents after 100 rads to the whole body in man (Ref. 4).

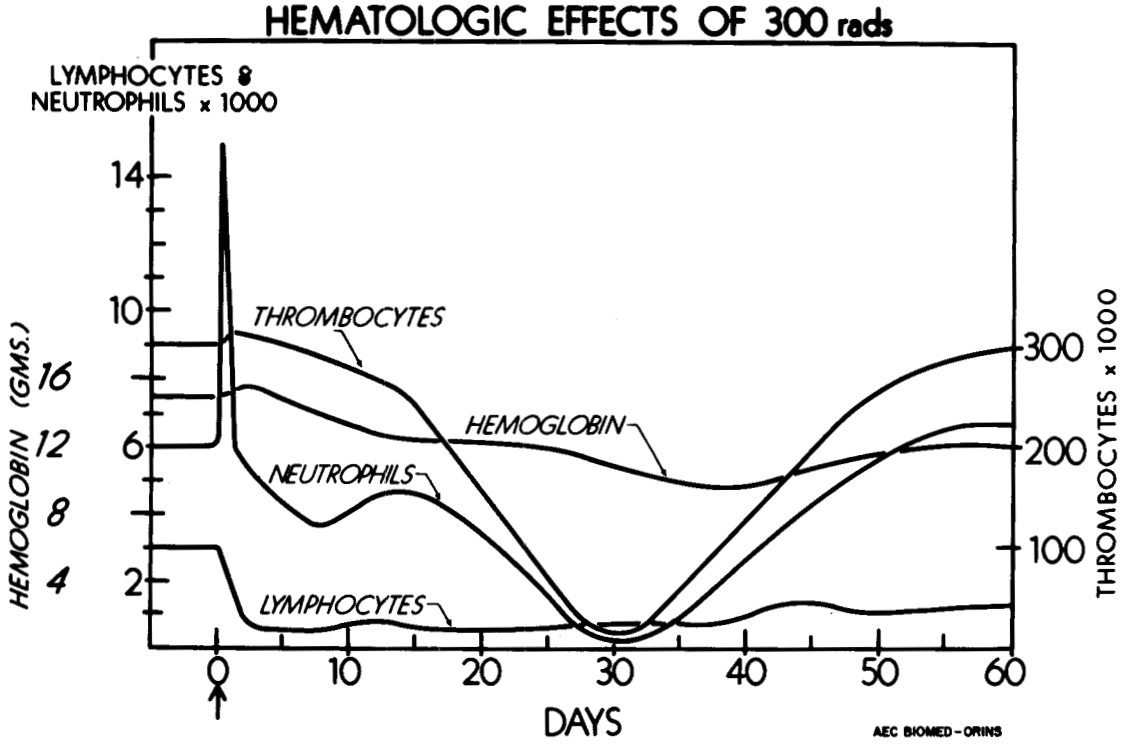

Fig. 14. Chart of the usual changes in parameters of peripheral blood morphologic contents after 300 rads to the whole body in man (Ref. 4).

III. 4

EFFECTS OF TOTAL- AND PARTIAL-BODY THERAPEUTIC IRRADIATION IN MAN

Eugene L. Saenger

College of Medicine
University of Cincinnati
Cincinnati, Ohio

It is thought-provoking to consider the reasons for presenting experiences derived from therapeutic total- and partial-body radiation in man to the problems of accelerator radiation. The experience of radiobiologists concerned almost exclusively with human beings is derived from extensive work with sparse radiation. In these circumstances we can draw on knowledge of total, partial, and regional radiation given for a variety of diseases and on an extensive literature in experimental radiobiology carried out in animals. In the use of accelerators experience with both human beings and animals has necessarily been far more limited. In this latter circumstance, radiation effects have been studied in small animals and in various cultures of tissues and organisms, and--to an even more limited degree--in regional radiation therapy in humans. [1]

In this communication, some findings resulting from total- and partial-body exposure of human beings are presented and implications for workers in accelerators are discussed.

The program at the University of Cincinnati was initiated in 1960 to study the effects of radiation on patients who received total- and partial-body irradiation for cancer. It is our belief that these studies concerning radiation effects in the human being can yield valuable information in these subjects, even though the characteristics of cancer must be kept in mind in the evaluation of the data.

The major objectives of this investigation are to study

(a) therapeutic effects on the clinical course,

(b) hematological changes,

(c) protective effect of autologous bone marrow,

(d) psychological and psychiatric changes,

(e) effects of total- vs partial-body radiation.

III. 4

Design of Study

Each patient serves as his own control, utilizing a preirradiation period of 1 to 2 weeks. During this time several sham irradiations are given to permit accurate dosimetry and to obtain cooperation of the patient. There is no discussion with the patient of possible subjective reactions which might be attributable to radiation. However, patients are appraised of the risks of therapy.

Patients with metastatic or incurable neoplasms are given total- or partial-body radiation for palliation of their disease. Patients for detailed studies are selected from the above group if they satisfy the following criteria:

(a) presence of "solid" tumors (patients with lymphoma are excluded);

(b) relatively good nutritional status (ability to maintain weight);

(c) normal renal function;

(d) stable hemogram in the control period.

Absorbed midline tissue doses of 50 to 200 rad of total-body radiation (TBR) and 100 to 300 rad of partial-body radiation (PBR) were given, using a cobalt-60 teletherapy unit and dose rates of 3 to 6 R/min. The distance from the source to patient midline is 282 cm. Half the planned dose is given to each lateral aspect. The relative depth-dose distribution for the lateral fields is shown in Fig. 1. The beam area for the 50% isodose curve at the patient midline is a square of about 73×74 cm (Fig. 2). The patient is placed in a sitting position with legs raised and head tilted slightly forward. For partial-body radiation, the teletherapy collimator is used to restrict the beam. The isodose curves (Fig. 3) and relative dose distributions for upper and lower body radiation[2] (Figs. 4 and 5) show that for the upper body about 40% of the body volume is included and for the lower body about 60% is included.

Clinical Findings

Forty patients have received total-body radiation. Three patients received upper-body radiation and ten received lower-body radiation.

The relation to dose of the frequency and severity of prodromal symptoms of anorexia, nausea, and vomiting are of particular interest. No prodromata were found below 100 rad. In 14 patients receiving 100 rad, only four patients showed prodromal symptoms. At doses of 150 and 200 rad, two-thirds of the patients showed these symptoms (Table 1). Table 2 shows the probability of development of prodromata for the midline dose in rads and for integral doses in megagram rads.

Many of these patients had previously received extensive courses of regional radiation therapy and systemic chemotherapy. In the early part of this study it seemed that patients who had received such earlier treatment had a higher incidence of prodromata; yet, as the study progressed, this trend did not continue. Hence individuals who have received extensive previous therapy have not shown an increased incidence of prodromata.

For the three patients who received upper-body radiation with doses of 100 to 200 rad, none showed prodromata. Of the ten patients receiving lower-body radiation, five showed prodromal symptoms (Table 3).

Symptoms during the stage of manifest illness were minimal. In many individuals it was difficult to distinguish symptoms of radiation from those attributable to the neoplasm.

A number of standard psychological tests were utilized according to the design of the study; certain new psychiatric tests have been developed to attempt evaluation of performance decrement following radiation.[2] It has been difficult to evaluate these studies, in part because of the low educational levels and intelligence quotients of these patients. Psychic depression seemed to parallel changes in physical state. Anxiety was high prior to sham or actual treatment and decreased subsequently.

Mortality

The effect of radiation on lethality in this group of selected patients has been difficult to interpret. Several models can be considered. Lushbaugh et al.[3] assume that any patient dying in less than 60 days has died of radiation. The difficult aspect of this problem is to determine the effect of cancer on mortality and also the possible effects of radiation on the course of the neoplasm. Other hypotheses can be that the cancer process itself leads to early death and also that total- or partial-body radiation in some way tends to defer the time of death.

In the TBR patients the median survival time of 37 patients was 200 days. Eleven patients died within 40 days. Two patients receiving 50 and 150 rads each died respectively on the 9th and 10th days. They were eliminated from the calculation since, at those doses, radiation death is too early. Three patients, given 25, 100, and 100 rad, are alive at this time surviving 1074 days, 514 days, and 2099 days (as of March 1, 1967). One patient was lost to follow-up.

When the mean and median days to death of 36 patients were calculated (Table 4), a progressive decrease in survival was found, as would be expected were radiation the principal factor, except for the 200-rad group. In this group the mean and median survival times show a marked increase. Thus if the hypothesis of death under 60 days due to radiation is accepted, one must also accept the

hypothesis that in properly selected patients, this type of radiation may prolong life. Similar calculations of mortality following partial-body radiation show a progressive increase in survival with increase in dose.

It is possible that the higher radiation doses were given to patients whose clinical condition seemed better to the therapist. Once the patient was selected for this type of treatment, the determination of the dose to be administered was made by the radiation therapist. One difficulty in this type of study is that there are no survival figures available for comparable groups of patients who have been treated by other methods, as any selection method would introduce biases in either direction. It would be possible to select controls who were either much sicker or less sick than these patients. It would also be difficult to obtain concurrent patients with neoplasms similar in extent and pathological type. Hence the type of data given in Table 4 seems to be about as reliable as one can obtain.

If, however, one follows the absolute lymphocyte count, one observes a marked and persistent lymphopenia ranging from 800 to 200, often remaining low for 40 to 60 days. In two of the partial-body cases, the lymphocytes did not begin to fall for 48 to 72 hours after exposure, and it would have been difficult to detect radiation in this manner. (These cases received 100 and 200 rad respectively to the lower body.)

If one compares the hematological changes in partial-body radiation with those in total-body radiation, one is struck by the paucity of change in total white count, platelets, and hematocrit, particularly since four of the eight patients receiving 200, 300, and 300 rad had prodromal symptoms. We have not yet established the partial-body radiation dose which produces the degree of change seen at 100 to 150 rad of total-body radiation in the human being. Nor has the amount of marrow being irradiated in the human being been similarly evaluated. It is quite likely that the degree of hematological depression is more a function of the volume of marrow irradiated for a given dose than of dose alone. The incidence of prodromal symptoms seemed dose-dependent for both total- and partial-body irradiation. On the contrary, depression of granulocytes and platelets was minimal or absent in partial-body irradiation. Even lymphocyte depression seemed to be less marked for comparable doses in partial-body irradiation.

Michelson et al.[4,5] have irradiated beagles and compared lethality of partial- and total-body radiation. The dividing point for upper- and lower-body radiation was the xiphoid. The $LD_{50/60}$ for total-body irradiation was 310 rad; for upper-body irradiation it was 2150 rad, and for lower-body irradiation 900 rad. If one compares the fall in white blood cell counts in dogs receiving doses at the $LD_{50/60}$ level, one finds in the totally irradiated dog (receiving 225 to 300 rad) that the WBC fell to 20% of the pretreatment level in 7 to 25 days, after which time recovery began. In the dogs in whom treatment was given to the upper body (1700 to 1850 rad), the WBC fell to 30% of the initial value for 5 to 10 days, followed by recovery. In dogs receiving treatment to the lower body (700 to 875 rad) the WBC levels fell to 35% at about the 15th day and then recovery began. It is of course

impossible to give radiation doses to humans of the same order of magnitude as used in these animals. It is possible that there would be differences in the effects of upper- vs lower-body irradiation in humans had more patients been studied; additional comparisons will have to await further studies.

Discussion

The reason for presentation of these observations to this meeting is to point out that carefully controlled clinical observations on human beings can continue to expand our understanding of acute radiation injury, in addition to yielding information on the palliative effect of this form of treatment.

There have been a number of other studies similar to ours.[6,7] In all of these studies there are important limitations. It has not been possible to study certain aspects of the radiation event. The effect of dose rate under carefully controlled circumstances is not known. For example, our radiation has been given over about 30 to 60 minutes. What clinical effects would be different if the dose rates were much higher? In respect to symptoms, signs, psychological behavior, or laboratory findings, would the results differ if 200 rad were administered in 1 minute or less? At present, our thoughts are inferential. Recently I participated in a discussion of a mass of experimental data involving about nine species of animals exposed under a great variety of conditions. It was difficult to obtain opinions regarding species differences, and even more of a problem to extrapolate pertinent information to the human being. My opinion is not presented from the viewpoint of a theoretical radiobiologist but as a clinician whose responsibility is to care for colleagues who are injured by radiation.

Dosimetry, relative biological effectiveness, and degrees of injury can be estimated for exposures at an occupational level. At the level of clinical injury we lack information. To illustrate this point, one need only recall the interesting studies of supervoltage therapy by Milton Friedman, which provided tissue tolerance for supervoltage and neutron therapy, and studies by the late R. S. Stone, which provided human data for late effects of neutron irradiation. Yet, with increased understanding, supervoltage therapy has become a life-saving contribution to many cancer patients. At present, neutron therapy is being re-evaluated.

As in all great advances in physics, the family of accelerators is developing primarily because of interest to physicists. Gradually certain biomedical problems and interests develop--usually years after the advances in physics and engineering. With the esoteric particles and their complicated interactions, the biological investigations lag behind those interests which certain of us have at a clinical level. With the exception of certain human studies utilizing very-small-field irradiation and relatively low energies, little work appropriate to the type of studies described here is being planned or carried out. A distinguished physicist once told me that with our present biological knowledge, it is entirely possible to foretell all effects

in humans from any of these newer radiations. This viewpoint may be questioned only after several episodes of human injury have been recorded.

Thus serious consideration needs to be given now to providing increased opportunity for clinical investigation of many of these radiations, both for their possible clinical benefits in cancer patients and for concomitant evaluation of their deleterious effects. It is doubtful that a principal problem is one of exchange of information between physicist and biologist, or even of getting time on existing machines for biological experiments. As we have seen from relative biological effectiveness and linear energy transfer, it matters little whether we provide 50 or 100 inches of shielding or whether the quality factor is 2, 10, or 20 for occupational exposure. These are the easy problems.

The difficult problems are diagnosis, therapy, and prognosis of acutely and seriously injured man. The need is for more accelerators with large fields and pertinent radiations which can be applied therapeutically to add pertinent clinical understanding for acute human overexposure!

III.4

References

1. J. H. Lawrence and C. A. Tobias, Heavy Particles in Medicine, in Progress in Atomic Medicine, J. H. Lawrence, Ed., 1:127-146. Grune and Stratton, Inc., New York, 1965.

2. E. L. Saenger, B. I. Friedman, J. G. Kereiakes, and H. Perry, Metabolic Changes in Humans Following Total-Body Radiation, DASA-1844. Defense Atomic Support Agency, Department of Defense, Washington, D. C. 20301, 1966.

3. C. C. Lushbaugh, F. Comas, and R. Hofstra, Clinical Studies of Radiation Effects in Man: A Preliminary Report of a Retrospective Search for Dose-Response Relationships in the Prodromal Syndrome, Workshop Conference on Space Radiation Biology, University of California, Berkeley, California, September 8, 1965.

4. S. M. Michaelson, L. T. Odland, and J. W. Howland, Mechanisms of Injury and Recovery from Whole- and Partial-Body Exposure to Ionizing Radiation. AEC Research and Development Report UR-615. U. of Rochester, Rochester, N. Y, September 18, 1962.

5. W. J. Quinlan, K. Scheer, R. W. Neidlinger, S. M. Michaelson, and J. W. Howland, Late Manifestations of Whole- and Partial-Body Ionizing Radiation in the Dog: A Two Year Summary. AEC Research and Development Report UR-609, U. of Rochester, Rochester, N. Y., June 23, 1962.

6. L. S. Miller, G. H. Fletcher, and H. E. Gerstner, Radiobiologic Observations on Cancer Patients Treated with Whole-Body X-Irradiation. Radiation Res. 4: 150 (1958).

7. G. A. Andrews, C. C. Lushbaugh, R. M. Kniseley, D. A. White, and B. I. Friedman, Hematologic Effects of Total-Body Radiation in the Human Being, International AEC Panel on the Effects of Various Types of Ionizing Radiations from Different Sources on the Haematopoietic Tissues, Vienna, Austria, May 17-20, 1966.

Table 1. Frequency of prodromal symptoms[a] following total-body irradiation (Cincinnati data).

Midline dose (rads)	Frequency
50	0/8
100	4/14
150	8/12
200	4/6

a. Nausea, vomiting, etc.

b. Patients with syndrome/total patients in group.

Table 2. Stimulus (prodromal symptoms[a]) at which proportion P would be expected to respond (Cincinnati data).

P	Midline dose (rads)	Integral dose (Mg-rads)
0.10	58	1.4
0.20	86	4.3
0.30	107	6.4
0.40	125	8.1
0.50	141	9.7
0.60	157	11.4
0.70	175	13.1
0.80	195	15.2
0.90	224	18.1
0.99	292	24.9

a. Nausea, vomiting, etc.

Table 3. Incidence of prodromal symptoms[a] following partial-body irradiation (Cincinnati data).

Midline dose (rads)	Frequency
100	0/3
150	1/2
200	2/6
300	2/2

a. Nausea, vomiting, etc.

b. Patients with syndrome/total patients in group.

Table 4. Elapsed time to death following total- and partial-body radiation.

Midline dose (rads)	N	Days from irradiation to death	
		Mean	Median
Total-body			
50	6	242	96
100	12	257	198
150	12	197	64
200	6	348	246
Partial-body			
100	3	72	38
150	2	101	--
200	6	138	133
300	2	212	--

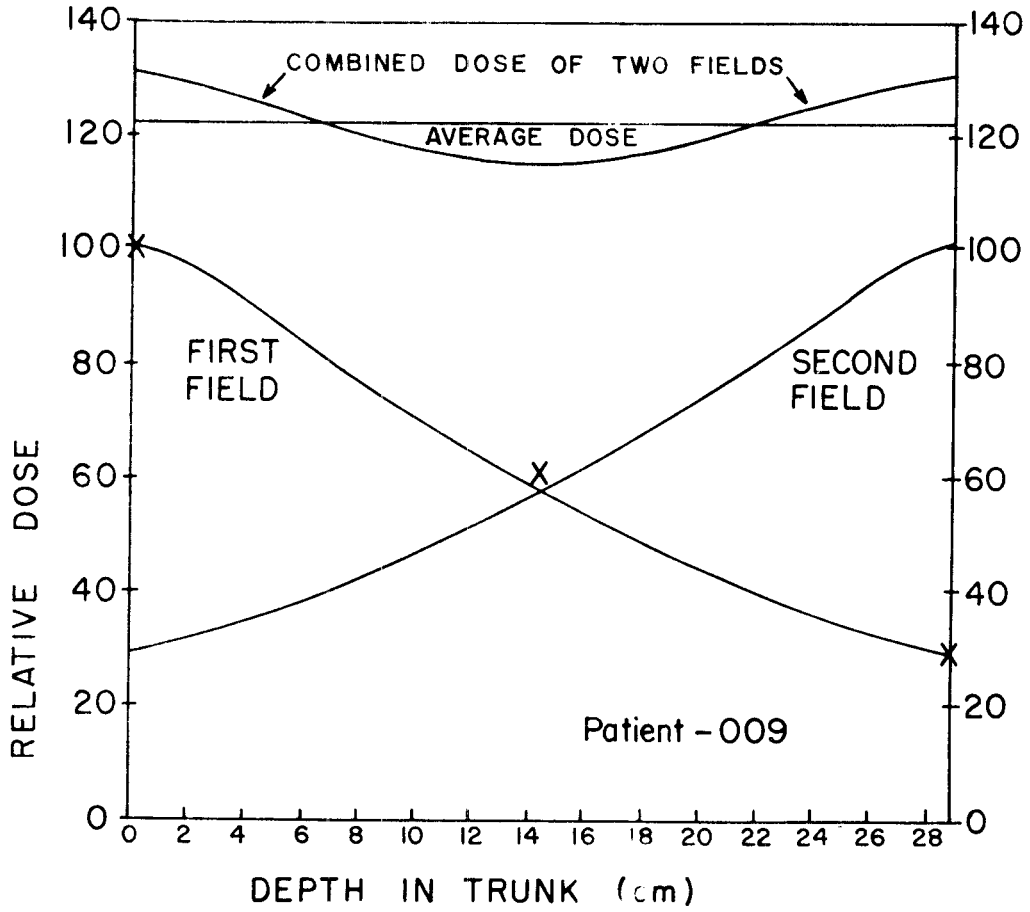

Fig. 1. Relative depth-dose distribution for lateral fields.

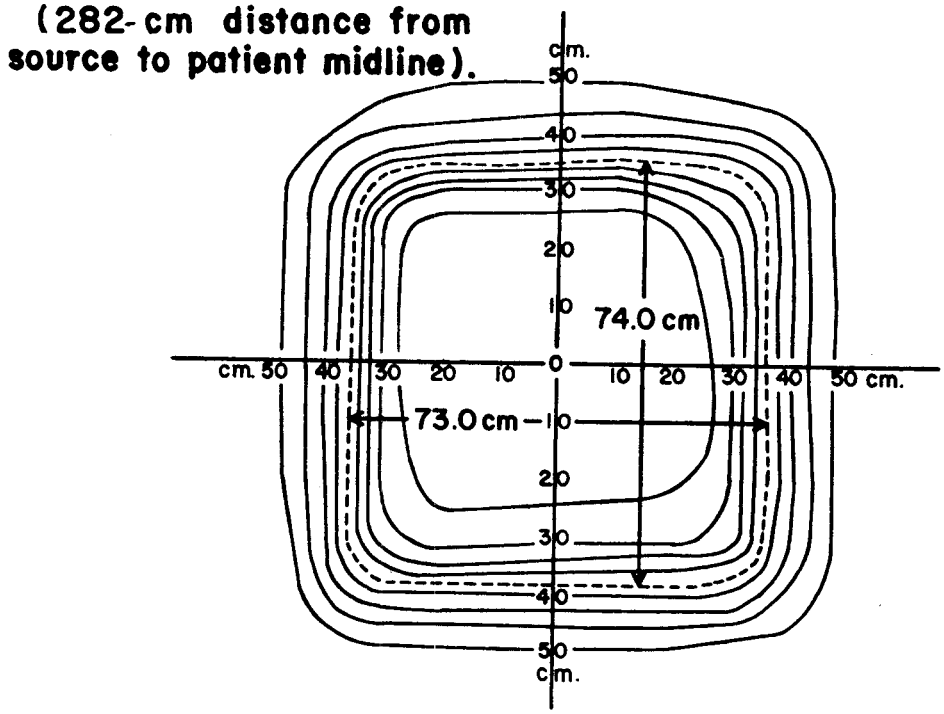

Fig. 2. Cobalt-60 field for total-body irradiation (282-cm distance from source to patient midline).

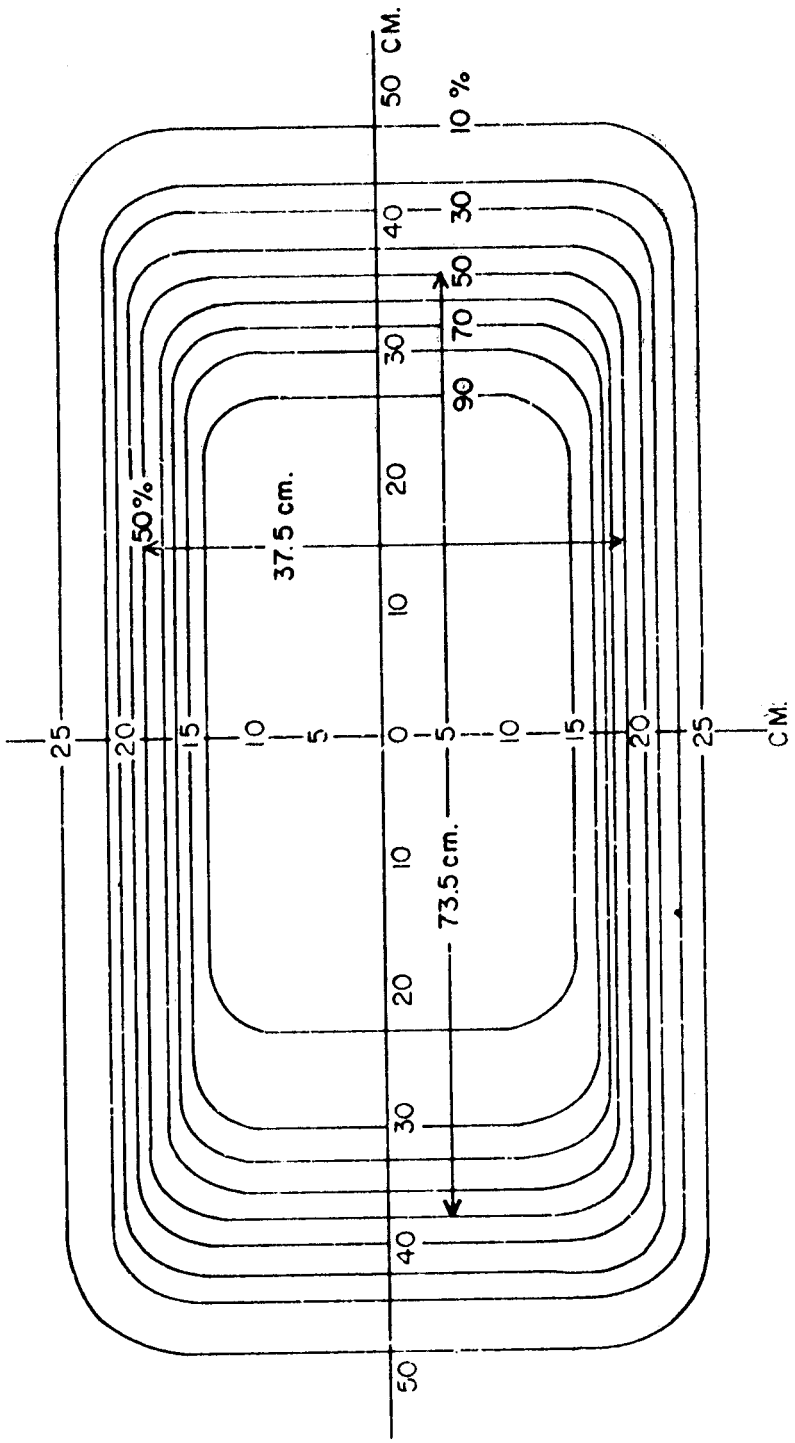

Fig. 3. Cobalt-60 field for partial- (half-) body irradiation.

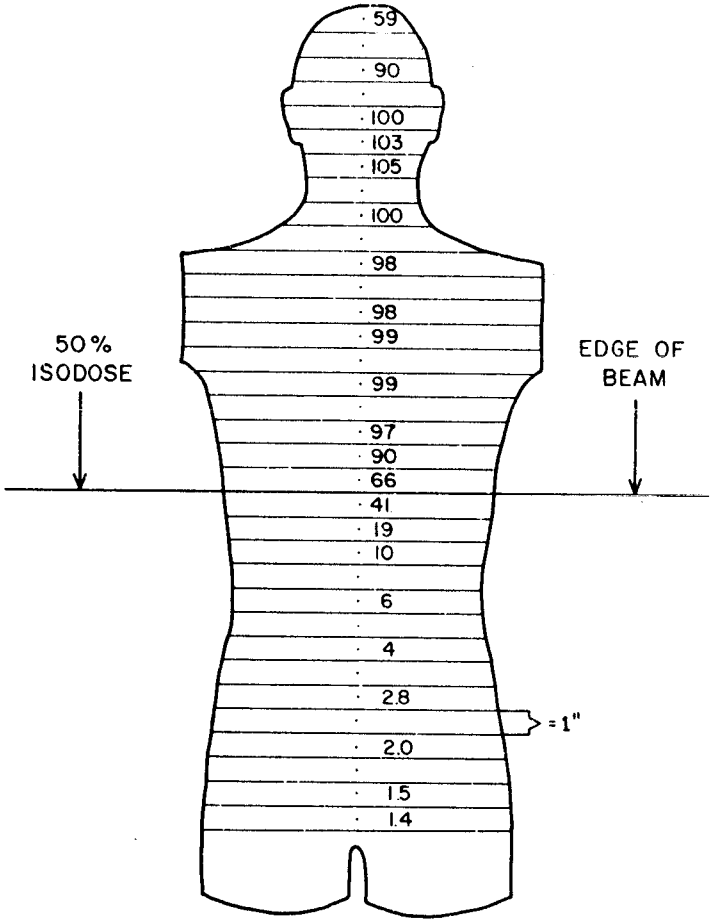

Fig. 4. Relative doses for ^{60}Co partial-body (upper) irradiation as measured with TL-100 powder at center of Rando phantom lateral irradiation.

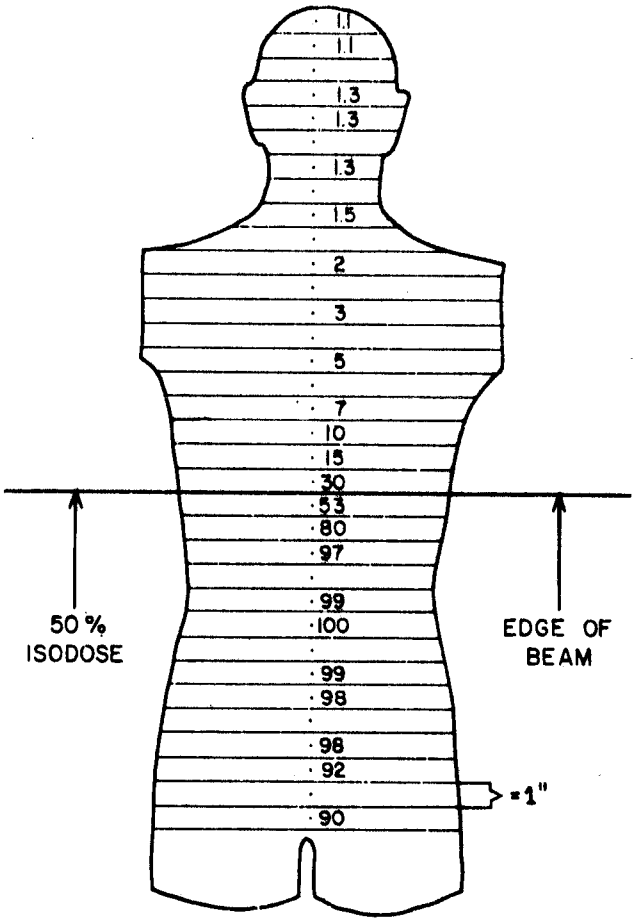

Fig. 5. Relative doses for ^{60}Co partial-body (lower) irradiation as measured with TL-100 powder at center of Rando phantom lateral irradiation.

IV.5

DATA FROM ANIMAL EXPERIMENTS

J. F. Fowler

Postgraduate Medical School
Hammersmith Hospital
London, W. 12.

1. Introduction

I shall attempt to deal only with somatic damage in animals, and that only in the organs with which I am familiar. Dr. Oakberg has dealt with genetic and gonadal aspects, and Dr. Sullivan with intestinal and gonadal injury. My experience is mostly concerned with the fast neutron beam from the M. R. C. Cyclotron at Hammersmith Hospital; in addition we have carried out experiments jointly with Dr. Barendsen, both on the neutron beam and on beams of deuterons and α particles of six different well-defined LETs.

The spread of LET in a fast neutron beam is wide (Fig. 1) and "mean LETs" cannot be satisfactorily specified either to obtain RBE values or to calculate other effects such as the oxygen enhancement ratio (see below, also Ref. 6).

This paper presents some results from the skin of pigs, mice, and rats irradiated with cyclotron neutrons, and will discuss the relevance of these to more fundamental cell-survival studies.

2. The Distinction Between RBE and QF

An RBE value is the result of one set of experiments on a given biological system. Quality Factor, on the other hand, is an arbitrary series of dose ratios of the same dimensions as RBE values, but chosen by the ICRP[17] to represent a series of reasonable values, solely for the purpose of radiation protection precautions. QFs are specified for given values of LET. They apply only to such low doses as are appropriate to personnel monitoring. There are two main problems about QF. One is that LET is difficult to specify, since all radiation fields contain a mixture of LETs, and there is no satisfactory way of obtaining a useful mean value. Neither track average nor dose average is adequate for calculating both oxygen enhancement ratio and RBE in mammalian cells.[1] It is likely that methods will be necessary which take account of distributions of local energy density at the submicroscopic level.[22] There are methods of measuring distributions of LET in mixed radiation fields;[21] also techniques by which each component of LET is multiplied by the ICRP value of QF before summing to give a single figure in "rem." This last method is convenient, especially for summing doses in very-low-dose monitoring, but the information is blurred, and should appreciable doses be recorded further analysis would be necessary.

The second problem about QF is that it is, by definition, no guide whatever to the possible clinical outcome of any significant overexposure. It would be grossly misleading to use the QF of 20 in the event an appreciable dose were received accidentally by the whole body--i.e., by the haemopoietic system--or locally by the skin.

Figure 2a shows the variation of RBE with LET summarised by Alper[1] for plant, mammalian, and enzyme systems. Figure 2b shows more detailed experimental values for LD_{50}--30 days in mice plotted against LET, together with the ranges of LET of several types of radiation. The $LD_{50/30d}$ is presumed to be correlated with depletion of leucocytes following cellular depopulation of bone marrow.

Figure 3 shows more recent data on RBEs for somatic damage. The lower dotted lines are the RBEs for proliferative survival of human kidney T cells in tissue culture obtained from Barendsen's experiments with track segments of charged particles.[2,3] The peak in RBE occurs at about the same LET as for the LD_{50} in mice. The increase of the peak RBE with decreasing level of damage--i.e., with decreasing dose, specifically dose per cell cycle--is clearly shown. Some RBEs for thymus weight loss in the rat[4] fall into the same range of RBE and dose, although the choice of mean LET for Bateman's neutrons was difficult to make. The significant result is that Neary, Munson, and Mole found RBEs of about 10 in mice exposed to dose rates of the order of 1 rad per day of fission neutrons or x rays.[20] These RBEs are higher than those for cell killing by larger doses, and the curve relating QF and LET goes through the chronic irradiation values. QF then remains high, although the RBEs for somatic damage decrease at higher LETs, where the length of single-particle track becomes less than the diameter of a nucleus.

3. Principles of Dependence of RBE upon LET

a. RBE depends upon the "LET distribution," or, better, upon the distribution of local energy density at the submicroscopic level. There is no satisfactory "mean value" of LET.

b. RBE depends upon the size of individual dose necessary to produce the given end point. This is due to a greater curvature in the x-ray dose response curves than in those for higher LET radiation (Fig. 4). In cell survival, this means a smaller relative amount of intracellular recovery from sublethal injury (see below).

c. RBE depends upon dose rate. This is obvious when the time of irradiation rises above about an hour, so that intracellular recovery occurs before all the dose is given, and similarly when the dose per cell cycle becomes small, as in continuous irradiation. There are also some unexplained findings in dose-rate dependence of 4-day death in mice, presumed due to killing of the cells populating the crypts and villi in the intestinal mucosa. Hornsey et al. found a 30% increase in $LD_{50/4d}$ when the dose rate was 6000 rad/min instead of 100 rad/min.[15] Sondhaus et al. reported a similar effect.[23] Marcus and Sticinsky[18] and Fritz-Niggli[14] have reported increased efficiency in killing drosophila eggs at high dose rates. Marcus' experiments involved spacing dose fractions apart by seconds or by milliseconds. More experimental work is required here.

d. RBE depends upon the cellular sensitivity of cells in an organ, i.e., upon D_0 and extrapolation number, which in turn may depend upon the phase of cell in the cell cycle, i.e., upon whether the cell is "resting in G_0" or in some equivalent state; and upon whether the cells have been partially synchronized by previous irradiation or by any other means.

e. RBE may also depend upon the kinetics of the cells in an organ. This dependence may be in subtle ways connected with synchrony perhaps, since the gross proliferative rate of a cell population does not appear to be different after x rays or after high-LET radiation. Figure 5 illustrates this lack of difference for mouse skin irradiated with 250-kV x rays or by cyclotron neutrons with a modal energy of 6 MeV and a maximum energy of 18 MeV. Further, Westra and Barendsen[27] have found no difference in cell colony size distribution for the kidney cells after irradiation by x rays or polonium α particles. These observations are consistent with our earlier results on the skin of swine.[7] In an intact animal, the variation of RBE with LET may take the form that a different organ becomes predominant as a cause of death as the LET or dose is changed.

4. Evidence for Less Intracellular Recovery of Sublethal Injury After High-LET Radiation

Experiments with split doses on the skin of mice, pigs, and rats have shown that the amount of recovery which takes place in 24 hours--this includes the intracellular repair of sublethal injury, which is complete within a few hours, followed by progression of the partially synchronized cell population through the metabolic cycle, together with a certain amount of repopulation--is between half and two-thirds of that after x rays or 15-MeV electrons.

Figure 6 illustrates such experiments; the single-dose response curve is shown on the left, the split-dose response curve with a 24-hour interval between two equal fractions is shown on the right. If D_1 is the single dose required to produce the same average skin reaction (over 8 to 30 days--see Fig. 5) as the dose D_2 given as two fractions 24 hours apart, then $D_2 - D_1$ gives the 24-hour "recovery." Table 1 summarises the results, and shows that the recovery after cyclotron neutron irradiation is approximately half of that after x rays or electrons, in mouse skin. The lower half of the table gives results for pig skin, where six individual fractions of about 180 rads of neutrons or 600 rads of 8-MV x rays were found to give the same skin reaction as single doses of 800 or 2000 rads respectively. Again, the short-term "recovery" averaged over the five 3- or 4-day intervals is for the neutrons half as great as that for x rays. In rat skin, for five fractions in 4 days the average recovery in the 24-hour intervals is smaller, being about one third instead of one half.

In both the two-dose and six-dose fractionations, a proportion of the "recovery" is due to synchrony induced by the first dose and to some cellular repopulation. The proportions of these are not known, but synchrony even after a large first dose such as in the two-dose experiments is unlikely to increase $(D_2 - D_1)_{24h}$ by as much as the value of D_0.[28] The relative magnitudes of synchrony produced by x rays or fast neutrons are not known, and constitute a field where study is needed. It is possible that the two-fraction experiments demonstrate more synchrony and the six-fraction experiments more repopulation, so that the ratio of one half found in both cases for the recovery after fast

neutrons compared with x rays may be a coincidence. If so, the amount of "recovery" which corresponds to the "shoulder" of the cell survival curve may be somewhat less than one half, as suggested by the results on rat skin. It is, however, a practical value for considerations of radiotherapy using fast neutron beams.

Hornsey et al. found,[16] in split-dose experiments on 4-day death of mice, much less recovery after cyclotron neutrons than after x rays. Their values of $D_2 - D_1$ were 0 to 30 rads of neutrons and about 400 rads of x rays. The results were consistent with no recovery at all from the fast neutron irradiation, for an interval of 6 hours, during which most of the recovery in skin has already occurred. This shows that different organs show different degrees of short-term recovery, and we know little about such differences as yet.

5. Variation of RBE With Size of Single Dose in Mouse and Rat Skin, and in Rat Tumors

It has previously been pointed out that for skin reactions in pigs, the RBE decreased as the size of individual doses increased (Sec. 3b; Ref. 7). Table 2 summarises these results. Figure 7 shows this trend for the lower levels of damage, but at higher doses the hypoxic component of skin tissue controls the response, and the x-ray dose-response curve flattens out. This leads to higher RBEs at higher single doses--in some cases very much higher RBEs. This is to be expected if a proportion of the tissues is hypoxic, but would not be seen for rather small individual fractions.

Figure 8 shows an entirely similar result for the skin of rats' feet.[9] The RBE decreases to a minimum value of 1.48 just before the "breakaway" level at which the hypoxic response begins to predominate. Figure 9 shows that in a tumor in the same rats, where a greater proportion of hypoxic cells is present ($\geq 1\%$), the same effect is even more marked. The tumor is Dr. Thomlinson's RIB_5, an anaplastic fast-growing transplantable fibrosarcoma.[24, 25] The end point measured is the delay which the irradiation causes in the time to grow to 25 mm diameter.

Figure 10 compares the results (at top) with schematic cell survival curve expectations, and shows that they are in good agreement.

6. Comparison of the Effects of Fast Neutrons and x Rays on Skin and Tumors in Rats

Field, Thomlinson, and Jones have carried out a careful study of the relative skin and tumor responses in rats as described above, for one, two, and five fractions. They are seeking the best combination of high tumor response and low skin damage, as a guide to application of cyclotron neutrons in radiotherapy.[5, 10, 12, 13, 19] The results mentioned above, together with similar results for the two- and five-fraction schedules (with 24-hour intervals) allow a rather complete picture to be presented, with two provisos. One is that only these two tissues in the rat are compared; other pairs of tumor and normal tissue may give different results. The second is that experiments are required for larger numbers of fractions, especially to determine whether multifractionation with x rays can give better results than any number of neutron fractions, large or small.

Bearing these provisos in mind, we see in Fig. 11 a plot of tumor response (ordinates) vs skin damage (abscissa). The most advantageous results in radiotherapy are of course for maximum tumor response and minimum tumor injury, i.e., results in the upper left corner of the graph. Figure 10 shows that two or five fractions of x rays are better than a single dose; that one or five fractions of fast neutrons are better than the x rays; and that two fractions of neutrons give the best tumor response for a given degree of skin injury. The fact that the two-fraction curves are relatively high both for x rays and for neutrons may indicate some induced synchrony.

These results can only be taken to apply to the skin of rats' feet and to the fast-growing fibrosarcoma RIB_5. These results are, as far as they go, encouraging for fast-neutron therapy, but different pairs of normal tissues and tumors may give different results. Other exposures, such as might be received in accidental overdoses, would have to be evaluated on the basis of a knowledge of the effect of x rays or fast-neutron doses of the appropriate magnitude on the irradiated organs.

7. Acknowledgments

The author has pleasure in acknowledging stimulating discussions with Dr. T. Alper, Dr. S. Hornsey, Dr. R. H. Thomlinson, Dr. D. K. Bewley, Dr. G. W. Barendsen, Miss J. Denekamp, and Dr. S. B. Field. Thanks are due to Dr. Field, Dr. Thomlinson, and Dr. Jones and to the Editors of the British Journal of Radiology for permission to publish Figs. 8, 9, 10, and 11. Figures 4, 5, and 6 are published by permission of the Editor of Radiation Research.

8. References

1. T. Alper, Ann. Rev. Nucl. Sci., 10 (1960).

2. G. W. Barendsen, in Biophysical Aspects of Radiation Quality, Tech. Report Series No. 58 (IAEA, Vienna, 1966).

3. G. W. Barendsen, M. H. Walter, J. F. Fowler, and D. K. Bewley, Radiation Res., 18: 106 (1963).

4. J. L. Bateman, H. H. Rossi, V. P. Bond, and J. Gilmartin, Radiation Res., 15: 694 (1961).

5. D. K. Bewley, Brit. J. Radiol., 36: 81 (1963); Radiology, 86: 251 (1966).

6. D. K. Bewley, in Report of 2nd Panel on Biophysical Aspects of Radiation Quality (IAEA, Vienna, 1967).

7. D. K. Bewley, J. F. Fowler, R. L. Morgan, J. A. Silvester, B. A. Turner, and R. H. Thomlinson, Brit. J. Radiol., 36: 107 (1963).

8. J. Denekamp, J. F. Fowler, K. Kragt, C. J. Parnell, and S. B. Field, Radiation Res., 29: 71 (1966).

9. S. B. Field, R. H. Thomlinson, and T. Jones, Brit. J. Radiol. (in press).

10. J. F. Fowler, in Modern Trends in Radiotherapy, T. J. Deeley and C. A. P. Wood, Eds. (Butterworths, London, 1967), Chap. 8.

11. J. F. Fowler, and J. Denekamp, 1966. Abstract No. 340, 3rd Int. Conf. Rad. Res., Cortina.

12. J. F. Fowler and R. L. Morgan, Brit. J. Radiol, 36: 115 (1963).

13. J. F. Fowler, R. L. Morgan, and C. A. P. Wood, Brit. J. Radiol., 36: 77 (1963).

14. H. Fritz-Niggli, private communication, 1967).

15. S. Hornsey and T. Alper, Nature, 210: 212 (1966).

16. S. Hornsey, S. Vatistas, D. K. Bewley, and C. J. Parnell, Brit. J. Radiol., 38: 878 (1965).

17. ICRP, Report of the RBE Committee, Health Physics, 9: 357 (1963).

18. B. Marcus and E. Sticinsky, Strahlentherapie, 115: 394 (1963).

19. R. L. Morgan, in Modern Trends in Radiotherapy, T. J. Deeley and C. A. P. Wood, Eds. (Butterworths, London, 1967), Chap.

20. G. J. Neary, R. J. Munson, and R. H. Mole, Chronic Radiation Hazards (Pergamon Press, 1957).

21. W. Rosenzweig and H. H. Rossi, Radiation Res., 10: 532 (1959).

22. H. H. Rossi, Radiology, 78: 530 (1962).

23. C. A. Sondhaus, J. K. Ashikawa, C. A. Tobias, L. L. Kayfetz, S. O. Stephens, and M. P. Donovan, 3rd International Conference on Radiation Research, Cortina, 1966, Abstract No. 821.

24. R. H. Thomlinson, in Fundamental Aspects of Radiosensitivity (Brookhaven Symposia in Biology No. 14), p. 204, 1961.

25. R. H. Thomlinson, in Scientific Basis of Medicine Annual Reviews (Athlone Press, 1965).

26. R. H. Thomlinson, in Modern Trends in Radiotherapy, T. J. Deeley and C. A. P. Wood, Eds. (Butterworths, London, 1967).

27. A. Westra and G. W. Barendsen, 3rd International Conference on Radiation Research, Cortina, 1966, Abstract No. 934.

28. J. M. Young, private communication, 1967.

Table 1. Recovery in skin.

24-Hour recovery in mouse skin
(Denekamp et al., Ref. 8)

Radiation	Single Dose	$D_2 - D_1$ (rads)	$(D_2 - D_1) \times$ RBE
Cyclotron neutrons	1100 - 1700	135 - 190	230 - 325
250-kV x rays	2000 - 3000	420 - 540	420 - 540
15-MeV electrons	2500 - 3500	480 - 680	380 - 540

Short-term recovery in pig skin
(from 6 fractions in 17 days--Bewley et al., Ref. 7)

	D_1	$(D_6 - D_1)/5$	$\frac{D_6 - D_1}{5} \times$ RBE
Cyclotron neutrons	800	60	150
8-MV x rays	2000	300	300

Short-term recovery in rat skin (from 5 fractions in 4 days--Field, Thomlinson, and Jones, Ref. 9)

	D_1	$(D_5 - D_1)/4$	$\frac{D_5 - D_1}{4} \times$ RBE
Cyclotron neutrons	1000	60	120
250-kV x rays	2000	400	400

Table 2. Variation of single-dose RBE in skin with size of dose.

Skin of rats' feet (Ref. 9)

Neutron dose	x-Ray dose	x Rays/neutrons ratio
600	1260	2.10
900	1440	1.60
1200	1770	1.48
1500	2540	1.70
1800	3770	2.10

Skin of mice's feet (Ref. 8)

Neutron dose (rads)	RBE relative to x rays	RBE relative to 15-MeV electrons
800	---	1.62 - 2.34
1000	1.35 - 1.57	1.56 - 2.0
1200	1.5 - 1.7	1.67 - 2.57
1400	1.6 - 1.7	1.7 - 2.9
1500	1.9 - 2.3	---
1700	2.2 - 2.4	---

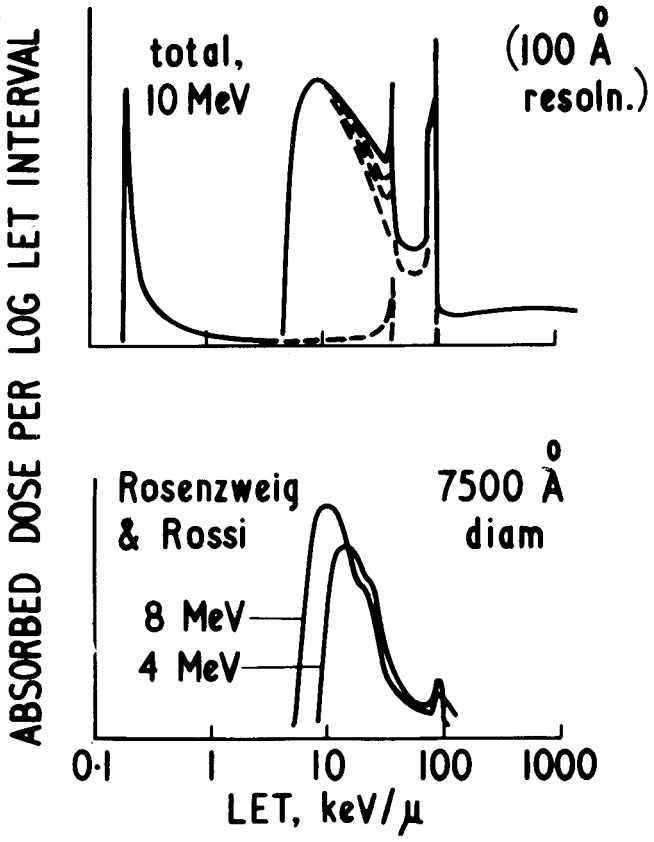

Fig. 1. Fast neutron spectra (calculated after Howard-Flanders). Below: as measured by a tissue-equivalent proportional counter.

T. Alper, 1960 503

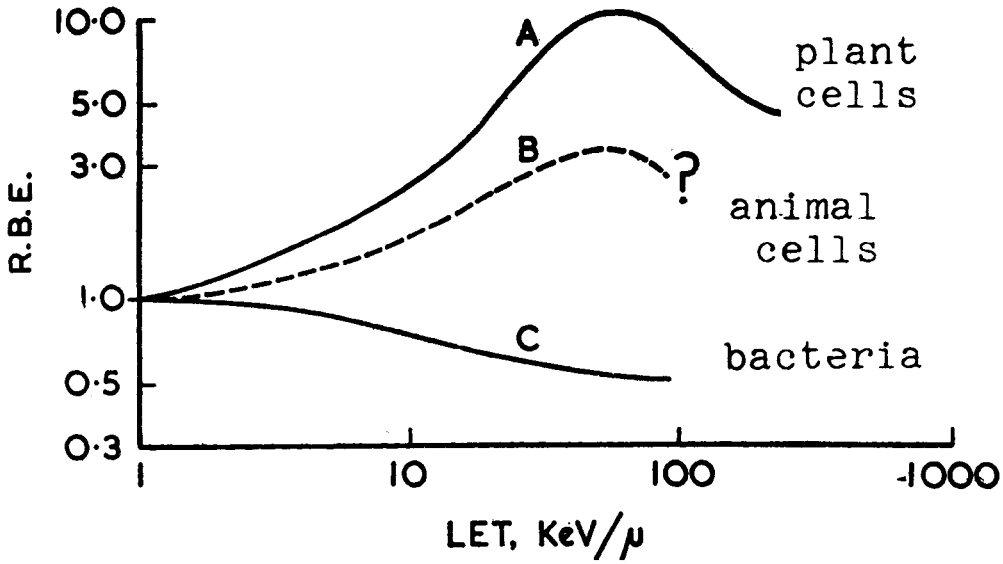

Fig. 2a. RBE versus LET for three different types of biological system: schematic (Ref. 1). Upper curve: Plant systems. Middle curve: Mammalian systems. Lower curve: Virus and enzymes.

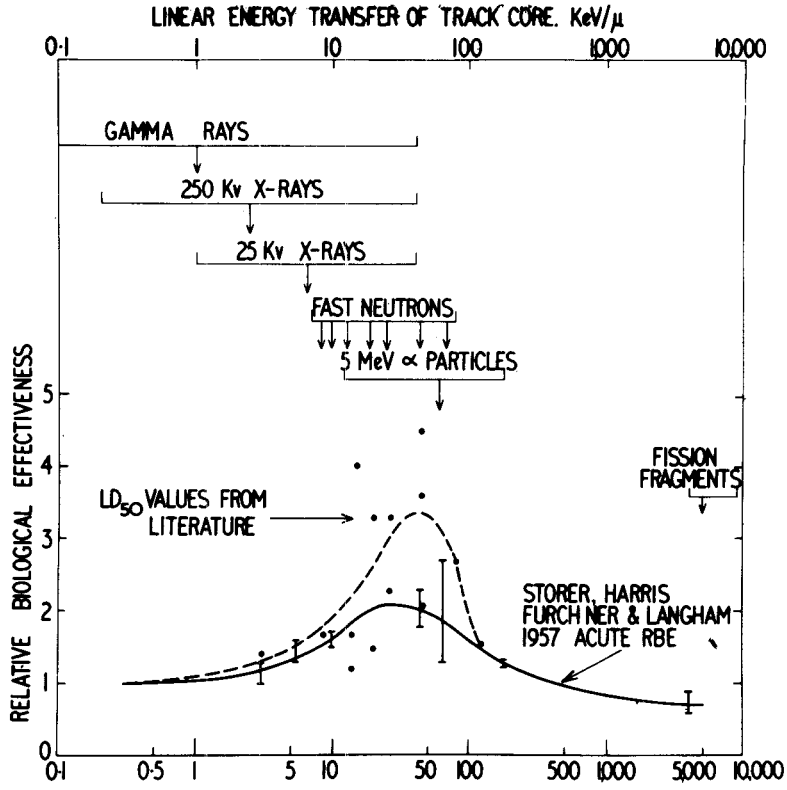

Fig. 2b. RBE for LD_{50} - 30 day death of mice versus LET (Ref. 13).

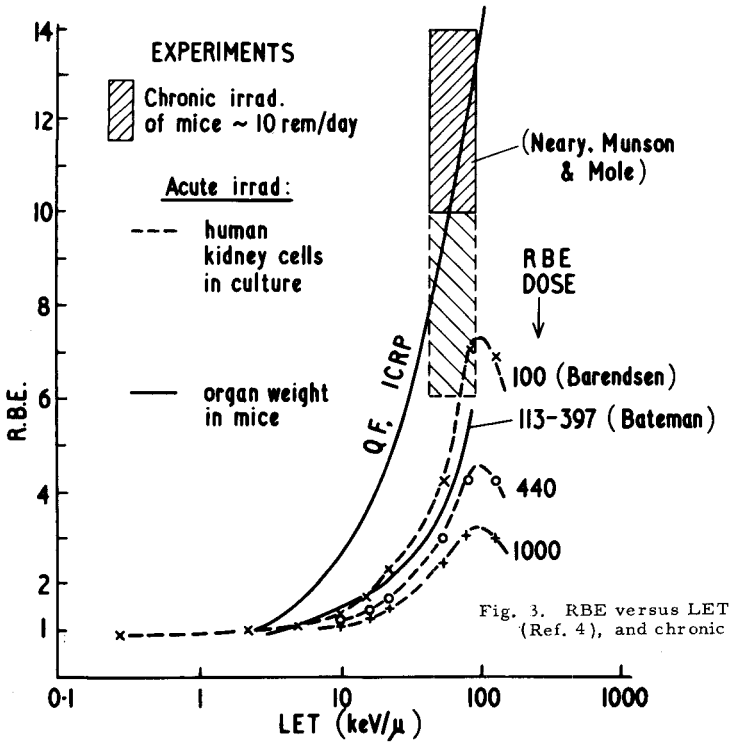

Fig. 3. RBE versus LET for cell killing (Ref. 2), organ weight loss in mice (Ref. 4), and chronic irradiation of mice with fission neutrons (Ref. 20).

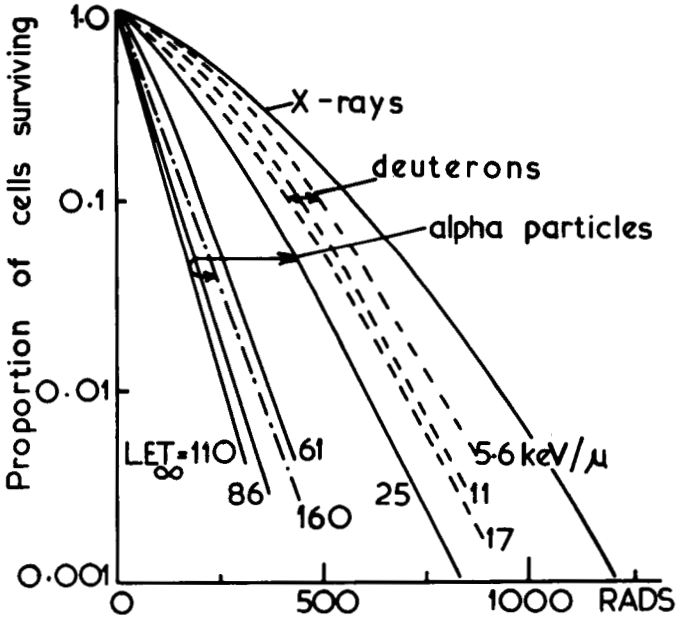

Fig. 4. Proliferative survival of kidney T-cells in tissue culture at various values of LET_{∞} (particle track-segment experiments, Ref. 3).

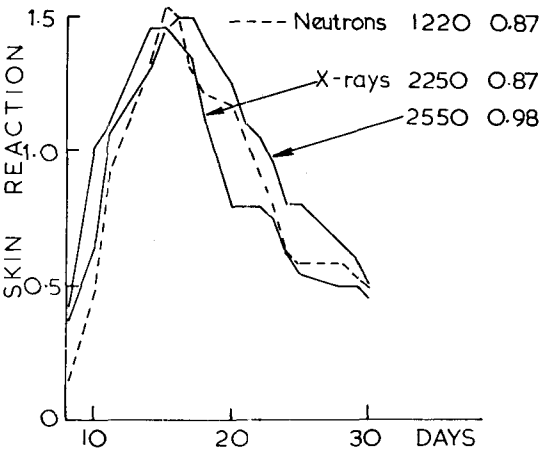

Fig. 5. Daily skin reactions in two groups of mice irradiated by cyclotron neutrons and one by 250-kV x rays. The maximum responses are matched; the test is to see whether the rates of increase and decrease differ (Ref. 8).

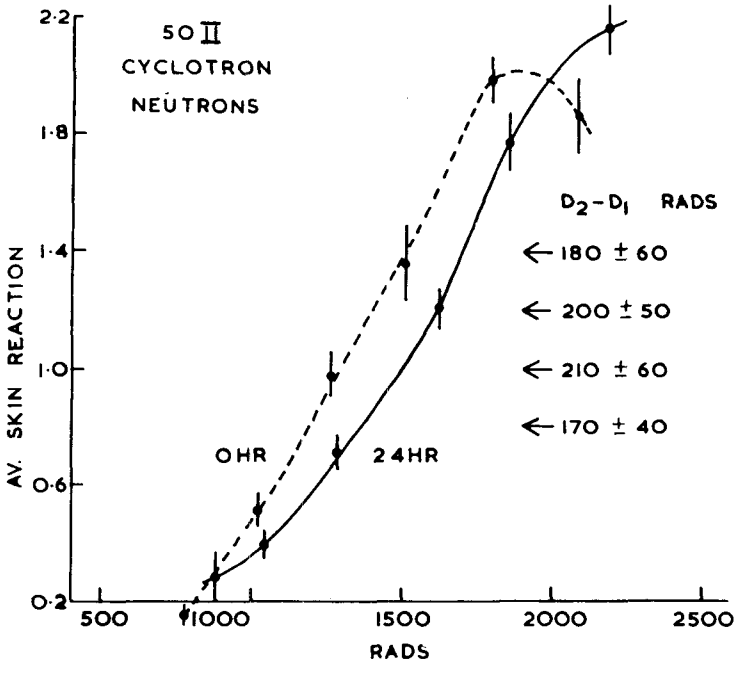

Fig. 6. Split-dose experiment on mouse skin with cyclotron neutron irradiation. Left-hand curve, single doses. Right-hand curve, two equal doses given at 24-hour intervals. The displacement of this second curve gives the total "recovery" (D_2 - D_1) occurring in 24 hours after a first dose of 1000 to 2000 rads of fast neutrons (Ref. 8).

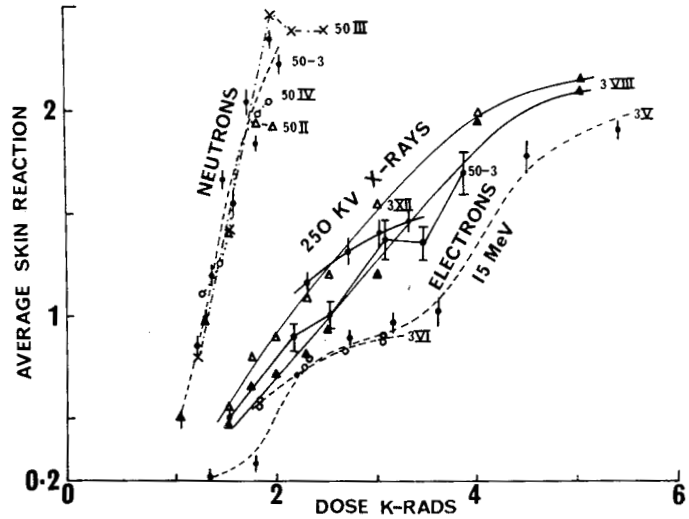

Fig. 7. Single-dose response curves for skin reactions (8 to 30 days) in mouse feet, for neutrons, 250-kV x rays, and 15-MeV electrons. The increase of RBE above x-ray or electron doses of about 2000 rads is attributed to hypoxia of the skin (Ref. 8).

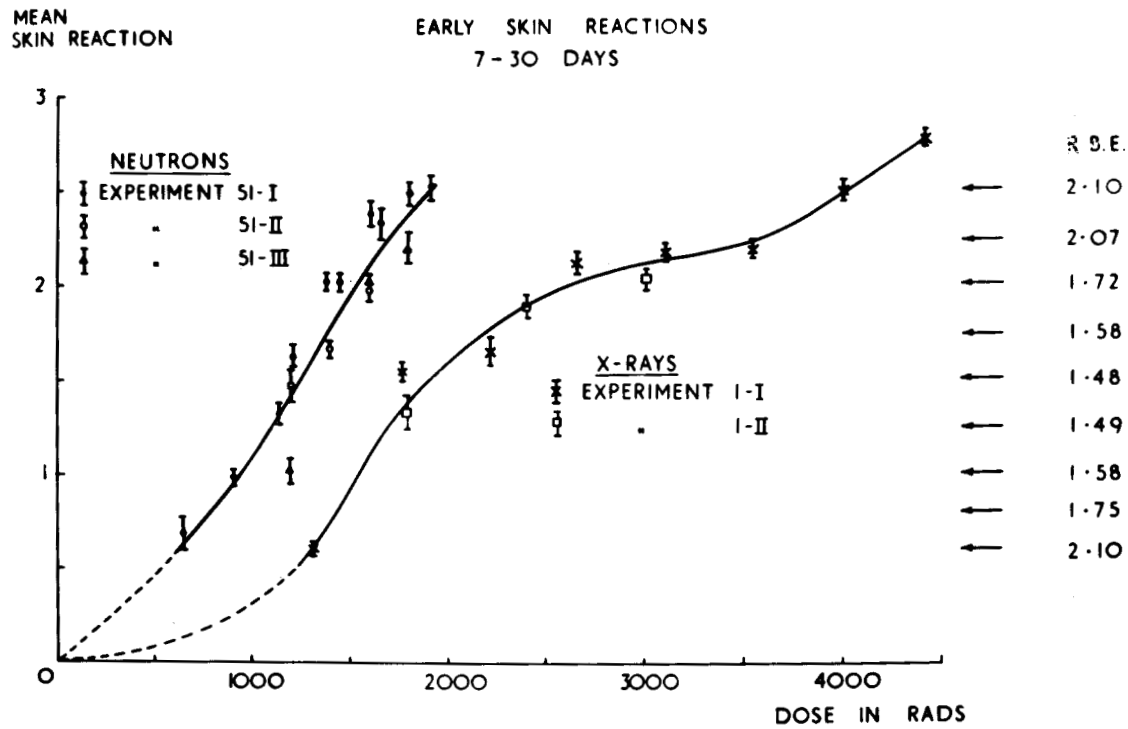

Fig. 8. Single-dose response curves for skin reactions in rat feet after fast neutron or 250 kV x-irradiation (Ref. 9).

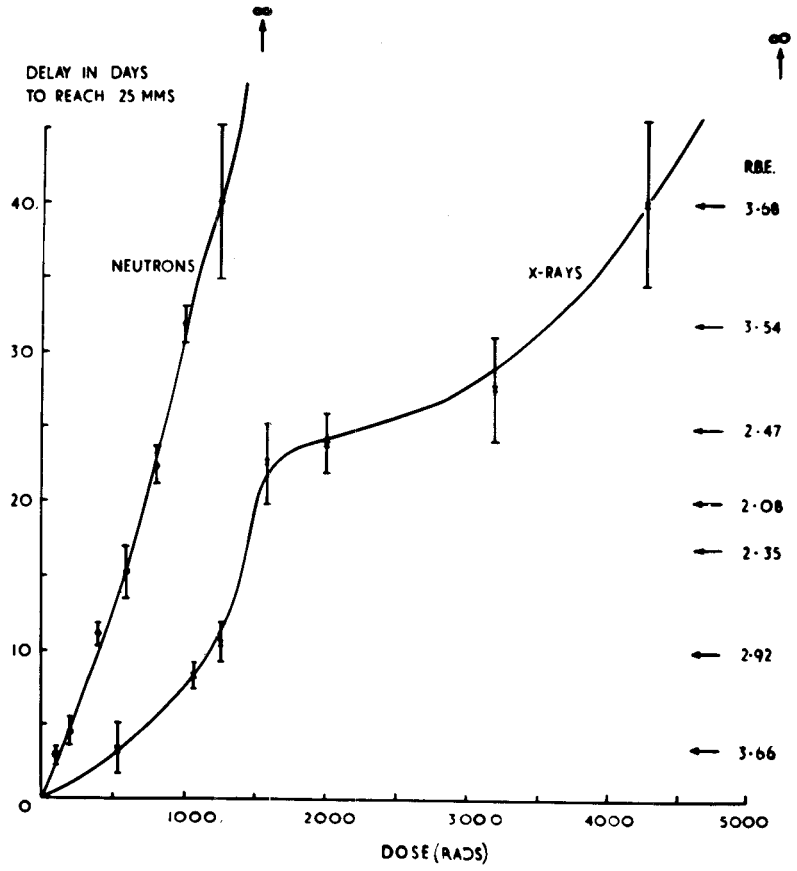

Fig. 9. Delay in growth of RIB_5 rat fibrosarcoma to 25 mm diameter (difference from unirradiated tumors) versus single dose of fast neutrons or 250-kV x rays.

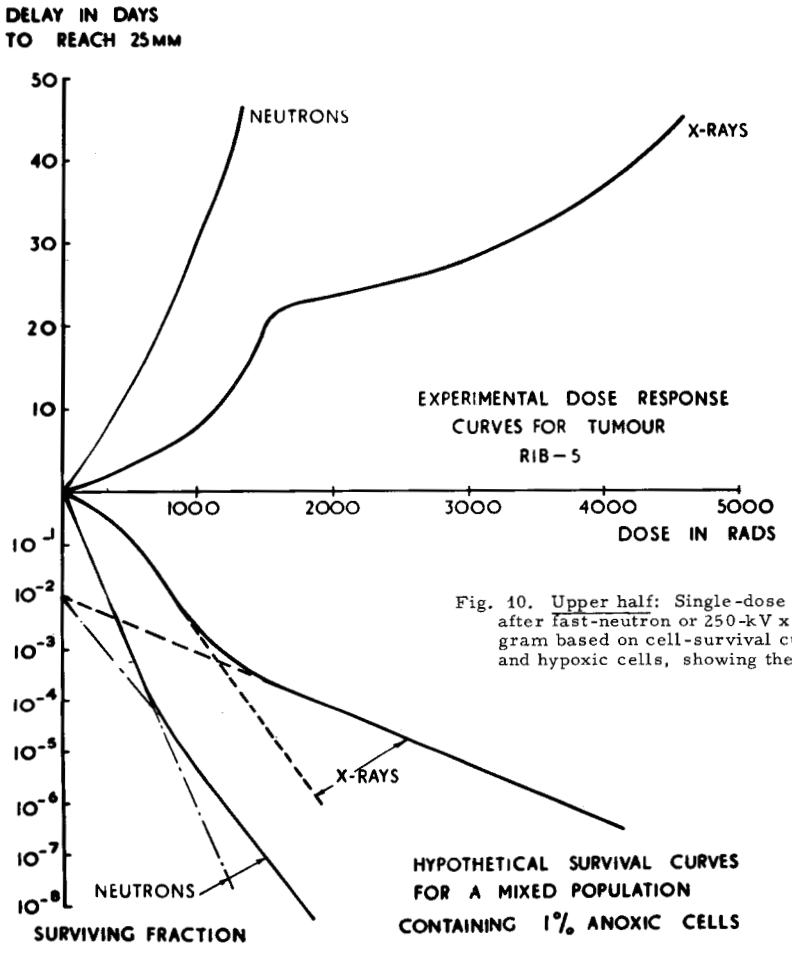

Fig. 10. Upper half: Single-dose response curves for delay in tumor growth after fast-neutron or 250-kV x irradiation. Lower half: Schematic diagram based on cell-survival curves for a mixed population of oxygenated and hypoxic cells, showing the similarity of results (Ref. 9).

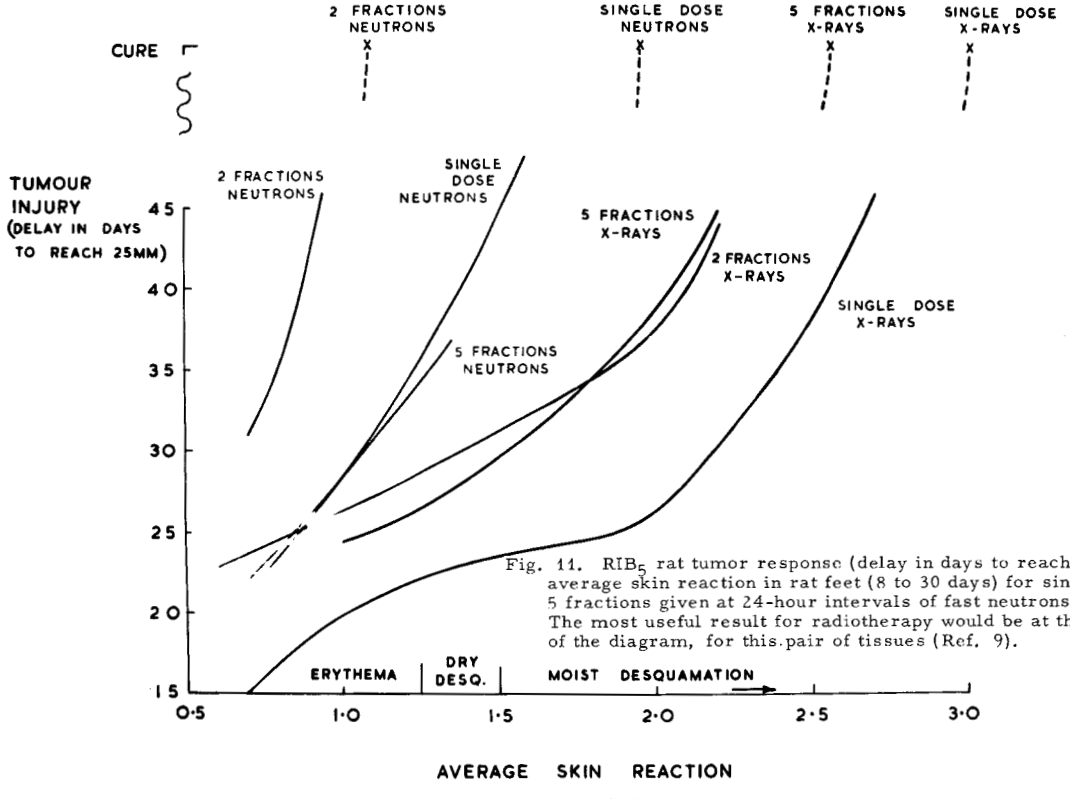

Fig. 11. RIB_5 rat tumor response (delay in days to reach 25 mm) versus average skin reaction in rat feet (8 to 30 days) for single dose or 2 or 5 fractions given at 24-hour intervals of fast neutrons or 250-kV x rays. The most useful result for radiotherapy would be at the upper left corner of the diagram, for this pair of tissues (Ref. 9).

RECENT STUDIES AMONG PERSONS EXPOSED TO RADIATION FROM MILITARY OR INDUSTRIAL SOURCES: A REVIEW

LEONARD A. SAGAN, M. D.
DIVISION OF BIOLOGY AND MEDICINE
U. S. ATOMIC ENERGY COMMISSION

The largest group of persons exposed to large amounts of radiation have received such exposures for therapeutic purposes. The smaller group of non-clinically exposed persons, however, provides information not otherwise available. Radiation effects examined in persons therapeutically irradiated are subject to bias because of patient selection, possible effects of other therapeutic modalities and of the underlying disease itself. Accidents to healthy humans provide information not handicapped by these confounding variables. The following review summarizes recent studies among persons exposed externally either in industrial accidents or from military sources. The acute radiation syndrome among accidentally exposed persons has recently been summarized.[1]

Sources of information:

1. Industrial exposures. (Table 1)

2. Marshall Island exposures. On March 1, 1954, due to an unexpected shift of winds, sixty-four persons on Rongelap Island, 105 miles from the Bikini Test Site, were accidentally exposed to fallout irradiation.[14] The mean dose to the population was estimated to be 175 rads whole-body gamma radiation plus contamination of the skin sufficient to result in beta burns and slight internal absorption of radioactive materials through inhalation and ingestion. These persons, in addition to Marshallese who were away from the island at the time but who subsequently returned and serve as controls, have been examined at yearly intervals since.

3. In the same episode as cited above, 23 Japanese fishermen were irradiated aboard the fishing boat, Lucky Dragon.[15] Estimates of the doses for the individual crew members range from 170 to 700 rads. One of the heavily irradiated men subsequently died although the relationship of his death to previous radiation exposure is not clear. These survivors have also been examined at regular intervals.

4. Hiroshima and Nagasaki survivors of the atomic bomb. Under auspices of the National Academy of Sciences, a selected sample of Japanese survivors of the two bombings of Hiroshima and Nagasaki together with controls have been carefully studied for late effects of radiation exposure at the Atomic Bomb Casualty Commission (ABCC). Radiation dose for each individual, including a consideration of shielding, has been calculated, but remains tentative.

TABLE 1

ACCIDENTAL EXPOSURE TO IONIZING RADIATION IN INDUSTRY

	Location	Date	Persons Exposed	Reference
1.	Los Alamos	1945	2	2
2.	Los Alamos	1946	8	2
3.	Argonne	1952	4	3
4.	U.S.S.R.	?	2	4
5.	Oak Ridge	1958	8	5
6.	Vinca	1958	6	6
7.	Los Alamos	1958	3	7
8.	Lockport	1960	9	8
9.	Wisconsin	1961	1	9
10.	Hanford	1962	3	10
11.	Mexico	1962	5	11
12.	Illinois	1965	1	12
13.	Belgium	1965	1	13
			53	

5. Residents of southwestern Utah. Residents of Utah were exposed to fallout from the Nevada Test series ending in 1962. Although considerable uncertainty exists, one estimate of mean exposure to the thyroid gland of children living in the area from radioiodine (195 2-6) is 50 rads.[16] Others have speculated that certain individuals may have received far more.

Leukemia

Because the leukemogenic effect of radiation, being rather weak, can only be detected in large populations, one would not anticipate statistical evidence of this effect in a population less than several thousand in size. Therefore, of the various populations under consideration here, only the ABCC population is of sufficient size and character to allow study of radiation leukemogenesis. Within the past year, a summary of leukemia studies at the Atomic Bomb Casualty Commission has been published.[17] Several conclusions can be drawn from this work that are of interest:

1. In addition to the first incidence peak that occurred in about 1952, there was a second peak in 1958.

2. Whereas the first peak consisted about equally of cases of chronic and acute leukemia, the second peak was predominantly of acute leukemia.

3. There were five times as many persons less than thirty years of age at the time of bombing who developed acute leukemia during the first peak whereas during the second peak acute cases among younger and older persons were about equal.

4. Chronic leukemia was found most commonly among those very young at the time of bombing during both peak periods.

In conclusion, the relationship between radiation and subsequent leukemogenesis is a complex one and involves many variables, all of which are not understood; for instance, the above noted studies are at considerable variance with the data of Court-Brown,[18] who noted a peak incidence of leukemia at 3-5 years following irradiation in contrast with a peak among Japanese survivors at 8 years. The explanation for this difference is not clear.

Although hematologic effect during the acute response to whole-body irradiation has long been recognized, more subtle cytogenetic changes have only recently been recognized as techniques have become available for their demonstration. Cytogenetic studies in several populations have demonstrated persistent chromosomal anomalies. These several studies are summarized in Table 2. At the present time all of these persons seem to be otherwise well and there seems to

TABLE 2

CYTOGENETIC CHANGES IN ACCIDENTALLY EXPOSED PERSONS

Population		Fraction of Persons Exposed Demonstrating Exchange-Type Anomalies	Control	Reference
1. Japanese Fishermen	1954	7/11	0/11	15
2. Atomic Bomb Casualty Commission	1945	33/94	1/94	19
3. Oak Ridge Employees	1958	6/6	-	20
4. Marshallese	1954	16/43	0/8	21

be no clear-cut relationship between dose and degree of abnormality, nor is there any understanding of a relationship between karyotypic changes and leukemias, if any. Dr. Goh of Oak Ridge Institute of Nuclear Studies has described, in addition to exchange-type chromosomal changes, an abnormally formed chromosome of the G group which resembles the Philadelphia chromosome of chronic myelogenous leukemia.[20] These abnormal forms have been found in all six of the exposed Oak Ridge workers who have so far been examined. Whether or not these forms are identical to the Philadelphia chromosome or what relationship they may bear to it is not known.

Thyroid

Although thyroid disease had been described in clinically irradiated populations[22] there were no reports of thyroid pathology in nonclinically irradiated populations until 1963, since which time three different studies have generated new information on the effects of both X irradiation and radioiodine on the thyroid gland.

In 1963, reporting a summary of clinical examinations of survivors in both Hiroshima and Nagasaki, Socolow[23] noted histologic demonstration of thyroid carcinoma in seven subjects under 20 years of age and in 12 subjects over 20 years of age, incidence rates about equal. These were detected through clinical examination and biopsy and were largely asymptomatic lesions.

A second study of thyroid carcinoma among survivors was carried out in the ABCC autopsy population by Zeldis.[24] The thyroid gland in 1253 consecutive autopsies was examined. Although thyroid carcinoma showed a dose dependency, none of the lesions had contributed to mortality.

These ABCC studies noted above are quite consistent with clinical experiences in which thyroid carcinogenesis has been noted with x-ray exposures above 100 rads.[22] On the other hand, information regarding the relative neoplastic effect of radioiodine has not been available until recently. Animal studies would indicate far less neoplastic potential from radioiodine than with x ray.[25] Therefore, the following two studies are of particular interest.

Within the past year, a report of findings of thyroid pathology among Marshallese who were exposed to whole-body external radiation as well as that from absorbed radioiodine has been published.[26] Of the 19 children accidentally irradiated with estimated thyroid dose of 700 to 1400 rads, plus an additional 175 rads whole-body radiation, 68 percent have now developed thyroid nodules and an additional two children were found to have hypothyroidism.[27]

Among those above age 10 at the time of exposure, 3 of 44 or about 9 percent developed thyroid nodules-one of which was found to be malignant. Estimated dose to the adult thyroid was 300 rads.

Another population presumably exposed to radioiodine from fallout which has been recently studied is the 2000 children living in the area of Utah northeast of the Nevada test site. Although no publications of this data are yet available, preliminary analyses of the data do not indicate the presence of radiation-related lesions.[28] A single case of previously unsuspected hypothyroidism was uncovered.[29]

Hypothyroidism has also been found among two of the Marshallese children[26] and one of the persons accidentally irradiated[30] at Los Alamos in 1946 was subsequently found to be myxedematous in 1956. All of these cases have appeared at about 10 years post-irradiation; however, a causal relationship remains highly speculative. Nevertheless, these clinical findings together with some recent experimental studies in dogs[31] in which thyroid atrophy followed only moderate doses of x irradiation justify attention.

Early Aging

Although a great deal of information has been collected demonstrating accelerated aging among various animal populations,[30] this effect has not yet been persuasively demonstrated among humans, either through physiologic measurements[31] or through mortality studies.[32] A recent publication does indicate increased hexosamine: collagen ratios among tissues of survivors as compared with controls,[33] but the significance of this finding remains to be elucidated.

Fertility

Recently published studies of spermatogenesis following accidental radiation bear on radiation effects on the gonads.

Survivors of the Hiroshima bombing demonstrated depressed sperm counts,[34] particularly within 0.9 mile, where only 13% of men tested had sperm counts above 40,000/cm^2 compared to 60% beyond that distance. This effect was transient and was manifest only during the immediate post-attack period.

Of the 23 Japanese fishermen accidentally radiated on the Lucky Dragon on March 1, 1954, with estimated whole-body radiation of 170-700 R, all became relatively aspermic, sperm counts returning to normal levels in about two years. No children were born to the wives of the group during 1954 or all of 1955; however, several normal children were born subsequently.

These data are in agreement with experimental human data,[35] which indicate aspermia universally with exposures above 100 rads with duration of suppression related to degree of exposure. Doses of 15 R will produce a moderate oligospermia.

Morphologic evidence of testicular atrophy following an acute radiation insult has been long known[36] but only recently have chronic changes been described.[37] Jordan et al, examining autopsy material among atomic bomb survivors, have found a highly significant excess of tubular sclerosis and vascular hyalinization in testicular tissues. These differences became even more significant when the study sample was limited to exposed survivors with estimated exposures of more than 300 rads.

Studies of live births to survivors of both cities shows no relationship to distance from the hypocenter at time of bomb. Birth rates for the small number of exposed women of Rongelap have been greater than those of the Marshallese as a whole.

It would appear, then, that reproductive capacity is unimpaired among irradiated females although a temporary infertility following exposure is not excluded.

Growth and Development

The first suggestion of growth retardation among irradiated children was published by Reynolds[39] in 1954. His study of atomic bomb survivors was hampered, however, by the problem of matching controls for nutritional and other socio-economic factors. More recent study[40] of exposed Marshallese children substantiates such an effect, particularly among younger boys, but not among girls. Following publication of those findings, two of the most severely retarded boys were found to be hypothyroid[24] and two other children have what appears to be incipient hypothyroidism, thus supplying a possible mechanism for at least some of the growth retardation. Subsequent to therapy, both hypothyroid boys have shown a growth spurt.

Cataracts

Although there can be no question that radiation produces cataracts, dose-response relationships here have been extremely difficult to establish. Changing clinical procedures, inter-observer variation, and lack of a clear definition of radiation cataract makes interpretation of data difficult if not impossible.

Several studies from ABCC have produced contradictory results, although in each case radiation cataracts were detected.[41] Visual impairment was rare. The most recent and extensive study has not yet been published. Cataracts have also been reported among the Marshallese, and the Los Alamos criticality victims. Woods[42] report of a study of 13 cyclotron workers estimated that 80 rads of fast neutrons is a cataractogenic dose producing visual impairment.

Discussion and Summary: Although a clear understanding of human radiation effects must await an understanding of the mechanism of action of radiation

at a cellular and subcellular level, studies of persons exposed to radiation through industrial and military sources will continue to shed light on sequaelae of radiation exposure. It is therefore important that records of such persons so exposed and the degree of exposure be maintained. Studies of the subsequent health of these persons will provide information not otherwise available on acute radiation effects among healthy persons.

Animal studies and human studies suggest problem areas that lend themselves to investigation among these human populations. They are as follows:

1. Dose - response relationships. Although this may be the most critical problem facing investigators of human radiation effects, the difficulty of assembling sufficiently large populations with low-level exposure and suitable controls may be insurmountable.

2. Synergistic effect of other environmental hazards with radiation in the induction of late effects.

3. Dose - rate effects. Although it is well known that the acute radiation syndrome is highly dose-rate-dependent, it is not known whether or not late effects are also dose-rate-dependent to the same degree; recent evidence with respect to repair mechanisms would suggest that it is.

4. Accelerated aging. Although accelerated aging is widely accepted to be an effect of radiation, at least as interpreted from animal studies, neither the nature of aging nor the mechanisms of radiation effects are understood. The matter has widespread biologic significance and requires resolution.

5. Relative biologic effectiveness of particular radiation.

REFERENCES

1. V. P. Bond, T. M. Fliedner, and J. O. Archambeau, Mammalian Radiation Lethality, Chapter 6, Academic Press, New York, 1965.

2. L. H. Hempelmann, H. Lisco, and J. G. Hoffman, The Acute Radiation Syndrome, A Study of Nine Cases and a Review of the Problem, Ann. Intern. Med. 36, 280-510, 1952.

3. R. J. Hasterlik and L. D. Marinelli, Physical Dosimetry and Clinical Observations on Four Human Beings Involved in an Accidental Critical Assembly Excursion, Proc. Intern. Conf. Peaceful Uses Atomic Energy, Geneva, 2, 25-34, 1955.

4. A. K. Gerskova and G. D. Baisogolov, Two Cases of Acute Radiation Disease in Man, Proc. Intern. Conf. Peaceful Uses Atomic Energy, Geneva, 3, 35-44, 1956.

5. M. Brucer, Compiler, the Acute Radiation Syndrome, A Medical Report on the Y-12 Accident, June 16, 1958, USAEC Report-ORINS, April, 1959.

6. B. Pendic, the Zero Energy Reactor Accident at Vinca in Diagnosis and Treatment of Acute Radiation Injury, Proc. Sci. Meeting Atomic Energy Agency and World Health Organ., Inter. Doc. Service (Columbia Univ. Press) New York 1961.

7. T. L. Shipman (Ed.), Acute Radiation Death Resulting From an Accidental Nuclear Critical Excursion, J. Occupational Med. (Spec. Suppl.) 3, 146-192, 1961.

8. J. W. Howland, M. Ingram and C. L. Hansen, The Lockport Incident: Accidental Partial Body Exposure of Humans to Large Doses of X-Irradiation, in Diagnosis and Treatment of Acute Radiation Injury, Proc. Sci. Meeting Intern. Atomic Energy Agency and World Health Organ., Intern. Doc. Serv. (Columbia Univ. Press) New York, 1961.

9. C. Rossi, A. H. Thorngate and C. F. Larson, Acute Radiation Syndrome Caused by Accidental Exposure Cobalt-60, J. Lab. Clin. Med., 59, 655-666, 1962.

10. P. A. Fuqua, Final Medical Report of Accidental Excursion, Recuplex Operation 234-5 Facility, 4/7/62, Hanford Lab. Rept. HW 81010, 1964.

11. G. Andrews, Mexican Co^{60} Radiation Accident, Isotopes and Radiation Technology, 1, 200-201, 1963-64.

12. L. H. Lanzl, M. L. Rozenfeld, and A. R. Tarlov, High Dose Human Exposure From a 10-Mev Linear Accelerator, Proc. USAEC First Symposium Accelerator Radiation Dosimetry and Experience (Brookhaven) Div. Tech. Inform. USAEC 1965.

13. H. Jammet, R. Gongora, R. LeGo, and G. Marble, Observation Clinique et Traitment D'Un Cas D'Irradiation Globale Accidentelle. Abstract #164, First Internat. Congress of the International Radiation Protection Assoc. Sept. 5-10, 1966, Rome, Italy.

14. K. A. Conard et al, Medical Survey of the People of Rongelap and Utirik Islands Nine and Ten Years after Exposure to Fallout Radiation (March 1963 and March 1964) Brookhaven National Laboratory, BNL 908 (T-371).

15. T. Kumatori, T. Ishihara, T. Veda, and K. Miyoshi, Medical Survey of Japanese Exposed to Fallout Radiation in 1954, National Inst. of Radiological Sciences (Japan) Dec. 1965.

16. A. R. Tamplin and H. L. Fisher, Estimation of Dosage to Thyroids of Children in the U. S. from Nuclear Tests Conducted in Nevada During 1952 Through 1956, UCRL-14707 Lawrence Radiation Laboratory, University of California, Livermore, California, May 10, 1966.

17. O. J. Bizzozero, K. G. Johnson, A. Ciocco, Radiation - related leukemia in Hiroshima and Nagasaki, 1946-1964, New Eng., J. Med. 274, 1095, 1966.

18. W. M. Court Brown, R. Doll, Mortality from Cancer and other Causes after Radiotherapy for Ankylosing Spondylitis, Brit. Med. J. 2, 1327, 1965.

19. A. D. Bloom et al., Cytogenetic Investigation of Survivors of the Atomic Bombings of Hiroshima and Nagasaki, Lancet, 672, Sept. 24, 1966.

20. K. Goh, Smaller G. Chromosome in Irradiated Man, Lancet 1, 659-660, 1966.

21. H. Lisco, Progress Report to the Atomic Energy Commission, 1966.

22. R. H. Murray and L. H. Hempelmann, A Review of the Tumor Incidence in Children Irradiated for Benign Conditions, 282-293 Radioactivity in Man, G. R. Meneely, ed., Charles C. Thomas, Springfield, Ill., 1961.

23. E. L. Socolow, A. Hashizome, S. Heriishi, and R. Niitani, Thyroid Carcinoma in Man after Exposure to Ionizing Radiation: A Summary of the Findings in Hiroshima and Nagasaki, New Eng. J. Med. 268, 406, 1963.

24. L. T. Zeldis, S. Jablon, and M. Ishida, Current Status of ABCC-New Studies of Carcinogenesis in Hiroshima and Nagasaki, Ann. N. Y. Acad. Sci. 114, Article 1, 225-240, 1964.

25. E. L. Saenger, R. A. Seltzer, T. D. Sterling, and J. G. Kereiakes, Carcinogenic Effects of I^{131} Compared With X-Irradiation - A Review, In Biology and Radioiodine, Ed. L. K. Bustad, Pergamon Press, Oxford, 1964.

26. R. A. Conard, J. E. Rall, and W. W. Sutow, Thyroid Nodules as a Late Sequela of Radioactive Fallout, New Eng. J. of Med. 274, 1392-1399, 1966.

27. R. A. Conard, Report to the Atomic Energy Commission, 1966.

28. E. Weiss, Personal Communication.

29. M. L. Rallison, Unpublished Data.

30. L. Hempelmann, Eighteen Year Follow-up of Survivors of the 1945 and 1946 Nuclear Accidents at Los Alamos, Progress Report to the Division of Biology and Medicine, U. S. Atomic Energy Commission.

31. S. M. Michaelson, W. Quinlan, G. W. Casarett and W. B. Mason, Radiation-Induced Thyroid Dysfunction in the Dog, Rad. Res. 30, 38, 1967.

32. Upton, A. C., Ionizing Radiation and Aging Process, J. Geront. 12, 306, 1957.

33. J. W. Hollingsworth, A. Hashizume, and S. Jablon, Correlations Between Tests of Aging in Hiroshima Subjects - An Attempt to Define "Physiologic Age," Yale J. Biol. and Med. 38, 11, 1965.

34. S. Jablon, M. Ishida, M. Yamasaki, JNIH-ABCC Life Span Study Hiroshima and Nagasaki, Report 3. Mortality from October 1950-September 1960, ABCC TR 15-63.

35. R. E. Anderson, The Hexosamine Collagen Ratio as a Measure of Biochemical Age in Hiroshima Atomic Bomb Survivors, Am. Heart J., 70, 283, 1965.

36. A. W. Oughterson, and S. Warren, Medical Effects of the Atomic Bomb in Japan, 159, McGraw-Hill, New York, 1956.

37. C. G. Heller, P. Wooton, M. J. Rowley, M. F. Lalli, and D. R. Brusca, Action of Radiation Upon Human Spermatogenesis, Proc. VI Pan-American Congress of Endocrinology, 408-410, Mexico City, 1965.

38. W. R. Oakes and C. C. Lushbaugh, Course of Testicular Injury Following Accidental Exposure to Nuclear Radiations, Radiology, 59, 737-743, 1952.

39. S. W. Jordan, C. M. Hasegawa, and R. J. Keehn, Testicular Changes in Atomic Bomb Survivors, Arch. Path. 82, 542-554, 1966.

40. D. G. Seigel, Frequency of Live Births Among Survivors of Hiroshima and Nagasaki Atomic Bombings, Radiation Research 28, 278, 1966.

41. E. L. Reynolds, Growth and Development of Hiroshima Children Exposed to the Atomic Bomb. Three Year Study (1951-53) Atomic Bomb Casualty Commission, Technical Report, 20-59, 1954.

42. W. W. Sutow, R. A. Conard, and K. M. Griffith, Growth Status of Children Exposed to Fallout Radiation on Marshall Islands, Pediatrics, 36, 721, 1965.

43. S. C. Finch and S. Jablon, Opthalmology Programs at ABCC, A Brief Review and Preliminary Plan ABCC Technical Report, 12-61.

44. A. C. Woods, Cyclotron Cataracts, Amer. J. Opthal., 47(5) Part II, 20, 1955.

IV.7

DOSIMETRY AND RBE AT THE ENDS OF PROTON TRAJECTORIES

P. Bonét-Maury, T. Kahn, A. Wembersies, R. Choquest,
A. Bernet, J. de Sagey, and L. Cieur

Institut du Radium
Laboratoire Joliot-Curie
Orsay (S. & O.), France

We have shown[1] that the dosimetry and the biological effects of protons of 140 to 600 MeV are practically the same as those of γ rays, provided that we use the first part of the proton beam, where the LET is about 0.5 keV/μ and varies only slightly across the dosimeter or across the animal. This work has confirmed the experiments of Tobias et al.[2] that high-energy particles have virtually the same biological effect as 200-keV x rays. This is proved by the experimental observation that, with both these types of radiation the RBE for LD_{50} to mice is close to unity. There is general agreement today among the majority of authors that an RBE of about 1 ± 0.2 should be ascribed to most of the path of high-energy protons. When the energy does not exceed a few hundred MeV, the nuclear reactions (cascades and evaporation) caused by inelastic collision do not play an important part in the production of biological effects. With irradiation in air, secondary radiation such as α particles, neutrons, and protons contributes little (a few percent) to the absorbed dose.[3] Thus we have found, in experiments performed in collaboration with Baarli at CERN, that 592-MeV protons have the same effect on C57/BL6 mice behind a 1-cm aluminum absorber as with no absorber. Secondary radiation may become significant as the energy of the primary radiation increases, since this increases the frequency of the nuclear interactions. Thus, irradiating mammals with 2.2-GeV protons, Legeay et al.[4] found that secondary radiation is responsible for more than 25% of the total effect. Secondary radiation has also been found significant by the same authors and Baarli at CERN in experiments in which mice were irradiated with 600-MeV protons.

However, the above remarks do not apply if the dosimeter or the animal is irradiated with the terminal part of the proton track, i.e., the Bragg region, where the absorbed dose and the LET are greatly increased. This property of the end of the trajectory of high-energy beams was first exploited by the Berkeley group, who used narrow beams of well-defined geometry in cancer therapy and for neurosurgery. The present authors have studied effects of the ends of the trajectories of broad proton beams in connection with the hazards near accelerators and in space flight, as well as with fundamental radiobiology. The flux, the LET, and the absorbed dose of such proton beams are significantly different over the last few centimeters of the trajectory, and so, therefore, are the biological effects. More specifically, the following changes are observed: (a) the flux

decreases, at first slowly (region of nuclear reactions) and then rapidly (region of increasing ionization); (b) the mean LET of a proton steadily increases, at first slowly and then rapidly; and (c) the absorbed dose follows the usual Bragg curve, with a peak as seen in Fig. 1. In the region of the Bragg peak and toward the end of the track, the LET increases to about 15 and 25 keV/μ, respectively (Table 1). Near the end of the proton's range the LET increase is counterbalanced by a drastic drop in the proton flux and in the absorbed dose (as seen in Fig. 2), making it difficult to predict the biological effect in this terminal region. To check this experimentally, we measured the absorbed dose and the RBE in the region of the Bragg peak by exposing various parts of the animals to protons at the ends of their trajectories.

Experimental Arrangement

A proton beam was led through an evacuated tube from the synchrocyclotron without being focused. After leaving the tube through an aluminum window, and passing through a 6-mm-thick lead screen and a 4.5-m-thick air layer, the beam was broad and homogeneous, as shown in Figs. 3 and 4. The isodose curves were approximately circular, as seen in Fig. 5, and the initial energy of 152 MeV had been reduced to about 140 MeV. The dosimeters and the animals were placed behind Lucite walls in such a way that the Bragg peak fell at the selected depth in the animal. The surface dose was measured with various small air-ionization chambers (Baldwin-Farmer, Victoreen, and Philips) or with film glass, and LiF dosimeters. These results are compared in Fig. 6. The comparison also includes the ferrous sulfate dosimeter, with which we found G = 15.8 ± 0.3 for 150-MeV protons.

Determination of the Absorbed Dose

The absorbed dose in the region of the Bragg peak was determined with thin dosimeters, namely Kodak C B and dental dosifilms (about 1 mm thick), LiF (2.5 mm), French glass (3.9 mm), and Japanese glass (4 mm), as seen in Figs. 7 through 11. These dosimeters were calibrated with ^{60}Co γ radiation and the readings were expressed in rads.

(a) Dosifilms

Fifty such films are arranged in a stack with an aggregate thickness of about 5 cm, behind a Lucite screen, in such a way as to incorporate the Bragg peak. The Lucite screen was composed of 1-cm-thick sheets with films placed between them, so as to determine the curve of the absorbed dose for the whole track (see Fig. 12). C B films were fitted with water-tight cases, and the same experiment was done with water instead of Lucite.

Table 1. Linear energy transfer (LET) and relative biological effectiveness (RBE) as a function of the residual range in mm of water. The LET is seen to rise monotonically through the Bragg peak.

							Bragg Peak	
Residual Range, mm	30	20	10	8	6	4	2	~0
LET keV/μ	1.4	1.6	3	4.5	7	10	14	25
RBE (ICRP)		1		1 to 2		2 to 5		

(b) Glass dosimeters and LiF

These dosimeters were placed in Lucite blocks fitted with holes and suitable covers. The holes were so arranged that each dosimeter fell in a different range. The dosimeters were offset by 5 mm, but additional holes for LiF dosimeters reduced this distance to 2 mm in the vicinity of the Bragg peak, as seen in Fig. 13. These devices permitted determination of the response curve of each dosimeter along the entire proton trajectory, and notably around the Bragg peak. From these curves one could establish the distribution of the various absorbed doses from broad beams in soft tissues, since the reaction of Lucite with respect to high-energy particles is very similar, if not identical, to the reaction of soft tissues.

It has thus been found that the dosimeters all together indicate a Bragg-type curve, with a maximum and with an abrupt decline toward the end of the proton range. The measured values agree with the theoretical values as a function of energy. However, the shapes of the curves differ from those of the theoretical curves, and the experimental values are as yet insufficient to fix the exact heights of the peaks, except for the C B film, whose curve is practically the same as the theoretical curve and has the same peak height.

The complete absence of a response beyond the proton range shows the absence of diffused secondary radiation downstream from the Bragg peak. Moreover, the response curve for the C B film shows the absence of diffused radiation, which could flatten the peak. There is a surprising difference between French and Japanese glass and film dosimeters: whereas French glass and particularly C B film dosimeters give well-defined peaks, the Japanese glass and dental-film dosimeters indicate curves with virtually no peaks. No satisfactory explanation of this phenomenon has yet been proposed.

Though only preliminary, these results show that the absorbed-dose curves are not modified around the Bragg peak by an increase in the LET or by secondary radiation. The curve recorded with C B film coincides perfectly with the theoretical curve with a peak height of about 4 times the level of the entrance-surface dose. However, the region of the Bragg peak must be investigated further.

Determination of RBE

The experimental RBE values around the Bragg peak were determined by observing the lethal effect of a proton beam on a thin layer of bacterial culture. A suspension of E. coli in physiological serum having a concentration of 10^9 microorganisms per ml was placed in flat Lucite cells. The overall thickness of the cells was 5 mm, and the 1-ml suspension formed in them a 2-mm layer. The cells were placed along the proton beam, with Lucite screens between them in the first part of the path. The radiation dose received by some of the Lucite cells was

determined by replacing them with identical cells filled with ferrous sulfate solution and irradiating them under the same conditions.

The survival rate after irradiation with an entrance dose of 25 000 rad was estimated by counting in Petri dishes. The curve for the absorbed dose vs the lethal effect on this E. coli strain was determined with ^{60}Co γ rays, so that one could correlate with each survival rate a γ dose having the same effect. Figure 14 shows the resulting proton doses along the track. The experimental curve is seen to virtually coincide with the expected Bragg curve, and has the same peak height (4 times the surface dose).

It has thus been found that the increase in the LET near the Bragg peak does not appreciably affect the RBE of protons, which retains its value of 1, observed at the beginning of the track for lethal effect on a bacterial culture. For bacterial populations, however, the RBE probably increases only slowly with the LET, and may even decrease.

Guppies

Corresponding experiments are being carried out with more complex organisms, namely guppies, which, because of their sturdiness and small size, lend themselves to this work. The thickness of these aquarium fish is less than 2 mm at 1 month and 4 to 5 mm when adult. The radiosensitivity of these fish to γ rays needs to be studied, since the effects are different from those in mice. The temperature factor, for example, is very important in the determination of the radiosensitivity.

Experiments on Mice

Male C57BL6 mice were placed in Lucite tubes or blocks, and these were placed parallel or perpendicular to the beam axis in such a way that the section of the beam corresponding to the Bragg peak passed through various parts of the mice (abdomen, side, head, and hindquarters). See Figs. 15 through 22, which summarize these experiments. The irradiated mice were then kept under the same conditions as the controls, and were examined periodically for local skin and general effects, specifically mortality in 30 days, average life span, leucopenia (the leukocyte level on the third day), shrinkage of testicles by the 30th day, skin lesions, and "bleaching" of hair. Observations of the carcinogenic effect are in progress.

The integral absorbed doses for some parts of the animals were determined with the aid of tubes of the same size as the mice, filled with a solution of ferrous sulfate. When the Bragg peak fell inside the tube, ratios beween the integral and the surface dose were 1.95, 1.7, and 2.2. Checking was done by attaching film, glass, and LiF dosimeters to the animals.

Local Effects

The increase in the dose in the region of the Bragg peak is clearly manifested by enhanced bleaching and well-defined areas of epilation and radionecrosis (sublethal doses ≤ 600 rad) (see Figs. 18, 19, 21, and 23). By contrast, general irradiation in the initial parts of proton beams leads to uniform bleaching without epilation and radionecrosis (see Fig. 17). It may be added that protons cause bleaching sooner than the same surface dose of ^{60}Co γ rays.

General Effects

Irradiation of the entire animal with protons in the initial parts of the beam was compared with the irradiation of only certain parts of the animal with the section of the proton beam that incorporates the Bragg peak. This comparison showed that the dose increase in the region of the Bragg peak more than compensates for halving the irradiated volume of the animal. This is why general irradiation with 600 rad is not lethal, whereas irradiation of only the anterior part of mice with the same dose in such a way that the Bragg peak lies in the abdomen leads to 75% mortality and a lifespan of 14 days, and lateral irradiation with 530 rad (with the Bragg peak region lying lengthwise through the center of the body) leads to 100% mortality and a lifespan of 6.5 days, as summarized in Fig. 22. The maximum effect is therefore obtained when the Bragg peak lies at the center of the mouse.

The weight decrease of the testicles (critical organs) caused by partial irradiation varies according to whether or not the testicles lie in the beam. If they do not, the damage appears to be less than with general irradiation. The testicles showed an appreciable decrease in weight even when they were not directly irradiated. The testicles were never placed in the Bragg region.

Leukopenia arising from partial irradiation of the abdomen is more serious than that caused by general irradiation. Leukopenia offers an interesting quantitative indication of the biological effect, since a constant linear relationship has now been found between the number of leukocytes on the third day and the logarithm of the absorbed dose of protons, photons, and deuterons.

The observations described above prove that partial irradiation with the Bragg region of a beam involves a greater hazard than general irradiation with the same surface dose if the terminal part of the beam falls in the abdominal region, where most of the radiosensitive tissues are situated.

The dose of whole-body irradiation that produces the same biological effect as a given dose of partial irradiation can be found from the dose-effect relationship based on mortality, life span, and leukopenia. It is interesting to note that the doses thus calculated are higher than the surface dose, but less than twice the latter, i.e., of the order of the integral doses found with a ferrous

sulfate dosimeter. It should be mentioned, however, that the position of the Bragg peak inside the animals was fixed only roughly, and a more accurate location in the region of the most highly radiosensitive tissues may lead to more pronounced effects.

Conclusions

Mice and E. coli cultures were irradiated with monoenergetic unidirectional protons at the ends of their trajectories, and the results suggest that the increase in the biological effects at the Bragg peak is explained qualitatively and quantitatively by the increase in the absorbed dose in this region. The increase in the LET at ends of trajectories seems to play an insignificant part, and the RBE seems to retain a value close to 1 even in the terminal part of proton beams.

References

1. P. Bonét-Maury, J. Baarli, T. Kahn, G. Dardenne, M. Frilley, and A. Deysine, Biological Effects of Neutron and Proton Irradiation, Vol. I, p. 261-77, IAEA, Vienna, 1964.

2. C. A. Tobias, H. O. Anger, and J. H. Lawrence, Radiological Use of High-Energy Deuterons and Alpha Particles, Am. J. Roentgen, Radium Therapy, Nucl. Med., 67: 1 (1952).

3. V. P. Afanas'ev, I. F. Keirium-Marcus, S. S. Kuznetsova, E. G. Litvinova, I. K. Sokolova, and E. Stukina, p 1-19, Biological Action of Neutron Irradiation, IAEA, Vienna 1963 (Preprint No. SM-44/57, translation).

4. G. Legeay, Ph. Tardy-Joubert, and N. de Bottom, The Relative Biolgical Effectiveness of 3-GeV Protons on Mice. Analysis of Secondary Particles Contribution, P/47 Health Phys. 12 [8]: 1177 (1966).

5. J. Neufeld, W. S. Snyder, J. E. Turner, and H. Wright, Calculation of Radiation Dose from Protons and Neutrons to 400 MeV, Health Phys., 12: 227 (1966).

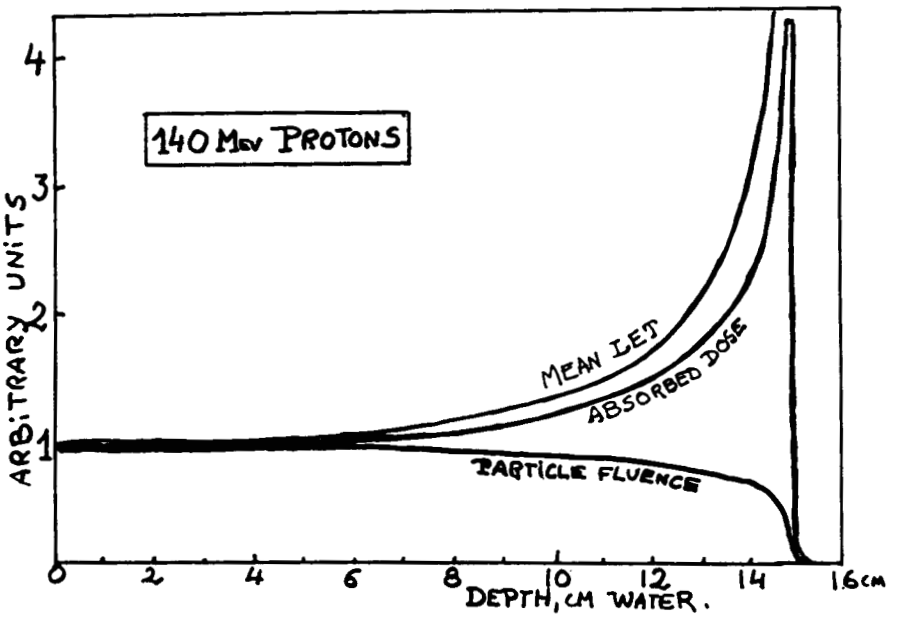

Fig. 1. The mean LET, absorbed dose, and particle fluence as a function of the depth in water for 140-MeV protons. The region of nuclear reactions seen at higher energies in the first part of the proton track is relatively unimportant at 140 MeV. The absorbed dose and mean LET follow each other closely as the particle fluence decreases at the end of the track.

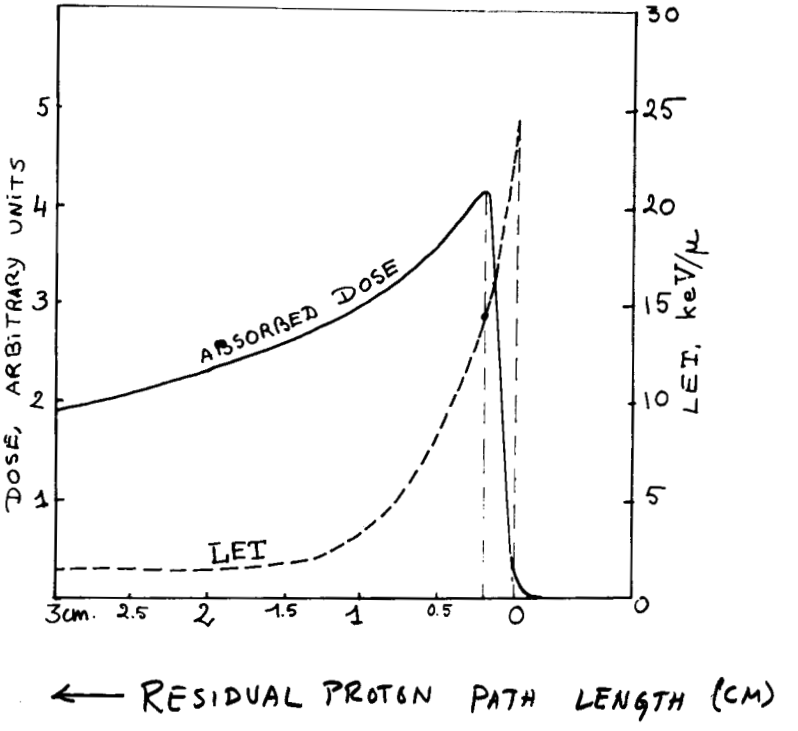

Fig. 2. The absorbed dose and LET as a function of the residual range in water, shown in greater detail than in Fig. 1. The very rapid change in both quantities in the first 0.25 cm of residual range makes the evaluation of the biological effect in this terminal region difficult to predict.

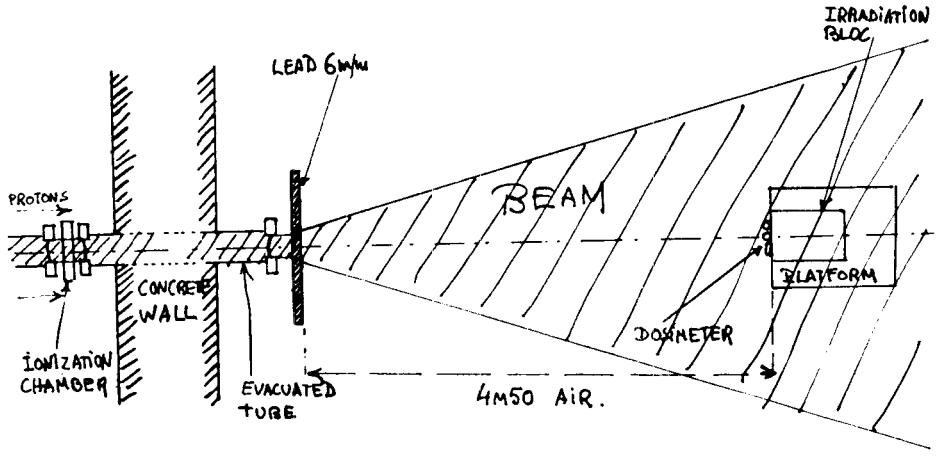

Fig. 3. The experimental arrangement for irradiating mice with the cyclotron beam.

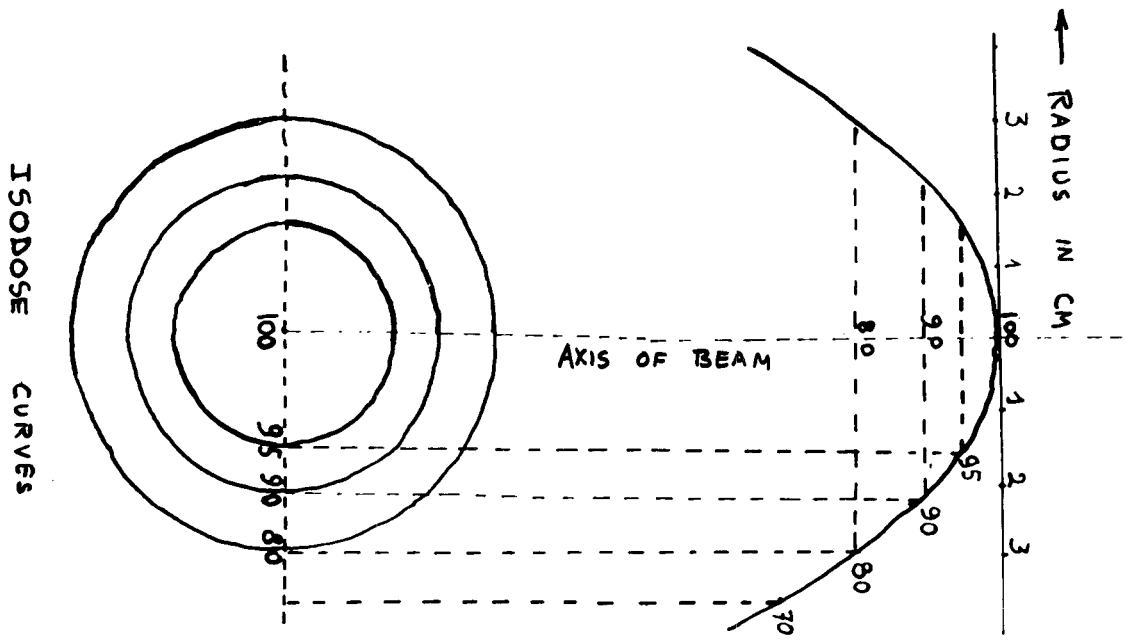

Fig. 4. Experimentally determined isodose curves for the 152-MeV proton beam after it has been reduced to 140 MeV by the lead screen. There is seen to be a close approximation to cylindrical symmetry. These values were measured near the lead screen.

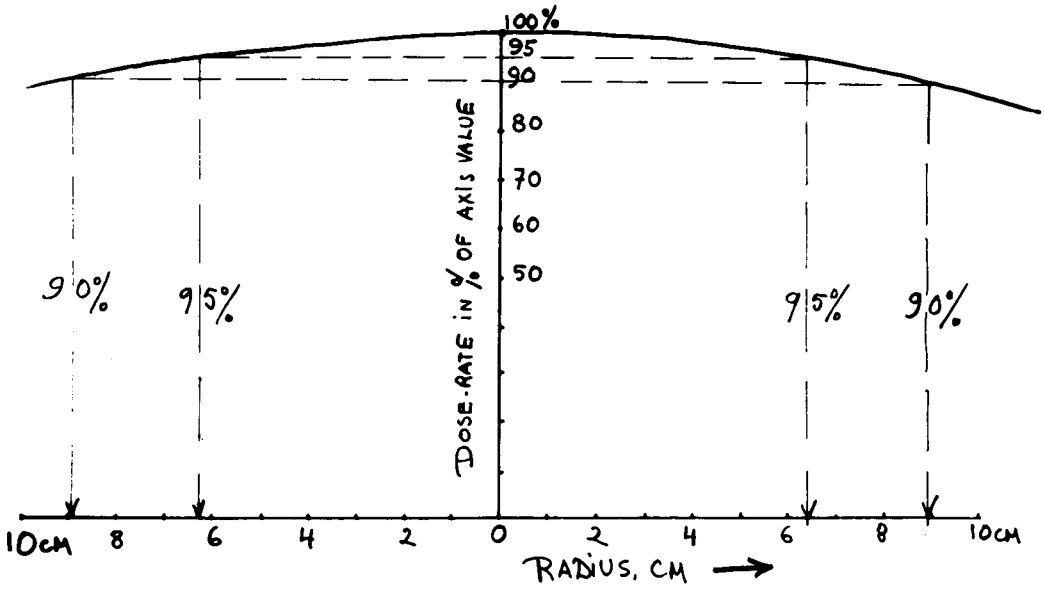

Fig. 5. Dose rate as a function of the radius measured at the position of the experimental animals after the beam has spread out through 4.5 m of air. The beam has passed through 6 mm of lead, 4.5 m of air, and 30 mm of Lucite. The dose distribution has become much flatter than that shown in Fig. 4.

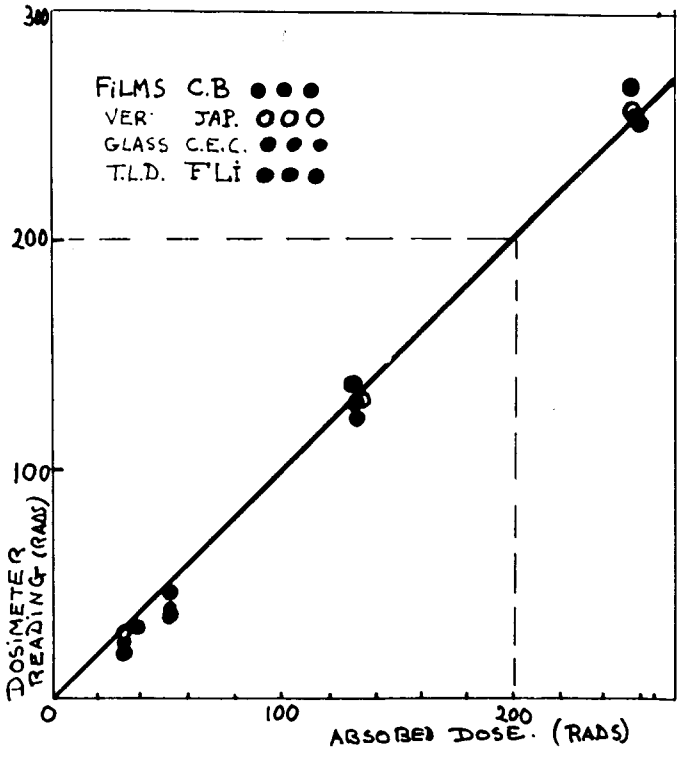

Fig. 6. A comparison of several dosimeters used to evaluate the surface dose.

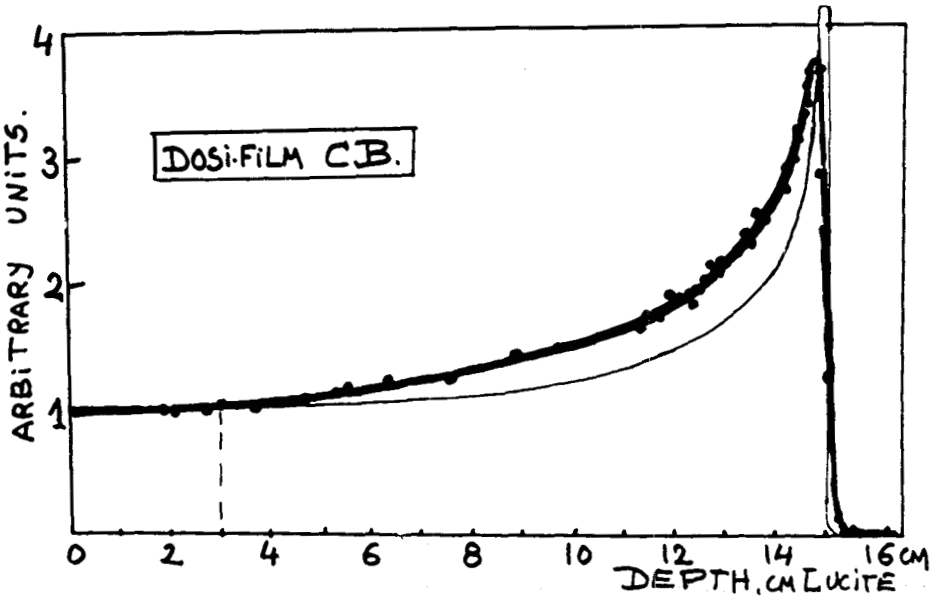

Fig. 7. The depth-dose response of CB film (about 0.8 mm thick) in Lucite to protons. The theoretical dose curve is shown as a light line.

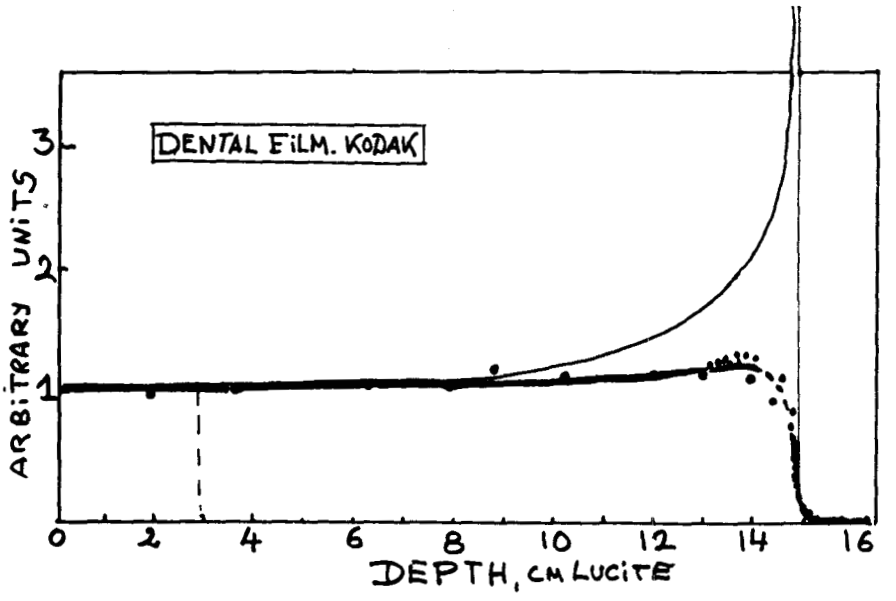

Fig. 8. The depth-dose response of Kodak dental film (1.3 mm thick) in Lucite to protons. The theoretical dose curve is shown as a light line. It is seen that this film does not show the peak so clearly as in Figs. 7, 9, and 10.

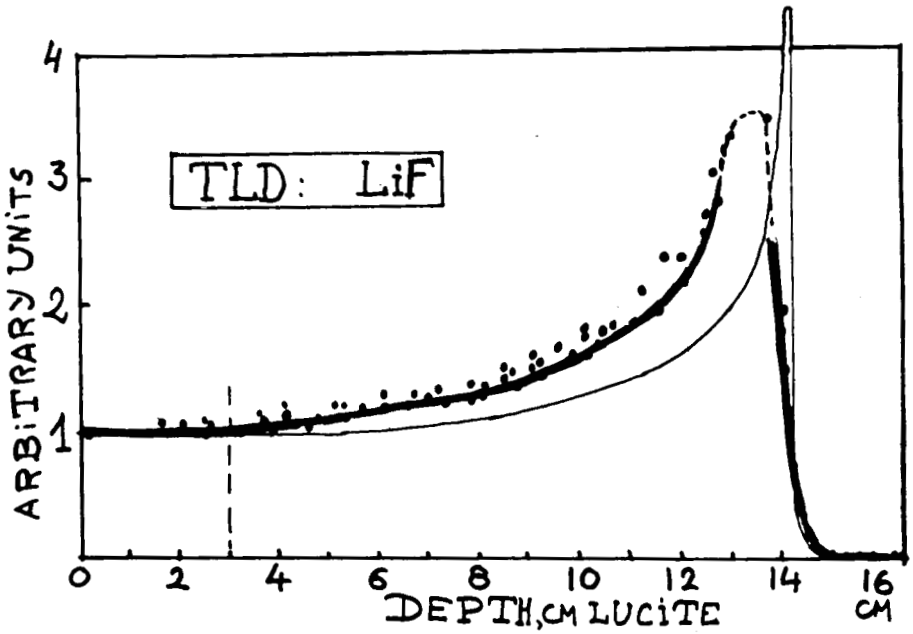

Fig. 9. The depth-dose response of LiF dosimeters (cylinders 18 mm long, 5 mm in diameter, with long axis perpendicular to the beam) in Lucite to protons. The theoretical dose curve is shown as a light line.

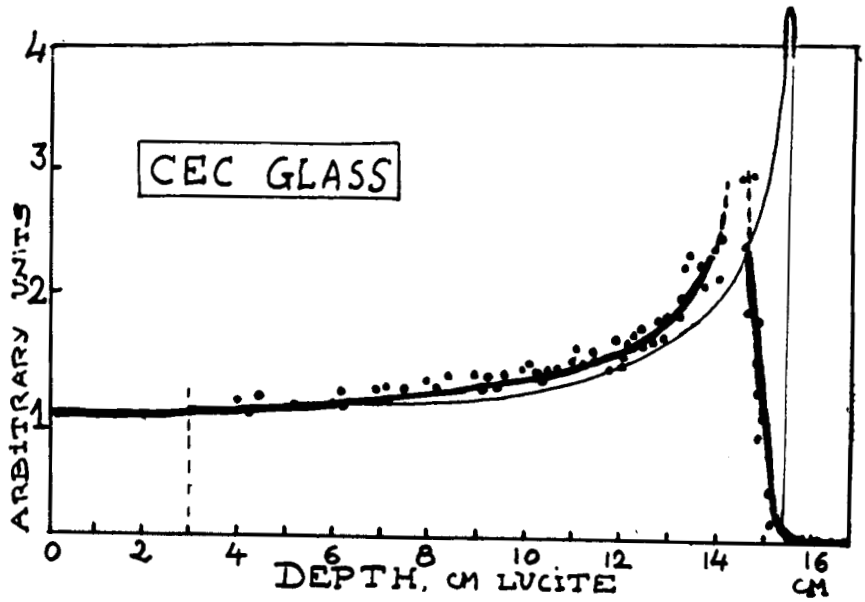

Fig. 10. The depth-dose response of CEC glass rods (6 mm long, 3.7 mm in diameter) with long axis perpendicular to the beam) in Lucite to protons. The theoretical dose curve is shown as a light line.

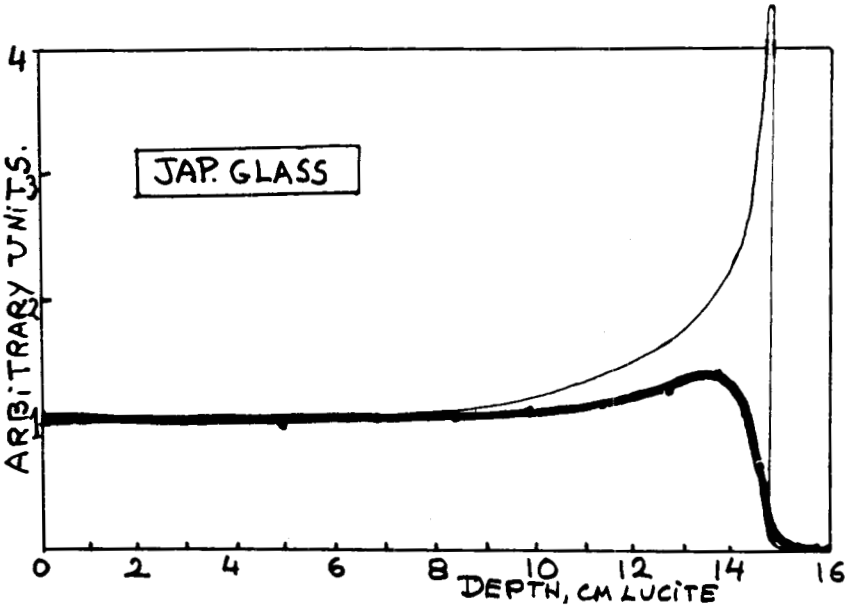

Fig. 11. The depth-dose response of Japanese glass (rectangles 9×9 mm by 5 mm in the beam direction) in Lucite to protons. The theoretical dose curve is shown as a light line. It is seen that this glass does not show the Bragg peak so clearly as in Figs. 7, 9, and 10.

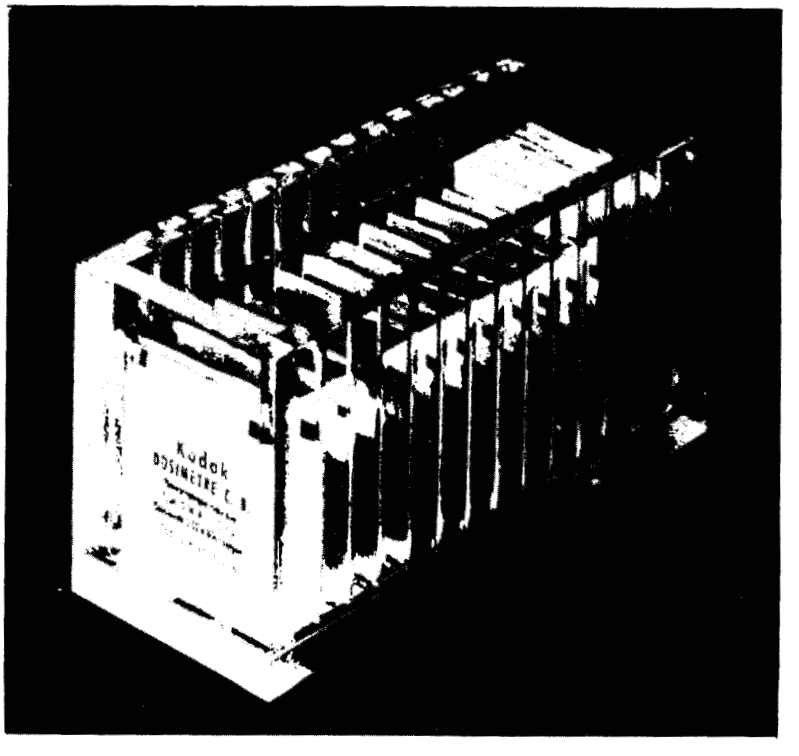

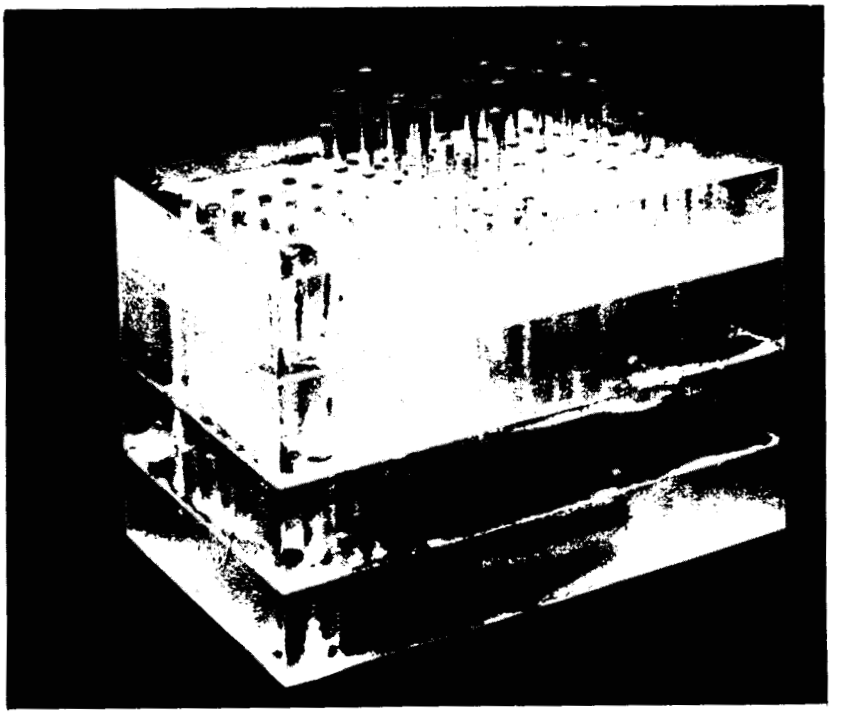

Fig. 13. Lucite block containing holes to space both glass and LiF dosimeters throughout the region of the Bragg peak.

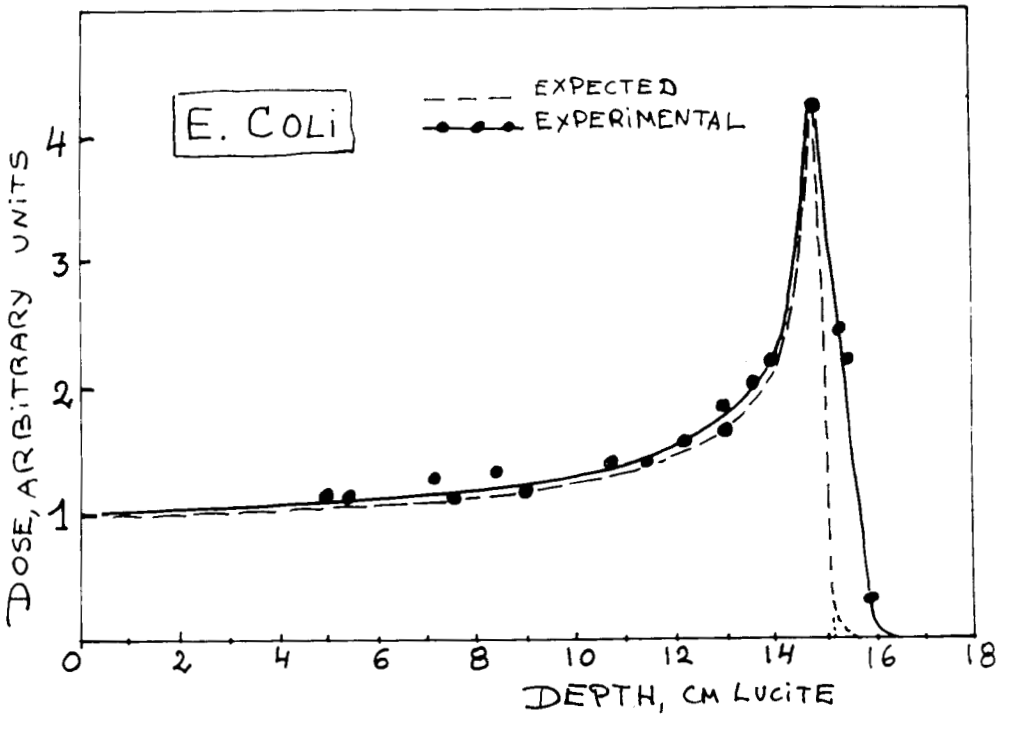

Fig. 14. Experimental depth-dose curve measured with E. coli by use of the lethal effect calibrated against ^{60}Co γ rays. The experimental curve is seen to correlate very well with the theoretical curve, shown as a dashed line. The peak-to-entrance dose ratio is seen to be 4:1 for both curves.

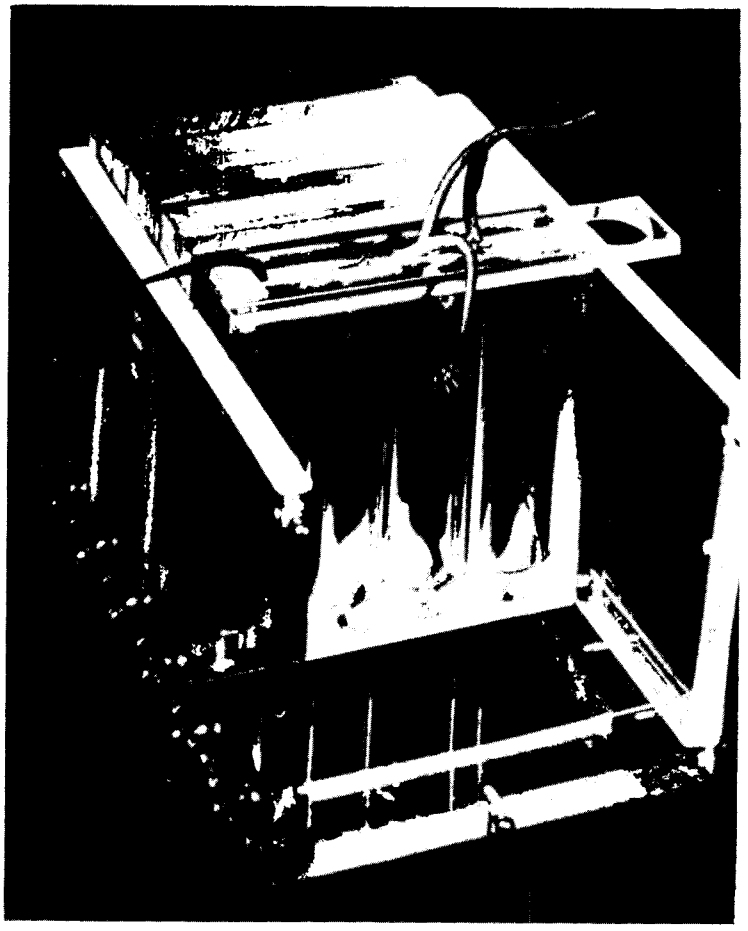

Fig. 15. Arrangement of the mouse-holding tubes and Lucite absorber screens which allows the Bragg peak to fall at a preselected depth in the mouse.

Pol2 SURFACE DOSE 460 RADS	1 LETALITY AFTER 30 DAYS	2 MEAN SURVIVAL (DAYS)	3 LEUCOCYTES (% CONTROL) AFTER 3D | 30D
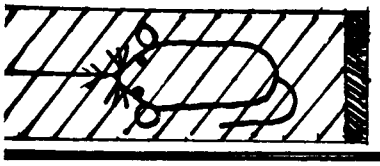	0	>30	7 → 38
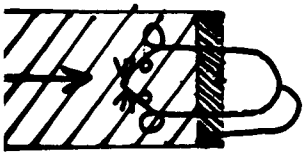	0	>30	2 → 90
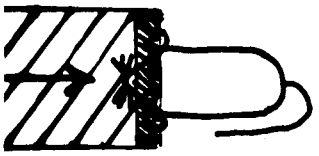	0	>30	93 → 92

Fig. 16. Schematic arrangement and results of three different geometries of irradiation with 460-MeV protons.

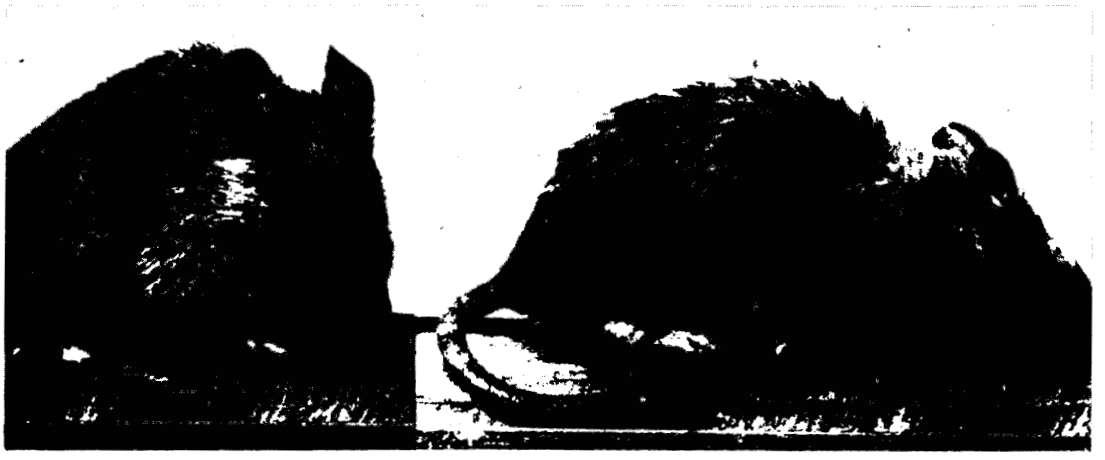

Fig. 17. Mouse irradiated in the entrance plateau portion of the 460-MeV proton beam. The grey hair which has grown out after the exposure is seen to be fairly uniform over the animal.

Fig. 18. Mouse some time after irradiation with 460-MeV protons from the side. The Bragg peak was located in a saggital plane somewhat to the left of the midplane. Both sides of the same animal are shown.

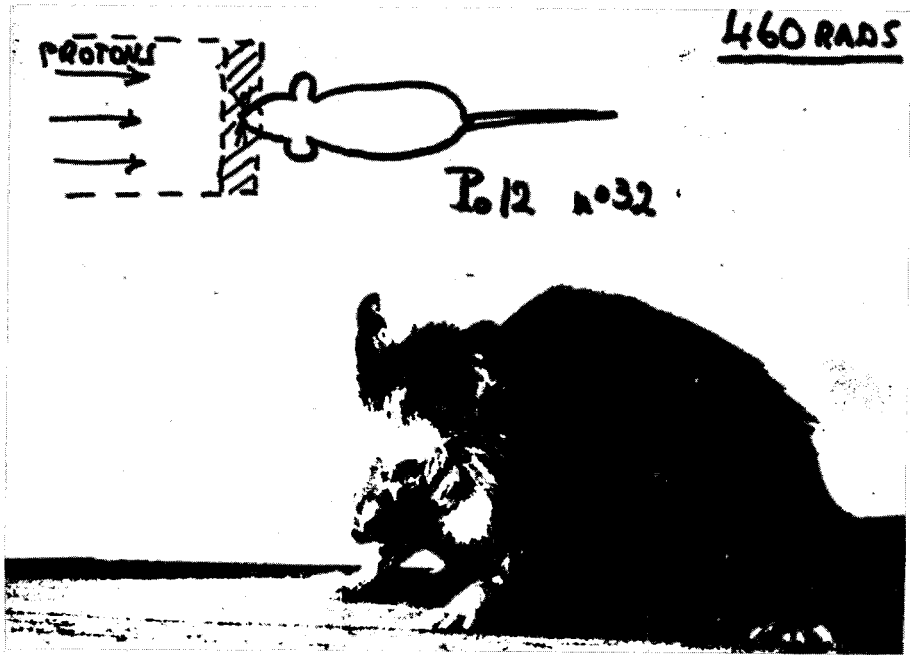

Fig. 19. Mouse irradiated with 460-MeV protons in such a way that the Bragg peak fell on the head.

P.12 SURFACE DOSE 530 RADS	1 LETALITY AFTER 30 DAYS	2 MEAN SURVIVAL (DAYS)	3 LEUCOCYTES (% CONTROL) AFTER 3D | 30D
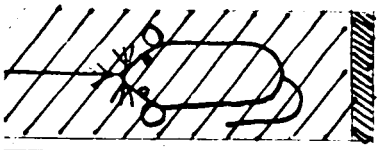	25 %	18D	10 → 31
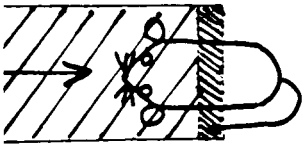	100 %	8D	6 → 0
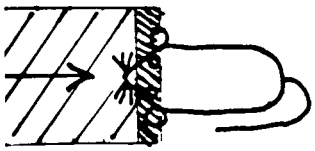	0	>30D	70 → 130

Fig. 20. Schematic arrangement and results of three different geometries of irradiation with 530-MeV protons.

Fig. 21. Mouse after irradiation with 500-MeV protons from the head to the midtorso, with the Bragg peak falling in the shaded region as shown in the sketch.

P.15 SURFACE DOSE 600 RADS	1 LETALITY AFTER 30 DAYS	2 MEAN SURVIVAL (DAYS)	3 LEUCOCYTES (% CONTROL) AFTER 3D | 30D	4 TESTIS WEIGHT (% CONTROL) AFTER 30 DAYS
	0	>30	8 → 33	35
	0	>30	1 → 100	31
	75%	14_D	2 → 5	
	0		3 → 100	54
	100%	6.5_D	1 → 0	

Fig. 22. Schematic arrangement and results of five different geometries of irradiation with 600-MeV protons.

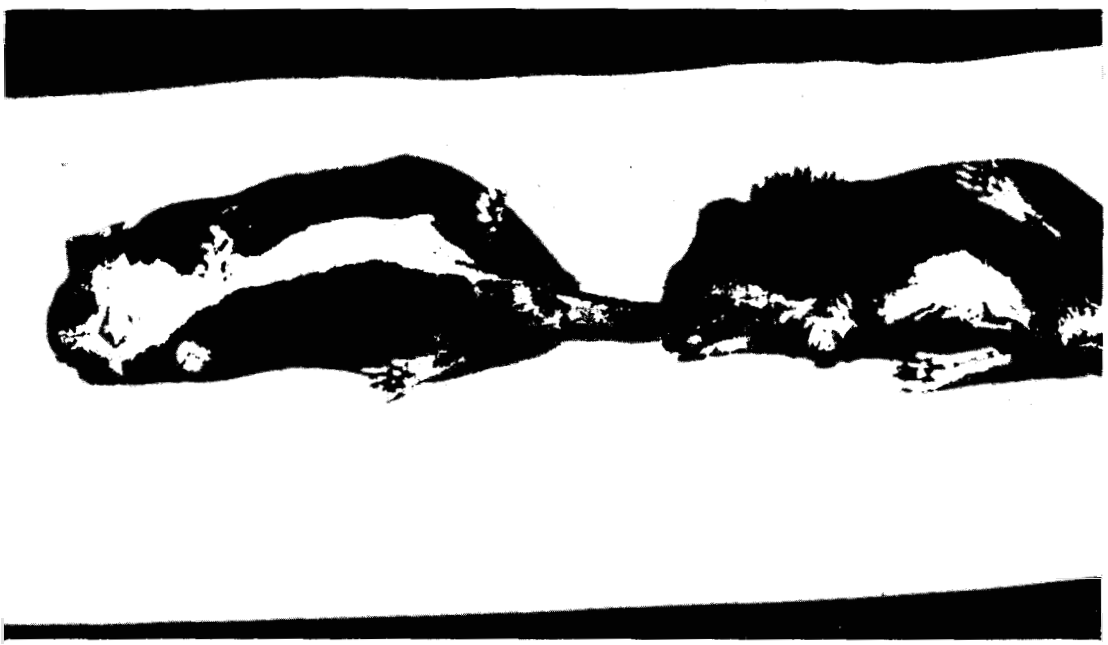

Fig. 23. Mice exposed to 600-MeV protons in the last arrangement shown in Fig. 22, where the saggital location of the Bragg peak fell on the midplane.

IV.8

Relative Biological Effectiveness of Gamma Rays, X-rays, Protons, and Neutrons for Spermatogonial Killing*

E. F. Oakberg

Oak Ridge National Laboratory

INTRODUCTION

High sensitivity to radiation-induced cell death and ease of quantitation of surviving cells make spermatogonia of the mouse a good radiobiological test system (Oakberg, 1957). With appropriate techniques, the effect of doses in the range of 2 rads to 1000 rads can be studied. These attributes have led to the present experiments on the comparison of the biological effectiveness of different types of radiation.

Three types of spermatogonia can be recognized in the mouse (Oakberg, 1956a). Type A spermatogonia are the stem cells of the seminiferous epithelium, and through the process of stem cell renewal (Leblond and Clermont, 1952) maintain their own numbers while giving rise to an unlimited number of differentiated cells. Intermediate spermatogonia are derived from type A, and divide once to form spermatogonia of type B. B spermatogonia divide once to form primary spermatocytes (Oakberg, 1956a).

Intermediate and B spermatogonia are of homogeneous sensitivity, and when log-survival is plotted against dose, give survival curves with a shoulder at doses of 10 R or less, and a steeper, exponential decrease in survival at higher doses. LD_{50}'s in the range of 21-25 R of Co_{60} gamma rays have been reported for these cells (Oakberg, 1957). Survival at 100 R is essentially zero.

Type A spermatogonia are of heterogeneous sensitivity, with survival comparable to intermediate and B types at doses below 25 R. The survival curve then flattens markedly at doses of 50-1000 R, presumably because of a resistant component in the population. Thus at doses of 25 R or less, data on survival of type A spermatogonia can be combined with that of late type A and intermediate spermatogonia to obtain larger numbers of cells and greater statistical reliability of estimates of radiation effects. The resistant component of the A population can be used for doses in the range of 100 to 1000 R.

MATERIALS AND METHODS

Male F_1 hybrid mice from the cross of inbred 101 strain females with inbred C3H males have been used exclusively. All animals were 12 weeks old at the time of irradiation.

Mice were killed 72 hours after irradiation when doses were 200 R or less and five days after irradiation for doses of over 200 R. Testes were fixed in

*Research jointly sponsored by the National Aeronautics and Space Administration, and by the U. S. Atomic Energy Commission under contract with the Union Carbide Corporation.

Zenker-formol, embedded in paraffin, sectioned at 5μ, and stained by the PAS technique. One hundred tubule cross sections, distributed among the stages of the cycle of the seminiferous epithelium on the basis of a previously determined frequency distribution for control mice (Oakberg, 1956b) were scored for each mouse. Apparently normal spermatogonia in all tubules, and pre-leptotene spermatocytes in stage VII were counted. Data were expressed as experimental/control ratios.

RESULTS

Survival curves for 250 kv X-ray exposures made at the Lawrence Radiation Laboratory and for 280 kv X-ray exposures made at Massachusetts General Hospital were not significantly different. Accordingly, the data were pooled to provide a more reliable base of comparisons for the preliminary estimates of RBE given in Table 1. Slopes were fitted to Log survival by the least squares method and the ratio of the slopes compared to obtain the RBE. At present, data are restricted to late A and late A plus intermediate spermatogonia. Although the actual values vary from 0.76 for 130 and 730 Mev protons for late type A to 1.38 for Co_{60} gamma rays for late A plus intermediate spermatogonia, RBE's of approximately 1 can be accepted for these radiations in estimation of hazards.

In an earlier study (Oakberg and Clark, 1961), the relative effectiveness of 2.5 Mev and 14.1 Mev neutrons to Co_{60} gamma rays was compared. These data are given in Table 2. Two sets of RBE's were computed, one for each cell type over the entire dose range, and a second set for the combined survival of all spermatogonial types at low doses. The RBE for both levels of neutron energies is greater than 1, and probably about 2 when the comparison is based on all the data. Restriction of the comparison to low doses raised the point estimate to 8 for 14.1 Mev and to 3 for 2.5 Mev neutrons. Since the confidence limits are approximate, and they overlap, the RBE's for 2.5 and 14.1 Mev energies probably are not significantly different.

Recently, cell survival after irradiation with fission neutrons with an average energy of 1-2 Mev has been measured (Figure 1). These data are for cells irradiated and scored as type A spermatogonia, i.e., a different cell type from those represented by the data of tables 1 and 2. Co_{60} gamma rays, 250 kv X-rays, and 730 Mev protons gave equal survival. The neutron RBE, however, was based only on the X-ray data. A value of 6.5 was obtained for neutron doses of 18-101 rads, and of 4.7 for doses of 172-258 rads.

DISCUSSION AND SUMMARY

Statisitical analyses of the data are not complete, especially for cells irradiated and scored as type A spermatogonia. On the basis of preliminary results presented here, it is reasonable to accept an RBE of 1 for 250 kv X-rays, 280 kv X-rays, 130 Mev protons, 730 Mev protons, and Co_{60} gamma rays for estimates of radiation hazards.

Previously, we had attributed the lack of a difference in RBE between 14.1 and 2.5 Mev neutrons to a "wasting" of energy with the more densely ionized track of the 2.5 Mev neutrons (Oakberg and Clark, 1961). This explanation no longer appears tenable in view of the RBE's of 6.5 and 4.7 for fission neutrons, with an average energy of 1-2 Mev. Obviously, there is no simple relationship

between LET and biological effect, as already pointed out by Smith and Rossi (1966).

The phenomenon of higher neutron RBE's at low doses, as given in Table 2 and Figure 1, has been observed previously. The logical explanation of this phenomenon is that there is a region of less slope (shoulder) on the X- and gamma ray survival curves; whereas the neutron dose curves are linear. Accordingly, divergence of X or gamma ray and neutron curves will be greatest at low doses. This presentation is obviously over-simplified, for a continuous scale of RBE values probably exists for each energy comparison. The RBE of neutrons vs. X- and gamma rays therefore is quite arbitrary owing to the comparison of a dose-effect curve which is curvilinear (X- and gamma rays) with a linear dose-effect relationship (neutrons). Use of systems which give linear effects with ionizing radiation is not the answer either, since qualitative differences in biological effect usually occur.

In summary, X-rays, gamma rays, and 130 as well as 730 Mev protons all appear to have an RBE of approximately 1. Neutron RBE's are a function of LET and dose, being greater both with low doses and higher LET. No simple relationship exists, however, between RBE and either dose or LET.

ACKNOWLEDGEMENTS

The author wishes to express his appreciation to Dr. A. H. Koehler and other staff members of the Harvard Cyclotron Laboratory for the 130 Mev proton irradiation; to the staff of the Lawrence Radiation Laboratory at Berkeley, California, for the 730 Mev proton irradiation; to Dr. M. L. Randolph for the 2.5 and 14.1 Mev neutron irradiations; to the Health Physics Division of ORNL for the fission neutron exposures; and to Dr. D. G. Gosslee for statistical analysis of the data.

REFERENCES

1. Leblond, C. P., and Y. Clermont, Spermiogenesis of rat, mouse, hamster, and guinea pig as revealed by the "periodic acid-fuchsin sulfurous acid" technique. Am. J. Anat., 90: 167 (1952).

2. Oakberg, E. F., A description of spermiogenesis in the mouse and its use in analysis of the cycle of the seminiferous epithelium and germ cell renewal. Am. J. Anat. 99: 391 (1956a).

3. Oakberg, E. F., Duration of spermatogenesis in the mouse and timing of stages of the cycle of the seminiferous epithelium. Am. J. Anat. 99: 507 (1956b).

4. Oakberg, E. F., Gamma-ray sensitivity of spermatogonia of the mouse. J. Exp. Zool. 134: 343, 1957.

5. Oakberg, E. F., The effects of dose, dose rate and quality of radiation on the dynamics and survival of the spermatogonial population of the mouse. Jap. J. Genet. Suppl. to V. 40: 119 (1964).

6. Oakberg, E. F., and E. Clark, Effect of dose and dose rate on radiation damage to mouse spermatogonia and oocytes as measured by cell survival. J. Cell Comp. Physiol. Suppl. 1, V. 58: 173 (1961).

7. Smith, H. H., and H. H. Rossi, Energy requirements and relative biological effectiveness for producing cytogenic phenomena in maize by irradiating seeds with X-rays and monoenergetic neutrons. Rad. Res. 28: 302 (1966).

Estimates of RBE's of Co_{60} gamma rays, 730 Mev protons, and 130 Mev protons to 250 and 280 kv X-rays based on spermatogonial killing

I. Late A spermatogonia		II. Late A + Intermediate spermatogonia	
Source	RBE	Source	RBE
730 Mev Protons	.765	730 Mev Protons	.973
130 Mev Protons	.755	130 Mev Protons	1.013
60 Gamma	.799	60 Gamma	1.379
250-280 Kv X	1.000	250-280 Kv X	1.000

Table 2

RBE of neutrons to Co^{60} γ rays for spermatogonial killing

Neutron energy	Cell type irradiated	RBE		
		Lower 95 % confidence limit	Point estimate	Upper 95 % confidence limit
		Based on all doses		
14.1 Mev	A	1.41	1.76	2.76
	Late A	2.19	2.52	2.89
	Late A + Intermediate	2.11	2.38	2.69
2.5 Mev	A	1.26	1.89	3.32
	Late A	1.22	1.85	2.53
	Late A + Intermediate	0.73	1.10	1.49
		Restricted to low doses		
14.1 Mev	Pooled*	4.39	8.18	16.42
2.5 Mev	Pooled*	0.68	3.03	6.80

*All three cell types combined for low dose ranges only: (1-23 rad for Co^{60} γ rays, 0.5-5.0 rad for 14.1 Mev neutrons, 0.25-7.42 rad for 2.5 mev neutrons).

(From Oakberg, E. F., and E. Clark, J. Cell Comp. Physiol. Suppl. to Vol. 58: 173-182, 1961.)

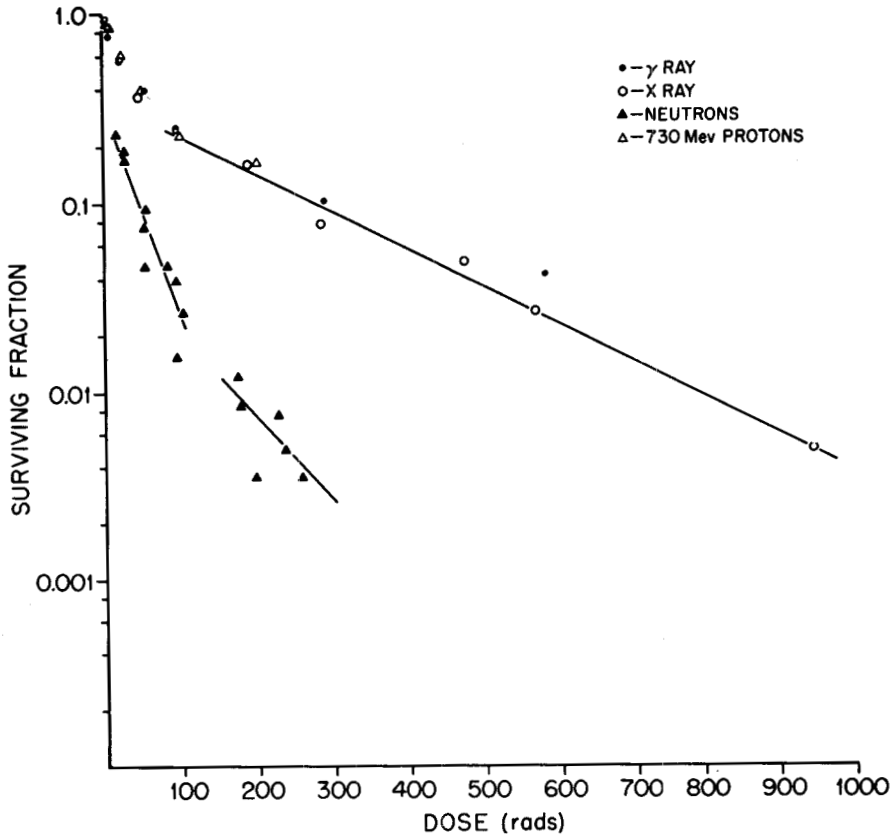

Figure 1 Survival of type A spermatogonia of the mouse after gamma-ray, X-ray, 730 Mev proton, and fission neutron irradiation.
(. = gamma rays, o = X-rays, △ = 730 Mev protons, ▲ = neutrons).
(From Oakberg, E. F., Jap. J. Genetics 40: 119-127, 1964).

INTESTINAL AND GONADAL INJURY AFTER EXPOSURE TO FISSION NEUTRONS

Maurice F. Sullivan

Biology Department
Battelle Memorial Institute
Pacific Northwest Laboratory
Richland, Washington

ABSTRACT

INTESTINAL AND GONADAL INJURY AFTER EXPOSURE TO FISSION NEUTRONS. It has been well established that there are distinct differences in the predominant sites of action by neutrons or X rays. The gastrointestinal tract and the gonads are particularly vulnerable to the effects of fast neutrons. Rats were exposed to doses between 150 and 310 rad of fission neutrons in the Hanford Physical Constants Test Reactors. Intestinal injury was determined after exposure by measuring the excretion of ^{131}I-labeled polyvinylpyrrolidone (PVP) after intravenous injection. The leakage of PVP into the intestine was proportional to the neutron dose and was decreased by pre-irradiation treatment of the rats with cysteine (1.0 g/kg). An RBE of 3.0 was determined for fission neutrons based on PVP data, which was about the same as the RBE determined by mortality. The time of death indicated that hematopoietic injury was a major cause of death from these exposures.

Most of the information on gonadal response after neutron irradiation has been obtained with mice. The rats surviving this study on acute intestinal injury were mated to obtain additional information on fecundity in that species. All males surviving the exposure were sterile three months after exposure but the females produced litters one month after exposure at all dosage levels. On subsequent matings males exposed to the lowest dose became fecund and the females gave birth to litters that decreased in size with increasing neutron doses. Testes of males at the higher doses were still atrophic at the conclusion of the study.

These results demonstrate the sensitivity of both the intestine and the gonads to neutron irradiation and indicate the usefulness of specific indicators for measuring injury from neutron irradiation.

INTRODUCTION

The conspicuous relative radiosensitivity of the gastrointestinal tract and reproductive organs to fast neutron exposures is well known. Methods to quantitate that distinctive effect would be particularly useful for establishing RBEs and for use as indicators of injury in radiotherapy. The use of protein leakage as a measure of intestinal damage from X rays has now been well established[1-4] and has also been found[5,6] useful for measuring damage from fast neutron exposures. In the experiments reported here it was used to determine an RBE for intestinal injury from fission neutrons. It was also used to show that protection could be afforded to the intestine by pre-treatment with cysteine or AET and a dose reduction factor calculated for these drugs on that basis. The effect of X rays and fission neutrons on PVP excretion was also mimicked by nitrogen mustard and that effect reduced by drug prophylaxis.

Because of the scarcity of information about the effect of fission neutrons on rat reproductive capacity the survivors of this acute study were mated. The results indicate that there are distinct differences between the effects of X or gamma rays and those of neutrons on rat gonads.

MATERIALS AND METHODS

The fission neutrons used in these experiments were produced by irradiating a uranium-235 foil which was wrapped around a lead cylinder (7.0 cm wall thickness) with thermal neutrons from the Hanford Physical Constants Test Reactor. Rats were exposed by the arrangement shown in Figure 1. The modal neutron energy was 800 kV and the maximum energy 2 Mev, as seen on the spectrum shown in Figure 2 along with a similar spectrum of the neutrons from a Los Alamos Godiva type reactor. Dosimetry for the animal experiments employed sulphur activation and silicon diodes for neutron measurements, and silver-activated phosphate glass rods, 6 mm diameter (Toshiba), for gamma-ray measurements. These dosimeters were taped to a wood probe and positioned beside each rat. Total body exposures to X radiation was done in order to have a basis for neutron comparison by rotating the rats in a lucite container on a turntable under a vertical beam. Partial body irradiation was achieved under pentobarbital sodium anesthesia, 40 mg/kg. The region of the body exposed included all the GI tract distal to the squamous stomach and excluded only a few cm of the terminal colon, while the remainder of the body was protected by 35-mm-thick lead shield. The physical factors were 250 kVp, 30 ma, 0.25 mm Cu, and 1.0 mm Al added filtration.

The rats, obtained from Charles River Farms and weighing 200 gm, were given KI in their drinking water to saturate their thyroid glands after irradiation and injected intravenously with 20 μCi/kg of ^{131}I-PVP at two days after exposure. Free iodine was removed from the PVP prior to injection by dialysis against an Amberlite anion-exchange resin (I.R.A.-400 chloride). The radioprotective drugs cysteine, 1.0 g/kg, and AET, 2-(aminoethylisothiouronium) bromide hydrobromide, 150 mg/kg, were injected intraperitoneally 10 minutes prior to neutron or X-ray exposure. The nitrogen mustard, methyl bis 2-(chloroethyl) amine hydrochloride (HN2) was injected intraperitoneally, 1.0 mg/kg. Protective agents were administered 30 minutes prior to injection of the nitrogen mustard.

Fecal collections of excreted PVP were made daily for five days and counted for radioactivity with a single-channel gamma spectrometer.

Fertility was tested at 10 weeks after exposure of the males and three weeks after irradiation of the females with fission neutrons, using the survivors of the PVP study. Each male was caged with four females of the same age for 10 days and irradiated females caged with both unirradiated females and a male in the same one-to-four male/female ratio. The offspring were killed at 10 days after birth and the mothers re-mated a week later. This procedure was followed through three matings. If the reproductive capability of control animals became doubtful, substitutions were made with normal animals of the same age. At three months after the last mating (8 months following exposure), the males were killed, their testes fixed in 10 percent formalin and stained with hematoxylin-eosin for histological analysis.

EXPERIMENTAL RESULTS

PVP Excretion after X-ray, Fission-Neutron, or Nitrogen Mustard Treatment. About 70 percent of the ^{131}I activity from the injected PVP usually appeared in the urine during the first day or two after injection.(2) Most of that passing into the intestine was eliminated between three and six days after exposure, when intestinal damage was most severe and when diarrhea was apparent. The quantity appearing in the feces was proportional to the radiation dose over the range of 500 to 1500 R, Figure 3. At that higher radiation dose, however, survival time was usually about 3.5 days. This necessitated the use of abdominal exposures, which gave a survival time long enough for fecal collections representative of the intestinal damage to be obtained.

The total quantity of PVP appearing in the feces from two to seven days after injection of neutron-irradiated rats was also directly related to the radiation dose over the range studied, Figure 4. Some of the animals at the higher end of the range exhibited gross signs of intestinal radiation injury and died before the collection was completed. Pre-treatment of the rats with cysteine reduced PVP leakage markedly.

The data for PVP excretion were plotted against the radiation dose in rad for whole-body exposure to both fission neutrons and 250-kV X rays, Figure 5. By drawing a horizontal line connecting the best straight lines at an arbitrary point, 7.5 percent, and subtracting the gamma contamination dose from the X-ray dose, an RBE of about 3 was obtained. The gamma contamination was unfortunately substantial, 50 percent of the neutron rad dose, but not sufficient by itself to alter the quantity of PVP excreted. The RBE calculated by this method, which is essentially that used by Turner and Fowler,(5) varied slightly depending upon the level of response chosen for the comparison. By using an approximate RBE of 3 to calculate the effective radiation dose from neutrons, the data in Figures 3 and 4 can be compared and the dose reduction factor (DRF) of the protective agents calculated from the results. These data are shown in Table 1 and indicate that the DRF for PVP leakage after cysteine prophylaxis of neutron-irradiated rats is about 1.4, and about 2.0 for X rays.

Histologic damage to the mucosa and the time at which signs of intestinal injury were obvious after treatment with the nitrogen mustard, HN2, was similar to that seen after X irradiation. Although no mortality occurred after injection of 1.0 mg/kg of HN2, the PVP leakage shown in Figure 6 exceeded that resulting from lethal doses of X rays, 1000 and 1500 R. Pre-treatment with cysteine substantially reduced the quantity of PVP lost into the intestine after HN2, but AET was not as effective.

Reproductive Capacity of Neutron Irradiated Rats. The literature on related studies done after X irradiation led us to believe that at these levels of exposure male fertility should have recovered at 11 weeks after exposure. Eleven males exposed to 130 or 160 rad of neutrons were, therefore, initially mated with both neutron-irradiated and with normal females. None of them were fertile, however, although fecundity had returned to two of four rats exposed to 130 rads by the next mating, five weeks later. All of the eight

TABLE 1. PVP Excretion Data.

Type of Exposure	Estimated dose: Combined* (rem)	X ray (R)	Neutron (rad)	Gamma (rad)	Protective agent**	No. of Rats	PVP Excretion† (% of dose)
Control	-	-	-	-	-	14	5.7 ± 0.7
X ray	500	500	-	-	-	6	4.8 ± 0.6
Reactor	525	-	150	75	-	6	3.7 ± 0.4
Reactor	645	-	185	90	-	6	5.4 ± 0.7
Reactor	735	-	210	105	-	6	8.3 ± 1.4
X ray	750	750	-	-	-	6	7.0 ± 1.0
Reactor	960	-	275	135	-	6	7.3 ± 1.1
X ray	1000	1000	-	-	-	8	10.6 ± 0.9
Reactor	1085	-	310	155	-	3	14.2 ± 3.5
Reactor	735	-	210	105	Cysteine	6	4.7 ± 0.3
Reactor	960	-	275	135	Cysteine	6	5.4 ± 1.3
X ray	1000	1000	-	-	Cysteine	6	5.1 ± 0.9
X ray	1000	1000	-	-	AET	6	4.8 ± 1.0

* An RBE of 3 assumed for neutrons.
** Cysteine dose: 1000 mg/kg. AET dose: 150 mg/kg.
† Fecal excretion of PVP during five days postinjection with standard deviation of the mean.

rats exposed to 160 or 210 rad survived the study but none recovered fecundity. At sacrifice eight months after exposure spermatogenesis was completely absent in three of four rats given 210 rad, and the testes of the other animal exhibited only an occasional tubule showing spermatogenesis. The smaller arterioles exhibited a thickening of the walls and those most severely affected, a fibrinoid necrosis. The testes of the four rats given 160 rad were also almost devoid of spermatogenesis but fibrinoid necrosis was not evident in the blood vessels. At 130 rad damage was variable and the tubules ranged from ones which were markedly aspermic to those showing active spermatogenesis. The blood vessels were also less severely involved, showing only minimal hyaline changes.

Female fertility data are shown in Table 2. The average control litter size for all three matings was 10.5. Some of the irradiated rats died during the course of the experiment from delayed effects of the exposure. Neutron irradiation did not cause infertility before the first mating at $3\frac{1}{2}$ weeks postirradiation, but a dose-dependent decline in both fertility and in litter size became evident by the second and third matings when only 9 of the 58 females tested bore young.

DISCUSSION

The marked sensitivity of both the intestine and the gonads to fast neutron irradiation is a well documented observation,[7,8] but the reason for this specificity is not well understood. These effects are not markedly influenced by the presence of oxygen, and prophylactic agents are relatively ineffective for preventing death from over-exposure. Although this preferential effectiveness for damaging the GI tract would seem to make neutrons superior to other, less specific radiations for studying intestinal damage, relatively little of our present information has been obtained from their use. This probably stems from our inadequate methods of dosimetry and for measuring damage to specific sites of injury.

The epithelium and capillaries of the gastrointestinal tract constitute one of the most sensitive systems to acute radiation injury.[9] Acute radiation damage to that organ results in a loss of protein into the lumen of the intestine[10,11] that can be measured by various methods.[12-14] The group at Hammersmith[5] recognized the potential value of using protein leakage to establish RBEs for intestinal injury and assigned an RBE of 2.8 to cyclotron-generated neutrons (6 Mev) in comparison to 250-kV X-rays. Vatistas and Hornsey later suggested[6] that, although PVP excretion might be useful in radiotherapy, morphologic damage to the intestine and functional damage resulting in PVP leakage are not closely related. Dalla Palma[15] used it in radiotherapy but did not get a dose-dependent response. The uncertainty of these results that question the validity of using protein leakage as a measure of intestinal radiation injury may lie with the region of the intestine that is irradiated. We found,[2] for example, in rats that unless the upper small intestine were irradiated PVP excretion and mucosal damage were definitely not closely related. This was consistent with autoradiographic data of Ullberg *et al.*,[16] which showed that ^{131}I-labeled albumin catabolism and excretion by cats occurred in the upper small bowel. Clinical data has also been reported[17,18] suggesting that the jejunum may be a major site for protein-losing enteropathy.

TABLE 2. Female Rat Fertility After Neutron Irradiation.

Number of Rats†	Dose (rad)	Mortality (%)	No. Fertile/No. Tested First Mating	Second Mating	Third Mating
		Control			
11	0	0	10/11 (10.8)*		
16	0	0		13/16 (9.4)	
16	0	0			13/16 (11.5)
		Irradiated			
6	150	0	1/3 (6)	3/6 (6.3)	2/6 (7)
6	185	17	2/3 (6)	1/6 (1)	0/5
6	210 + cysteine	17	2/3 (8.5)	1/6 (1)	0/5
6	210	33	1/3 (10)	0/4	1/4 (2)
3	240	66	0/1	0/1	0/1
6	275 + cysteine	50	2/2 (5.5)	0/3	0/3
6	275	50	1/3 (4)	0/3	0/3
	Total (neutron exposed)		9/18	5/29	3/27

* Average litter size
† Number of rats initially mated

The effect of the nitrogen mustards on the intestine is similar to that caused by exposure to radiation, and damage can be reduced by pre-treatment with thiol protective agents. Dose-reduction factors as high as 4.2 were obtained[19] for some of these drugs, using cysteine as the protective drug and spleen weight or mortality as an index of protection. It was suggested by these investigators that the non-uniformity of the protective action of these drugs could be advantageous for obtaining a localized therapeutic concentration. The results of the present study indicate that a DRF could be established for protection against HN2 on the basis of PVP excretion. They also suggest that this drug has a greater effect on the intestinal epithelial function responsible for PVP leakage than does either X or neutron radiations when comparisons are made on a mortality basis.

Protection against fast neutrons by cysteine[20] or by a combination of protective agents[21] has given DRF's of only about 1.1, using death as an endpoint. Survival is, no doubt, the ultimate endpoint for measuring protection against accidental exposure, but a measure of damage at a specific site, such as PVP excretion, could be useful for measuring a therapeutic exposure dose in which radiation effectiveness is restricted to certain localized areas by drug prophylaxis. We were able to show that cysteine pre-treatment gave a DRF for the intestine of 1.4 for fission neutrons. The DRF for X rays afforded by either cysteine or AET was approximately 2.0.

The RBE for testicular injury based on weight loss in mice from fission neutrons has been found by Spalding *et al.*[22] to be as high as 6.5, while Batchelor *et al.*[22] obtained a value of 4.6. Silini *et al.*[24] obtained a value of 4.9 by comparing cyclotron-generated 6-Mev neutrons with 8-Mev X rays. No attempt has been made in the present study to derive an RBE for damage to the male gonads, but Pitcock stated[25] that permanent sterilization of rats cannot be induced by acute sub-lethal irradiation. From the present study one must conclude that this possibility does indeed exist for exposures to 160-210 rad of fission neutrons.

These result suggest that the RBE for sterilization of the testes by neutrons may be similar to those obtained on the basis of testicular atrophy.

Female fertility exhibited a dose-dependent decrease which progressively worsened with time as evidenced by the number and size of the litters. Although no quantitation was attempted there was an obvious increase in the incidence of still-births and neonatal deaths among the offspring of the irradiated female.

ACKNOWLEDGEMENTS

The pathologic damage interpretations by Dr. T. D. Mahony, the dosimetric and spectrophotometric measurements by Mr. P. E. Bramson of the Radiological Protection Operation, the reactor operation by Mr. H. Henry and his staff of the Physical Instruments Laboratory, and especially the faithful service of Mrs. A. L. Crosby for technical assistance, is sincerely appreciated.

REFERENCES

1. M. F. Sullivan, Polyvinylpyrrolidone labeled with ^{131}I as an agent for the diagnosis of radiation injury in rats, Int. J. Radiat. Biol., 2: 393 (1960).
2. M. F. Sullivan, Intestinal vascular permeability changes induced by radiation and nitrogen mustard, Am. J. Physiol., 201: 951 (1961).
3. H. P. Witschi, S. Baradun, and H. Cottier, On the pathogenesis of postirradiative hypoproteinemia, Schweiz. Med. Wochschr., 92: 104 (1962).
4. A. R. Bromfield and P. W. Dykes, Radiation-induced protein leakage into the small intestine, Nature, 201: 633 (1964).
5. B. A. Turner and J. F. Fowler, The RBE of fast neutrons in producing intestinal and skin injury in rats, Brit. J. Radiol., 36: 101 (1963).
6. S. Vatistas and S. Hornsey, Radiation induced protein loss into the gastrointestinal tract, Brit. J. Radiol., 39: 547 (1966).
7. R. Ghys, Comparison of the biological efficiency of fast neutrons and caesium gamma-rays on 'August' rats, Int. J. Radiat. Biol., 2: 399 (1960).
8. J. F. Fowler and R. L. Morgan, Pre-therapeutic experiments with the fast neutron beam from the Medical Research Council cyclotron: a review, Brit. J. Radiol., 36: 115 (1963).
9. G. Birke, S.-O. Liljedahl, L.-O. Plantin, and J. Wetterfors, Acute radiation injury: pathophysiological aspects of the massive leakage into the gastrointestinal tract, Nature, 194: 1423 (1962).
10. R. F. Palmer and M. F. Sullivan, Effect of intestinal tract irradiation on serum proteins of the rat, Proc. Soc. Expt. Biol. Med., 101: 326 (1959).
11. W. Friedberg, Serum-albumin metabolism in X-irradiated mice with implanted rat bone-marrow, Int. J. Radiat. Biol., 2: 186 (1960).
12. K. N. Jeejeebhoy and N. F. Coghill, The measurement of gastrointestinal protein loss by a new method, Gut, 2: 123 (1961).
13. K. Hødt-Rassmussen, E. Kemp, B. Møller-Petersen, and L. Hansen, The measurement of gastrointestinal protein loss by ^{131}I-labeled protein and resin, Gut, 5: 158 (1964).
14. K. Rootwelt, Direct intravenous injection of ^{51}chromic chloride compared with ^{125}I-polyvinylpyrrolidone and ^{131}I-albumin in the detection of gastrointestinal protein loss, Scand. J. Clin. Lab. Invest., 18: 405 (1966).
15. L. Dalla Palma, R. Masi, and L. Cionini, Study of the permeability of the intestinal wall to polyvinylpyrrolidone-I^{131} in patients irradiated in the abdominal-pelvic region, Nuntius Radiol., 29: 531 (1963).
16. S. Ullberg, G. Birke, E. Ewaldsson, E. Hansson, S.-O. Liljedahl, L.-O. Plantin, and J. Wetterfors, The role of the gastrointestinal tract in the elimination of serum albumin, Acta. Med. Scand., 167: 421 (1960).
17. M. Schwartz and S. Jarnum, Gastrointestinal protein loss in idiopathic (hypercatabolic) hypoproteinemia, Lancet, I: 327 (1959).
18. S. Jarnum, Protein-losing enteropathy, Lancet, 1: 417 (1961).
19. G. Calcutt, T. A. Connors, L. A. Elson, and W. C. J. Ross, Reduction of the toxicity of "radiomimetic" alkylating agents in rats by thiol pretreatment. Part II. Mechanism of production, Biochem. Pharmacol., 12: 833 (1963).
20. H. M. Patt, J. W. Clark, and H. H. Vogel, Jr., Comparative protective effect of cysteine against fast neutron and gamma irradiation in mice, Proc. Soc. Exptl. Biol. Med., 84: 189 (1953).
21. H. H. Vogel, Jr., N. A. Frigerio, and D. L. Jordan, Prophylactic and therapeutic treatment of neutron-irradiated mice (Abstr.), Radiat. Res., 12: 483 (1960).

22. J. F. Spalding, S. B. Hawkins, and V. G. Strang, The relative effectiveness of neutrons of 1.4-Mev and 14-Mev energies and gamma rays in the reduction of fertility in the male mouse, Radiat. Res., 9: 369 (1958).
23. A. L. Batchelor, R. H. Mole, and F. S. Williamson, Effect on the testis of the mouse of neutrons of different energies, in Biological Effects of Neutron and Proton Irradiations, Vol. 2, International Atomic Energy Agency, Vienne, 1964.
24. G. Silini, S. Hornsey, and D. K. Bewley, Effects of X-ray and neutron dose fractionation on the mouse testis, Radiat. Res., 19: 50 (1963).
25. J. A. Pitcock, Late testicular lesions in irradiated monkeys, in Effects of Ionizing Radiation on the Reproductive System, W. D. Carlson and F. X. Gassner eds., The MacMillan Co., p. 153 (1964).

Figure 1

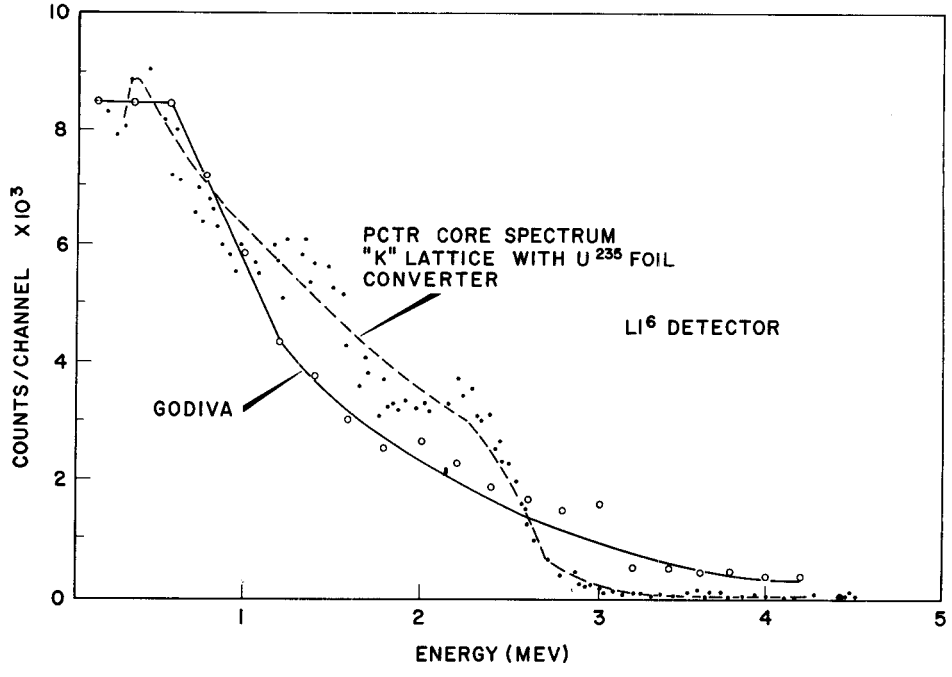

Figure 2

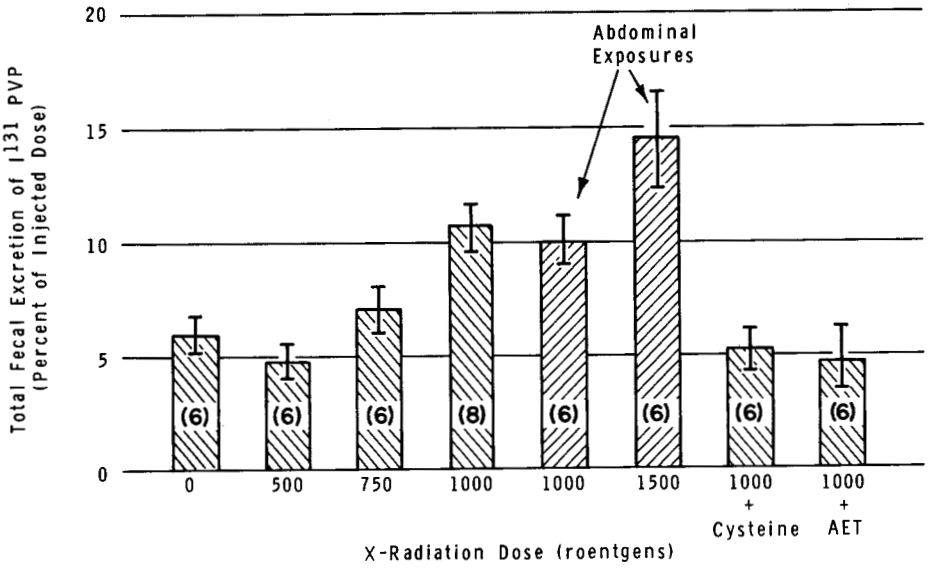

Figure 3

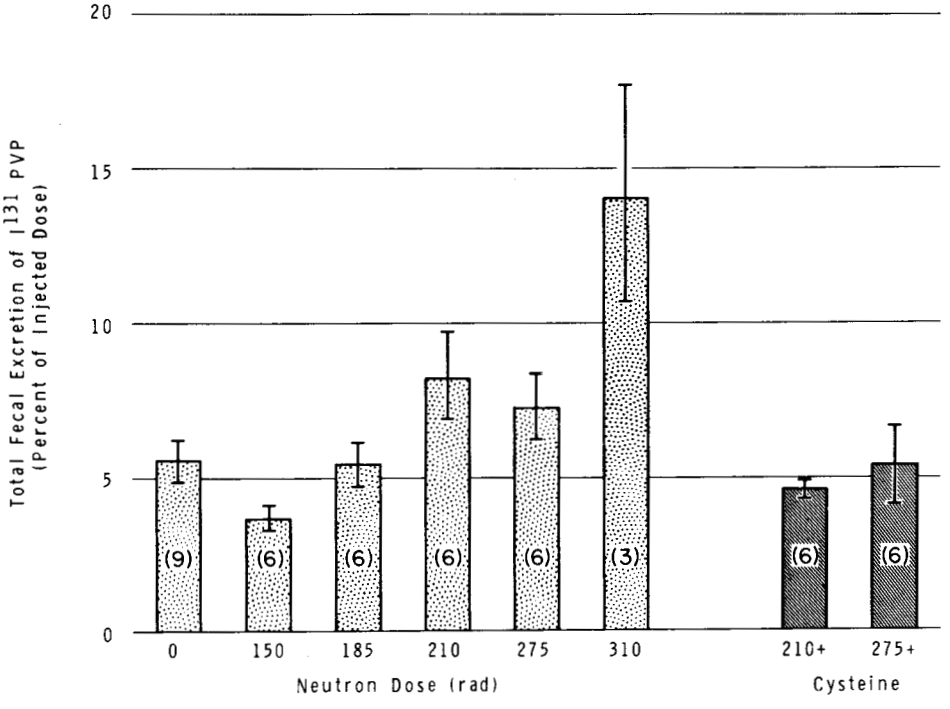

Figure 4

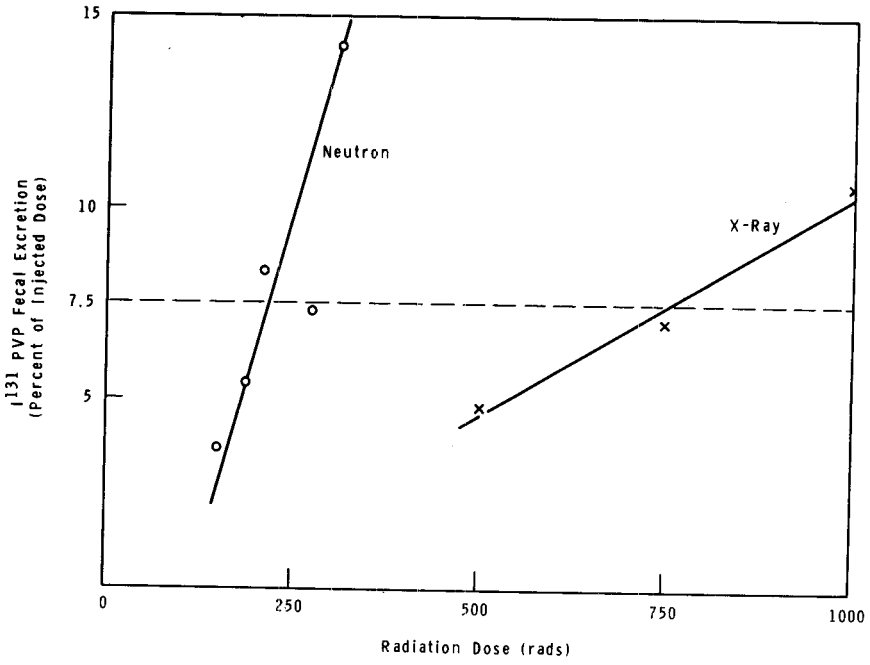

Figure 5

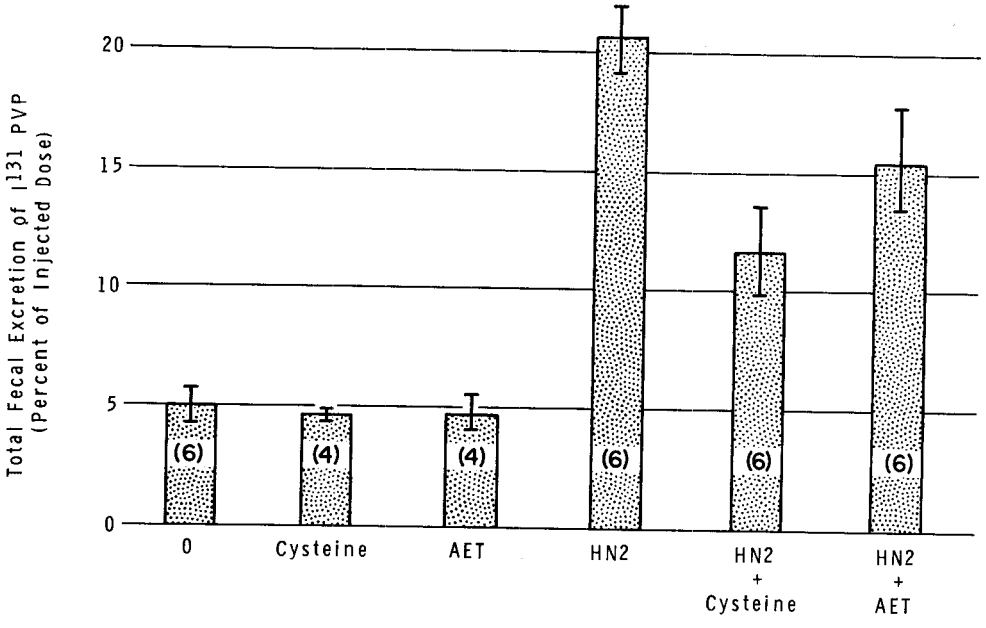

Figure 6

Banquet Address

THE CONTRIBUTION OF BIOLOGY TO STANDARDS OF RADIATION PROTECTION

Samuel M. Nabrit, Commissioner
U. S. Atomic Energy Commission

I am privileged to meet with you this evening and to participate in this timely conference. As I took note of the interesting work being presented at this meeting I could not help reflect on the considerable developments that have occurred through the years. Although I have not actively practiced my profession of biologist for some time, I certainly can recognize and feel a sense of appreciation toward those past and present who have contributed to the field of radiobiology.

It seems significant for us here to make the passing observation that at the time of the great discovery of x rays by Wilhelm Roentgen in November 1895 and spontaneous radiation a year later in November 1896 by A. H. Becquerel, there was a widespread notion in the world of science that all which was to be discovered had been discovered. It remained only to polish off the findings to another few decimal places!

To us today it may seem that an extremely presumptuous conclusion had been reached in the closing years of the 19th century. We can avoid similar complacency by looking back at some of the renowned discoveries and contributions made since the closing years of the 19th century. The procession of great names includes the Curies, associated with the discovery of radioactivity through isolation of radium and polonium, Thomson and the electron, Chadwick and his discovery of the neutron, Anderson and the positron, and many others.

A particularly interesting observation following the initial use of x rays was that of the biological effects of this form of radiation. Naturally the earliest noticeable effects were on the most visible portion of the body--the skin. It seems that in the United States a Dr. E. H. Grubbé developed an x-ray dermatitis of the hands. He was being treated by a fellow physician who noted the damage to skin tissue and suggested the possible value of using the x rays for cancer therapy. Dr. Grubbé responded to the suggestion and began to employ radiation experimentally for therapeutic purposes. Apparently he is the first physician to have used x rays for treatment of cancer of the breast.

With the introduction of fluoroscopic diagnostic techniques, radiologists received even higher and more prolonged exposure to x rays. Generally speaking, these early workers were hesitant to accept the idea that prolonged exposure during fluoroscopic examinations could injure them, and as a consequence many were indeed injured by this new discovery.

During the first few years x rays were used almost entirely empirically. After 1900, serious attempts were made to relate the biological action to the disease process in a scientific way. To accomplish this some idea of dose and dose rate was needed. In short, methods of measurement were needed. Names like Guido Holzknecht, Sabourand, Noire, Kienback, and Benoist are among the pioneers in this field. Duane and Glasser developed small ion chambers suitable for measuring x rays. This led, during the International Congress of Radiology in Stockholm in 1929, to the suggestion for the first time of an international unit to

define x-ray dose, but this was not adopted until the Fifth Congress in 1937.

The use of radium was not far behind that of x rays. As early as 1905 Robert Abbé and Francis Williams in the United States and MacKenzie Davidson in England were using radium by surgically implanting radium-containing tubes within tumors.

While important strides were being made on the disease therapy front, other scientists were looking at some other important aspects of radiation. In 1927 my former Professor, Dr. Hermann Muller, a vigorous and imaginative researcher, demonstrated to the world the important phenomenon of radiation-induced mutations in the fruit fly, Drosophila. For this notable contribution to science, Dr. Muller was awarded a Nobel Prize.

The fundamental explanation of biological action of radiation still eludes us today. Biologists continue to seek a better understanding of the effect of ionizing radiations on living systems. New techniques such as the ability to grow cells in culture and induce division for chromosomal studies, and the many advances in biochemical methods, have broadened our approaches to radiation research. Applications of some of these approaches are being discussed at this meeting.

Recently, increasing attention has been given to the concept of cellular repair mechanisms. Dr. Setlow of the Biology Division, Oak Ridge National Laboratory, has used ultraviolet irradiation of a bacterial system for such studies. Ultraviolet light apparently damages the bacterial cell by altering individual bases of deoxyribonucleic acid (DNA), the polymer which contains the genetic information. His work has shown that certain types of injured bacteria that are uv resistant can recognize the error and through specific enzymatic activity eliminate the error from the DNA strands. One repair mechanism, the dark repair process, involves the excision of the damaged DNA strand and the synthesis of new DNA using the complementary strand as a template--thus restoring the normal sequence of bases in the DNA. The more uv-resistant the bacteria, the more rapidly they are able to correct such errors. Research in the Laboratory of Radiobiology at the San Francisco Medical Center is now attempting to extend similar work to human cells. It has been observed that after irradiation of these cultured human cells, synthesis of DNA occurs in a manner completely different from that in the normal unirradiated cells. This postirradiation DNA synthesis may represent a type of repair to genetic material of the cell.

Considerable evidence of a mechanism for the repair of genetic material has also been reported in mice by Dr. William Russell's group of the Oak Ridge National Laboratory. For example, when a period of time elapses before conception following irradiation of the mother, fewer mutations are observed in the offspring than if conception occurs immediately after irradiation. It has been further shown by this group that apparent repair of "premutational" damage occurs following 50 rad of acute exposure. That is, the ultimate effects of irradiation on the frequency of induced mutations are less than would be expected if one assumes the effects of 50 rad to be linearly proportional to the effects of higher doses up to 600 rad given in an acute exposure.

The problem in the past which continues to elicit the most interest today is

the relationship between dose, dose rate, and biological effect. It is well known that the Relative Biological Effect for a particular kind of radiation may be dependent upon such factors as the specific biological effect under consideration, the tissue irradiated, the radiation dose, and the rate at which it is delivered. As you are aware, the Federal Radiation Council, of which I am pleased to be a member, summarizes in its series of reports the knowledge of the biological effects of ionizing radiation on animals and man pertinent to the problem of defining radiation protection standards, since this is our ultimate interest. Dose-effect information has been accrued through experimental evidence in animals and observations in humans, as well as through assumptions and hypotheses. The available data describing immediate effects which have been considered in the development of radiation protection standards include:

1. Medical data on effects following the therapeutic use of external sources such as x rays and of radionuclides such as radium, iodine-131, etc.,
2. Occupational data on exposure of radiologists, cyclotron workers, and workers in nuclear industry as a result of certain accidents, and
3. Population observations on atomic bomb survivors and on persons irradiated by heavy fallout in the vicinity of the Marshall Islands.

Information concerning delayed effects has been inferred from animal evidence, epidemiological-statistical observations, and a few medical and industrial cases. Further data are needed to refine our knowledge of dose-effect relationships. However, as you are aware, certain stumbling blocks continue to exist. Age-effect relationships extrapolated from animal data are limited because of the maturation and senescence variables between man and animal. In the light of these problems new techniques and methods are being sought.

Another interesting challenge to the radiobiologist and the health physicist has been created with the advent of the high energy accelerator. Of the 240 accelerators currently operating within the AEC program, 40 machines produce particles with energies greater than 20 MeV--among them such giants as the Bevatron, AGS, SLAC, ZGS, PPA, and CEA. The energy region above 20 MeV is characterized for our purposes here as one in which substantial uncertainties exist in dose estimation. The provisional estimates of the National Committee on Radiation Protection and Measurement and the International Commission on Radiological Protection for radiation above 20 MeV are based on mathematical models used in conjunction with data on biological effects obtained at lower energy regions. I believe it is essential to obtain more direct biological data in the higher energy region to verify these extrapolations. Attention needs to be given to the distribution of energy per unit volume on a microscopic scale as well as energy dissipated per unit volume. In this connection the Atomic Energy Commission in its biomedical research program is attempting to foster and strengthen research efforts in the field of what might be called molecular biophysics as it may relate to ionizing radiation effects. Further studies closely linking the dosimetry of accelerator beams of known type and energy with biological studies in the same beams should be encouraged.

Interestingly enough, an integral part of the problem of more clearly defining the direct biological effect to the human organism is the need to increase our knowledge in fundamental dosimetry. Improved measurement techniques and equipment which will permit identification of or differentiation between the various components of the dose, such as energy spectrum and type of radiation, are

prerequisites to the better understanding of the dose-effect relationship.

While the radiobiologist looks to the research health physicist for answers in identifying the radiation environment, the health physicist is also looking to the radiobiologist for biological parameters to be considered in the development of instrumentation. Even if instrumentation existed which would readily describe the accelerator radiation field in adequate detail (such as intensity and energy distribution of each component) there would still remain perplexing problems of interpretation. As you are aware, for gamma rays RBE values are missing above 3 MeV, and for neutrons above 30 MeV only calculated values exist (which have not been fully adopted).

Finally, as you are aware, there is a need for further development of concepts which would be more useful in relating the physical parameters of the radiation to biological effect. Areas of uncertainty exist in the application of the Quality Factor as well as the fluence, kerma, first collision dose, and other terms used to convert "dose" to effect. At present the rad-to-rem conversion is at best an approximation.

A resolution of these uncertainties and development of improved concepts will depend to a large extent on progress made in radiobiological research and instrumentation development.

In summary, we have come a long way in our knowledge of radiation and its biological effects. But as one can see, there are still some knotty problems which pose a challenge to radiation biologists, radiation physicists, and the molecular biophysicist. Since the end point of all this work is effect on man, work should continue in close collaboration with biologists to ask from living systems whether parameters such as LET, spatial distribution, time rate, and other factors are appropriate ones to describe radiation effects in tissue.

Our future horizons include the support and use of two new and unique facilities. The first of these is the Omnitron accelerator, to be located at Lawrence Radiation Laboratory, Berkeley, which will provide many unique radiations for research in radiobiology, chemical biodynamics, medical research, nuclear physics, and chemistry research. The accelerator, which was first proposed by the Medical Physics Group at the Lawrence Radiation Laboratory, will be capable of accelerating nuclei as heavy as argon to 400 or 500 MeV per nucleon (18 BeV). The radiobiological studies of radiation effects at varying depths in tissue planned for this machine include the production of a converging beam which will allow precise focusing into cancerous tissue. It should be possible with this device to produce lesions, for example in brain tissue, through broad areas of the brain at almost any desired depth and much more sharply.

It will also be possible to produce for the first time in a substantial way the spectrum of space radiations and to study the effects of these on critical tissues of the body that do not regenerate.

The second facility is called the Meson Physics Facility. The biomedical specialists enthusiastically support construction of this facility at Los Alamos Scientific Laboratory; it will provide, as a by-product and on a noninterfering basis, an abundance of π^- mesons for treatment of cancer and for other biomedical

investigations. Exploratory studies carried out jointly by Dr. Chaim Richman of the Graduate Research Center of the Southwest, Dallas, Texas, and Dr. John Lawrence and Dr. Cornelius A. Tobias of the Lawrence Radiation Laboratory indicate that it is almost a certainty that π^- mesons, with their star formation in deep-seated tumors and minimal dose to the skin and intervening normal tissues, may offer a real advantage over presently available modes of treatment. The work of both groups, at the Lawrence Radiation Laboratory and at the Los Alamos Scientific Laboratory, using these important tools for investigation should yield much information of fundamental importance to the advancement of radiobiology.

In addition to these, other machines, such as the 200 BeV accelerator, will provide many unique radiations for biologically oriented scientists to use in their quest for new knowledge on the biological effects of radiation. Without a doubt, the information will provide a much firmer basis for assessing the significance of radiation protection standards.

PHYSICAL, GEOMETRICAL, AND TEMPORAL FACTORS DETERMINING BIOLOGICAL RESPONSE TO HEAVY CHARGED PARTICLES

Charles A. Sondhaus

California College of Medicine
University of California
Irvine, California

The biological response to any radiation depends not only on "absorbed dose," but also on its distribution within tissue in both space and time. In this brief discussion, I would like to try to summarize what physical measurements ought to be made with high-energy charged particles to specify the dose distribution, and why. In order to do this I want to concentrate on the basic phenomena that take place when a beam of high-energy charged particles interacts with matter.

To relate these phenomena to the problem of what one should measure, we might start by recalling that in order to characterize an exposure completely one must know something about five quantities. In most cases it is possible to simplify or make assumptions about some of these, but when one is dealing with high-energy particles whose interactions are less well known it is important to know as much as possible. These five are (a) the accumulated absorbed dose; (b) its time profile--i.e., the dose rate and how it has varied over a period of time-- (c) the fraction or region of the body which has been exposed; (d) the depth-dose distribution; and (e) the LET, energy density, or any other information on a microscopic scale which characterizes the nature of the local energy deposition. Obviously no one device can satisfy all these requirements.

It would be desirable, of course, to have as many dosimetric devices as possible at different points on the body of a person who is likely to be exposed. One generally can't do this, however; there is often only a dose taken in air in the region to be occupied by the person, or that measured in a volume of tissue-equivalent material. The latter alternative is particularly important for the proton case, as will be discussed shortly.

A system of instruments could be designed to measure fluence, or preferably fluence plus energy distribution, but in general even with a complete description of both fluence and energy distribution the computation of dose is quite complex, because it depends on so many local circumstances. Some of these are the geometry of the exposure and its variation if a person changes position near a shield or in the vicinity of a beam; the effects of angular incidence and self-shielding; and in particular the fact that we really don't have very accurate physical data on the interaction properties between high-energy radiation and tissue. Historically, the roentgen unit was introduced for low-energy γ radiation just to remove the necessity for such calculations; it does not represent fluence nor even the amount of energy being transferred to tissue, but simply because of the difficulties in measuring those quantities, was defined

only in terms of the ionization that the beam was producing in air. Later on, when the constancy in the amount of energy required to ionize gas molecules by photons of different energies was recognized, it was possible to associate the energy absorbed from the beam by air with both fluence and energy absorbed in tissue; the first one of these three quantities is now called exposure. In high-energy charged-particle beams there is no analogous quantity defined; thus difficulties at the start make it necessary to refer to absorbed dose as much as possible.

One can therefore summarize as follows: the measurements a health physicist needs to make must aid in describing (a) the microdose, which has been discussed in detail during the last two days; (b) what might be called the macrodose distribution; and (c) the relationship of the field itself and of its parameters of fluence and energy to the absorbed dose. All three of these areas present special problems in the case of high-energy charged particles.

First, let us briefly consider the essential properties of the interaction of high-energy particles with matter and how they relate to the interpretation of both macro- and microdose distributions and their consequent biological effects. Depending on the type and energy of the incident radiation, a complex spectrum of primary and secondary particles is produced; these particles in turn produce very specific local energy density and dose distributions in the tissues. The process begins with the two kinds of interactions that the primary high-energy charged particles undergo when they pass through matter. The first type is nonnuclear and electromagnetic; the energy of the particle is decreased as it traverses material by interactions with the orbital electrons of the atoms in the tissue or shield. As a result the particle has a range which depends on its initial energy, and the process, being random, is subject to fluctuations. Dr. Maccabee is going to discuss the effect of these fluctuations on very thin dosimeters, the Landau effect, a little later on. The results of the first type of interaction are the familiar processes of ionization, excitation, and heat transfer; each event represents a small energy loss. The process is well described by the Bethe-Bloch formula, as Dr. Robertson has discussed. This formula breaks down at low energies near the end of the path of the particle, where its charge varies due to electron pickup; it also breaks down at the point of maximum ionization, the Bragg peak. However, the phenomenon is well enough understood to permit calculation of primary dose. The bulk of the energy is actually deposited by this mechanism, either by the primary charged particle itself or by the secondary heavy charged particles which it in turn produces through nuclear interactions; the latter are the second type of interaction which the particle undergoes. (Elastic nuclear scattering may also be grouped with the first type of interaction not involving nuclear phenomena; not much energy is lost, but it can be dosimetrically important in the way it influences the angular distribution of the fluence.)

The second type of interaction is an inelastic collision of the heavy particle with a nucleus of the absorbing material (for neutrons, of course, this is the only kind of interaction that takes place). The higher the energy of the primary particle the more nuclear collisions will occur before it reaches the end of its range. For example, in a 150-MeV proton beam about 15% of the protons will have undergone inelastic nuclear collisions before stopping, according to an estimate by Strauch.

These inelastic interactions produce a variety of secondary particles with distributions of velocity and energy. These secondary particles in turn interact with both nuclei and atomic electrons in the material, producing the extranuclear cascade. The cascade adds so much dose to that from the primary beam that it is a prime consideration both in the design of shielding and in the dose distribution in tissue. The probability of this second type of interaction is measured by the attenuation or removal cross section; a great many measurements of it have been made with both protons and neutrons for a variety of elements.

Figure 1 is a schematic indication of the three major types of inelastic and near-elastic collisions that can take place. These are the elastic, the quasi-elastic, and the multiple collisions. The nucleus and its energy levels are also depicted in the figure. Because of the three kinds of interaction, a particle spectrum of secondaries is produced as shown in Fig. 2; this is merely a representative diagram (due to Strauch); not all these peaks are present in all cases. Close to the incident energy (T_{inc}) is the elastic peak of secondary particles; it is followed closely by a series of peaks related to the shell structure and energy levels in the nucleus. Further on, the peak denoted by T_{inc}-20 is due to excitation through a dipole state associated with photoproduction. Still further on, at a somewhat lower energy, the quasi-elastic peak is observed; it has a width which depends on the momentum distribution of the nucleons in the target nucleus. Finally, a rising continuum of cascade particles extends down either to 2 MeV (for a neutron interaction) or to the Coulomb barrier energy for a proton interaction.

Figure 2 summarizes all possible features of the secondary particle spectrum in a high-energy nuclear reaction, but the relative importance of these peaks depends on the energy of the incident nucleon and on the atomic number of the target nucleus. Whether any or all peaks were observed would also depend on the energy resolution and the experimental setup. For purposes of describing the angular distribution of the cascade particles and its influence on dose, the processes can be summarized as follows: (a) the secondary particles due to near-elastic events peak rather strongly in the forward direction, similarly to those resulting from elastic scattering, (b) the quasi-elastic events produce an angular distribution which is similar to that from free nucleon-nucleon collisions; (c) the intranuclear cascade particles are generally emitted in the forward direction, the more so the higher the energy; and, finally, (d) the low-energy evaporation particles are emitted isotropically, all in the center-of-mass system.

The experimental results obtained in a number of laboratories agree quite well with the general features of this model. Figure 3, from an experiment by Hess and Moyer here in Berkeley, is for 330-MeV protons incident on a carbon target. This is a distribution of energy vs differential cross section at the scattering angle of 40 deg. It resembles fairly closely the results of some Russian work at Dubna at about the same time (1959), which show a similar distribution: a quasi-elastic peak that dominates the secondary spectrum in light elements, and for the heavier elements an intranuclear cascade becoming more important. These spectra of secondary particles have also been obtained for neutrons, and they too show near-elastic and quasi-elastic peaks in the same way. Most of the measurements so far have been carried out at limited angles

only, and a great increase in usefulness will occur when cross sections can be obtained for a wider angular region. To summarize: a particle beam passing through matter undergoes a gradual energy loss due to ionization and excitation, and will also be attenuated and scattered by the nuclear interactions that result in the production of these secondary particles. The secondaries have energies ranging all the way from a few hundred keV to a large fraction of the primary particle energy, and they may undergo further interactions that produce the cascade. The highly excited nuclei that have been struck lose their energy by evaporating off more nucleons and heavier particles of much lower energy. The numbers and kinds of secondary particles depend on the composition and density of the absorber, and the nature, energy, and charge of the incident particle. Not only secondary protons and neutrons, but also electrons, x, and γ rays are all produced, and at proton energies above about 350 MeV the production of mesons begins to occur.

Although we are here considering only the production of secondaries by incident protons, the general features of cascade phenomena hold equally well for other charged particles. Metropolis treated this phenomenon analytically a few years ago. Figure 4 plots his calculation of the number of cascade protons emitted per incident proton for a variety of target materials. One sees that although in the higher energy region the lower-A materials emit fewer cascade particles, they actually have a higher production rate than the higher-A materials below 500 MeV.

Figure 5 shows a typical energy spectrum of secondary particles, also due to Metropolis; this was discussed by Wallace et al. at the 1962 Gatlinburg Symposium. It shows how the distribution of the emitted proton energies runs all the way down to small values. Several other authors have also treated the evaporation phenomenon. Figure 6 shows the number of evaporation protons per incident proton for different A, plotted against the energy of the incident proton or neutron. One sees that the number of evaporation protons is fairly constant at about a 1-to-1 ratio over a fair-sized energy range. The energy spectrum of evaporation particles has usually been obtained by estimating an excitation energy for the nucleus and treating it as if it were a source of thermal energy evaporating off the nucleons. The excitation energy is not very sensitive to incident proton energy over several hundred MeV. Figure 7, using data from Moyer, shows the total neutron production per proton striking a target as a function of proton energy for four materials, the particle coming completely to rest in the target. One can make similar estimates for neutrons, protons, or heavier particles.

The passage of high-energy protons is different from that of lower-energy ones, mainly because the high-energy ones survive far enough into the absorber to have a reasonable number of these inelastic interactions take place. The cascade which results dominates the problem of predicting dose distributions and certainly has a great influence on the uniformity of the dose patterns that result. A knowledge of the cascade is thus essential to dealing with this problem, both for shielding and for dosimetry. Figure 8 shows the typical idealized intensity-depth curve which results from the nuclear cascade in material; it is taken from Shen, who made experimental studies of the cascade at the Brookhaven Cosmotron. The thickness of the material is on a linear scale,

whereas the intensity or fluence is on a log scale. This intensity-depth curve is usually called the transition curve. In this figure the function $f_{det}(x, T_o)$ represents the detected component of the flux at some depth x in the absorber, with T_o the total thickness of the absorber. The point x is moving through a given absorber and does not represent adding absorber in front with nothing behind. This quantity can also be considered as proportional to the energy deposition, or the dose, or some other function of the fluence or component of fluence. The dashed straight line $f_{prim}(x)$ represents intensity due to the primaries alone; the detected component may or may not include this part. The curve may be regarded as made up of four regions, following Shen: (a) the premaximum, (b) the approach, (c) the equilibrium, and (d) the exit region. If the finite absorber were infinitely extended in both directions up and down the beam, then the intensity-depth curve would no longer have this shape, but would instead be the straight line $f_{det}(x, \infty)$. The deviation of the actual curve from this line except in this equilibrium region can be thought of as being due just to the missing parts of the absorber on either side. The missing front part fails to supply the forward-moving particles; they would fill the area between the curve and the straight line in the approach and premaximum regions. In a similar way the missing rear part fails to supply the backward-moving particles, or albedo, which would fill the corresponding area in the exit region. This deviation in shape from the straight line is called the transition effect; the first two regions make up the entrance transition and the last one the exit transition. If, now, instead of having an absorber of fixed thickness one were to use an absorber of variable thickness and detect behind it, the dotted intensity-thickness curve $f_{det}(T)$ would result. The lower curve $f_{det}(T)$ is derived from the upper one, $f_{det}(x, T_o)$, simply by subtracting the albedo flux all the way back through the material at every depth except in the exit region, where it is already absent.

Four quantities are of particular interest: first, the location of the transition maximum, x_{max}, sometimes called the optimum depth; second, the critical depth, where the value of $f_{det}(x_c)$ is the same as at the entrance $f_{det}(0)$, and x_c is some finite distance in the absorber where the buildup has come down again; third, the buildup factor, which is the ratio f_{det}/f_{prim} at any depth x, and fourth, the maximum-to-primary ratio $f(x_{max})/f(0)$. A quantity of particular interest in both shielding and dosimetry is the critical depth x_c. For example, for monoenergetic primaries any shield thinner than the critical depth would do more harm than good, because the resultant fluence emerging from it would be greater than the incident primary fluence. When one has a distribution of primary particle energies, then one has to add a series of such curves together and weight each one by the intensity in each energy interval. In such a case the maxima may smear out sufficiently to mask the transition effect and result in a continuously decreasing depth-dose profile; its intensity will nevertheless be higher everywhere than primary interactions alone would account for.

Figure 9 shows some results of a computer program at LRL developed by Palmer Steward as part of the research efforts centering around irradiation of mammals in a simulated space radiation field. The program was developed to calculate depth dose in spheres of tissue for isotropically incident monoenergetic protons of various energies. It is applicable to accelerator beams as well, since it also generates dose rate versus depth in a slab of water due to a normally incident, parallel beam. Figure 9, for the parallel beam case,

shows the calculated dose rate in rads per hour per unit fluence of 10^4 protons per square centimeter per second, for several different energies. Of course these are idealized curves for single particles, and the height of the Bragg peak is subject to all the qualifications discussed in previous papers. In any real situation the finite number of particles, the straggling, and other effects would bring this peak down. These corrections aren't too important in the isotropic case, however, where one has particles entering from all directions, since for 4π geometry things tend to smear themselves out.

The spectra and the number of cascade and evaporation protons were based on the Metropolis data mentioned earlier, and approximate analytic expressions for each contribution to dose rate were used. Only the first generation of secondaries was considered. Comparison of this code with some results of experiment as well as with other calculations, notably those of the Oak Ridge group, have shown that very little accuracy was sacrificed. At each depth the dose rate deposited by protons in each of eight energy intervals was also summed separately; no multiplication by QF or any other factor was carried out. Figure 10 shows some results of the Oak Ridge code based on the Monte Carlo method first set up by Bertini. This calculation was made for a different material, and it sums not only the contribution of primary protons but secondary and heavy particles as well, but when one converts the fluence-to-dose ratio to the units of Fig. 9 they are very close to each other for each of the energies in the Oak Ridge code up to 400 MeV.

Figure 11 shows a comparison of the Oak Ridge code with experiment for one case, one of the few results with which it has been possible to compare the code experimentally. It happens to be for neutrons, from Shal'nov's work in Russia. The experimental data are for 140-MeV neutrons incident in water. The dose calculated for 100-MeV protons was compared with the experimental data; though the energy was different, the agreement is still close enough to be quite good. Figure 12 shows a comparison of the Berkeley code with experimental data recently obtained by Tanner and Baily on the 730-MeV beam; Dr. Baily has done considerably more work on this, which he will present in a later paper. The agreement is seen to be very close; it should be noted that in contrast to Fig. 11, which was not normalized but was an absolute comparison, the two curves in Fig. 12 have been normalized at a depth of 1 cm. In any case, for a clean beam without any energy degradation or interactions beforehand one sees clearly the steep buildup of dose, as the transition curve of Fig. 8 predicts. It can be seen that the assumptions regarding the parameters of the different kinds of intranuclear reactions have accounted for this transition fairly well. The important point is that if one makes the dose measurement in the beam and then puts an animal in place of the dosimeter this buildup occurs. The transition effect provides at this energy an increase of more than 40% at maximum dose over that from the primary beam alone at the surface; for lower energies the same thing occurs to a lesser extent.

Figure 13 shows the extent of disagreement between the simple model and some experimental data obtained with a beam that had been passed through a carbon target of sufficient thickness to degrade the energy to 260 MeV by multiple nonnuclear (Coulomb) reactions. Although the calculations led to an extraordinarily high Bragg peak, the experimental data did not show this peak,

but instead showed that secondaries--either gammas or neutrons--appeared to cause the curve of dose taken with an extrapolation chamber to extend even further than the range of the primaries themselves. The initial buildup is still present, although somewhat reduced.

Isotropic fluence calculations were performed for a number of sphere sizes. Figure 14 shows the general assumptions made: the beam entered an element of surface in an arbitrary direction and the dose was summed in an element inward along a radius from some point at the surface. Contributions from the secondaries were taken into account by use of the so-called straight-ahead approximation and the simplifications that were mentioned above.

Figure 15 shows that there are three modes of dose deposition, depending on the volume of the tissue sphere and the energy of the incident particle. The first dose pattern is that in which the primary proton has energies too low for it to cross the sphere. In the second type of interaction the particles pass the center of the sphere but come to rest before they get out of it. If one considers the dose as a function of the radius it is usually found that the cross contribution produces maxima with relatively higher dose at certain depths, depending, of course, on both energy and the radius of the tissue sphere. These maxima occur only for monoenergetic protons with no contamination by either neutrons or γ rays. In an irregularly shaped animal the principal significance of this depth-dose pattern is its indication that large doses may occur in shells within the volume being irradiated if some segment of the surface has the proper curvature. The third radiation pattern due to high-energy protons going through the sphere does not produce any areas of high dose; a fairly flat profile results. This last case is the one usually encountered in the laboratory.

Figure 16 shows that for the 730-MeV beam about half the total dose in a sphere of this radius is actually due to the secondary protons. At lower energies, such as 250 MeV, there still is a substantial contribution from them. This produces the second pattern mentioned above, with a peak at an intermediate depth. This peak is a smeared-out overlapping of Bragg peaks; Fig. 17 shows that at 60 MeV the peak is quite obvious.

Table 1 shows a sample breakdown of the total dose and the dose rate at different depths in several energy intervals for 60 MeV. In the low-energy intervals, where the LET is highest, only a few percent of the total dose is produced. The greatest high-LET component of dose occurs at a depth of 2 cm, just before the Bragg peak, where the overlapping of Bragg peaks causes the buildup to start. By contrast, in the 730-MeV case shown in Table 2 the dose is fairly evenly distributed in depth.

A calculation by Schaefer, shown in Fig. 18, illustrates the important differences between the distribution of proton energies in a solar flare extending to low energies, and that of fission-spectrum neutron recoil protons; also shown is the LET of protons plotted against their kinetic energy. Figure 19, also calculated by Schaefer, shows the difference between the LET distribution at the end of a proton track and that at the end of an electron track.

To conclude this brief and admittedly incomplete discussion of physical factors in high-energy charged-particle exposures, we point out several instances where biological response or its interpretation has been influenced by them.

Figure 20 shows two examples of animal exposures in which a proton or α-particle beam was used to irradiate mice. The percent mortality is plotted as a function of the time postirradiation; the curves represent data from several hundred mice. For protons, the predominant mode is a peak of early "gastrointestinal" death at 4 days for a dose producing 98% mortality. For 250-kVp x rays, a dose high enough to produce this same degree of mortality produces a peak of "hematopoietic" death, mainly occurring at 11 days. Alpha particles appear to produce both peaks. This distinct separation at 98% lethality is statistically significant. Figure 21 shows a dose-rate effect; decreasing the dose rate appeared to reduce the early peak and shift mortality to the later mode.

In view of the calculations that we have just mentioned, neither the change with dose rates shown in Fig. 21 nor the mortality distribution shift seen in Fig. 20 can be explained by LET differences. We believe that the explanation lies in the difference in microdose distribution in the bone marrow cavity; x rays may produce electron secondaries in small marrow cavities that can, as Spiers first showed in 1949-50, produce 50% higher dose in marrow cavities of a few micra. Apparently this situation has always been present, at least at the lower-energy x-ray exposures, but does not prevail for the protons. As will be shown in a later paper, the dose at an interface between materials with different Z may differ, relative to the standard γ-ray case, for protons.

Figure 22 shows the depth-dose pattern due to solar flare protons, which is seen to be very steep. The important property of this distribution is the macro nonuniformity, which is quite pronounced. This can also occur in the vicinity of accelerators. Dr. Bond has covered this in the first paper. Figure 23 shows Jackson's experiment, in which he compared a uniform depth-dose exposure with a steeply varying exposure produced by a wedge filter. A cobalt source was used, and rats were compressed into cylinders and rotated in front of the wedge to produce the steep pattern of depth dose; the LD_{50} value is shown.

Figure 24 is from a study of maximum depression in white blood cell count in primates, made by Taketa et al. at NASA, Sunnyvale, in collaboration with LRL. When the results for gamma-irradiated and proton-irradiated primates are plotted as a function of the midline air dose, the protons appear to be relatively more effective. Figure 25, in contrast, is in terms of the absorbed dose at the midline of the animal (lithium fluoride dosimetry was used.) The fact that the gamma exposure was not entirely uniform but had the characteristic dip in the midline, whereas the proton exposure, due to the buildup of secondaries, was actually higher in the midline than at the edges, had the effect of reversing the apparent ratio of effectiveness of these two radiations.

In conclusion, then, it seems clear from the foregoing that the interpretation of biological response to high-energy charged-particle exposure requires both caution and a considerable increase in the exactness with which both gross and microscopic dose distributions must be described. In fact, this may be its greatest challenge to the radiological protection specialist.

Bibliography

1. K. Strauch, Measurements of Secondary Spectra from High-Energy Nuclear Reactions, in Proceedings of the Symposium on the Protection Against Radiation Hazards in Space, Gatlinburg, 1962, Vol. 2, p. 409, USAEC-TID-7652, 1962.

2. W. N. Hess and B. J. Moyer, Production of Deuterons in High-Energy Nuclear Bombardment of Nuclei and the Bearing on Nuclear Charge Distribution, Phys. Rev., 101: 337-350 (1956).

3. R. W. Wallace and C. A. Sondhaus, Techniques Used in Shielding Calculations for High Energy Accelerators: Applications to Space Shielding, in Proceedings of the Symposium on the Protection Against Radiation Hazards in Space, Gatlinburg, 1962, Vol. 2, p. 829, USAEC-TID-7652, 1962.

4. S. P. Shen, Some Experimental Data on the Nuclear Cascade in Thick Absorbers, in Proceedings of the Second Symposium on Protection Against Radiation in Space, Gatlinburg, 1964, p. 357, NASA-SP-71, 1964.

5. Palmer Steward, Depth Dose in Tissue Irradiated by Protons, M. S. Thesis, Lawrence Radiation Laboratory Report UCRL-10980, July 1964.

6. W. E. Kinney and C. D. Zerby, Calculated Tissue Current-to-Dose Conversion Factors for Nucleons of Energy Below 400 MeV, in Proceedings of the Second Symposium on Protection Against Radiation in Space, Gatlinburg, 1964, p. 171, NASA-SP-71, 1964.

7. M. I. Shal'nov, Tissue Doses of Fast and Ultrafast Neutrons, Soviet J. Atom Energy, 5: 735 (1958).

8. N. Baily, (UCLA), personal communication.

9. C. A. Sondhaus, P. Steward, and R. Wallace, Primary and Secondary Proton Dose Transition Curves in Tissue--Comparison of Theory With Experiment, (abstract), Radiation Res., 27: 539 (1966).

10. R. W. Wallace, P. Steward, and C. A. Sondhaus, Primary and Secondary Proton Dose Rates in Spheres and Slabs of Tissue, in Proceedings of the Second Symposium on Protection Against Radiation in Space, Gatlinburg, 1964, p. 301, NASA-SP-71.

11. H. J. Schaefer, Local LET Spectra in Tissue for Solar Flare Protons in Space and for Neutron-Produced Recoil Protons, in Biological Effects of Neutron and Proton Irradiation, Vol. I, p. 297, International Atomic Energy Agency, Vienna, 1963.

12. C. A. Sondhaus, Effects of High-Energy Protons and Alpha Particles on Small Animals, in Proceedings of the Second Symposium on Protection Against Radiation in Space, Gatlinburg, 1964, p. 97, NASA-SP-71, 1965.

13. J. K. Ashikawa, C. A. Sondhaus, C. A. Tobias, A. G. Greenfield, and V. Paschkes, Difference in Injury Mode, Dose-Rate Dependence, and RBE of 730-MeV Protons, 100-kVp x rays, and 250-kVp x rays, in Biological Effects of Neutron and Proton Irradiation, Vol. I, p. 249, International Atomic Energy Agency, Vienna, 1964.

14. H. J. Schaefer, Time Profile of Tissue Ionization Dosage for Bailey's Synthetic Spectrum of a Typical Solar Flare Event, Bu. Med. Project MR005, 13-1002, Subtask I, Report 22, USN School of Aviation Med., 1962.

15. K. L. Jackson, The Lethal Effectiveness of a Solar Flare-Type Dose Distribution Delivered to the Rat, in the Proceedings of the Symposium on Protection Against Radiation Hazards in Space, Gatlinburg, 1962, Book I, p. 375, USAEC-TID-7652, 1962.

16. S. T. Taketa, B. L. Castle, W. H. Howard, C. C. Conley, W. Haymaker, and C. A. Sondhaus, Effects of Acute Exposure to High Energy Protons on Primates, Radiation Res. (in press).

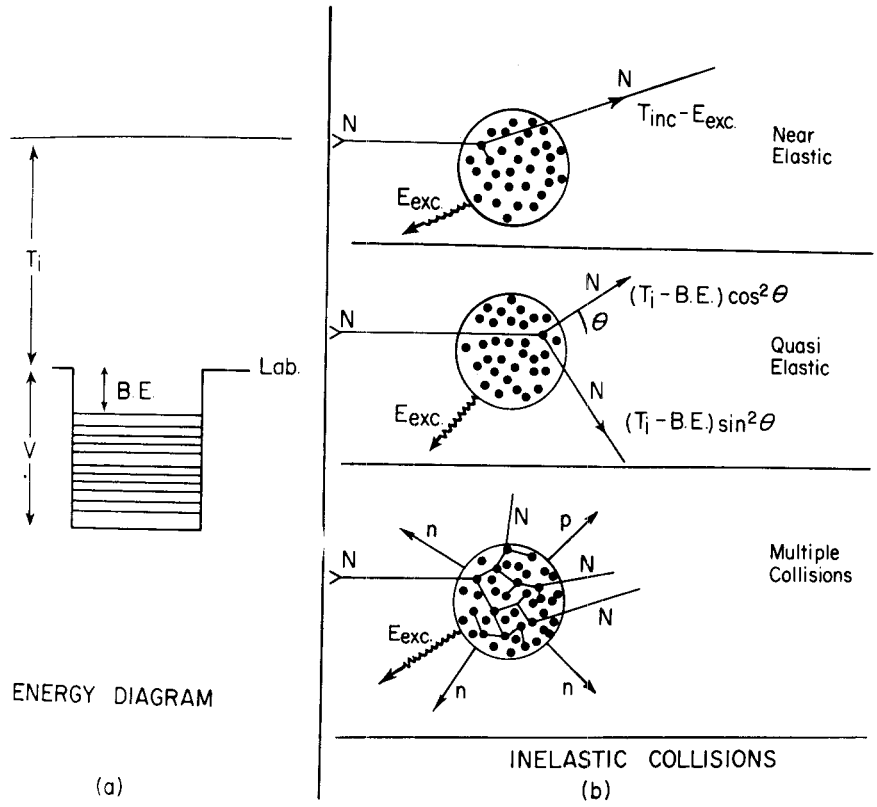

Fig. 1. Types of inelastic nuclear collision. (Strauch)

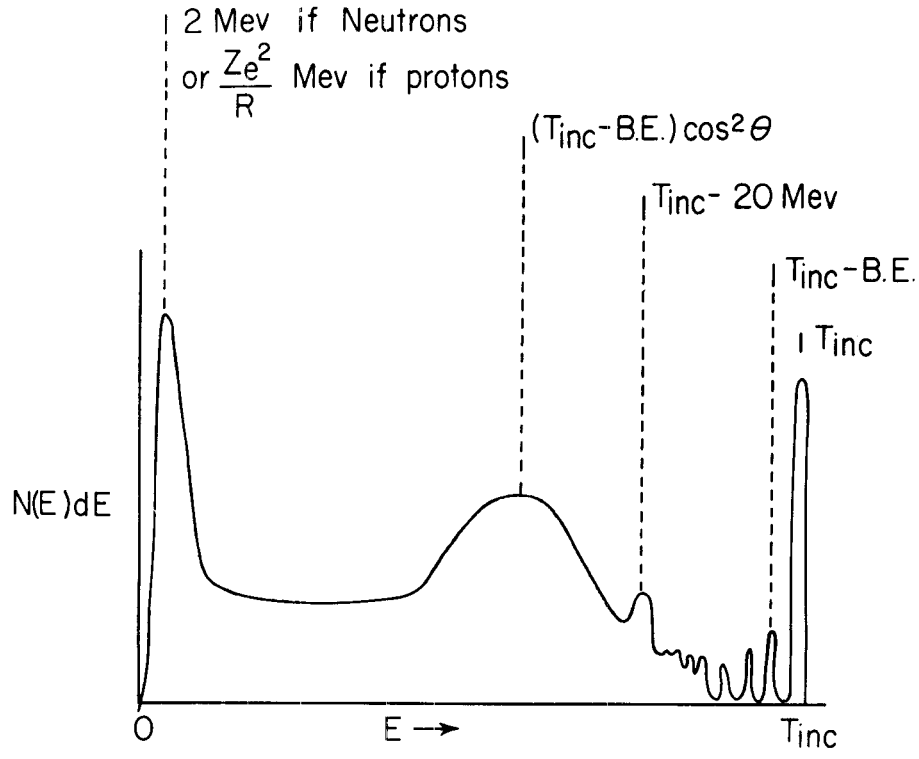

Fig. 2. Hypothetical secondary-particle spectrum at angle θ. (Strauch)

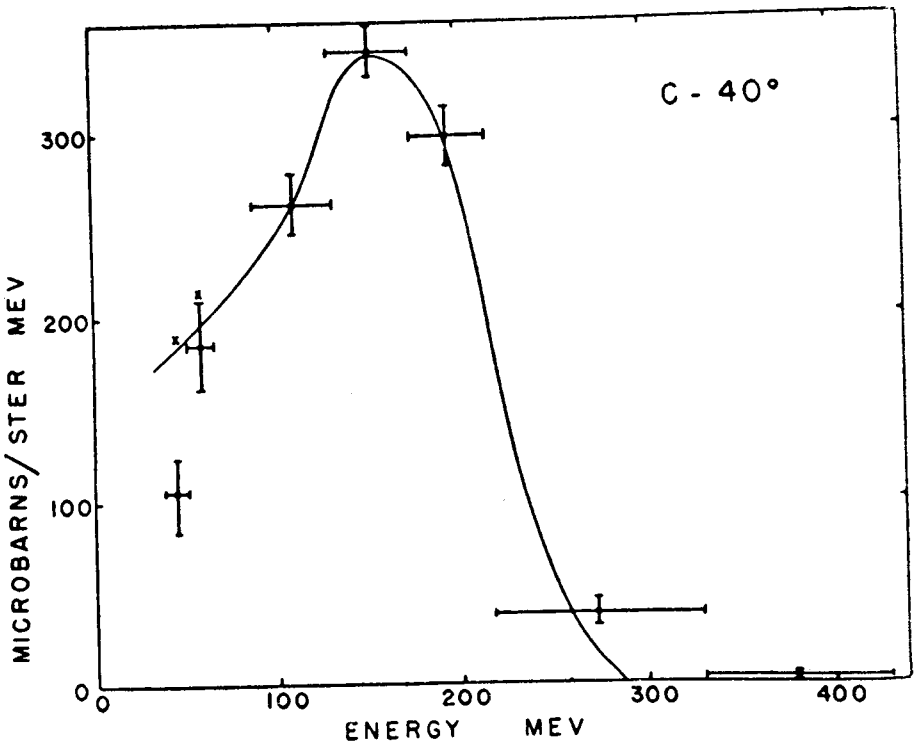

Fig. 3. Differential cross section vs energy for 330-MeV protons on carbon at 40 deg. (Hess and Moyer)

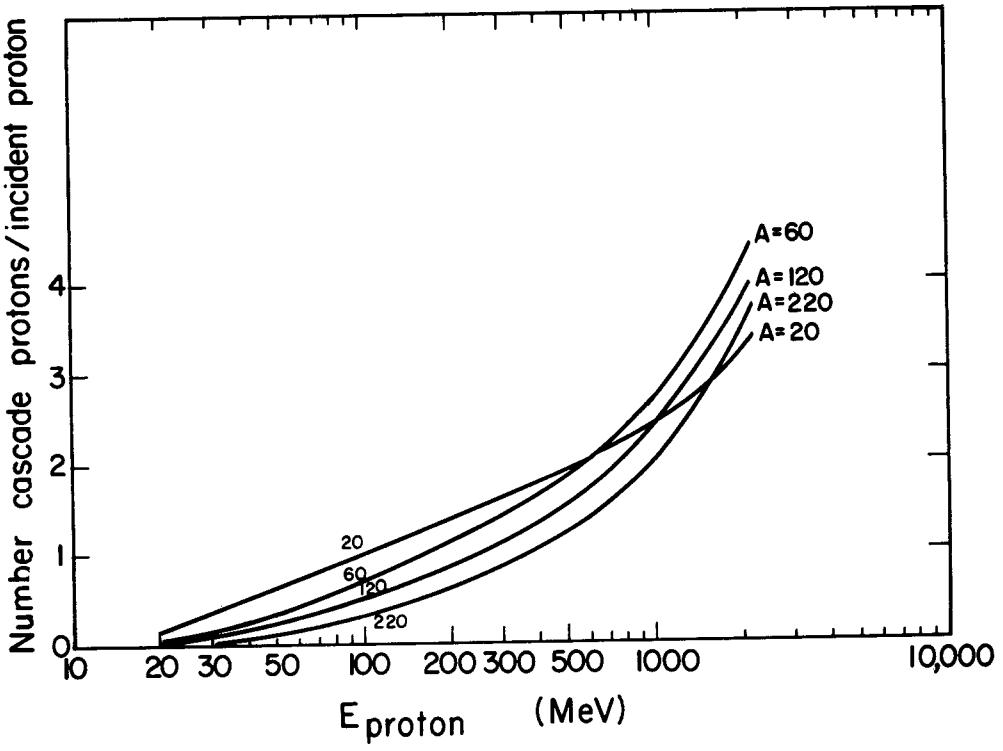

Fig. 4. Number of cascade protons emitted per incident proton vs incident proton energy and target mass number. (Wallace and Sondhaus)

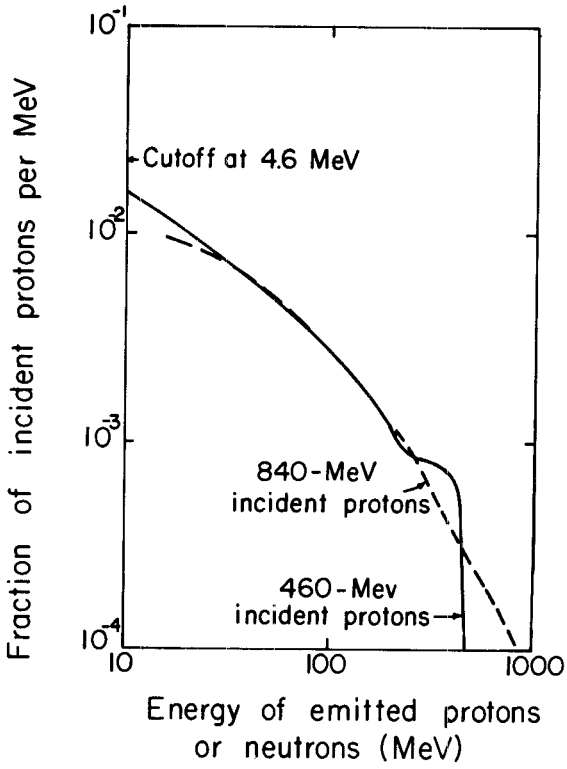

Fig. 5. Relative numbers of emitted secondary protons or neutrons vs secondary-particle energy for two primary proton energies. (Wallace and Sondhaus)

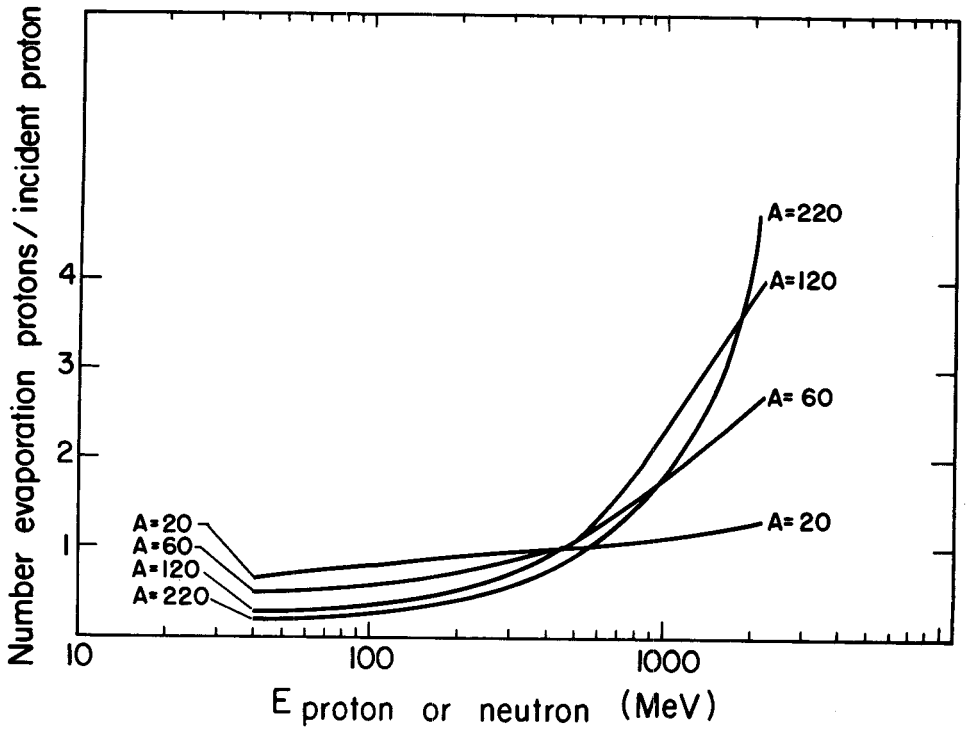

Fig. 6. Number of evaporation protons emitted per incident proton vs incident proton energy and target mass number. (Wallace and Sondhaus)

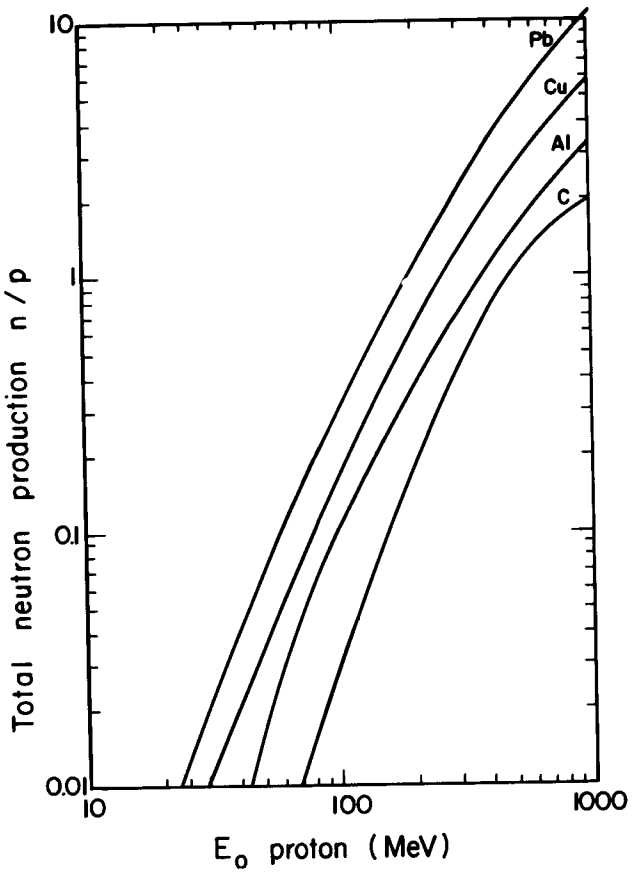

Fig. 7. Total thick-target neutron production per incident proton vs incident proton energy. (Wallace and Sondhaus)

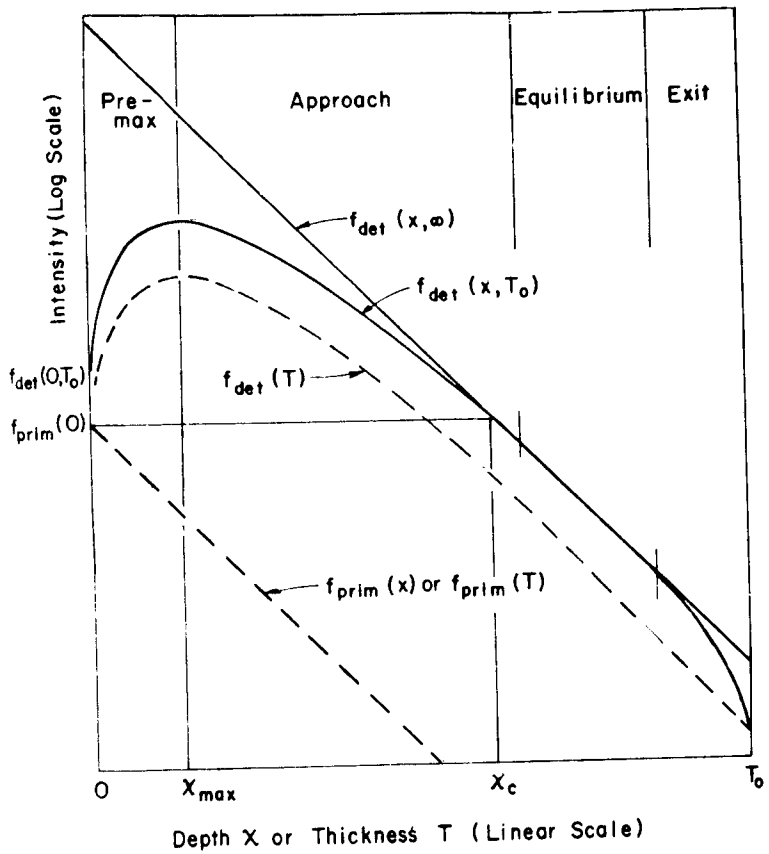

Fig. 8. Idealized intensity-depth curve from nuclear cascade in material, or transition curve. (Shen)

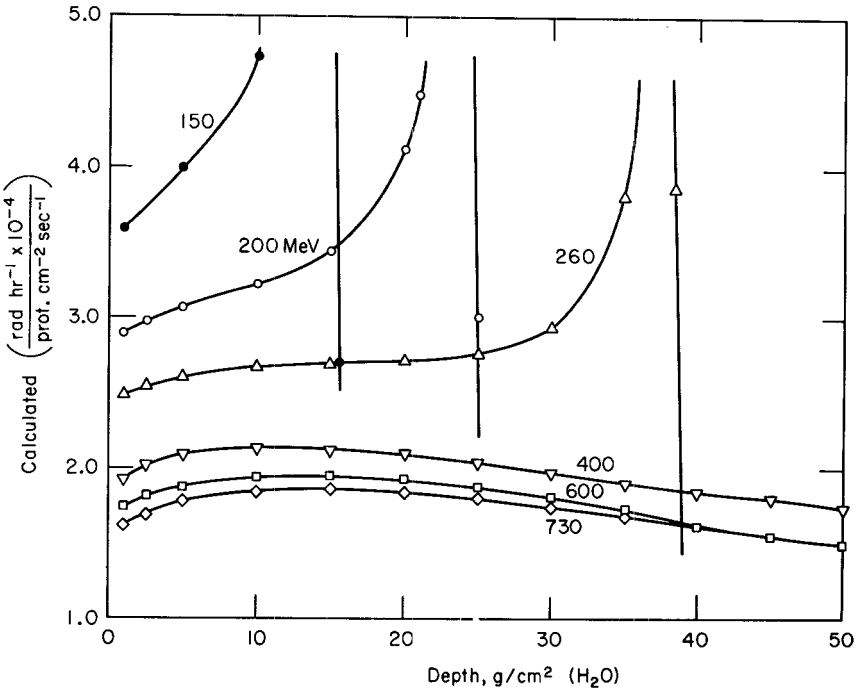

Fig. 9. Calculated dose rate vs depth per 10^4 protons per cm^2 incident normally on a semiinfinite slab of H_2O for various energies. (Steward)

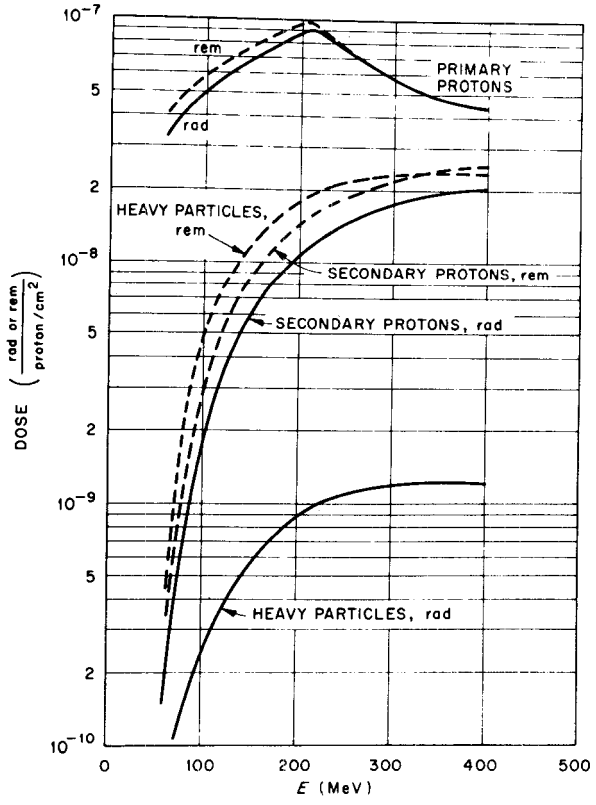

Fig. 10. Entrance (surface) dose per proton per cm^2 vs proton energy for protons incident normally on semiinfinite tissue-equivalent slab. Primary-, secondary-, and heavy-particle dose components are indicated in rad and rem. (Kinney et al.)

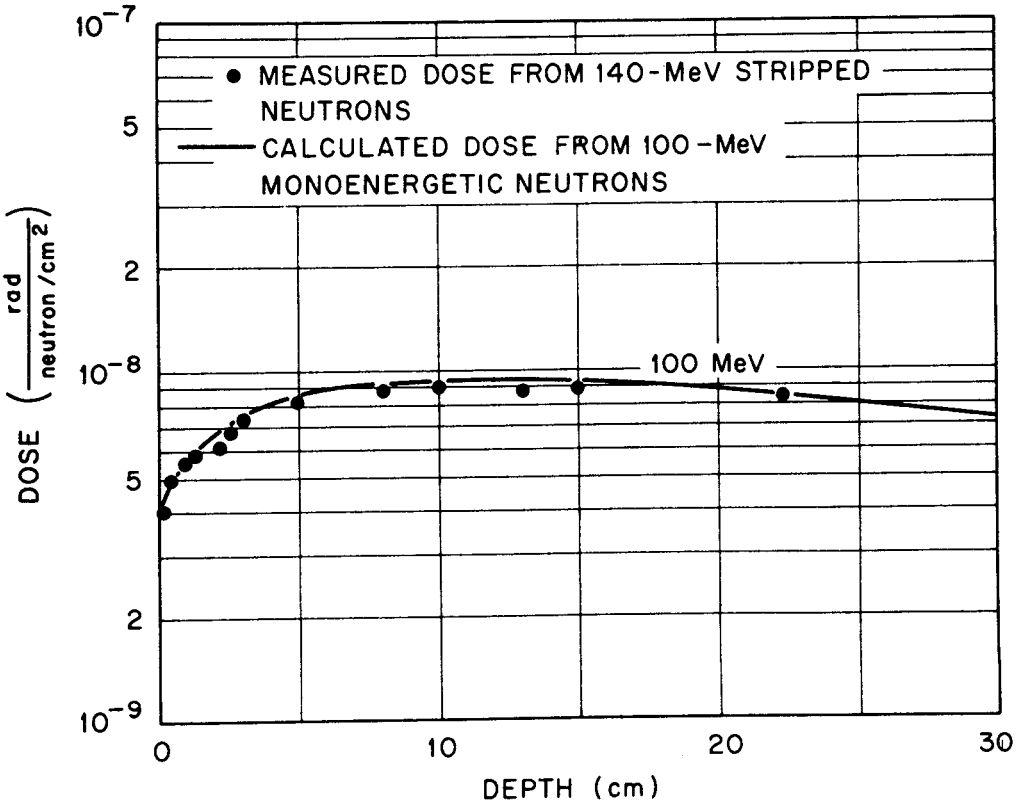

Fig. 11. Comparison of ORNL-code-calculated depth-dose curve for 100-MeV neutrons with experimentally measured depth-dose curve for 140-MeV protons (Kinney et al., and Shal'nov)

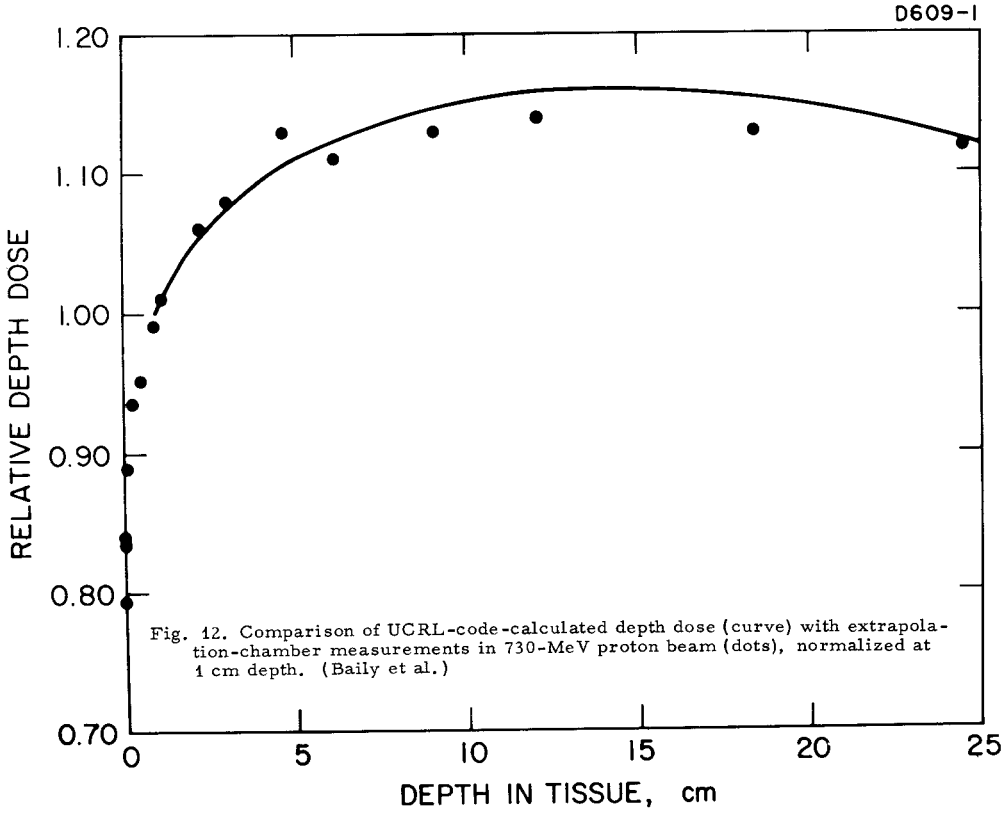

Fig. 12. Comparison of UCRL-code-calculated depth dose (curve) with extrapolation-chamber measurements in 730-MeV proton beam (dots), normalized at 1 cm depth. (Baily et al.)

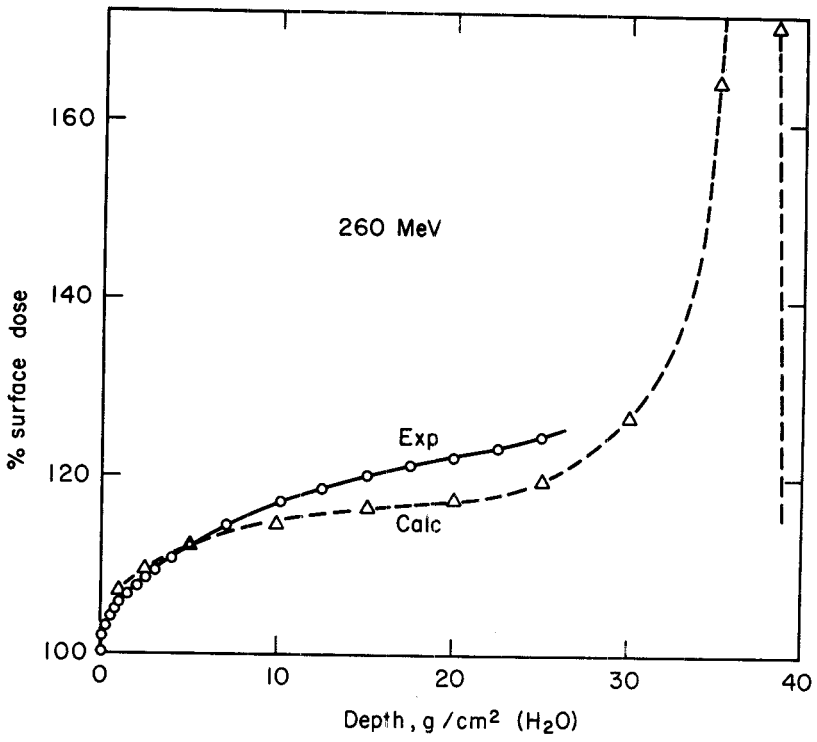

Fig. 13. Comparison of UCRL-code-calculated depth dose with extrapolation-chamber measurements in 730-MeV proton beam degraded to 260 MeV by passage through carbon. (Sondhaus et al.)

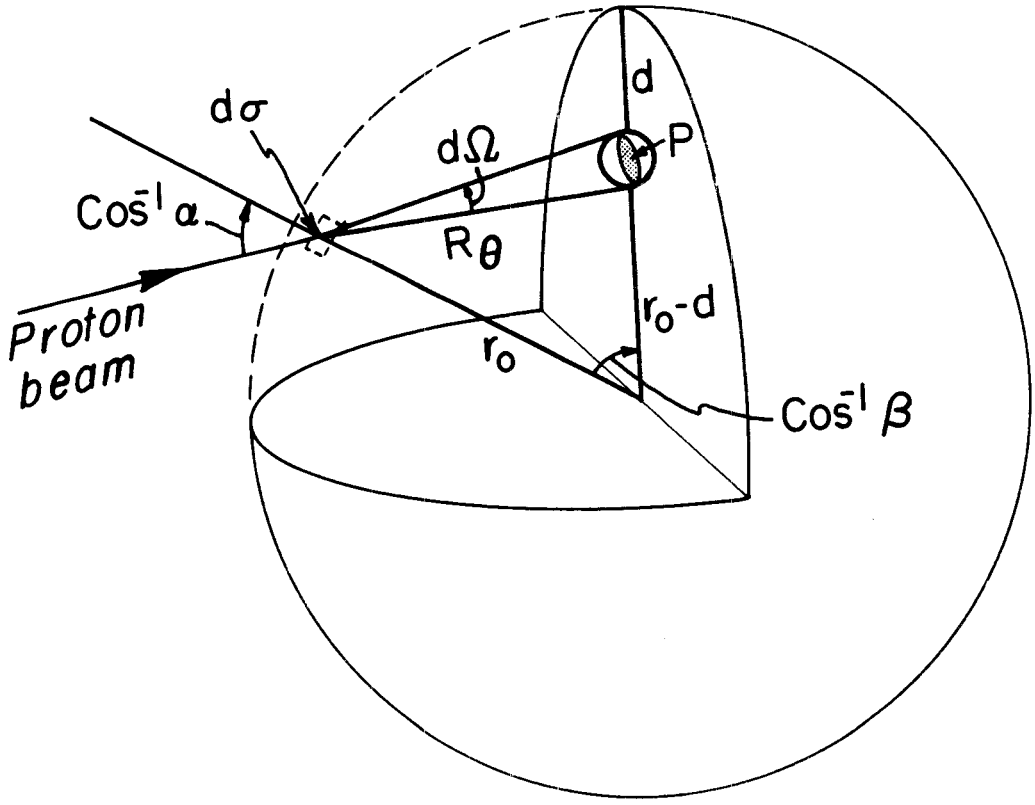

Fig. 14. Geometry assumed for UCRL calculation of depth dose in sphere exposed to isotropic proton fluence. (Steward)

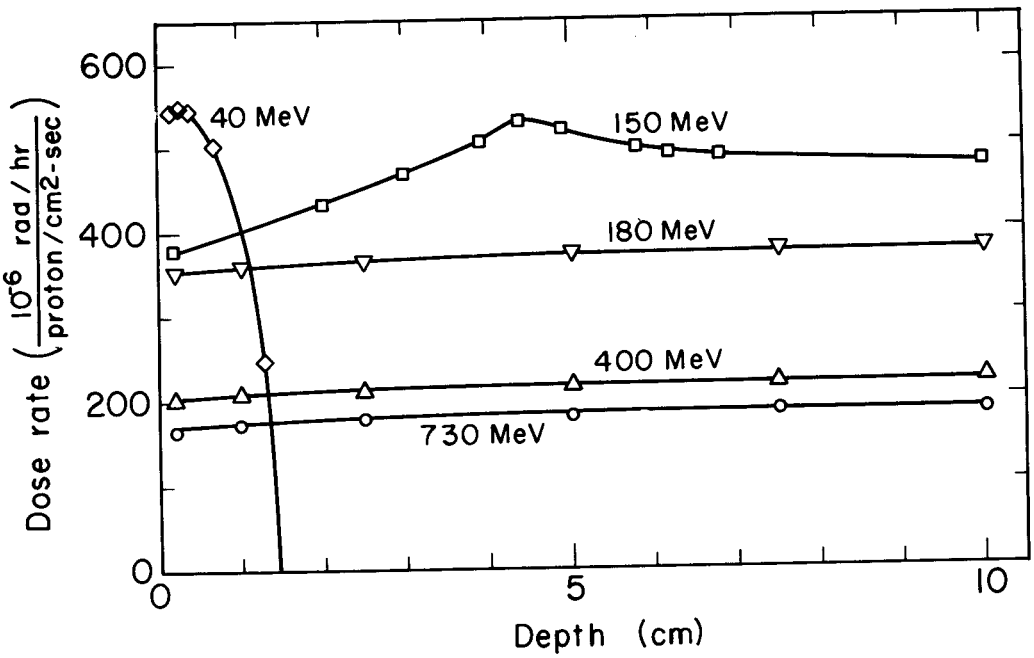

Fig. 15. Depth dose in sphere of 10 cm radius per unit isotropic proton fluence for several proton energies. (Wallace et al.)

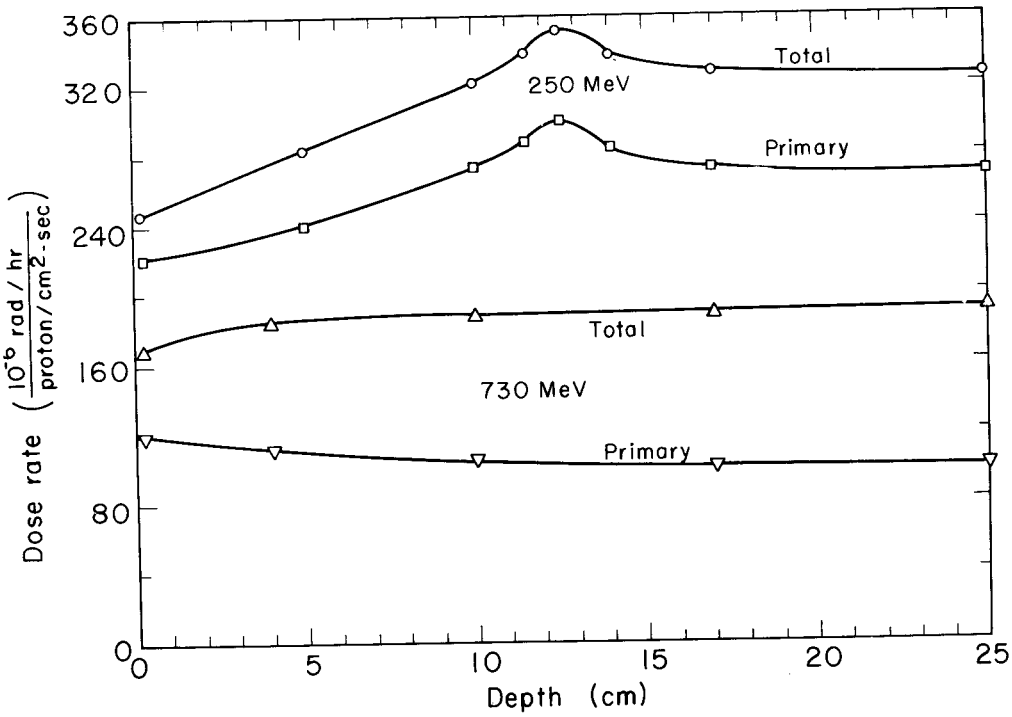

Fig. 16. Depth dose in sphere of 25 cm radius per unit isotropic proton fluence for 730-MeV and 250-MeV protons. Primary- and secondary-proton dose components as indicated. (Wallace et al.)

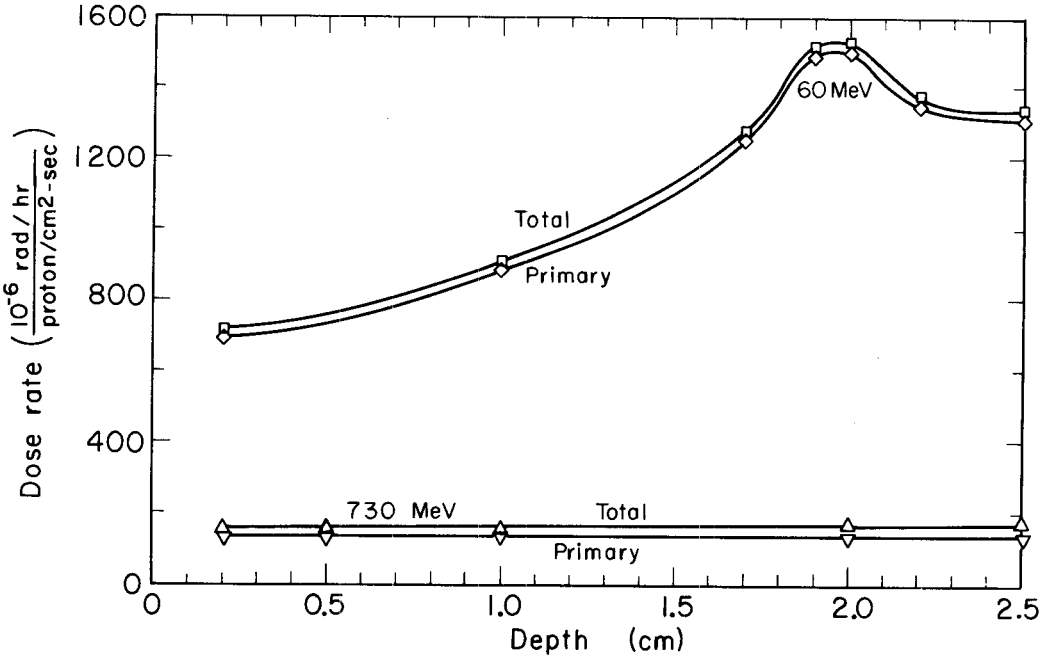

Fig. 17. Depth dose in sphere of 2.5 cm radius per unit isotropic proton fluence for 60-MeV and 730-MeV protons. Primary- and secondary-proton dose contributions as indicated. (Wallace et al.)

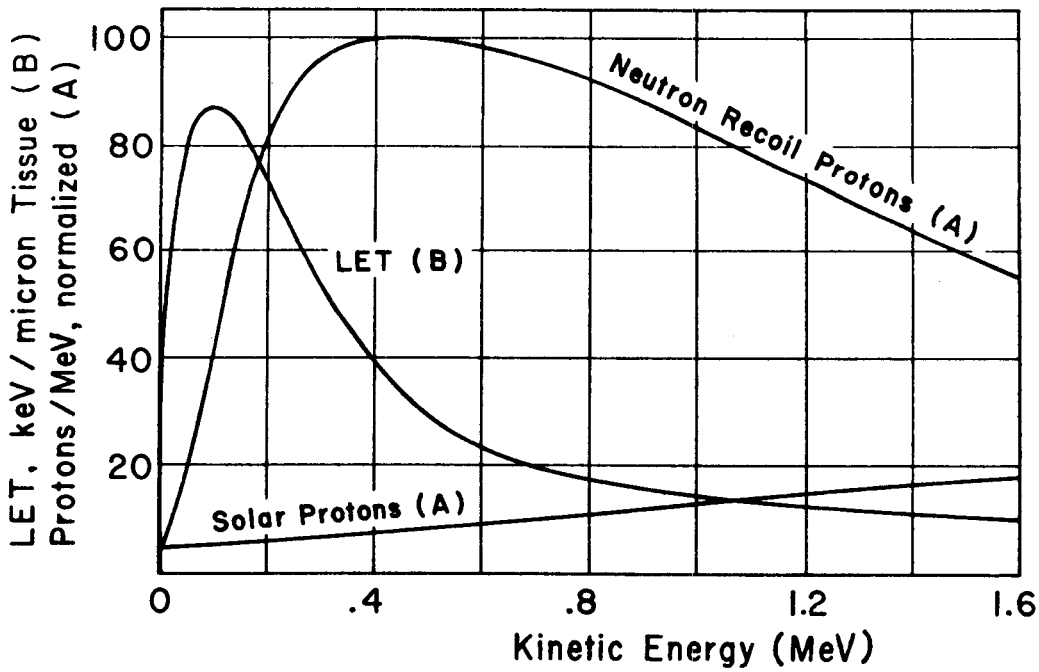

Fig. 18. Calculated relative number-energy distributions of solar protons and fission-spectrum neutron recoil protons (curves A) and calculated average LET vs proton energy (curve B). (Schaefer)

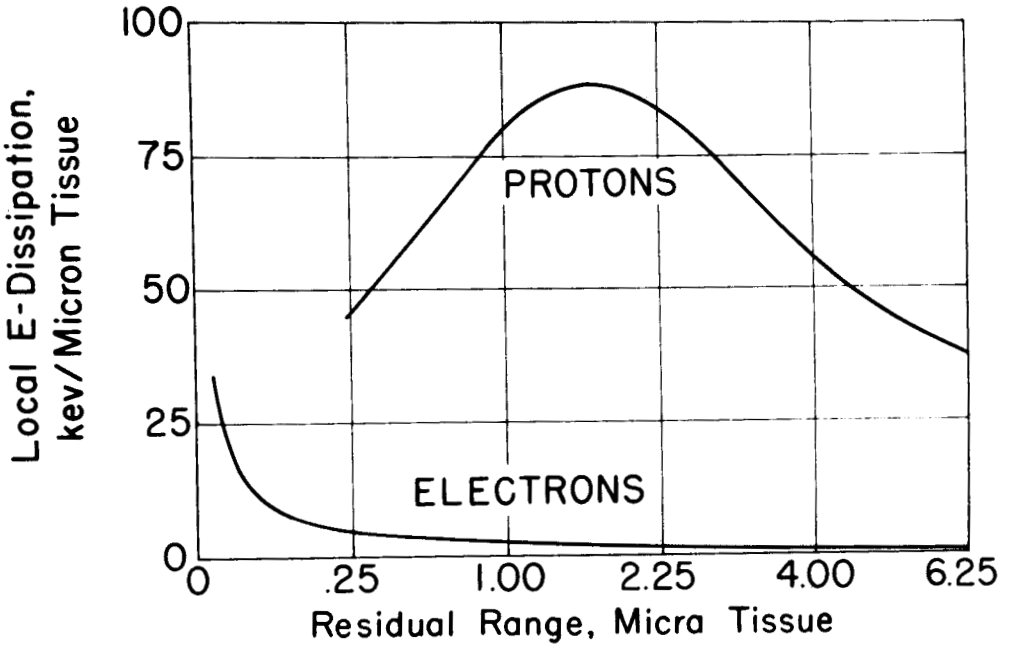

Fig. 19. Local energy dissipation of protons and electrons in the terminal sections of their tracks. (Schaefer)

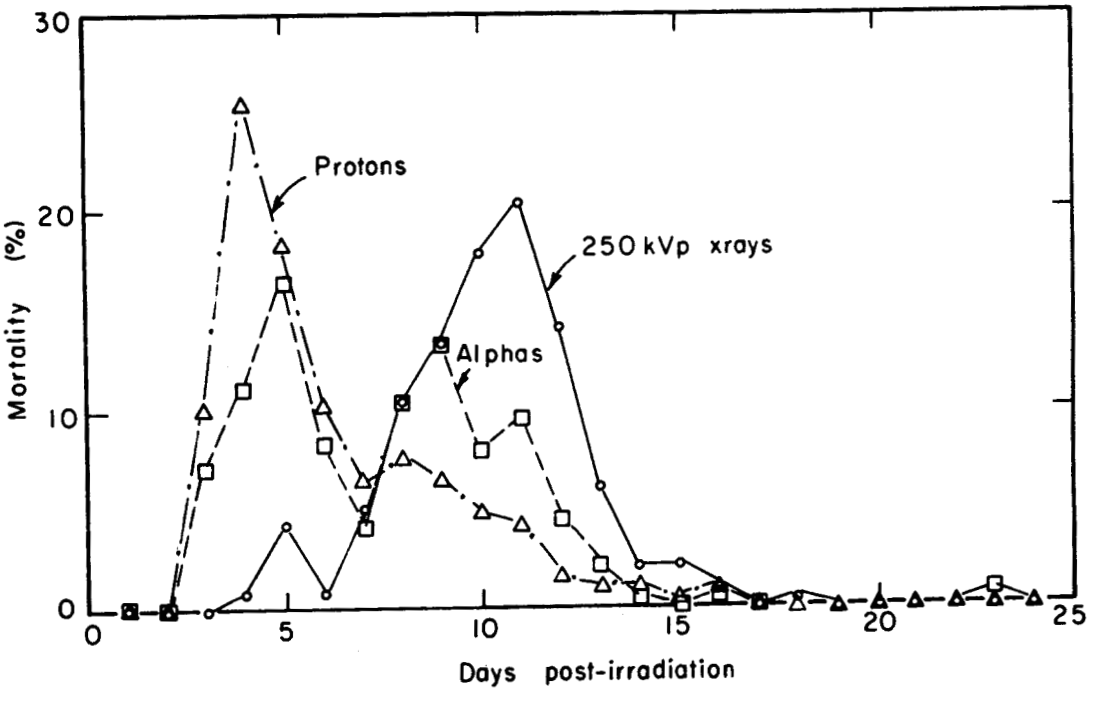

Fig. 20. Postirradiation mortality for 730-MeV protons, 910-MeV alpha particles, and 250-kVp x rays in mice. (Sondhaus)

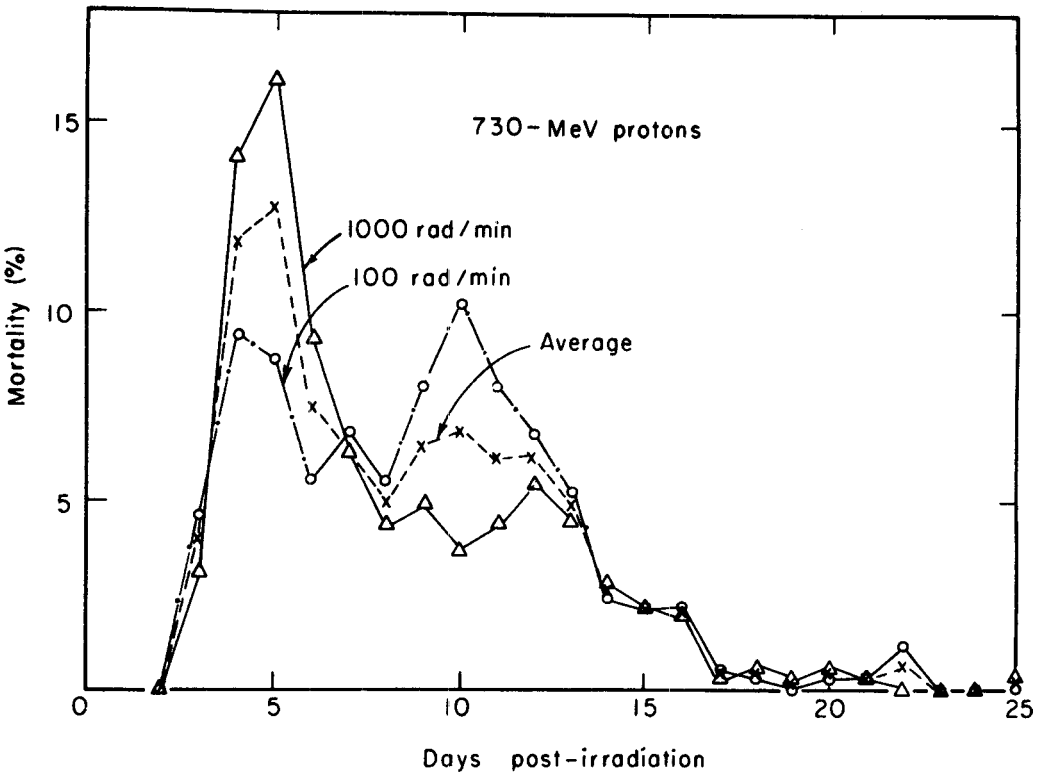

Fig. 21. Postirradiation mortality in mice for 730-MeV protons at 1000 and 100 rad/min. (Ashikawa et al.)

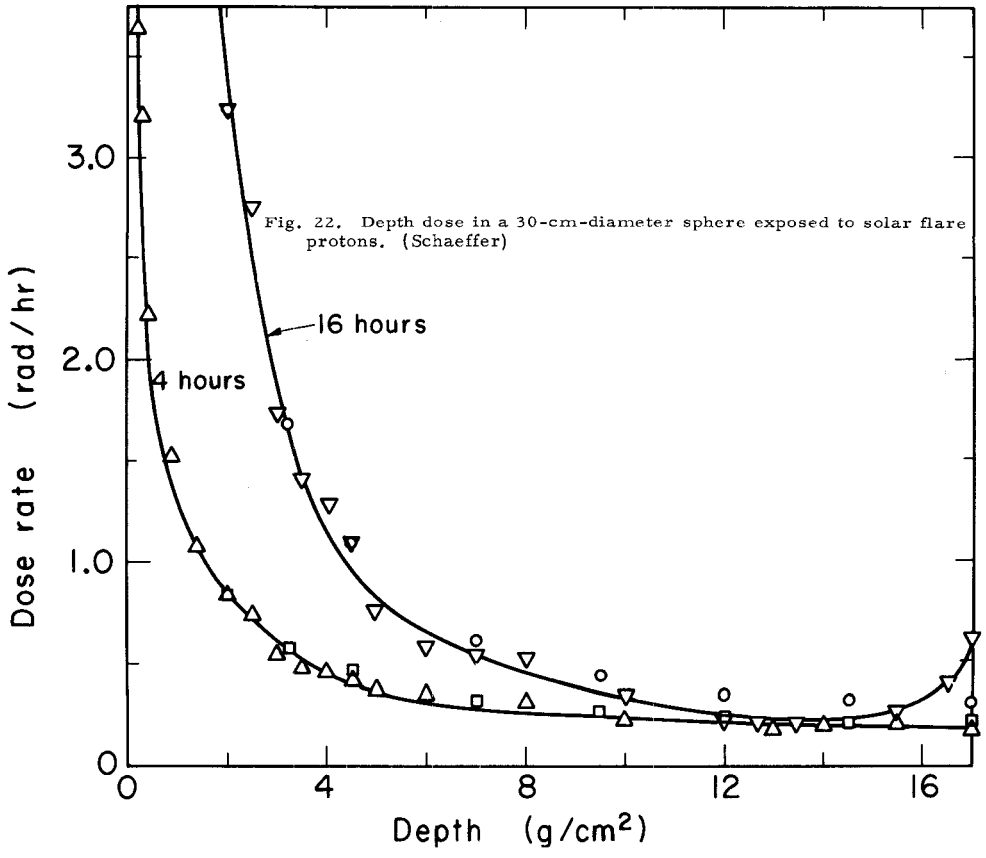

Fig. 22. Depth dose in a 30-cm-diameter sphere exposed to solar flare protons. (Schaeffer)

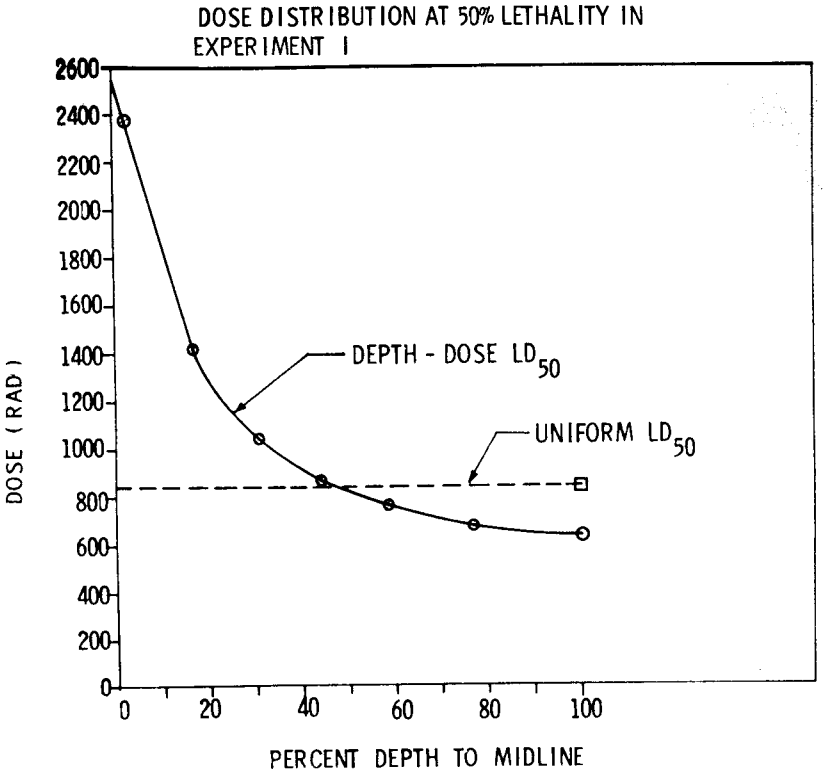

Fig. 23. ^{60}Co dose distributions for 50% lethality in rats, for uniform and nonuniform exposure geometries. (Jackson)

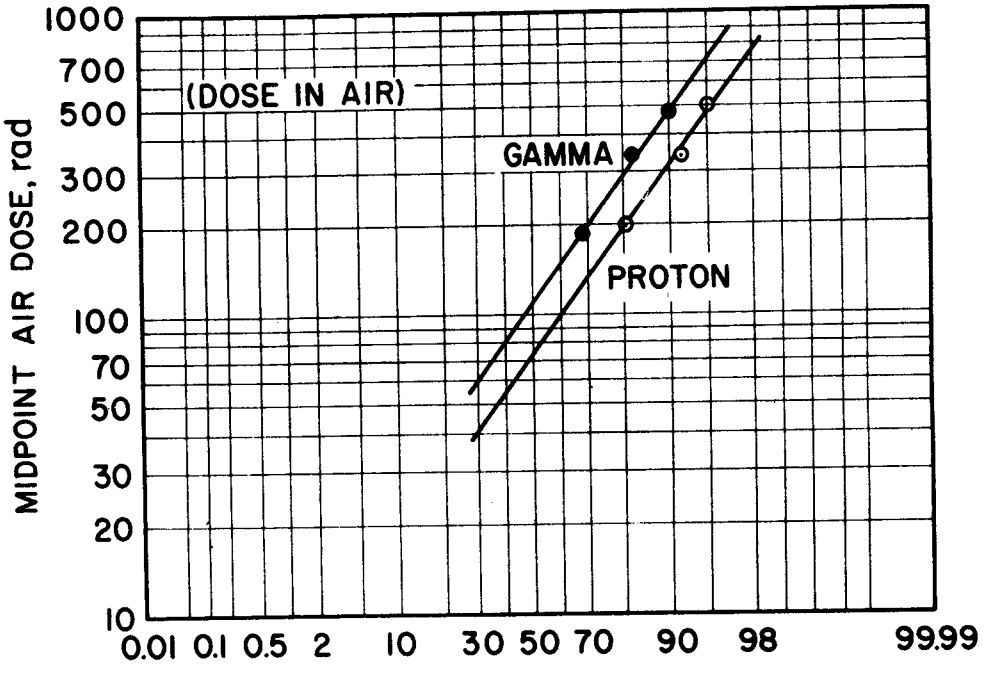

Fig. 24. Maximum WBC depression (percent of preexposure counts), vs midline air dose. (Taketa et al.)

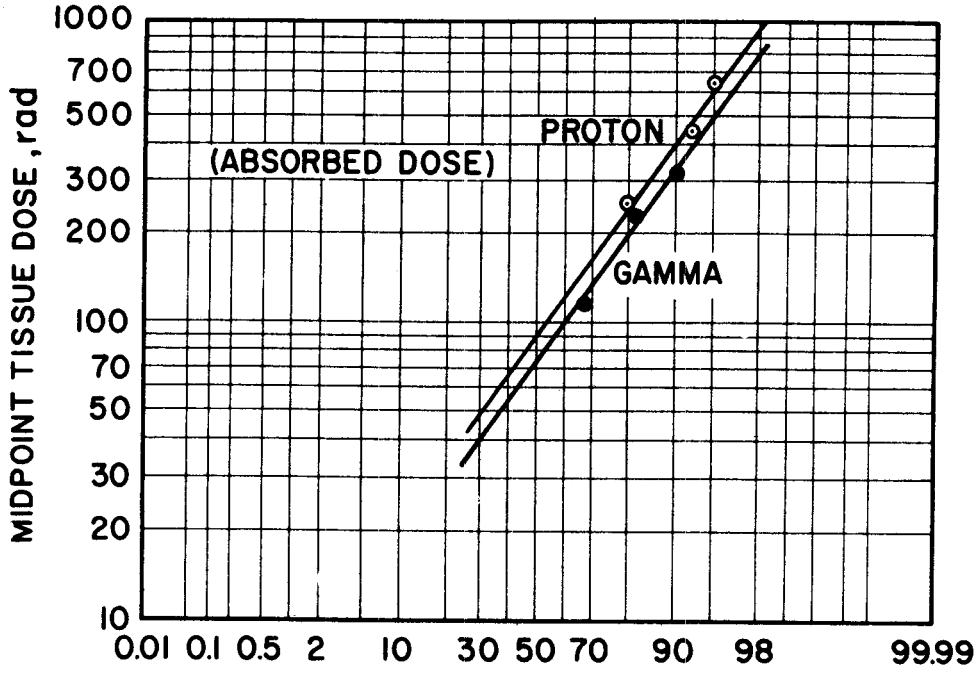

Fig. 25. Maximum WBC depression (percent of preexposure counts), vs midline absorbed dose. (Taketa et al.)

Table 1. Total (primary plus secondary) proton depth dose data for 60-MeV protons incident upon the 2.5-cm-radius sphere of tissue-equivalent material.

Depth (cm)	Total dose rate	Dose rate per energy interval $\left(\frac{10^{-6}\ \text{rad/hr}}{\text{proton/cm}^2\text{-sec}}\right)$							
		Energy interval (MeV)							
		0.02-1	1-2	2-5	5-10	10-20	20-40	40-80	80-∞
0.2	711	6.84	7.06	21.6	36.0	70.5	150	419	0
1.0	907	13.4	13.7	41.7	70.0	143.0	364	261	0
1.7	1275	27.6	28.4	85.6	144.0	300.0	690	0	0
1.9	1519	37.2	38.3	115.0	194.0	406.0	728	0	0
2.0	1526	1.70	1.85	41.0	234.0	490.0	757	0	0
2.2	1374	1.50	1.71	5.50	7.40	492.0	866	0	0
2.5	1337	1.45	1.65	5.49	7.46	9.70	1310	0	0

Table 2. Total (primary plus secondary) proton depth dose data for 730-MeV protons incident upon the 2.5-cm-radius sphere of tissue-equivalent material.

Depth (cm)	Total dose rate	Dose rate per energy interval $\left(\frac{10^{-6}\ \text{rad/hr}}{\text{proton/cm}^2\text{-sec}}\right)$							
		Energy interval (MeV)							
		0.02-1	1-2	2-5	5-10	10-20	20-40	40-80	80-∞
0.2	161	0.44	0.47	1.74	3.22	4.75	3.90	2.98	144
0.5	165	0.52	0.55	1.98	3.57	5.26	4.53	3.62	144
1.0	167	0.55	0.58	2.08	3.73	5.57	5.03	4.20	145
2.0	169	0.58	0.61	2.16	3.87	5.81	5.42	4.71	146
2.5	169	0.58	0.61	2.17	3.93	5.82	5.46	4.75	146

IONIZATION FLUCTUATIONS IN CELLS AND THIN DOSIMETERS

H. D. Maccabee and M. R. Raju

Lawrence Radiation Laboratory
University of California
Berkeley, California

Abstract

Since fast charged particles lose energy in matter by a collision process which is discrete and random, statistical fluctuations are expected in the energy loss of such particles when traversing "thin" absorbers. The theory of ionization fluctuations has been developed by Bohr, Landau, Symon, Vavilov and others, and has been verified by several experimenters, including Maccabee and Raju. Cells and thin dosimeters acts as thin absorbers for many types of particulate radiation, and thus significant fluctuations in energy deposition are to be expected. We discuss the application of the theory to these cases, and the effect of energy-loss straggling on the Bragg peak of charged particle beams.

I. Introduction

When energetic charged particles pass through matter, they lose energy predominantly by a series of inelastic collisions with the electrons of the material, resulting in ionization and excitation of the atoms of the material. Since the collisions are discrete and random, statistical fluctuations in ionization are expected.

In first approximation, the probability of energy loss ϵ in a single electronic collision is proportional to ϵ^{-2}. If this collision spectrum is summed over all possible collision energy losses, we obtain an expression for the average linear rate of energy loss due to ionization and excitation. The standard formula for this quantity (for particles heavier than electrons*) is:

$$\frac{dE}{dx} = - \frac{4\pi e^4 z^2 NZ}{mv^2} \left[\ln \frac{2mv^2}{I(1-\beta^2)} - \beta^2 - \frac{C}{Z} - \frac{\delta}{2} \right], \qquad (1)$$

*Note on electrons: although many of the arguments presented here are valid for electrons, we consider only heavy charged particles in the following treatment.

where
- e = electron charge,
- z = particle charge number,
- N = number of atoms per cm^3 of material,
- Z = atomic number of material,
- m = electron mass,
- v = particle velocity,
- I = mean excitation potential of material $\approx 13.5\ Z$(eV),
- β = particle velocity $\div$ speed of light,
- $\frac{C}{Z}$ = shell correction (negligible for protons >1 MeV),
- $\frac{\delta}{2}$ = density correction (negligible for protons < 1 GeV).

This quantity is often called the stopping power S; if all the energy lost is "imparted locally" to the medium, then S is identical with L, the linear energy transfer (often denoted by LET). The product of the linear energy transfer and the particle fluence Φ (the number of particles entering per unit area) yields the energy imparted per unit volume, which may be multiplied by the density to give the absorbed dose.

In a thin slab of matter (one in which the energy loss is small compared with the total kinetic energy of the particle) we can assume that the average energy loss rate is approximately constant through the slab, and thus write for the average total energy loss $\bar{\Delta}$ in thickness x:

$$\bar{\Delta} = \left(\frac{dE}{dx}\right)(x). \tag{2}$$

The ϵ^{-2} dependence of the collision spectrum implies that collisions resulting in a large energy transfer to an electron are relatively rare compared with small-energy-transfer collisions. Although they are relatively infrequent, the large-energy-transfer collisions account for a significant proportion of the total energy loss. The relatively high energy electrons resulting from these rare collisions are often called delta rays. In a thin absorber, the probable number of large-energy-transfer collisions may be so small that the random statistical variations in this number are relatively large, and result in significant fluctuations in the energy lost in this mode; thus fluctuations occur about the average total energy loss, $\bar{\Delta}$. These fluctuations are often called energy-loss straggling.

II. Theory

Since the fluctuations depend on the number of large-energy-loss collisions, a dimensionless parameter which provides an estimate of this number should be useful to characterize the distribution of total energy losses. Such a parameter, κ (kappa), was introduced by Vavilov in his exact theoretical treatment of ionization fluctuations.[1]

$$\kappa \equiv 0.150 \left(\frac{sZz^2}{A}\right)\left(\frac{1-\beta^2}{\beta^4}\right), \tag{3}$$

where
- s = thickness of absorber in $g/cm^2 = \rho x$,
- A = atomic weight of absorber,
- Z, z, and β are as defined above.

As the absorber thickness increases and the particle velocity decreases, κ increases, corresponding to the increased number of particle-electron collisions in the highest collision-energy interval. The case of $\kappa \gg 1$ was treated in 1915 by Bohr,[2] who found that the distribution of total energy losses is Gaussian, with variance given by

$$\sigma^2 = 0.157\ sZz^2/A \quad [\text{in (MeV)}^2], \tag{4}$$

and the most probable energy loss equals the mean.

For thinner absorbers and higher particle velocities, κ decreases and fluctuations become much more severe. The case of $\kappa \leq 0.01$ was treated in 1944 by Landau, who found a broad asymmetric distribution characterized by a long high-energy-loss "tail" and a most probable energy loss which is considerably less than the average.[3] The full width of the Landau distribution at half maximum is given by

$$\text{FWHM} = 0.611\ sZz^2/A\,\beta^2 \text{ (in MeV)}, \tag{5}$$

and the most probable energy loss is

$$\Delta_{mp} = \frac{2\pi e^4 z^2 NZ}{mv^2} \times \left[\ln \frac{4\pi e^4 NZx}{I^2(1-\beta^2)} - \beta^2 + 0.37\right]. \tag{6}$$

There are many cases corresponding to intermediate values of κ, i.e., $0.01 \leq \kappa \leq 1$; these cases were treated approximately by Symon[4] in 1948, and exactly by Vavilov[1] in 1957. See Fig. 1. As might be expected, the energy-loss distributions for these cases form a smooth transition between the narrow symmetric Gaussian and the broad highly-skewed Landau distribution. The Vavilov theory is general, and includes the Gaussian and Landau distribution as its special cases. The numerical quadrature of Vavilov's rigorous but complicated solution was performed by Seltzer and Berger[5] in 1964. They provide a systematic and comprehensive tabulation of the Vavilov distribution in terms of the parameters κ and β^2, and furnish tables relating κ and β^2 to the absorber thickness and particle energy.

III. Experiment

There is extensive experimental evidence for the validity of the Bohr and Landau theory of energy-loss fluctuations, but until recently there have been few data in confirmation of the more general Vavilov formulation. Maccabee and Raju have used solid-state silicon semiconductor detectors to measure the energy-loss distributions of protons up to 730 MeV and alpha particles up to 910 MeV in order to verify the quantitative theory of ionization fluctuations over virtually the whole range of the significant parameter κ (Ref. 6). Semiconductor detectors have several advantages for this type of measurement: their density (and thus their stopping power) is about a thousand times that of a gas, yielding that many more energy-loss collisions per unit path length. Also the energy required to create a charge pair in silicon is 3.6 eV (approximately a tenth of the value for gas), yielding ten times as many charge pairs. The result of these properties is to improve the charge statistics and thus yield superior energy resolution. In addition, the semiconductor detectors have relatively uniform sensitive thicknesses, highly linear response, and short pulse duration. The method of the experiment is to pass a parallel monoenergetic beam of heavy charged particles (from an accelerator) through the detector and measure the pulse-height spectrum with a multichannel analyzer. The system is calibrated by using standard sources.[6] Since the pulse height is directly proportional to the energy loss in the detector, the pulse-height distribution may be simply processed to yield the energy-loss distribution, i.e., a plot of relative probability versus energy loss.

The results of a few of these experiments follow. Figure 2 shows the energy-loss distribution of 45.3-MeV protons in 0.265 g/cm^2 silicon (about 1mm) with $\kappa = 2.23$. The distribution is very close to a symmetric Gaussian with the most probable energy loss only 0.7% less than the mean energy loss, and an rms deviation (σ) of 145 keV, in agreement with the Bohr theoretical prediction.

Figure 3 shows the energy-loss distribution of 910-MeV alpha particles (He^{2+} ions) in 0.206 g/cm^2 silicon, with $\kappa = 0.318$. This curve is a good example of the intermediate values of κ, in which the distribution is asymmetric, with the beginnings of a high-energy-loss tail, and a most probable energy loss which is significantly (6%) less than the mean. For this curve, the value of the full width at half maximum is 22% of the mean energy loss, in agreement with the prediction of the Vavilov theory.

Figure 4 shows the energy-loss distribution resulting from 730-MeV protons passing through 0.413 g/cm^2 silicon, with $\kappa = 0.021$. This is a good example of the lower range of κ, where the Landau theory is valid: the curve is highly asymmetric, with a long high-energy-loss tail, and a most probable energy loss which is 18% less than the mean. The full width at half-maximum is 180 keV, in agreement with the Landau theory. In general, there is very good agreement between the measured experimental energy-loss distributions and the Vavilov theoretical predictions over virtually the whole significant range of κ (from $\kappa = 2.23$ to $\kappa = 0.003$).

Measurements of this type have been performed in gas detectors by several groups. Gooding and Eisberg[7] found good agreement with the Symon theory for 37-MeV protons in 1957, and Rosenzweig and Rossi[8] did a detailed study of energy-loss straggling for 5.8-MeV alpha particles in a variable-thickness proportional counter in 1963. They found general agreement with the Symon theory for κ values from 0.11 to 3.56, provided that corrections were applied for the effects of electron binding and delta-ray escape from their detector. Glass and Samsky have found agreement with the Vavilov theory of ionization fluctuations for protons of energy as low as 1 MeV in a gas detector equivalent to 0.5 micron of tissue. These results imply that the theory of ionization fluctuations can be applied to absorbers as small as cells and their constituents.

There is a limitation on the Bohr-Landau-Vavilov theory of ionization fluctuation, however. The theory is formulated in terms of continuum statistics, and thus depends on a large number of collisions occurring in at least the lowest collision-energy interval. Thus if the absorber is so thin that the mean energy loss is not much greater (say a factor of 20) than the mean excitation potential, there are so few collisions altogether that continuum statistics are invalid, and discrete Poisson statistics must be used. Examples of measurements for solids in this energy-loss region are given by Rauth and Simpson[10] for 20-keV electrons and Morsell for 992-keV protons.[11]

IV. Applications

It is generally accepted that one of the most important parameters for characterizing radiation effects is the absorbed dose. As shown above, there are wide fluctuations in the energy loss for many cases of charged particles passing through thin absorbers, and thus we can expect fluctuations in the dose delivered by each individual particle. The result of this phenomenon can perhaps best be understood by considering another important parameter of radiation effects, the local energy deposition. The effect of energy-loss straggling is that, even for monoenergetic incident particles, the local energy transfer is not single-valued, but spread over a spectrum. The theory of ionization fluctuations can be used to predict the energy transfer spectrum, if corrections are made for the energy that is not imparted locally. In fact, measurements of the

type shown above are actually measurements of the energy transfer spectrum in the detector.

There is a factor that mitigates the effect of energy-loss straggling to some extent: The largest fluctuations are due to the few highest energy collisions, which are just the collisions that produce the delta-rays that are most likely to escape the volume in question. The net effect is to transfer events from the high-energy-loss tail of the spectrum to the low-energy-loss end. One way of estimating the effect of delta-ray escape is by computing the "restricted" stopping power, i.e., the average energy-loss rate due to all collisions whose energy is less than that of a secondary electron that can just escape the volume in question. The approximate formula for the restricted stopping power was given by Bethe:[12]

$$\left.\frac{dE}{dx}\right|_{\epsilon<\epsilon_\delta} = -\frac{2\pi e^4 z^2 NZ}{mv^2}\left[\ln\frac{2mv^2\epsilon_\delta}{I^2(1-\beta^2)} - \beta^2\right], \qquad (7)$$

where ϵ_δ is the energy of a delta-ray electron whose range is equal to the dimension of the specimen, and it is assumed that $\epsilon_\delta << (2mv^2)/(1-\beta^2)$.

It is clear that biological cells act as "thin" absorbers for most forms of particulate radiation, and that significant energy-loss fluctuations will occur in many cases. For example, consider 10-MeV protons traversing slab-like cells of 5-micron thickness. In this case dE/dx is 4.7 keV/micron and thus the mean energy loss in the cell will be about 24 keV. With $\rho \approx 1$ g/cm^3 and $Z/A \approx 0.5$, parameter $\kappa = 0.150\ s\ (Z/A)\ z^2(1-\beta^2/\beta^4) \approx 0.15\ (5\times10^{-4})\ 0.5(0.98/4.4\times10^{-4}) \approx 0.08$. Thus the Vavilov distribution holds, and the most probable energy loss in the cell will be only about 82% of the mean, and the full width of the energy-loss distribution at half maximum will be 8 keV.

Of course most cells are not slab shaped and most incident radiations are neither monoenergetic nor parallel. Thus in order to estimate the true distribution of energy deposition in the cell, the energy-loss distribution must be "folded in" with the path-length distribution in the cell and the effects of the distribution of energies in the incident radiation.

Several experimental methods have been developed to measure the parameters of dose quantity and quality in masses comparable to that of the cell. Notable among these thin dosimeters are the tissue-equivalent ionization chambers and proportional counters in slab and cylindrical geometry, and the system of spherical microdosimeters developed by Rossi and his colleagues.[13] Even a cursory examination of the results of such experiments is sufficient to show that ionization fluctuation is one of the primary factors determining the shape of the measured distributions, and that fluctuation theory should be applied in the analysis of the data. It should be remembered, however, that relative biological effectiveness is probably only a slowly varying (e.g., logarithmic) function of specific ionization, and thus even fluctuations of energy loss by a factor of 3 about the mean should not make a large difference in the results of a biological exposure. If an energy threshold exists for a biological effect, however, the effect of fluctuations should be more severe.

Naturally, if there are fluctuations of the energy lost in a given small thickness, one expects fluctuations in the total thickness traversed by particles in losing all their energy. This phenomenon is called range straggling and is the cumulative effect of energy-loss straggling over a large thickness of absorber. Since there are a large number of collisions at all energies, the range distribution is approximately Gaussian:

$$P(R) \approx \frac{1}{(2\pi)^{1/2}\sigma_R} \exp[-(R-\bar{R})^2/2\sigma_R{}^2], \qquad (8)$$

where P(R) is the probability of range R, $\bar{R}$ is the mean range, and $\sigma_R{}^2$ is the variance. Berger and Seltzer[14] give a more thorough discussion of this subject and multiple scattering, and tabulate σ_R, which varies between 1 and 2% of the mean range for protons of 300 to 2 MeV in light elements. The net effect of range straggling and multiple scattering on a monoenergetic charged particle beam is to broaden considerably the peak of the Bragg ionization curve. The physical explanation of this effect is that some of the particles are stopping (and therefore ionizing heavily) while others still have enough kinetic energy to travel farther. The consequences of this effect can be clearly seen in Fig. 5, which shows the energy distribution of a 910-MeV alpha particle beam at the Bragg peak, and the corresponding LET values, as measured by Raju.[15] Note that the modal energy at the peak is much higher than one might expect. This case, along with our measurements on a 50-MeV proton beam and measurements at the Harvard cyclotron, indicate that one can use a general rule of thumb that the most probable energy at the Bragg peak is about 10% of the initial kinetic energy.

Acknowledgments

This work was supported by the U. S. Atomic Energy Commission and the National Aeronautics and Space Agency.

References

1. P. V. Vavilov, Soviet Phys. -JETP 5, 749 (1957).
2. N. Bohr, Phil. Mag. 30, 581 (1915).
3. L. Landau, J. Phys. USSR 8, 201 (1944).
4. K. R. Symon, Ph. D. Thesis, summarized in B. Rossi, High Energy Particles (Prentice-Hall, New York, 1952), p. 10.
5. S. Seltzer and M. Berger, in Studies in Penetration of Charged Particles in Matter, NAS-NRC Publ. No. 1133, 1964, p. 187.
6. H. D. Maccabee, Ph. D. Thesis, UCRL-16931 (1966), to be published.; H. D. Maccabee and M. R. Raju, Nucl. Instr. Methods 37, 176 (1965).
7. T. Gooding and R. Eisberg, Phys. Rev. 105, 357 (1957).
8. W. Rosenzweig and H. H. Rossi, Columbia Radiological Research Laboratory Report NYO-10716 (1963), unpublished.
9. W. A. Glass and D. N. Samsky, Rad. Res. (in press).
10. A. M. Rauth and V. A. Simpson, Rad. Res. 22, 643 (1964).
11. A. L. Morsell, Phys. Rev. 135, A1436 (1964).
12. H. Bethe, Ann. Physik 5, 325 (1930) and Z. Physik 76, 293 (1932).
13. H. H. Rossi et al., Radiology 64, 404 (1955); 66, 105 (1956); Rad. Res. 10, 522 (1959); Rad. Res. Suppl. 2, 290 (1960); Rad. Res. 15, 431 (1961).
14. M. Berger and S. Seltzer, see Ref. 5, p. 69.
15. M. R. Raju, Lawrence Radiation Laboratory Report UCRL-16354 (1965) Presented at Workshop Conference on Space Radiation Biology, Sept. 7, 1965. (Proceedings to be published in Radiation Research.)

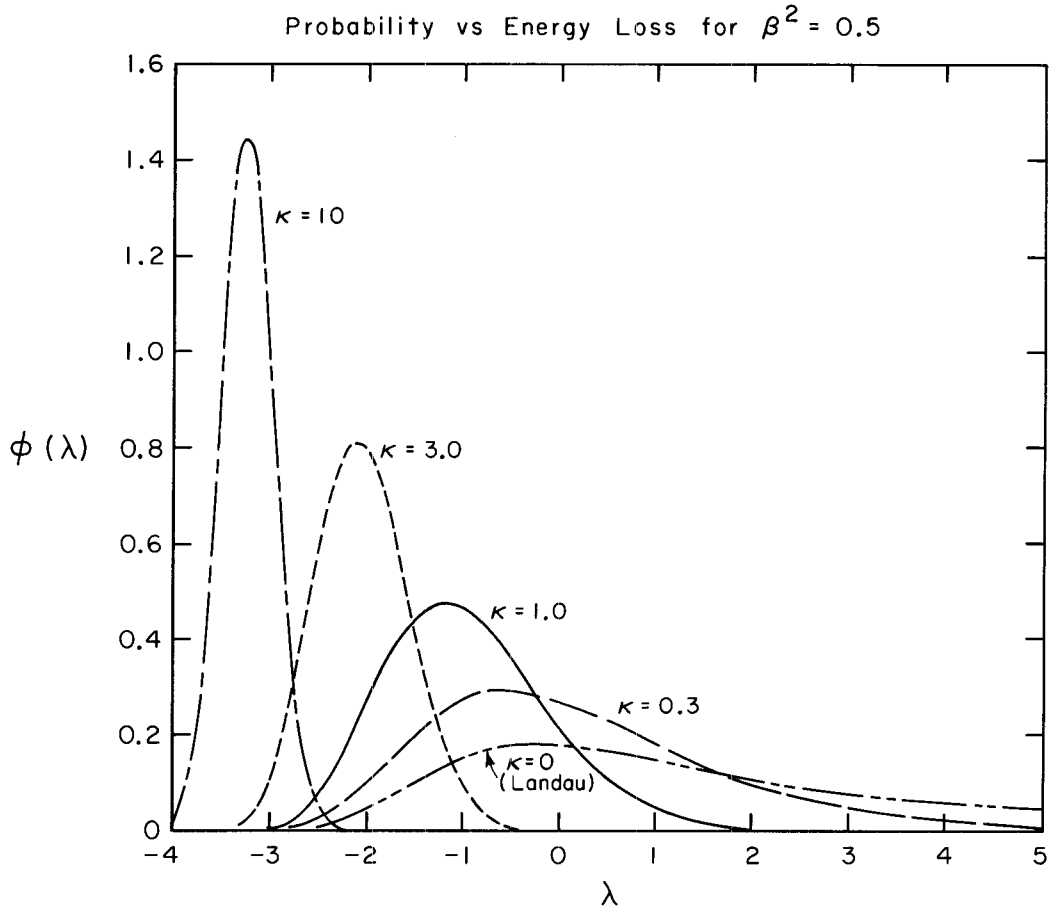

Fig. 1. Normalized probability $\phi(\lambda)$ versus Landau's energy-loss parameter λ, for $\beta^2 = 0.5$. Note the smooth transition between the energy-loss distributions as parameter κ decreases from 10 to 0.

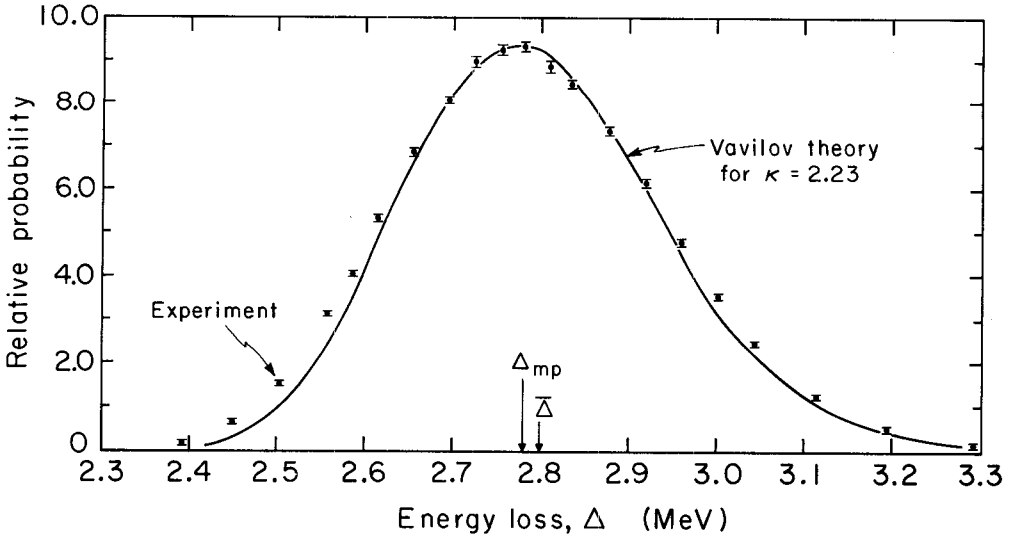

Fig. 2. Energy-loss distribution of 45.3-MeV protons in 0.265 g/cm^2 silicon; $\kappa = 2.23$.

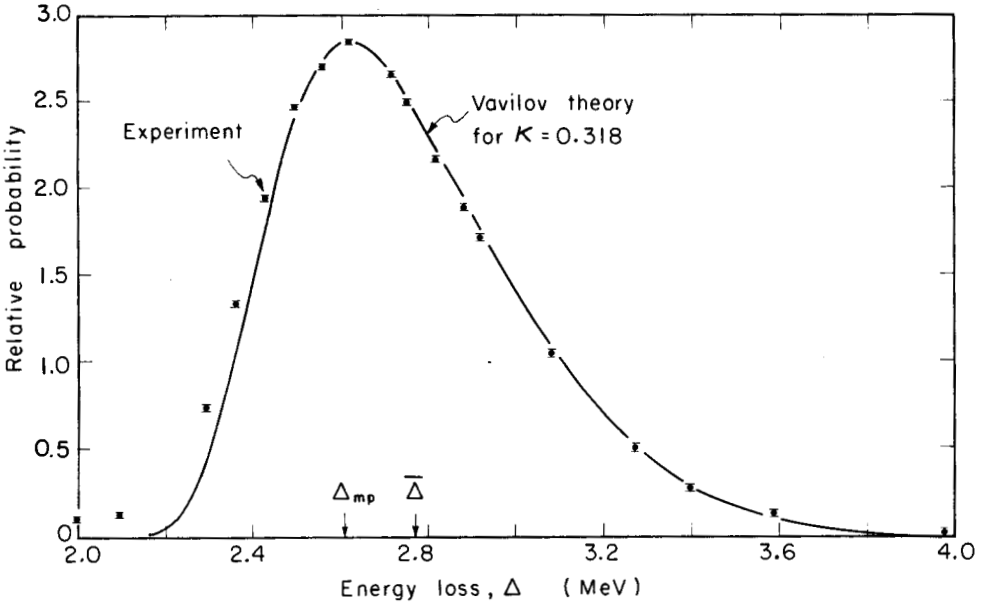

Fig. 3. Energy-loss distribution of 910-MeV alpha particles in 0.206 g/cm^2 silicon; $\kappa = 0.318$.

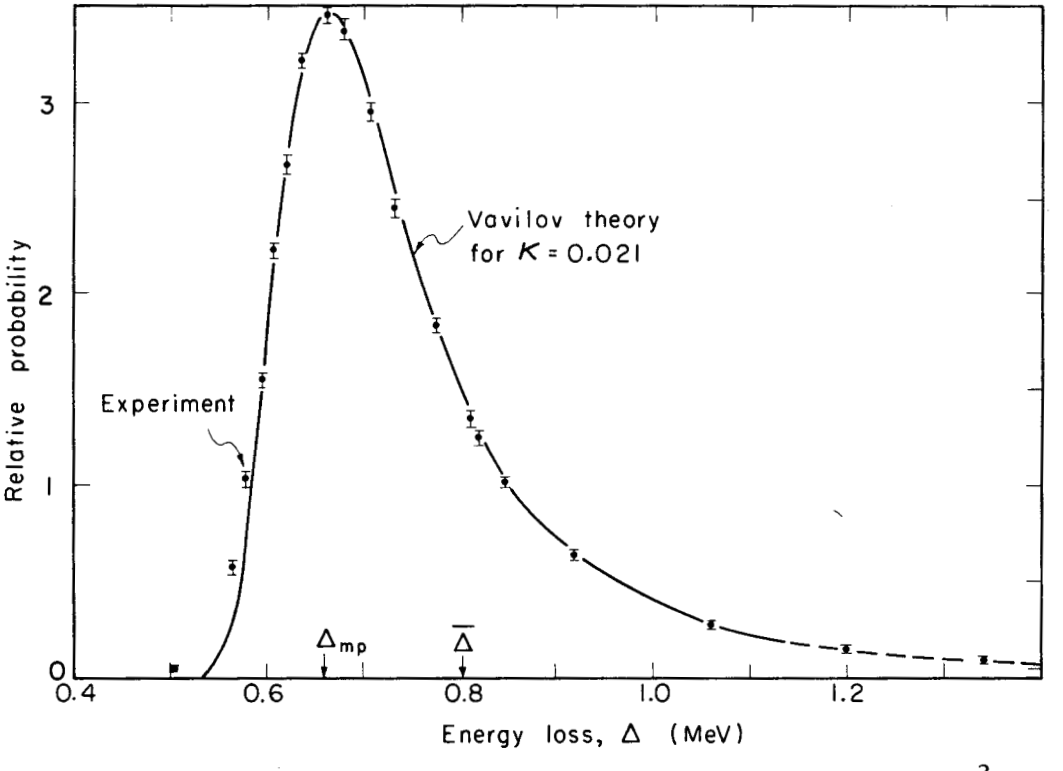

Fig. 4. Energy-loss distribution of 730-MeV protons in 0.413 g/cm^2 silicon; $\kappa = 0.021$.

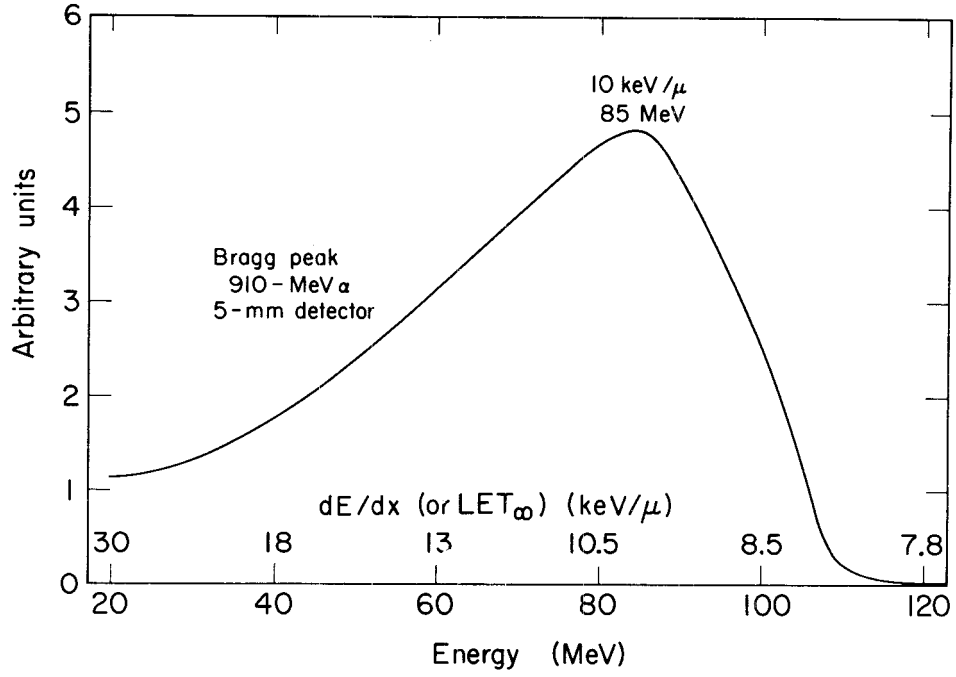

Fig. 5. Energy distribution measured at the Bragg peak of a 910-MeV alpha particle beam. LET values computed for water.

V.3

TWO HAZARD-EVALUATION CRITERIA--DOSE EQUIVALENT AND FRACTIONAL CELL LETHALITY

Stanley B. Curtis

Lawrence Radiation Laboratory
University of California, Berkeley, California

In a situation in which there is a potential hazard from radiation, it is important for the health physicist to know what physical parameters to measure, how to use the measurements to arrive at an evaluation of the hazard, and the limitations imposed on the accuracy of the evaluation by any lack of necessary biological and physical data. We consider here two methods of evaluation: the first is a straightforward approach with the use of a dE/dx or LET spectrum and the appropriate quality factor (QF) leading to a calculation of the dose equivalent (DE); the second is the concept of FCL (fractional cell lethality)--the use of inactivation cross sections to arrive at the fractional number of cells inactivated in an organ. The advantages and disadvantages of each approach will be indicated. It should be mentioned at the outset that each has strong limitations and may find fruitful application in very different situations.

QF and dE/dx Spectra

The standard method of evaluation is by means of a dE/dx or LET spectrum coupled with a QF or quality factor. This factor and its dependence on dE/dx has been decided upon by the International Commission on Radiological Protection! The QF agreed upon by the RBE Committee of the ICRP is supposed to be a conservative extrapolation (i.e., an upper limit) of experimental RBE's down to low doses and dose rates. The expression given[1] is

$$QF = 0.8 + 1.6 \times 10^{-2} L \qquad (1)$$

for $QF < 20$. Here L is the average dE/dx of the radiation in tissue in units of MeV-cm^2/g. We discuss how a more realistic QF might be used.

The LET or dE/dx spectrum provides the information on the distribution of dE/dx in the absorbed dose. In what follows, it is assumed that δ-ray corrections are small and that the locally absorbed energy loss per unit length may be approximated by the total ionization loss, dE/dx, or LET_∞, as it is sometimes called in the literature. We first form the differential dose element, dD, in terms of the differential energy spectrum of particles at the point, dN/dE, and the dE/dx, L, of particles with energy E:

$$dD = \frac{dN}{dE} L \, dE. \qquad (2)$$

We now define a function, the dE/dx spectrum, F(L), such that

$$F(L)dL = dD. \tag{3}$$

Equating the right side of Eq. 2 with the left side of Eq. 3 and solving for F(L) gives an expression for the dE/dx distribution,

$$F(L) = \frac{dN}{dE} \frac{L}{dL/dE}. \tag{4}$$

Because of the wide range of L present in many situations, it is convenient to plot such distributions as a function of log L. Thus, in order to give equal distances along the abscissa equal weight, it is customary to redefine the distribution as

$$F'(L)\, d(\log L) = dD. \tag{5}$$

The corresponding function, F'(L), is given by

$$F'(L) = 2.303 \frac{dN}{dE} \frac{L^2}{dL/dE}. \tag{6}$$

Examples of this function in various radiation environments are shown in Figs. 1, 2, and 3. Figure 1 gives the normalized LET spectra for two solar particle events behind two shielding thicknesses.[2] Figure 1a presents sharply falling initial momentum spectra behind shielding of 5 g/cm^2 of water. Figure 1b shows flatter spectra behind thinner shielding of 1 g/cm^2 of water. The initial total fluence of protons relative to α particles and M particles (ions of atomic number Z between 6 and 9) was held constant at values consistent with experiment. The "spikes" in the spectra occur at the point where the slope of the dE/dx-vs-E curve is zero (i.e., dL/dE = 0; see Eq. 6). This causes F'(L) to diverge. The area under these spikes is small compared with the rest of the area and so contributes little to the total dose.

Figure 2 gives the dE/dx spectrum for galactic cosmic rays at solar minimum behind 0.2 g/cm^2 water shielding for the various components.[3] Note the wide range of dE/dx represented. Here the "spike" is at the low end of the contribution from each class of particles. This is a result of the highly energetic character of the radiation. The spike occurs at the minimum ionizing point of the dE/dx-vs-E curve.

Figure 3 is an example of a dE/dx spectrum from a negative pion beam in the region where the pions stop and produce nuclear interactions.[4] Here the initial beam was assumed to contain 25% electrons and 10% muons. Such beams are presently being used to explore possible radiotherapeutic applications, as is

to be discussed later in this Symposium.[5] The contributions from the various kinds of particles are indicated in the figure.

Dose Equivalent

Now the straightforward approach consists first of measuring the dE/dx spectrum with a suitable instrument at the point of interest. Possibly the best type of device developed so far is a Rossi-type ionization chamber.[6-8] In addition, the dose rate should be measured, since the severity of biological effects produced in many radiation environments depends on the dose rate. Finally, the spectrum at the organs of most interest should be measured, since in many cases there is a strong dependence of the spectrum upon depth within the body. With the above data and the latest information from radiobiological experiments on the dependence of RBE or what is here called specific QF on dE/dx, for the organ and dose rate under consideration, the dose equivalent, DE, or the equivalent x-ray dose, can be computed from

$$DE \text{ (in rem)} = \int F'(L)\, QF(L)\, d(\log L). \tag{7}$$

Here the QF acts as a weighting factor which weights the higher dE/dx components more than those with lower dE/dx. We make the implicit assumption in forming this integral that rem from different radiations are additive.

Such a program might be carried out in the following way. A plastic dummy, constructed of tissue-equivalent material and perhaps even with the bones in place, would be moved to the position where the radiation environment was to be evaluated. A small easily movable proportional counter would be inserted into the region of the dummy where the spectrum was to be measured. The pulses received by the counter could be displayed on a pulse-height analyzer, or the spectrum of pulse heights could be electronically differentiated, if necessary, for subsequent analysis.[7] In addition, if the health physicist had at his disposal a loose-leaf notebook, containing the latest up-to-date information (or, if you wish, best guesses) on specific QF for the various organs of interest and dose rates of importance as a function of dE/dx, he could choose an appropriate dependence of this weighting factor on dE/dx and calculate an approximate equivalent x-ray dose (dose equivalent) in rem from Eq. 7.

Limitations

As in any simplified approach to a complex problem, difficulties arise which, at present at least, are not easily surmountable. Several of the major problems are discussed briefly here.

1. Lack of organ localization

As discussed by Bond[9] at this conference, the marrow in the body is not at a constant depth, and so a distribution factor must be applied in this case as another factor in the evaluation, and the advantage of placing the detector at various depths is to a large extent nullified. Because of the different penetrating power of different types of radiation, this factor evidently varies with the kind of radiation as well as with its energy spectrum. Perhaps applicable factors will be developed which may be adequate for the suspected types of radiation environments to be found around accelerators (e.g., high-energy particles or neutron fluxes). At any rate the lack of a unique position in the body for the system or organ complicates the assessment of the appropriate dE/dx spectrum. Of course if enough detectors were available and properly placed, an "average" spectrum might be obtained, so that a reasonably accurate dose equivalent could be calculated.

2. Neutrons

As Barendsen has pointed out in this Symposium,[10] neutrons may pose a special problem. At least for human kidney cells in tissue culture, biological quantities such as RBE and oxygen-enhancement ratio (OER) cannot be predicted theoretically by using the calculated dE/dx spectrum and RBE-vs-dE/dx or OER-vs-dE/dx curves obtained experimentally[11] with various charged particles having single-valued dE/dx (the so-called "track segment" experiments).[12] Although the reasons for this discrepancy are not clear at present, a reasonable qualitative explanation is that the very short carbon, nitrogen, and oxygen recoils which occur in the neutron irradiation are more effective per unit dose (i.e, have a higher RBE) than particles with the same dE/dx in the "track segment" experiments. At any rate, one must be careful in using RBE's measured with charged particles to predict biological effects from neutrons.

3. The significance of dE/dx as a biologically meaningful parameter

As indicated, the measurement of a dE/dx spectrum is not always sufficient to determine the biological effects that will occur. The dE/dx of a particle in this approach is assumed to be a continuously varying quantity, whereas in reality the particle loses energy intermittently in varying amounts over small distances, and the dE/dx as calculated by the Bethe-Bloch formula is only an average value over a sufficiently large number of collisions. As shown by Maccabee in this Symposium,[13] large fluctuations can occur in the energy loss over small distances. Sufficiently small volumes, such as occupied by biologically important molecules or portions of cells, can receive an energy deposition significantly larger than that calculated by multiplying the standard dE/dx value by the track distance. The finite size of the important molecule or volume is of great importance, and undoubtedly a parameter that is a function of both the size of the biologically important volume and the amount of energy

actually deposited in that volume will emerge as the relevant parameter to describe biological effects, as has been suggested by Rossi.[14] In any case, it is clear that the validity of dE/dx alone as a biologically important parameter is limited. At present it should be considered a relevant parameter only because it is the best we have. We should not be surprised if, in the future, dE/dx distributions--which are so well-defined and calculable (and even roughly measurable) and therefore so pleasing to the physicist--fall into disuse as we find out more about the mechanisms by which radiation damage manifests itself in biological systems.

Fractional Cell Lethality and Inactivation Cross Sections

The second method of hazard evaluation is at present more speculative, since few of the required data are available at present for its utilization. This approach lends itself most readily to situations in which accumulated irreparable damage may become important, such as in extended space flight outside the shielding provided by the earth's magnetic field. In addition, the approach employs the dE/dx distribution and so is open to the criticism discussed in point 3 of the preceding section.

This approach does eliminate the necessity of dealing with RBE's or QF's, however, and substitutes the concept of a cross section, which is actually a probability. Thus the approach has an intrinsic appeal to the physicist. The inactivation cross section, σ, is the probability of inactivation of a cell per incident particle per cm^2, in exact analogy to a nuclear interaction or scattering cross section in nuclear physics. It is a function of the energy of the particle and appears to be a universal function of dE/dx. The number of inactivations per cell is then given by

$$\mathcal{N} = \int \frac{dN}{dE}\, \sigma(E) dE. \tag{8}$$

Cross sections have been measured for few biological systems. Figure 4 presents experimental data obtained by Todd[15] on cross sections for human kidney cells in culture of the type used by Barendsen. The biological end point employed here was destruction of the colony-forming ability of the cells. The experimental results are explained by assuming two types of damage mechanisms, a single-hit irreversible mechanism described by σ_1 and a multihit reversible mechanism described by σ_2. The survival curve for a particle irradiation by a given energy is well described by the expression

$$S = e^{-N\sigma_1} \left[1 - (1 - e^{-N\sigma_2})^n \right], \tag{9}$$

were S is the fractional survival, N is the number of particles incident per cm^2, and n can be interpreted as the number of hits necessary to inactivate the cell by the multihit mechanism.

We now define the fractional cell lethality,[16] FCL, as

$$FCL = 1 - S. \tag{10}$$

For low doses, it can be assumed that reparable damage is repaired and the multihit mechanism is not important. When an energy spectrum is involved we have

$$FCL = 1 - e^{-N\sigma_1} = 1 - e^{-\int dN/dE\ \sigma_1\ dE}, \tag{11}$$

where $N\sigma_1$ is the number of inactivation hits by the irreversible mechanism. From Eqs. 2, 5, and 8 it is easy to show that

$$N\sigma_1 = \int F'(L)\,\frac{\sigma_1(L)}{L}\,d(\log L). \tag{12}$$

Here we note that without the factor σ_1/L this integral would just be the dose. The factor σ_1/L, then, becomes a weighting factor which takes the place of an RBE or QF in the first approach. In Fig. 2, σ_1/L is plotted against L on an arbitrary scale. The shape of this curve is strikingly similar to RBE-vs-dE/dx curves for mammalian systems. Thus we have replaced the RBE factor or QF with another factor involving the probability for inactivation. FCL can be calculated from Eqs. 11 and 12 whenever the dE/dx spectrum can be calculated and the inactivation cross section is known. Unfortunately, few cross sections for human cells are known, and none are known for the most critical organs of the body.

After the fractional number of cells inactivated is estimated for a given organ, the final step in a hazard evaluation is a determination of the degradation of organ function due to the estimated FCL. That is, suppose it is known that 30% of the cells of an organ, say the eye, are inactivated. It must be determined what this means in terms of loss of function of the eye. Much must be done in this area before this approach is feasible as an accurate working means of hazard evaluation.

Summary

Two approaches to the problem of radiation hazard evaluation have been examined. The first uses the dE/dx distribution at the point of interest and the best curve for RBE or QF vs dE/dx for the organ under consideration, with due regard for the dose rate involved. A technique for carrying out an evaluation by this means is described. Several important difficulties to this approach are discussed. It appears that in some cases additional distribution factors must be included to account for the nonlocalization of the organ or system under consideration. Also, a separate neutron detector should probably be included because of certain problems in the proper weighting of neutron dE/dx distributions. Finally,

certain fundamental limitations on the validity of the dE/dx concept itself as a biological parameter are discussed.

In the second approach, the fractional number of cells inactivated (FCL) is calculated with the use of an inactivation cross section. Here the ratio σ/L replaces the RBE or QF. Few cross sections are known at present for mammalian cells, however, and there is little known about the correlation of FCL with organ malfunction. This approach may find some application in situations in which irreparable damage from radiation is allowed to build up over a long period of time, such as might occur on extended space flight.

References

1. Report of the RBE Committee to the ICRP and ICRU, Health Phys., 9: 357 (1963).

2. S. B. Curtis, D. L. Dye, and W. R. Sheldon, Hazard from Highly Ionizing Radiation in Space, Health Phys., 12: 1069 (1966).

3. S. B. Curtis, Energy-Loss Distributions and Fractional Cell Lethality, in Proceedings of the Special Sessions on Radiation Transport and Biological Effects, ANS-SD-4, 99 (1967).

4. S. B. Curtis and M. R. Raju, Physical Characteristics of Negative Pion Beams: Energy-Loss Distribution and Bragg Curves, to be submitted to Radiation Res.

5. M. R. Raju, C. Richman, and S. B. Curtis, A Review of the Physical Characteristics of Pion Beams, this Symposium, VII.3.

6. H. H. Rossi and W. Rosenzweig, A Device for the Measurement of Dose as a Function of Specific Ionization, Radiology, 64 [3]: 404 (1955).

7. H. H. Rossi, W. Rosenzweig, M. H. Biavati, L. Goodman, and L. Phillips, Radiation Protection. Surveys at Heavy-Particle Accelerators Operating at Energies Beyond Several Hundred Million Electron Volts, Health Phys., 8: 331 (1962).

8. T. R. Overton, Experience with a Linear Energy Transfer (LET) Chamber at CERN, CERN Document CERN 66-33, 1966.

9. V. P. Bond, Cellular Radiobiology in the Mammal, this Symposium I.1.

10. G. W. Barendsen, Fundamental Aspects of the Dependence of Biological Radiation Damage in Human Cells on the Linear Energy Transfer of Different Radiations, this Symposium, II. 5.

11. G. W. Barendsen, C. J. Koot, G. R. Van Kersen, D. K. Bewley, S. B. Field, and C. J. Parnell, The Effect of Oxygen on Impairment of the Proliferative Capacity of Human Cells in Culture by Ionizing Radiations of Different LET, Intl. J. Rad. Biol., 10: 317 (1966).

12. D. K. Bewley, An Analysis of the Response of Mammalian Cells to Fast Neutrons, to be submitted for publication.

13. H. D. Maccabee and M. R. Raju, Ionization Fluctuations in Cells and Thin Dosimeters, this Symposium, V.2.

14. H. H. Rossi, M. H. Biavati, and W. Gross, Local Energy Density in Irradiated Tissues. I. Radiobiological Significance, Radiation Res., 15: 431 (1961).

15. P. Todd, Biological Effects of Heavy Ions, in Second Symposium on Protection Against Radiations in Space, NASA SP-71, 105, 1965.

16. S. B. Curtis, D. L. Dye, and W. R. Sheldon, Fractional Cell Lethality Approach to Space Radiation Hazards, Second Symposium on Protection Against Radiations in Space, NASA SP-71, 219, 1965.

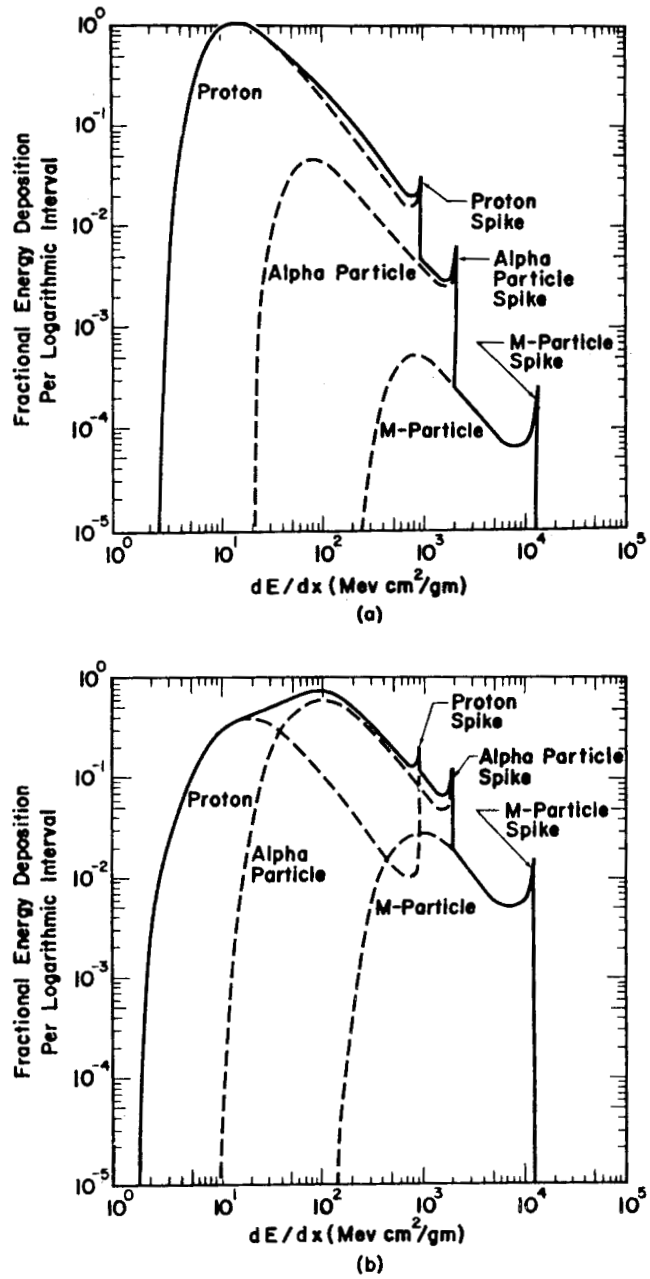

Fig. 1. Two examples of normalized dE/dx distributions behind water shielding. (a) Shielding thickness of 5 g/cm^2 for a solar particle event with a steep incident spectrum; (b) shielding thickness of 1 g/cm^2 for a solar particle event with a flatter spectrum.

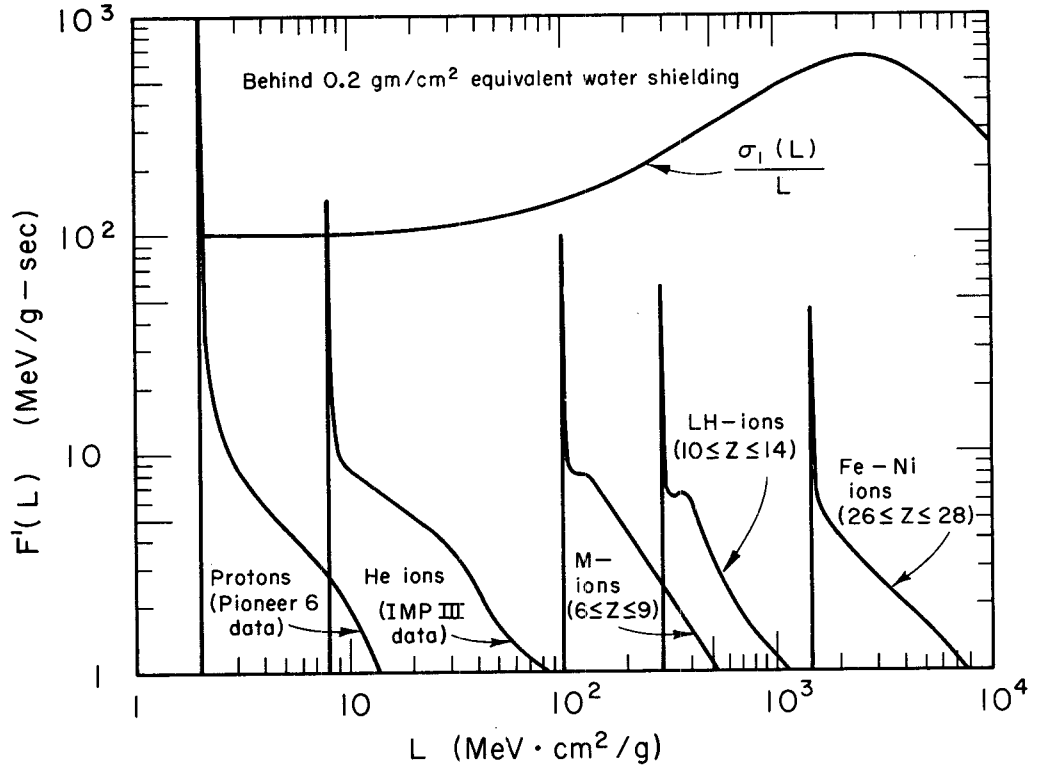

Fig. 2. The dE/dx distribution from galactic cosmic rays behind 0.2 g/cm^2 water shielding. The upper curve gives the weighting factor (L)/L on an arbitrary scale.

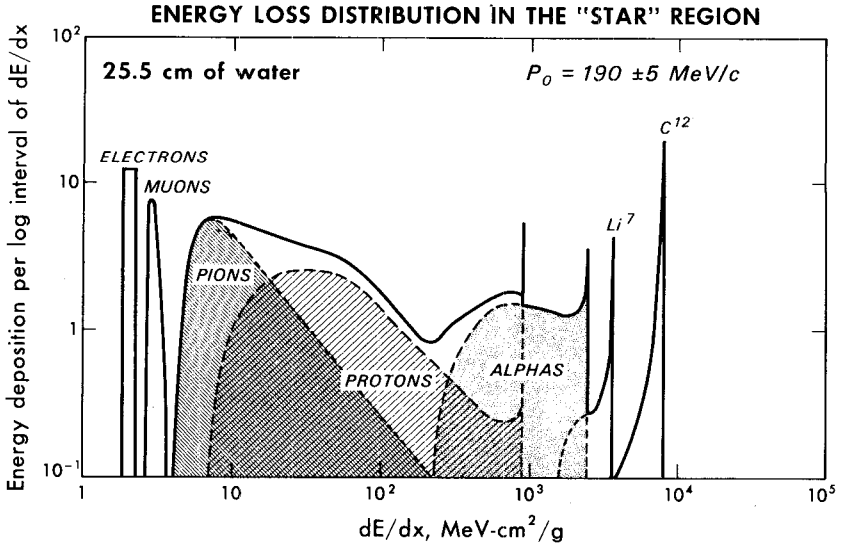

Fig. 3. The dE/dx distribution of a contaminated negative pion beam at 25.5 cm of water in the stopping pion region, calculated for an incident Gaussian momentum distribution: 190 ± 5 MeV/c. The ordinate is in MeV/(g × logarithmic interval of dE/dx × incident pion/cm^2).

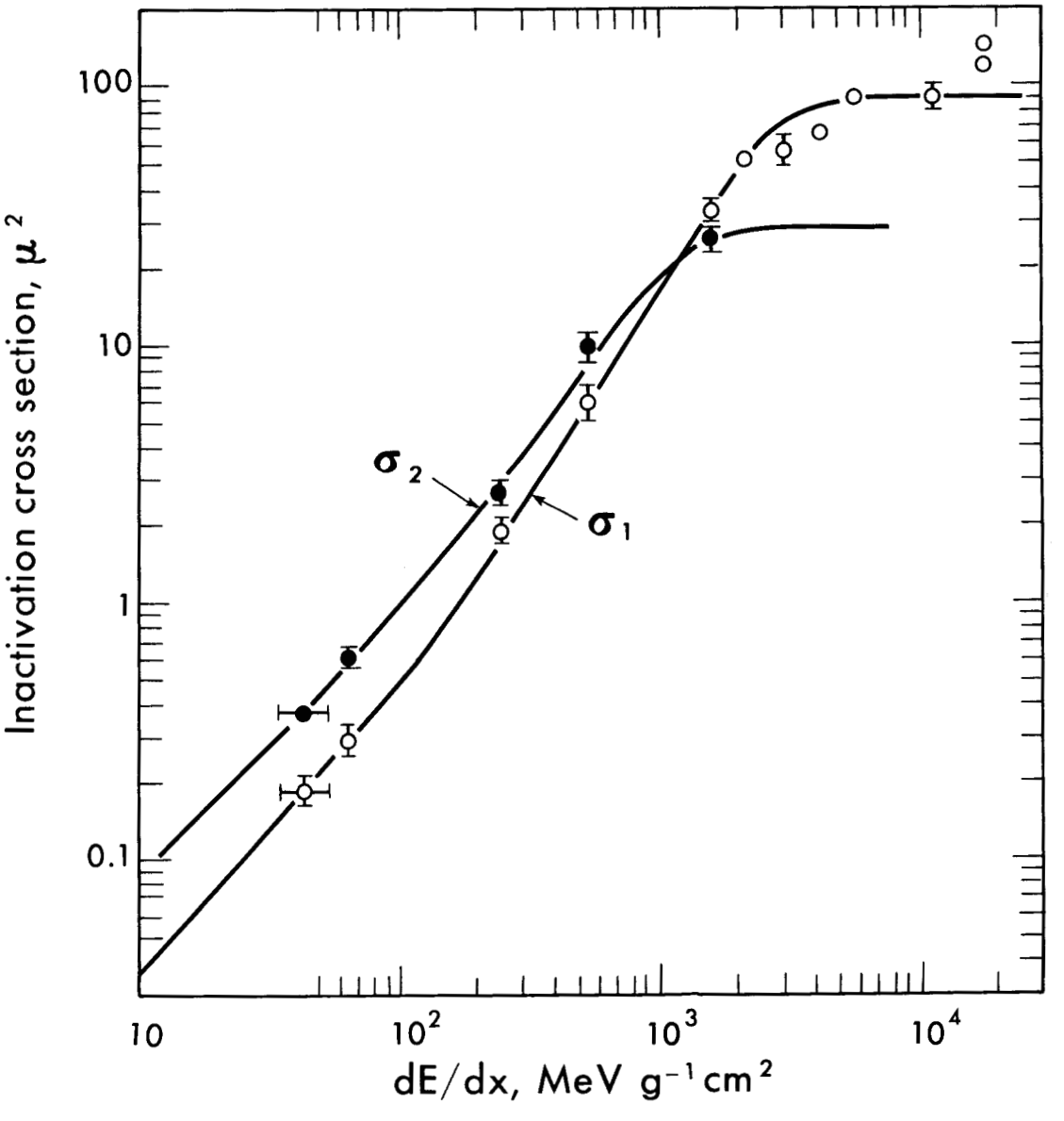

Fig. 4. Inactivation cross sections for irreversible (σ_1) and reversible (σ_2) damage to the colony-forming ability of human kidney cells as a function of dE/dx, as measured by Todd (Ref. 15).

ELECTRON FLUX SPECTRA IN ALUMINUM; ANALYSIS FOR LET SPECTRA AND EXCITATION AND IONIZATION YIELDS*

R. D. Birkhoff, W. J. McConnell, R. N. Hamm, and R. H. Ritchie
Health Physics Division, Oak Ridge National Laboratory
Oak Ridge, Tennessee 37830

ABSTRACT

Measurements were made of the electron flux generated in effectively infinite Al media by uniformly distributed sources of ^{198}Au and ^{64}Cu. Above 100 kev the shapes of the flux spectra are determined by the integral primary beta spectrum. Between 100 kev and 5 kev the flux is constant. Between 5 kev and 100 ev the flux rises as $1/E$ and below 100 ev rises as about $1/E^3$. On an absolute basis the experiment is in agreement with the Spencer-Fano theory above 10 kev but exceeds the theory by as much as a factor of 4 at 400 ev. The results were analyzed to obtain LET spectra as well as K-shell and L-shell ionization, volume plasmon excitation, and electron-electron interaction yields. The conclusions drawn from the analysis were that electrons with energies less than 55 ev contribute as much to the flux in LET space as do electrons with energies greater than 55 ev, that electrons are nearly mono-LET particles, and that volume plasmon excitation accounts for nearly all of the energy delivered to an aluminum medium by an electron slowing down in it.

I. INTRODUCTION

Previous experimental studies on electron flux spectra in metals have determined the electron flux as a function of energy in media of intermediate[1,2] and high[3] atomic numbers. It was desirable to extend these measurements to a medium of low atomic number to more nearly approximate tissue equivalence in order to make the observations of more applicability to radiobiological problems. Unfortunately, media of tissue-equivalent plastic were unsuitable because such materials can withstand neither the reactor irradiation used to activate the sources nor the subsequent beta irradiation. Thus, alloys of ≈99% Al and 1% of either Au or Cu were used instead. In previous studies little effort has been devoted to determining how the energy was absorbed or the relative importance of the various energy regions with respect to radiation effects. This was due in part to the lack of cross sections and stopping powers, either theoretical or experimental. The recent availability[4,5] of such fundamental data in Al led us to choose it as a slowing down medium over other non-organic low-Z materials.

*Research sponsored by the U. S. Atomic Energy Commission under contract with Union Carbide Corporation.

A very brief discussion of the theory of electron slowing-down is given in section II. The electron spectrometer and the source are described in section III. Data corrections are discussed in section IV and the flux spectra are given in section V. Flux spectra are analyzed to yield LET spectra in section VI. In section VII the K-shell and L-shell ionization, volume plasmon excitation, and electron-electron interaction yields are calculated using our data and appropriate theoretical cross sections. Conclusions are given in section VIII.

II. THEORY

A general theory of electron slowing-down has been presented by Spencer and Fano.[6] They modified the continuous slowing-down approximation to include secondary electrons produced by the few violent collisions experienced by the primary electrons and to include the effects of bremsstrahlung. McGinnies[7] has tabulated the results of calculations using the Spencer-Fano theory for monoenergetic sources in various media. A simplified treatment of the Spencer-Fano theory has been given by Spencer and Attix[8] and reviewed by Birkhoff.[9] A modification of the Spencer-Attix treatment which allows calculation by successive generations has been given by Hamm, McConnell, Birkhoff, and Berger.[10]

The theory which we have used to compare with experiment was obtained from the McGinnies tabulation. The slowing-down spectra in aluminum for monoenergetic sources was weighted with the ^{64}Cu and ^{198}Au beta spectra and the results were summed to obtain spectra from these non-monoenergetic sources.

III. APPARATUS

The Keplertron,[11, 12, 13] a spherical electrostatic-focusing spectrometer, shown in Figure 1 was used to measure the electron flux. The Keplertron has an energy resolution of 6% and a transmission of 25%. Electrons leaving the source on the inner sphere are focused by an inverse-square electric field between the two spheres and detected using a Faraday cup and a vibrating-reed electrometer. The Keplertron operates over the energy range from 1 ev to 65 kev. Energy selection is accomplished by varying the outer sphere potential. The sources used for the measurements consisted of two parallel coaxial discs about 1 cm in diameter and 0.3 cm apart. The thickness of each disc was equal to the range of the electrons. Thus a plane between the discs represented a plane in an infinite, homogeneous, isotropically irradiated medium. The edges and outer sides of these sources were shielded to prevent the escape of electrons from these surfaces.

IV. DATA CORRECTIONS

The expression used to obtain the experimental flux, y, in units of electrons cm^{-2} ev^{-1} per primary cm^{-3} from the Faraday cup current is

$$y(T + T_B) = \frac{4\pi}{(A\Delta\Omega)_{eff}} \frac{1}{D} R(T) B(T) P(T) \left(\frac{16}{T}\right) \times \{I(T) - I(0)\}, \qquad (1)$$

where T is the electron energy in ev with respect to the vacuum level and $T_B = E_F + \varphi$ where E_F is the Fermi energy and φ is the work function. The quantity $(A\Delta\Omega)_{eff}$ represents the product of the effective source area and solid angle seen by the Keplertron and has a value of 0.402 cm^2 steradians. The experimental fluxes were normalized by dividing by D, the disintegration rate cm^{-3} sec^{-1}. A correction is made for the response of the spectrometer, operating at low energy, to the high-energy electron components of the source. It has been shown experimentally that electrons with energy greater than 40 kev produce a constant background current in the Keplertron which is equal to the current I(0) at zero sphere potential. The correction for electrons of these energies is the subtraction of the zero-potential currents I(0) from the observed currents I(T).

The spurious background current due to electron components in the source having less than 40 kilovolts was obtained as follows. Experimental studies of the line profile shape of the Keplertron for monoenergetic electrons revealed a low-energy tail extending from the line profile down to zero energy. This tail was typically about 0.15% of the peak current in the line profile.[13] Thus, as shown in equation 2, the incremental spurious current at energy T' is proportional to the incremental true current at energy T, where T is greater than T',

$$dI_{spur}(T') = .0015\, dI_{true}(T) \qquad T > T'. \tag{2}$$

The integral of this equation is shown as equation 3,

$$I_{spur}(T') = .0015 \int_{T'}^{40\ kev} dI_{true}(T). \tag{3}$$

Now the spurious current at T' is equivalent to the product of the spurious flux at T' and the energy window of the spectrometer T'/16. Also the incremental true current is equal to the flux at T multiplied by dT. If one makes these substitutions as shown in equation 4,

$$y_{spur}(T')\frac{T'}{16} = .0015 \int_{T'}^{40\ kev} y_{true}(T)dT, \tag{4}$$

then the flux at energy T' is as shown in equation 5,

$$y_{spur}(T') = \frac{.024}{T'} \int_{T'}^{40\ kev} y_{true}(T)dT. \tag{5}$$

The true flux is determined at every energy below 40 kilovolts by subtracting the spurious flux from the observed flux. The ratio of the true to observed flux is designated as R(T) and is a multiplicative factor, as shown in equation 1. It varied from about unity near 10 ev and 40 kev to a minimum of 0.8 between 50 ev and 1 kev.

A correction B(T) was made for the energy barrier at the surface which the electrons must overcome when moving from the metal into the vacuum.[1] This correction ranges from 22 at 1 ev to 1.1 at 1.4 kev. The spectrometer detects only negative electrons when a negative outer sphere potential is used. As a result, the primary positrons from the decay of ^{64}Cu are not detected but the negative secondary electrons which they produce are. The factor P(T) is a correction[1] applied to the ^{64}Cu data to raise the primary part of the experimental flux to the value it should have if the Keplertron detected positrons as well as negatrons. At 60 kev P is equal to 1.5 and below 100 ev is equal to unity. A final correction is made for the energy window of the spectrometer. This window is proportional to the electron energy. To obtain the current per unit energy, the observed current must be divided by the window width, T/16. A more complete discussion of these corrections may be found elsewhere.[1]

V. ELECTRON FLUX DISTRIBUTIONS

Figures 2 and 3 show the experimental fluxes as a function of electron energy. The spectra have a shape which can be broken down into four regions. Above 100 kev the shape is determined by the integral primary beta spectrum. Below this energy the primary spectrum declines due to the increase in the stopping power. However, the decline is matched by an increase in the number of secondary electrons in such a way that the flux is essentially constant down to about 5 kev. Between 5 kev and 100 ev the flux rises approximately as 1/E and below 100 ev the flux rises more nearly as $1/E^3$. Figures 2 and 3 also show the Spencer-Fano theory. Both the theory and experiment are shown on an absolute basis. The experiment agrees very well with the theory above about 10 kev but exceeds the theory by as much as a factor of 4 at 400 ev. It is not clear why the theory fails to predict this large increase of low-energy secondaries. However, it should be noted that the theory is based on the Möller free-electron-scattering formula for the production of secondary electrons. As a result, it accounts neither for the large energy losses resulting from inner-shell ionization nor the injection of additional electrons due to the Auger cascade following inner-shell ionizations.

VI. LET DISTRIBUTIONS

A LET distribution of the electron flux was obtained using the relation

$$y(T)\, dT = F(L)\, dL \quad . \tag{6}$$

Equation 6 states that the flux of y of electrons between T and T + dT must equal the flux F of electrons between LET values L and L + dL. This equation may be solved for F(L) to obtain

$$F(L) = \frac{y(T)}{dL/dT} \quad . \tag{7}$$

Values of dL/dT were obtained from the stopping power[4,5] for aluminum shown in Figure 4. We have assumed that LET and stopping power are identical. While this does result in some small error it does not effect the conclusions we draw from the results. The dashed portion of the curve above 10 kev is the Bethe-Bloch theory. The solid line is a theory derived by Ritchie[4] which includes the electron-plasmon and electron-electron interactions in the conduction band, and electron-electron interactions in the L-shell. The points around 1 kev are measurements made by Garber, Nakai, and Birkhoff[5] by comparison of the transmission of electrons through thin films of various thicknesses. Figures 5 and 6 show the electron flux as a function of LET. It is composed of two contributions - one from electrons with energy greater than 55 ev (the energy at which the stopping power is maximum) and another from electrons with energy less than 55 ev. Both energy regions make roughly equal contributions to the flux and decrease from 10^{-9} electrons cm^{-2} LET^{-1} per primary electron cm^{-3} at 10^{7} ev/cm to a high LET tail which has a value of about 2×10^{-12} electrons cm^{-2} LET^{-1} per primary electron cm^{-3}. The peak at 4.5×10^{8} ev is due to the shoulder on the theoretical stopping-power curve due to L-shell ionization which appears at about 300 ev. These data verify the assumption that electrons are essentially mono-LET particles since the low LET flux is about 3 orders of magnitude above the high LET flux.

VII. EXCITATION AND IONIZATION YIELDS

The electron fluxes as a function of energy were used also to obtain the number of interactions per cm^{-3} per primary electron cm^{-3} for K-shell ionization, L-shell ionization, volume plasmon excitation, and electron-electron collisions. The number N of interactions cm^{-3} per primary cm^{-3} is given by

$$N = \int_{T_{th}}^{T_{max}} y(T)\lambda^{-1}(T)dT, \tag{8}$$

where y is the electron flux in units of electrons cm^{-3} ev^{-1} per primary electron cm^{-1}, λ^{-1} is the inverse mean free path or macroscopic cross section in cm^{-1}, and T_{th} is the threshold energy for the interaction. Equation 8 can be put into more convenient form by multiplying and dividing by T to get

$$N = \int_{E_{th}}^{E_{max}} Ty(T)\lambda^{-1}(T)d(\ln T) \quad . \tag{9}$$

Further, if $Ty(T)\lambda^{-1}(T)$ is plotted versus lnT,[14] an area under this curve between any two energies T_1 and T_2 is equal to the number of events occurring within the energy range $T_2 - T_1$. The inverse mean free paths used in the calculations are shown in Figure 7 as the solid lines. Values of N given in Table 1 were determined by graphical methods from plots of $Ty(T)\lambda^{-1}(T)$ as a function of log (T) as shown in Figures 8-10. A plot of $Ty(T)\lambda^{-1}(T)$ as a function of log T for electron-electron

Table 1

Interactions cm^{-3} per Primary Electron cm^{-3}

Interaction \ Electron Source	^{64}Cu	^{198}Au
K-Shell Ionization	2.6	4.0
L-Shell Ionization	266	324
Volume Plasmon Excitation	17,420	18,320

interactions is shown in Figure 11. The excitation of a volume plasmon in aluminum requires 15 ev; thus the amount of energy expended in exciting volume plasmons was 260 kev for the ^{64}Cu source and 275 kev for the ^{198}Au source. These can be compared with the average energies of the beta spectra which are 230 kev for ^{64}Cu and 315 kev for ^{198}Au.

VIII. CONCLUSIONS

In summary we have drawn five conclusions from our data. The electron flux in energy space can be divided into four regions: a region in which the flux is determined by the integral primary beta spectrum; a region in which the flux is roughly constant; a region in which the flux goes as E^{-1}; and a region in which the flux goes as E^{-3}. Theory and experiment are in good agreement at high energies, but the theory is much too low at lower energies. Electrons with energy below 55 ev contribute as much to the flux in LET space as do electrons with energy greater than 55 ev. As is generally assumed, electrons are essentially mono-LET particles. Finally, when an electron slows down in a metal, nearly all of the energy goes ultimately into volume plasmon excitation.

REFERENCES

1. W. J. McConnell, H. H. Hubbell, Jr., R. N. Hamm, R. H. Ritchie, and R. D. Birkhoff, Phys. Rev., 138: A1377 (1965).

2. W. H. Wilkie and R. D. Birkhoff, Phys. Rev., 135: A1133 (1964).

3. W. J. McConnell, H. H. Hubbell, Jr., and R. D. Birkhoff, Health Phys., 12: 693 (1966).

4. R. H. Ritchie, to be published.

5. F. W. Garber, Y. Nakai, and R. D. Birkhoff, Bull. Am. Phys. Soc., II: 534 (1966).

6. L. V. Spencer and U. Fano, Phys. Rev., 93: 1172 (1954).

7. R. T. McGinnies, Nat'l. Bureau of Std. (U.S.) Cir. 597 (1959).

8. L. V. Spencer and F. H. Attix, Rad. Res., 3: 239 (1955).

9. R. D. Birkhoff, in Handbuch der Physik, edited by S. Flügge (Springer-Verlag, Berlin, 1958), Vol. 34, p. 53.

10. R. N. Hamm, W. J. McConnell, R. D. Birkhoff, and M. Berger, Bull. Am. Phys. Soc., 10: 477 (1965).

11. R. H. Ritchie, J. S. Cheka, and R. D. Birkhoff, Nucl. Instr. Methods, 6: 157 (1960).

12. R. D. Birkhoff, J. M. Kohn, H. B. Eldridge, and R. H. Ritchie, Nucl. Instr. Methods, 8: 164 (1960).

13. H. H. Hubbell, Jr., W. J. McConnell, and R. D. Birkhoff, Nucl. Instr. Methods, 31: 18 (1964).

14. This method of plotting has been used previously in atomic physics [R. L. Platzman, Int. J. Appl. Rad. Isotopes, 10: 116 (1961)] and in nuclear physics [G. S. Hurst, R. H. Ritchie, F. W. Sanders, P. W. Reinhardt, J. A. Auxier, E. B. Wagner, A. D. Callihan, and K. Z. Morgan, Health Phys., 5: 179 (1961)]. In the former case Platzman has calculated electron flux spectra in He for 10 kev and 100 kev sources and obtained the number of various excitation and ionization events as a function of energy.

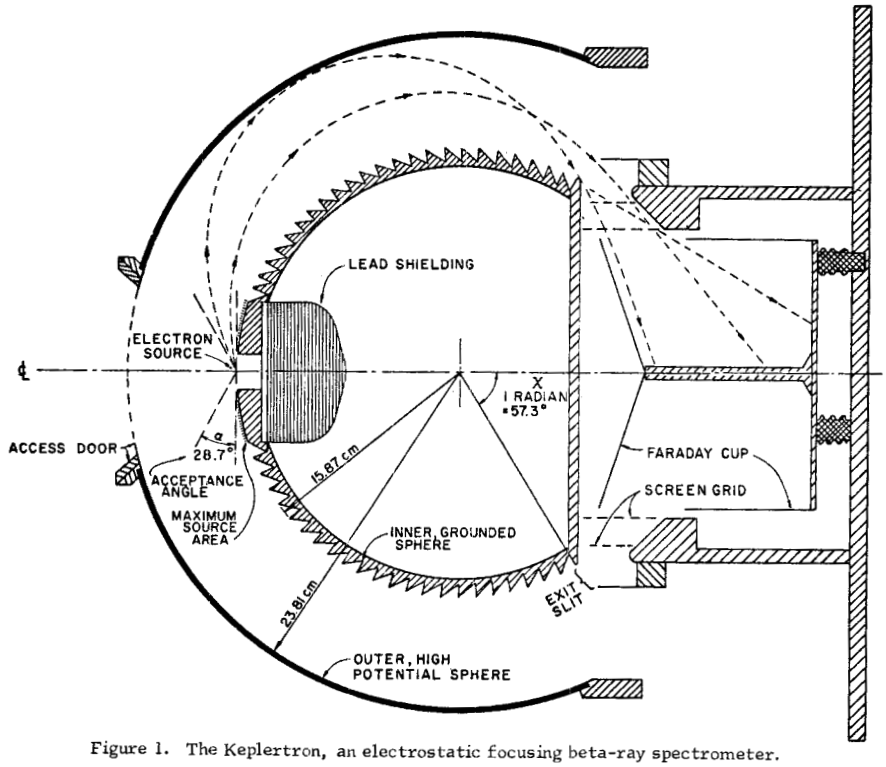

Figure 1. The Keplertron, an electrostatic focusing beta-ray spectrometer.

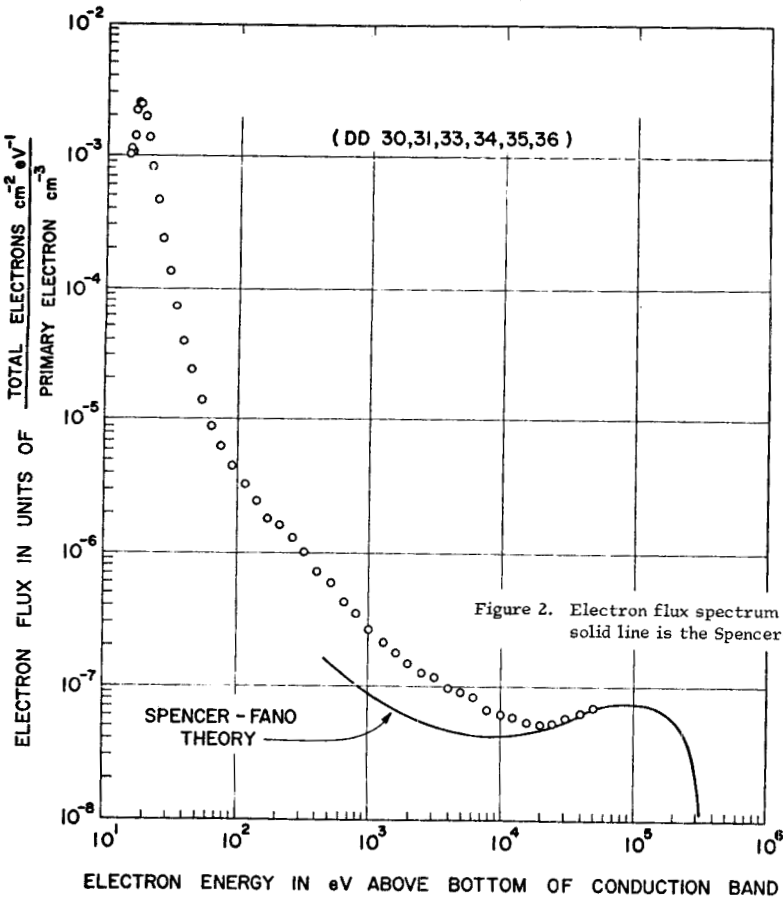

Figure 2. Electron flux spectrum from ^{64}Cu beta rays absorbed in aluminum. The solid line is the Spencer-Fano theory.

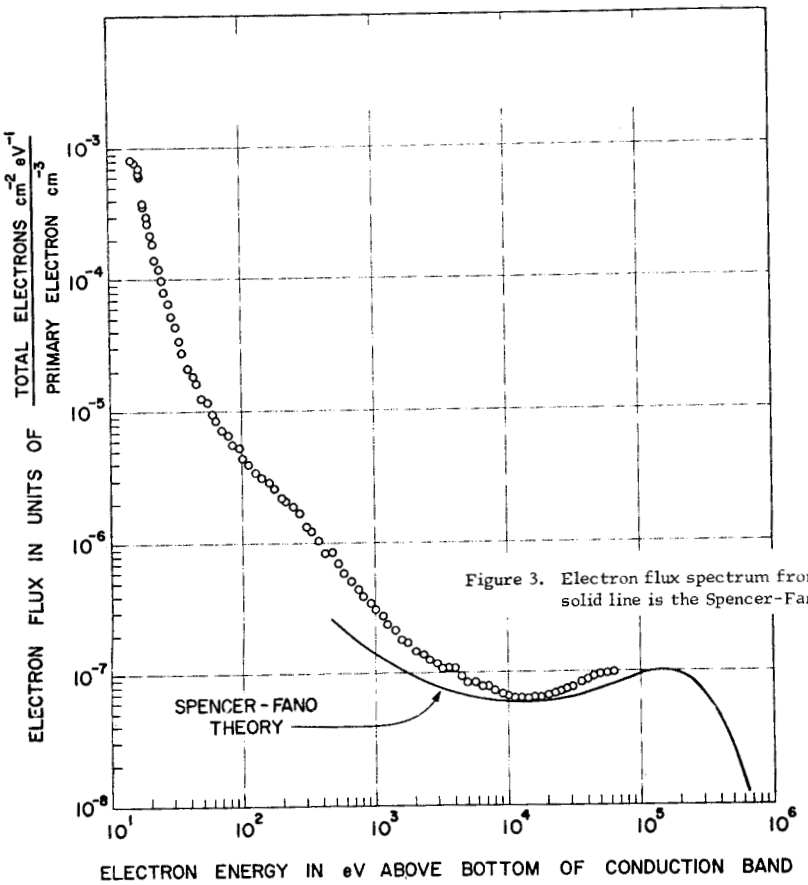

Figure 3. Electron flux spectrum from ^{198}Au beta rays absorbed in aluminum. The solid line is the Spencer-Fano theory.

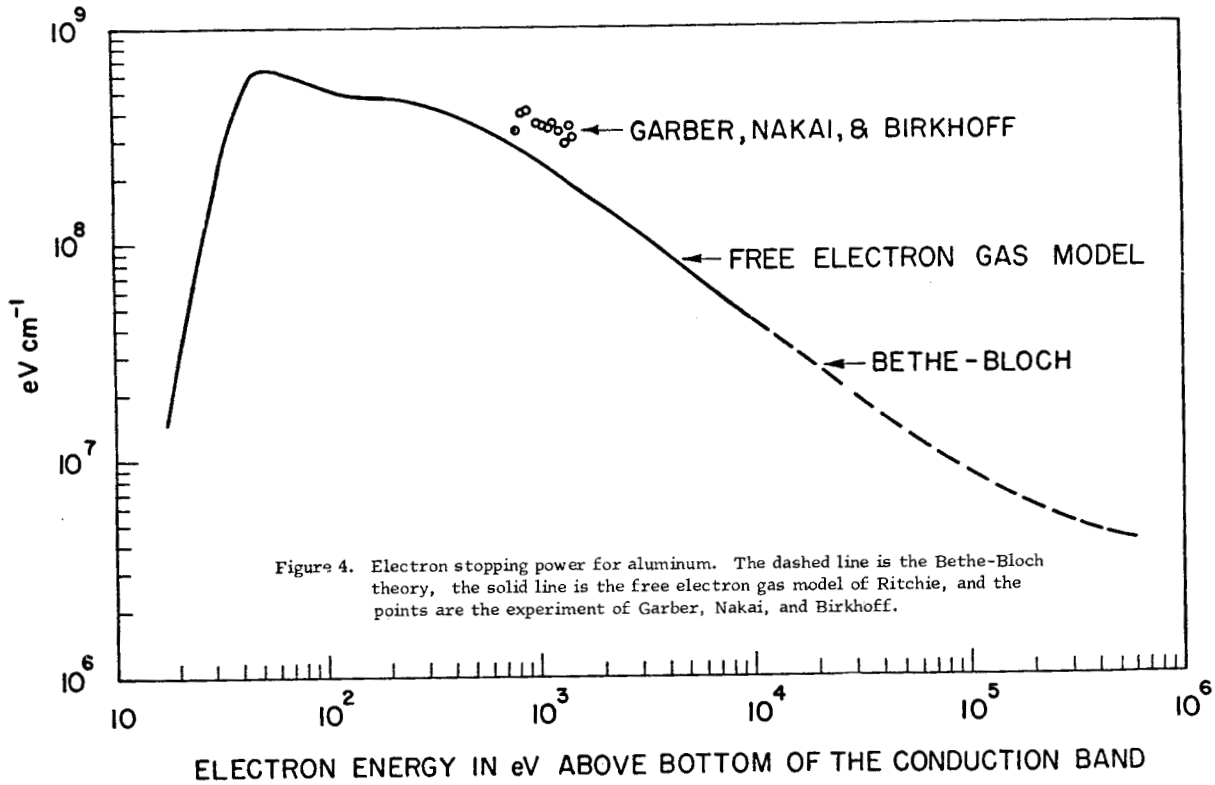

Figure 4. Electron stopping power for aluminum. The dashed line is the Bethe-Bloch theory, the solid line is the free electron gas model of Ritchie, and the points are the experiment of Garber, Nakai, and Birkhoff.

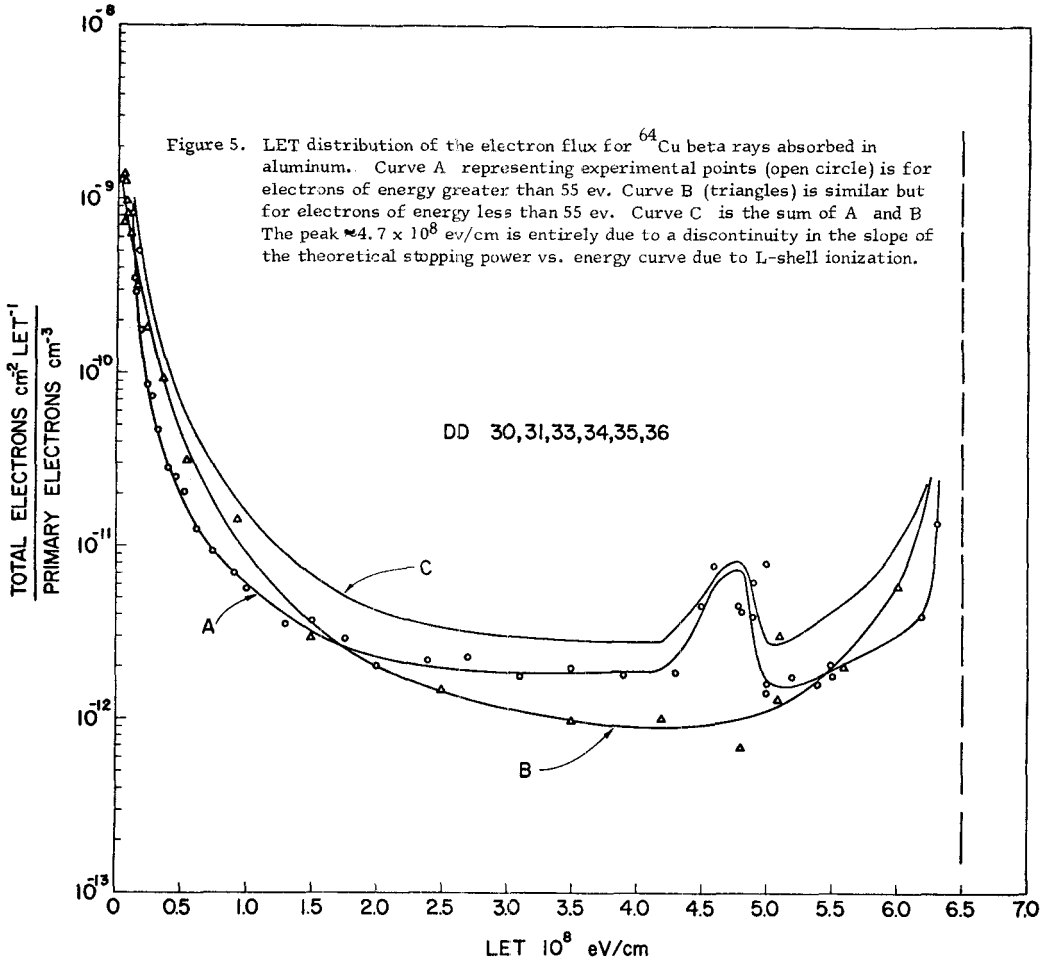

Figure 5. LET distribution of the electron flux for ^{64}Cu beta rays absorbed in aluminum. Curve A representing experimental points (open circle) is for electrons of energy greater than 55 ev. Curve B (triangles) is similar but for electrons of energy less than 55 ev. Curve C is the sum of A and B The peak ≈4.7 x 10^8 ev/cm is entirely due to a discontinuity in the slope of the theoretical stopping power vs. energy curve due to L-shell ionization.

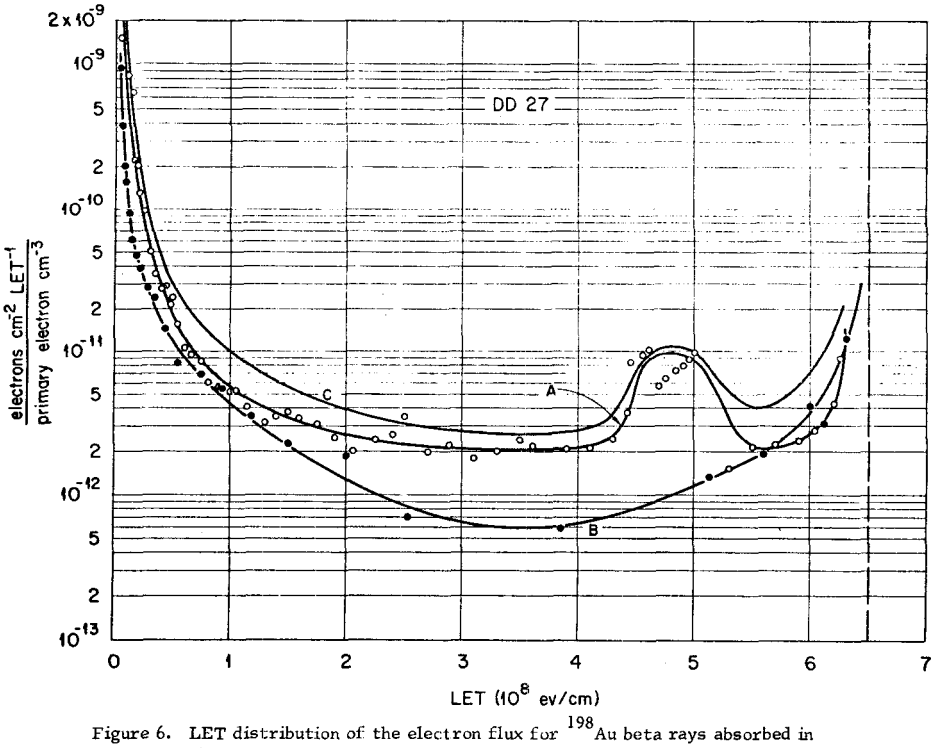

Figure 6. LET distribution of the electron flux for ^{198}Au beta rays absorbed in aluminum. Curve A, representing experimental points (open circle),is for electrons of energy greater than 55 ev. Curve B (triangles) is similar but for electrons of energy less than 55 ev. Curve C is the sum of A and B. The peak ≈4.7 x 10^8 ev/cm is entirely due to a discontinuity in the slope of the theoretical stopping power vs. energy curve due to L-shell ionization.

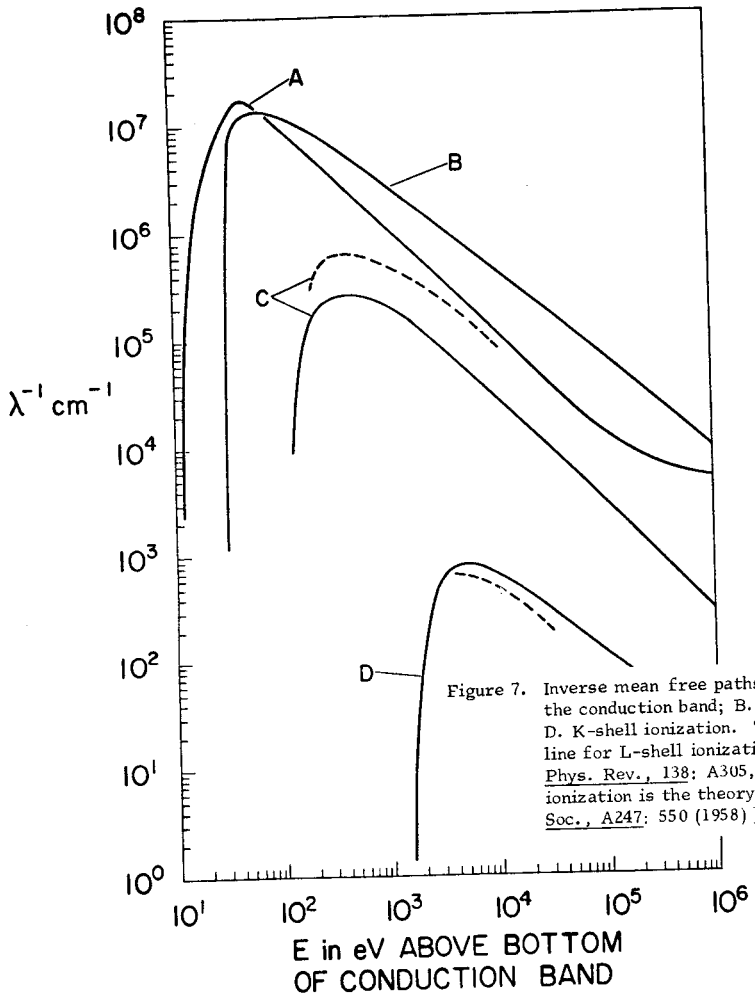

Figure 7. Inverse mean free paths in aluminum. A. Electron-electron interactions in the conduction band; B. Volume-plasmon excitation; C. L-shell ionization; D. K-shell ionization. The solid lines are theory by Ritchie; the dashed line for L-shell ionization is a Gryzinski-type calculation [M. Gryzinski, Phys. Rev., 138: A305, A322, A336 (1965)]; the dashed line for K-shell ionization is the theory of A. M. Arthurs and B. L. Moiseiwitsch [Proc. Roy. Soc., A247: 550 (1958)].

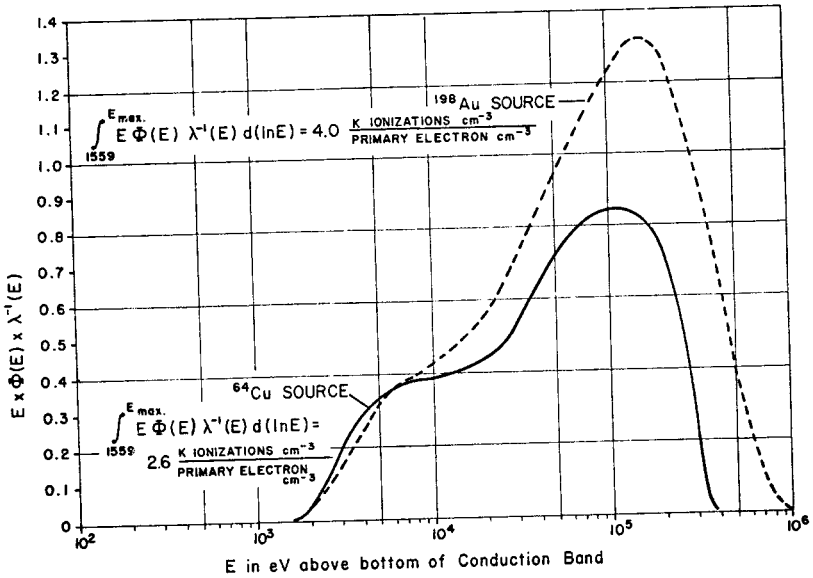

Figure 8. K-shell ionization in aluminum. Solid line ^{64}Cu source, dashed line ^{198}Au source.

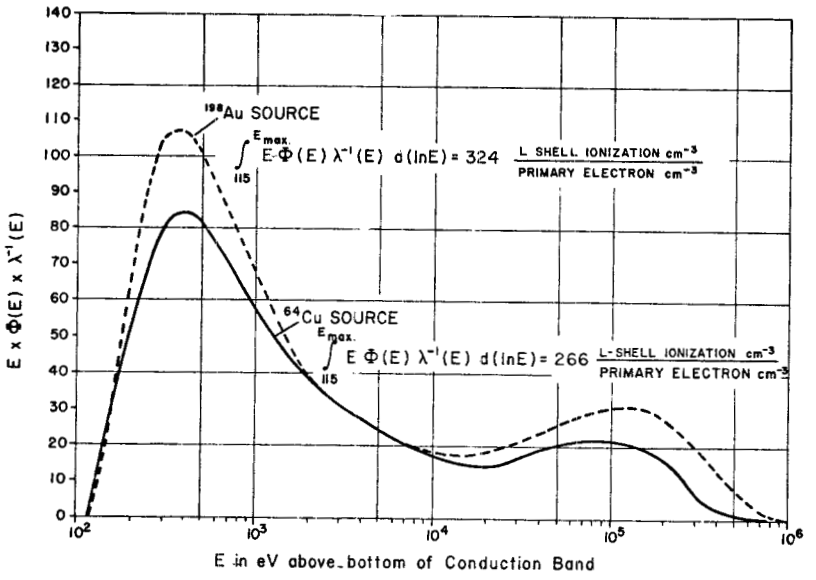

Figure 9. L-shell ionization in aluminum. Solid line ^{64}Cu source, dashed line ^{198}Au source.

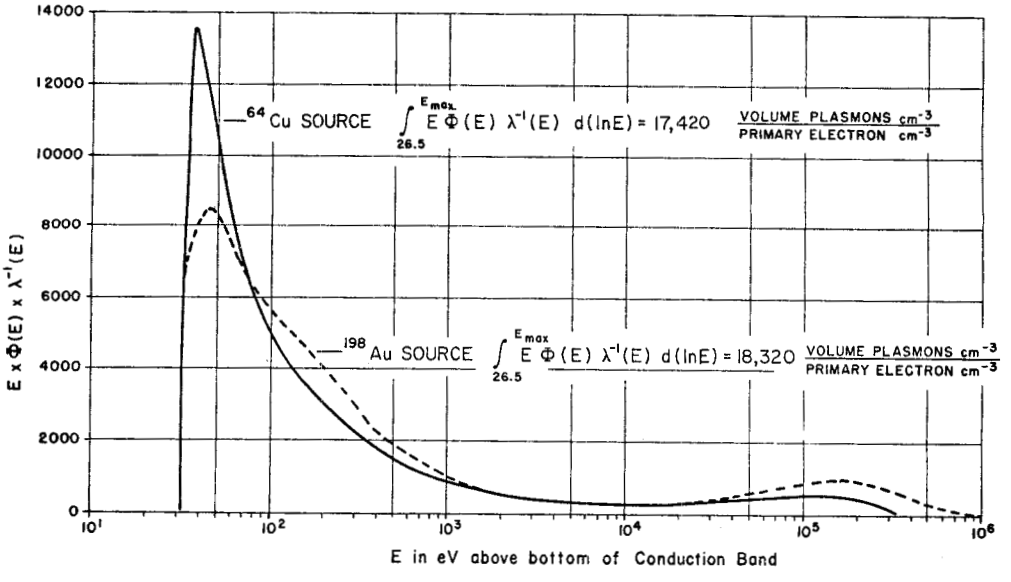

Figure 10. Volume plasmons excited in aluminum. Solid line ^{64}Cu source, dashed line ^{198}Au source.

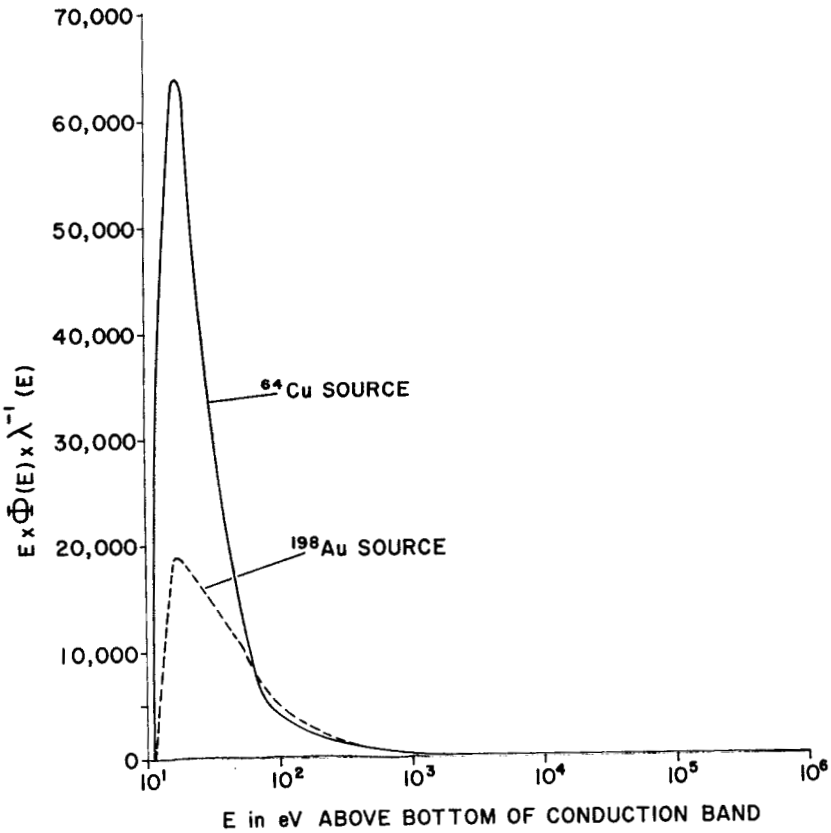

Figure 11. Electron-electron interactions in the conduction band of aluminum. Solid line ^{64}Cu source, dashed line ^{198}Au source.

A METHOD OF INFERRING QUALITY FACTOR USING THE BONNER SPECTROMETER*

George R. Holeman

Yale University

New Haven, Connecticut

Introduction

As the use of accelerators increases, it is becoming increasingly more important to accurately determine the dose equivalent due to the mixed, stray radiation around accelerators. Mixed-radiation dosimetry is usually accomplished by one of two methods. In the first method, attention is focused on the radiation field itself and measurements made of the intensity and energy distribution of the various radiation components. This information is then used to obtain a description of the absorbed dose rate due to the radiation environment or, for example, to compute the dose equivalent to individuals. The second method describes the radiation field in terms of its interaction with matter; actually a sum over the complete energy distribution of the field is obtained which results in a measurement of the absorbed dose. For Health Physics and legal purposes an evaluation of the radiation field in terms of dose equivalent is desired. In order to obtain the dose equivalent from the first method, the appropriate quality factors are applied to the individual components, depending upon the energy distribution. In the second approach the composition and energy distribution are not known; therefore, accurate quality factors cannot be applied. However, when the composition and energy distribution are unknown, it has been common practice to assign a conservative quality factor to the radiation field to obtain the dose equivalent. This paper is a description of an approach which attempts to determine the first-collision dose, dose equivalent, and quality factor for a given field of mixed accelerator-produced radiation which is predominantly neutrons.

A 10-in.-diameter polyethylene sphere containing a lithium iodide crystal has a response approximating the inverse of the dose-equivalent curve for neutrons from thermal energies to at least 7 MeV.[1] This detector, used together with a Bonner or multisphere spectrometer[2] consisting of a bare detector, cadmium-covered detector, 2-, 3-, 5-, 8-, and 12-in. polyethylene spheres, was used to infer the quality factor from data on accelerator-produced neutron radiation. By calibrating the single 10-in. spherically moderated detector with a PuBe neutron source, the detector may be used to measure the dose equivalent directly in mrem/hr. The computer program BON,[3,4] written by the Radiation Physics Division, HASL, USAEC, is capable of unfolding the neutron spectra using the data from a multisphere spectrometer. BON also provides the rads/(n/cm^2) and the

* Work supported in part by the United States Atomic Energy Commission and United States Public Health Service Grant, 3-TI-RH-70-01-A1.

particle fluence (Φ) in n/cm^2. Therefore, the first-collision dose rate in rads/hr may be obtained and the quality factor inferred. A recent radiation survey of the Wright Nuclear Structure Laboratory at Yale* provided the data used in this study.[5] During the survey 19.2-MeV protons were impinging upon a water-cooled aluminum target.

Instrumentation and Method

The instrumentation used consisted of a 10-in. spherically moderated detector and a multisphere spectrometer. The 10-in. spherically moderated detector consisted of a ^{6}Li I (Eu) crystal located at the center of a 10-in.-diameter polyethylene sphere. The associated electronics was biased to discriminate against gamma-ray background. The neutron response of this instrument has been discussed extensively by Hankins.[1,6] The neutron response closely approximates the inverse of the dose-equivalent curve and is compared with it in Figure 1. From Figure 1, it can be seen that for thermal neutrons the response is nearly that of the dose-equivalent curve (± 4 percent), and for fast neutrons the response is within ± 15 percent. Above 7 to 10 MeV the response of the detector drops rapidly and the error increases rapidly until at 14 MeV the response is about 50 percent of the dose equivalent. For accelerator-produced neutrons below approximately 10 MeV the instrument response is reported[6] to be within ± 15 percent of the dose equivalent.

A neutron spectrometer used to analyze stray accelerator radiation should be capable of responding to neutrons over a wide energy range depending upon the accelerator operating characteristics. Few neutron spectrometers have the wide energy range that is desirable; however, the multisphere spectrometer has this desirable, wide energy range. The spectrometer used was the array described by Burrus[7] consisting of an unmoderated detector, one covered with a 30-mil cadmium cover, and detectors inside 2-, 3-, 5-, 8-, and 12-in. polyethylene spheres. The detector assembly was composed of ^{6}Li I (Eu) crystal, placed at the center of the various spheres. The spectrometer data was used to obtain solutions to the homogeneous Fredholm equation of the first kind. The equation to be solved is

$$g(x) = \int_a^b k(x,y)\, f(y)\, dy, \qquad (1)$$

where g (x) represents the measurement from which the neutron spectrum, f (y), is to be inferred and k (x,y) is the response function.

* Operated under Contract AT-(30-1)-3223 with the United States Atomic Energy Commission.

The technique of obtaining solutions to equation 1 by the method of iterations, used in this paper, was originated by Scofield[8] and Gold.[9] Response matrices for the multisphere spectrometer have been published by various authors.[3,7,10] However, the values we used for the response functions were those used by O'Brien, which were taken in part from the calculations of Hansen and Sandmeier,[11] McGuire,[12] and Burrus.[7] The response matrix used was 7 x 52 and ranges from 1 x 10^{-2} to 1.6 x 10^{8} eV. Figure 2 depicts some of the response functions used in determining the matrix. BON, written by O'Brien,[3] utilizing the above-mentioned 7 x 52 response matrix, takes the seven pieces of data and solves for a log-log smoothed neutron spectrum by an iterative method.

The single 10-in. spherical detector was calibrated in mrem/hr by using a one-curie PuBe neutron source with a source strength of 1.8 x 10^{6} n/sec. The quality factors included in this calibration were those recommended by the NCRP.[13] In a given neutron field, the dose equivalent was measured with the calibrated 10-in. spherical dosimeter. At the same time the array of seven detectors was exposed and the neutron energy spectrum obtained. Using the appropriate conversion factors the energy spectrum was converted to a first-collision dose rate in rads/hr. Then from the following relationship the neutron quality factor was inferred:

$$QF_n = \frac{\int k(E)N(E)QF(E)dE}{C\int N(E)dE}, \qquad (2)$$

where QF_n = neutron quality factor,

$k(E)$ = energy-dependent conversion factor, particle fluence rate to first-collision dose rate,

$QF(E)$ = quality factor,

C = average conversion factor, particle fluence rate to first-collision dose rate,

$\int N(E)dE$ = integrated neutron spectrum in n/cm^2 per time.

The quantity $\int k(E)N(E)QF(E)dE$ was obtained from the calibrated single 10-in. detector, the quantity C and $\int N(E)dE$ were obtained by analyzing the data obtained from the multisphere spectrometer.

Once the neutron quality factor was known then a total or effective quality factor was calculated by the following relationship:

$$QF_T = \frac{DR_n \times QF_n + DE_\gamma}{DR_m}, \qquad (3)$$

where QF_T = the effective or total quality factor,

DR_n = first-collision neutron dose rate in mrad/hr,

QF_n = neutron quality factor,

DE_γ = gamma dose equivalent rate in mrem/hr,

DR_m = dose rate of mixture in mrad/hr.

The quantity DE_γ used in equation 3 was obtained from the exposure rate measured with a gamma-sensitive survey meter and assuming a quality factor for gamma of one.

A similar technique has recently been reported by Awschalom[10]; however, he used a tissue-equivalent ionization chamber in conjunction with a multisphere spectrometer to obtain his absorbed and first-collision doses, and a different method of inferring the quality factor.

Results

For calibration purposes the quality factor of a one-curie PuBe neutron source was determined. The neutron energy spectra and dose equivalent were measured both at 17 cm and at 91.4 cm. Figure 3 is the neutron spectra obtained at these locations and compares the spectra with that of Stewart.[14] There seems to be a reasonable agreement between the multisphere and Stewart's spectra considering the lack of detail of the log-log smoothed curve and the wide energy range. Table 1 is a comparison between the previously calculated quality factor of Distenfeld[15] and those determined by the multisphere technique.

Recently the Yale MP Tandem Van de Graaff accelerator met and exceeded design specifications for beam intensity and energy,[16] and at that time a radiation survey was made to establish the effectiveness of the shielding.[5] During the survey the accelerator was producing a 10-uA proton beam at

Table 1

PuBe Quality Factor	
Method	Quality Factor
Calculated	7.55
Multisphere, 17 cm	7.3
Multisphere, 91.4 cm	8.5

19.2 MeV which was allowed to strike a water-cooled aluminum target. Some measurements were also made when the beam was stopped in a tantalum-lined Faraday cup located in the accelerator vault. Figures 4 and 5 show the locations where measurements were made. Figures 6 and 7 depict the neutron energy spectra obtained from the multisphere technique. Table 2 is a listing of quality factors obtained where the neutron energy spectra were utilized to calculate the inferred quality factors.

Discussion

When determining the neutron energy spectra of the PuBe neutron source, the main difficulties were overcoming the problem of obtaining good geometry and minimizing the effect of scatter. The distance 17 cm was chosen to be the same as that of Stewart's, and the distance 91.4 cm was chosen as an attempt to overcome the effect of varying solid angle subtended by the detector and various moderator arrangements. When the two spectra (at 17 and 91.4 cm) are compared with a normalized Stewart spectrum they both agree quite well between 5×10^5 and 10^7 eV with the difference, varying from a factor of 1 to approximately 7 for the 17-cm spectrum and from 1 to approximately 6 for the 91.4-cm spectrum.

The reason for the quality factor at location 14 having a value as high as 15 is not clear. The high value may be due to several reasons; however, the most likely seem to be either machine instability at high voltage over prolonged periods due to lack of sufficient conditioning, or the over-estimate of dose equivalent of the 10-in. spherical dosimeter due to a preponderance of intermediate-energy neutrons.

It is also of interest to note the different quality factors for location 11, for the two conditions: beam striking target in target room 1 and beam being stopped in the Faraday cup in the accelerator vault. The increase in quality factor from 1 to 9 is due to the larger proportion of fast neutrons reaching the monitoring location when the beam is stopped in the accelerator vault.

The method described above for determining the implied quality factor of neutrons seems to be a feasible approach. Some of the advantages of this approach are: (1) the quality factor information is a by-product of obtaining dose equivalent and energy spectra at a given location, (2) time-consuming calculations are performed

Table 2

Inferred Quality Factors

Yale MP Tandem Accelerator

Location*	Neutron Quality Factor	Total Quality Factor
1	4.1	1.5
2	3.2	2.3
4	3.4	2.3
5	9.8	4.3
6	2.1	1.3
8-V	3.7	3.1
11	1.0	1.0
11-V	8.9	7.1
12	6.5	5.2
14	15.0	1.5
16	10.0	2.0

*See Figures 4 and 5 for locations.

The locations with a "-V" in the notation, indicates that the beam was being stopped in the Faraday cup located in the accelerator vault.

by computer, and (3) covers wide energy range from thermal energies to 7 or 10 MeV and the energy range can be extended with additional data points using larger spheres. Some of the disadvantages are: (1) accuracy above 7 to 10 MeV is questionable, (2) program errors involved are not too well understood, (3) spectra void of detail and other methods are definitely better when only fast neutrons between 0.5 and 10 MeV are present, (4) presently calibrated with PuBe but additional calibration points should be obtained, (5) long time needed for complete survey of accelerator laboratory and changes in beam characteristics during this time will affect survey results, and (6) fast computer needed to analyze spectra.

From the data in Table 2 it appears that a quality factor of 5 contains adequate safety for the radiation fields outside the accelerator vault and target areas. Although a quality factor of 10 is recommended for fields where the neutron spectra are unknown, the shielding employed in the Wright Nuclear Structure Laboratory appears to sufficiently degrade the neutron energy to justify use of an average quality factor of 5.

Acknowledgements

The author wishes to express his appreciation to J. C. Overley and the staff of the Wright Nuclear Structure Laboratory, Yale, for their assistance; and to K. O'Brien, HASL, for discussions and a copy of the BON computer program.

REFERENCES

1. D. E. Hankins, A Neutron Monitoring Instrument Having a Response Approximately Proportional to the Dose Rate From Thermal to 7.0 MeV, USAEC Report LA-2717, Los Alamos Scientific Laboratory, 1962.

2. R. L. Bramblett, R. I. Ewing, and T. W. Bonner, A New Type of Neutron Spectrometer, Nucl. Inst. and Meth.,9:1 (1960).

3. K. O'Brien, R. Sanna, and J. McLaughlin, Inference of Accelerator Stray Neutron Spectra from Various Measurements, in USAEC First Symposium on Accelerator Radiation Dosimetry and Experience, November 3-5, 1965, USAEC Report Conf-651109, pp 286-304, 1965.

4. K. O'Brien, USAEC Health and Safety Laboratory, personal communication, January 28, 1966.

5. J. C. Overley, G. R. Holeman, P. D. Parker, and D. A. Bromley, Radiation Shielding for an MP Tandem Accelerator Installation (submitted to Nucl. Inst. and Meth.).

6. D. E. Hankins, Determination of the Neutron Contribution to REM Dose, in USAEC First Symposium on Accelerator Radiation Dosimetry and Experience, November 3-5, 1965, USAEC Report Conf-651109, pp 163-171, 1965.

7. W. R. Burrus, Bonner Spheres and Threshold Detectors, USAEC Report ORNL-3360, pp 296-305, Oak Ridge National Laboratory, 1962.

8. N. E. Scofield, A Technique for Unfolding Gamma Ray Scintillation Spectrometer Pulse Height Distributions, USN Report USNRDL-TR-447, 1960.

9. R. Gold, Iterative Solutions for the Matrix Representation of Detector Systems, USAEC Report TID-18304, 1960.

10. M. Awschalom, The Use of the Multisphere Neutron Detector For Dosimetry of Mixed Radiation Fields, USAEC Report PPAD-59E, Princeton-Pennsylvania Accelerator, 1966.

11. G. E. Hansen and H. A. Sandmeier, Neutron Penetration Factors Obtained By Using Adjoint Transport Calculations, Nucl. Sci. Engng., 22:315 (1960).

12. S. A. McGuire, A Dose Monitoring Instrument For Neutrons From Thermal to 100 MeV, USAEC Report LA-3435, 1965.

REFERENCES (continued)

13. Protection Against Neutron Radiation Up to 30 Million Electron Volts, National Bureau of Standards, Handbook 63, 1957.

14. L. Stewart, Neutron Spectrum and Absolute Yield of a Plutonium-Beryllium Source, Phy. Rev., 98: 740 (1955).

15. C. H. Distenfeld and A. M. Markoe, Determination of Quality Factor Through the Utilization of a Balanced, Tissue Equivalent, Ionization Chamber, Nucl. Inst. & Meth., 45: 181 (1966).

16. D. A. Bromley, Bull. Am. Phys. Soc. II, 11: 464 (1966).
Bull. Am. Phys. Soc. II, 12: 44 (1967).

17. Recommendations of the International Commission on Radiological Protection, ICRP Publication 4, 1964.

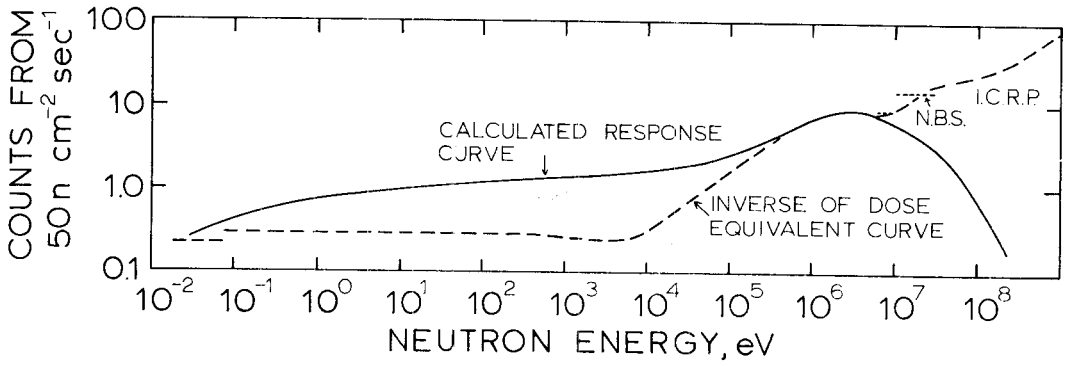

Figure 1. Calculated response of a 10-in. single-sphere instrument versus energy (from reference 1). NBS refers to reference 13 and ICRP refers to reference 17.

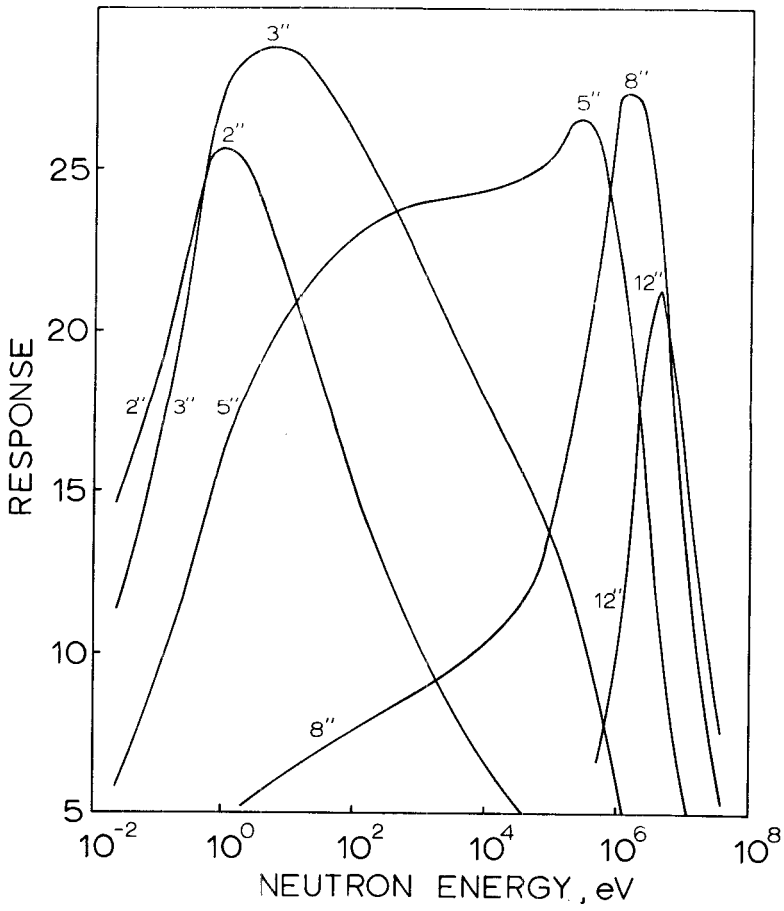

Figure 2. Response functions for the multisphere spectrometer (references 3 and 12).

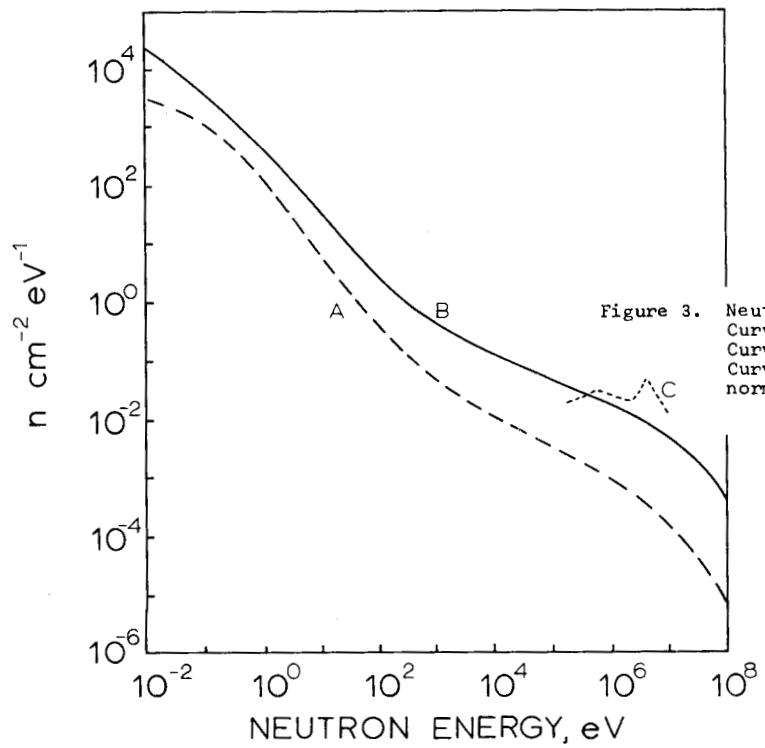

Figure 3. Neutron spectra from PuBe neutron source.
Curve A - multisphere spectrum at 91.4 cm.
Curve B - multisphere spectrum at 17 cm.
Curve C - Stewart's (reference 14) spectrum normalized to conditions of Curve B.

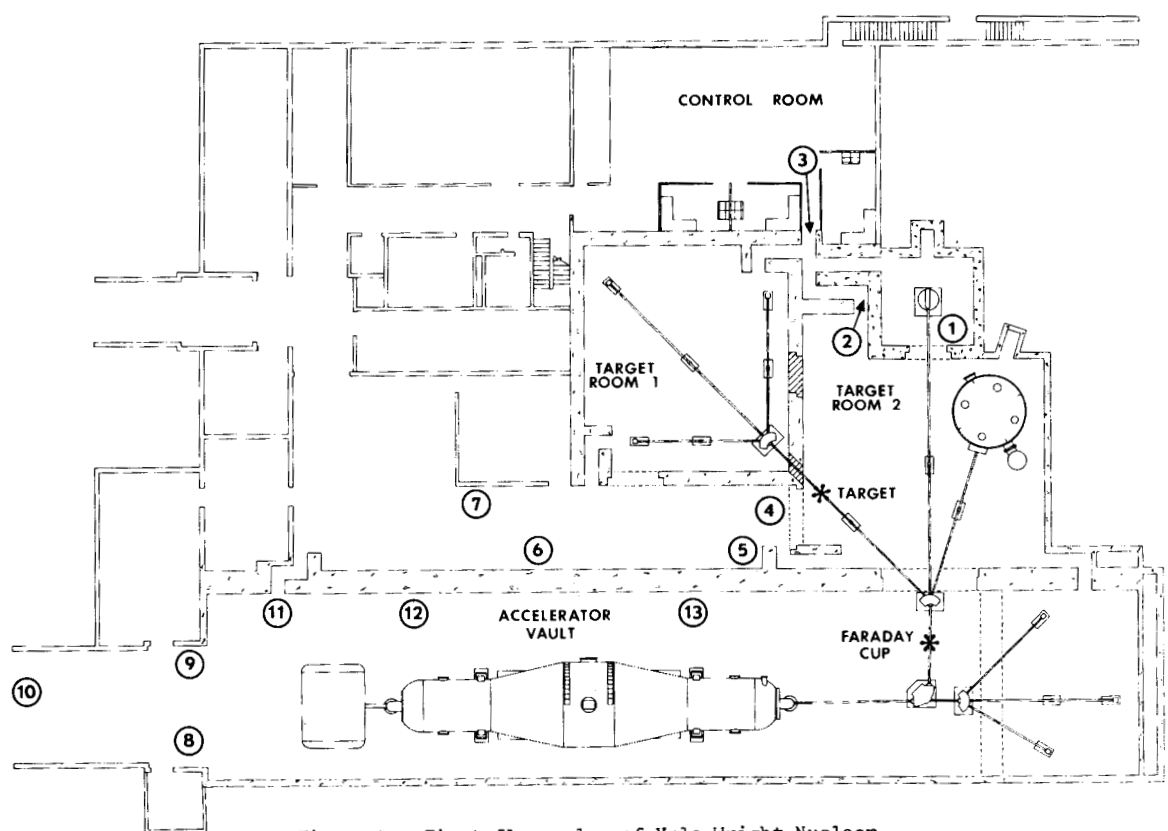

Figure 4. First-floor plan of Yale Wright Nuclear Structure Laboratory showing monitoring locations.

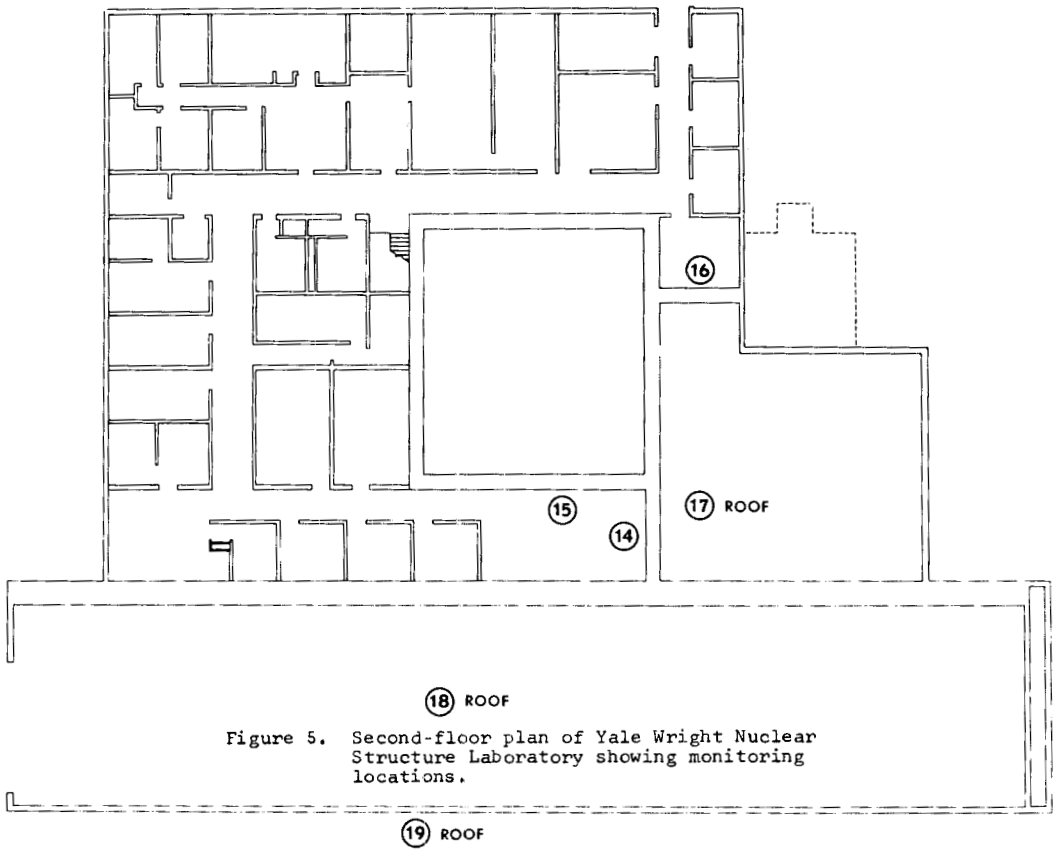

Figure 5. Second-floor plan of Yale Wright Nuclear Structure Laboratory showing monitoring locations.

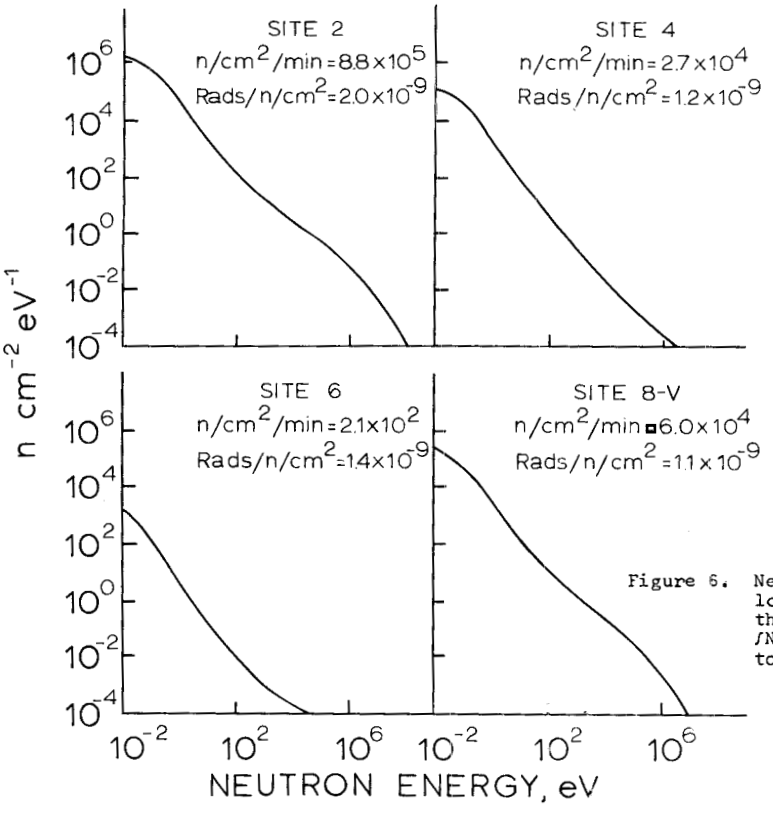

Figure 6. Neutron spectra at various monitoring locations and the numerical values of the quantities C (rads/n/cm²) and $\int N(E)dE$ (n/cm²/min). (Spectra normalized to time of one minute).

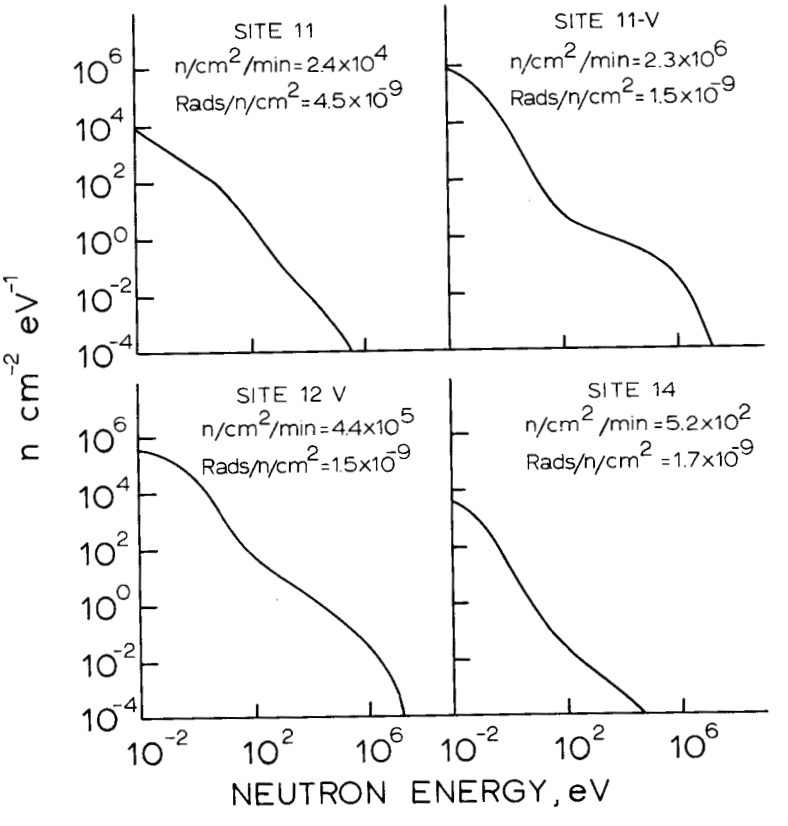

Figure 7. Neutron spectra at various monitoring locations and the numerical values of the quantities C (rads/n/cm^2) and $\int N(E)dE$ (n/cm^2/min). (Spectra normalized to time of one minute).

DOSE ESTIMATION IN THE CONTEXT OF HEALTH PHYSICS REGULATIONS AND RESPONSIBILITIES

Walter S. Snyder

Oak Ridge National Laboratory
Oak Ridge, Tennessee

The definition of health physics or, alternatively, the question of the proper role and function of the health physicist, seldom fails to arouse a lively discussion whenever the topic is raised in a group of cognoscenti. Even among those closely concerned with this discipline, the image of the health physicist ranges from that of an individual who is concerned with taking routine measurements and comparing them slavishly with numbers in a handbook to an Olympian individual who untangles the almost inextricably complicated web of benefits and risks and, having balanced them, legislates the proper procedures for protecting individuals and even the human race against the direst consequences. If an official definition is needed, the founding fathers of the Health Physics Society have provided one,[1] and it clearly indicates that, in their view, health physics includes the scientific and professional aspects of radiation protection as well as all levels of the technological disciplines involved in carrying out radiation protection programs. I intend to discuss my subject from this broad point of view; that is, to consider a health physics program as including professional as well as technological aspects and to outline these broadly, but with special attention to a radiation protection program for an accelerator facility. Thus, while the day-to-day monitoring and advising that constitute so large a fraction of the working effort in a health physics program will not be ignored, the professional aspects also will be noticed. A profession is considered here to consist of the practitioners of a technical discipline whose exercise involves a large measure of judgment and in which the practitioner has an obligation to act and make decisions even though all uncertainty is not resolved, and further has the obligation to act in the interest of others not so technically competent as himself in this discipline. I believe this statement is a reasonably accurate general statement of the health physicists' responsibilities, and consequently I view health physics as a profession in the same sense as medicine or law are so considered.

The formal or quasi-legal aspects of a health physics program will be considered first. These consist in establishing a program by which the recommendations or requirements of various authoritative bodies are implemented so far as possible. These requirements range from the recommendations of the ICRP and NCRP, which are advisory in character, to the formal and legal requirements of the FRC, of various state or local governments, or of management. These recommendations and guides operate with varying degrees of force in determining the health physics program, but those of the ICRP are perhaps typical of the general nature of such guidance and it is essentially the ICRP's recommendations which will be used here to illustrate my thesis. These recommendations are rather general in nature, and give the health physicist great latitude in planning and carrying out his program. Obviously, at

the working level these general recommendations will be replaced with much more detailed and specific procedures and rules which will vary greatly with the type of facility and the operating program.

The ICRP uses dose equivalent (DE) as the basic concept by which radiation exposure is evaluated. Table 1 contains the basic recommendations for occupational exposure as formulated in Publication 9, [2] page 14.

Table 1. ICRP: Summary of dose limits for individuals.

Organ or tissue	Maximum permissible doses for adults exposed in the course of their work	Dose limits for members of the public
Gonads, red bone-marrow	5 rems in a year[a]	0.5 rem in a year
Skin, bone, thyroid	30 rems in a year[a]	3 rems in a year[b]
Hands and forearms; feet and ankles	75 rems in a year[a]	7.5 rems in a year
Other single organs	15 rems in a year[a]	1.5 rems in a year

a. Subject to the limitations given in paragraphs 54 and 57, up to one-half of the annual dose limit, or one-half of the annual permissible dose commitment, may be accumulated in any period of a quarter of a year (see, however, special recommendation for women of reproductive capacity—paragraph 62).

b. 1.5 rems in a year to the thyroid of children up to 16 years of age.

These general criteria will be discussed now in slightly more detail, keeping in mind the context of a health physics program for an accelerator operation.

The limits in Table 1 are to be averaged over a year, but the Commission also limits individual doses. Thus, for occupational exposure, it only permits half the annual limit to be received in any one quarter except in very special circumstances. It discourages permitting two such exposures to occur in a short period of time. Under these special conditions which are defined as Planned Special Exposures, doses up to twice the annual limit may be given,

but this is further limited by requiring that the total occupational dose to gonads or red bone marrow accumulated by the individual in his entire career not exceed the formula 5(N - 18), where N is his age in years. This provides for substantially the same flexibility as was permitted previously. The Commission also considers that doses of up to five times the annual limits may be received in very exceptional cases, but that these should not occur more than once to any individual. It is not the intention here to attempt to give in detail the circumstances under which such exposures are permitted. Rather, the intent is only to indicate that there is considerable flexibility possible within the recommendations and to refer the reader to the text for details.

In general, doses are to be averaged over the organ or tissue of interest. Conventionally, the red bone marrow is taken to be at a depth of 5 cm below the surface of the body. For accelerator radiation of great penetrating power the depth-dose curve is usually rather flat except when a monodirectional and monoenergetic beam occurs, with the Bragg peak present in the body. Such a case is shown in Fig. 1, which is taken from Turner et al.[3] In Fig. 2 is the corresponding depth-dose distribution for an isotropic source of monoenergetic protons, and the Bragg peak is not in evidence because of the averaging over depth which results from the spread of the angular distribution. It is clear that the peak will not be in evidence in the depth-dose curve if the source has a continuous energy spectrum or a continuous angular distribution, or if the body moves substantially during the exposure. The peak might be present if one adjusted a target by sighting into the beam. In most practical situations the smoothed depth-dose curve would seem to be the better approximation to the actual situation. The health physicist should consider what cases, if any, warrant an estimate of dose based on the peak. The dosimetric significance of bone as contrasted with soft tissue is discussed by Turner et al. in another paper of this symposium. The sharp drop in the depth-dose curve seen in Fig. 1 is also present in monoenergetic electron beams, where the dose drops practically to zero at the end of the range. The health physicist must be aware of the nature of the source and plan his monitoring program accordingly.

In Table 1 the lenses of the eyes occur in the category of "other organs" for which 15 rem/yr is recommended as the MPD. This seeming change in the recommendations is rather a matter of terminology, and illustrates the flexibility permitted by the present definition of dose equivalent as the product of dose in rads, the quality factor, and any appropriate modifying factors. In the lenses of the eyes, cataract is the relevant end point, and the biological data on which the formerly recommended MPD of 5 rem/year was based relates primarily to exposure to radiation of high LET. Thus radiation of low LET was not the primary standard. In order to continue to use QF = 1 for the low-LET radiation which is relatively ineffective for cataract production, it was only necessary to raise the MPD to 15 rem/yr and to insert an additional modifying factor of 3 in the case of radiation for which QF is 10 or more. Other values of this modifying factor are to be interpolated for intermediate values of QF (Ref. 1, Par. 16). Thus, the health physicist needs to estimate QF at a depth corresponding to the lenses of the eyes if he is to avoid the possibly overconservative practice of using the modifying factor of 3 for all radiation for which QF is greater than 1.

In estimating dose to skin, it should be noted that the dose is averaged over the body if the dose is fairly homogeneous, but for exposure of a very small area the Commission recommends that dose be averaged over a square centimeter of surface in the region receiving the highest dose (Ref. 2, Par. 28). In fact, the existence of beams of radiation in any working area poses monitoring problems which the health physicist cannot ignore. It is necessary that he effectively prevent persons from intercepting a beam unless he can monitor the exposure and show that exposure is within the recommended limits; either alternative poses practical problems of considerable difficulty.

The flexibility permitted for special planned exposures has been mentioned and the health physicists should consult ICRP Publication 9 for full detail on this point. The Commission further recognizes that emergency exposures, e.g., when a life or an installation of immense value is at risk, will cause individuals to deliberately — and perhaps properly — exceed the levels recommended for routine operations. In addition, there are accidental exposures to be considered. In all these cases where exposure is high the health physicist has the obligation to make as prompt and accurate an assessment of dose as circumstances permit. If the dose is well above permissible levels, the ultimate disposition of the case will be in the hands of the medical profession. It was the fashion some years ago to maintain that dosimetric information is of little use for medical treatment of severe radiation exposure cases and that doctors will prefer to be guided by the clinical course as observed. Certainly one would not want to recommend that the dosimetric information be the sole or preponderant consideration for the doctor who is responsible for the case. However, two extremely severe cases of partial body exposure in recent years point up the importance of knowing with all reasonable precision the actual pattern of dose within the body.[4,5] In both cases an elaborate dosimetric investigation was conducted, and it is not too much to say that the results did greatly influence the treatment of the case. In an accelerator situation the possibility of partial-body irradiation will often be present, and the health physicist should plan procedures which might be used in such situations as seem to offer some potentiality for severe exposure.

Thus far I have discussed only the formal requirements of a health physics program in the context of the ICRP recommendations. In some cases the recommendations or guides or rules of NCRP, FRC, states, or management may differ in some details, but the ICRP recommendations are rather typical of the spirit if not of the letter of these other sources of guidance. Actually it is not feasible to do justice here to the full scope and carefully conceived guidance the ICRP and the NCRP offer. The responsible health physicist will make himself thoroughly familiar with the relevant publications of these organizations as well as with the rules of the FRC and the AEC, which have legal force when applicable to his situation. If he will absorb the spirit of the ICRP and NCRP recommendations he will have through this alone a well-grounded basis for his program.

However, the health physicist as a professional man should go beyond the letter of the rules. As one responsible for the well-being of others he has the obligation to be aware of new developments and concepts that are relevant to his activities. He acts in behalf of others and he does not deserve to be considered professional unless he feels an obligation to be worthy of that trust. I

will mention here only a few examples of additional information he might consider, and these are chosen only to illustrate this position:

(a) Distribution of Dose Within the Body. This has been discussed somewhat above in the context of the ICRP recommendations. Probably doses to various body organs will seldom be made a matter of record. In most cases certain measurements are made, and these insure that the maximum dose is low enough that none of the MPD are exceeded. Certainly I do not want to recommend that the health physicist grind out and record a large number of dose estimates for all the tissues and organs for which MPD are given. I do believe he should not be content to obtain only the crude "air doses" or other monitoring information that assures him the doses are well below the MPD. Important as this assurance is, I think he should give some attention to the actual doses to body tissues and organs and be prepared for the cases—which one hopes never will occur—which might require detailed estimates of dose within the body. Even if such cases do not occur he will have fulfilled his obligation to the people for whom he has some responsibility, and he will understand the whole rationale of his program better for having considered the basis and reasons for his procedures.

(b) Estimation of Radiation Quality. As indicated above in a particular case, the health physicist may need to estimate LET for the radiation of concern. He may need to do this merely to meet the formal requirements of his program so he can estimate QF and hence the DE. But I would have him go further. There are other pertinent indices of radiation quality; for example, the distributions studied by Rossi,[6] or the distribution of δ rays. Admittedly these are not now formal requirements of the book of rules, but as a professional man the health physicist should be aware of what is significant in assessing the hazard of radiation exposure, and these and other measures of radiation quality are certainly relevant whether required or not.

(c) "Stars" and Tracks of Densely Ionizing Particles. The health physicist should be aware of the questions, as yet unanswered, concerning the biological significance of very high and local concentrations of ionization and dose. He will be aware of the work of Curtis,[7] which demonstrates that they can produce observable biological effects, i.e., graying of hair due to the passage of a single particle having a very densely ionized track. Although none of the formal rules require this, I think he should try to estimate what fraction of the doses he typically measures is of this kind. Even if he is never called upon to produce his estimates he will be the better health physicist for having gone beyond the minimal requirements of his work.

(d) The Concept of Cell Lethality. I would have our health physicist be aware of new dosimetric concepts that arise from time to time. For example, Curtis et al.[8] have recently discussed the concept of fractional cell lethality. No doubt this fraction is infinitesimal for doses below the MPD, but the health physicist does not assume all exposures will be low, and even without this practical interest, he should have a professional interest in new developments related to the basic concepts of his profession.

The above-mentioned examples are only a few of many that could be cited but whose import is simply this: that the health physicist is not merely concerned with carrying out a routine job of meeting formal criteria in a routine way. There is a minimal formal set of criteria he must meet to some degree, but as a professional man he should go somewhat beyond this minimal program. I am not saying he must do research in these and other areas,

although he might well consider this as a possibility. A glance through the technical journals will reveal that many health physicists do find it possible to do some research along with their primary work in the regular course of a health physics program.

Finally, the health physicist must ponder deeply the obligations of his profession. On the one hand he is responsible to his management for carrying out an efficient and a high-quality program and on the other hand he has an even greater and primary responsibility for the people he is protecting. Superficially, there might seem to be a conflict of interest here but this is not really the case. No management can long afford to have a health physics program of poor quality if there is a real potential risk of high exposures, as there usually is in work with accelerators. The health physicist must be prepared to defend his program and to inform management of the rationale of his program and of its needs, and a properly informed management cannot afford to ignore the real demands of a good program. Here again health physics is intrinsically of a professional nature, requiring judgment beyond the scope of a routine application of formalized procedures, and demanding the highest qualities of character to serve the best interests of those for whom he acts.

The matter of keeping records of exposure of radiation workers has been under discussion recently.[9] Some have expressed the view that records of doses received are only indices of the adequacy of the health physics program and are not worthy of consideration if and when any biological effects are in question. From what I have said it is evident I take strong issue with this point of view. As you are doubtless aware, the AEC has under way a study to determine whether it is feasible to use dosimetric records collected in the past as a basis for correlation with whatever effects might be observed.[10] The position I have tried to outline above is, essentially, that as health physicists we should try to obtain the information now believed to be relevant, and that the data we collect should be as reliable as modern techniques permit. In this way the health physicist can truly fulfill his responsibilities to the radiation workers he protects and to the management he serves, and fully qualify as a professional man in the highest and best sense of the term.

REFERENCES

1. Health Physics, 11: 1126 (1965).

2. "Recommendations of the International Commission on Radiological Protection (Adopted September 17, 1965)," ICRP Publication 9, 14 (1966).

3. J. E. Turner, C. D. Zerby, R. L. Woodyard, H. A. Wright, W. E. Kinney, W. S. Snyder, and J. Neufeld, Health Physics, 10: 783 (1964).

4. L. H. Lanzl, M. L. Rozenfeld, and A. R. Tarlov, Health Physics, 13: 241 (1967).

5. Abstracts 162-164, Health Physics, 12: 1815 (1966).

6. H. H. Rossi, Radiation Research, 10: 522 (1959).

7. Proceedings of the Symposium on the Protection Against Radiation Hazards in Space, Gatlinburg, Tennessee, November 5-7, 1962, U. S. Atomic Energy Commission Report TID-7652 (2 books), 1962.

8. S. B. Curtis, D. L. Dye, and W. R. Sheldon, Health Physics, 12: 1069 (1966).

9. Hearings (Aug. 30, 31 and Sept. 20, 21, 22, 1966) before the Joint Committee on Atomic Energy, Congress of the United States, 89th Congress, Second Session, on Proposed Legislation (HR 16920 and S 3722) Related to Uniform Record Keeping and Workmen's Compensation Coverage for Radiation Workers.

10. T. F. Mancuso, M. D., B. S. Sanders, and A. Brodsky, Feasibility Study of the Correlation of Lifetime Health and Mortality Experience of AEC and AEC Contractor Employees with Occupational Radiation Exposure, Progress Report No. 2, April 3, 1965 - May 31, 1966.

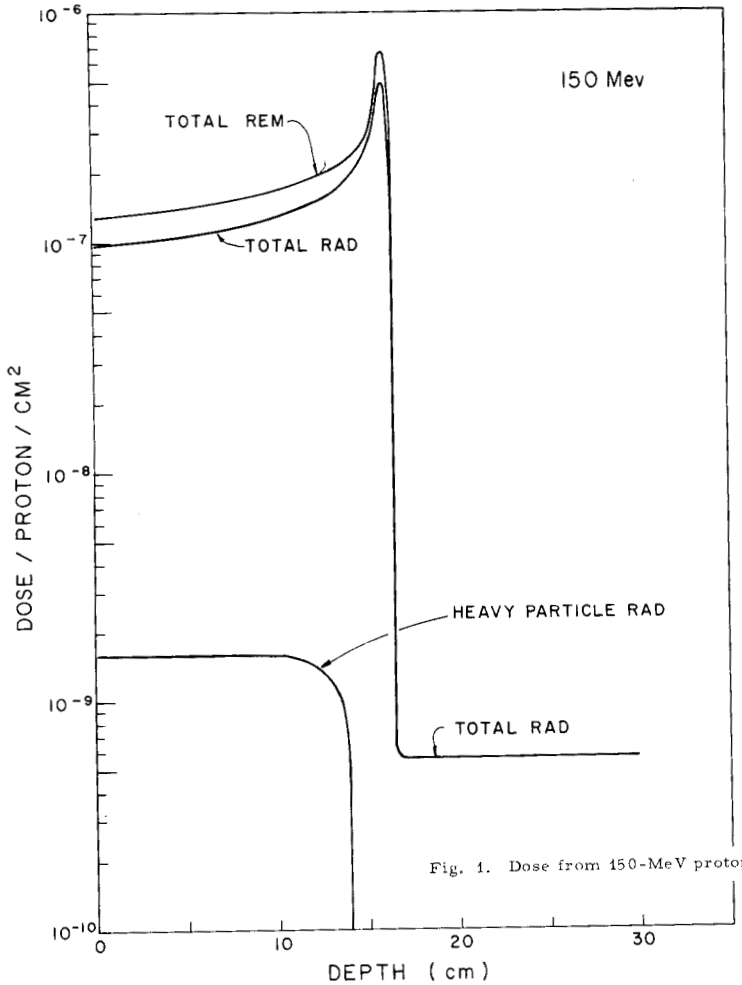

Fig. 1. Dose from 150-MeV protons normally incident on 30-cm tissue slab.

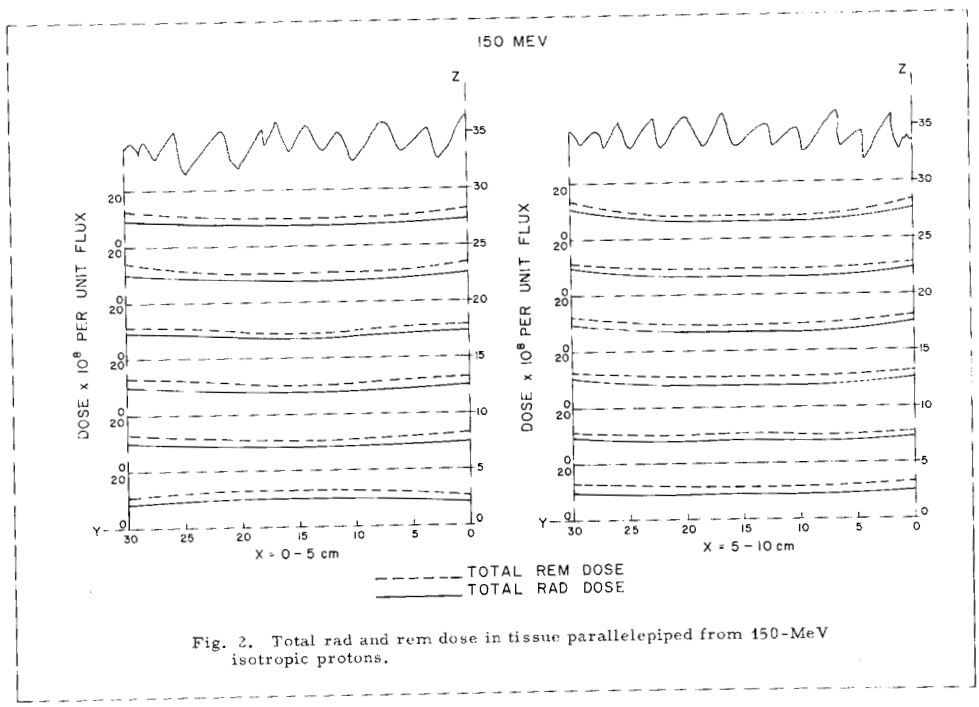

Fig. 2. Total rad and rem dose in tissue parallelepiped from 150-MeV isotropic protons.

RADIATION ENVIRONMENT PARAMETERS AND THE BIOPHYSICIST*

John T. Lyman

Lawrence Radiation Laboratory
University of California
Berkeley, California

April 1967

In this conference it was planned that you, the health physicist, would hear papers summarizing our current knowledge of the biological effects of radiation. By now you should know some of our problems; there has been much talk about dose, dose rate, dose distribution, LET distribution, oxygen effect, strain differences, and so on. There have been discussions about the physical aspects of the dose distribution, FLET, slowing-down flux, macro- and micro-dosimetry, dosimetry at an interface. By now you may be asking yourself the question, "How does this affect me, the health physicist?"

I feel that you, who are in charge of the measurement of the radiation environment, have the responsibility for furnishing the biophysicist with the dosimetric information he needs to evaluate the effects of various exposures to accelerator-produced radiation.

Today there are probably only three things that a biophysicist will want to know about the dosimetric features of an exposure:[1] (a) the absorbed dose at all points of interest, (b) the time distribution of the dose, and (c) the variation on a microscopic scale of the local energy density. Other information is very useful, regardless of the details with which these fundamental dosimetric data are given; this would include the type or types of radiation emitted by the source, the relative intensity of each type, their energy distributions, any filtration or moderation, the effective size of the source, the distance between the source and the irradiated object, and the angular distribution of the radiations. I don't think a biophysicist would ask for more today, but several years from now the questions a biophysicist would ask may be different. Then the questions might be, what was the momentum transfer? or the dose at a bone—bone-marrow interface, or the FLET distribution, using either a sliding cutoff or a fixed cutoff energy?

I think that the point Dr. Madey was trying to make is that at this time we cannot become fixed in our thinking about the cutoff energy for a delta ray. There are not enough biologic data available to say what should be used. There probably are different cutoffs for different biologic effects, and there may be different cutoffs for ions having different velocities, but we may not know until after much more work.

So what should you measure? My answer is that anything you measure, if you do it accurately, will probably be of help. But the most useful measurements will be those from which you can derive the other quantities of interest.

*This work was done under auspices of the U. S. Atomic Energy Commission.

I think you should measure the basic physical parameters. These would be the type of radiation, the flux of each radiation, the effective source size, the angular distribution of the radiation, the energy distribution of the radiation, the distance from the effective source to the object being irradiated, certain parameters that would specify the object being irradiated, any intervening filtration or moderation, and appropriate time factors. These are the measurements which I think are the most useful, and from these basic physical exposure parameters the information desired by the biophysicist could be calculated.

The radiotherapist has access to computer programs which enable him to obtain depth dose distribution from rather complicated limited-field exposure by cobalt-60 sources.[2] These same programs have been modified to calculate dose distributions from electron accelerators. These programs even account for macroscopic inhomogeneities in tissue density. There are programs for calculating range and dE/dx for heavy charged particles,[3] and programs for calculating the dose due to the transport of nucleons through matter.[4]

When you consider the magnitude of the responsibility that has been entrusted to you it does not seem such a large problem to put these programs together so that any of the dosimetric features of an exposure that a biophysicist might want would be available. With this approach it would be easy to include RBE values for estimate of exposure, or QF values to estimate the hazard of a particular environment, or to include inactivation or malfunction cross sections for the appropriate cells in different parts of the body and to also calculate fractional cell lethality.

Now if a computer program were assembled so that when you supplied information about the radiation environment the computer could calculate the dosimetric features of the exposure, then your problem would be supplying the necessary radiation environment parameters. I think the input to such a program, if it were to be a general program, would be:

The types of radiations
For each type, the angular distribution and the energy distribution
The effective source size
The distance from the effective source to the object of interest
Any filtration or moderation of the radiations occurring between the effective source and the object of interest
Parameters that would specify the object of interest
Appropriate time factors.

The final decision as to what measurements are to be made is yours, but remember to think about the future. The quantities of interest tomorrow may be different from what they are today, but if you have made the right measurements, you should be able to calculate all the desired quantities.

References

1. Radiobiological Dosimetry, Recommendations of the International Commission on Radiological Units and Measurements. NBS Handbook 88 ICRU Report 10e 1962.
2. Theodor D. Sterling, Harold Perry, and James J. Weikam, Automation of Radiation Treatment Planning, VI, Brit. J. Radiol. (to be published).
3. Palmer G. Steward and Roger Wallace, Calculation of Stopping Power and Range-Energy Values for any Heavy Ion in Nongaseous Media, USAEC Report UCRL-17314, Lawrence Radiation Laboratory, Dec. 1966.

4. J. E. Turner et al., Calculation of Radiation Dose from Proton to 400 MeV, Health Physics, 10: 783-808 (1964).
5. C. D. Zerby and W. E. Kinney, Calculated Tissue Current-to-Dose Conversion Factors for Nucleons Below 400 MeV, USAEC Report ORNL-TM-1038, Oak Ridge National Laboratory, May 1965.

The Role of Cellular Radiobiology in Radiation Protection*

Harald H. Rossi

Radiological Research Laboratory, Department of Radiology

Columbia University, New York, N.Y.

Present-day standards of radiation protection are derived from a great diversity of causes. Some of these are historical: it is possible to trace one or two presently accepted concepts for periods that can approach half a century. Some are empirical: our steadily lengthening experience of human exposure provides a measure of confidence at least in the area of long-term somatic radiation effects. Other important considerations are practical, such as formulation of standards with a view towards both adaptation to various situations and ease of enforcement, or conserving, such as a desire to minimize alterations of numbers that are part of legal codes. Considerations pertaining to the balancing of risk and benefit may even be philosophical, ethical, or sociological.

It is only natural to assume that the most important considerations should be scientific, if only because scientists are primarily responsible for the formulation of radiation protection regulations. However, science is not necessarily indispensable. Thus scientific considerations are virtually absent in the formulation of those traffic regulations which deal with speed limits, a subject that is in many ways akin to maximum permissible dose.

The significance of scientific contributions to the subject of radiation protection has in fact been questioned on the basis of two major arguments. One of these maintains that although progress in radiobiology may have made radiation one of the better understood hazards, our knowledge of basic radiobiological mechanisms is still insufficient for firm recommendations. On the other hand it is also argued that accurate radiobiological information is of limited value since it can only provide the answer to the easier of the two questions involved in the balancing of risk versus benefit. Thus the decision as to whether to raise the permissible dose to the general population by a certain amount is hardly facilitated by increasingly precise information on the relation between dose and the frequency of abnormal offspring.

It can also not be denied that in the past the "scientific" basis for radiation protection criteria was rather poor. Thus early permissible doses were designed to avoid erythema or changes in the white blood count. This is now considered naive, and we are concerned with more subtle effects such as carcinogenesis and genetic mutation. However, one cannot help wondering whether twenty

*This investigation was supported by Contract AT-(30-1)-2740 for the U.S. Atomic Energy Commission and U.S. Public Health Service Research Grant RH-99, National Center for Radiological Health.

years from now present-day concerns will seem also naive.

Despite such reservations radiobiology has had a strong influence on radiation protection and will very likely continue to do so in the future. We simply have no choice but to adapt our recommendations to the best current knowledge of radiobiology. On balance it would appear from the experiences gained thus far that this only rational course has stood us in good stead.

Radiobiological effects may be divided into tissue (or organ) responses and cellular responses. Near maximum permissible radiation levels, cells are only sporadically affected and prompt tissue responses are negligible. It is therefore generally assumed that one should focus attention on injury to individual cells and its amplified manifestation in genetic mutation or carcinogenesis. However, in special cases (e.g. the lens of the eye), damage to a very small fraction of the cells may severely impair the function of an organ. The possibility must also be considered that carcinogenesis may require damage to several neighboring cells.[1]

The quantities of importance to the biological effect of radiation can be divided into two groups (Table 1). Two of the three biophysical parameters listed are explicitly taken into account in the formulation of radiation protection regulations. The third, dose rate, is subject to a long-term (3 month) basis of accumulation.

Of the biological parameters only one - organ sensitivity - is explicitly considered. Age is regarded only in a lower limit for occupational exposure. The most important, the volume subject to irradiation, is ignored if it includes critical tissues. Thus the permissible dose is the same whether one cc of bone marrow or the entire body is exposed.

The biophysical parameters are subject to a strong mutual interaction. The principal aspects of lethal action on mammalian cells are shown in Figure 1, which is taken from the report of the RBE Committee of the ICRP and the ICRU.[2] This diagram may be summarized as follows:

1. If the charged particles that deliver the dose have a high LET (i.e., the -dE/dx is of the order of 100 keV per micron of tissue) the logarithm of the surviving fraction decreases linearly with dose. Hence, the fraction of the cells inactivated at low doses is simply proportional to dose. Exponential cellular survival to high-LET radiation is one of the most universal rules in radiobiology. Apparently the only exception holds for microorganisms in which there is genetic redundancy (several nuclei or at least several sets of chromosomes).

2. The survival of cells irradiated with high-LET particles depends little if at all on dose rate.

(1.) and (2.) suggest that high-LET particles inactivate the cell in single rather than multiple events. This conclusion is also strongly supported by physical evidence which shows that for sufficiently high LET the number of cells killed is just about the same as that in which one particle has traversed the nucleus.

3. In the case of low-LET radiation the shape of the response curve is more complex - at least when the dose rate is high. In this case the logarithm of the surviving fraction decreases more rapidly as the dose increases. There is some

Table 1

Major Variables Controlling

Biological Effect

Biophysical Parameters	Biological Parameters
Dose	Fraction of Organ Irradiated
Dose Rate	Organ Sensitivity
Radiation Quality	Age
	Individual Variability

argument as to whether the curve ever attains a constant slope but there seems to be general agreement that it does so at least approximately. However, an even more important question concerns the shape of the survival curve at low doses. It is not entirely established whether it meets the ordinate with a slope that is zero or finite.

4. At high doses the shape of the dose-effect curve for low-LET radiation depends strongly on dose rate, with survival increasing as the dose rate is reduced. As a consequence the curvature of the entire curve must become less, but it is at present again not definitely known whether it becomes a straight line and if it did whether its slope would be zero.

It is evident that inactivation of mammalian cells by low-LET radiation occurs usually through the agency of more than one particle. The question arises whether this is always the case. Curves of the type shown in Fig. 2a would imply that it is. The types shown in Fig. 2b would obtain if inactivation can occasionally be caused by a single particle - a process that must predominate at low doses. If Fig. 2a is correct, it is conceivable that steady reduction of the dose rate could eliminate the appearance of observable effects, since in the eventuality of recovery from one "hit" before the next one occurs one would never observe the effect. On the other hand if Fig. 2b is correct, there is a finite possibility of inactivation by single particles, and this is of course dose-rate-independent.

Depending on the validity of either curve the RBE (relative biological effectiveness) of high-LET radiation relative to low-LET radiation approaches either infinity or some high but limited value as the dose and/or dose rate is reduced.

It will be appreciated that the question as to which model is correct has very important implications to radiation protection. This is particularly true since most of our experience with human exposure has been with low-LET radiation. If Fig. 2a is correct the hazards of high-LET injury are of a different nature and could be much greater than this experience might indicate.

Inactivation in multiple events could occur on the basis of two distinct processes which have often been termed multi-hit and multi-target. According to the multi-hit model, cells contain sensitive sites in which radiation must deposit some minimal energy before inactivation results. The number of such sites per cell is probably more than one, but except for purposes of numerical calculations this is really immaterial as long as excess of the energy threshold in any site leads to inactivation. Presumably the required energy can usually be delivered by a single high-LET particle but only by several low-LET particles.

However, low-LET radiation may be expected to occasionally deposit as much energy in a site as does high-LET radiation. This is illustrated in Fig. 3, which shows the pattern of energy deposition in 1-micron spherical regions within tissue irradiated by radiations of greatly different average LET (Co-60 γ rays and 1 MeV neutrons). Y, the event size, is defined as the quotient of energy deposited by sphere diameter in keV/μ. Since here $\mu = 1$, Y is simply equal to the energy deposited. F(Y) is the frequency of such deposition per unit logarithmic interval of Y and per rad of absorbed dose. It will be seen that the distributions overlap. There are good reasons to believe that the diameter of sensitive sites is less than one micron. In this case the degree of overlap must be expected to be even greater.

According to the multi-target model a certain minimum energy must be depos-

ited in each of several sites (typically two). It is again of minor importance to these considerations whether the number of such sets of associated sites is one or more than one per cell as long as inactivation can be initiated in any one of the sets. It is assumed that a single high-LET particle going through all the sites of a set delivers sufficient energy to each but that it is unlikely that several particles inactivate a set (as already mentioned there is about one high-LET particle per nucleus of inactivated cells). At low LET the reverse situation is postulated. Neary[3] has developed such a model in detail in order to account for plant chromatid aberrations. There is also evidence that this type of inactivation mechanism is involved in opacification of the lens of the eye.[4]

According to Fig. 3 energy deposition by low-LET radiation can be equal to that produced by high-LET radiation but it tends to become quite rare at large Y. If it were to be required in two targets the relative probabilities would need to be squared, which might make the difference very much larger. In this case one-step inactivation by low-LET radiation might become so unlikely as to be negligible even in the radiation protection range. Because of this necessary multiplication of probabilities the multi-target model generally tends to favor the situation depicted in Fig. 2a.

Another factor indicating a progressively decreasing inactivation rate at decreasing doses of low-LET radiation is a steady rise in RBE. There appear to be no experiments that indicate that the RBE becomes constant below some radiation dose. Fig. 4 is based on data by Bateman et al.[5] and indicates that in the case of opacification of the lens of the mouse eye there are no signs of a leveling off, and RBE values become quite high even in acute irradiations. It would seem that these studies were carried out at the lowest neutron doses investigated in mammalian systems to date.

Although the choice between the alternatives depicted in Fig. 2 can not be made with certainty, 2b, which assumes a linear initial portion of the curve, is more cautious in that it assumes that any dose of radiation has some effect that can not be eliminated by a reduction of dose rate. It has been necessary for reasons of prudence to design radiation protection on this assumption. This establishes a philosophy according to which the permissible dose of any radiation (high or low LET) represents a limited risk rather than a condition of safety, and its magnitude, however chosen, must be arbitrary. Needless radiation exposure should be avoided and the risk attending an exposure must be justified in terms of a corresponding benefit. The postulate that any amount of radiation is harmful is particularly bothersome when considered in connection with the well-known fact that no amount of shielding can entirely suppress the radiation emitted from most sources.

On the other hand, linearity of the dose-effect curves and virtual absence of dose-rate effects in the permissible range make the dose by itself a good index of hazard. However, one would then expect that the integral dose, defined as the product of dose and mass of tissue exposed, would be the best index. Thus the mean dose to an organ should be a better index than the maximum dose in any one cc - which is the limiting quantity according to present recommendations.

Our present knowledge of somatic cellular effects is not sufficiently specific to deal with the problems of differential organ sensitivity or the numerical value of the maximum permissible dose. However, an annual dose of 5 rems to any cell system would be expected to have any effect on only very few cells if the rem is interpreted according to its original meaning as the absorbed dose of any radiation that elicits the same biological response as one rad of x rays.

The adoption of the model in Fig. 2b minimizes the biophysical effects of dose rate only to the extent that dose rate is unimportant as long as the dose is delivered in a period short enough so that the characteristics of the cell do not change during irradiation. Movement through the cell cycle, division, differentiation, etc. will, of course, change sensitivity. Tissues and entire organisms can clearly repair damage by cell replacement and do so more effectively when the damage is low. There are also further considerations, such as the length of latent periods for manifestation of injury and the simple practical requirement that in order to continue his exposure to radiation an individual can not have already received his allotted life-time dose. All of these reasons require a limited rate of dose accumulation. The formula according to which the total dose equivalent received at age N must be less than 5(N - 18) rem and the dose per 3-month period less than 3 rem would also not seem unreasonable in the light of whatever quantitative data we have on cellular injury.

Perhaps the only aspects of present protection recommendations that may be disturbing from the viewpoint of cellular radiobiology are the numerical values assigned to the quality factor (QF), which has a maximum value of 20 although recent ICRP regulations may be construed to make this 60 for the lens of the eye. Apart from this possible exception the quality factor applies to all organs and can not be equated to the RBE for any particular one. However, it should not be greatly different from the maximum RBE for any of them. The model in Fig. 2b is more conservative if one is concerned with effects of low-LET radiations. The model in Fig. 2a is more conservative if one wishes to formulate QF values on the basis of protection experiences with low-LET radiations, since it suggests the possibility of very high RBE values which are also indicated in Fig. 4. It should be emphasized that these data deal with minor injuries and that one can not extrapolate with any certainty from mouse to man. It is, however, also evident that further data on the RBE at low doses are urgently needed.

This presentation has been principally based on our experiences with somatic cellular effects for the simple reason that I am more familiar with these than with genetic effects. It would appear, however, that most of the conclusions are the same for genetic effects. For these the model of Fig. 2b seems firmly established.

Effects such as aging and carcinogenesis are much more pertinent to human radiation injury- and they are doubtlessly much more complex- than lens opacification or inability of tissue-culture cells to divide indefinitely. However, they must derive from the same fundamental cause of cellular impairment. We must continue to explore this phenomenon in all of its forms. The understanding thus gained will always be of essential help to our formulation of radiation protection recommendations.

References

1. G. Failla, Considerations bearing on permissible accumulated doses for occupational exposure, Radiology, 69: 23 (1957).

2. International Commissions on Radiological Protection and on Radiological Units and Measurements, Report of the RBE Committee, Health Phys., 9: 357 (1963).

3. G.J. Neary, Chromosome aberrations and the theory of RBE. 1. General considerations, Int. J. Radiation Biol., 9: 477 (1965).

4. H.H. Rossi, The role of associated absorption events in lenticular radiation injury, to be presented at International Atomic Energy Agency Panel on Biophysical aspects of radiation quality, Vienna, Apr. 10-14, 1967, and to be published in the proceedings.

5. J.L. Bateman, H.H. Rossi, B.J. Biavati, and V.P. Bond, Dependence of RBE on the energy of fast neutrons. V. Lens opacities at low doses, in preparation.

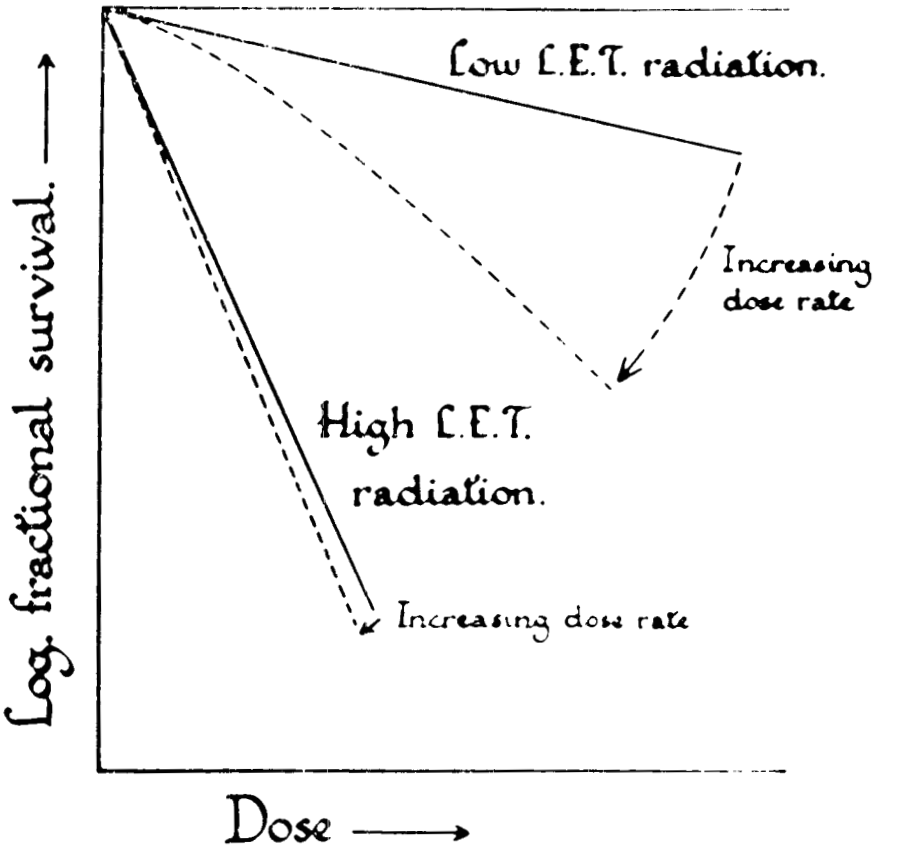

Fig. 1: Dependence of cellular radiation effects on dose, dose rate, and LET (From ICRP-ICRU RBE report[2]).

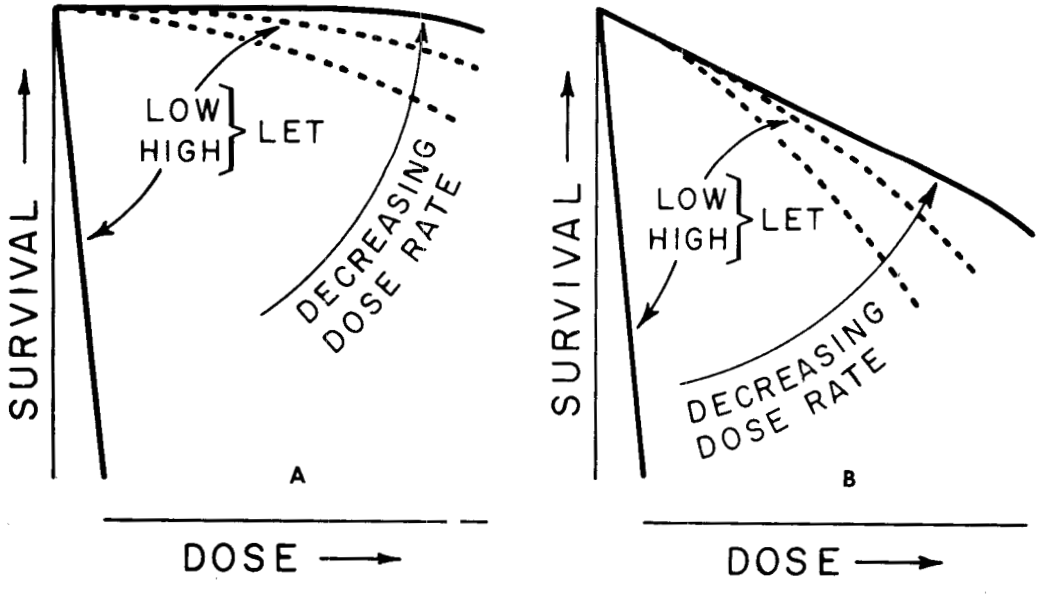

Fig. 2: Possible magnified views of the curves in Fig. 1 near intersections with ordinate. A single-event component in low-LET injury is absent in a but present in b. The change of shape for low-LET radiation depends not only on the absolute dose rate but also on the degree of recovery between events. The limiting straight lines apply in the extreme case of complete recovery between successive events.

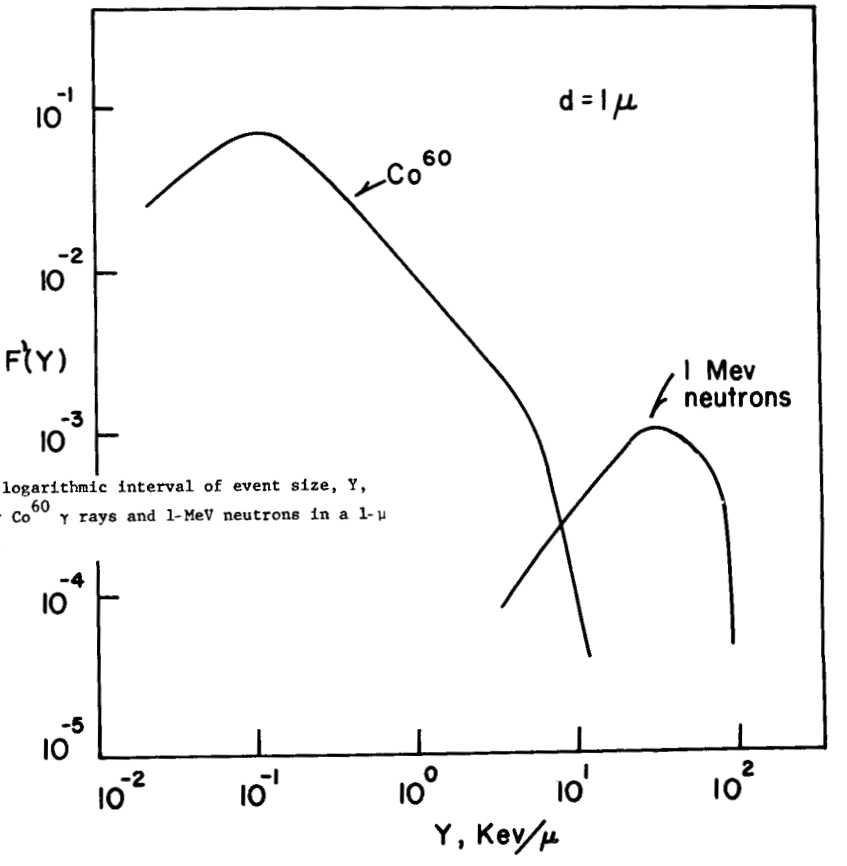

Fig. 3: Event frequency, F'(Y), per logarithmic interval of event size, Y, versus Y. The data are for Co^{60} γ rays and 1-MeV neutrons in a 1-μ spherical region of tissue.

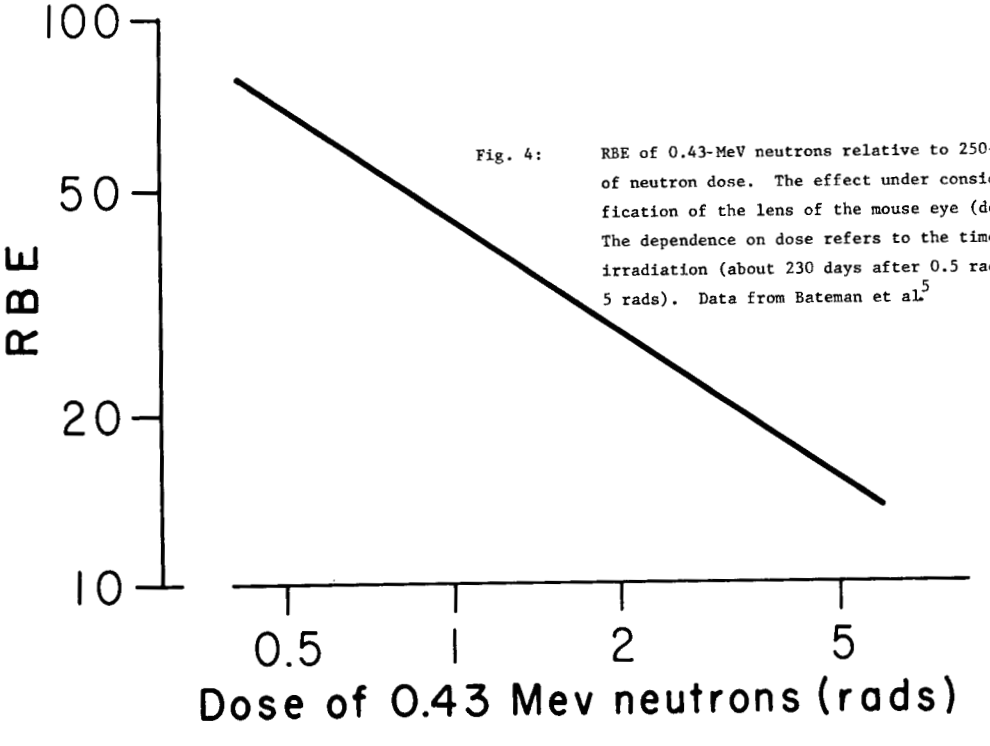

Fig. 4: RBE of 0.43-MeV neutrons relative to 250-kV x rays as a function of neutron dose. The effect under consideration is a minor opacification of the lens of the mouse eye (denoted by Bateman as 2.5%). The dependence on dose refers to the time when it appears after irradiation (about 230 days after 0.5 rad and about 140 days after 5 rads). Data from Bateman et al.[5]

VI. 9

RADIATION EXPOSURE LIMITS AND THEIR BIOLOGICAL BASIS

Hardin B. Jones

Donner Laboratory and Lawrence Radiation Laboratory
University of California, Berkeley, California

INTRODUCTION

The concept of threshold dominated thoughts about radiation exposure hazard in the first half of this century. And there was ample basis for this view. Even as late as 1956, the position paper of the National Academy of Sciences held that radiation exposure of less than 100 roentgens is without evident physiological effect. This concept was the result of years of acquaintance with the relations between dose and response for various chemical toxins, and comparison of these phenomena with the immediate effects of ionizing radiation. As exposure to the chemical agents declines from levels causing great harm, the magnitude of the harm induced decreases much more rapidly than the dose, so that in all cases there are levels which do not evoke a perceptible physiological change. These levels are thus below the threshold of injury. Early radiation exposure limits were based on the observation that immediate radiation injury similarly failed to appear when the dose was below some threshold level. Fortunately, those who had set the guide for caution in radiation exposure had placed the maximum for safe daily exposure to be 0.1 R/day, approximately 1/1000 of the apparent threshold level for response to a single exposure. The working conditions of many installations involving occupational radiation exposure in the 1950's permitted individuals to be exposed to levels of the order of 0.1 R/day and many persons were in fact exposed to these amounts daily.

Exposure-effect information on the induction of genetic mutations in the fruit fly, first noted by H. J. Muller and later developed by Curt Stern, established a direct proportional relationship for the risk of mutation per roentgen over a wide range of exposure. Muller's work was necessarily based on high exposure doses; but Stern had particularly established that the mutation frequencies associated with 25 and 50 roentgens were proportionally reduced from the mutation rates observed at levels orders of magnitude higher. Indeed, by 1954 there was reason to believe that there was no threshold associated with mutagenic effects of radiation. Subsequently, Bentley Glass was able to extend the observation of proportionality to exposures lower by another order of magnitude.

While the hypothesis of proportionality for radiation effects was becoming well established with regard to the genetic response, the long-standing belief in the threshold hypothesis for injurious effects in general remained ingrained, and

thresholds were reported as observed in a number of experiments in which the data might have been fitted as well or better by the concept of proportionality. By analyzing the data of many investigators, I was able to show that, for cell killing, induction of cancer, and aging effects, proportionality held throughout the regions studied and no inference of a threshold seemed warranted. In the middle 1950's, the risk of leukemia associated with radiation exposure of the populations of Hiroshima and Nagasaki was linked to a threshold interpretation in the first follow-up report on these populations. Immediately, E. B. Lewis and I separately undertook reanalysis of the data and justified a proportional-risk interpretation of the same information.

With this cue to suggest the possibility that other long-accepted threshold relationships might not be valid, I began to look at the dose-effect relationships for various carcinogens. Selected examples of the fit of induced cancer frequencies to the quantitative exposure to carcinogen are shown in Figs. 1 through 4. In Fig. 1, the chemical carcinogen dibenzanthracene, which produces cancerous nodules in the lung, is seen to have no apparent threshold, as nearly as the data can demonstrate.

In Fig. 2, the logarithm of effect is related linearly to dose for the bone-seeking radionuclides strontium-90 and calcium-45, without any evident threshold. Figure 3 similarly shows no threshold for the chemical carcinogen methylcholanthrene. An exception seems to occur in the case of lymphoma induction in the mouse by radiation. In Fig. 4, Kaplan and Brown's data on dose versus logarithm of effect suggest that a threshold does exist. In general, however, both chemical carcinogens and ionizing radiation cause an increase in cancer that is either linearly or logarithmically proportional to exposure. Many other examples of proportionality could have been shown, and the weight of evidence is now on this side.

In observations on the effect of radiation in decreasing life span, I have continually held that it is reasonable to show the effect as a simple proportional reduction, while at the same time pointing out that the experimental observations have been limited to exposures over 100 R and that radiation exposure effects have not been tested directly in the range of the order of 1 R. Nevertheless, we are justified in assuming that these are the best estimates of the risk of radiation effect to be made at this time.

Some comparison to other environmental hazards is helpful in placing the radiation hazard in perspective and appreciating its relative risk to populations. I have found it useful to translate the hazards of disease, toxic agents, and other adverse factors into equivalent years of effective aging, using the age-specific death rates as an index of the effective age of any group or population we select for study. Similarly, favorable factors for longevity may be translated into "negative aging" and can be shown as equivalent years of life prolongation. In

Fig. 5, the risk of death from tuberculosis is shown to decline fairly uniformly decade by decade during recent calendar time, and with proportional decline at all ages in the population. With respect to this one disease, for example, the figure shows the same death rate in 1960 for persons aged 80 as prevailed in 1950 for persons aged 47, so that an effective improvement of 33 years (minus 33 years of aging) measures the gain at that age level in our battle against tuberculosis. It is not too different at other ages; age 50 in 1960 has the same mortality rate as age 19 in 1950--minus 31 years. The effect of imprisonment in some concentration camps of World War II is shown in Fig. 6; again there is a proportional increase in the risk of death in all ages and to the same relative extent. By sliding any one line horizontally to coincide with another and noting the number of years it must be moved, we can interpret conditions in the one camp as a relative aging with respect to those in another. In Fig. 7, chronic radiation exposure of mice (the relation is similar for other mammals) is shown to increase the rate of aging, as indicated by the change in slope of the lines corresponding to accelerated increase in death risk with age as exposure rate increases. An assortment of selected environmental and constitutional variables and their effects on life span is shown in Table 1. For those factors which can assume a range of values, the effects on life span are generally proportional to the magnitude of the variable factor.

The acceptance of the hypothesis of proportionality with respect to the risk associated with radiation has caused some social and political problems when the risk has been considered out of context and exaggerated. Conceivably a very small exposure to ionizing radiation could be the cause of a cancer, even though the statistical risk of generation of disease is extremely small. It is impossible to prove that radiation is the cause in any particular case because exactly the same kind of cancer can occur for many other reasons as well. The person affected is just as ill whether his illness arose spontaneously or followed a massive exposure to radiation that might have been its cause. The importance of the principle of proportionality as a guide to controlling radiation exposure is that, on the average, the risks will be least if the exposure is kept low, and that such exposure as is incurred should be in exchange for significant benefit.

In the evaluation of exposure to agents which are hazardous to life and health, it is helpful to gain perspective by comparisons with familiar circumstances. For example, it helps to know what levels of risk most people accept calmly in their daily lives. The life span of the chronic smoker is reduced about 7 years at a pack-per-day smoking rate; and, throughout all of the years he spends as a smoker, he lives his life at a lower level of resistance to disease and hence probably at a lower level of vigor. We may use this as a basis of comparison with those who survived the effects of atomic bombing in Japan and who were severely exposed to ionizing radiation. The survivors probably did not receive much more than 300 R. Both directly, through the medical follow-up of that population, and indirectly through general comparisons with experimental radiation of animal

populations and corresponding life-shortening observations, we can estimate this particular effect of atom-bombing to be approximately the same as that of smoking a package of cigarettes per day. Both agents of harm are appreciable at this level; yet, as the degree of exposure is reduced, the effect may be regarded as proportionally reduced. At some degree of reduction, for all reasonable purposes the average person may cease to regard the small effect as a real harm, just as the person who smokes undoubtedly does with respect to a single cigarette. The biological basis for setting exposure limits then depends largely on the value placed on health by society and the extent to which harm can be estimated and evaluated within the experience of the people concerned.

Table 1. Relative displacements of physiologic age by factors that accentuate aging or loss of life span (minus time) or retard aging (plus time).

REVERSIBLE	Years
Country vs city dwelling	+ 5
Married vs single, widowed, divorced	+ 5
Overweight	
25% overweight group	-3.6
45% overweight group	-6.6
67% overweight group	-15.1
Occupational exercise vs sedentary occupation	+5.0
Smoking	
1 pack cigarettes per day	- 7
2 packs cigarettes per day	- 10
Atherosclerosis	
Fat metabolism	
In 25 percentile of population having "ideal" lipoprotein concentrations	+ 10
Having average lipoprotein concentrations	0
In 25 percentile of population having elevated lipoproteins	- 7
In 5 percentile of population having highest elevation of lipoproteins	- 15
Diabetes	
Controlled with insulin	- 10
Antibiotics	+

PERMANENT	Years
Female vs male sex	+ 3
Familial constitutions	
Mother lived to age 90	+ 3
Father lived to age 90	+4.4
Both mother and father lived to age 90	+7.4
Mother died at 60	-0.7
Father died at 60	- 1.1
Both mother and father died at 60	- 1.8
Recession of childhood and infectious disease over past century in Western countries	+ 15
Rheumatic heart disease	-11 to -18
Rapid pulse	- 3.5
Varicose veins	- 0.2
Epilepsy	-20.0
Skull fracture	-2.9
Tuberculosis	- 1.8
Nephrectomy	-2.0
Trace of albumin in urine	- 5.0
Moderate albumin in urine	- 13.5

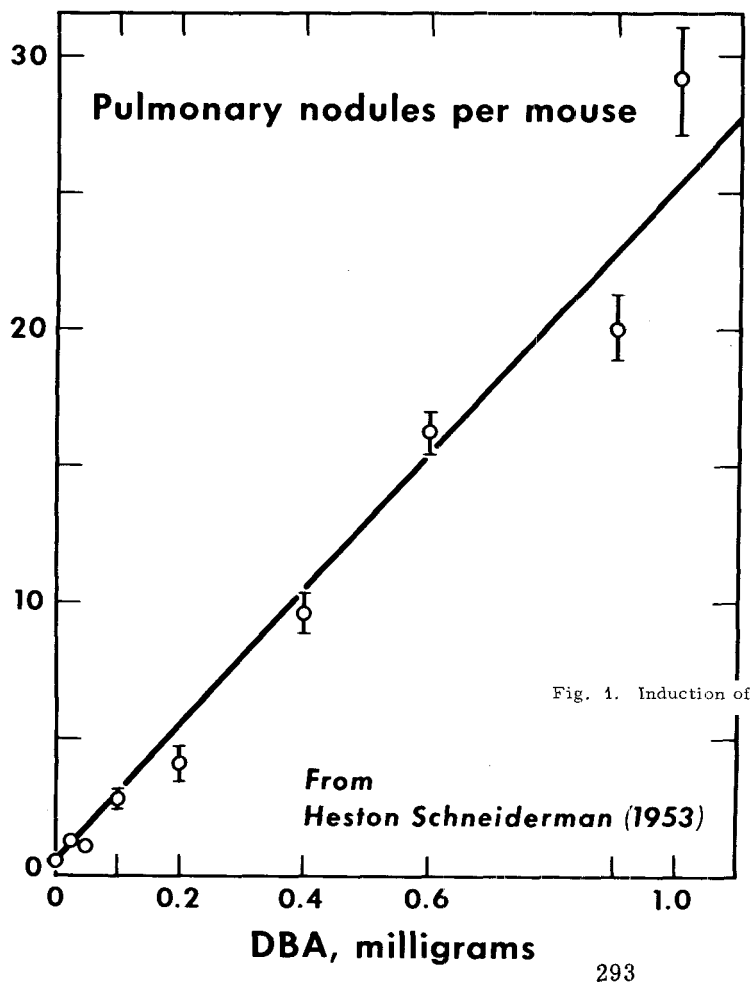

Fig. 1. Induction of pulmonary tumors in mice by dibenzanthracene

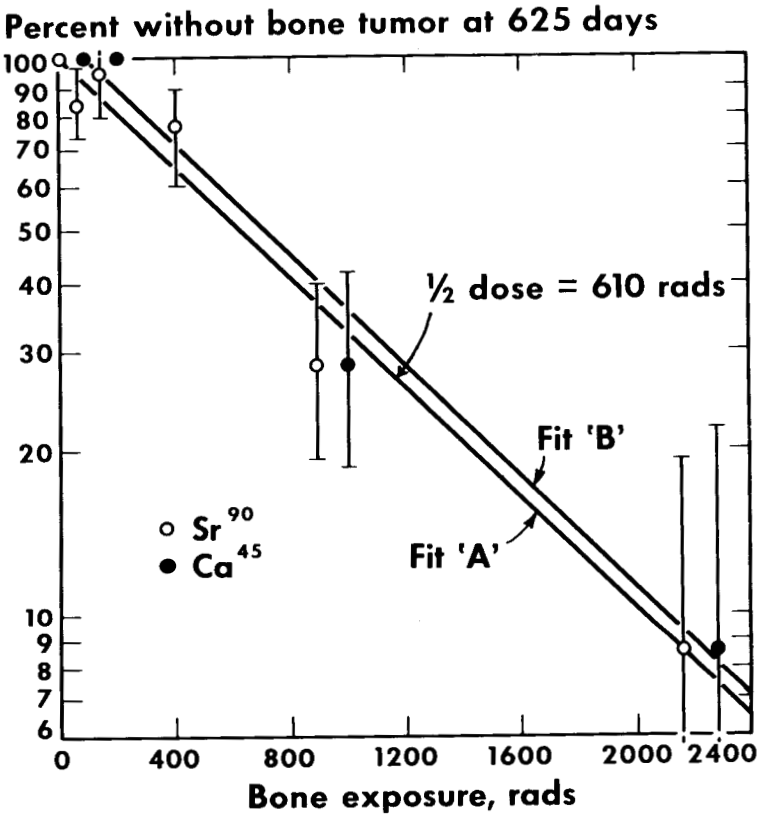

Fig. 2. Induction of bone tumors in mice following intravenous injection of ^{90}Sr or ^{45}Ca. From data of Finkel and Scribner, 1956.

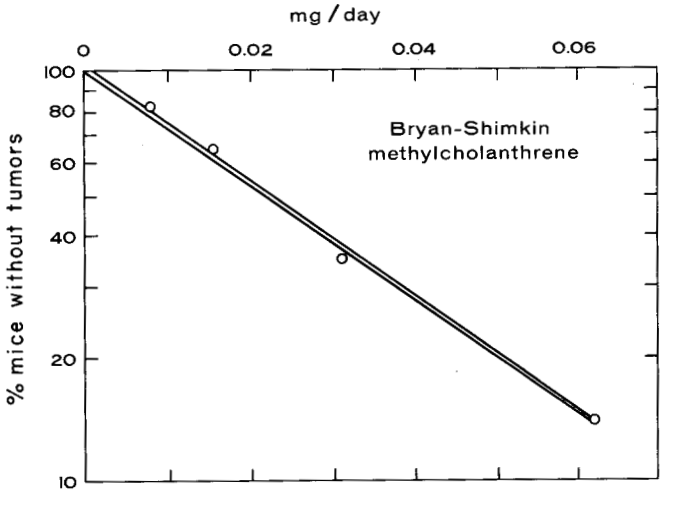

Fig. 3. Induction of subcutaneous tumors in mice by injection of methylcholanthrene.

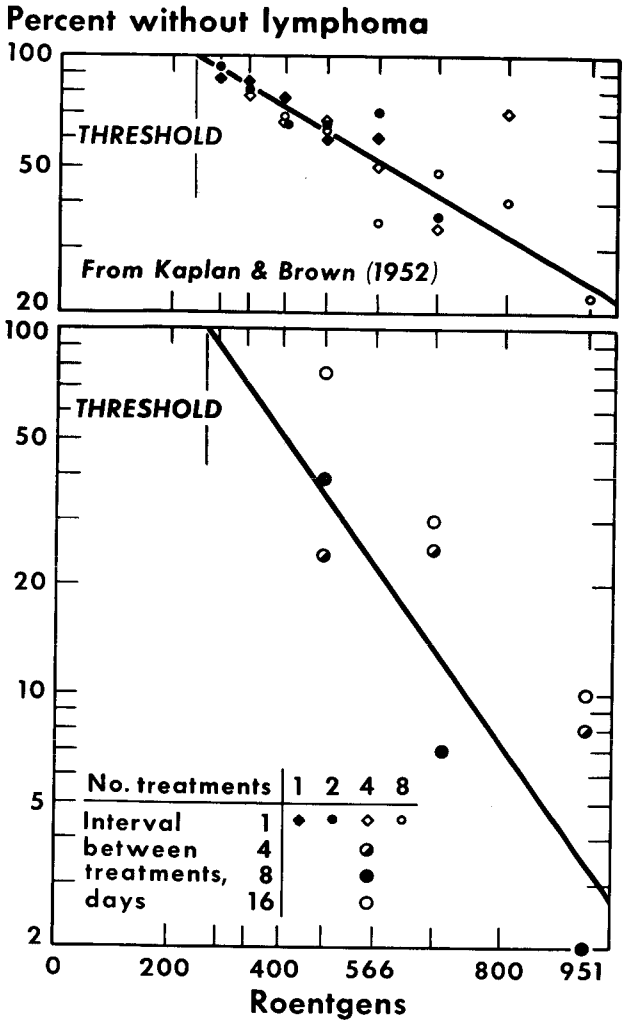

Fig. 4 Induction of lymphoid tumors in mice by irradiation.

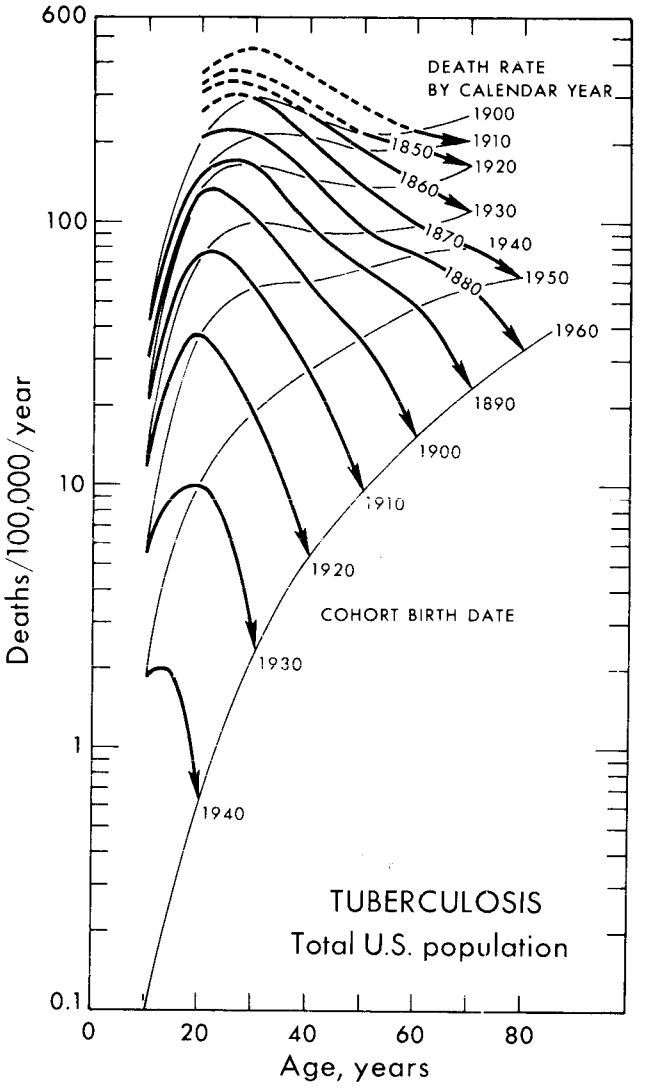

Fig. 5. Annual death rate due to tuberculosis in total population of United States of America, 1900-1960.

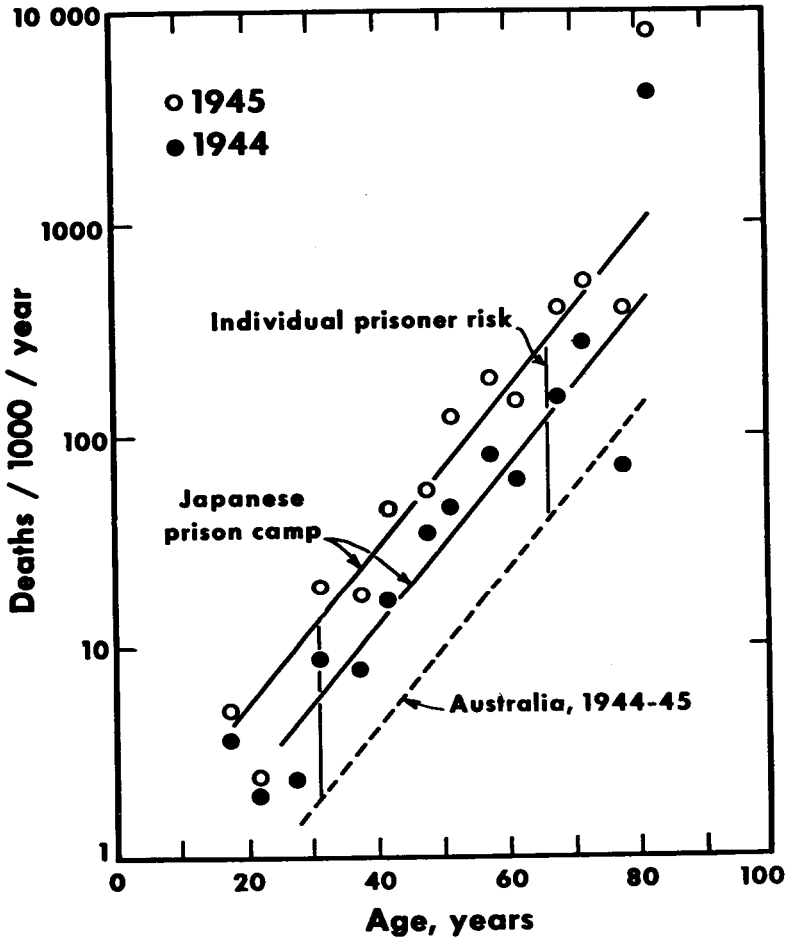

Fig. 6. Annual death rates by age in World War II prisoner-of-war camps.

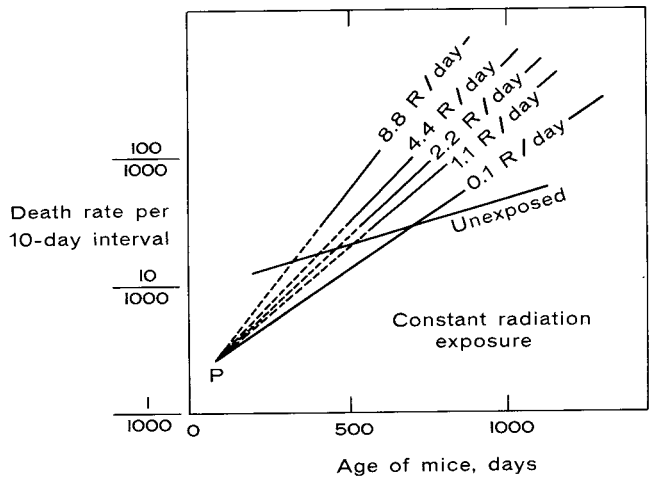

Fig. 7. Death rates by age for mice exposed to continuous gamma irradiation. From data of Lorenz, Heston, Eschenbrenner, and Deringer, 1947.

A MODEL FOR THE ACTION OF RADIATION ON SIMPLE BIOLOGICAL SYSTEMS*

W. C. Roesch

Pacific Northwest Laboratory
Battelle Memorial Institute
Richland, Washington

The hit hypothesis in radiobiology is that deposition of energy concentrated along the tracks of charged particles in the irradiated material, rather than spread uniformly throughout the medium, is responsible for the potency of the radiation and for the shape of the observed dose-effect curves. Most investigators accept the hypothesis, but past mathematical elaborations of it have been only partially successful in explaining observed phenomena[1]. In particular, dose-rate and fractionation effects are difficult to explain. Also, the fairly general tendency of survival curves to be asymptotically exponential has been explained as due to the presence in each individual of more than one site that must be destroyed by the radiation. Current biological evidence is against the presence of such multiple sites[2]. This paper is concerned with explaining these phenomena by developing a different mathematical elaboration of the hypothesis.

Past elaborations of the hypothesis have assumed that the passage of a determinable number of charged particles (hits) through a critical region of a cell, bacterium, virus, etc. will "kill" it. Classical one-hit theory assumes that only a single hit is necessary; two-hit theory, that two are necessary; etc. The present theory assumes instead that a single hit is sufficient to cause death but that it may not always do so, i.e., there is a conditional probability that the entity will survive a hit. Similarly, it is assumed that a reaction leading to death may occur between the products of two hits, but again there is a conditional probability for survival. This probability will depend on the time interval between the hits. Since neither type of death is certain to occur, the analysis must include allowance for either type occurring. Also, death may not result from the first hit or first pair of hits; it may result from any hit or any pair of hits among a possibly large number of hits.

Similar modifications of classical hit theory have been taking shape in the work of several authors. Recent papers include: Neary[3] showed that chromosome aberration phenomena could be explained as the result of single hits or the interactions between the results of single hits rather than as the result of the accumulation of a large number of hits. He suggested a similar explanation for cell killing. Fowler[4] showed that experimental survival curves could be explained by distributions in the number of hits required to produce death. He felt that the distributions resulted from differences in the number of hits required to produce a necessary inactivation energy. They could equally well be explained as single-hit deaths with a conditional probability of survival. Kellerer and

*Work performed under Contract AT(45-1)-1830 between the Atomic Energy Commission and Battelle Memorial Institute.

Hug[5] have produced a generalized model of radiation effects with probabilities of radiation-induced changes of state and of recovery.

Hit Theory with Conditional Probabilities

The equation from the present theory that gives the fraction, S, surviving a single irradiation is

$$S = \sum_{n=0}^{\infty} e^{-m}\, m^n\, (n!)^{-1}\, S_1^{\,n}\, s_0^{\,n-1}\, s_1^{\,n-2} \cdots s_{n-2}. \qquad (1)$$

It arises in the following way: $\underline{m}$ is the average number of hits in an individual (it is proportional to the absorbed dose); $e^{-m}\, m^n\, (n!)^{-1}$ is the Poisson probability of there being $\underline{n}$ hits when the average number is $\underline{m}$. S_1 is the probability of surviving the effects of a single hit, and $S_1^{\,n}$ is the probability of surviving such individual effects of $\underline{n}$ hits; $\underline{s}_j$ is the probability of surviving the effects of interactions between the products of two hits whose occurrence is separated in time by the occurrence of j others. These are obtained from a more fundamental quantity, s(t), the probability of surviving interactions between two hits that occur a time $\underline{t}$ apart. Figure 1 illustrates a particularly simple case of what this function might be like. In general, the hits have their best chance of interacting (lowest value of s) when they occur nearly simultaneously, and the least (s=1) when there is a very long time between them. The $\underline{s}_j$ are determined from $\underline{s}$ by

$$s_j = \frac{\int_0^T c^{j+1}\, t^j\, e^{-ct}\, s(t)\, dt}{\int_0^T c^{j+1}\, t^j\, e^{-ct}\, dt}. \qquad (2)$$

Here $c^{j+1}\, t^j\, e^{-ct} \div \int_0^T c^{j+1}\, t^j\, e^{-ct}\, dt$ is the probability of a time between $\underline{t}$ and t + dt between two hits separated by j others when T is the length of the irradiation. The number of each $\underline{s}_j$ required for $\underline{n}$ hits is readily determined; for example, Figure 2 shows the possible interactions in the case of 5 hits. Finally, the probabilities for survival for all values of $\underline{n}$ must be summed.

The probabilities of a single hit or a pair of hits causing death depend on just where the tracks cross the system. These probabilities can be averaged over the spatial coordinates, just as Equation (2) is an average over the time coordinate. S_1, $\underline{s}$, and the $\underline{s}_j$ are such averages.

Survival Curve Shapes and Dose-Rate Effects

Figure 3 illustrates the survival curves that result for a given S_1 and $\underline{s}$ but for different dose rates [i.e., different $\underline{c}$, where c = (dm/dt)]. For this example it was assumed that $s = 1 - a\, e^{-bt}$, where $\underline{a}$ and $\underline{b}$ are constants. It is necessary to make a specific assumption about $\underline{s}$ in order to obtain data for the curve; however, the conclusions in Equations (3) through (9) follow for any form of s(t) that has the general shape shown in Figure 1.

At very low dose rates it takes a long time, T, to accumulate hits. Then, Equation (2) indicates that all the s_j equal 1, and

$$S_{low} = e^{-m(1-S_1)}. \tag{3}$$

This equation results whenever interactions between hits are not possible. In other words, when the time between hits is large enough, they have little chance of interacting and death results only from the individual effects of each hit.

At very high dose rates, T is very small, Equation (2) gives all $s_j = (1-a)$, and

$$S_{high} = \sum_{n=0}^{\infty} e^{-m} m^n (n!)^{-1} S_1^{\,n} (1-a)^{1/2\, n(n-1)} \tag{4}$$

This surviving fraction decreases faster than exponentially with m; when the logarithm of S_{high} is plotted versus m, it gives a continually steepening curve.

At intermediate dose rates the survival curves are asymptotically exponential. This is apparent in Figure 3 and can be deduced from Equation (1). Equation (1) can be written

$$S = \sum_{n=0}^{\infty} e^{-m} m^n (n!)^{-1} S_1^{\,n} \frac{(s_0 s_1 \cdots s_{n-2})^n}{(s_0 s_1^{\,2} \cdots s_{n-2}^{\,n-1})}. \tag{5}$$

In the asymptotic region m is large. For large m almost any postulated form for s will give s_j's from Equation (2) that are independent of m and that tend to 1 as j increases. Also, for large m the numerically important terms in Equation (5) are those for large n. But, for large n and for the s_j just described, the products involving the s_j can be replaced by the corresponding infinite products. Then

$$S = \sum_{n=0}^{\infty} e^{-m} m^n (n!)^{-1} S_1^{\,n} A B^n \tag{6}$$

$$= A\, e^{-m(1-BS_1)}.$$

The extrapolation number, A, is

$$A = (s_0 s_1^{\,2} s_2^{\,3} \cdots)^{-1}. \tag{7}$$

The number $1-BS_1$ is proportional to what is often called the sensitivity; $(1-BS_1)^{-1}$ is proportional to what is denoted by D_o or D_{37} and called the mean lethal dose. B is given by

$$B = s_0 s_1 s_2 \cdots . \qquad (8)$$

These survival curve shapes and their general behavior with dose rate closely resemble those often found experimentally.

Fractionation

The effect of dividing the dose into fractions delivered separately can be analyzed by the present theory also. It is necessary to allow both for interactions between hits within a fraction and for interactions between hits in different fractions. It is possible to show that for two fractions giving average numbers of hits m_1 and m_2, where m_1 and m_2 are both large enough for the survival to be in the asymptotically exponential region,

$$S = (A^2/\alpha)\, e^{-(m_1+m_2)}\, (1-BS_1). \qquad (9)$$

Here α is an extrapolation number obtained in the same way A is obtained, from s(t), except that the time origin is displaced to the right (in Figure 1) a time equal to the time $\underline{d}$, between the two fractions. This surviving fraction is A/α times that surviving a single dose to m_1+m_2. From the description of α, it is clear that $(A/\alpha) = 1$ for $d = 0$ and $(A/\alpha) = A$ for large enough $\underline{d}$, i.e., the survival increases by a factor equal to the extrapolation number as the time between fractions increases. Figure 4 shows a curve of A/α versus $\underline{d}$ calculated for $s = 1 - a\, e^{-bt}$, as above; it is of interest that it does not change exponentially. The present theory does not predict the Elkind-Sutton effect; however, this effect is thought to be due to changes of sensitivity during the cell cycle[6] and would be deduced if a mixture of S_1's and $\underline{s}$'s were used in the theory.

RBE

In the present theory the difference in effect of different radiations is explained as due to differences in S_1 and $\underline{s}$. A priori one would guess that high-LET radiations would be more effective in killing than low-LET ones and would therefore have lower values of S_1 and s. Figure 5 shows the two limiting survival curves (Equations 3 and 4) for two values of S_1 and for $s(0) = 0$. The two limits define the region within which the curves for all dose rates must lie. For high S_1, 0.9, the region is very broad. For low S_1, 0.3, the band is so narrow that experimental detection of dose-rate effects is unlikely even though they are there, in principle. Also, the two latter limits are so nearly exponential that it is not surprising that low-S_1 high-LET radiations are usually reported as giving exponential survival curves.

To make more precise predictions about the effects of different radiations requires making more assumptions. It is convenient to use the low-dose-rate limit, Equation (3), for this purpose. Doing so does not exclude the effects of interactions. Although all the $\underline{s}_j$ are 1, S_1 includes an effect of interactions, because if interactions are possible between the products formed along different tracks they are also possible between products from different parts of the same track. As a first, elementary attempt at analysis it can be assumed that the average number of death-producing events of the kind requiring interactions is proportional to the square (since two parts of the track are involved) of the stopping power, L, and those not requiring interactions are proportional to the

first power. Then, if the events are Poisson distributed,

$$S_1 = e^{-(fL+gL^2)}, \tag{10}$$

where f and g are constants. The absorbed dose is proportional to both m and L; hence, where Equation (3) applies, the RBE is proportional to $(1-S_1)/L$, or

$$RBE \propto (1/L)\,(1 - e^{-(fL+gL^2)}). \tag{11}$$

Figure 6 shows RBE curves calculated from this equation for different values of f and g. The curves were adjusted to give RBE = 1 at L = 1 keV/μm and to have their maxima at L = 100 keV/μm. The curves are of qualitatively correct shape and range of values.

Chemical Effects

Suitable chemical agents can alter the probabilities we have been discussing. As a simple example of how this might happen, the average number of the non-interaction events might change according to a first-order kinetic law. Then fL of Equations (10) and (11) would be multiplied by a factor, [M/(M+k)], where M is the concentration of the agent and k is a constant. Then the ratio of the "sensitivities", $(1-S_1)$ at concentration M and $(1-S_1)_0$ at M = 0, would be

$$\frac{(1-S_1)}{(1-S_1)_0} = \frac{[(fL+gL^2)/gL^2]\,M + k}{M + k} \tag{12}$$

for small L. This is the same form as the law found by Alper and Howard-Flanders[7] and others for oxygen enhancement. It is obtained by keeping two terms in the expansion of the exponential in Equation (10). For larger values of L, the ratio of sensitivities approaches 1, because the exponential would become negligible. Also, in this theory, the extrapolation number would not be changed by changes in the agent, because the quantities in Equation (7) would not be affected by changes in the probabilities of the non-interaction events.

References

1. K. G. Zimmer, Quantitative Radiation Biology, Hafner Publishing Company, Inc., New York, 1961.

2. T. Alper, Cellular Radiobiology, in Annual Review of Nuclear Science, Vol. 10, pp. 489-530, Annual Reviews, Inc., Stanford, California, 1960.

3. G. J. Neary, Chromosome Aberrations and the Theory of RBE, 1. General Considerations, Int. J. Rad. Biol., 9: 477 (1965).

References (Continued)

4. J. F. Fowler, Distributions of Hit-numbers in Single Targets, in Biophysical Aspects of Radiation Quality, pp. 63-80, International Atomic Energy Agency, Vienna, 1966.

5. A Kellerer and O. Hug, Zur Kinetik der Strahlenwirkung, Biophysik, 1: 33 (1963).

6. M. M. Elkind and W. K. Sinclair, Recovery in X-irradiated Mammalian Cells, in Current Topics in Radiation Research, Vol. I, pp. 167-220 (M. Ebert and A. Howard, eds.), North-Holland Publishing Co., Amsterdam, 1965.

7. T. Alper and P. Howard-Flanders, Role of Oxygen in Modifying the Radiosensitivity of E. Coli B., Nature, 178: 978 (1956).

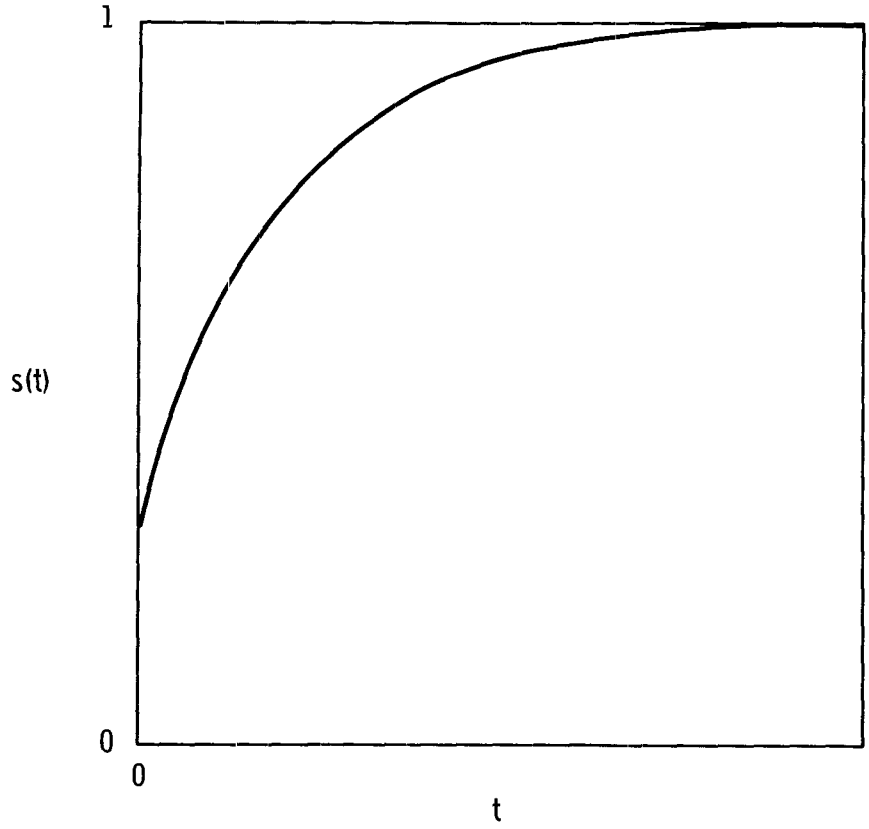

1. An example of the dependence of the probability of surviving interactions between the products of two different hits, s(t), on the time, t, between them.

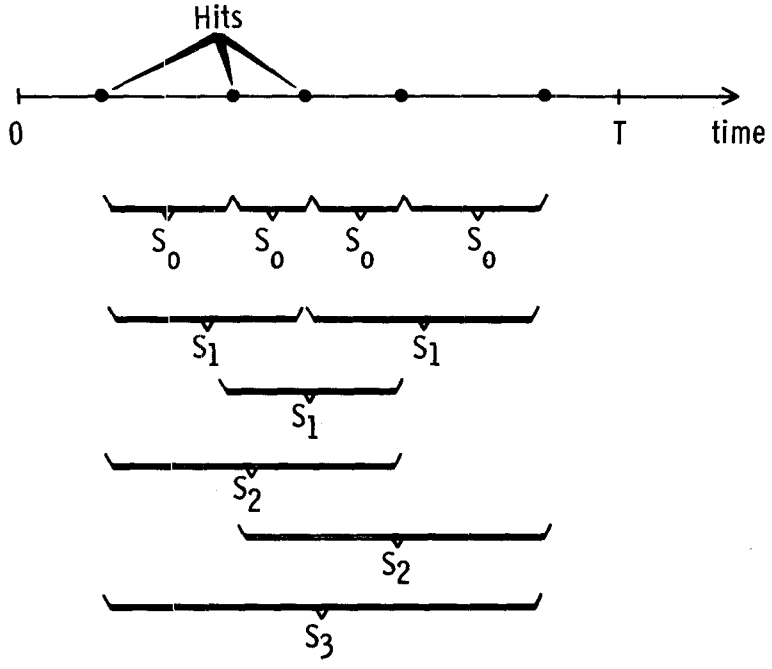

2. The possible interactions between five hits.

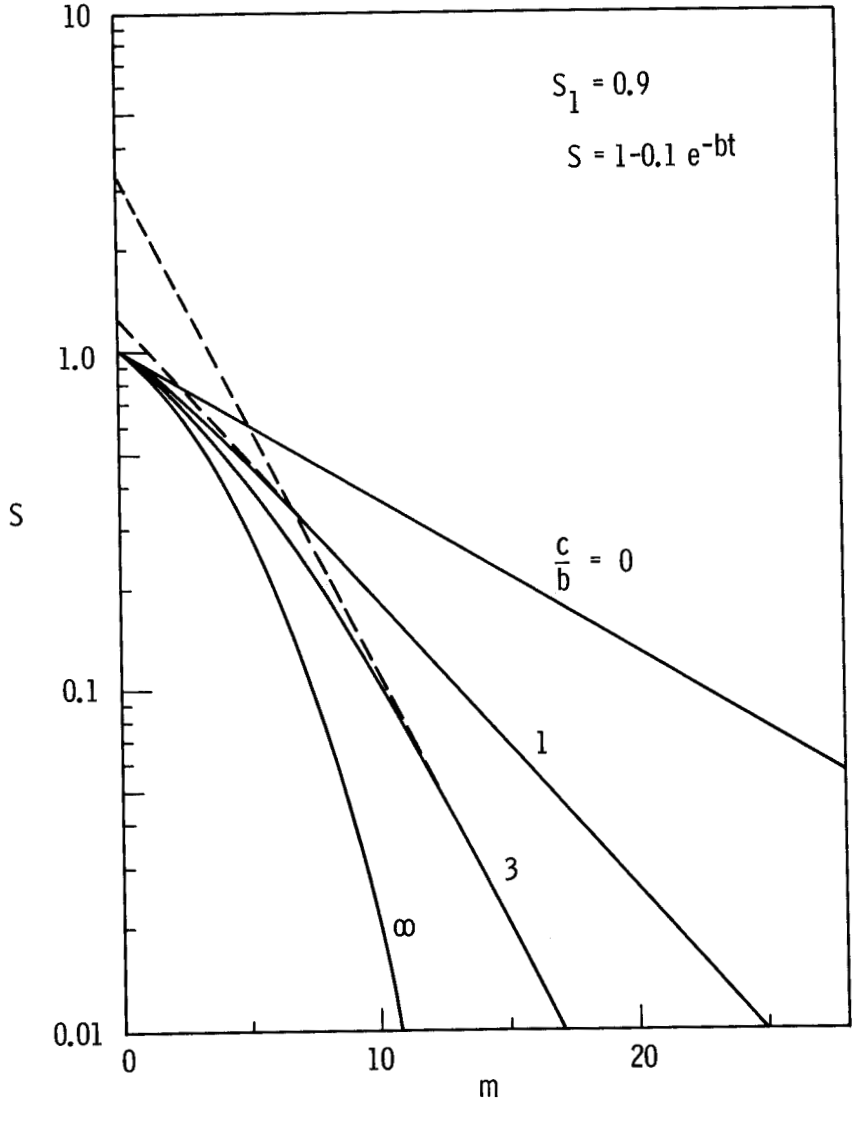

3. The fraction, S, of a population surviving irradiation to an average number of hits, m (proportional to absorbed dose), for different dose rates (proportional to c/b). The dashed lines are asymptotic exponential curves.

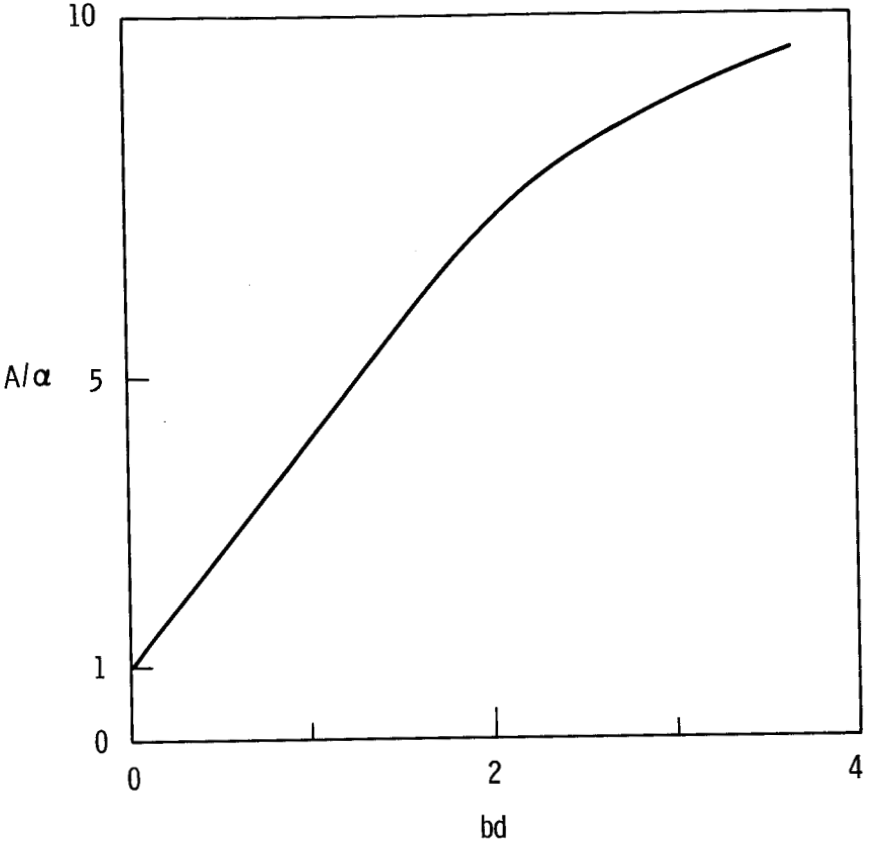

4. The increase in survival due to fractionation.

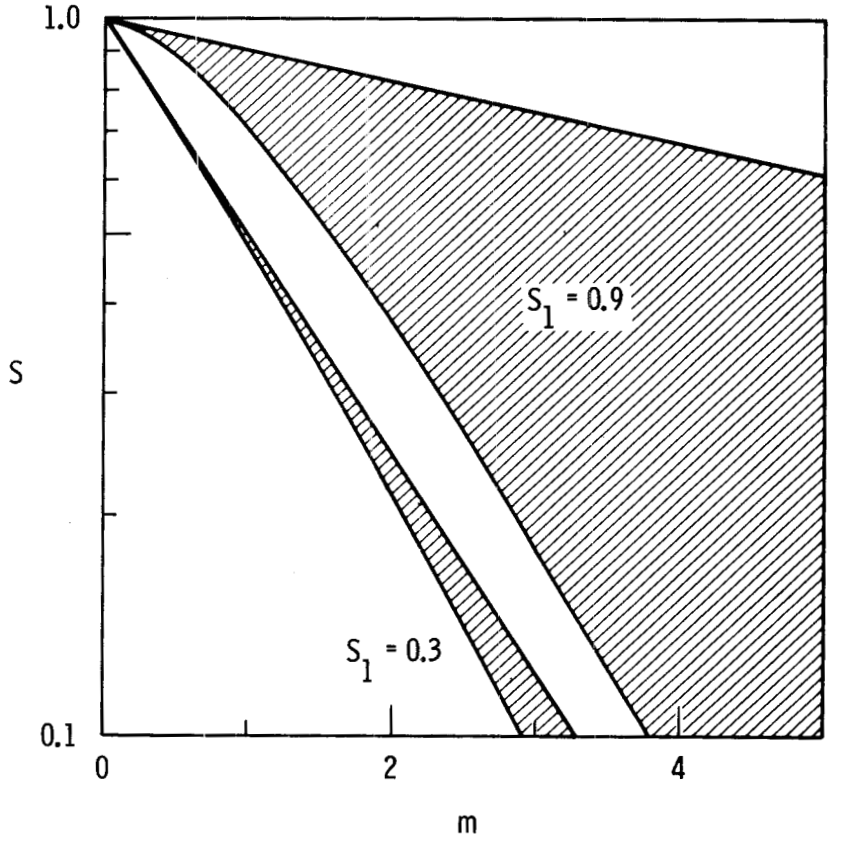

5. Limiting survival curves for two values of S_1. Survival curves for different dose rates must lie in the shaded regions.

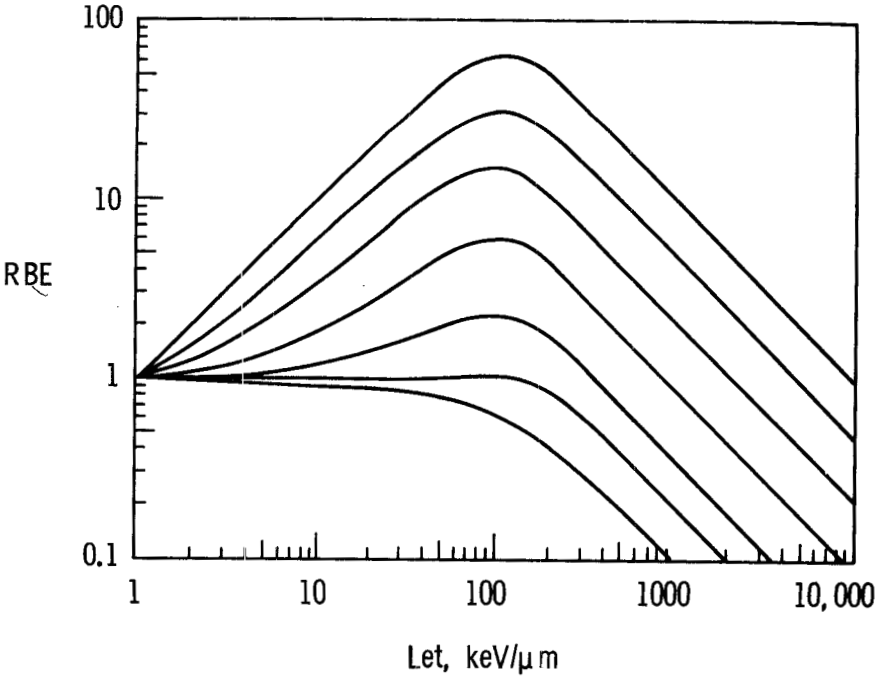

6. Theoretical RBE curves.

DOSE FROM HIGH-ENERGY RADIATIONS AT AN INTERFACE BETWEEN TWO MEDIA*

J. E. Turner, V. E. Anderson, H. A. Wright, W. S. Snyder, and J. Neufeld
Health Physics Division, Oak Ridge National Laboratory
Oak Ridge, Tennessee 37830

ABSTRACT

Build-up at an interface between two media is important for the interpretation of radiation dose. This paper reports the results of studies of dose from high energy protons and neutrons at an interface between soft tissue and bone. Because of their different atomic compositions, the contribution to dose from nuclear interactions in the two media is different. By using the Monte Carlo technique, calculations were made of the dose from nucleons with energies of 100 and 400 Mev in two phantoms composed of bone and soft tissue parts. One phantom was a cylinder, having a diameter of 2.5 cm and a length of 8 cm, made in three concentric annular rings, the middle ring containing bone. The other phantom was a 20 x 31 x 60 cm soft tissue parallelepiped with a solid bone center. With 400 Mev nucleons incident laterally on the cylinder the build-up of dose equivalent in going from the outside to the inside of the cylinder appears to be increased some when the middle annular ring is made of bone rather than soft tissue. A decrease in the quality factor of 400 Mev neutrons from ≈ 8.6 to ≈ 6.5 was found in the middle ring when soft tissue was replaced by bone. In the parallelepiped, the presence of the bone center, rather than soft tissue, apparently makes little difference.

I. INTRODUCTION

In this paper we report numerical results of calculations of dose and dose equivalent in non-homogeneous phantoms of finite extent from incident protons and neutrons with energies of 100 and 400 Mev. The Monte Carlo calculations were done with computer codes for nuclear interactions and nucleon transport developed by the Neutron Physics Division at Oak Ridge National Laboratory and described elsewhere.[1,2] Because these codes neglect the production of pions, they are not applied to nucleon energies above 400 Mev.

The work to be reported here supplements in two ways previous publications[3,4] which dealt primarily with dose in homogeneous, soft-tissue slabs of infinite lateral extent. First, large and small phantoms consisting of both soft tissue and embedded bone structures are treated here. Second, particular attention is given to the behavior of radiation dose across an interface separating soft tissue and bone.

*Research sponsored by the U. S. Atomic Energy Commission under contract with Union Carbide Corporation.

The investigation was motivated initially to see whether dose build-up occurs when high-energy nucleons penetrate through soft tissue into bone.[5] Whereas the amounts of energy deposited per unit mass by interactions with atomic electrons in the two media are comparable, the denser bone, containing heavier elements, might receive a higher dose or dose equivalent due to nuclear interactions. In particular, we wanted to compare the calculated radiation dose in a cylindrical cavity of marrow surrounded by bone with dose values found previously[3,4] in targets consisting entirely of soft tissue.

II. DESCRIPTION OF TARGETS AND INCIDENT RADIATION

Figures 1 and 2 show the phantoms used in these studies. The cylinder in Fig. 1 is 8 cm in length and 2.5 cm in diameter and consists of a cylindrical soft tissue center enclosed in concentric bone and soft tissue rings. This target was used to simulate the geometry of a bone with marrow cavity in the arm or leg of a small primate. The larger soft-tissue parallelepiped slab in Fig. 2 has outside dimensions 20 cm x 31 cm x 60 cm, approximately the size of a human torso. This slab was used with a 10 cm x 15 cm x 30 cm bone center to try to assess the effects of target size on the relative dose to bone and soft tissue. Monoenergetic nucleons were incident laterally on the cylinder in such a way as to simulate rotation of the cylinder in a uniform broad beam perpendicular to its axis. Isotropically incident monoenergetic nucleons were used with the parallelepiped slab. Protons and neutrons with energies of 400 Mev and 100 Mev were studied with both targets shown in Figs. 1 and 2. Unless otherwise stated, the calculation of dose in a given target from nucleons of a given energy were made from the energy deposited as a result of 5,000 incident protons or 10,000 incident neutrons.

For analysis, the cylinder was divided into three concentric annular cylindrical regions containing the inside soft tissue, the bone, and the outside soft tissue, as shown in Fig. 1. The absorbed dose was calculated in each region from the total energy absorbed there and the dose equivalent in each was determined by weighting the absorbed energy according to its LET distribution, as explained below. The diameters of the cylindrical regions are 0.5 cm, 1.5 cm, and 2.5 cm. We shall refer to the outside, middle (bone), and center cylinders as regions 1, 2, and 3.

The slab was divided for dose analysis into smaller parallelepipeds by intersecting planes parallel to the slab surfaces. The planes passed through the points X = 0, 8, 23, 31 cm; Y = 0, 5, 10, 15, 20 cm; and Z = 0, 15, 30, 45, 60 cm. This method of subdivision is shown in Fig. 3, which is drawn with a portion of the slab removed. Every smaller parallelepiped consisted entirely of either bone or soft tissue, region 8 being bone. When the incident radiation is isotropic, the dose need be calculated in only one octant of the slab. Because of symmetry, therefore, the dose in regions bearing the same number is, apart from statistical fluctuations, the same.

The compositions and mean excitation energies used for soft tissue and for bone are shown in Tables 1 and 2. The atomic composition of soft tissue is the one used in

previous calculations,[3] and the composition of bone is that of the wet tissue.[6] The mean excitation energies used in the Bethe stopping-power formula[7] are taken from the NAS-NRC Report No. 1133.[8]

III. NUMERICAL RESULTS

Detailed descriptions of the calculational methods used here are given in (3) and (4). Briefly, nuclear cascade and evaporation processes are handled by computer codes that utilize Monte Carlo techniques. Cascades produce secondary nucleons (pion production is neglected) and evaporation can produce particles with mass numbers up to four. The histories of all primary and secondary particles are traced until a particle either interacts with a nucleus, escapes from the target, or loses all of its energy in the target. Charged-particle slowing down is calculated by means of the stopping-power formula.[7] In the present calculation particle histories were analyzed and the absorbed dose (rad) and dose equivalent (rem) were computed in each of the regions shown in Figs. 1 and 3. The assignment of quality factors used in obtaining dose equivalent was made according to the recommendations of the National Committee on Radiation Protection and Measurements for long-term occupational exposure to radiation, as described in (3). These values, which are also recommended by the International Commission on Radiological Protection,[9] are based on the values of the linear energy transfer (LET) of radiation.

Figure 4 shows the calculated values of absorbed dose (rad) and dose equivalent (rem) per unit fluence in the three regions of the cylinder from 400 Mev incident neutrons. A total of 20,000 incident neutrons was used in the calculation. The error bars on the rem curves show the spread in values obtained in two runs of 10,000 particles each. The relative volumes of the three regions are 16:8:1, and the smaller number of nuclear collisions in region 3 is reflected in the relatively large difference in dose equivalent obtained in the two runs. With 10,000 incident 400 Mev neutrons, some 810 secondary nucleons having energies greater than 50 Mev were produced by cascades together with nucleons of lower energies. In addition, some 3500 nucleons and approximately 100 heavier particles are generated in evaporation processes. As was done in previous work,[3] a quality factor of 20 was assigned both to these heavier particles and to the recoil nuclei after a cascade.

Division of the dose equivalent by the absorbed dose gives the effective quality factor (QF) in each region. The most striking feature of the results shown in Fig. 4 is the smaller QF in the bone compared with the adjacent soft tissue. To study this finding, an additional 10,000 neutrons were run with a homogeneous soft-tissue cylinder — in effect, replacing the bone ring by one of soft tissue. The results thus obtained are compared with those for which bone is present in Fig. 5.* It is found that, in the homogeneous soft-tissue cylinder, the QF is essentially constant throughout. The

*The error bars on the left show the extremes obtained in two calculations with 5,000 incident neutrons each. Whereas the values on the left were calculated with 10,000 neutrons, those on the right were obtained with 20,000.

difference in QF in the middle ring when the soft tissue is replaced by bone occurs as a result of the different nuclear compositions of those two media, since the number of electrons per gram is approximately the same. Using the atomic densities in Tables 1 and 2, we find that the ratio of the linear cross sections for nuclear interaction in bone and soft tissue (1.93) is approximately the same as the ratio of the densities (2.04). As a result, the number of nuclear collisions per gram per unit fluence in the two media is about the same. This being the case, the higher quality factor in soft tissue implies that a large fraction of the energy deposited there occurs with a high LET as compared with bone. A study is now underway to determine the extent to which this depends on the different distributions of recoil nuclei energies and heavy particle energies from evaporation in the two media.

Figure 6 shows the results of bombardment of the cylinder with 5,000 protons with an energy of 400 Mev. An increase in the quality factor with depth was found. Since a large fraction ($\approx$80%) of the dose is due to ionization caused by the primary protons, the QF of this radiation is smaller than that of neutrons of the same energy. As contrasted with Fig. 4, no decrease in QF in the bone is found. Figure 7, which is analogous to Fig. 5, shows that, with incident protons, the presence of bone apparently increases somewhat the dose equivalent in the center region.

Figures 8 and 9 show the results of bombarding the cylinder with 100 Mev neutrons and protons. To within the statistical accuracy of the calculations, the absorbed dose and dose equivalent are uniform in the target, the magnitudes of these quantities having the values shown.

When 400 Mev neutrons bombard the parallelepiped slab isotropically the values of dose and dose equivalent found in the eight regions of Fig. 3 are shown in Fig. 10. A measure of the statistical precision of the results is given by a comparison of the values of QF in regions having the same number. When statistical fluctuations are negligible, both the rad and rem doses are the same. As with the smaller target in Fig. 4, the dose equivalent appears to be smaller in bone than in soft tissue. The corresponding data for 400 Mev isotropically incident protons, like those in Fig. 6, show no significant difference between the radiation doses in the two media. Calculations with 400 Mev protons incident isotropically on a homogeneous soft-tissue slab of almost identical dimensions[3] give the same values of dose and dose equivalent as when the bone center is present.

Calculations with 100 Mev isotropically incident neutrons and protons on the slab showed a decrease in dose in going into the interior of the slab due to the absorption and stopping of nucleons. (The range of a 100 Mev proton is $\approx$7.9 gm/cm^2.) No pecularities were noted due to the presence of the bone center.

IV. SUMMARY

The foregoing calculations indicate that there is no significant build-up in dose in soft tissue from nucleons with energies up to 400 Mev directly attributable to the presence of bone near the soft tissue. With the quality factor QF = 20 used for heavy particles in earlier calculations, the dose equivalent in bone inside a small target is apparently reduced by approximately one-fourth compared with its value in a homogeneous soft tissue target.

REFERENCES

1. H. W. Bertini, Low-energy Intranuclear Cascade Calculation, Phys. Rev., 131: 1801 (1963). Errata, Phys. Rev., 138: AB2 (1965).

2. W. E. Kinney, Nucleon Transport Code, NTC, Oak Ridge National Laboratory Report ORNL-3610 (1964).

3. J. E. Turner, C. D. Zerby, R. L. Woodyard, H. A. Wright, W. E. Kinney, W. S. Snyder, and J. Neufeld, Calculation of Radiation Dose from Protons to 400 Mev, Health Phys., 10: 783 (1964).

4. C. D. Zerby and W. E. Kinney, Calculated Current-to-Dose Conversion Factors for Nucleons below 400 Mev, Nuclear Instr. and Meth., 36: 125 (1965).

5. The possibility that this might be important in primate experiments was suggested by Dr. G. V. Dalrymple in a conversation with J. E. Turner. See also the papers of G. V. Dalrymple and coworkers, Rad. Res. Suppl., 28: 365 (1966).

6. Revision of Report on the Standard Man, Committee 2 on Internal Exposure, International Commission on Radiological Protection. The authors are grateful to M. J. Cook of Oak Ridge National Laboratory for making these data available prior to final publication of the revised report.

7. See, e.g., Eq. (1) in reference 3 for the Bethe formula.

8. J. E. Turner, Values of I and I_{adj} Suggested by the Subcommittee, Report No. 6 in Studies in Penetration of Charged Particles in Matter, National Academy of Sciences-National Research Council Publication 1133, pp. 99-101, Washington, D.C. (1964).

9. Recommendations of the International Commission on Radiological Protection, ICRP Publication 9, Pergamon Press, Oxford (1965).

Table 1. Description of Soft Tissue [Ref. (3)] (Density = 0.961 gm/cm^3)

Element i	Atomic Number	Atoms per cm^3 N_i	Mean Excitation Energy (ev) I_i
Hydrogen	1	5.98×10^{22}	18
Oxygen	8	2.45×10^{22}	98
Carbon	6	9.03×10^{21}	78
Nitrogen	7	1.29×10^{21}	85

Table 2. Description of Wet Bone [Ref. (6)] (Density = 1.96 gm/cm^3)

Element i	Atomic Number Z_i	Atoms per cm^3 N_i	Mean Excitation Energy (ev) I_i
Hydrogen	1	9.64×10^{22}	18
Carbon	6	3.39×10^{22}	78
Oxygen	8	3.00×10^{22}	98
Nitrogen	7	3.15×10^{21}	85
Calcium	20	3.07×10^{21}	228
Sodium	11	1.92×10^{20}	142
Sulfur	16	8.34×10^{19}	191
Magnesium	12	6.21×10^{19}	152
Potassium	19	5.35×10^{19}	219
Chlorine	17	3.93×10^{19}	170

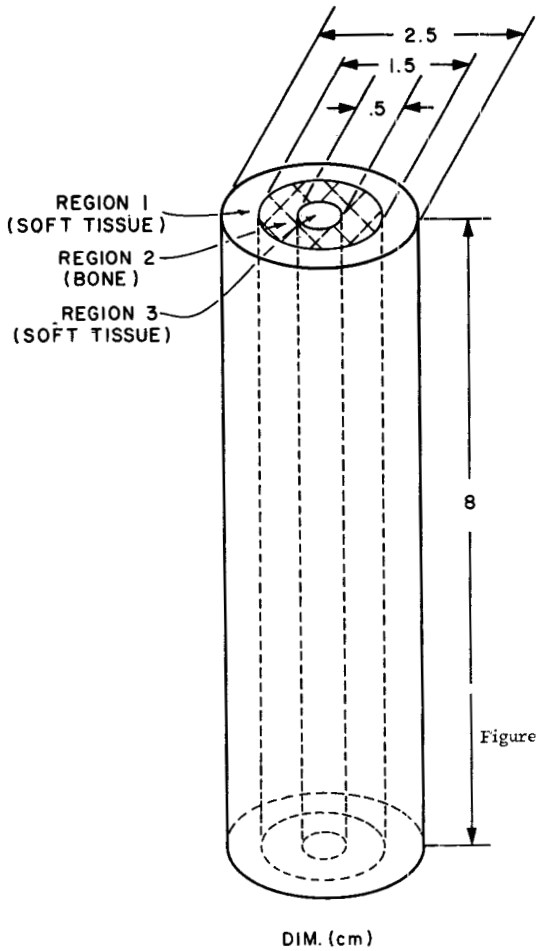

Figure 1. Cylinder of soft tissue surrounded by concentric annular cylinders of bone and soft tissue.

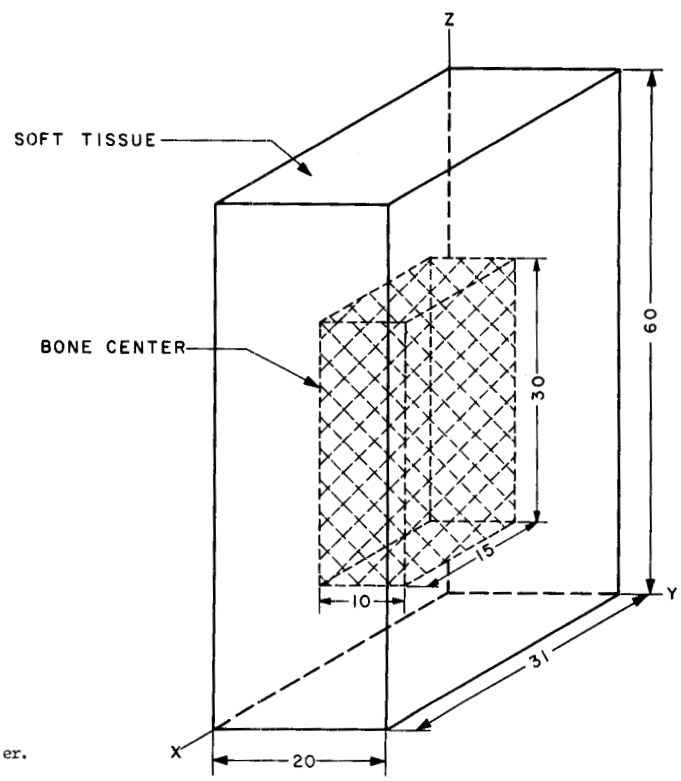

Figure 2. Soft tissue parallelepiped slab with solid bone center.

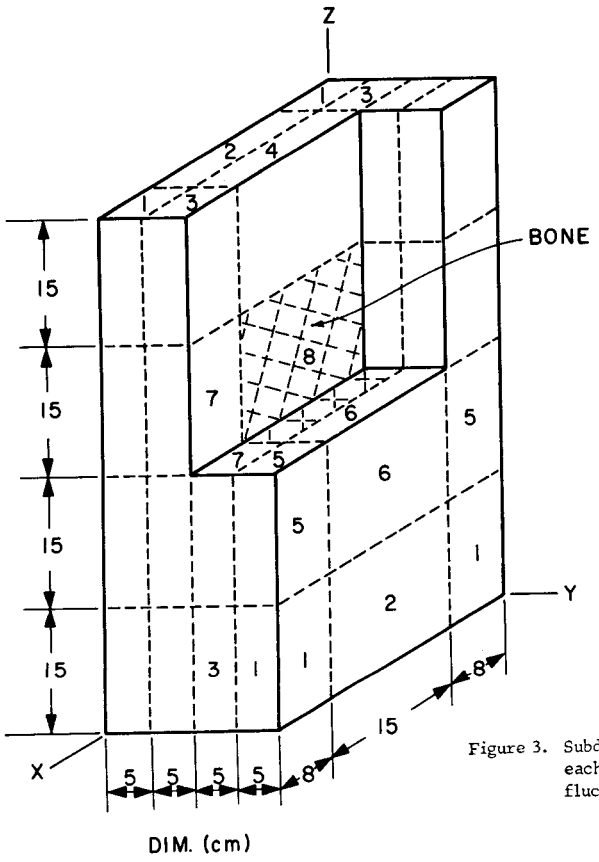

Figure 3. Subdivision of parallelepiped slab for dose analysis. By symmetry, dose in each region having the same number is the same, apart from statistical fluctuations. Regions 1···7 are soft tissue and region 8 is bone.

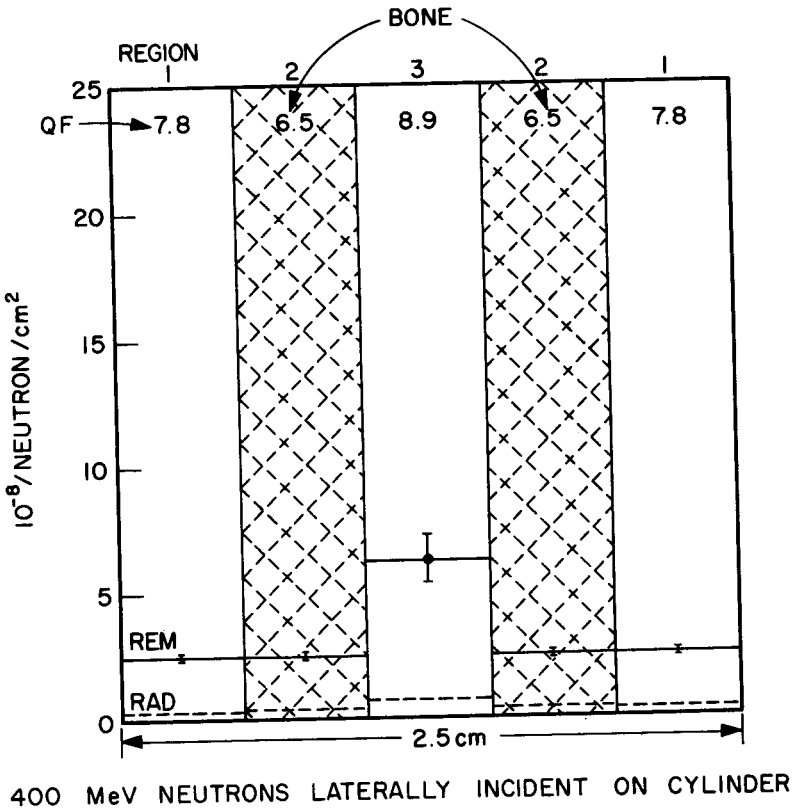

Figure 4. Absorbed dose and dose equivalent in cylinder with bone from 400 Mev laterally incident neutrons.

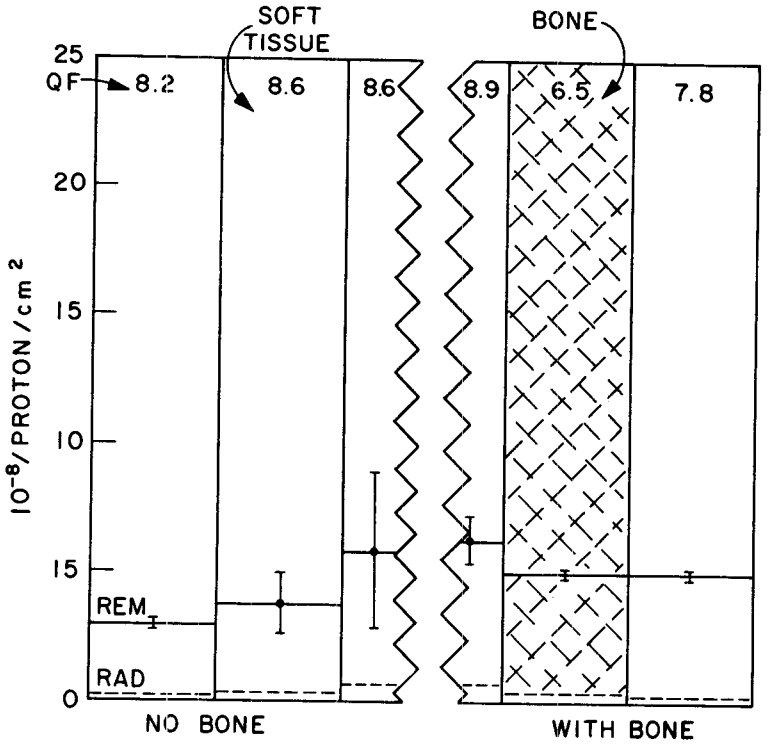

Figure 5. Comparison of absorbed dose and dose equivalent in cylinder with bone present (shown on right) and with bone replaced by soft tissue (on left). The data on the right are taken from Figure 4.

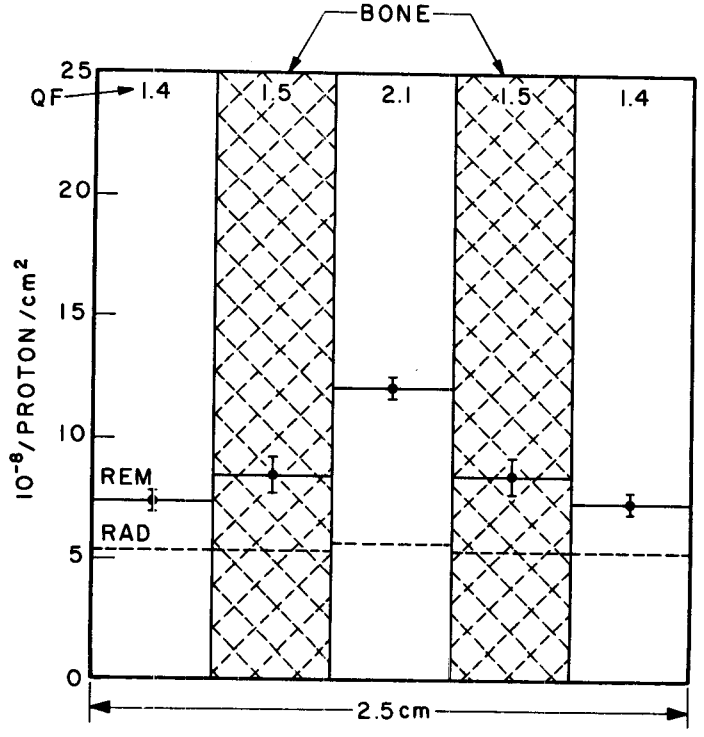

Figure 6. Absorbed dose and dose equivalent in cylinder with bone from 400 Mev laterally incident protons.

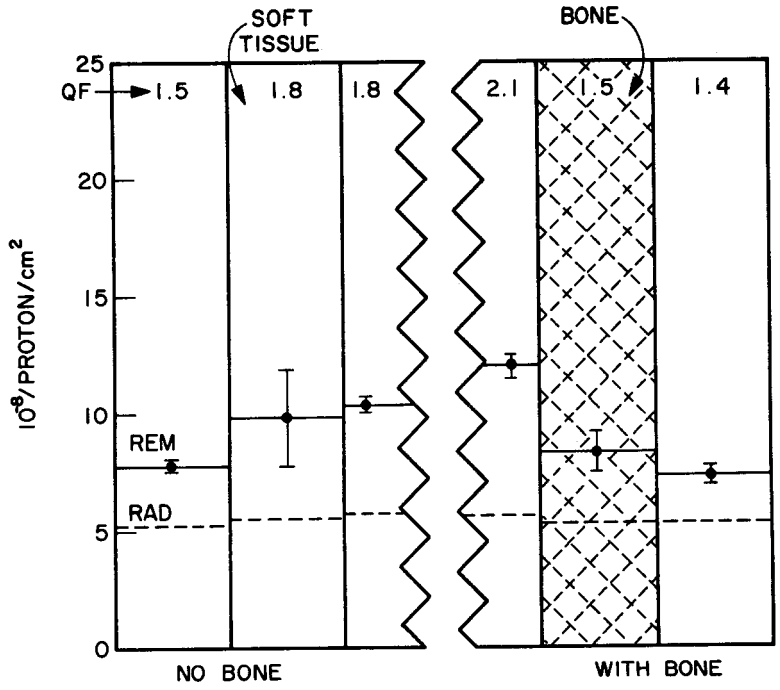

Figure 7. Comparison of absorbed dose and dose equivalent in cylinder with bone present (shown on right) and with bone replaced by soft tissue (on left). The data on the right are taken from Fig. 6.

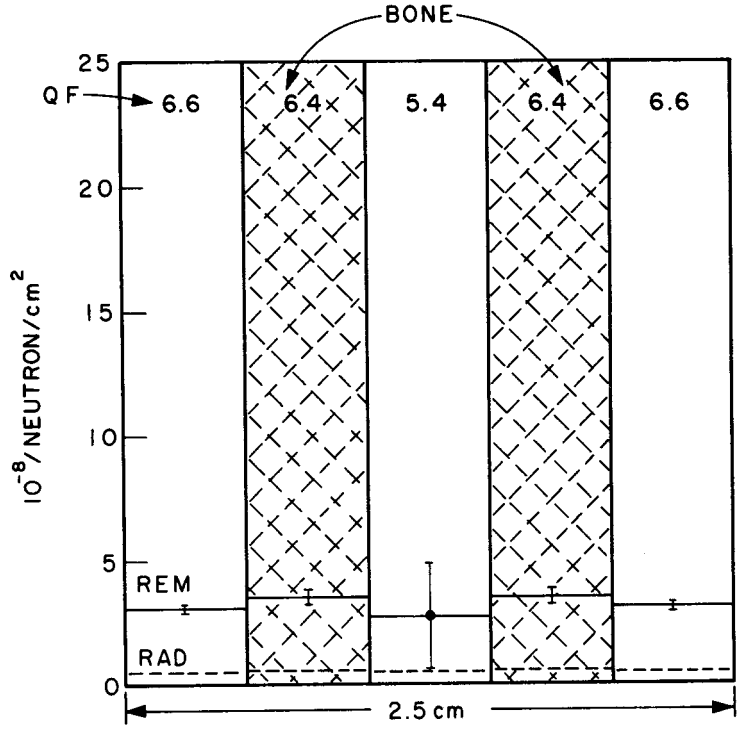

Figure 8. Absorbed dose and dose equivalent in cylinder from 100 Mev laterally incident neutrons.

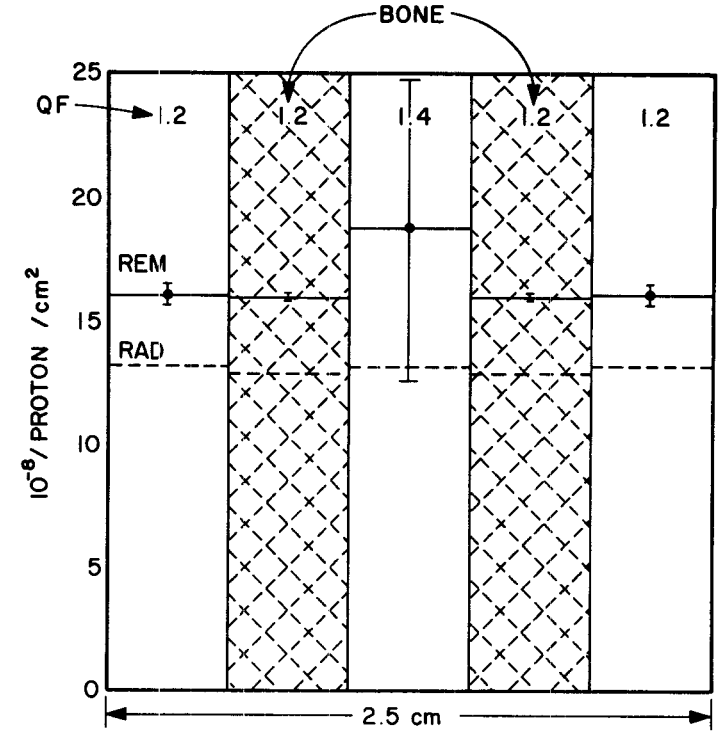

Figure 9. Absorbed dose and dose equivalent in cylinder from 100 Mev laterally incident protons.

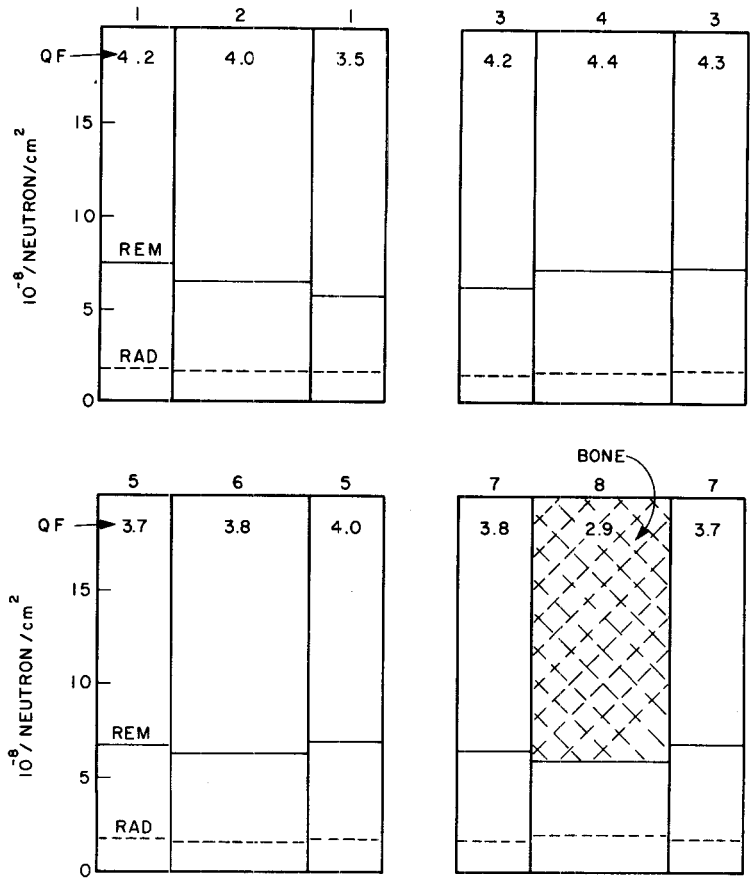

Figure 10. Absorbed dose and dose equivalent in slab from 400 Mev isotropically incident neutrons.

TECHNIQUES IN DOSIMETRY AND PRIMATE IRRADIATIONS WITH 2.3-BeV PROTONS*

G. H. Williams, C. V. Parker, J. B. Nelson and I. L. Morgan
Texas Nuclear Corporation, Austin, Texas

J. C. Mitchell and K. A. Hardy
School of Aerospace Medicine, San Antonio, Texas

Introduction

This paper will describe the physical experimentation and dosimetry involved in the whole-body irradiation of the primate Macaca mulatta with 2.3 BeV protons obtained from the Cosmotron facility at the Brookhaven National Laboratory. The work is part of a study involving whole-body exposures of the primate to protons of various energies in the range 32 MeV to 2.3 BeV. By extension, the effects of ionizing radiation on man and possible hazards experienced by extended travel in space can be estimated. The physical aspects, dosimetry, and resultant biological effects have already been reported[1] for exposures to protons of 32 MeV, 55 MeV, 138 MeV, 250 MeV, and 400 MeV.

A total of 117 primates were irradiated with doses ranging from 28 to 3400 rads. The basic dosimetry measurement was the integrated proton flux incident on the animals. The flux was then related to average body dose in rads by making exposures of glass and lithium fluoride microdosimeters embedded in primate phantoms. Measurements indicated that the rad dose received by the animals was 43% higher than that based on the stopping power of the incident protons alone. The primates were exposed while in a horizontal position parallel to the beam axis, half the total proton flux being incident on the head, and half incident on the feet. Biological results of the exposures are briefly reported.

Experimental Method

Quadrupole defocussing was used to enlarge the beam size to obtain a uniform proton flux over the primates. It was not possible to spread the 2.3 BeV beam out greater than about 10 cm. This prevented the animals' being irradiated in a sitting position as had been the practice in our previous proton exposures.[2] Instead, the animals were exposed while in a horizontal position, being placed in cylinders rotating parallel but off axis to the proton beam at the rate of 2 rpm. Figure 1 indicates the arrangement used during the exposures. Protons from the Cosmotron passed through a total flux monitoring, parallel-plate ionization chamber, then through a quadrupole magnet used for defocussing the beam at the position of the irradiation subject.

During irradiation the primates were contained in a rotating Lucite cylinder, 5-1/2" in diameter and 30" long. The cylinder walls were 1/8" thick and the end plates 1" thick. The quadrupole optics system spread the beam into an irregular-shaped profile. Several trial positions of the cylinder axis relative to the beam axis were examined before a satisfactorily uniform proton flux was obtained across the face of the rotating

cylinder. Figure 2 shows the approximate shape of the beam and its position relative to the end face of the rotating cylinder to give a ± 5% flux uniformity. The profile of the proton flux over the cylinder end was measured by polystyrene foil activation using the reaction

$$C^{12}(p,pn)C^{11} \xrightarrow[\text{half life}]{20.4 \text{ min}} B^{11} + \beta^{+}.$$

A row of 3/8"-diameter by 1/8"-thick discs was placed diametrically across the front face position of the primate container and irradiated for ten minutes while rotating. Subsequent counting of the gamma rays from induced activity in the foils and correction for decay time yielded a measure of the flux profile. Figure 3 shows the proton profile deemed suitable for the animal irradiations. The uniformity was checked periodically during the 50-hour period of the irradiations. Slight changes in the pattern as indicated in Figure 3 occurred, but the uniformity remained at ± 5% across the face of the primate container.

All irradiations were made relative to the total flux monitoring ionization chamber. This chamber was calibrated in terms of the proton flux at the front face of the rotating cylinder. The polystyrene activation method[2,3] was used to determine the flux. Four 1"-diameter 1/8"-thick polystyrene discs were placed across a diameter at the front face position of the animal container cylinder. With the outer support cylinder rotating these foils were exposed to the proton beam for a given time interval. The positron activity of these foils due to the $C^{12}(p,pn)C^{11}$ reaction was then measured. Using the standard radioisotope production formula[4] and a cross section[3] for the reaction at 2.3 MeV of 27.2 millibarns, the integrated proton flux for the foil exposure was calculated. This was then related to the reading obtained from the total flux monitoring ionization chamber.

The basic measurement involved in the exposures was the proton flux given to each subject. As in the case of the beam uniformity, the flux calibration was checked throughout the experiment period. The proton flux was then related to the rad dose received by the animals by exposing microdosimeters under similar circumstances while embedded in primate phantoms.

Dosimetry

To determine the extent of dose buildup due to secondary dose production, a series of dosimetry studies was carried out. A phantom constructed by encasing a primate skeleton in a unit density plastic (Epibond-Furane) had to be used due to the irregular shape of the animals. This phantom

is described elsewhere.[5] The phantom was traversely sectioned into eight segments, allowing microdosimeters to be embedded throughout the volume. Glass rods and lithium fluoride dosimeters were used. The glass rods were Bausch and Lomb Hi-Z silver phosphate microdosimeters, read on a Bausch-Lomb Model 33-66-02 reader. Conrad Type 7 lithium fluoride was used as the thermoluminescence dosimeter; the 55 mg samples were read out on a Conrad Model 412A reader.

Figure 4 shows the results of one experiment in which the phantom was exposed in an identical manner to that of the animals. The dose response of the microdosimeter is measured relative to the response to Co^{60} gamma rays. Basing dose on the stopping power of the protons only, the illustration is for the case where 1000 rads were given to the phantom in the rotating cylinder, 500 rads to each face. For 2.3 BeV protons the mass stopping power in tissue is 2.00 MeV cm^2/g and the dose due to ionization by the primary beam only is given by

$$\text{Dose} = 3.204 \times 10^{-8} \text{ rads/proton/cm}^2.$$

Figure 4 shows that a substantial buildup of dose takes place due to nuclear reactions giving rise to secondary radiation. On the assumption that the response of the microdosimeters is directly correlated against the response due to a similar dose of Co^{60} gamma rays, the body dose relation is given by

$$\text{Average Body Dose} = 4.58 \times 10^{-8} \text{ rads/proton/cm}^2.$$

The above relation was used to determine the dose received by the animals and is 43% higher than that based on stopping power alone.

To evaluate the dose buildup, depth dose measurements were also carried out using right circular cylindrical phantoms of Lucite and Masonite. These phantoms were 10 cm in diameter, traversely cut into segments containing holes for holding the microdosimeters. Figure 5 shows the results for the case where the unit density Masonite cylinder was exposed to a flux of 3.12×10^{10} protons/cm^2 incident to one face of the rotating container. This flux is equivalent to 1000 rads due to stopping power only.

The response of the dosimeters indicated an immediate buildup at the front surface of the Lucite end cap of 24%. This is in agreement with the results published by Phillips and his coworkers.[6] Using a tissue-equivalent ionization chamber, they found a surface dose on a large paraffin phantom due to 3 BeV protons to be 26% higher than the air dose. This immediate

buildup is due to local secondary dose produced by cascade and evaporation protons and neutrons and heavy ions. The dose increases to a maximum at a depth of 8 cm inside the Masonite cylinder before an almost linear decrease due to scattering out of the phantom and to a smaller extent the slight divergence of the primary beam. The shape of this depth-dose curve resembles the relative depth-dose curve obtained by Gross and Bell[7] with 2.2 BeV protons at the same facility. In their experiment a 5-inch-diameter phantom was used together with a tissue-equivalent ionization chamber; no proton flux or absolute dose measurements were specified in this work.

In-air exposures of the microdosimeters were also made. Table 1 gives the results for doses from 500 rads to 3000 rads. These doses are based on stopping power only. Close agreement is obtained between the calculated dose and the response calibrated against Co^{60} gamma-ray doses. The lithium fluoride results are on the whole about 5% higher. This may be due to the size, resulting in a secondary dose effect taking place.

It had been planned to compare the response of the microdosimeters against that of a tissue-equivalent ionization chamber. Instrumentation difficulties prevented this being carried out. A program is presently underway in which comparison of ionization chamber response with that of microdosimeters will be made over a wide range of proton energies. For phantom dose measurements the size and convenience in use of the microdosimeters can offer a distinct advantage over ionization chambers.

Animal Exposures

Eleven groups of the primate Macaca mulatta were exposed to 2.3 BeV protons, receiving doses ranging from 28 rads to 1130 rads at a dose rate of 25 rads/minute, and 1700 rads and 3400 rads at 110 rads/minute. The animals were irradiated while in a horizontal position. In each case half of the dose was given head on and the other half was given with the feet incident to the beam. Through the course of the irradiation, the animals were rotated on the long axis at approximately two revolutions per minute. Table 2 lists the exposures. The mean weight of the animals was 3.2 kg ± .4 (S.D.). The average body trunk diameter was about 10 cm, and in a horizontal position the length from head to foot averaged 56 cm. The animal care practices were similar to those described elsewhere.[8]

The fifteen animals receiving the high doses of 1700 rads and 3400 rads were given to various institutions for study. The animals exposed to the doses from 1130 rads to 28 rads have been under examination by J. C. Traynor and his group at the School of Aerospace Medicine. Traynor[9] indicates that the

general pattern of the clinical course of these animals paralleled those reported for 2 MeV x-ray[8] and other penetrating proton exposures.[1] Animals receiving 730 rads or more developed signs of severe gastrointestinal injury characterized by mucous and bloody diarrhea. The animals surviving beyond 9 to 10 days developed hemorrhagic diathesis as evidenced by petechiae and epistaxis. An LD-50/30 of 475 ± 21 (S.D.) rads was calculated by probit analysis from mortality data.

Acknowledgments

We wish to express our appreciation to W. M. Moore, the staff, and operating crew of the Cosmotron facility for their hospitality and assistance during the course of this work.

References

1. Radiation Research Supplement, Radiation Res., 28: 365 (1966).

2. G. H. Williams, J. D. Hall and I. L. Morgan, Whole-body irradiation of primates with protons of energies to 400 MeV, Radiation Res., 28: 372 (1966).

3. J. B. Cumming, Monitor reactions for high energy proton beams, Ann. Rev. Nucl. Sci., 13: 261 (1963).

4. R. D. Evans, The Atomic Nucleus, pp. 484-486, McGraw-Hill, New York, 1955.

5. G. V. Dalrymple, I. R. Lindsay and J. J. Ghidoni, A primate phantom for use in radiobiology, USAF Report SAM-TDR-64-84, USAF School of Aerospace Medicine, December 1964.

6. L. F. Phillips, R. J. King, and F. F. Cowan, Depth-dose studies with 3 BeV and 33 BeV proton beams, Nucleonics 21 No. 12: 55 (1963).

7. W. Gross and W. B. Bell, Dosimetry of 2.2 BeV protons, in Annual Report on Research Project, USAEC Report NYO-2740-3, Columbia University, January 1966.

8. G. V. Dalrymple, I. R. Lindsay, and J. J. Ghidoni, The effect of 2 MeV whole-body x-irradiation on primates, Radiation Res., 25: 377 (1965).

9. J. C. Traynor, School of Aerospace Medicine, San Antonio, Texas, personal communication, 1967.

TABLE 1

In-air response of the microdosimeters to 2.3 BeV protons. Calculated dose based on dE/dX only. Microdosimeter response calibrated to equivalent Co^{60} dose.

Calculated Dose Rads	Glass Rods Response, Rads	LiF Response Rads
500	529	598
1000	1019	1088
1570	1519	1588
2000	1980	2150
3000	2940	3087
8070 Total	7987 Total	8511 Total

TABLE 2

The 2.3 BeV proton exposure program carried out on the primate, *Macaca mulatta*.

No. of Animals	Flux Protons/cm^2	Dose, Rads	Dose Rate, Rads/Min.
7	7.37×10^{10}	3400	110
8	3.68	1700	110
11	2.46	1130	25
15	1.96	900	25
14	1.60	730	25
14	1.23	560	25
14	8.60×10^{9}	395	25
14	4.91	225	25
11	2.46	113	25
7	1.23	56	25
2	6.14×10^{8}	28	25

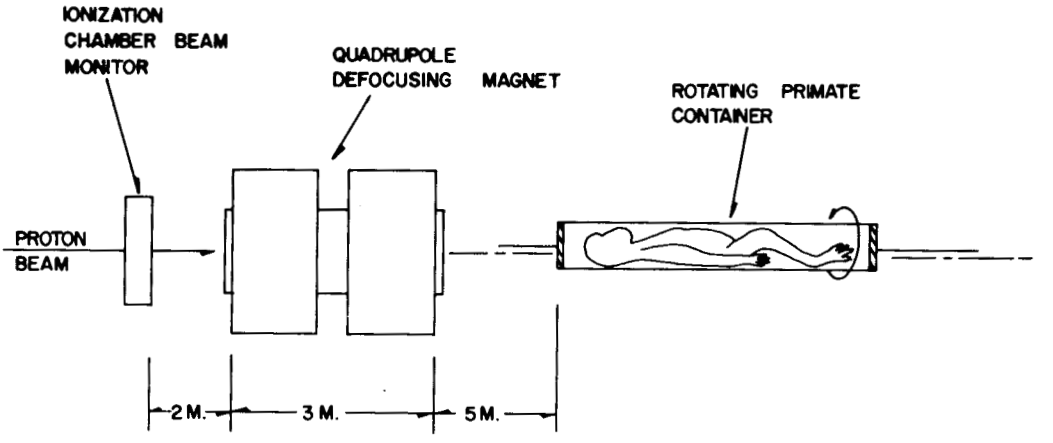

Figure 1 Experimental arrangement for primate irradiations with 2.3 BeV protons.

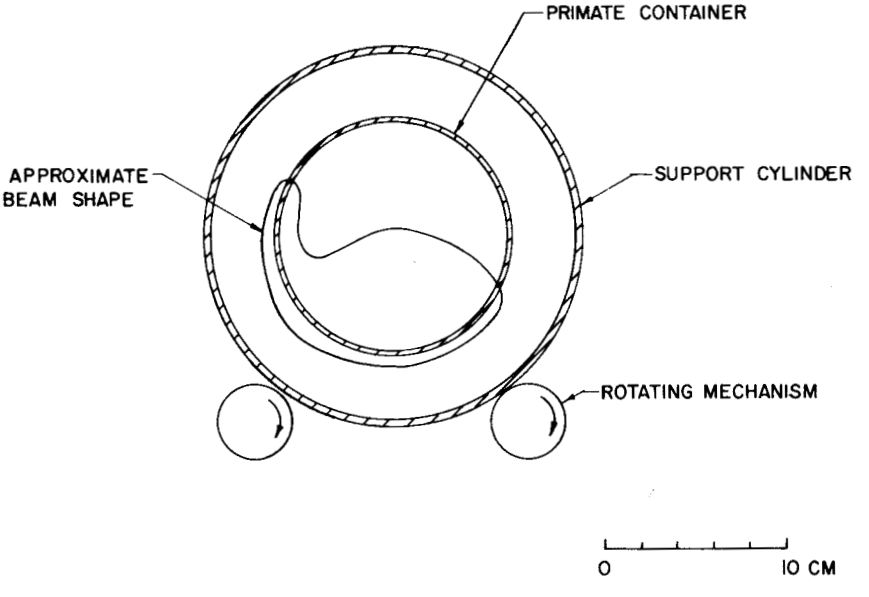

Figure 2 The approximate shape of the defocused 2.3 BeV proton beam relative to the front face of the primate container.

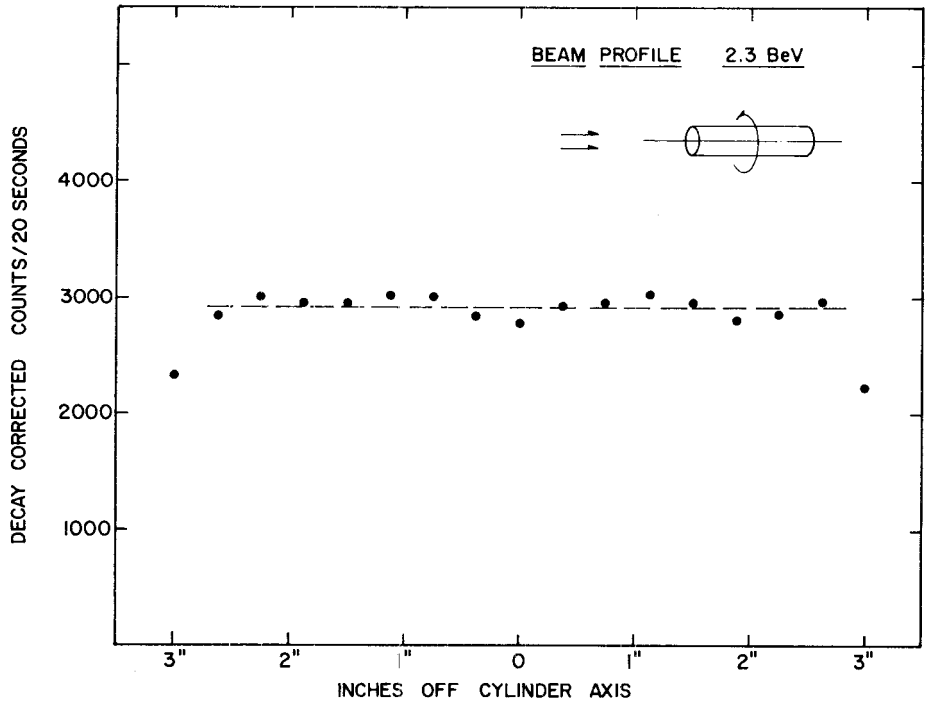

Figure 3 Beam intensity profile across front face of rotating system.

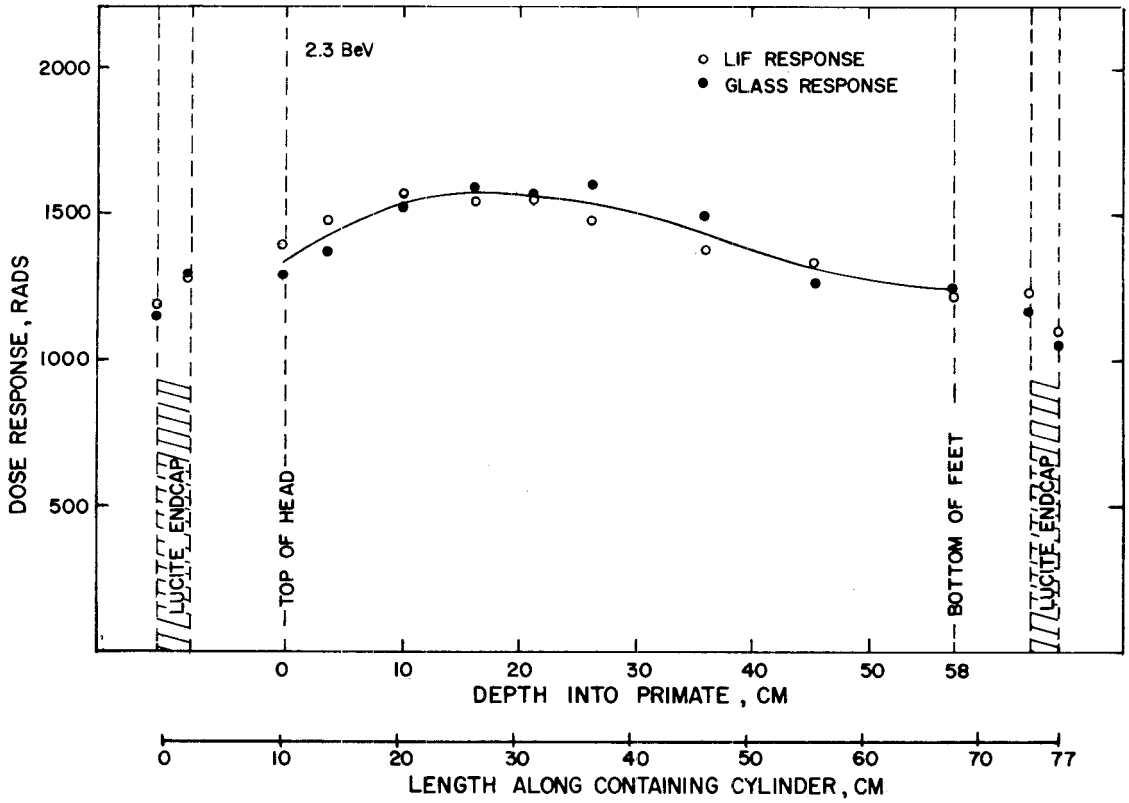

Figure 4 Dose distribution in primate phantom as measured by LiF and glass rod microdosimeters, 1.56×10^{10} protons/cm^2 to each face of the rotating container cylinder.

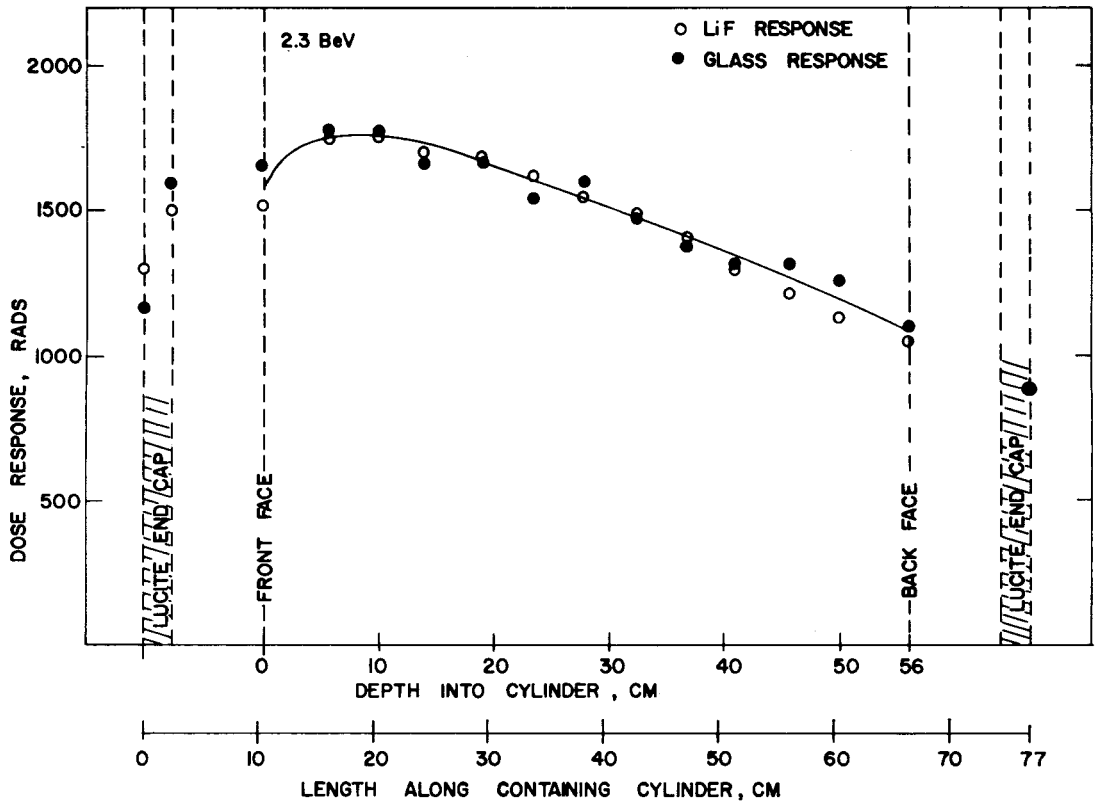

Figure 5 Dose distribution in a masonite cylinder, 10 cm diameter, 3.12×10^{10} protons/cm^2 to one face of the rotating container cylinder.

VII.2

RECENT RESULTS IN MACRO AND MICRO DOSIMETRY OF HIGH-ENERGY PARTICULATE RADIATION

Norman A. Baily

Department of Radiology, University of California at Los Angeles
Los Angeles, California

Introduction

Dosimetry for health physics purposes at or around high-energy accelerators is complex, since invariably we must measure both absorbed dose and quality for an unknown radiation field. The field can be and usually is composed not only of the degraded primary radiation, but also of secondary radiations produced by interactions of the primary beam with accelerator components, target, and shielding materials. In health physics work associated with high-energy accelerators, a typical problem involves protons, neutrons, mesons, γ rays, and even electrons.

In considering new developments centered about these types of problems, the health physicist, in addition to providing reliable data on absorbed dose, must concentrate on perfecting reliable methods for evaluating the quality factor associated with these. Underestimates can be dangerous, overestimates can be costly. Methods of measuring these quantities must be made in the light of the biological application that is going to be made. The interpretation or conversion of spectral data, particle analysis, and flux measurements for biological or health physics purposes has not yet reached the point where a high degree of confidence can be placed in the biological interpretation of such data. To date the most reliable and most easily interpretable data are those derived through use of tissue-equivalent dosimetric techniques.

A third quantity of growing importance, primarily due to an increasing knowledge of radiobiology, is the fraction of the total absorbed dose that is due to highly ionizing particles. This is treated separately, since for health physics purposes we shall see that the trend has been to measure an average quality factor. This QF approach has been used because of the great simplification which can be made in the required instrumentation. However, from the viewpoint of long-term, low-dose-caused effects, the additional information (on highly ionizing particles) would be very desirable.

VII.2

Methodology

During the past 20 years there have been many developments in instrumentation, and indeed in new methods, for recording the total absorbed dose delivered by neutrons, x and γ rays, and electrons. Simplifications and improvements in circuitry, development of solid-state electrometers, the perfection of thermoluminescent materials--all have made the more routine measurements required by the health physicist simpler and more accurate, and pushed the minimum dose level recordable to significantly lower levels. However, an extension of these techniques to high-energy charged particles is not a simple one. Due attention must be paid to the differences in their interactions with the atomic components of tissue. Much of the energy transferred is in the form of nuclear interactions. Such interactions produce secondaries of short range, thereby resulting in large local energy depositions, and in some instances high-energy (long range) highly ionizing particles. The problem is of course complicated by the great variety and energy range of such secondaries. To deal with these properly and attain meaningful measurements requires that strict attention be paid to both geometric and atomic simulations.

From an instrumental point of view we must take due accord of the wide range of particle stopping powers which will exist within the detector used. In a tissue-equivalent device this quantity will vary from about 0.2 keV/μ to greater than 100 keV/μ with reference to unit density. However, because many of the interactions may lead to spallation, the products of such reactions, and indeed even heavy recoils, can produce very dense clusters of ionization whose local value is greatly in excess of the upper value of the linear stopping power. The cross section for such reactions is of the order of the geometric cross section of the atoms in the stopping material. For protons such interactions have a threshold in the range of 150 to 200 MeV. At depth in the body, about 50% of the total dose delivered by 700-MeV protons is due to cascade protons produced as a consequence of nuclear interactions. Behind thick shielding inevitably the major portion of the dose delivered to workers around such installations is due to secondary radiations generated in the shield.

For protection purposes it is necessary that we make measurements which completely define the radiation dose equivalent. This means absorbed dose, quality factor, and dose distribution with respect to vital organs. Although the importance of microdosimetry will be demonstrated in another section of this paper, for health physics purposes quality factor means a quantity dependent only on an average LET_{∞}. This makes the task of incorporating such a factor into an instrument response a good deal easier than a concept based on local energy deposition. The values of the quality factor recommended by the NCRP[1] are given in Table 1.

The general situation is one therefore that calls for the development of methods whereby we can make correct measurements of the absorbed dose and

dose distribution, and an evaluation of the quality factor independent of the incident radiation type and energy. These must be accomplished in a manner which correctly evaluates the contributions of the nuclear interactions and the biological damage to be expected from these. A deeper and fuller understanding of the problems involved will almost certainly be achieved by experiments--both physical and biological--carried out in well-defined particle beams ("well-defined" in this instance meaning monoenergetic and mono-type). These are important, since the dose-to-flux relationships of the various secondary components have been shown to vary considerably among themselves, and may differ markedly from those for the primaries. However, the dose equivalents (DE) have been shown to have remarkably close equivalences at some tissue depths while differing markedly at others. This has been well demonstrated by Baarli.[2] Some typical results are given in Table 2. The data in this table are measured values, and will be further discussed in later sections of this paper. The data refer to pure beams and are different from those for attenuated high-energy radiations.

The data given in Table 2 indicate, first, that the flux-to-dose ratio may vary considerably for the different kinds of strongly interacting particles and for different degrees of degradation.

Second, it is apparent that a quantity similar to an energy event distribution in volumes whose size and shape are similar to those of biological importance should be examined as a function of the amount of tissue penetrated. The statistics of the energy deposition in small volumes may differ significantly at the different tissue depths, since large changes in distribution have been found when energy losses go from very small to moderate. Similarly nuclear reaction products or track endings can produce very high local energy deposition contributing to those effects exhibiting poor or no recovery.

In the above discussion the use of "LET" has been deliberately avoided. Instead, the concept of a distribution of energy deposition in single events has been adopted. There are at least two basic difficulties in the LET concept. First, we must always remember that the loss of energy of a charged particle as it passes through matter is a series of discrete energy transfers and consequently subject to the usual statistical fluctuations. However, for small increments (as compared with the particle energy), such as we expect in cellular or chromosomal volumes, Landau[3] has shown these to be even greater than one would predict from ordinary statistical treatments. Recent results (which will be presented) show that for the volumes and energy losses being discussed in this paper the statistical spread is much greater than Landau's calculations predict. This is due to the neglect, in his treatment, of the second moment of the distribution, which then tends to minimize the high-energy end of the distribution. In more familiar terms, when one irradiates a thin biological sample of thickness ΔX with a homogeneous beam of charged

particles having a LET or dE/dX value of L, the energy, ΔE, expended by individual particles deviates from the mean value $L\Delta X$ to an extent that depends on the magnitude of ΔX, as well as on the energy which the particles can transfer in a single collision. The smaller ΔX is, or the larger the value of ΔE that is possible the greater will be the spread (on the high ΔE side) of the energy loss (ΔE) spectrum.

The second major difficulty with the LET concept is that only a quantity sometimes designated as $(LET)_\infty$ is equal to dE/dX. This can mean a large volume in those cases in which high-energy secondaries having long ranges in tissue are generated. If we try to modify this concept by defining LET in terms of energy locally absorbed, it becomes extremely difficult to meaningfully define the δ-ray energies to be considered. Further, even high-energy δ rays deposit some energy in the volume of interest. The same dose delivered in the same LET interval can conceivably be delivered along a few long track sections or along many short ones, depending on the character and energy of the primary particles. When such track sections become as long as, or approach the dimensions of, the sensitive biological volumes the effects produced may be drastically different. It is because of such considerations that I regard the concepts of microdose or energy event distributions as basic to the high-energy health physics problem.

Absorbed Dose

The measurement of absorbed dose combined with depth-dose distribution from high-energy particulate radiation requires extreme care in selecting instrumentation and in reproducing geometry. This is due to the rapid buildup characteristics at the surfaces and both the rapid buildup and fall-off at the Bragg peaks. A particularly good instrument for carrying out such measurements is the extrapolation chamber.[4] An adaptation of this concept specifically designed for use with high-energy particles is shown in Fig. 1.[5] This chamber has a top electrode made of 0.00025-in. aluminized Mylar, which acts as the entrance window. The other electrode is fabricated from Shonka[6] plastic or can be fabricated from any other conducting material. We have used a muscle-equivalent conducting plastic, and are planning to work with bone-equivalent plastics to investigate absorbed dose delivered by high-energy protons to transition regions. Air-equivalent materials are also available. The air gap or collecting volume may be made as small as a few tenths of a millimeter.

The data obtainable[5] by using this technique are illustrated in Figs. 2 and 3. Figure 2 shows the depth-dose distributions produced by monoenergetic, parallel proton beams incident on an infinite phantom. Curves A, B, C, and D are for 730, 630, 590, and 300 MeV, respectively. Of importance to note is the degree of buildup, which was not predicted by theory and not shown by

measurements made with other techniques. The rapidity with which this buildup takes place is well illustrated by the data shown in Fig. 3. Here curves A and B represent the initial portions of curves A and B shown in Fig. 2. Nuclear absorption processes combined with some straggling account for the exponential decrease of the dose for depths greater than that at which the peak appears. The peaking represents an equilibrium between these processes and the production rate of the cascade protons.

A pertinent example of geometrical or ionization chamber induced artifacts and some data on 70-MeV negative pions are shown in Fig. 4.[2] The dotted curve shows the dose rate in air along the beam axis and indicates a 22% change in 15 cm due to divergence of the beam. The two peaks in the range curve correspond to a pion energy of 70 MeV (14.8 cm) and a meson energy of 82 MeV (23 cm). The depth-dose measurements were made with both air- and tissue-equivalent ionization chambers. Baarli attributes the difference in the two sets of depth-dose data to a geometrical difficulty, stating that the cross section of the tissue-equivalent ionization chamber was greater than the lateral half value of the pion beam. However, since this chamber had a 1-liter volume, it is obvious that the peak value would also be low due to an averaging of the rate of ionization across the dimensions of the particle path within the chamber. The radiation quality or QF measurements shown are discussed in the following section. However, it is worth noting at this point the change in QF values with depth of penetration.

The second area or region that it is important to investigate and for which the extrapolation chamber technique is particularly well suited is that around the Bragg peak. An example of this type of investigation is illustrated by the data in Fig. 5.[5] These data illustrate the absorbed dose distribution in this region for protons of 138 MeV (curve A), 45.8 MeV (B), and 21.4 MeV (C). Because of the rapid change in the energy absorption pattern the extrapolation chamber technique is about the only way to obtain such curves accurately. The patterns found dramatically illustrate the effects of straggling on both the height and half-width of the Bragg peak. It is obvious that these characteristics are very much a function of the past history of the particle. The mean energy of the particles arriving at the depth at which the peak occurs is a function of the initial particle energy. Similarly the spread in number and spread in energy of the particles arriving at this point are both functions of the amount of material traversed and the number of collisions undergone by the incident beam.

Making accurate calculations from theory is extremely difficult in this region. This is clearly illustrated by Baarli's work[2] with negative pions. Figure 6 shows a comparison of his experimental and theoretical results. It is significant that a value of 20 MeV per stopped pion due to nuclear absorption processes occurring at the end of its range gives good agreement with the experimental data.

Many experiments have been misconceived and many health physics situations overcalculated because of a common assumption that particles reaching depths at which the Bragg peak occurs had high LET values. It has recently been shown experimentally by Raju[7] that the mean energy of the particles arriving at a depth corresponding to that at which the peak occurs is approximately 10% of the initial energy of the incident particles. This had been previously pointed out by Bichsel.[8] However, very little attention had been paid to this fact by either the radiological or health physics community.

It is important to recognize that after passage through large amounts of material the depth-dose distributions are considerably different from those produced by pure beams. Figure 7 is illustrative of the changes caused by such degradation. Curve A represents the depth-dose distribution along the central axis of the beam in an infinite scattering media (tissue) of a 730-MeV parallel proton beam after passage through 44-in. of carbon. The resultant proton energy incident on the phantom was 220 MeV and the residual range 31 cm of tissue. Curve B was observed under similar conditions except that 10.76-in. of copper was substituted for the carbon absorber. The energy of the protons in this case was 260 MeV and they had a residual range of 41 cm (tissue). Comparison with Fig. 2 points out the very significant changes which have occurred in the depth-dose distribution. These curves are characteristic of the high-energy secondaries (neutrons and γ rays) produced by the primary protons in their passage through the absorbers.

Microdosimetry

Before discussing the instruments or results associated with the average quality factor it is instructive to look at the more fundamental aspects of this quantity. The determination of energy event distributions, in volumes of interest to radiobiology, due to charged particles is at a very early stage. Only very preliminary results are available. However, these have been dramatic, since they emphasize the inadequacy of available theoretical treatments for dealing with this problem. These treatments are unable to handle energy losses that are small compared with the mean atomic ionization potentials. For high-energy particles this is always the case. The resultant distributions are very much broader, with the broadening occurring on the high-energy side of the distribution. An example of the type of distribution obtained is shown in Fig. 8. The data shown here represent the distribution in the energy losses suffered by 46-MeV protons in passing through 1.3 μ of tissue. The number of high-energy events is greatly in excess of what would be expected if the distribution were similar to that found for greater mean energy losses. Such data are extremely important when considering radiation damage on a cellular level. Such considerations could conceivably lead to a revision of our current concepts of quality factor and its interpretation.

To date there has been only one experimental method developed for the determination of an average quality factor in a beam of unknown composition that is readily adaptable for health physics or survey use. Sullivan and Baarli[9] have devised and built an ionization chamber capable of evaluating the QF of an unknown beam based on its proportional response to the average LET of the particles traversing it. This is a tissue-equivalent parallel-plate high-pressure ionization chamber. The chamber operates at a field strength below which complete collection of the ion pairs is achieved. Since the type of recombination which takes place is a columnar phenomenon, surrounding the particle track, the recombination is therefore a function of the ionization density along the track. In turn, therefore, it becomes by definition a function of QF. It has been found that the current in such a chamber obeys the relationship

$$I = kV^n.$$

The exponent (n) is independent of dose rate, directionality of the incident particle, etc. However, it is directly proportional to QF. In fact, in addition to being proportional to the QF, it has the additional effect of averaging it over any mixture of incident radiations. The response of Baarli's chamber[2] is shown in Fig. 9.

Using the same principle, Zel'chinskii et al. developed an instrument having dual ionization chambers, one operating at saturation for measuring dose and the other below voltage saturation for measuring the average QF. The operating conditions are such that the average QF is a unique function of the current ratio of the chambers. This current ratio is read directly by a divider circuit.

For the first time consideration has been recently given to a passive device which will allow evaluation of QF. It has been found that heavy charged particles produce tracks in certain materials and that different materials have different thresholds of ionization density for the production of such tracks.[11] By using dosimetry packets containing some pertinent combination of such materials, it should then be possible to obtain information on the relative number of particles having LET or QF values greater than some given threshold value. To date results have been obtained only for α particles, heavy ions, and fission fragments. Materials and methods applicable for use with less highly ionizing particles are being actively investigated.

Conclusions

1. Tissue-equivalent dosimetry correctly used is the most accurate method for assessing the biological effects of high-energy radiations.

2. The extrapolation chamber method is the only completely reliable method for measuring absorbed dose in regions of rapidly changing energy deposition, and is pertinent to the dosimetry of high-energy beams to be used for radiobiological experiments.

3. Microdosimetric techniques are important for the interpretation of the radiobiological consequences of high-energy particulate radiations.

4. Assessment of the average QF is required for health physics surveys of high-energy accelerator facilities.

5. A passive dosimetry system to supplement the film badge at high-energy facilities is required, and work towards achieving a reliable system should be actively pursued.

References

1. Permissible Dose from External Sources of Ionizing Radiation, N. B. S. Handook 59, 1954.

2. J. Baarli, Radiological Physics of Pions, CERN paper #DI/HP/80, 1965.

3. L. Landau, On the Energy Loss of Fast Particles by Ionization, J. Phys., 8: 201 (1944).

4. G. Failla, The Measurement of Tissue Dose in Terms of the Same Unit for All Ionizing Radiation, Radiology, 29: 202-215 (1937).

5. R. L. Tanner, N. A. Baily, and J. W. Hilbert, High Energy Proton Depth Dose Patterns, Radiation Res., in press.

6. F. R. Shonka, J. E. Rose, and G. Failla, Conducting Plastic Equivalent to Tissue, Air and Polystyrene, in Proceedings of the Second Conference on Peaceful Uses of Atomic Energy, 21: 184-187 (1958).

7. M. R. Raju, Heavy-Particle Studies with Silicon Detectors, in Semiannual Report, Biology and Medicine, USAEC Report UCRL-16613, page 6, Lawrence Radiation Laboratory, Jan. 1966.

8. H. Bichsel, Relative Ionization of Protons Near the End of Their Range, Phys. Rev., 120: 1012-1014 (1960).

9. A. H. Sullivan and J. Baarli, An Ionization Chamber for the Estimation of the Biological Effectiveness of Radiation, CERN report #63-17, 1963.

10. M. Zel'chinskii, V. N. Lebedev, and M. I. Salatskaya, Instrument for Determination of Recommended Relative Biological Effectiveness of Radiation, Pribory i Tekh. Eksperimenta, 6: 73-76 (1964).

11. R. L. Fleischer, P. B. Price, R. M. Walker, and E. L. Hubbard, Phys. Rev., 156: 353 (1967).

Table 1. Recommended values of the quality factor for radiations of different specific ionizations.

Average linear energy transfer (LET) to water (KeV/μ)	Ion pairs/μ	Quality factor
3.5 or less	100 or less	1
3.5 - 7.0	100 - 200	1 - 2
7.0 - 23	200 - 650	2 - 5
23 - 53	650 - 1500	5 - 10
53 - 175	1500 - 5000	10 - 20

Table 2. Physical factors measured for some high-energy particles in pure beams.

Beam	QF at 1 g/cm^2	Buildup factor	QF at max. buildup	Particles/cm^2-sec per mrem/hr
70 MeV - π^-	1.0	2.2	3.5	1.1
400 MeV - n	3.5	2.5	2.0	16.0
600 MeV - p	12.0	1.2	1.2	6.3

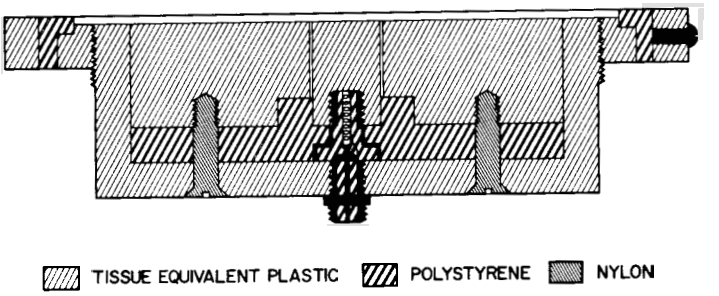

Fig. 1. Tissue-equivalent extrapolation chamber designed for use with high-energy particulate beams.

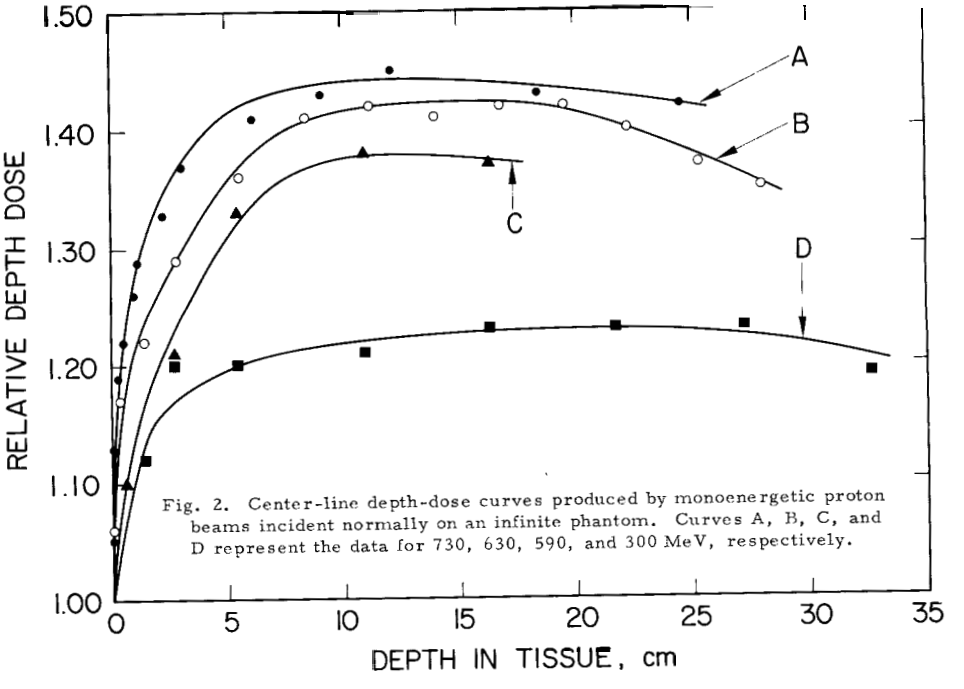

Fig. 2. Center-line depth-dose curves produced by monoenergetic proton beams incident normally on an infinite phantom. Curves A, B, C, and D represent the data for 730, 630, 590, and 300 MeV, respectively.

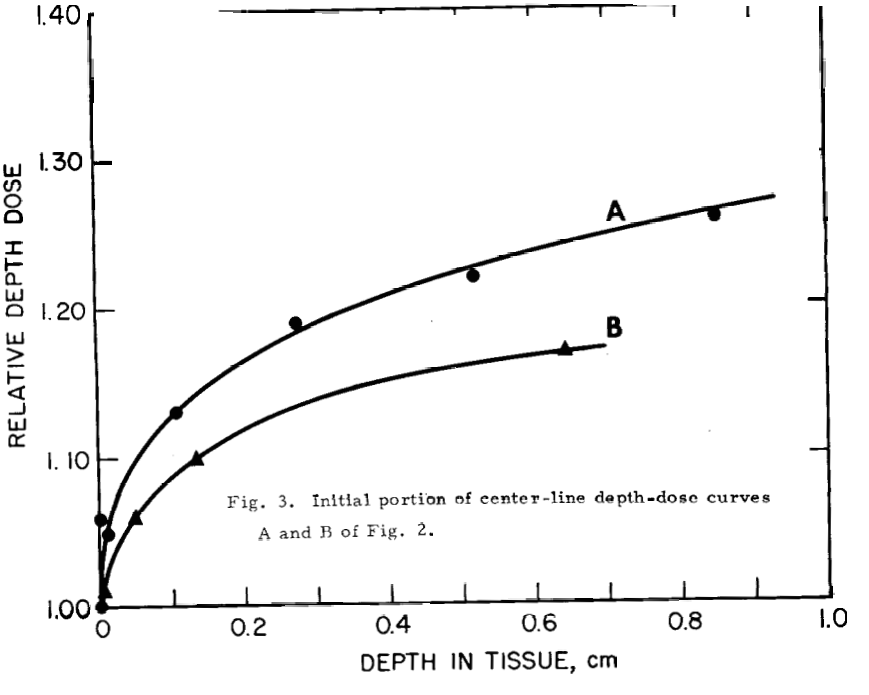

Fig. 3. Initial portion of center-line depth-dose curves A and B of Fig. 2.

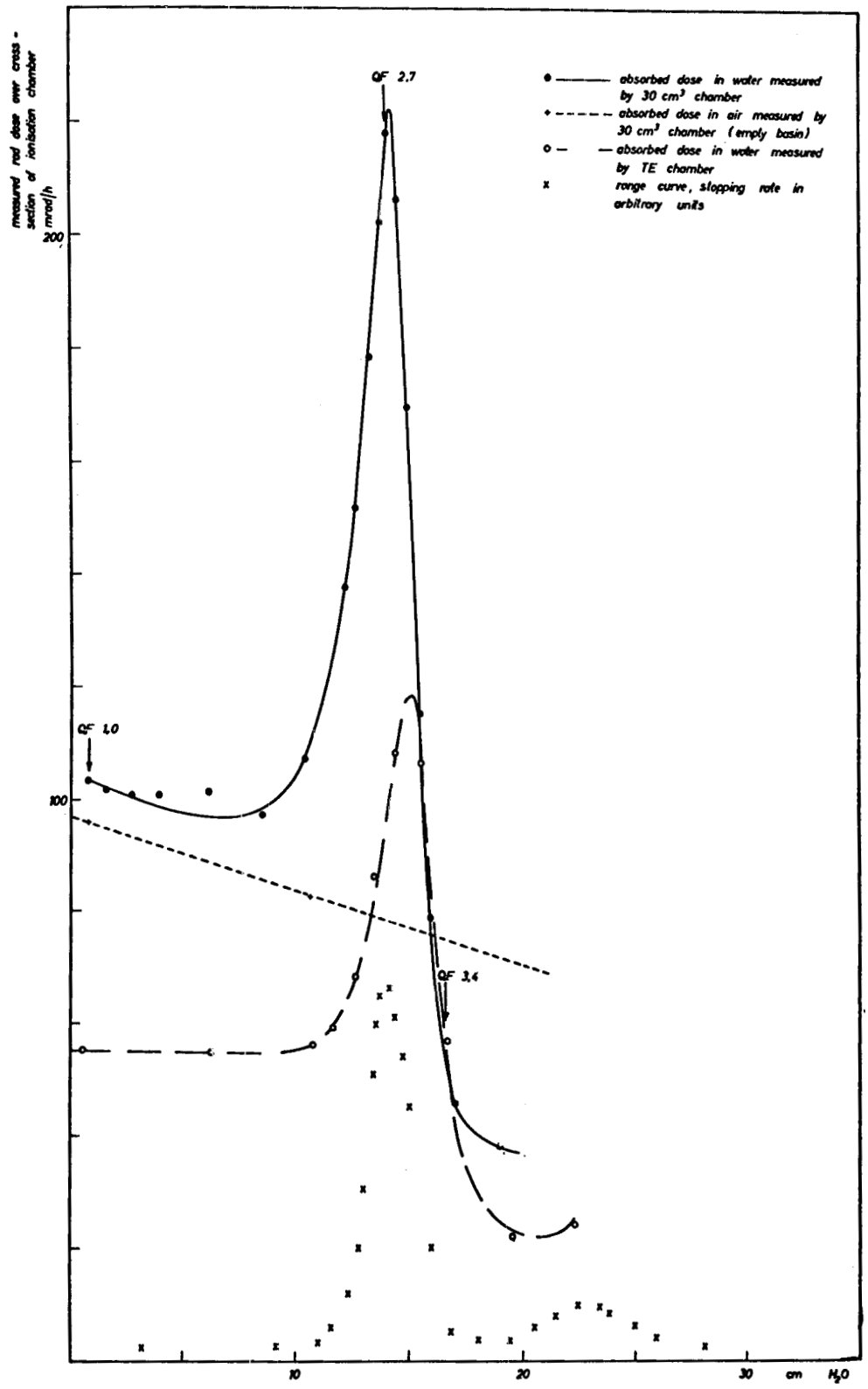

Fig. 4. Measured dose distributions in a water phantom exposed to a 70-MeV π^- beam. The QF values measured at various depths are also shown.

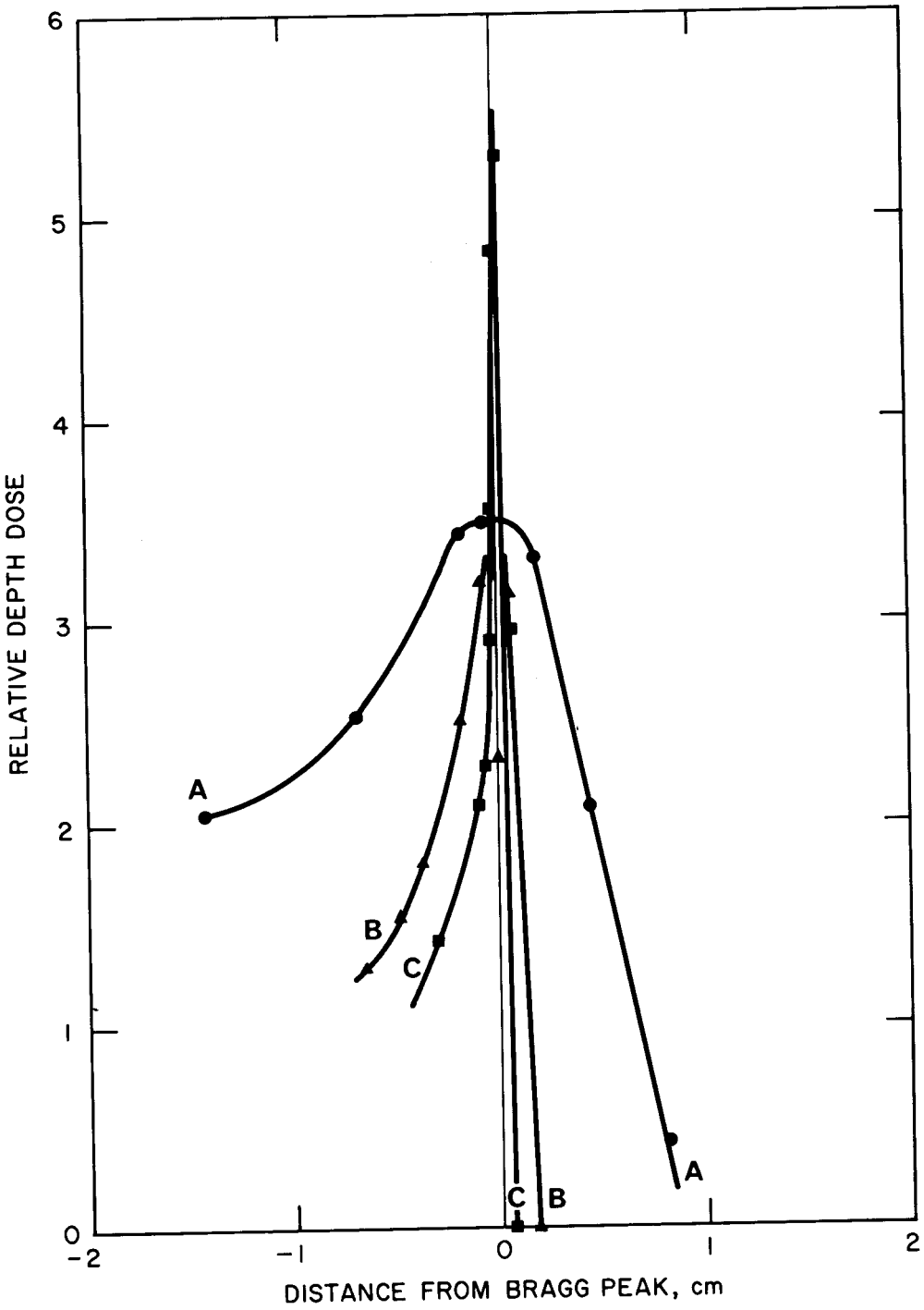

Fig. 5. Characteristics of Bragg peak regions (in tissue) for monoenergetic proton beams incident normally on infinite phantoms. Curves A, B, and C are for 138, 45.8, and 21.4 MeV, respectively.

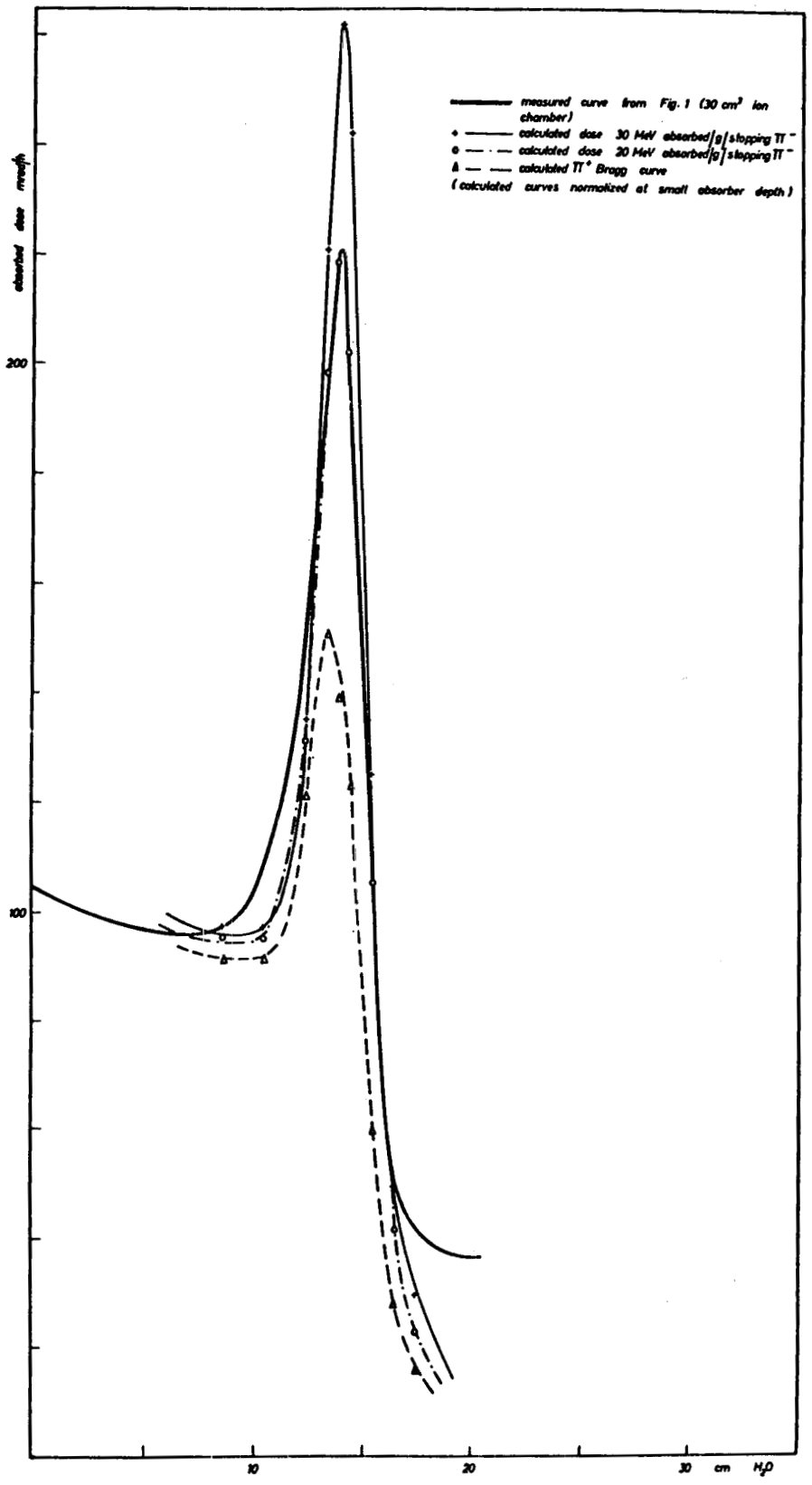

Fig. 6. Calculated and measured depth-dose distribution of a 70-MeV π^- beam in water.

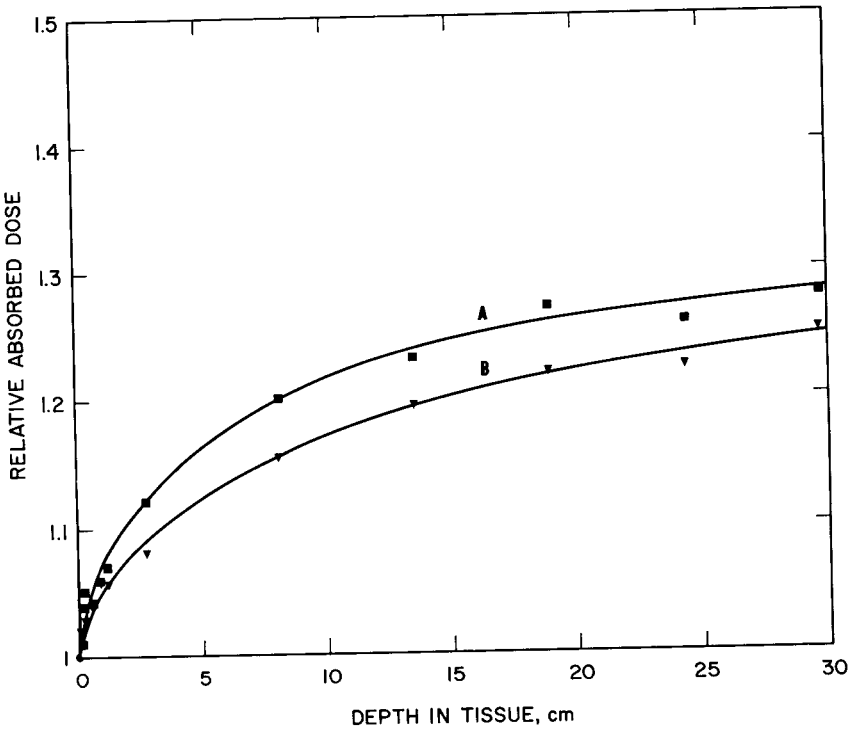

Fig. 7. Depth dose distributions of a degraded 730-MeV proton beam. Curve A is the pattern produced after passage through 44-in. of carbon. Curve B is that produced after passage through 10.76-in. of copper.

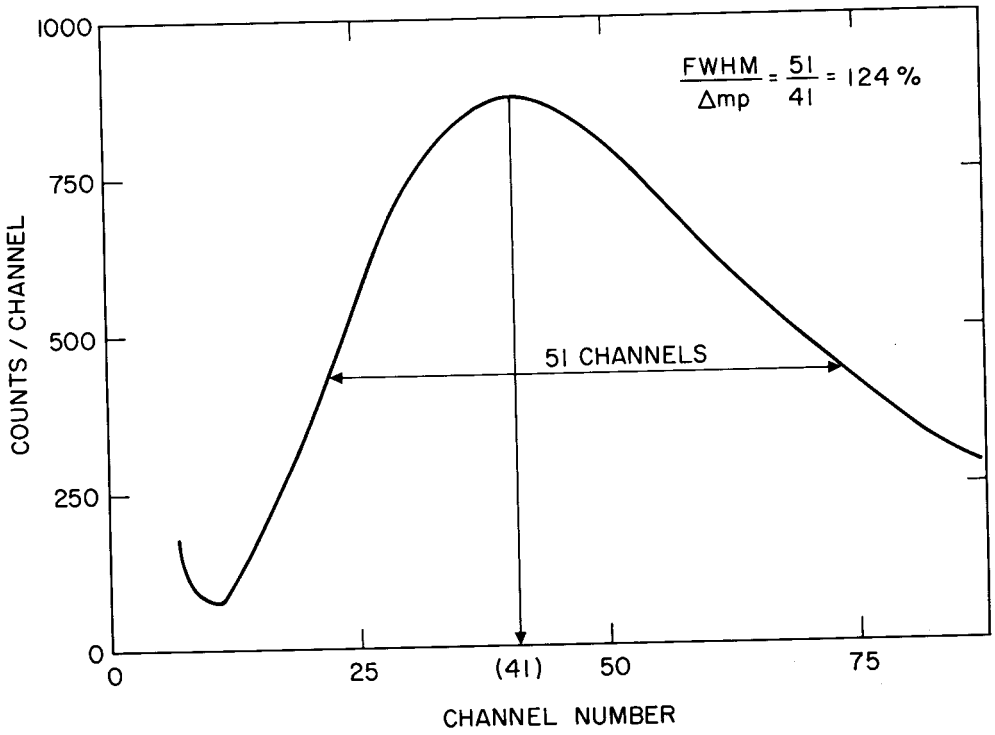

Fig. 8. Energy-loss event distribution of a 46-MeV proton beam in passing through 1.3 μ of tissue.

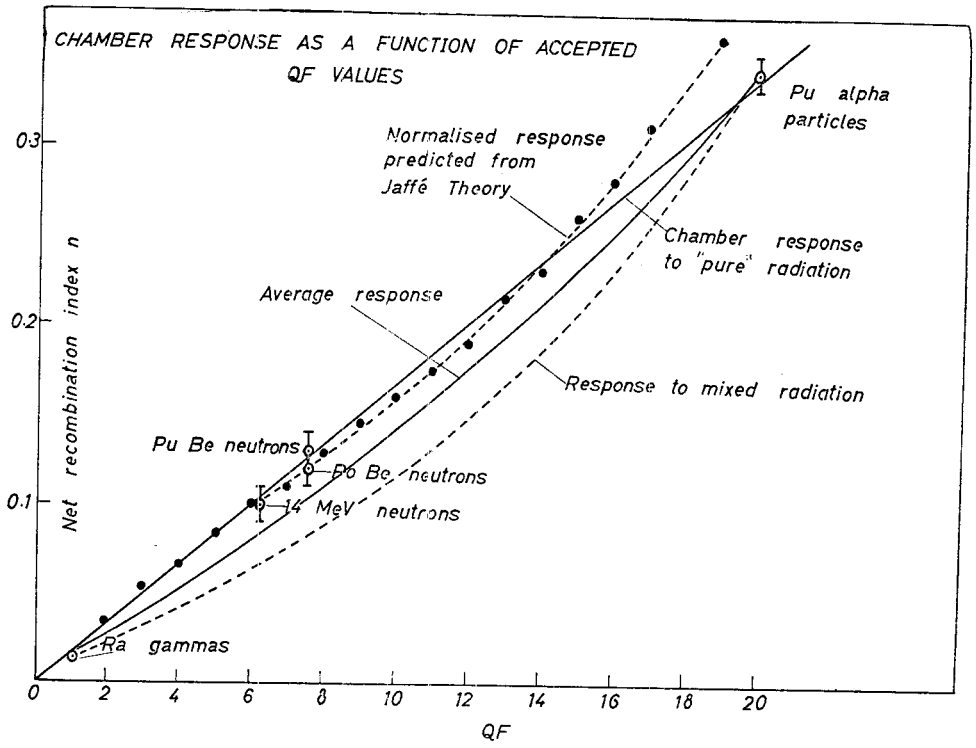

Fig. 9. Measured chamber response as a function of accepted QF values.

VII.3

π^- MESONS, RADIOBIOLOGY, AND CANCER THERAPY

Chaim Richman

Southwest Center for Advanced Studies
Dallas, Texas

Nature of the π^- Beam

Mudundi Raju and José Feola have presented the experimental results of the work on pion beams, and these are the important things that needed to be said. There are some things that can be added, here and there, to fill in the picture of the nature of the π^- beam, the radiobiological work, and the outlook of the π^- beam for the treatment of cancer.

Peter Fowler, who in collaboration with Don Perkins did the first calculations of the dose to be expected from negative pions, has emphasized an interesting point: Of all the radiations that have been discovered in the past 10 years or so in high energy physics, the π^- meson is the only one that has the properties that might be able to improve cancer therapy. This is certainly true, and it is therefore of great importance to do the experiments that will show what can be done therapeutically.

The π^- meson is what would certainly be called a penetrating particle. For a given energy it goes a long way in tissue, in other words it is a lightly ionizing particle in flight. At the 184-inch cyclotron the 90-million-volt pion traverses about 25 cm of tissue before stopping; an α particle requires 900 MeV to go through about 30 cm of tissue. Also, the pion delivers in the region of stopping a dose of which a large fraction is of high LET. It is therefore clear that here is a particle that in a manner of speaking changes its character in the tumor region, and it must be appreciated that this is a most unusual phenomenon.

The pion beam is a secondary beam which is made by letting the 732-MeV protons strike a beryllium target. The pions come off at all angles from the target, and a portion is taken off to make the beam. The beam is large in cross-sectional area. It is quite different, therefore, from proton and α-particle beams, which are usually small in cross section. Now it must be said that this is the kind of beam that is needed for therapy; a therapeutic beam must cover a large field.

This fact also means that detailed isodose measurements must be made in the experiments in which four mice in a single compartmented holder are exposed to the beam.

To be quite frank, it must be said that when the first measurements of the augmented Bragg peak were made with ionization chambers and later with lithium-drifted silicon detectors, the peak-to-plateau ratios were disappointingly small, and some remarks should be made about this fact: Many people know that in using a Bragg peak in therapy, that for large tumors these peaks have to be overlapped, so to speak, and in doing this the plateau dose is raised, which often means that in treating a large tumor, the peak-to-plateau ratio may fall to figures between 1 and 2. The early calculations by Fowler and Perkins were

made for small tumors, about 2 cm in diameter. In therapy, the tumor that presents the anoxic problem is the large tumor, more like 5 cm in diameter. The peaks used in our experiments are almost always broad, between 4 and 5 cm, as appeared in the previous slides. Dr. Stanley Curtis has made calculations of the dose distribution for wide peaks and he finds that they agree farily well with the experimental results. However, more work is certainly needed here; especially on the peak-to-plateau ratios for beams of given momentum spread.

I would like to say something about the electron background. This background originates with the neutral pion, which is also produced in the target, and at present it constitutes 25% of our beam. The electron weighs about 1/300 the weight of the pion. Now it is possible with a technique that is commonly used on the Bevatron to eliminate such a particle from a beam by means of an electrostatic separator. It would be well if at some time in the future an electrostatic separator were to be installed in the beam-handling system and the electrons were eliminated. Mr. John Sperendi has calculated that the electrons can be removed entirely. This is not true for the muons, however, which constitute in any case only 10% of the beam. For radiobiology this separation is at this time prohibitive because the loss in intensity is too large.

It would seem that the best way to do the dosimetry is with the lithium-drifted silicon detectors and the linear amplifiers in use at present, but then go over to a small computing machine like the PDP-5 and store all the information. Any kind of integral or partial integral can then be called for from this system. This is not the most convenient approach, but may well turn out to be the best approach to the problem.

Radiobiology of π^- Mesons

It is impressive and gratifying to find that much can be learned and accomplished here, even with the low-intensity beam that is now available on the cyclotron. I feel that much more can be learned about the RBE of pions and the oxygen effect with pions with the appropriate biological systems. The oxygen effect especially merits a great deal of attention and effort.

The work of Steve Richman and Henry Aceto with Vicia faba, the work of William Loughman on the induction of polyploidy in ascites tumor cells, and especially the studies of José Feola on the inhibition of the proliferative capacity of the ascites tumor cells, all agree on the strong effects produced by the dose at the peak. When the accuracy of the dosimetric measurements is improved, and when more runs have been made with the mice with these tumor cells, there is no reason why good values for RBE should not be forthcoming.

This conference has brought forth some surprising and interesting results on the oxygen-enhancement ratio of different radiations. It appears from the work presented by Dr. Barendson and the work of Dr. Fowler with neutrons that we can expect an appreciable effect on the OER with the LET spectrum that exists in the pion peak. It appears that the LET spectrum in the peak is not too low nor certainly too high.

VII.3

On Cancer Therapy with π^- Mesons

As far as radiotherapy is concerned, there is one point that hardly needs making at this time: In treatment with this beam there is very little dose after the Bragg peak compared with neutrons, and in any case the dose after the peak and before the peak has always very low LET and is therefore much less damaging to the healthy tissue than a neutron beam which has an exit dose. This is not a minor point, since there are cells in the human body which are normally anoxic, and it is unfortunate when these cells are oxygenated (as in the hyperbaric chamber) so that they are damaged by cobalt-60 α rays, or would be damaged more with neutrons. In other words, with pions, we preserve the normal protection that these cells have.

The other point--a very intriguing one--is that there is quite a new possibility here for fractionation. Since the LET in the healthy tissue is low, which means that recovery processes can take place, and since the LET distribution in the tumor is much higher and recovery processes are minimized, fractionation in this case would mean that the healthy tissue would recover and at the same time the tumor would not recover. The possibility for saving healthy tissue would therefore seem to be increased in a manner that takes advantage of the radiobiological knowledge that has been accumulating for such a long time.

The dosimetric techniques and results can of course be taken over right away to more intense beams. The biological experiments are certainly low-dose-rate experiments, with all the questions that are left unanswered; nevertheless, they give a framework and a beginning on the questions and problems that lie ahead.

A REVIEW OF THE PHYSICAL CHARACTERISTICS OF PION BEAMS*

Mudundi R. Raju, Chaim Richman, and Stanley B. Curtis

Donner Laboratory and Lawrence Radiation Laboratory
University of California, Berkeley, California

and

Graduate Research Center of the Southwest
Dallas, Texas

Introduction

Localization of radiation dose in a region of interest, for example, in tumor tissue, while sparing the normal tissue is one of the essential requirements for radiotherapy. It has been known for a long time that the blood supply has a great effect on the sensitivity of tissue to radiation, and clinical studies have shown that tumors with good blood supply are more sensitive to radiation. In most types of neoplasma there are likely to be cells deficient in oxygen. As such cells are relatively insensitive to radiation, they survive the usual forms of radiotherapy and cause recurrence of the tumor growth. However, this oxygen effect diminishes considerably for high-LET radiations. Hence the radiation to be used for cancer therapy preferably should have the properties of delivering a highly localized radiation dose of high LET. Conventional x rays have limited penetrating qualities and are of low LET; hence they cause damage preferentially to the oxygenated tissue. High-energy radiation such as ^{137}Cs, ^{60}Co, and high-energy x rays and electrons have better penetrating qualities, but again the LET is low.

The fast neutrons of modal energy 6 MeV have penetration similar to that of 250 kVP x rays, but in interacting with tissue produce recoil protons with LET high enough to overcome the oxygen effect considerably.

A few years after the discovery of the neutron, fast neutrons obtained from small cyclotrons then developed at Berkeley were tried[1] for tumor therapy but without success because of the lack of knowledge in radiobiology and the then erratic operation of the cyclotrons.[2] More work with fast neutrons is now being done at Hammersmith Hospital, London, and this technique may prove to be beneficial for tumor therapy. Unfortunately, there is always a necessary compromise between getting a higher LET by using low-energy neutrons and getting better depth dose by using high-energy neutrons.

*Work done under the auspices of the U. S. Atomic Energy Commission, the American Cancer Society, and the Office of Naval Research.

The highly accelerated heavy charged particles such as protons, deuterons, and α particles are of special interest because of their physical properties. Since the mass of singly charged heavy particles is many times that of the electron, the angle of Coulomb scattering for a given velocity is reduced approximately by the ratio of the masses of the incident particle and the electron; thus undesirable side scattering can be reduced to a minimum. The radiation fields of heavy charged particles can also be shaped with greater precision than those of x rays and gamma rays. The heavy-charged-particle beam has a definite range of penetration that depends on its energy. It proceeds through a medium in very nearly a straight line; the increase in dose delivered by it as the particles slow down gives rise to a sharp maximum known as the Bragg peak near the end of the range. Hence intense irradiation of a strictly localized region within the body is possible with relatively small dose at the skin.

However, the Bragg peak is too narrow to permit uniform irradiation of most tumors, and the LET at the Bragg peak position is also much lower than one would normally[3] expect (for example at the Bragg peak of 910 MeV α beam the LET corresponding to the modal energy is ~ 10 keV/μ). It is possible to irradiate the entire tumor region by transforming the Bragg peak into flat maxima using variable absorbers, but when this is done the LET will be lowered further. Hence heavy charged particles such as protons, deuterons, and α particles may not provide much oxygen advantage for cancer therapy; however, they are very useful for hypophysectomy in which anoxic cells are not involved. Heavier ions such as neon may prove to be useful for tumor therapy.[4]

The negative pi mesons (pions) are also heavy particles, and have a mass 276 times the electron mass. When a negative pion is brought to rest in a medium, say tissue, it is captured by a constituent nucleus, which explodes into a "star" consisting of short-range and heavily ionizing fragments capable of delivering a large localized radiation dose resulting in an augmented Bragg peak. The heavily ionizing fragments should be capable of overcoming the oxygen effect considerably. The pion capture can be made to take place in the tumor by proper selection of the pion energy. Negative pions pass through healthy tissue as minimum ionizing particles of very low LET (< 1 keV/μ) and stop in the tumor region, delivering a large localized dose at much higher LET. Hence the use of negative pions in principle should be very promising for therapeutic applications. A few people, including Richman appreciated this possibility as early as 1952. Fowler and Perkins calculated the dosage to be expected from negative pions in tumors and in the surrounding tissue.[5] Their results clearly demonstrate that for negative-pion beams, the dose delivered in the tumor should be many times that in adjoining regions. The presently available negative-pion beams are low in intensity compared with that required for therapeutic applications. At present there are four groups in the world working on this problem: Lawrence Radiation Laboratory, Berkeley; Brookhaven National Laboratory; Wills Physics Laboratory, England; and CERN, Switzerland. The pion beam at LRL at present is the most intense ($\approx 10^6$/sec) with reasonably low background. The work at the above-mentioned places will be reviewed briefly and a detailed up-to-date account of the work that has been done at this Laboratory is presented here. Some of our results have already been published,[6-9] and a short account of these published results is also included here.

Interaction of Charged Pions With Tissue

Charged pions travel through tissue similarly to any heavy charge particle, and stop after traveling a given range that depends on energy; e.g., a 50-MeV pion travels through about 10 cm of tissue. Unlike other charged particles like electrons or protons, the charged pion is unstable; it decays in free space into a muon and a neutrino with a lifetime of $\approx 2\times10^{-8}$ sec. Hence there will always be a contamination of muons in a pion beam. The characteristic

difference in behavior between a positive and a negative pion occurs at the end of the range. When the positive pion comes to rest, the coulomb repulsion between its positive charge and that of the nucleus keeps it from interacting with the nucleus. It goes through two decay processes:

$$\pi^+ \rightarrow \mu^+ + \nu$$

$$\mu^+ \rightarrow e^+ + \nu + \bar{\nu}.$$

The ν and $\bar{\nu}$ are neutrinos and do not contribute to the dosage. The μ^+ is a short-range 4.12-MeV muon which contributes a small dose. The positron has a distribution in energy with a peak around 30 MeV. Examples of this type of decay are shown in Fig. 1.

Tissue is composed mainly of hydrogen, carbon, nitrogen, and oxygen; when a negative pion is brought to rest in such a medium, it may be captured by any one of these atoms. When captured by hydrogen, however, the resulting neutral mesic atom diffuses through the medium and when it gets close to a heavier nucleus, the pion is transferred to it because the resulting energy is lower. As a result, the pion is captured by the main tissue elements and cascades down the atomic levels to the ground state of the atom in a time that is short compared with its lifetime. From the ground state it is captured by the constituent nucleus, which explodes into a star consisting of short-range heavily ionizing fragments. In such interactions, about 20% of the total rest-mass energy (140 MeV) appears in the form of α particles, protons, and heavier fragments with ranges less than 1 mm in tissue. A further 40 MeV is expended in breaking up the nucleus, and the remaining 70 MeV is carried off by neutrons.[10] A few examples of negative-pion capture in carbon, nitrogen, or oxygen as observed in photographic emulsions are shown in Fig. 2.

The type of disintegration of a nucleus such as that of carbon and nitrogen has been studied with a diffusion cloud chamber,[11] and considerable energy was found to be in the ionizing fragments of the light elements.

The dominant reaction for carbon (accounting for $\approx 25\%$ of the captures) is

$$\pi^- + {}^{12}C \rightarrow 2\alpha + 1p + 3n.$$

The dominant reaction in nitrogen (19% of the captures) is

$$\pi^- + {}^{14}N \rightarrow 3\alpha + 2n.$$

The other reactions yield from zero to five charged particles, which at times include a heavy ion.

The relative frequency with which different elements capture pions is closely proportional to their relative abundance by mass. In bone-free parts of the body we expect 73% of the captures to be in O, 20% in C, and 3% in N, which leaves only 4% in heavier atoms. It is important, therefore, to know the characteristics of capture in oxygen nuclei. Mayes and Fowler made measurements on tracks of particles stopping in wet and dry emulsions in order to get the data on pions captured in oxygen alone.[10] They found that interactions with oxygen produce tracks of multiply-charged particles. The common form of disintegration of oxygen is into three α particles and a proton. The energy partition for π^- capture in water as given by Fowler[10] is shown in Table 1.

Mayes and Fowler also measured the differential energy spectra of the various particles emitted in the nuclear interaction of the negative pion with the oxygen nucleus. From these data it is possible to calculate the energy-loss distribution for a point in the stopping-pion region.[12] If some reasonable assumptions are made about the momentum spread of the incident beam and the amount of contamination by muons and electrons, the contribution from these sources can be included. The results of such a calculation are shown in Fig. 3. Conditions here were chosen to parallel those existing in the meson cave of the Berkeley cyclotron. The incident particle beam momentum was chosen as 190 MeV/c with a Gaussianly distributed momentum spread of standard deviation 5 MeV/c. The incident beam was chosen to have a 25% electron and a 10% muon contamination. The point of computation was the center of the star region at 25.5 cm of water. The contributions from the various components in the beam are shown in the figure.

The integral under the curve is proportional to the dose deposited at the computation point. If these integrals are computed for various depths and normalized to the entrance dose, a central-axis depth-dose curve (Bragg curve) can be constructed. The result of such integrations is shown for the contaminated beam in Fig. 4. The contributions of the various components are indicated. Our beam has such a large cross section (50 cm^2) that multiple-scattering corrections are negligible on the central axis. Because of the broad distribution in incident momenta, straggling corrections are negligible compared with the range spread due to the momentum distribution. It is seen from the figure that the peak-to-plateau dose ratio rises to almost 3:1 and that the width of the peak is about 4 cm.

For comparison, the depth-dose distribution for pure pions is shown in Fig. 5. Here the width of the peak is about the same as for the contaminated beam, but the peak-to-plateau dose ratio has risen to almost 3.5:1.

Production of Pion Beams

Pions can be produced in a nuclear interaction by any strongly interacting particle if its energy is great enough. They are generally produced by a primary beam of protons. Our experiments at Berkeley are carried out at the 184-inch synchrocyclotron. This machine provides an accelerated beam of 732-MeV protons that in their outer orbit strike a 5-cm thick beryllium target and produce neutral, positive, and negative pions. The experimental arrangement is shown in Fig. 6. The negative pions are deflected out of the cyclotron by the cyclotron fringe field, and after leaving the cyclotron tank through a window, enter a small quadrupole focusing magnet (meson quad), then along a channel (dashed line in Fig. 6) through the main cyclotron shielding (hatched area). The pions then enter the meson cave, where various arrangements of magnets are used for energy selection and focusing of the pion beam. A bending magnet is used for momentum selection. The cyclotron produces pions in a range of energies from 0 to about 450 MeV (the upper limit being determined by the energy of the primary proton beam). In all our experiments, we used pions of energy around 90 MeV, because at this energy the yield of pions is good with reasonably low background. In the change from a negative to a positive pion beam, all the magnetic fields, including that of the cyclotron, are reversed. The magnetic-lens system remains unchanged for pions of the same energy, regardless of charge.

The negative pions are produced in the reaction of the proton beam with the neutrons in the beryllium nucleus:

$$p + n \rightarrow p + p + \pi^-.$$

The positive pions are produced in two ways:

$$p + n \rightarrow n + n + \pi^+$$

$$p + p \rightarrow p + n + \pi^+ .$$

Neutral pions are also produced. They have a very short lifetime, $\approx 10^{-16}$ sec, and decay into two γ rays in the target. The gamma rays get converted into electron-positron pairs that go mainly in the forward direction. The electrons from this conversion constitute the electron background in the negative-pion beam.

Physical Measurements

Some of the early measurements of isodose curves of a 70-MeV pion beam obtained from the 600-MeV proton beam at the CERN cyclotron have been reported by Baarli.[13] The beam had a 30% contamination of muons and electrons. The dose at the Bragg peak as measured by a small tissue-equivalent ionization chamber was found to be 2.2 times the dose at the beam entrance. Measurements of quality factor were 2.7 at the Bragg peak and 3.4 in the middle of the downward slope of the Bragg curve. Their experimental Bragg curve was in good agreement with the calculated curve if the local energy deposition was assumed to be 20 MeV per nuclear star. Further measurements have been made recently by using an LET chamber to measure the contribution of dose due to stars formed by negative-pion capture.[14] Their results at the Bragg-peak position of negative pions indicate that a substantial part of the dose is delivered at LET values appropriate to α particles with energies between 5 and 15 MeV, the peak value of the spectrum being at an LET value appropriate to an α particle of energy[14] 6 MeV. It is quite probable, however, that saturation of their system at high LET prohibited the higher LET portion of the distribution to be accurately measured. A comparison of their spectrum with that in Fig. 3 shows a rather sharp drop to zero in the region where the lower energy α particles should be making a significant contribution.

Dosimetric studies of negative pions have also been carried out at Brookhaven National Laboratory with the negative-pion beam produced at the Cosmotron. The beam had a momentum of 156 MeV/c and a range of about 15 cm in water. The electron and muon contamination of this beam is much higher than the contamination of the CERN and Berkeley beams because very high-energy protons ($\approx$ 2 BeV) from the Cosmotron were used to produce the pion beam, and because the distance between the target and the experimental area was large. Because of the considerable beam contamination, a telescope consisting of particle counters was used for discriminating against the background electronically.[15] A Cerenkov counter was also used for eliminating the dose contribution from the beam contamination, and NaI (Tl) or CsI (Tl) crystals were used as an ionization detector. The ionization spectra were measured as a function of absorber depth. The ionization curve was computed from the pulse-height spectra produced in NaI (Tl) or CsI (Tl) crystals. The data are not yet completely analyzed.

The group from England headed by Peter Fowler has made some calculations of negative-pion dose distributions and the oxygen-enhancement ratio.[5, 10] In addition, they made measurements at the CERN facility of negative-pion capture in oxygen, using wet emulsions as described previously.[10] They do not have a negative-pion beam facility at present for this investigation; however, they are now planning to use Nimrod.

The intensity of the negative pion beam at the 184-inch synchrocyclotron at Berkeley is 5 rads/hr for a beam size of $\approx$ 7 cm by 7 cm. The beam has a contamination of 25% electrons and 10% muons. This beam intensity is two

orders of magnitude lower than that needed for therapeutic application; nevertheless, dosimetric experiments can be done quite well, and with care, limited biological experiments can also. The physical and biological experiments have been done since 1963. A detailed account of the biological experiments will be covered in a separate paper. Most of the physical measurements have already been published,[6-9] and a detailed summary of the results to date will now be given here.

Integral Range Curve

As it passes through the medium, the pion beam is attenuated because of elastic and inelastic interactions with nuclei in the medium. Hence the number of pions passing through an absorber decreases as the thickness of the absorber is increased. This particle loss is important, since the dose at the Bragg-peak position depends on the intensity of the particles there. A plot of the number of particles that reach a given absorber thickness as a function of thickness is called an integral range curve or a number-distance curve. The integral-range measuring apparatus used consists of two plastic scintillators connected in double coincidence to monitor the beam intensity. A third plastic scintillator measures the beam intensity after the particles pass through the variable absorber. The intensity of the transmitted beam through the absorber is given by a triple coincidence between all three scintillators. The integral range curve is the plot of the ratio of the triple coincidences over the double coincidences (incident beam intensity) as a function of the absorber thickness. Such a plot for a pion beam of energy 100 MeV (or momentum 195 MeV/c) with its muon and electron contamination taken in Lucite is shown in Fig. 7. The attenuation of the pion beam before the pions stop is represented by the curve between zero absorber and the point A shown in the figure. Forty percent of the particles from the beam are lost before they reach the pion-stopping region (AB in the figure); the muon and electron contamination is represented from point B onwards. The energy spread and the average energy of the pion beam can be calculated from the integral range curve by taking the energies corresponding to the ranges at points A and B (94.5 and 108 MeV, respectively) from range-energy tables of pions in Lucite. Because of the mass difference between pions, muons, and electrons, for a contaminated pion beam of the same momentum, the muons will have a range 30% greater than pions and the electrons will have a much higher range than muons. Hence, knowing the ranges of pions and muons, we can estimate the contamination of muons and electrons in the pion beam.

Time-of-Flight Measurements

The time-of-flight measurements reveal more vivid information on contamination. In a contaminated pion beam of a given momentum, muons and electrons will travel faster than pions. In these experiments, one measures the time taken by each particle in the beam to travel an extended path (23 feet). A plastic scintillation counter is placed at each end of the flight path. The geometry of this experiment is therefore different from that of the other experiments. The velocity spectrum of the particles, as expressed by the time delay between the two scintillation counters, is fed first to a time-to-pulse-height converter and then to a pulse-height analyzer. Figure 8 shows four Polaroid pictures of the PHA display for a negative-pion beam after it passes through 2-1/8, 6-1/8, 8-5/8, and 13-1/8 inches of Lucite absorber. For absorber thicknesses of 2-1/8 and 6-1/8 inches, the beam is clearly differentiated into three distinct peaks representing the pions, muons, and electrons. Summation of a single peak gives the total number of particles represented by that peak. This procedure was repeated at several different depths in Lucite. The percentage of electrons in the 180 MeV/c beam increases linearly from 23% at the entrance to 40% at the Bragg-peak position in Lucite.

Semiconductor Detector Measurements

Semiconductor detectors are also used for investigating pion beams because of their many advantageous properties, which include their linear response with the deposited energy. A lithium-drifted silicon detector of thickness 0.61 g/cm^2 was employed to analyze both the positive- and negative-pion beams[6] with their contaminants when the particle passed through different depths of Lucite. The experimental details are discussed in an earlier paper.[6]

Figure 9 shows the results obtained with a 95-MeV π^+ beam (189 MeV/c whose muon and electron contamination is very small) after it passed through various thicknesses of Lucite. A number of features of this data are interesting. The resolution is in reasonable agreement with the Landau effect. The peaks are shifted to higher energies by 7-1/2 inches of Lucite, i.e., roughly 1 in. less than the range of pions, a small peak at 1.15 MeV occurs in addition to the 1.98-MeV π^+ peak (Fig. 9b). This small peak is due to μ^+ particles formed by the decay of π^+ mesons. When the beam is degraded by 8-1/2 inches of Lucite, which corresponds to the Bragg-peak position (Fig. 9c), the muon and pion peaks are shifted to higher energies. At 9-1/2 inches of Lucite plus 3/8 inches of copper (copper is used to substitute for a thicker sheet of Lucite because of the lack of space), which is beyond the range of pions and muons, only the positron peak at 0.92 MeV shows (Fig. 9d).

Unlike the π^+ beam, the π^- beam is contaminated with approximately 25% electrons and 10% muons. Figure 10 shows the results obtained with a 95-MeV π^- beam (189 MeV/c) with its muon and electron contamination passing through various thicknesses of Lucite. Two peaks at 0.87 and 1.05 MeV can clearly be seen in Fig. 10(a), and they are due to electrons and pions, respectively. The muon contamination, being relatively small, is hidden in the broad distribution of electrons and pions. Notice that as the absorber thickness increases, the relative height of the pion peak decreases in comparison with the electron peak. This result is due partly to the large loss of pions due to nuclear collisions, and partly to electron build-up due to shower formation. The results of the time-of-flight measurements also confirm this behavior. As the thickness of Lucite increases, the peak due to electrons remains at the position corresponding to about 0.87 MeV, but the peak due to pions shifts to higher energies. This is because the electrons of initial momentum 189 MeV/c are still in the minimum ionizing region, but the pion energy losses increase considerably as the thickness of the Lucite absorber increases. Beyond the range of pions (i.e., for thickness greater than 8-5/8 in. of Lucite), the pion peak is absent and the electron peak persists (Fig. 10d).

The experimental values of the most probable energy losses of pions (both positive and negative) agreed well with the values predicted by theory.

The energy distribution of the negative-pion stars in silicon was also measured. Using ionization chambers, we obtained the Bragg peak at 8-5/8 in. of Lucite. Most of the pions stop in this region and create stars. Hence, a lithium-drifted silicon detector placed at this position will stop many negative pions, and stars will be formed in silicon. Most of the star's energy will be absorbed in the detector itself. In order for the detector to "see" the energy distribution of the pion stars alone, the energy deposited by the pions, muons, and electrons while passing through the detector has to be eliminated. This elimination is done with another semiconductor detector in anticoincidence with the analyzing detector. The results of such measurements are shown in Fig. 11. It can be seen from the figure that the number of stars is constantly decreasing with increasing energy, and this star energy extends beyond 60 MeV. The computed average energy of the star stopped in detector (0.61 g/cm^2) is 21 MeV.

Depth-dose Distribution of Pion Beams

Our early measurements were made by using two 7-in. diameter ionization chambers filled with a mixture of 96% argon and 4% carbon dioxide, at a pressure of 3 psi over atmospheric pressure. The depth-dose distribution of pion beams was measured by using one chamber as monitor, followed by different thicknesses of Lucite absorber, and then using the second chamber as a detector. Measurements were made for beams of both positive and negative pions. The Bragg peak due to the negative-pion beam should be enhanced due to the pion stars when compared with that from a positive-pion beam of the same energy. However, the Bragg ratio for both positive and negative pion beams was found[7] to be 2:1. This is partly due to the differences in the contamination for positive- and negative-pion beams. Also, because the positive-pion beam decayed into muons and positrons near the Bragg-peak position, the ionization chamber, being larger than the beam, will "see" more ionization from these long-range products than from the short-range star products from the negative-pion beam.

In addition to the depth-dose distribution of pion beams, it is important to measure also the ionization density at the points of interest. Lithium-drifted silicon detectors are also being used for such measurements by operating them as pulse-radiation dosimeters.[8]

The charge liberated in the lithium-drifted silicon detector is directly proportional to the energy deposited in it. A charge-sensitive preamplifier yields a voltage pulse proportional to the energy deposited in the detector. At room temperature, the leakage current of the lithium-drifted silicon detector is $\approx 2\ \mu A$, depending on the thickness of the detector, and this current is comparable to the current generated in the detector due to pions passing through it. (The total pion intensity seen by the detector is 10^4/sec). The detector leakage current has been blocked by ac amplification used in the system, as shown in the block diagram in Fig. 12. Simple capacitive coupling is not adequate because of cancellation of the positive signal by the negative overshoot. This cancellation necessitates a polarity-clipping circuit to eliminate the overshoot contribution to the subsequent integration. The integration consists of a standard operational amplifier with feedback capacitor. It is electronically reset by a diode pump that furnishes an accurate amount of charge to the capacitor. To measure the dose due to pulses corresponding to the energy deposition in the detector greater than a particular value or over a particular range of energies, we used a single-channel pulse-height analyzer (or discriminator), gated linear amplifier, and a delayed amplifier. Such threshold measurements yield information on the distribution of ionization density at the measured position.

This system was used to measure the depth-dose distribution of a 190 MeV/c pion beam in water. The most probable energy losses in the 3-mm detector used in this investigation are 1 MeV by the electrons and 1.2 MeV by the pions, and the energy lost by the muons is intermediate between these values. At the end of the range the negative pions stop and produce stars, thereby depositing in the detector energies at times exceeding 60 MeV. Hence the systems should be linear at least from 0.6 MeV to 60 MeV. When checked out with a calibrated pulser, the system was found to be linear within 5% over the energy region from 0.6 to 60 MeV.

Two plastic scintillators connected in coincidence were used to monitor the fluctuating pion beam. The lithium-drifted silicon detector was housed in a small waterproof Lucite-box and could be moved remotely in a water phantom. The integrated charge from the lithium-drifted silicon detector was measured during the time the monitor scintillator system accumulated a fixed number of counts. This procedure was repeated for each position of the detector in the

water phantom. For comparison, measurements were also made for a positive-pion beam, with the results shown in Fig. 13. As can be seen from the figure, the negative-pion beam gave rise to a much higher dose than that of the positive-pion beam near the end of the range.

The depth-dose distribution of a negative-pion beam in water as measured with a silicon detector agreed reasonably well with the calculated dose in water shown in Fig. 4. The similarity between the two results indicates that the nuclear interactions occurring when pions are captured in silicon do not produce significantly different particle types and spectra from those occurring in water. Thus, silicon detectors appear to be useful dosimeters for these investigations, although the dose measured is not strictly the tissue dose.[12]

The integrated output of the lithium-drifted silicon detector was measured as a function of the discriminator setting (energy threshold) for positions designated 1, 2, 3, and 4 in Fig. 13. For comparison, the integrated output of the detector at zero threshold setting of the discriminator at the above-mentioned positions was normalized to unity. The resulting curves are shown in Fig. 14.

The two curves for the negative-pion beam at positions 1 and 2 corresponding to the peak and halfway down the falling portion of the depth-dose distribution curve are similar, thereby suggesting that the ionization density distributions at and beyond the peak of the negative-pion depth-dose curve may be similar. On the other hand, the curve corresponding to the position 3 halfway up the rising slope of the depth-dose curve falls below curves 1 and 2 with increasing threshold setting, thereby suggesting that the contribution from high ionization densities at that point is considerably less than at the other two points. As expected, the fractional dose for threshold settings greater than 10 MeV at position 4 of the positive-pion peak falls to zero quickly, as there are no stars contributing to the dose here. For the detector thickness used (3 mm), pulses greater than about 9 MeV cannot be due to the passage of pions through the detector. For negative pions, pulses greater than 9 MeV are definitely due to star formation and, as can be seen from Fig. 14, the stars contribute about 60% of the dose at the Bragg peak position.

It will be better to use thin detectors for measuring the depth-dose distribution because of the narrow width of the region where negative pions produce stars ($\approx$ 4 cm of water). Improvements in the linearity of the system are being made so as to permit use of thinner detectors. The depth-dose curve for a pure pion beam can be obtained by using a threshold Cerenkov counter in anticoincidence with the semiconductor detector so that the particles with velocities greater than pions (i.e., muons and electrons) will not be counted. Work in this direction is also in progress.

The electron contamination in the pion beam can be reduced considerably by using electrostatic separators; however, the existing muon contamination is relatively difficult to eliminate because its mass is nearly that of pion. Muons will deliver some radiation dose beyond the region of interest. The best way to minimize the muon contamination of the pion beams is to keep the experimental area a close to the target as possible. This will decrease the flight path of the pions, and hence fewer pions will decay into muons.

The results of the physical measurements and calculations indicate that the negative-pion beams may find a good place in radiation therapy. As mentioned before, the intensity of the presently available pion beams is two orders of magnitude lower than that needed for therapeutic application. Construction of machines that produce the necessary intensities is being planned, and one such machine is being considered for Los Alamos Scientific Laboratory with a special biomedical facility.

References

1. J. H. Lawrence, P. C. Abersold, and E. O. Lawrence, Comparative Effects of X-rays and Neutrons on Normal and Tumor Tissue, Proc. Natl. Acad. Sci. U.S. 22:543 (1936).
2. J. F. Fowler, Neutrons in Radiotherapy: Slow Neutrons, Fast Neutrons and Other Heavy Particles, Biological Effects of Neutron and Proton Irradiation, Vol. II, IAEA, page 185 (1964).
3. M. R. Raju, Heavy Particle Studies Using Silicon Detectors, USAEC Report, UCRL-16354, Lawrence Radiation Laboratory, August 1965; also in Proceedings of the Workshop Conference on Space Radiation Biology, Berkeley, California, Sept. 1965 (to be published in Rad. Res.).
4. The Omnitron – A Multipurpose Accelerator, USAEC Report, UCRL-16828, Lawrence Radiation Laboratory, July 1966.
5. P. H. Fowler and D. H. Perkins, The Possibility of Therapeutic Applications of Beams of Negative π-Mesons, Nature 189: 524 (1961).
6. M. R. Raju, H. Aceto, and C. Richman, Pion Studies with Silicon Detectors, Nucl. Instr. Methods 37: 152 (1965).
7. C. Richman, H. Aceto, M. R. Raju, and B. Schwartz, The Radiotherapeutic Possibilities of Negative Pions, Am. J. Roentogenol. Radium Therapy Nucl. Med. XCV1: 777 (1966).
8. M. R. Raju, E. J. Lampo, S. B. Curtis, J. M. Sperinde, and C. Richman, Lithium-Drifted Silicon Detector Used as a Pulse Dosimeter, USAEC Report, UCRL-16924, Lawrence Radiation Laboratory, Sept. 1966; also presented at the 13th Nuclear Science Symposium on Instrumentation in Space and Laboratory, Boston, Massachusetts, Oct. 19-21, 1966 (proceedings to be published by IEEE).
9. Henry Aceto, A Feasibility Study of the Therapeutic Possibilities of π-Mesons, USAEC Report, UCRL-11482, Lawrence Radiation Laboratory, June 1964.
10. P. H. Fowler, π Mesons Versus Cancer, Proc. Phys. Soc. (London) 85: 1051 (1965).
11. P. Ammiraju and L. M. Lederman, Diffusion Chamber Study of Very Slow Mesons. IV. Absorption of Pions in Light Nuclei, Nuovo Cimento 4: 283 (1956).
12. S. B. Curtis, M. R. Raju, and C. Richman, to be published.
13. J. Baarli, Radiological Physics of Mesons, to be published in the Proceedings of the Work Shop Conference on Space Radiation Biology, Berkeley, California, Sept. 1965 (to be issued as a Special Supplement to Rad. Res.).
14. T. R. Overton, Experience with a Linear Energy Transfer (LET) Chamber at CERN, CERN Report CERN 66-33, October 1966.
15. G. M. Tisljar-Lentulis, Method for Measurement of Ionization Curves by Means of Scintillation Counters, Rev. Sci. Instr. 37: 291 (1966).

Table 1. Energy partition for π^- capture in water.

	MeV
Rest mass of π^-	139.6
Average binding energy	40.0
Kinetic energy	
$Z > 2$	4.5 ± 0.5
$Z = 2$	8.0 ± 0.4
$Z = 1$	16.5 ± 0.6
Neutrons	70.0
	139.0

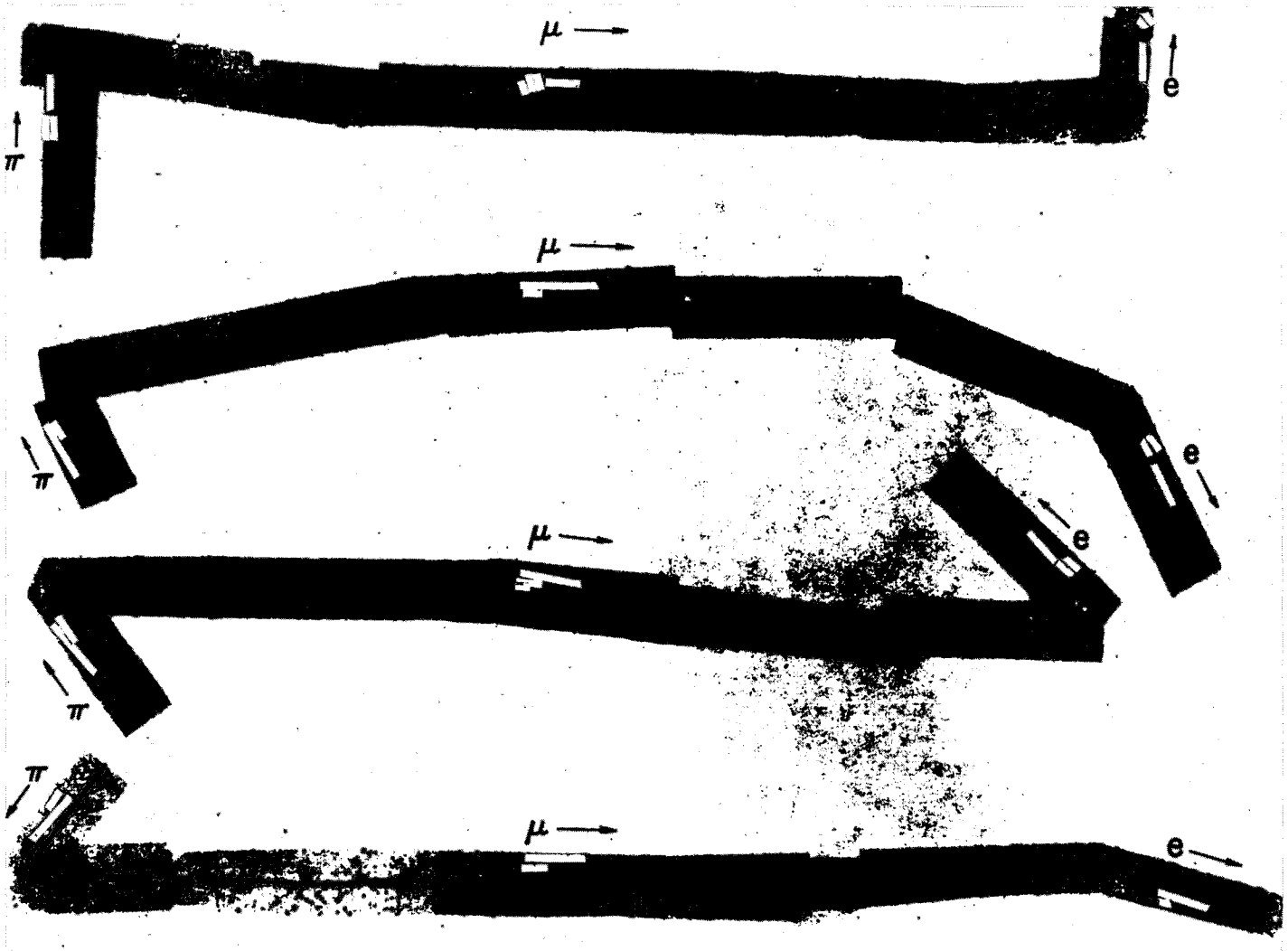

Fig. 1. Examples of π^+ decay as observed in nuclear emulsions. From C. F. Powell, P. H. Fowler, and D. H. Perkins, The Study of Elementary Particles by the Photographic Method, p. 669, Pergamon Press, N. Y., 1959.

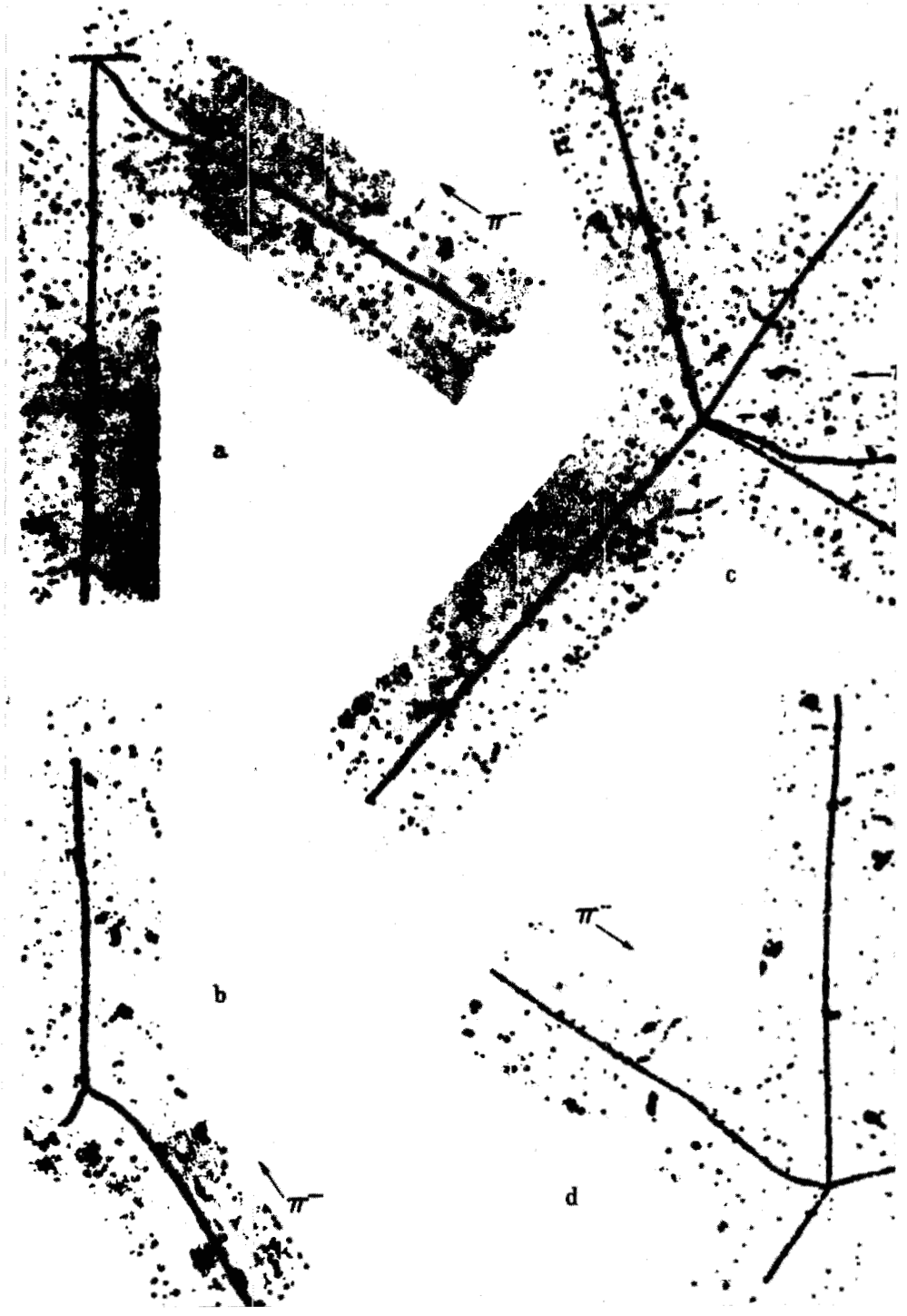

Fig. 2. Disintegration of light elements carbon, nitrogen, or oxygen by nuclear capture of π^- mesons as observed in nuclear emulsions. The pion tracks are labelled π^-; the stars produced following their capture have various numbers of prongs. From C. F. Powell, P. H. Fowler, and D. H. Perkins, The Study of Elementary Particles by the Photographic Method, p. 669, Pergamon Press, N. Y., 1959.

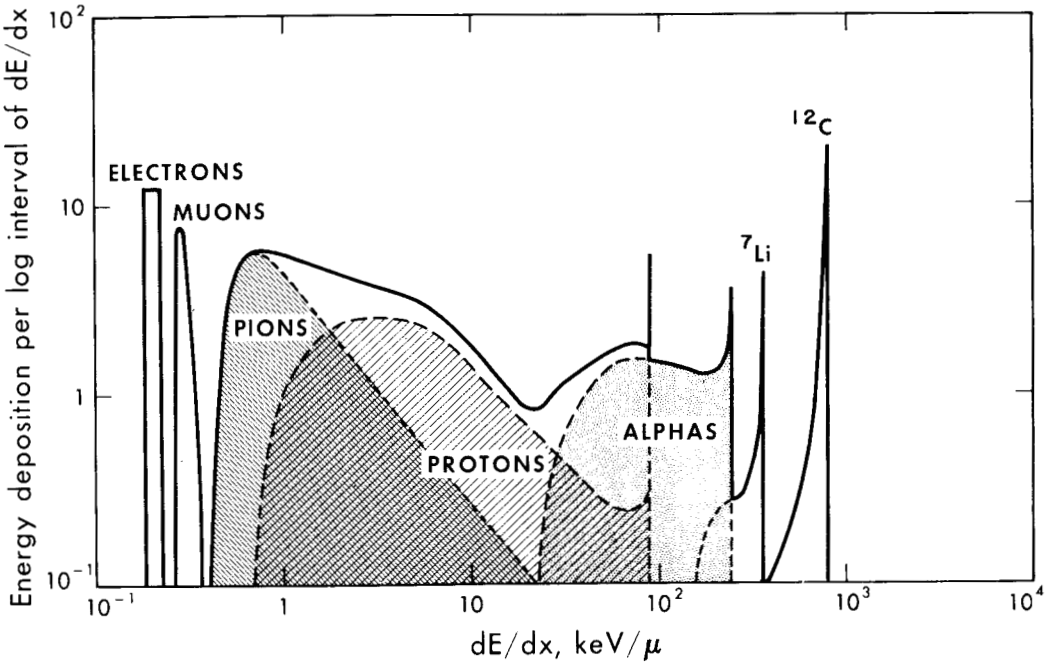

Fig. 3. Calculated energy-loss distribution at a point in the stopping negative-pion region in 25.5 cm of water. P = 190 ± 5 MeV/c.

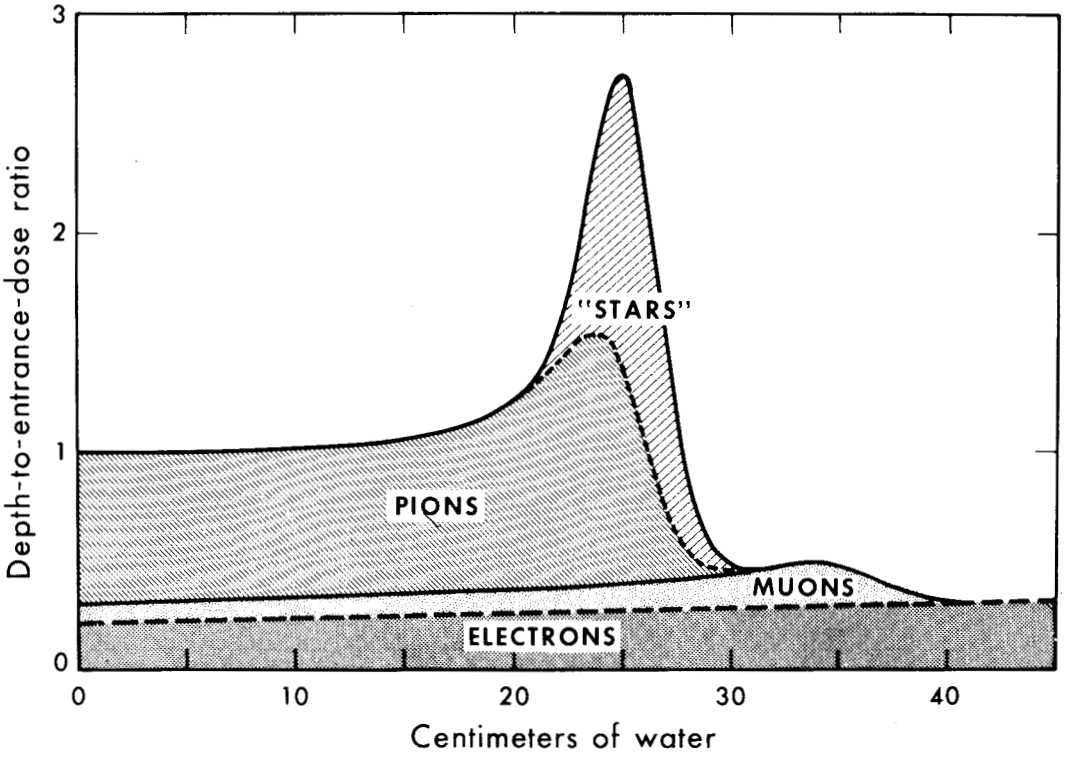

Fig. 4. Calculated central-axis depth-dose distribution of negative-pion beam with its contaminants in water. P = 190 ± 5 MeV/c. Incident beam is 65% pions, 25% electrons, and 10% muons.

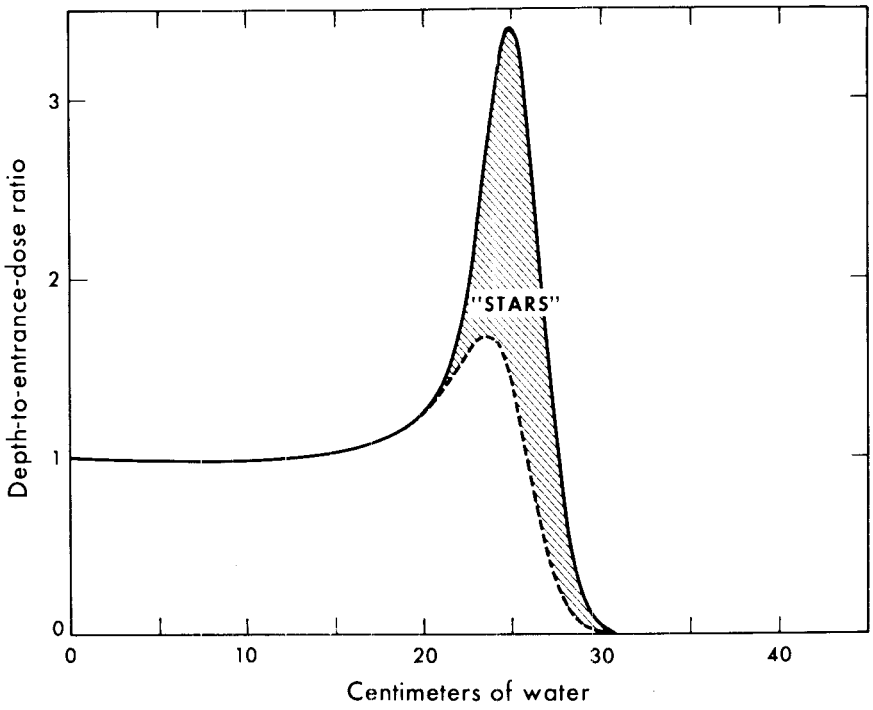

Fig. 5. Calculated central-axis depth-dose distribution in water of pure negative-pion beams. P = 190 ± 5 MeV/c.

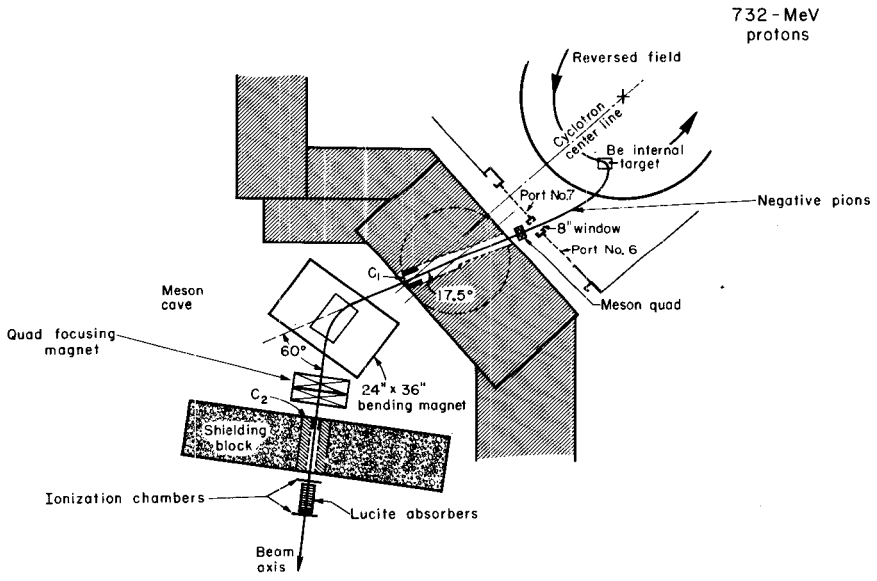

Fig. 6. Experimental setup for producing a negative-pion beam. For producing a positive-pion beam, all the magnetic fields and the direction of the proton beam are also reversed.

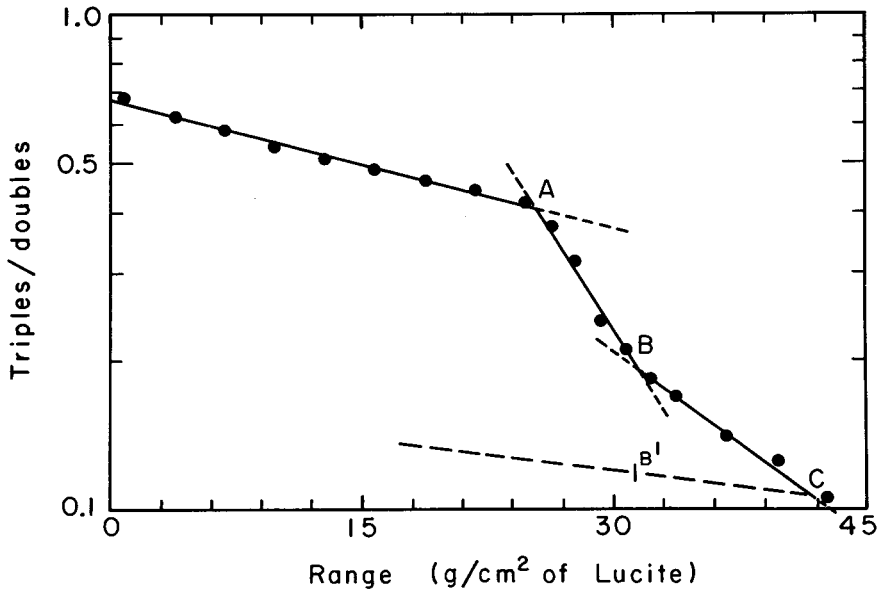

Fig. 7. Integral range curve of a negative 100-MeV pion beam.

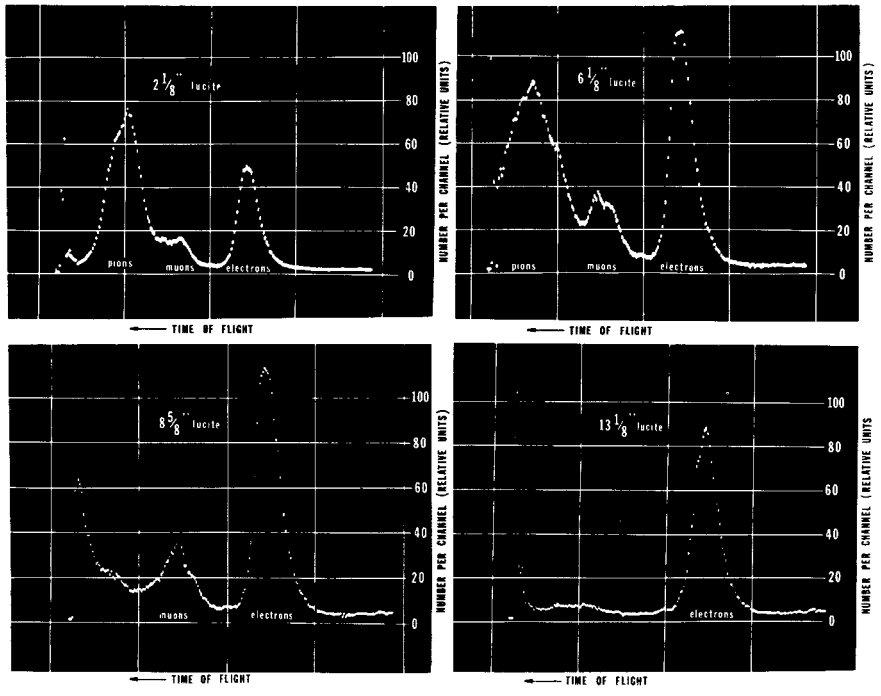

Fig. 8. Time-of-flight pictures of pion beam with its contaminants after passing through 2-1/8, 6-1/8, 8-5/8, and 13-1/8 inches of Lucite.

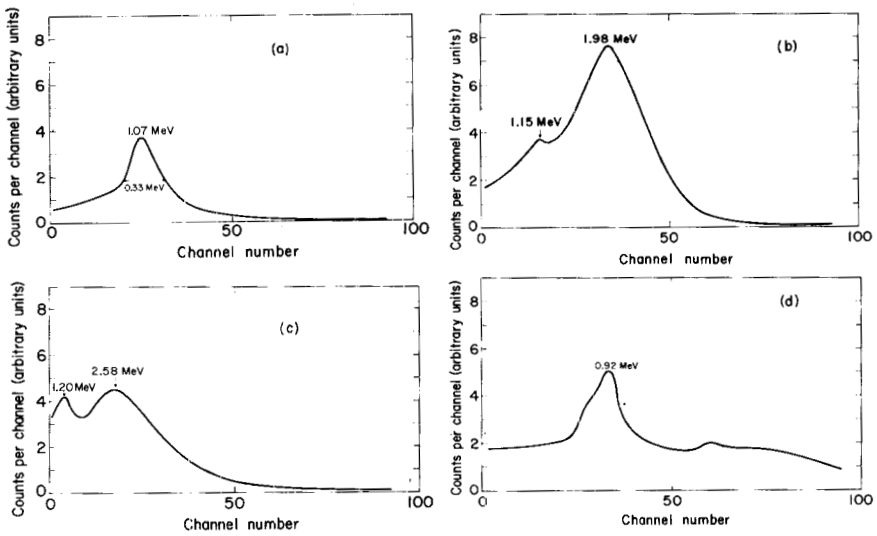

Fig. 9. Pulse-height spectra from lithium-drifted silicon detector for a 95-MeV π^+ beam after passing through various thicknesses of Lucite. (a) Direct beam; (b) beam degraded by 7.5 inches of Lucite; (c) beam degraded by 8.5 inches of Lucite; (d) beam degraded by 9.5 inches of Lucite and 3/8 inch of copper.

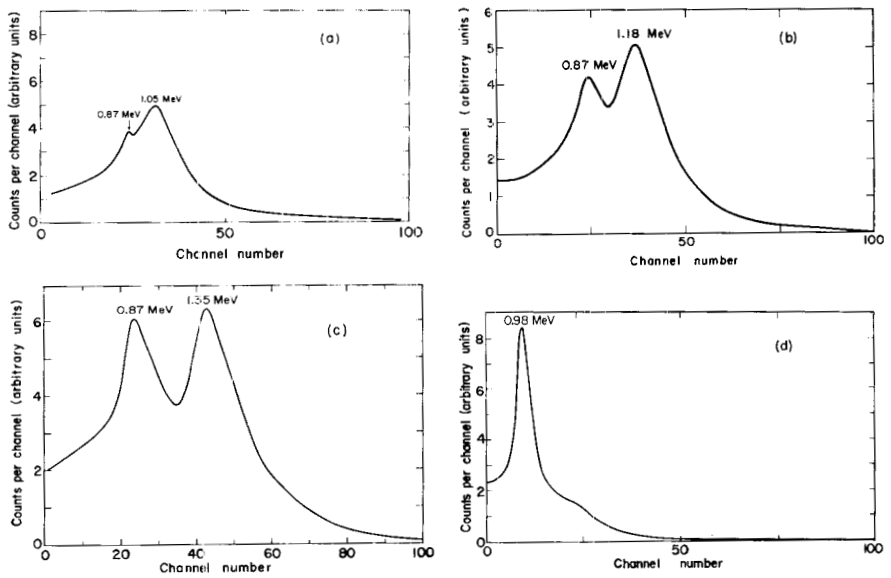

Fig. 10. Pulse-height spectra from a lithium-drifted silicon detector for a 95-MeV π^- beam with its contaminants after passing through various thicknesses of Lucite. (a) Direct beam; (b) beam degraded by 3 inches of Lucite; (c) beam degraded by 5 inches of Lucite; (d) beam degraded by 10 inches of Lucite.

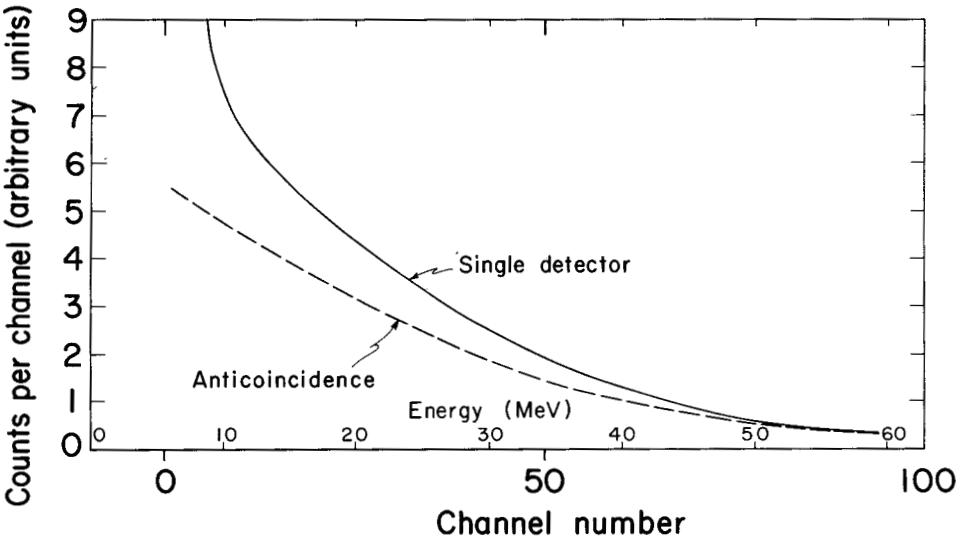

Fig. 11. Energy distribution of the negative-pion endings in silicon; this is very nearly the energy distribution of the pion stars. The curve without the anticoincidence detector includes the pulses of particles passing through but not stopping in the analyzer detector.

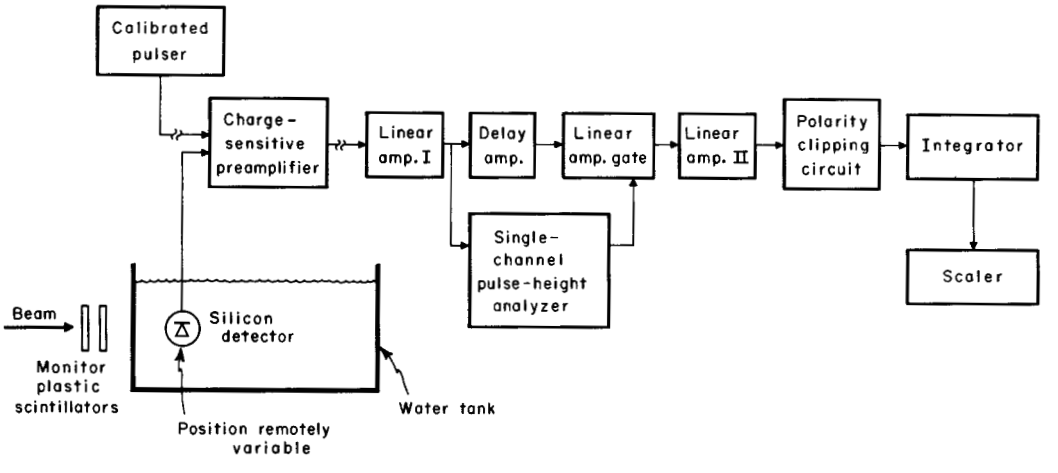

Fig. 12. Block diagram of the pulse radiation dosimeter setup.

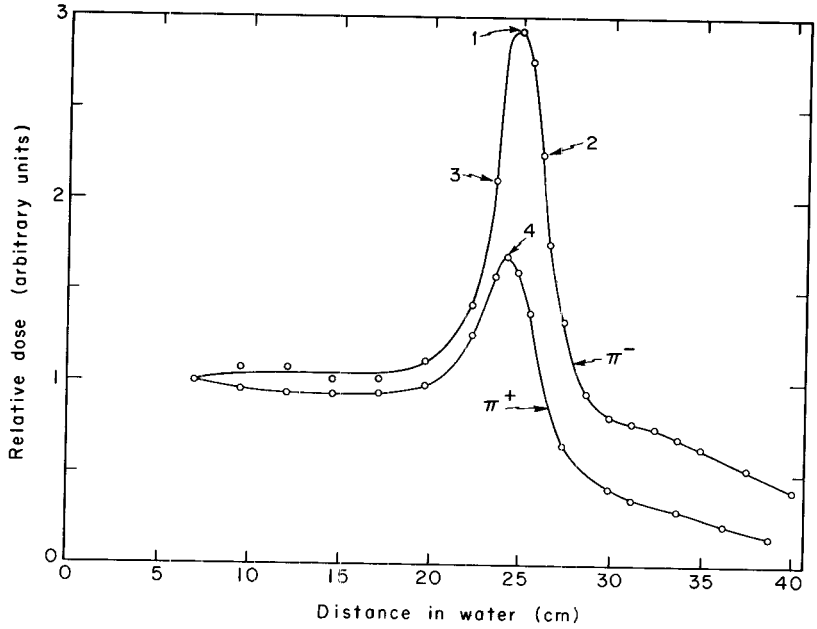

Fig. 13. Measured central-axis depth-dose distribution of 190-MeV/c π^+ and π^- beam in water.

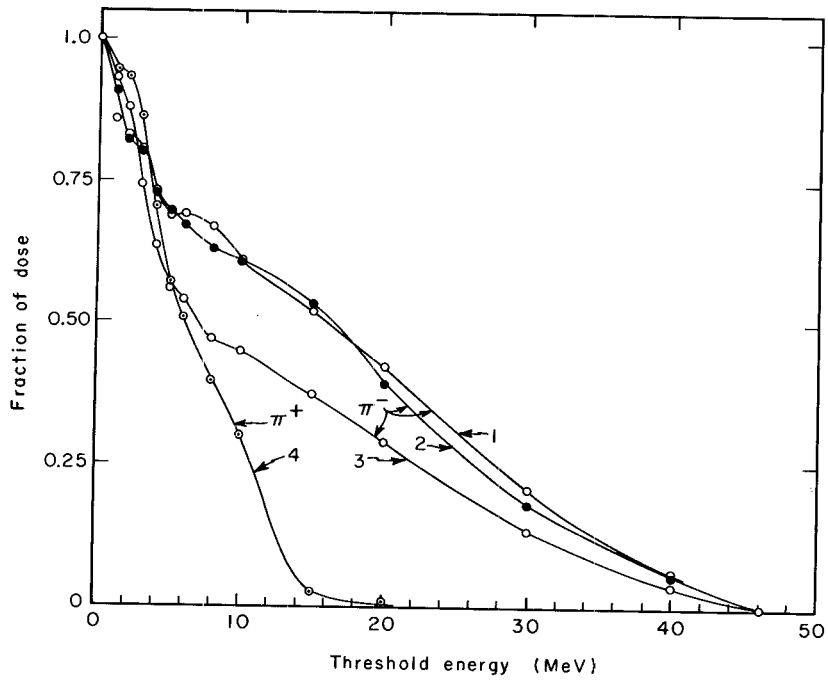

Fig. 14. Fraction of dose due to particles depositing energies higher than the threshold energy setting, shown as a function of threshold energy.

PION RADIOBIOLOGY

J. M. Feola, W. D. Loughman, and S. P. Richman

Donner Laboratory and Lawrence Radiation Laboratory
University of California, Berkeley, California

Fowler,[1] Fowler and Perkins,[2] Aceto,[3] and Richman[4,5] have suggested that negative pions (π^- mesons) might have applications in radiotherapy, provided that a beam of sufficient intensity could be made available. According to these authors, π^- beams should have a low ratio of surface dose to depth dose, a diminished oxygen enhancement ratio, and probably a high relative biological effectiveness.

Negative pions have the unusual property of being captured by an atomic nucleus when they come to rest in matter. In tissue, pion capture by the light elements (carbon, nitrogen, and oxygen) results in nuclear disintegration and a yield of short-range charged particles, mostly α particles and protons. This additional energy causes an enhancement of the ionization at the end of a charged particle's range over that given by the usual Bragg peak in a graph of ionization versus range. Furthermore, by choosing the pion energy properly, pions can be made to stop at a preselected distance within the volume to be treated. In the following discussion, the initial portion of the ionization curve will be called the "plateau" region and the portion of increased ionization near the end of the pion's range will be called the "peak" region.

Artificially produced π^- beams have been available since 1948, but biological investigations using π^- mesons were not performed until 1963. At that time, Micke et al.[6,7] used the 7- to 9-GeV π^--meson beam from the Brookhaven alternating-gradient synchrotron to irradiate seeds of Zea mays. Despite the low dose rate of tenths of rads per minute, these workers obtained an RBE of 3.23 for non-Bragg-peak π^- mesons.

In 1964 K. Sillesen and Y. Schmidlin, working in this Laboratory, attempted to measure pion RBE and the oxygen effect by irradiating mouse ascites tumors (lymphoma) in vivo. Initial difficulties with pion dosimetry and cell transplantation precluded definitive statements.

The physical characteristics of the π^- beam used by us in this and previous work are described elsewhere in these Proceedings, so that no details are given here. Figure 1 shows the setup for mice irradiations under temperature-controlled conditions, but a similar arrangement was used for the radiobiological experiments to be described below. Loughman et al.[8] also used LAF_1 mice carrying the L#2 lymphoma as an ascites tumor to study some cytological effects of the negative pions at plateau and at peak. Mice exposed in the plateau region received 65 to 80 rads, with the beam estimated to contain about 64% pions. Mice exposed in the peak region received 80 to 95 rads, with the beam estimated to contain less than 50% pions.

Lymphoma cells aspirated from mice at various times following pion irradiation were examined cytologically. Four characteristics were scored: mitotic index, frequency of polyploid metaphase cells, frequency of anaphase cells displaying "bridges," and chromosome counts of metaphase cells. Determinations of mitotic index indicate that it decreases with increasing age of tumor. An immediate drop in mitotic index is seen after irradiation, followed by an increase, reaching control values on about the second day after irradiation. Polyploid cells, usually approximately tetraploid, increased in frequency shortly after irradiation, and subsequently decreased to near control values. For at least 6 days following irradiation the frequency of polyploid metaphase cells in tumors exposed in the "star" region of the beam exceeded that in tumors exposed in the plateau region (see Fig. 2).

Anaphase "bridges," irrespective of type, increased in frequency following irradiation and then decreased to control values 5 to 6 days later. The frequency of bridges in lymphoma cells exposed in the star region exceeded that seen in cells exposed in the plateau region (see Fig. 3). Aneuploidy is increased following irradiation, with a larger spread of chromosome numbers per cell in tumors exposed in the star region than in the plateau region of the beam. Chromatid breaks and metacentric chromosomes, which were sometimes seen in the irradiated cells, were never seen in the controls. The irradiated cells showed an increased percentage of cells with multiple nuclei, micronuclei, and giant and bizarre nuclei. At 6 days following irradiation, the irradiated cells showed more karyorrhexis than did controls, and cells with multiple micronuclei were common.

The incidence of polyploidy and anaphase bridges was about five times as high in cells exposed in the star region of the beam as in cells exposed to the plateau region. It is difficult to interpret these findings in terms of RBE. However, since the radiation doses from plateau and star regions were similar, it would seem that star-region negative pions have a greater RBE than those in the plateau region.

In order to gain more information about the π^- beam, S. Richman et al.[9] used the Vicia faba root meristem because of its simplicity and sensitivity to relatively low doses (100 to 400 rads) of radiation. The roots were irradiated in water-filled Lucite boxes in the plateau region and at peak. Compressed air was bubbled through the boxes during the irradiation, which took about 20 hours. A dose of 100 rads was measured at plateau with LiF dosimeters calibrated with ^{60}Co γ rays. A peak-to-plateau ionization ratio of 1.5 was measured, so that the dose at peak was approximately 150 rads. Results of these experiments are summarized in Figs.4, 5, and 6. The primary cytological test was the scoring of abnormal anaphases. The word "anaphase" in Fig. 4 is in quotes because cells that were well in telophase were included in the scoring. This was simply a count of the number of anaphases containing bridges and fragments expressed as a percentage of the total anaphases seen. The fragments appearing at anaphase form micronuclei at telophase. These micronuclei remain in the cell for some time, and Fig. 5 shows the number of meristem cells containing one or more micronuclei as a function of fixation time after irradiation.

Figure 6 shows the results of two growth-rate experiments. Six days after irradiation the rate from peak irradiation dropped to about 0.45 and that from the plateau to about 0.75 of the control rate.

Although the dose at peak is greater than that at plateau, the significant differences found in the bean root tests seemed to indicate a higher RBE for the negative pions at peak than for the π^- at plateau. These results encouraged new experiments with the murine lymphoma cells.

The techniques used in preliminary studies on the effect of heavy particles on the proliferative capacity of ascites tumor cells grown in vivo[10, 11] were improved until a good degree of reproducibility and accuracy was attained.[12] An experiment was performed to gain information relative to the oxygen effect.[13] It was done without environmental control, attempting to detect the effect of anoxia on the surviving fractions of cells irradiated in vivo in the plateau region and at peak as described above. In this experiment four mice were exposed in each region, two of which had 3-day-old tumors (supposedly well oxygenated), and the other two had 7-day-old tumors (supposedly more anoxic). The irradiated cells were injected into 510 LAF_1 female mice at various dilutions.

The doses were measured with LiF dosimeters (^{60}Co calibration) distributed in front and back of the mice holders at peak and plateau. Since the LET of the pions in the plateau region is ≈ 1 keV/μ, LiF dosimetry is applicable. The situation in the peak region is more complicated,[14] and consists of a distribution of high-LET radiation. The ratio of ionization measurements at peak and plateau were taken as approximate dose ratios. This question is still open and is being investigated further. Proliferative capacity was evaluated at the end of 8 weeks by the percentage of animals developing tumors. LD_{50}'s (the number of cells necessary to produce tumors or death in 50% of the animals) and 95% confidence intervals were calculated by the method of Litchfield and Wilcoxon,[15] and surviving fractions were calculated by comparison with control groups. No difference was found due to anoxia, and the results were pooled and are as follows:

The surviving fraction (SF) in the plateau (PL) and the peak (PK) for a dose in the plateau of 150 ± 30 rads and a peak-to-plateau ratio of 1.3 were

$$(SF)_{PL} = 0.14 \pm^{0.24}_{0.05} \qquad 150 \pm 30 \text{ rads},$$

$$(SF)_{PK} = 0.03 \pm^{0.04}_{0.01} \qquad 195 \pm 45 \text{ rads}.$$

This gives a plateau-to-peak ratio of 4.7. Although this ratio suggested the greater effectiveness of the peak in impairing the tumor-forming ability of the lymphoma cells, the large standard errors shown above, and the fact that no estimation of the RBE was possible, encouraged further research aimed at obtaining survival curves.

Using the same animals and cells, Loughman et al.[16] confirmed the higher frequency of polyploid cells and anaphase bridges produced at the pion-stopping region than at plateau, as previously reported.[8]

Improved dosimetry,[17] as well as a better knowledge of the situation in the peak region, showed the possibility of using eight animals instead of four in this important position. Control of the environment was desirable. Accordingly,

two wooden boxes with Lucite ends for holding mice in place were used, one for the mice to be irradiated in the beam, and the other for control mice. The temperature of the air circulating through both boxes was continuously recorded and maintained at 21.5 ± 0.5°C by a thermostat with heater and blowers.

Lucite holders were built to hold eight mice each. Three of these holders were used for groups at peak and plateau regions of the π^- beam, and for the control group.

Twenty-four LAF_1 mice, 15 weeks old (Jackson Laboratory, Bar Harbor, Maine), were used in this experiment. The mice were maintained with wet food during the irradiation, which took 40 hours, and had four equally spaced 1-hour rest periods for eating and drinking at will.

Figure 7 shows the arrangement inside the temperature-controlled irradiation box. The π^- beam entered from the right and passed through 3 in. of Lucite absorber and through the holder with the "plateau" mice. After 4 in. more of Lucite the π^- beam entered the "peak" holder. The Jordan dosimeter is placed behind 1/2 in. of Lucite adjacent to the last holder and serves as a second monitor. The holder with the control mice is also shown. In the actual experiment this holder was in a separate temperature-controlled box away from the beam.

All the mice were injected with 10^6 L#2 lymphoma cells 3 and 5 days prior to the beginning of irradiation. The animals bearing 3-day-old tumors at the beginning of the experiment were used by Loughman et al. for their cytological studies, and the mice starting with 5-day-old tumors were used by Feola et al. to test the tumor-forming ability of the lymphoma cells after irradiation. The procedures followed have been summarized above, and complete results will be published elsewhere.[18,19] The total doses at plateau ranged from 145 to 250 rads, and the doses at peak ranged from 220 to 380 rads.

A parallel experiment using ^{60}Co γ rays was done using two dose-rates: 5 R/hr and 12.5 R/hr. The mice were kept in the holders for the same length of time as in the pion experiment to keep the stress the same. The doses ranged from 50 to 500 rads. A special irradiation was done at 20 R/hr to test the linearity of polyploidy induction up to the 1000-rad level.

Results of the cytological studies are summarized in Fig. 8. The RBE for the negative pions at peak was obtained by the ratio of the slopes of the lines shown, taking ^{60}Co γ rays as baseline. The RBE for the pions at peak (star-forming and high-LET pions), as well as the RBE for the star-forming pions, are calculated assuming an RBE = 1 for muons and electrons relative to ^{60}Co γ rays. The estimation of RBE's based on polyploidy induction gives

Beam	RBE
Star + π^- + μ^- + e^-	2.15
Star + π^-	2.37
Star only	3.64

If muon and electron dose contributions were underestimated, the RBE values for pions only and for stars only would be overestimated.

Survival curves for ^{60}Co γ rays and for peak negative pions, based on the tumor-forming ability of lymphoma cells, are given in Fig. 9.

The ratio of D_0 from the ^{60}Co data and D_0 from the pion peak region data gives an RBE of 5.4 ± 1.8 in the peak region relative to γ rays.

If an RBE of 0.8 is assumed for γ rays relative to x rays,[20,21] the RBE of the pions at peak becomes 4.3 ± 1.8 relative to x rays.

The biological experiments described in the foregoing paragraphs, although somewhat lacking in sophistication and precision, definitely indicate a higher RBE for peak-region π^- than for plateau-region π^-. The estimated RBE values, obtained in both plant and animal cell systems by observation of both cell-lethal and nonlethal effects, range from about 2 (Loughman 1966) to about 5 (Feola, 1966).These values were obtained with a low-intensity beam heavily contaminated with low-RBE particle fluxes, i.e., muons from pion decay and electrons present in the original beam as well as those originating from pion decay. The RBE estimates of Loughman[18] for a pure pion beam suggest that removal of contaminating particles by special devices (e.g., electrostatic separators) may increase peak-region pion RBE by approximately 10%. Additionally, narrowing the beam's momentum spectrum should result in a "sharper" Bragg peak region, further increasing peak-region pion RBE to an estimated maximum of 60% or so. This would result from an increase in the concentration of star events per unit volume in the Bragg peak.

If these increases can be attained in therapeutically practical π^- beams of higher intensity, then RBE figures for peak-region pions might range from about 3.5 for some non-cell-lethal effects (with considerable cell death present) to about 8.5 for cell-lethal effects. The energy deposition in tissue may be 50 to 100% more in the peak region than in the plateau region (Raju[17]). This fact, coupled with the high-peak-region RBE, may result in cell-lethal effects in the peak region which could be 17 or more times as high as in the plateau region, in "clean" negative pion beams.

The peak region's high LET (Curtis, these Proceedings) implies that the presence or absence of oxygen in tissues should have little effect on cell lethality. That is, π^- radiation in the peak region should be relatively free of the "oxygen effect" which protects hypoxic cells. The combination of advantages possible in π^- beams--high depth-to-surface dose ratio, high depth-to-surface RBE ratio, and oxygen-effect independence--suggest that π^- beams may have very high utility in tumor radiotherapy.

References

1. P. H. Fowler, 1964 Rutherford Memorial Lecture: Pi-Mesons Versus Cancer?, Proc. Phys. Soc. (London), 85: 1051 (1965).

2. P. H. Fowler and D. H. Perkins, The Possibility of Therapeutic Applications of Beams of Negative π^- Mesons, Nature, 189: 524 (1961).

3. Henry Aceto, Jr., A Feasibility Study of the Therapeutic Possibilities of π^- Mesons (Ph. D. Thesis), USAEC Report UCRL-11482, Lawrence Radiation Laboratory, June 1964.

4. C. Richman, H. Aceto, Jr., M. R. Raju, B. Schwartz, and M. Weissbluth, On the Dosimetry of Negative Pions with a View Toward Their Trial in Cancer Therapy, in Semiannual Report: Biology and Medicine, Donner Laboratory, USAEC Report UCRL-11387, pages 114-126, Lawrence Radiation Laboratory, July 1964.

5. C. Richman, H. Aceto, Jr., M. R. Raju, and B. Schwartz, The Radiotherapeutic Possibilities of Negative Pions, Am. J. Roent., 96: 777 (1966).

6. A. Micke, H. H. Smith, R. G. Woodley, and A. Maschke, Relative Cytogenetic Efficiency of Muons and Mesons in Zea mays (L.) and Its Modification by Postirradiation Storage, Radiation Res., 23: 537-550 (1964).

7. A. Micke, H. H. Smith, R. G. Woodley, and A. Maschke, Relative Cytogenetic Efficiency of Muons and π^- Mesons in Zea mays (L.), Proc. Natl. Acad. Sci. U.S., 52: 219 (1964).

8. W. D. Loughman, H. S. Winchell, H. Aceto, Jr., C. Richman, M. R. Raju, and J. H. Lawrence, Differential Cytologic Effects of Negative Pion Beams in Plateau and "Star" Regions: Preliminary Report, in Semiannual Report: Biology and Medicine, Donner Laboratory, USAEC Report UCRL-16246, pages 100-102, Lawrence Radiation Laboratory, July 1965.

9. S. P. Richman, C. Richman, M. R. Raju, and B. Schwartz, Studies of Vicia faba Root Meristems Irradiated with a π^- Beam, in Semiannual Report: Biology and Medicine, Donner Laboratory, USAEC Report UCRL-16613, pages 15-22, Lawrence Radiation Laboratory, Jan. 1966.

10. K. Sillesen, J. H. Lawrence, and J. T. Lyman, Heavy-Particle Ionization (He, Li, B, Ne) and the Proliferative Capacity of Neoplastic Cells "in vivo", Acta Isotopica, 3: 107-126 (1963).

11. Y. Schmidlin, J. H. Lawrence, K. Sillesen, G. Welch, and J. Lyman, Effect of Heavy Particles on the Proliferative Capacity of Ascites Tumor Cells (Lymphoma) Grown in vivo, in Semiannual Report: Biology and Medicine, Donner Laboratory, USAEC Report UCRL-11833, pages 80-94, Lawrence Radiation Laboratory, Dec. 1964.

12. J. M. Feola, J. H. Lawrence, and G. P. Welch, The Measurement of the Effects of X-Rays and Alpha Particles on the Proliferative Capacity of Lymphoma Ascites Tumor Cells in vivo, in preparation.

13. J. M. Feola, C. Richman, M. R. Raju, and J. H. Lawrence, Effect of Negative Pions on the Proliferative Capacity of Ascites Tumor Cells (Lymphoma L#2 Grown in vivo, in Semiannual Report: Biology and Medicine, Donner Laboratory, USAEC Report UCRL-16613, pages 23-26, Lawrence Radiation Laboratory, Jan. 1966, and Radiation Res., 27: 542 (1966).

14. M. R. Raju, H. Aceto, Jr., and C. Richman, Pion Studies with Silicon Detectors, Nucl. Instr. Methods, 37: 152-158 (1965).

15. J. T. Litchfield and F. Wilcoxon, A Simplified Method of Evaluating Dose-Effect Experiments, J. Pharmacol. Exptl. Therap., 96: 99-113 (1949).

16. W. D. Loughman, H. S. Winchell, M. R. Raju, and J. H. Lawrence, A Significant Difference in Mammalian Cell Polyploidy Induction Between Plateau and "Star" Regions of a Negative Pion Beam, in Semiannual Report: Biology and Medicine, Donner Laboratory, USAEC Report UCRL-16898, pages 11-13, Lawrence Radiation Laboratory, Fall 1966.

17. M. R. Raju, E. J. Lampo, S. B. Curtis, J. M. Sperinde, and C. Richman, Lithium-Drifted Silicon Detector Used as a Pulse Dosimeter, in Proceedings of Thirteenth Nuclear Science Symposium, Boston, Mass., Oct. 19-21, 1966, IEEE Trans. Nucl. Sci., NS-14 [1]: 559 (1967).

18. W. D. Loughman, J. M. Feola, M. R. Raju, and H. S. Winchell, RBE of π^- Beams in the Bragg Peak Region Using Polyploidy Induction in Mammalian Cells Irradiated in vivo, submitted to Radiation Res.

19. J. M. Feola, C. Richman, M. R. Raju, S. B. Curtis, and J. H. Lawrence, Effects of Negative Pions on the Proliferative Capacity of Ascites Tumor Cells (Lymphoma) Grown in vivo, to be submitted to Radiation Res.

20. J. B. Storer, P. S. Harris, J. E. Furchner, and W. H. Langham, The Relative Biological Effectiveness of Various Ionizing Radiations in Mammalian Systems, Radiation Res., 6: 188-288 (1957).

21. E. J. Hall, The Relative Biological Efficiency of X-Rays Generated at 220 kVp and Gamma Radiation from a Cobalt-60 Therapy Unit, Brit. J. Radiol., 34: 313-317 (1961).

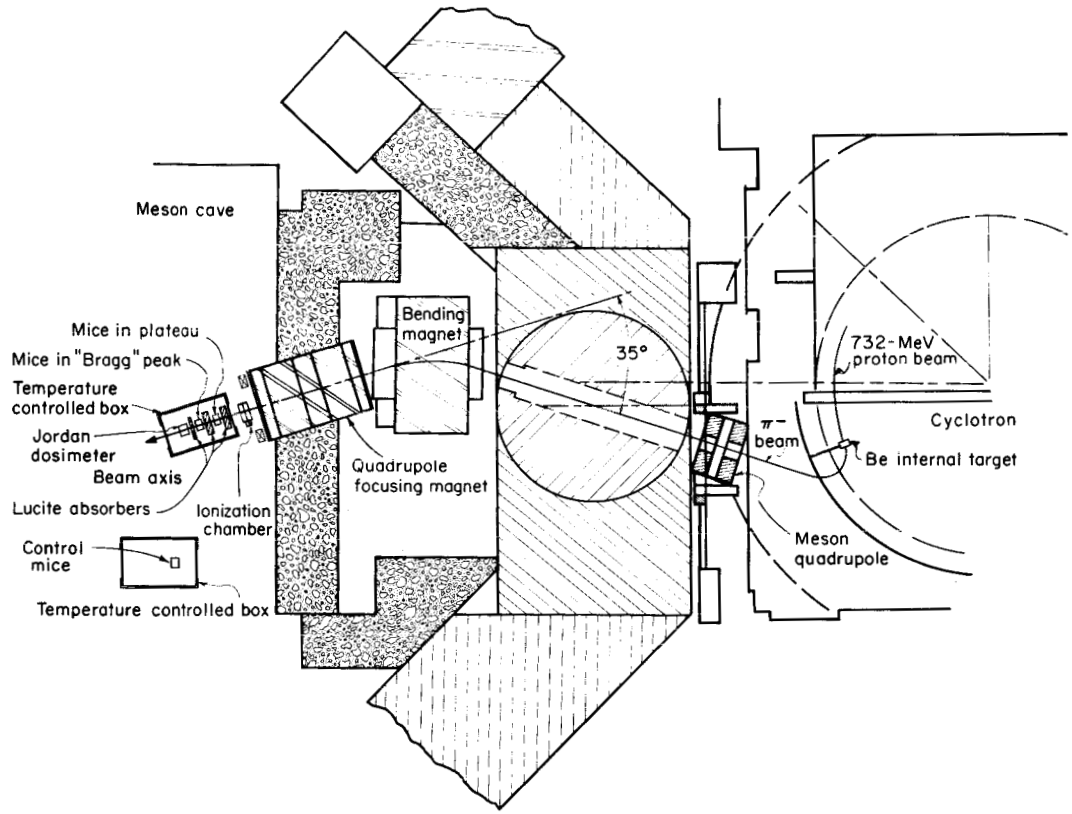

Fig. 1. Schematic drawing showing the production and focusing of the π^- beam. The positions of the ionization chamber, Jordan dosimeter, temperature-controlled boxes, and mice holders in the meson cave can be seen.

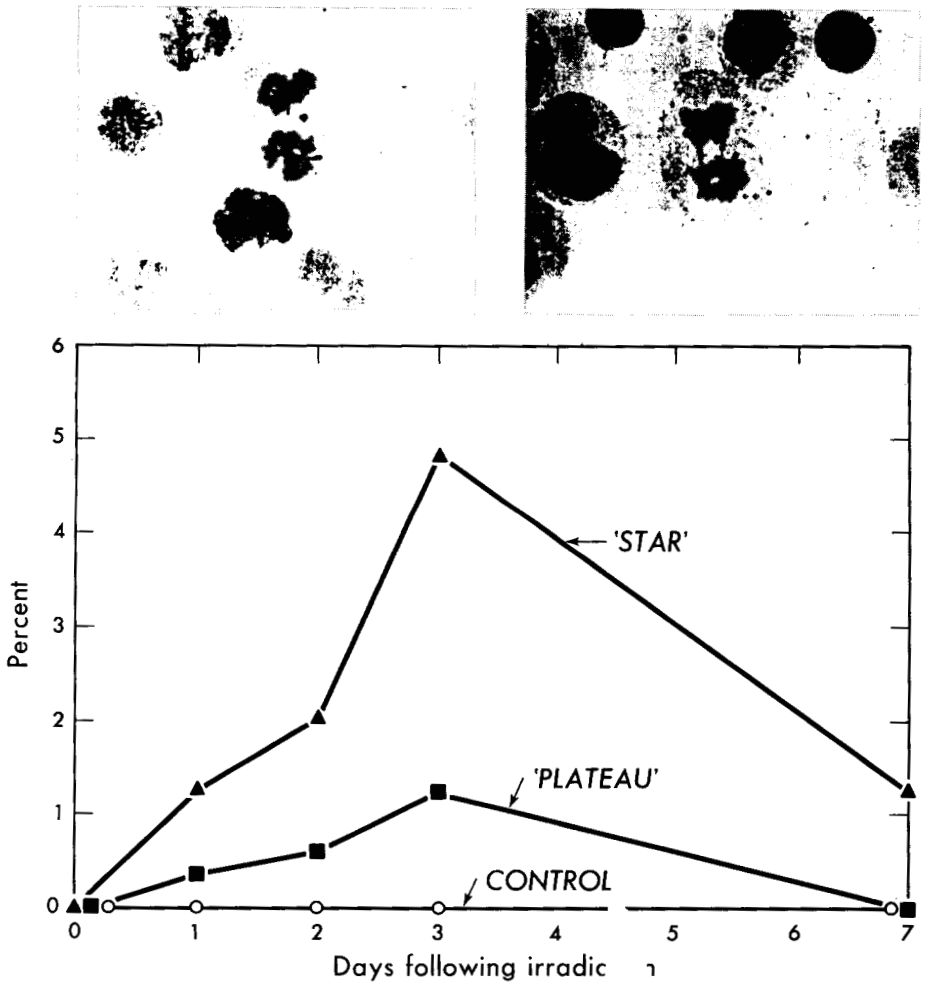

Fig. 2. Polyploid metaphase cells as a percent all metaphase cells scored in unirradiated control cells, cells exposed i: ıe plateau region of a π^- beam, and cells exposed in the "star" region Left photograph = normal Ly-2 metaphase. Right photograph = polyplo metaphase of extreme type.

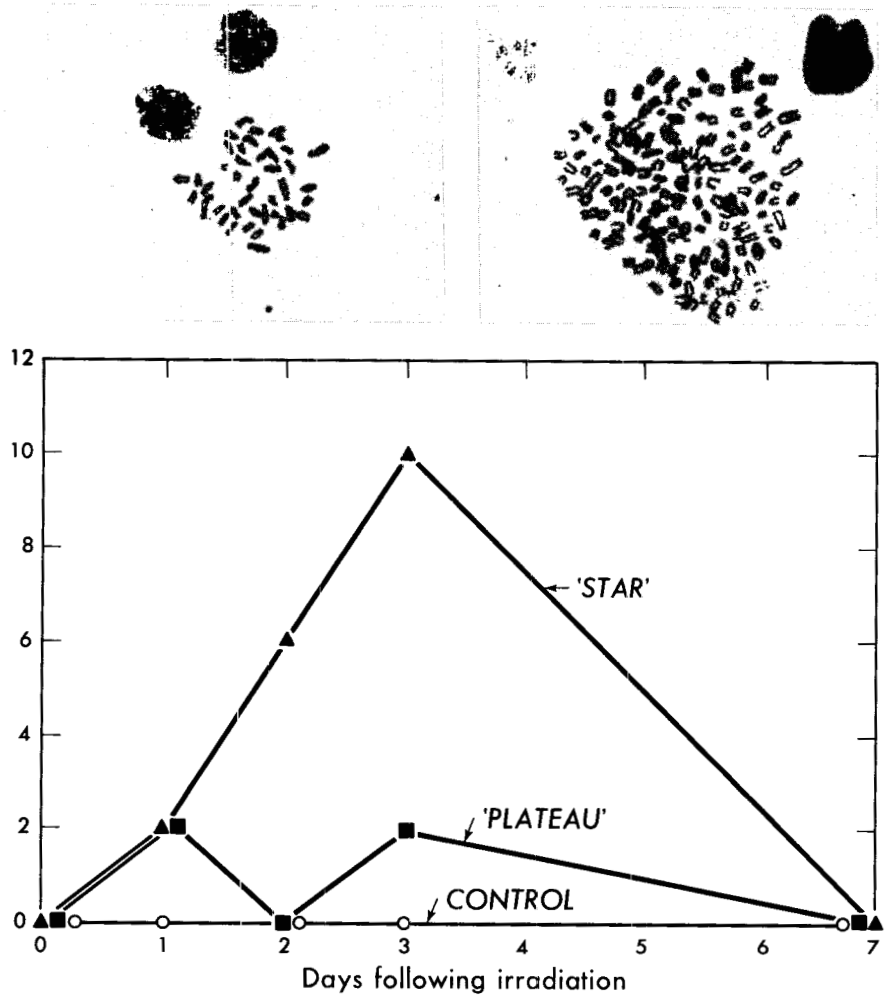

Fig. 3. Anaphase "bridges" as a percent of all anaphase cells scored in unirradiated control cells, cells exposed in the plateau region of a π^- beam, and cells exposed in the "star" region. Photographs = anaphase "bridges" found in irradiated cells.

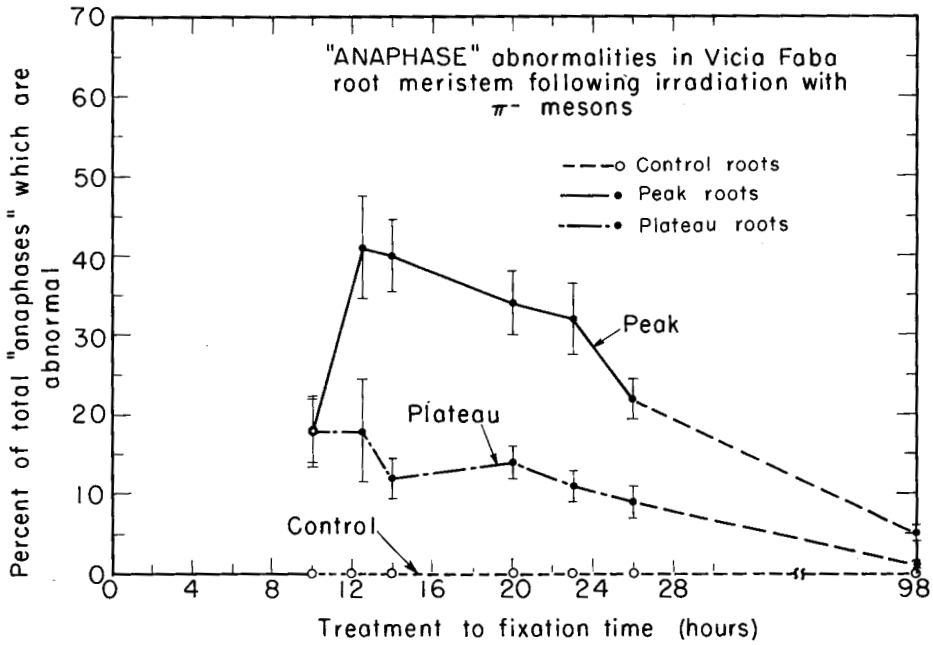

Fig. 4. The count of abnormal anaphases for the roots irradiated in the peak and in the plateau and for the control roots as a function of fixation time after irradiation. The average is 2.2:1. A second experiment gave 2.6:1.

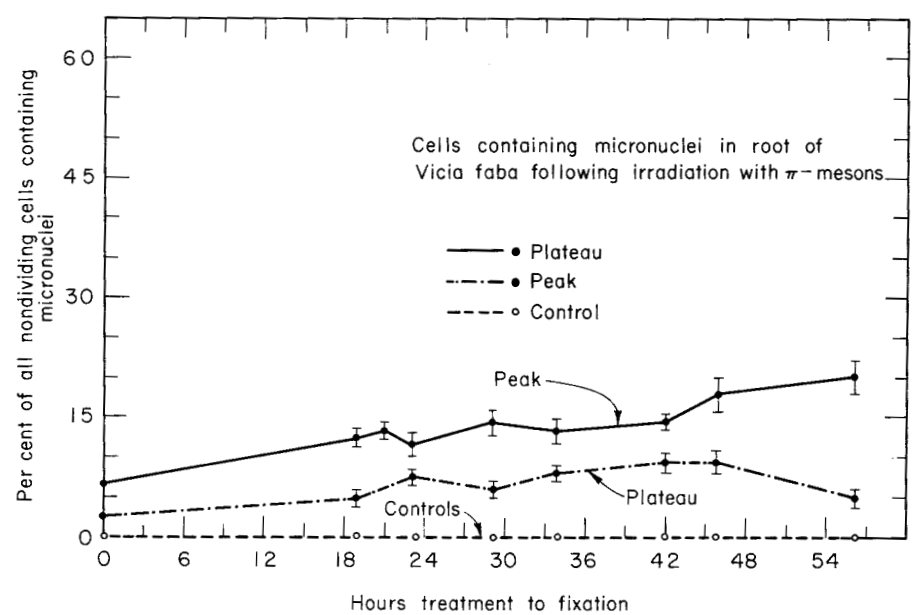

Fig. 5. The fraction of cells showing one or more micronuclei as a function of fixation time after irradiation.

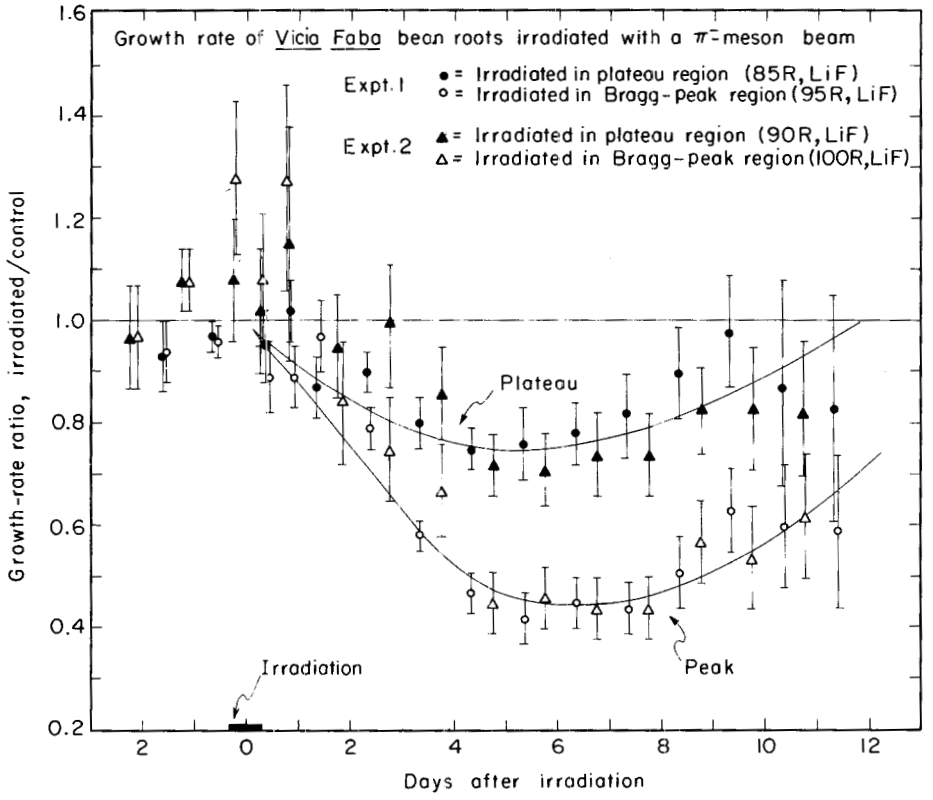

Fig. 6. The growth rate per day of roots irradiated in the peak and in the plateau of the Bragg curve compared with control roots, as a function of days after irradiation.

Fig. 7. Close-up view of mice in holders with dosimeters and absorbers. Environmental control box not shown. Pion beam enters from the right. Holder #2 is in Bragg peak position; holder #3 with the control mice is shown closer to the beam area than it was in the actual experiment.

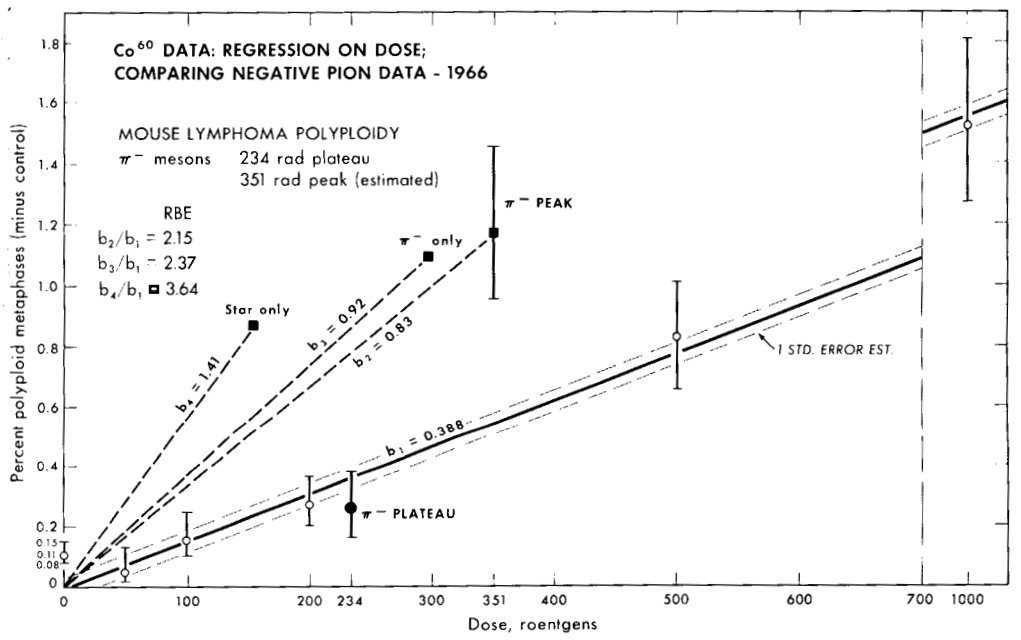

Fig. 8. Negative pion data compared with ^{60}Co data with derived estimates of RBE of negative pions.

Open circles = ^{60}Co data. Black circle and square = π^- data. Heavy line is drawn from the equation expressing the regression of polyploidy on dose: (% polyploidy) = [0.00155 (dose) - 0.0081]. Dashed line = regression line ± 1 standard error of the estimate ($S_{y.x}$ = 0.03).

Solid line = regression line from ^{60}Co data. Black squares = values of polyploidy vs dose for whole peak region π^- beam, pions only in peak region, and "stars" only in peak region. Respective RBE values are ratios of slopes of dashed lines to the solid (^{60}Co) line. Slopes of relevant lines are represented by b_1, b_2, b_3, and b_4.

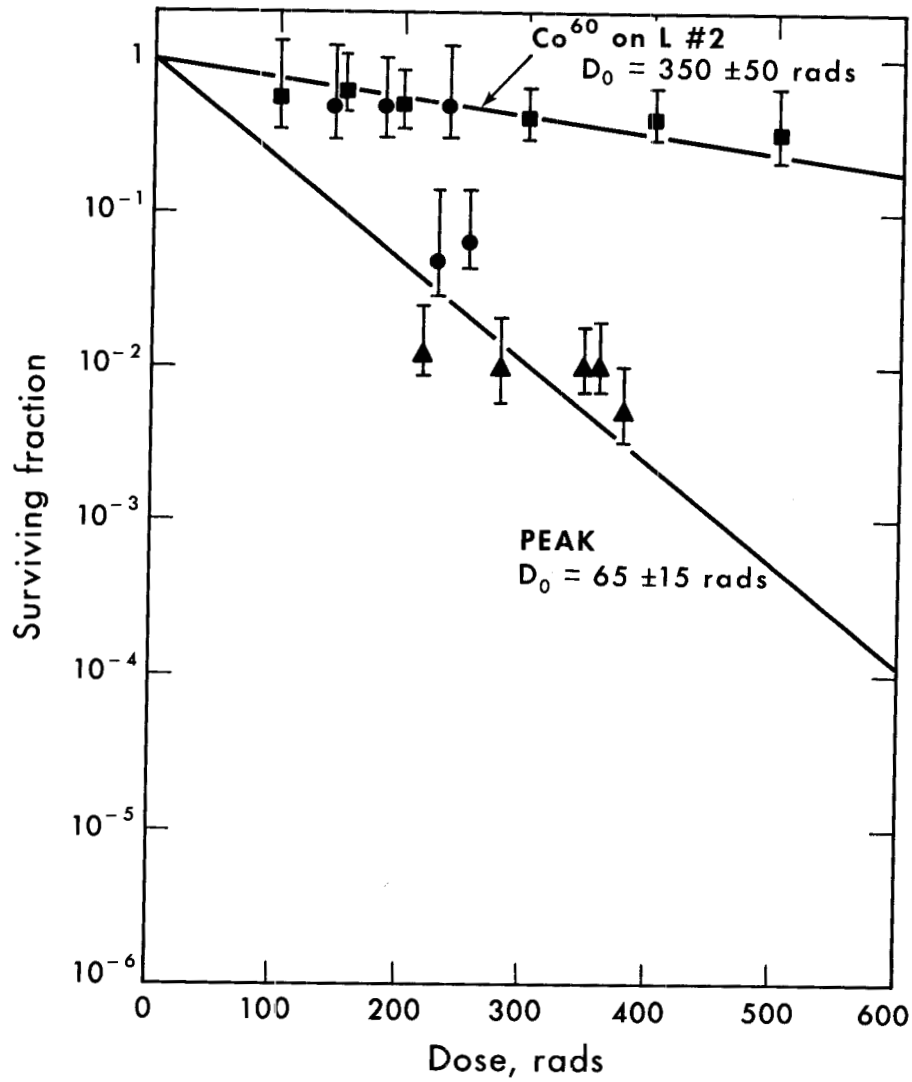

Fig. 9. Survival curves of lymphoma cells irradiated in vivo with a beam of π^- as compared with ^{60}Co γ-ray irradiation. Squares: ^{60}Co γ rays; triangles: π^- peak; circles: π^- plateau. No survival curve has been drawn for plateau points.

Use of Chromosome Aberrations for Dosimetry

Amos Norman
Department of Radiology, UCLA School of Medicine, Los Angeles, California 90024

A considerable body of work published in recent years [1-7] indicates that the frequency of chromosome aberrations in the lymphocytes taken from the peripheral blood may provide a useful measure of the absorbed dose. In this paper I shall review some of the problems involved in estimating the dose from the aberration frequency.

Figure 1 shows a photomicrograph of a normal lymphocyte obtained in a blood sample from a normal male. The karyotype, shown on the right, was prepared by cutting the chromosomes out of the photomicrograph and arranging them in conventional order. It can be seen that the forty-six chromosomes consist of twenty-two pairs of autosomes and an XY pair of sex chromosomes. Each chromosome consists of two identical chromatids joined by a centromere. Figure 2 shows a lymphocyte obtained from a man who had received three hundred rads of whole body X radiation. Structural alterations in the chromosomes can be easily seen. Perhaps most obvious are the dicentric (two centromeres) and the acentric (no centromere) fragments. The interest in chromosome aberrations arises primarily from the possibility that they are directly involved in the development of leukemia and other late effects of radiation.

Figure 3 provides a striking example of the possible involvement of chromosome aberrations in leukemia and also of the persistence over many years of radiation-induced chromosome aberrations. At the top, right, is shown a leukemic cell taken from a patient. The aberrant chromosomes from three such cells are shown at the bottom. At the top left is shown a lymphocyte obtained from the same patient. There are two dicentric chromosomes together with two associated acentric fragments; such aberrations are typical after high radiation doses. After the analysis had been made it was learned that the patient had been exposed accidentally to radiation some ten years prior to the development of his disease. Whether a cell damaged by radiation gave rise to the abnormal leukemic cells cannot be proved, but this may have been the mechanism for the development of the disease.

We cannot yet predict the risk of leukemia or other possible late effects of radiation from the frequency of chromosome aberrations--this is, of course, what we should like to do. But we can make a reasonable estimate of the dose received, particularly if it is an acute dose. The procedure essentially is to compare the frequency of aberrations observed with those produced in human lymphocytes *in vitro* by known radiation doses. Figure 4 shows the results of such *in vitro* experiments. The frequency of cells with dicentrics, rings, and tricentrics is shown as a function of acute doses of 2 Mev photons from a 6 Mev linear accelerator.[8] There are also shown data obtained in a single experiment with 40 Mev protons -- the aberration yields are not significantly different from those obtained with the photons. For both radiations the yield of dicentrics plus rings per cell is given rather well by $5.7 \times 10^{-6} D^2$, where D is the dose in rads. The yield of terminal deletions (acentric fragments not associated with dicentrics) is given by $1.0 \times 10^{-3} D$. Thus it can be seen that one class of

aberrations, the deletions, increases linearly with dose whereas the dicentrics and rings increase as the square of the dose. This is not true for all radiations. Uranium-fission neutrons, for example, produce rings and dicentrics with a frequency that varies linearly with the dose.(1) Nevertheless, it appears that radiations with LET comparable or less than that for 40-Mev protons will produce chromosome aberrations in human lymphocytes *in vivo* and *in vitro* with frequencies very similar to those reported here.

As the radiation dose increases the number of cells free of aberrations decreases. Figure 5 shows the frequency of chromosomally normal cells as a function of dose. The curve is quite similar to survival curves obtained with mammalian cells. However, there is not a simple relationship between chromosome aberrations and reproductive death. Moreover, only cells that are not reproductively dead can give rise to cancer. Thus the increased medical risks following radiation are very likely due to those cells that are genetically abnormal but not reproductively dead.(2,7)

Figures 4 and 5 also demonstrate another problem: at doses below 100 rad the frequency of cells with chromosome aberrations is very small. For example, after 50 rads only one cell in one hundred shows a dicentric. This frequency is significantly higher than that found in controls -- no dicentrics in 2,295 cells -- however, it is extremely tedious to analyze hundreds of cells by present techniques. For that reason many groups, including ours at UCLA, are working to automate the scoring of chromosome aberrations. Nevertheless, if we are willing to work hard, it is possible to make at least a rough estimate of dose even for doses of the order of ten rad. Examples of such estimates are shown in Table 1, but the uncertainties and the labor are both very great.

The frequency of aberrations in the lymphocytes is due only to the dose absorbed by the lymphocytes. Fortunately, the lymphocytes circulate so that a day or two after the radiation has been received the lymphocytes in the peripheral circulation probably give a measure of the average whole-body dose.(2) Moreover, when the dose is large, the distribution of aberrations can give an estimate of the uniformity of the dose over the lymphocyte population.(2) Finally, since the frequency of aberrant chromosomes decreases with time at a rate that is dependent on the type of aberration,(2) it is sometimes possible to estimate when the radiation was received. However, we are not usually concerned with large doses in the case of accidental exposures. When the dose is less than 50 rad it is feasible now only to make the sort of estimates shown in Table 1.

Much work remains to be done on yield of chromosome aberrations as a function of the distribution of dose in space and time and of the quality of radiation. Nevertheless, useful estimates can already be made of the dose absorbed by the circulating lymphocytes in people accidentally exposed to acute doses of radiation. The relationship of aberration frequency and medical risk for leukemia and other late effects of radiation remains for the future. A major drag on progress in this area will be removed when the scoring of chromosome aberrations is automated. At that time we shall be in a better position to guard the health of the chromosomes, and the chromosomes, after all, are our only biological legacy to the future generations of man.

References

1. M.A. Bender and P.C. Gooch, Somatic Chromosome Aberrations Induced by Human Whole-Body Irradiation: The "Recuplex" Criticality Accident, Radiation Res., 29: 568 (1966).
2. A. Norman, M.S. Sasaki, R.E. Ottoman, and A.G. Fingerhut, Elimination of Chromosome Aberrations from Human Lymphocytes, Blood, 27:706 (1966).
3. A. Norman, R.E. Ottoman, M. Sasaki, and R.C. Veomett, The Frequency of Dicentrics in Human Leukocytes Irradiated in vivo and in vitro, Radiology, 83:108 (1964).
4. A. Norman, M. Sasaki, R.E. Ottoman, and R.C. Veomett, Chromosome Aberrations in Radiation Workers, Radiation Res., 23:282 (1964).
5. P. Fischer, E. Gdob, E. Kunze-Muhl, A. Ben Haim, R.A. Dudley, T. Mullner, R.M. Parr, and H. Vetter, Chromosome Aberrations in Peripheral Blood Cells in Man Following Chronic Irradiation from Internal Deposits of Thorotrast, Radiation Res., 29:505 (1966).
6. S. Warren and L. Meisner, Chromosomal Changes in Leukocytes of Patients Receiving Irradiation Therapy, J. Am. Med. Ass., 193:351 (1965).
7. K.E. Buckton, P.A. Jacobs, W.M. Court-Brown, and R. Doll, A Study of the Chromosome Damage Persisting After X-ray Therapy for Ankylosing Spondylitis, Lancet ii:676 (1962).
8. A. Norman and M.S. Sasaki, Chromosome-exchange Aberrations in Human Lymphocytes, Int. J. Rad. Biol., 11:321 (1966).

Acknowledgement

The aberration frequencies reported here were obtained by Dr. M.S. Sasaki. This work was supported in part by Air Force contract AF 41(609)-2944.

Table 1

Estimation of dose received by four radiation workers

	No. of deletions	No. of cells	Deletions per cell	Estimated dose(rads)
Control	3	2,295	.0013	1.4 ± 0.8
1	5	300	.017	27 ± 12
2	3	100	.012	16 ± 9
3	2	100	.02	33 ± 23
4	4	300	.013	18 ± 9

The control group consists of three adult males. Film badge data indicate that subject 1 and 2 received 10 rem and 2 rem respectively. No adequate data available for subjects 3 and 4. The standard deviation given for each dose is based entirely on sampling error in the measurement of the frequency of deletions.

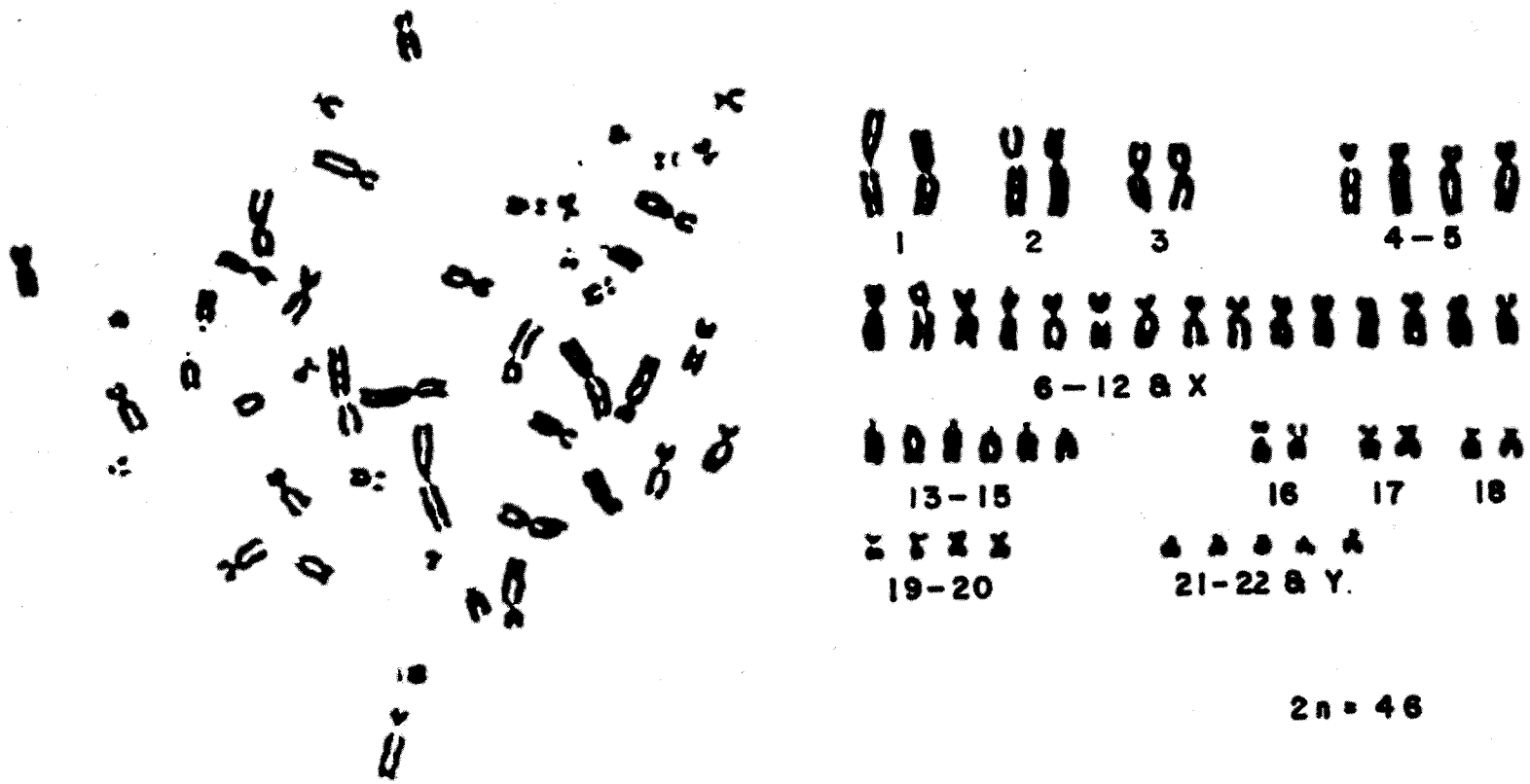

Figure 1 - Karyotype of a normal male lymphocyte together with the photomicrograph from which it was prepared.

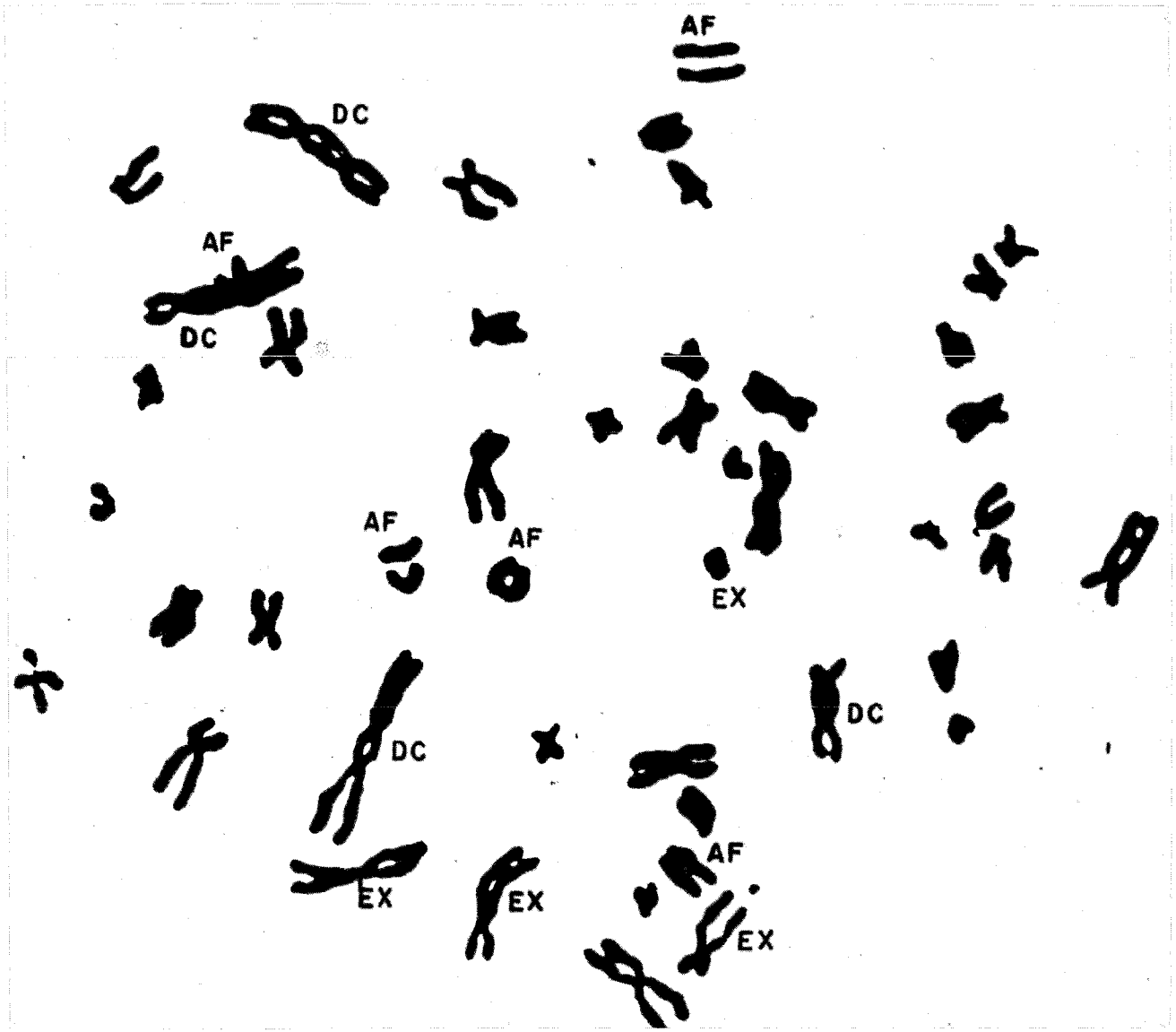

Figure 2 - Photomicrograph of a lymphocyte from a man who had received 300 rad whole body radiation. Dicentrics, DC, and acentric fragments, AF, are labelled.

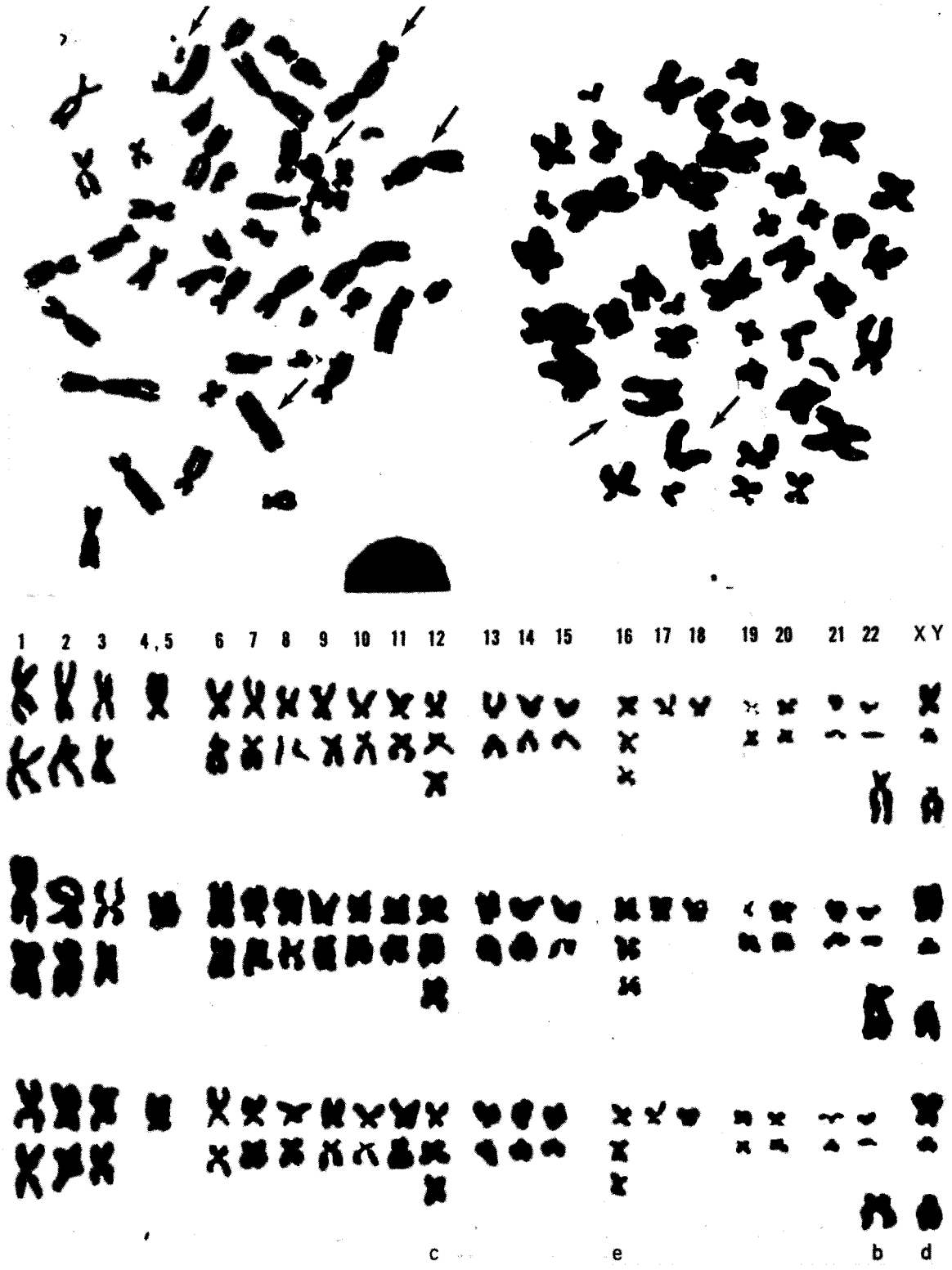

Figure 3 - A leukemic cell, right, and a lymphocyte, left, from the peripheral blood of a patient who had been accidentially exposed to radiation. The three karyotypes shown are from three leukemic cells.

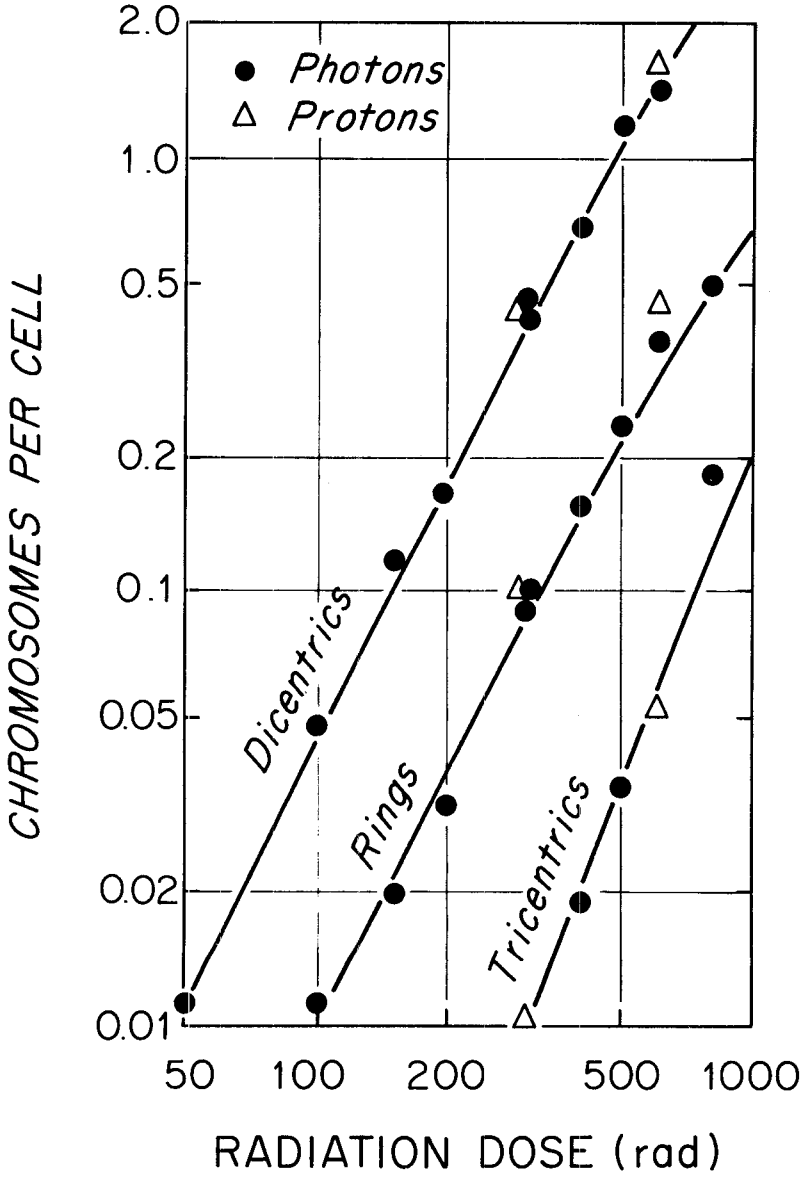

Figure 4 - Frequency of chromosome aberrations per cell as a function of the dose of 2 Mev photons and 40 Mev protons.

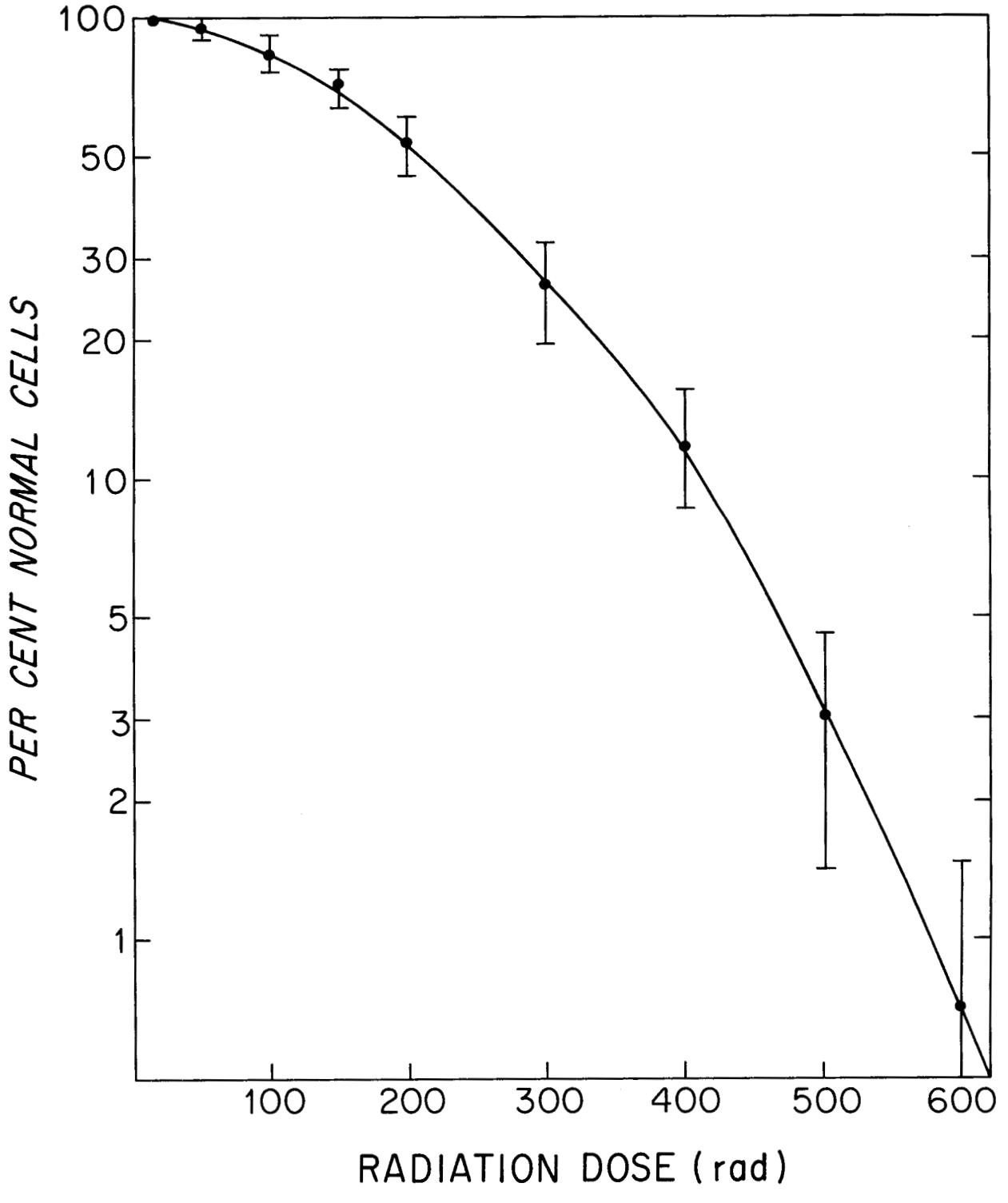

Figure 5 - Frequency of cells without chromosome aberrations.

LIST OF PARTICIPANTS

First International Symposium on the Biological Interpretation of Dose
from Accelerator-Produced Radiation
March 13-16, 1967

PARTICIPANTS

Henry Aceto
Biomedical Research
Lawrence Radiation Laboratory
Berkeley, California 94720

Peter Almond
University of Texas
M.D. Anderson Hospital and
Tumor Institute
6723 Bertner Avenue
Houston, Texas 77025

Lowell Anderson
Argonne National Laboratory
9700 South Cass Avenue
Argonne, Illinois 60439

Raymond G. Aune
Health Chemistry Department
Lawrence Radiation Laboratory
Berkeley, California 94720

A. Baietti
Tracerlab
2030 Wright Avenue
Richmond, California

Norman A. Baily
Hughes Research Laboratories
3011 Malibu Canyon Road
Malibu, California 90265

G. W. Barendsen
Radiological Institute of the Organization
for Health Research T.N.O.
151, Lange Kleiweg
Rijswijk Z.H., Netherlands

Nathaniel Barr
Division of Biology and Medicine
U.S. Atomic Energy Commission
Washington, D.C. 20545

Ray C. Barrall
Stanford University - Health Physics
171 Encina Hall
Stanford, California 94305

John W. Baum
Brookhaven National Laboratory
Upton, New York 11973

A. M. Beau
Department de la Protection Sanitaire
Commissariat à l'Énergie Atomique
Centre d'Etudes Nucléaires
Fontenay-aux-Roses, France

L. J. Beaufait
Safety and Technical Services Branch
U.S. Atomic Energy Commission SFOO
2111 Bancroft Way
Berkeley, California 94704

Harold Beck
Radiation Physics Division
Health and Safety Laboratory NYOO
376 Hudson Street
New York, N.Y. 10014

Burton G. Bennett
Radiation Physics Division
Health and Safety Laboratory NYOO
376 Hudson Street
New York, N.Y. 10014

Martin Biles
Division of Operational Safety
U.S. Atomic Energy Commission
Washington, D.C. 20545

R. D. Birkhoff
Oak Ridge National Laboratory
Oak Ridge, Tennessee 37830

Seymour Block
Lawrence Radiation Laboratory
Livermore, California

Richard Boggs
National Center for Radiological Health
1901 Chapman Avenue
Rockville, Maryland 20853

Frank Bold
General Atomic
P.O. Box 608
San Diego, California

Victor P. Bond
Medical Department
Brookhaven National Laboratory
Upton, New York 11973

P. Bonet-Maury
Institut du Radium
Laboratoire Joliot-Curie
B.P. No 1
Orsay (S. & O.), France

Max Boone
University of Texas
M.D. Anderson Hospital and
Tumor Institute
Houston, Texas 77025

Hans J. Bremermann
321 Campbell Hall
University Of California
Berkeley, California 94720

Tor Brustad
Norsk Hydro's Institute for
Cancer Research
The Norwegian Radium Hospital
Montebello, Oslo 3, Norway

William W. Burr
Division of Biology and Medicine
U.S. Atomic Energy Commission
Washington, D.C. 20545

Herbert P. Cantelow
Health Chemistry Department
Lawrence Radiation Laboratory
Berkeley, California 94720

Robert L. Clark
Nuclear-Chicago Corporation
333 East Howard Avenue
Des Plaines, Illinois 60018

D. M. James Compton
General Atomic
P.O. Box 608
San Diego, California 92112

Steven A. Coppola
National Center for Radiological Health
1901 Chapman Avenue
Rockville, Maryland 20853

Amasa Cornish
State Department of Public Health
Bureau of Radiological Health
2151 Berkeley Way
Berkeley, California 94704

W. G. Cross
Radiation Dosimetry Branch
Atomic Energy of Canada, Limited
Chalk River Nuclear Laboratories
Ontario, Canada

Stanley B. Curtis
Biomedical Research
Lawrence Radiation Laboratory
Berkeley, California 94720

Henry S. Dakin
Health Physics Department
Lawrence Radiation Laboratory
Berkeley, California 94720

H. T. Daw
International Atomic Energy Agency
Vienna, Austria

Carl Distenfeld
Brookhaven National Laboratory
Upton, New York 11973

Ernest L. Dobson
Donner Laboratory
University of California
Berkeley, California 94720

Patricia Durbin-Heavey
Biomedical Research
Lawrence Radiation Laboratory
Berkeley, California 94720

Morris Engelke
Los Alamos Scientific Laboratory
P.O. Box 1663
Los Alamos, New Mexico 87544

Robert D. England
State Department of Public Health
Bureau of Radiological Health
2151 Berkeley Way
Berkeley, California 94704

Gary R. Farmer
Oregon State Board of Health
State Office Building
P. O. Box 231
Portland, Oregon 97207

José M. Feola
Biomedical Research
Lawrence Radiation Laboratory
Berkeley, California 94720

Harold A. Fidler
Director's Office
Lawrence Radiation Laboratory
Berkeley, California 94720

Roland Finston
Health Physics
Stanford University
171 Encina Hall
Stanford, California 94305

Robert Flournoy
Naval Research Laboratory
Washington, D. C.

Trutz Foelsche
NASA Langley Research Center
Langley Station
Mail Stop 304
Hampton, Virginia 23365

Filbert T. Fong
U. S. Naval Radiological Defense
Laboratory
San Francisco, California 94135

J. F. Fowler
Department of Medical Physics
Royal Postgraduate Medical School
of London, Ducane Road
London, W. 12, England

Joseph Franaszek
California Division of Industrial Safety
455 Golden Gate Avenue
San Francisco, California 94102

C. B. Fulmer
Oak Ridge National Laboratory
P.O. Box X
Oak Ridge, Tennessee 37830

Francis E. Gallagher
California Institute of Technology
Pasadena, California

R. Gordon Gilbert
W. W. Hansen Laboratories of Physics
Stanford University
Stanford, California 94305

William Gilbert
Accelerator Study Group
Lawrence Radiation Laboratory
Berkeley, California 94720

Russell Gminder
Armed Forces Radiobiology
Research Institute
Defense Atomic Support Agency
Bethesda, Maryland 20014

Richard P. Grill
Health Chemistry Department
Lawrence Radiation Laboratory
Berkeley, California 94720

William A. Glass
Battelle Northwest Laboratory
P.O. Box 999
Richland, Washington 99352

H. Glauberman
U.S. Atomic Energy Commission NYOO
376 Hudson Street
New York, N.Y. 10014

Alexander Grendon
Donner Laboratory
University of California
Berkeley, California 94720

Kenneth A. Hardy
USAFSAM
Brooks AFB, Texas

William G. Hendrick
Space Radiation Effects Laboratory
11970 Jefferson Avenue
Newport News, Virginia 23606

John Hickman
University of California
Environmental Health and Safety
Davis, California 95616

George R. Holeman
Health Physics Division
1134 Kline Biology Tower
219 Prospect Street
New Haven, Connecticut 06520

Buddy Holley
Crocker Nuclear Laboratory
University of California
Davis, California 95616

John Holmes
Health Physics
Stanford University
171 Encina Hall
Stanford, California 94305

Don Honey
State Department of Public Health
2151 Berkeley Way
Berkeley, California

Harvey I. Israel
Los Alamos Scientific Laboratory
P.O. Box 1663
Los Alamos, New Mexico

C. D. Jackson
U.S. Atomic Energy Commission SFOO
2111 Bancroft Way
Berkeley, California 94704

Theodore M. Jenkins
Health Physics Department - SLAC
Stanford University
Stanford, California 94305

Hardin B. Jones
Donner Laboratory
University of California
Berkeley, California 94720

John H. Kane
Division of Technical Information
U.S. Atomic Energy Commission
Washington, D. C.

Elmer Kelly
Director's Office
Lawrence Radiation Laboratory
Berkeley, California 94720

Lola S. Kelly
Donner Laboratory
University of California
Berkeley, California 94720

S. Lakshmanan
Chemistry Department
University of Maryland
College Park, Maryland 20740

Lawrence H. Lanzl
Department of Radiology
The University of Chicago
Chicago, Illinois 60637

Harold V. Larson
Pacific Northwest Laboratory
Battelle Memorial Institute
Richland, Washington 99352

G. Legeay
D.P.S., Laboratoire de Radiopathologie
B.P. No 6-92
Fontenay-aux-Roses (Seine) France

Lionel M. Lieberman
Division of Operational Safety
U.S. Atomic Energy Commission
Washington, D. C. 20545

S. Allan Lough
Division of Biology and Medicine
U.S. Atomic Energy Commission
Washington, D. C. 20545

William D. Loughman
Donner Laboratory
University of California
Berkeley, California 94720

Lester F. Lowe
Air Force Cambridge Research Laboratories
L. G. Hanscom Field
Bedford, Massachusetts 01731

C. C. Lushbaugh
Applied Radiobiology
Oak Ridge Institute of Nuclear Studies
Oak Ridge, Tennessee 37830

John T. Lyman
Biomedical Research
Lawrence Radiation Laboratory
Berkeley, California 94720

Howard D. Maccabee
Biomedical Research
Lawrence Radiation Laboratory
Berkeley, California 94720

Richard Madey
Department of Physics
Clarkson College of Technology
Potsdam, New York 13636

C. W. Malich
Ames Research Center
Moffett Field, California 94305

Richard Marquiss
U.S. Naval Radiological Defense Laboratory
San Francisco, California

Shell Martin
NASA - Manned Spacecraft
Houston, Texas 77058 DC 32

R. C. McCall
Health Physics Department - SLAC
Stanford University
Stanford, California 94305

Joseph B. McCaslin
Health Physics Department
Lawrence Radiation Laboratory
Berkeley, California 94720

Edwin McMillan
Director's Office
Lawrence Radiation Laboratory
Berkeley, California 94720

A. J. Miller
Health Physics Department
Lawrence Radiation Laboratory
Berkeley, California 94720

Burton J. Moyer
Physics Department
Lawrence Radiation Laboratory
Berkeley, California 94720

Samuel A. Nabrit
Commissioner
U.S. Atomic Energy Commission
Washington, D. C. 20545

Amos Norman
Department of Radiology
The Center for the Health Sciences
University of California
Los Angeles, California 90024

John Novak
Argonne National Laboratory
9700 South Cass Avenue
Argonne, Illinois 60439

E. F. Oakberg
Biology Division
Oak Ridge National Laboratory
Oak Ridge, Tennessee 37831

Walter F. Ohnesorge
Oak Ridge National Laboratory
Oak Ridge, Tennessee 37831

Jean Paul Pages
Commissariat à l'Énergie Atomique
B.P. 511-15
75 - Paris 15ème, France

Howard Parker
Medical Department
Lawrence Radiation Laboratory
Berkeley, California 94720

Joseph R. Parker
Los Alamos Scientific Laboratory
Los Alamos, New Mexico 87544

Harvey M. Patt
Laboratory of Radiobiology
U.C. Medical Center
San Francisco, California 94122

H. Wade Patterson
Health Physics Department
Lawrence Radiation Laboratory
Berkeley, California 94720

John Pingel
USAEC Chicago Operations Office
9800 South Cass Avenue
Argonne, Illinois 60439

Donald G. Price
Radiation Control
University of Florida
Gainsville, Florida

M. R. Raju
Biomedical Research
Lawrence Radiation Laboratory
Berkeley, California 94720

Arthur Redmond
U.S. Naval Radiological Defense Lab
San Francisco, California 94135

Chaim Richman
Graduate Research Center of the
Southwest - P.O. Box 30365
Dallas, Texas 75230

James S. Robertson
Medical Physics Division
Brookhaven National Laboratory
Upton, L.I., New York 11973

William C. Roesch
Pacific Northwest Laboratory
Battelle Memorial Institute
Richland, Washington 99352

Harald H. Rossi
College of Physicians and Surgeons
of Columbia University
630 West 168th Street
New York, New York 10032

Jorma Routti
Health Physics Department
Lawrence Radiation Laboratory
Berkeley, California 94720

Eugene Saenger
Radioisotope Laboratory
University of Cincinnati College of Medicine
Cincinnati, Ohio

Leonard A. Sagan
Division of Biology and Medicine
U.S. Atomic Energy Commission
Washington, D. C. 20545

John W. Schaeflein
Veterans Administration Hospital
Long Beach, California 90804

Walter Schimmerling
Princeton-Pennsylvania Accelerator
Princeton, New Jersey 08540

Harlan Shaw
Tracerlab
2030 Wright Avenue
Richmond, California 94804

Alan R. Smith
Health Physics Department
Lawrence Radiation Laboratory
Berkeley, California 94720

Francis Smith, Jr.
Eberline Instrument Corporation
Livermore, California 94550

Walter S. Snyder
Health Physics Division
Oak Ridge National Laboratory
Oak Ridge, Tennessee 37830

Charles A. Sondhaus
Department of Radiological Sciences
University of California
California College of Medicine
1721 Griffin Avenue
Los Angeles, California 90031

Theodore Sopp
The Ohio State University Hospital
Office of Radiation Safety
410 West 10th Avenue
Columbus, Ohio 43210

Jerome W. Staiger
University Health Service
University of Minnesota
Minneapolis, Minnesota 55455

Lloyd D. Stephens
Health Physics Department
Lawrence Radiation Laboratory
Berkeley, California 94720

Palmer G. Steward
Health Physics Department
Lawrence Radiation Laboratory
Berkeley, California 94720

E. E. Stickley
Medical College of Virginia
Richmond, Virginia 23219

Warren Struven
SLAC - P.O. Box 4349
Stanford, California 94305

Maurice F. Sullivan
Pacific Northwest Laboratory
Division of Battelle Memorial Institute
Richland, Washington 99352

P. B. Tardy-Joubert
Commissariat à l'Énergie Atomique
B.P. 511-15
75-Paris 15ème, France

M. D. Thaxter
Health Chemistry Department
Lawrence Radiation Laboratory
Berkeley, California 94720

Ralph Thomas
Rutherford High Energy Laboratory
Chilton, Didcot, Berks., England

Cornelius A. Tobias
Donner Laboratory
University of California
Berkeley, California 94720

Eugene Tochilin
Radiological Physics Branch
U.S. Naval Radiological Defense Laboratory
San Francisco, California 94135

James E. Turner
Health Physics Division
Oak Ridge National Laboratory
Oak Ridge, Tennessee 37830

Edward J. Vallario
Division of Operational Safety
U.S. Atomic Energy Commission
Washington, D. C. 20545

M. Vialettes
Commissariat à l'Énergie Atomique
B.P. 511-15
75 - Paris 15ème, France

William W. Wadman III
Health Physics Department
Lawrence Radiation Laboratory
Berkeley, California 94720

Roger Wallace
Health Physics Department
Lawrence Radiation Laboratory
Berkeley, California 94720

Joseph Ward
California Department of Public Health
2151 Berkeley Way
Berkeley, California 94704

Martin S. Weinstein
U.S. Atomic Energy Commission
New York Operations Office
376 Hudson Street
New York, New York 10014

Max M. Weiss
Bell Telephone Laboratories, Inc.
Mountain Avenue
Murray Hill, New Jersey 07971

Graeme Welch
Biomedical Research
Lawrence Radiation Laboratory
Berkeley, California 94720

Robert Wheeler
Argonne National Laboratory
9700 South Cass Avenue
Argonne, Illinois 60439

Robert C. Will
Radiation Safety Office
University of Maryland
College Park, Maryland 20740

Donald Willhoit
University of North Carolina
P.O. Box 630
Chapel Hill, North Carolina 27514

G. H. Williams
Texas Nuclear Corporation
P.O. Box 9267
Austin, Texas 78756

Sheldon Wolff
Laboratory of Radiobiology
U.C. Medical Center
San Francisco, California 94122

Harold Wollenberg
Health Physics Department
Lawrence Radiation Laboratory
Berkeley, California 94720

Kim S. Wong
State of California
Division of Industrial Safety
455 Golden Gate Avenue
San Francisco, California

Ralph Worsnop
Radiology Department
U.C. Medical Center
San Francisco, California 94122

Paul Zurakowski
Hazards Control
Lawrence Radiation Laboratory
Livermore, California 94551

1

INDEX